

Studies in Systems, Decision and Control 342

Alla G. Kravets
Alexander A. Bolshakov
Maxim Shcherbakov *Editors*

Cyber-Physical Systems: Design and Application for Industry 4.0

 Springer

Studies in Systems, Decision and Control

Volume 342

Series Editor

Janusz Kacprzyk, Systems Research Institute, Polish Academy of Sciences,
Warsaw, Poland

The series “Studies in Systems, Decision and Control” (SSDC) covers both new developments and advances, as well as the state of the art, in the various areas of broadly perceived systems, decision making and control—quickly, up to date and with a high quality. The intent is to cover the theory, applications, and perspectives on the state of the art and future developments relevant to systems, decision making, control, complex processes and related areas, as embedded in the fields of engineering, computer science, physics, economics, social and life sciences, as well as the paradigms and methodologies behind them. The series contains monographs, textbooks, lecture notes and edited volumes in systems, decision making and control spanning the areas of Cyber-Physical Systems, Autonomous Systems, Sensor Networks, Control Systems, Energy Systems, Automotive Systems, Biological Systems, Vehicular Networking and Connected Vehicles, Aerospace Systems, Automation, Manufacturing, Smart Grids, Nonlinear Systems, Power Systems, Robotics, Social Systems, Economic Systems and other. Of particular value to both the contributors and the readership are the short publication timeframe and the world-wide distribution and exposure which enable both a wide and rapid dissemination of research output.

Indexed by SCOPUS, DBLP, WTI Frankfurt eG, zbMATH, SCImago.

All books published in the series are submitted for consideration in Web of Science.

More information about this series at <http://www.springer.com/series/13304>

Alla G. Kravets · Alexander A. Bolshakov ·
Maxim Shcherbakov
Editors

Cyber-Physical Systems: Design and Application for Industry 4.0

 Springer

Editors

Alla G. Kravets
Volgograd State Technical University
Volgograd, Russia

Alexander A. Bolshakov
Peter the Great St. Petersburg Polytechnic
University
St. Petersburg, Russia

Maxim Shcherbakov 
Volgograd State Technical University
Volgograd, Russia

The book was prepared with the financial support of the Russian Foundation for Basic Research, project No. 20-08-20032

ISSN 2198-4182 ISSN 2198-4190 (electronic)
Studies in Systems, Decision and Control
ISBN 978-3-030-66080-2 ISBN 978-3-030-66081-9 (eBook)
<https://doi.org/10.1007/978-3-030-66081-9>

© The Editor(s) (if applicable) and The Author(s), under exclusive license to Springer Nature Switzerland AG 2021

This work is subject to copyright. All rights are solely and exclusively licensed by the Publisher, whether the whole or part of the material is concerned, specifically the rights of translation, reprinting, reuse of illustrations, recitation, broadcasting, reproduction on microfilms or in any other physical way, and transmission or information storage and retrieval, electronic adaptation, computer software, or by similar or dissimilar methodology now known or hereafter developed.

The use of general descriptive names, registered names, trademarks, service marks, etc. in this publication does not imply, even in the absence of a specific statement, that such names are exempt from the relevant protective laws and regulations and therefore free for general use.

The publisher, the authors and the editors are safe to assume that the advice and information in this book are believed to be true and accurate at the date of publication. Neither the publisher nor the authors or the editors give a warranty, expressed or implied, with respect to the material contained herein or for any errors or omissions that may have been made. The publisher remains neutral with regard to jurisdictional claims in published maps and institutional affiliations.

This Springer imprint is published by the registered company Springer Nature Switzerland AG
The registered company address is: Gewerbestrasse 11, 6330 Cham, Switzerland

Preface

Industry 4.0 requires new approaches in the context of computer-aided design systems, new materials, and maintenance of cyber-physical systems as well as enhancing their interaction with humans. The book focuses on open issues of cyber-physical system design and its usage for the chemical industry and new material design as an essential component of Industry 4.0. Also, it discusses the implementation of breakthrough systems, models, programs, and methods that could be used in industrial processes for the control, condition assessment, diagnostics, prognostication, and proactive maintenance of cyber-physical systems.

The book contains 34 chapters joined into five parts. The first part Cyber-Physical Systems Design addresses the new ideas and results for improvement of cyber-physical systems in terms of reliability, efficiency, and decision making for humans interacting with machines. Seven chapters in part Cyber-Physical Systems in Chemical Industry provide interesting and novel results on how cyber-physical systems help to improve processes in the chemical industry and bring to another level of competitive ability. A part Cyber-Physical Systems for New Materials Design provides insight for engineers and R&D specialists from manufactures focusing on development and production of new materials using cyber-physical systems. A part Cyber-Physical Systems and Industrial Applications in Energetics presents chapters discussing issues in the energy domain such as reliability and guarantee of energy supply. Chapters in part Engineering Education for Cyber-Physical Systems Design highlight the essential aspect of professionals training who are able to design and support complex cyber-physical systems. Also, this book dwells with the analysis of the direction in engineering education, which helps the person who received it in creating cyber-physical systems. The authors describe the impact of education in the universities on the performance of industrial complexes and the organization of education for the development of cyber-physical systems.

The book is intended for practitioners, enterprise representatives, scientists, students, and Ph.D. and master's students conducting research in the area of cyber-physical system development and implementation in various domains. We

are grateful to the authors and reviewers for their ideas and contribution which make this book solid and valuable.

The book is dedicated to the 130th Anniversary of Kazan National Research Technological University and 35th Anniversary of the Computer-Aided Department at Volgograd State Technical University. Also, it is technically supported by the Project Laboratory of Cyber-Physical Systems of Volgograd State Technical University.

Volgograd, Russia
St. Petersburg, Russia
Volgograd, Russia
January 2021

Alla G. Kravets
Alexander A. Bolshakov
Maxim Shcherbakov

Contents

Cyber-Physical Systems Design

Patterns in Cyber-Physical Systems	3
Gennady Vinogradov, Alexey Prokhorov, and Georgy Shepelev	
Thermogradient Dimensional Stabilization of eddential Cross-Sections of the Carrying Structure of an Autonomous Object	17
Yulia Savelieva, Michael Livshits, Igor Adeyanov, and Ivan Danilushkin	
Minimum Defect Spline Multiwavelets and Parallel Computing for Big Data Compressing in Cyber-Physical Systems	33
Boris Shumilov	
Stress Computation and Reduction by Cyber-Physical Systems Controlling Printed Circuit Board Manufacturing Technology	49
Igor Kovtun and Vilen Royzman	
Geometric Parameters Optimization of Cable-Driven Parallel Robot with a Movable Gripper	61
Elena V. Gaponenko, Dmitry I. Malyshev, Victoria S. Kuzmina, and Larisa A. Rybak	
Decision Support System for Selecting Designs of Autostereoscopic Displays	73
Alexander A. Bolshakov and A. V. Klyuchikov	
The Rotor Speed Controlling Possibilities of a Promising Wind-Driven Power Plant Using Several Variable Elements of Its Geometry	89
Vladimir Kostyukov, Mikhail Medvedev, Dmitry Pavlenko, Andrey Mayevsky, and Nikolay Poluyanovich	
Repair Program Formation on the Basis of the Technical Condition Classifiers	107
Ruslan Voropai, Ivan Shcherbatov, Vladimir Agibalov, and Mikhail Belov	

Cyber-Physical Systems in Chemical Industry

Computer Modeling System for Energy- and Resource-Saving Control of Multi-Assortment Polymeric Film Production	119
-----------------------------------------------------------------------------------------------------------------------------	-----

Tamara Chistyakova and Andrey Polosin

Models and Algorithms for Selecting Safety Valves for Petroleum Industries	133
-----------------------------------------------------------------------------------------	-----

A. V. Nikolin and E. R. Moshev

Development of a Cyber-Physical Subsystem for Support and Decision Making of Managing Oil Production and Transportation Processes Under Uncertainty Conditions	145
-----------------------------------------------------------------------------------------------------------------------------------------------------------------------------	-----

Artur Sagdatullin and Gennady Degtyarev

Modeling of Vacuum Overhead System for Amine Mixtures Separation Unit	155
------------------------------------------------------------------------------------	-----

Eduard Osipov, Eduard Telyakov, and Daniel Bugembe

A Model of Rotational Mixing of Loose Environment on the Platform of Cyber-Physical Systems	167
----------------------------------------------------------------------------------------------------------	-----

A. B. Kapranova, D. D. Bahaeva, D. V. Stenko, and I. I. Verloka

Cyber-Physical Systems for New Materials Design

Computer System of Visual Modeling in Design and Research of Processes of Carbon Nanocluster Compounds Synthesis	181
-------------------------------------------------------------------------------------------------------------------------------	-----

Dmitriy Petrov, Tamara Chistyakova, and Nikolay Charykov

Intellectual System of the Life Cycle of Packaging Materials Characteristic Analysis	195
---------------------------------------------------------------------------------------------------	-----

Tamara Chistyakova, Aleksandr Razygraev, and Christian Kohlert

Model of Paired and Solitary Influence of Ingredients of Polymer Composition	205
-------------------------------------------------------------------------------------------	-----

Ilya V. Germashev, Evgeniya V. Derbisher, Vyacheslav E. Derbisher, and Tatyana P. Mashihina

The Indirect Methods of Conversion Monitoring Throughout Polymerization Processes in Bulk	219
--------------------------------------------------------------------------------------------------------	-----

Yuri P. Yulnets, Armen R. Avetisian, Roman Yu. Kulishenko, and Andrey V. Markov

Deformation and Filtration Characteristics of a Leather Semi-Finished Product	227
--------------------------------------------------------------------------------------------	-----

Shavkat Khurramov, Farkhad Khalturaev, and Feruza Kurbanova

Simulation Modeling for Drying Process of Pellets from Apatite-Nephenine Ores Waste	241
--------------------------------------------------------------------------------------------------	-----

Vladimir Bobkov, Maksim Dli, and Alexandr Fedulov

Optimal Control for Energy and Resource Efficiency in the Drying Process of Pellets from Apatite-Nepheline Ores 253
 Vladimir Bobkov and Maksim Dli

Cyber-Physical Systems and Industrial Applications in Energetics

Life Cycle Management of Power Grid Companies' Equipment 265
 Oleg Protalinskiy, Aleksandr Shvedov, and Anna Khanova

Developing an Energy Provider's Knowledge Base of Flow Charts 275
 V. A. Borodin, Oleg Protalinskiy, and Anna Khanova

A Method for Change Detection in Operating of Power Generating Equipment 285
 I. D. Kazakov, N. L. Shcherbakova, E. S. Rayushkin,
 and Maxim V. Shcherbakov

Forecast of the Cost of Electricity and Choice of Voltage Level for the Enterprise 299
 Nikita Ustyugov

Method of Operational Determination of Amplitudes of Odd Harmonics of Voltages and Currents in Power Supply Circuits of Powerful Electrical Installations 311
 P. K. Lange, V. N. Yakimov, E. E. Yaroslavkina, and V. V. Muratova

Uncertainty Region Decomposition Approach for Problem of Flexible One-Stage Heat Exchange Network Design 323
 T. V. Lapteva, Nadir Ziyatdinov, Ilya Emelyanov, and D. A. Mitsai

Optimal Heat Integration of Large-Scale Cyber-Physical Oil Refining Systems 335
 Alina Ryzhova, Ilya Emelyanov, Nadir Ziyatdinov,
 and Zufar Khalirakhmanov

Predictive Systems for the Well Drilling Operations 347
 O. V. Zhdaneev, K. N. Frolov, and Y. A. Petrakov

Engineering Education for Cyber-Physical Systems Design

Use of Computer Trainers for Teaching Management Manufacturing Personnel of Chemical Industries 371
 Tamara Chistyakova, Gunter Reinig, and Inna V. Novozhilova

Higher School Education Quality Forecasting by Regression Analysis Methods 383
 I. M. Kharitonov, E. G. Krushel, O. V. Stepanchenko, and O. O. Privalov

Increasing Student Motivation by Using Dynamic Rating: Approach and Implementation as Part of the LMS Based on Open-Source Software 399
Mikhail Ivanov and Victor Radygin

Student Activity Cognitive Preference Registration in Dynamic Computer Testing Simulators 413
I. V. Shadrin

Prospects of the Interdisciplinary Course “Computational Intelligence” in Engineering Education 431
Yuriy Skobtsov

Effective Tools and Technologies for Creating and Maintaining Web Resources Based on JavaScript Libraries 443
Ina Lukyanovich, Lidia Blinkova, and Uladzislau Sableuski

Cyber-Physical Systems Design

Patterns in Cyber-Physical Systems



Gennady Vinogradov, Alexey Prokhorov, and Georgy Shepelev

Abstract A robotic cyber-physical object is an informationally connected set of physical components, onboard measurement systems, onboard executive systems, an onboard computer system with implemented control algorithms, and a control station with displays and controls. Such an object must have the self-sufficient behavior that guarantees the fulfillment of a certain mission. The behavior intellectualization requirement makes us reconsider the logical and mathematical abstractions that are the basis for building their onboard control systems. The problem of developing such systems based on pattern theory is relevant. It is shown that this ensures the effective experience transfer into a cyber-physical system and ensures the compatibility of the theological approach and the cause-and-effect approach. There are the identification and pattern model construction problems are considered. It is proposed to use four information processing points for this purpose, and a method of logical inference on patterns is developed.

Keywords Decision making · Purposeful systems · Fuzzy judgement · Choice situation · Cyber-physical system

1 Introduction

A cyber-physical object is an informationally connected set of physical components, onboard measurement systems, onboard executive systems, an onboard computer system, with implemented control algorithms, and a control station with displays

G. Vinogradov (✉)

Tver State Technical University, Afanasy Nikitin Emb. 22, Tver 170026, Russia
e-mail: wgp272ng@mail.ru

A. Prokhorov · G. Shepelev

CJSC Research Institute “Centerprogramsystem”, 50 let Oktyabrya Ave. 3a,
Tver 170024, Russia
e-mail: forworkap@mail.ru

G. Shepelev

e-mail: shepelevgeorg@gmail.com

and controls. Such an object must have self-sufficient behavior that guarantees the fulfillment of a certain mission. It is possible to achieve the desired increase in the effectiveness of such complexes in an undetermined and poorly formalized environment mainly by improving the intelligent component of their control system. However, it should be noted that the vast majority of research in this area remains at the theoretical level [1–10]. There is a gap between primitive behavioral models of artificial entities, for example, in swarm robotics, their interaction models, and expectations from practice [11–13].

By now, it has become clear that it is possible to achieve the desired sharp increase in the efficiency of robotic systems, mainly by directing designers' and scientists' efforts to improve the control system intelligent component: (1) a set of algorithms for onboard control systems; (2) algorithms for the activities of the crew that controls a cyber-physical system. These components form the “cooperative intelligence” of a cyber-physical system, which allows creating a functionally integral object from a set of separate systems of onboard equipment aimed at performing the task of the current session of a functioning robotic system.

An autonomous intelligent system (hereinafter referred to as an agent) showing human-like behavior is a system that includes the following components (Fig. 1):

- onboard measuring devices (or a set of onboard measuring devices) that function as sensors which allow obtaining information about the environment state and their own state;
- onboard execution units (or a set of onboard execution units) that function as effectors which help the system to affect the external environment and itself;
- means of communication with other systems;
- “onboard intelligence”, which can include onboard computers, their software, as well as control center operators that are the carrier of a set of algorithms for solving problems of the subject area obtained due to training and experience

Such a system exists in time and space, interacts with other agents, with the environment when performing combat tasks and obligations using available mods

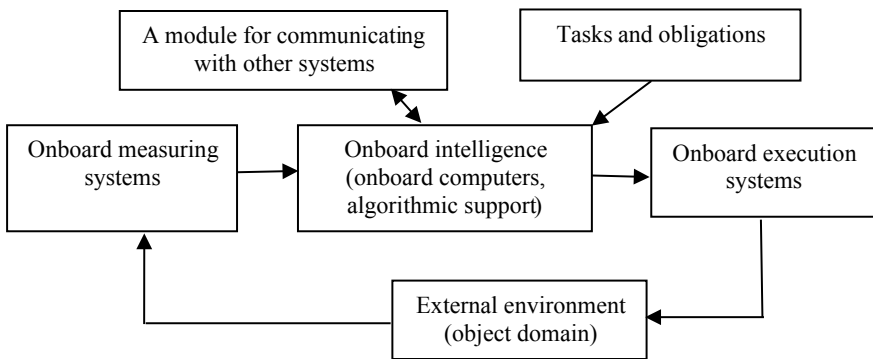


Fig. 1 An enlarged diagram of an intelligent autonomous system

of action. The agent performs the assigned tasks based on an understanding of his condition and subjective ideas about the state of the environment and the combat situation development, as well as the information received through a communication module. The agent is able to predict changes in the environment affected his actions and evaluate their usefulness.

2 Requirements for the Autonomy and Intelligence of Combat Cyber-Physical Systems

The role of automated systems when performing combat tasks should be considered from the standpoint of their impact on a human. They should help a commander by making his work easier and more efficient. At the same time, a commander must be an element of a control system (*human in the loop control*) of the cyber-physical system. Their interaction should ensure the experience transfer both from a human to the system and in the opposite direction, thereby providing the adaptive behavior. For example, the main difficulty for any autonomous system is the recognition of situations in the environment. The complexity and multiplicity of situations that arise during the mission performance make it impossible to identify them based on the results of multiple tests and form a knowledge base on their basis. Consequently, it is necessary to implement an additional monitoring scheme for the cyber-physical system to identify situation classes and successful modes of action in order to form behavioral models (patterns) based on data obtained in real conditions [14, 15]. This scheme guarantees a controlled evolution of self-sufficiency when solving tasks by combat units that include autonomous cyber-physical systems.

3 Initial Assumptions and Hypotheses

Usually, the situations that an autonomous system faces are difficult enough for their constructive formalization by traditional formal methods, but they are described well by natural language means. There also is their resolution experience and description, for example, by fuzzy logic means. The bearer of such experience is called a leader. Leaders share their experience through communication tools in the chosen language. Let us accept the hypothesis that human experience/behavior should be considered as a function of the interaction between a situation and a human. A situation can be interpreted as a component of the cause for its subjective reflection in a person. A person chooses a certain behavior based on a subjective representation of a situation, influences a situation, and changes it. At the same time, the processes occurring in a human mind when performing certain actions lead to expanding his ability structure (knowledge, experience). A cyber-physical system behavior model should also take into account this phenomenon of mutual influence. With this approach, the

concept of “typical situation” (TS) turned out to be constructive [16, 17]. This part of a cyber-physical system operation is functionally closed and has a clearly defined meaningful purpose. It appears as a whole in various (real) sessions, being detailed in them according to the conditions and the available ways of resolving problematic sub situations arising in TS [11]. When a cyber-physical system is fully intellectualized, TS, and the modes of action form an individual behavioral pattern as a reaction to it. A person, while mastering his experience, also aims to aggregate it by creating pattern models. Therefore, a pattern model should be considered as a unit of human experience, for which a person has a certain degree of confidence in obtaining the desired states in a situation similar to a typical one (cluster). V. Finn has shown that an ideal intelligent system should have 13 types of abilities. At the present stage, only a part of these abilities can be implemented and only in interaction with a person. For example, “this is a product of the sequence “goal-plan-action”, the ability to reflect, the ability to integrate knowledge, the ability to clarify unclear ideas, the ability to change the knowledge system when receiving new knowledge”. He notes that it is impossible to exclude a person from this mode. Therefore, an intelligent system for military purposes cannot be completely autonomous and must be considered as a partner human–machine system with a pattern as the unit of knowledge.

Definition. A pattern is the result of the activity of a natural or artificial entity associated with an action, decision-making, its implementation, etc., which was carried out in the past and is considered as a template (sample) for repeated actions or as a justification for actions according to this pattern.

4 The Model of a Behavioral Pattern Fuzzy Description

Behavior in TS is associated with a choice that occurs in a purposeful state situation [12]. Let us consider a behavioral model in the form of a fuzzy description of a choice situation model. It is proposed to build a possible variant of such construction using “paradigm grafting” of ideas from other sciences, for example [12, 18]. A purposeful state consists of the following components:

- a subject who making the choice (agent), $k \in K$.
- choice environment (S), which is a set of elements and their essential properties, a change in any of which can cause or produce a change in a purposeful choice state. Some of these elements may not be system elements and form an external environment for it. The impact of the external environment is described using a set of variables.
- Available modes of actions $c_j^k \in C^k$, $j = \overline{1, n}$ of the k -th agent that are known to him and can be used to achieve the i -th result (also called alternatives). Each mode of this set has a set of parameters called control actions.
- Possible results for environment S that are significant for an agent— $o_i^k \in O^k$, $i = \overline{1, m}$. The results are assessed using a set of parameters called the output parameters of a purposeful state situation.

- A method for assessing the properties of the results obtained after choosing a mode of action. Obviously, the assessment of the result should reflect the result value for an agent and thus reflect their personality.
- Constraints reflecting the requirements imposed by the choice situation on output variables and control actions.
- A domain model, which is a set of relationships that describe the dependence of control actions, parameters, and disturbances with output variables.
- An agent constraint model. It is described in detail in [17]. Regardless of a constraint description type, we will assume that the agent has a certain degree of confidence about the possibility of changing a part of constraints towards expanding a set of possible choice options (alternatives).

For the described components, let us introduce measures to assess the purposeful state.

1. We will assume that the agent is able to distinguish factors that are environmental characteristics $X^k = \{x_i^k, i = \overline{1, N}\}$. The agent evaluates the influence of each factor using a linguistic variable $\mu_x^k(x_i^k) : x_i^k \rightarrow [0, 1]$. Let us introduce a parameter for the agent to assess his situational awareness in a purposeful state situation

$$Es^k = \frac{\sum_{i=1}^N \mu_x^k(x_i^k) x_i^k}{\sum_{i=1}^N \mu_x^k(x_i^k)} \quad (1)$$

We can define the following constraint:

$$\sigma^k(Es^k) \geq \sigma_0^k,$$

where σ_0^k is a certain threshold level of agent's awareness due to using his own information sources.

2. We will assume that in order to describe the influence of the selected factors on the results $o_i^k, i = \overline{1, m}$, the agent uses an approximation in the form of the following production rules:

If x_1 is A_{r1}^k and if x_2 is A_{r2}^k and ... and if x_N is A_{rN}^k , then

$$o_i^k = f_{ir}^k(x_1, x_2, \dots, x_N), \quad r = \overline{1, R}, \quad i = \overline{1, m} \quad (2)$$

where R is the number of production rules, r is the current production rule number, $o_i^k = f_{ir}^k(x_1, x_2, \dots, x_N)$ is an explicit function that reflects the agent's idea of the causal relationship of input factors with possible results for the r -th rule; A_{ri}^k are fuzzy variables defined on $X^k = \{x_i^k, i = \overline{1, N}\}$.

Mathematical models, a verbal description, graphs, tables, algorithms, etc. might be used as a function $f_{ir}^k(\cdot)$.

Since c_j^k it is a function of the external environment state parameters taken into account and system properties, a set of assumptions about their possible values forms a scenario of the possible state of the external environment, the system functionality. The implementation of scenarios, for example, using the rules (2) allows forming an idea of possible results o_i^k . The ambiguity in choosing a mode of action might be described as the degree of confidence in the need to apply it to obtain a result o_i^k . This estimate can be described by the linguistic variable

$$\psi_j^k = \psi_j^k(c_j^k \in C^k | s_i \in S \rightarrow o_i^k) \in [0, 1].$$

This measure is an agent's individual characteristic, which can change after training and gaining experience, as well as a result of the communication interaction of agents with each other and with an operator. Therefore, $\psi_j^k = \psi_j^k(c_j^k \in C^k | s_i \in S, I^k \rightarrow o_i^k) \in [0, 1]$, where I^k is the information available to the agent at the time point t_k .

3. Choosing a mode of action c_j^k when the agent makes a decision in a purposeful state situation to achieve a result o_i^k is associated with building a quantitative assessment of the chosen solution properties, as shown in [12]. The list of properties and parameters is based on experience, knowledge, intelligence, and the depth of his understanding of a decision-making situation. A correct description of the properties and parameters of a mode of action is one of the main conditions for the choice c_j^k that will lead to the result o_i^k . The choice of the list of properties and their parameters that characterize them depends on the agent (his personality). Let us represent the possible results for a given environment for an agent's choice in the form $o_i^k \in \{o_{ij}^k, j = \overline{1, J}\}$, where o_{ij}^k is a set of possible results when choosing the j -th mode of action, $i \in I$ is a set of results that the k -th agent takes into account. It's obvious that $o_{ij}^k = o_{ij}^k(s_i)$, $s_i \in S$.
4. The value of the o_i^k results. Since $o_{ij}^k = o_{ij}^k(s_i)$ and $s_i = S(c_j^k)$, the value of the i -th type of result is estimated by the following linguistic variable $\phi_i^k(o_i^k(c_j^k)) \in [0, 1]$. The function $\phi_i^k(o_i^k(c_j^k))$ for the result o_i^k will be a monotonic transformation since $\phi_i^k(\cdot)$ it translates the range of the function $o_i^k(c_j^k)$ into the set of linguistic variable values. Since the base value of the linguistic variable corresponds to fuzzy variables, this transformation transfers the range of the function o_i^k into the range of the base fuzzy variables.

5 A Model for Choosing an Agent When Implementing a Pattern

The three linguistic variables $\mu_i^k(x_i^k)$, ψ_{ij}^k , E_{ij}^k introduced above form a model of the agent's ideas about the purposeful choice situation.

Since c_j^k it can be described in terms X_i^k and the agent has an idea of the dependence in the form of a rule base that links c_j^k the value of the possible i -th result o_i^k , it is

possible to determine the value of the purposeful state by the i -th result o_i^k for the k -th agent according to the rule [6, 17]:

$$E\phi_i^k = \frac{\sum_{j \in J} \phi_{ij}^k(o_{ij}^k(c_j^k)) \cdot o_{ij}^k(s^k)}{\sum_{j \in J} \phi_{ij}^k(o_{ij}^k(c_j^k))}.$$

In a similar way, we can assess the purposeful state value for the k -th agent by the efficiency of the i -th type of result:

$$EE_i^k = \frac{\sum_{j \in J} EE_{ij}^k(o_i^k(c_j^k)) \cdot \psi_i^k(c_j^k)}{\sum_{j \in J} \psi_i^k(c_j^k)}.$$

The agent's assessment of the desirability of a purposeful state by the i -th result and the effectiveness of its achievement in a choice situation is given in the form of a linguistic variable [19]

$$\chi_{i1}^k = \chi_1^k(E\phi_i^k) \in [0, 1], \quad \chi_{i2}^k = \chi_2^k(EE_i^k) \in [0, 1] \quad (3)$$

We can define the following restrictions:

$$\sum_i \chi_{i1}^k(E\phi_i^k) \geq \chi_1^0 \quad \text{and} \quad \sum_i \chi_{i2}^k(EE_i^k) \geq \chi_2^0$$

where χ_1^0 and χ_2^0 are the agent's expectations from the mission that reflect the balance between costs and achieve results o_i^k .

The model of the agent's choice situation in TS is the set of structural and functional properties that (in his opinion) the choice situation has and which affect his satisfaction or dissatisfaction with the situation.

There is another group of factors that determine the result implementation: will, risk proneness, self-esteem, motivation. These factors make it possible to talk about such an indicator as confidence $\rho_i^k(o_i^k)$ in obtaining a result o_i^k in a situation of choice when using one of the possible modes of action $c_j^k \in C^k$.

Based on the hypothesis of rational behavior, the agent forms a decision according to the rule

$$\begin{aligned} P_i^k(s \in S) &= \underset{c_j^k}{\text{Arg max}} \left(\sum_{j \in J} E\phi_i^k(o_i^k(c_j^k)) - EE_i^k(o_i^k(c_j^k)) \right) \\ c_j^k &\in C^k(I_i^k), \quad I_i^k \subseteq M, \quad o_i^k \in O^k \\ \sum_i \chi_{i1}^k(E\phi_i^k) &\geq \chi_1^0, \quad \sum_i \chi_{i2}^k(EE_i^k) \geq \chi_2^0 \\ \sigma^k(ES^k(X)) &\geq \sigma_0^k \end{aligned} \quad (4)$$

Since the choice is related to the agent’s ideas about the choice situation, it is necessary to include the knowledge base (2) in (4).

The relations (4) describe the agent’s (cyber-physical system) behavioral pattern when striving to achieve the i -th result. The agent considers (4) a pattern as a way of describing a problem, a principle, and an algorithm for its solution, which often arises, and its solution might be used many times without reinventing anything.

The value indicators of the purposeful state for the result $E\phi_i^k$ and the purposeful state value for the efficiency EE_i^k are elements of the integral value indicator of the purposeful state for the k -th individual $\sum_i E\phi_i^k \cdot EE_i^k$. Given his confidence degree in obtaining a result ζ_i^k , an expected specific value indicator will be the following:

$$EV_k = \frac{\sum_i (E\phi_i^k - EE_i^k) \cdot \zeta_i^k}{\sum_i \zeta_i^k} \tag{5}$$

This means that if two subjects are in the same situation of choice, then the difference in their behavior should be manifested in specific value estimates by the result and effectiveness and in the degree of confidence in achieving the goal.

The relationships (4-5) mean that when the agent wants to achieve some result, he has several alternative ways of achieving it with the methods of varying efficiency, and his confidence in obtaining the desired result is significant.

Such a model of autonomous agent’s individual behavior supposes forming a knowledge base by learning based on experimental experience, which makes it possible to implement the “cooperative intelligence” evolution due to an artificial cognitive process similar to that of natural entities [1, 20]. It should be noted that this capability is absent in knowledge-based systems since it lacks a computer model of adaptive behavior. Thus, the general principles of the agent’s reasoning are quite traditional and include the following three main phases (Fig. 2):

- Perception—receiving data and building a scene model in a loaded world;

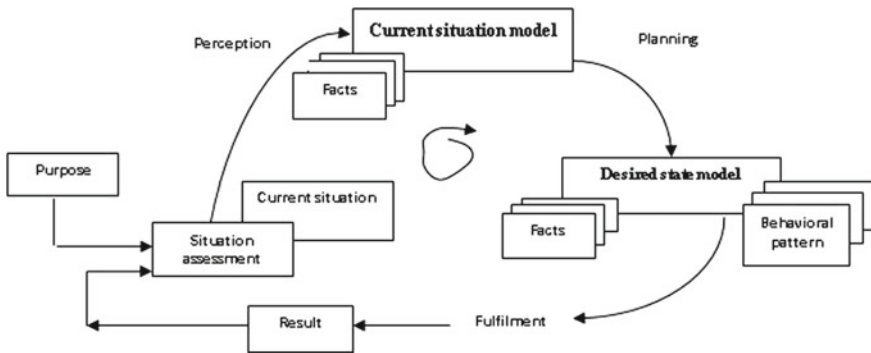


Fig. 2 The intelligent agent’s reasoning scheme (TOTE model)

- Cognition—analysis and forming a scenario of the subject’s actions to achieve the set goals;
- Execution of the intended scenario with a constant comparison of expected and observed results.

Unlike other similar systems, the system under consideration implements these phases through two basic mechanisms closely related to each other: abstraction and concretization.

6 Modeling Patterns. Basic Modeling Points

6.1 Modeling Patterns

Pattern modeling involves a limited natural language subset including modeling of case-based reasoning, which forms a specific part of human experience—meta-experience. To implement the described approach, there is a developed software system that allows modeling the environment (context) and the agent’s behavior pattern from different points. We have selected four basic perception points for collecting and interpreting information in order to identify a behavioral pattern model. They are: the first point (a person’s own point of view), the second point (situation perception from another person’s point of view), the third point (situation perception from an uninterested observer’s point of view), the fourth perception point implies considering the situation from the point of view of the involved system.

Since we assume that each point uses different visions of a situation and possible modes of action, the integration and coordination of viewpoints, allows the agent to expand his understanding of the purposeful state situation and a behavioral pattern.

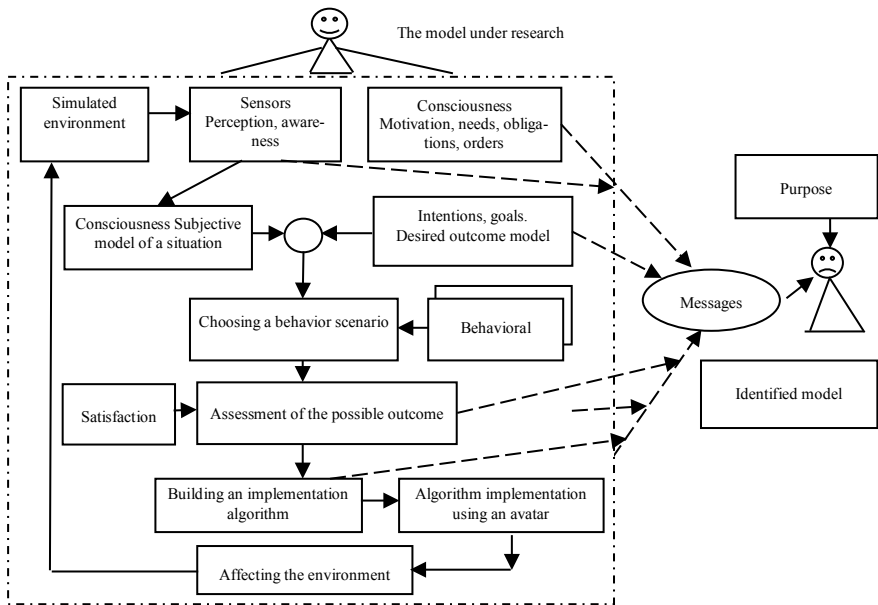
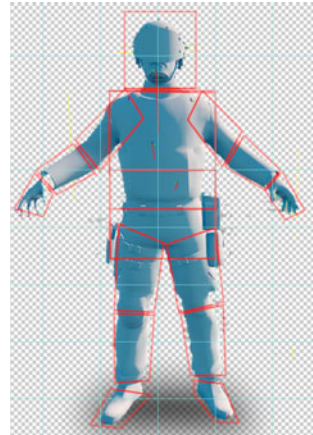
Modeling from the first point assumes that a person with experience in fulfilling a mission implements it in the system independently and examines the pattern(s) used in this case. A testee shows his behavior by performing voice control of an “avatar” (see Fig. 3).

Rectangles and the way of their positioning on the avatar are shown in red. The disadvantage of this method is that the accuracy of object recognition decreases, but at the same time, this method saves hardware resources and time for calculating intersections. This scheme for determining intersections will be used similarly to implement a hit in a fire contact situation. A testee performs actions in accordance with the scheme shown in Fig. 4.

The implementation of the agent model visual function represents seeing objects through simple forms, for example, in this case, they are cubes and their vertices, as well as ignoring objects that are not of value to the model, for example, walls and others.

The eye is implemented as an empty object that is used as an endpoint for constructing a visual ray located at the head level. To be realistic, it will also be animated for the cases of head rotation during character animation.

Fig. 3 A simplified representation of an avatar 3D model



These functions are for sorting, and therefore for speeding up object processing.

Fig. 4 A reflexive approach scheme for identifying a behavioral pattern from the first position is information flows

The entire visual part is reduced to 3 main functions:

1. determining whether the object is in sight;
2. determining the distance to the object;
3. constructing vectors from a simplified object model to an object responsible for the agent's eyes.

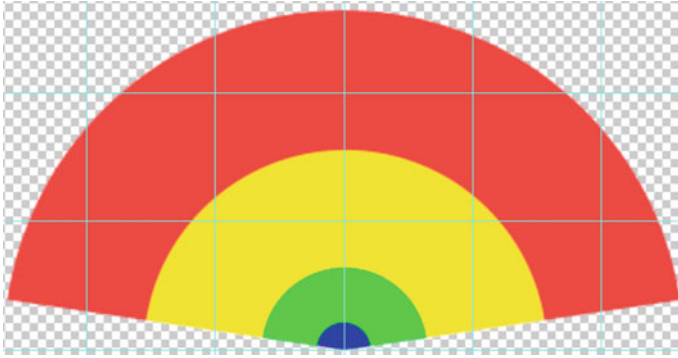


Fig. 5 The eye visibility scope

These functions are for sorting, and therefore for speeding up object processing.

6.2 The Function of Object Detection in the Eye Visibility Scope

The function makes it possible to see those objects that are in the eye visibility scope, thereby reducing the cost of detailed processing of all objects. A schematic implementation of the scope is shown in Fig. 5. The agent's location in the world is blue. The viewing angle is 120°.

6.3 The Function of Object Detection Within Eyesight

Another function for sorting objects and saving calculation time is an area divided into priorities (see Fig. 5).

Green is a high priority; objects in this area will always be selected. Now it is 20 m. Also in this zone, the objects will be named.

The yellow and red priority zones will be selected if there are no objects in the green priority zone. Now, these zones are 50 and 100 m, respectively.

In the future, it might be improved and in terms of time consumption, the objects that are located farther from the eye may require longer focusing time.

6.4 The Function of Object-Eye Intersection Detection

The function works on the principle of finding the intersection between the points of the rough object model and an “eye”. A ray is built between two points; if the ray hits an object, an “eye” does not see this point. If an “eye” sees at least one point of the object, then the entire object is visible.

The action pattern analysis is performed from the researcher’s point of view. It is important to emphasize that in order for the agent to describe already performed activities according to his own pattern (Fig. 4), the subject in question must leave his previous activity point and move to a new point that is external in relation to both already performed actions and the future projected activity. This is called the first level reflection: considering the agent’s previous position, his new point will be called the reflexive one, and the knowledge generated in it will be reflexive knowledge since it is taken in relation to the knowledge developed in the first point. The above reflexive output scheme will be the first abstract model characteristic of reflection in general.

The second position possibly assumes a full imitation of the agent’s behavior, when a researcher tries to think and act as close as possible to the agent’s thoughts and actions using the model obtained in the first point. This approach allows understanding at an intuitive level the essential but unconscious aspects of the modeled agent’s thoughts and actions, thus to refine a model. Modeling from the third point is to observe the modeled agent’s behavior as a disinterested observer. The third point assumes constructing a model of a mode of action from the point of view of a specific scientific discipline related to the agent’s subject domain. The fourth position presupposes an intuitive synthesis of all received ideas in order to obtain a model with maximum values of specific value indicators by a result and efficiency.

This approach involves implicit and explicit information. It is possible that the agent knows or understands the essence of some activity but is not able to perform it (conscious incompetence). Conversely, the agent is able to perform some actions well but does not understand the way to do them (unconscious competence). Having a perfect command of skill implies both the ability “to do what you know” and the ability “to know what you do”. Nevertheless, many behavioral and psychological elements that ensure the success of agents’ actions remain unconscious and only intuitive. As a result, they are unable to describe the mechanisms of any abilities directly. Moreover, some agents deliberately avoid thinking about what they are doing and how they are doing it due to fear that this knowledge will interfere with intuitive actions. Therefore, one of the modeling goals is to identify *unconscious competence*, and make it conscious in order to understand it better, improve and transfer a skill.

Cognitive and behavioral competences are modeled either “implicitly” or “explicitly”. *Implicit modeling* involves taking the second point in relation to the subject of modeling in order to achieve an intuitive understanding of the subjective experiences of a given person. *Explicit modeling* involves taking the third point in order to

describe an explicit structure of the modeled agent's experience so that it can be transmitted to others. Implicit modeling is primarily an inductive process for accepting and perceiving the structures of the surrounding world. Explicit modeling is a deductive process for describing and implementing this perception. Both processes are necessary for successful modeling. Without an implicit stage, there can be no effective intuitive base for building an explicit model. On the other hand, without an explicit phase, the modeled information cannot be translated into techniques or means and be transmitted to others. Implicit modeling itself helps a person develop personal, unconscious skills in relation to the desired behavior (this is how young children usually learn). However, creating a technique, mechanism or skill that can be taught or transmitted to others, requires explicit modeling.

Experimental studies involved relatively simple behavioral and cognitive patterns models, for example, when controlling an autonomous underwater vehicle, assessing the combat readiness of special reaction forces, and others. The implementation of the proposed procedures has resulted in models with synthesized: (a) intuitive understanding of the agent's abilities, (b) direct observation of the agent's work, and (c) researcher's explicit knowledge in the agent's subject domain.

Acknowledgements The work has been financially supported by the Russian Foundation for Basic Research (RFBR), project No.170100728.

References

1. Gorodetskii, V.I.: Self-organization and multiagent systems: II. Applications and the development technology. *J. Comput. Syst. Sci. Intern.* **51**, 391–409 (2012)
2. ACL—Agent Communication Language, <https://fipa.org/specs/fipa00061/SC00061G.pdf>. Last Accessed 19 01 2016
3. AgentBuilder—an integrated software toolkit that allows software developers to quickly develop intelligent software agents and agent-based applications, <https://www.agentbuilder.com>. Last Accessed 19 01 2016.
4. Bernon, C., Gleizes, M.P., Peyruqueou, S., Picard, G.: ADELFE: a methodology for adaptive multi-agent systems engineering. In: Proceedings 3th Internship Workshop on Engineering Societies in the Agents World pp. 156–169 (2002)
5. Bonomi, F., Milito, R., Zhu, J., Addepalli, S.: Fog computing and its role in the internet of things. In: Proceedings of the First Edition of the MCC Workshop on Mobile Cloud Computing (MCC 2012), pp. 13–16. NY, USA (2012)
6. Burrafato, P., Cossentino, M.: Designing a multi-agent solution for a bookstore with PASSI methodology. In: Giorgini, P., Lesperance, Y., Wagner, G. Yu, E. (Eds). Proceedings of Conference on Agent-Oriented Information Systems Intern 119–135 (2002)
7. Caire, G., Coulier, W., Garijo, F.J., Gomez-Sanz, J.J. (2002). Agent oriented analysis using MESSAGE/UML. In: Eds Agent-Oriented Software Engineering II 2222, pp. 119–125. Springer-Verlag LNCS
8. Cohen, P., Levesque, H.: Teamwork. *Nous* **25**, 487–515 (1991)
9. Cougaar Agent Architecture, <https://cougaar.org/wp/documentation/tutorials/>. Last Accessed 19 Jan 2016

10. Deloach, S.: Analysis and Design using MaSE and agentTool. In: Proceedings 12th Midwest Artificial Intelligence and Cognitive Science Conference on (MAICS). Miami University Press (2001).
11. Fedunov, B.E.: Constructive semantics for developing onboard intelligence algorithms for anthropocentric objects. *J. Comput. Syst. Sci. Intern.* **5** (1998)
12. Vinogradov, G.P.: Modeling decision-making by an intelligent agent. *Softw. Syst.* **3**, 45–51 (2010)
13. Vinogradov, G.P., Kuznetsov, V.N.: Modeling client behavior considering subjective ideas about the situation of choice. *Artif. Intell. Decision-Making* **3**, 58–72 (2011)
14. Deloach, S., Garcia-Ojeda, J.: The O-MaSE Methodology. In: Cossentino, M., Hilaire, V., Molesini, A., Seidita, V. (eds.) *Handbook on Agent-Oriented Design Processes*, 253–285. Springer-Verlag, Berlin-Heidelberg (2014).
15. Filatova, N., Bodrina, N., Sidorov, K., Shemaev, P., Vinogradov, G.: Biotechnical System for the study of processes of increasing cognitive activity through emotional stimulation. In: Kovalev, S., Tarassov, V., Snasel, V., Sukhanov, A. (eds.) *Proc. 4th International Scientific Conference on IITI'19. Advances in Intelligent Systems and Computing*, 1156 pp. 548–558. Springer Nature Switzerland AG 2020 (2020).
16. Zadeh L.: The concept of a linguistic variable and its application to approximate reasoning. *Inf. Sc.* **8**, 199–251, 301–357 (1975); **9**, 43–80 (1976)
17. Borisov P.A., Vinogradov G.P., Semenov N.A.: Integration of neural network algorithms, nonlinear dynamics models, and fuzzy logic methods in prediction problems. *J. Comput. Syst. Sci. Intern.* **1**, 78–84 (2008)
18. Dilts, R.: *Modeling with NLP*. Meta Publ. (1998).
19. Vinogradov, G.P.: A subjective rational choice. *JPCS* **803**, 012176 (2017)
20. Gorodetskii, V.I.: Self-organization and multiagent systems: I. Models of multiagent self-organization. *J. Comput. Syst. Sci. Intern.* **51**, 256–281 (2012).

Thermogradient Dimensional Stabilization of eddential Cross-Sections of the Carrying Structure of an Autonomous Object



Yulia Savelieva, Michael Livshits, Igor Adeyanov, and Ivan Danilushkin

Abstract The operating efficiency of autonomous objects of different purposes (underwater vehicles, spacecraft, etc.) substantially depends on the quality of the information received from heat-releasing apparatuses arranged on a carrying structure of the autonomous object. The thermal deformation of the carrying framework is caused by the irregularity of the temperature field due to a heat-releasing of devices, unsteady heat exchange with the ambient, and other reasons. In this case, the thermal deformation of the supporting framework, caused by the non-uniformity of the temperature field due to the heat dissipation of devices, unsteady heat transfer with the environment, and other reasons, is an important component of the complex distortion of information, especially optical measuring devices due to the displacement of the optical axis, focal length, etc., under the influence of a thermal gradient. Different systems of automatic thermal-stabilization are applied in order to decrease said distortions. The chapter is devoted to the mathematical modeling of thermal processes in the supporting framework during its automatic thermal gradient stabilization.

Keywords Autonomous object · Thermal-stabilization · Temperature distribution · Thermogradient stabilization system · Heat source

1 Introduction

Most devices arranged on a carrying structure of an autonomous object emits heat when operating, and it may cause thermal deformation, which, in turn, negatively affects the operation's efficiency of the information-measuring system comprising optical equipment [1–3]. The problem of stabilization of the average value of the temperature distribution as well as the reduction of its irregularity in order to exclude

Y. Savelieva (✉)

Branch of Samara State Technical University in Syzran, 45, Sovetskaya st, Syzran 446001, Russia
e-mail: Savelieva_yu_ol@mail.ru

M. Livshits · I. Adeyanov · I. Danilushkin

Samara State Technical University, 244, Molodogvardeyskaya st, Samara 443100, Russia
e-mail: usat@samgtu.ru

thermogradient instability of the carrying framework shape is of current interest. The irregularity of the temperature distribution can be significantly reduced by arranging additional controlled heat-releasing elements (means of thermal gradient stabilization—hereinafter referred to as MTGS) and/or using a liquid cooling system. To analyze the operating mode of the heat-releasing devices and MTGS, to synthesize effective stabilization systems for the temperature distribution of the carrying framework, a mathematical model of its (framework's) temperature state is required.

2 Problem Statement

The carrying framework of the information-measuring system of the autonomous object is considered. The said framework has a shape of a rectangular prism (plate) and is subject to the influence of various thermal deformation loads. The plate (Fig. 1a) is cooled under the effect from the environment (the boundary condition of the third kind is BC-3) and is heated at the points of contact with the heat-releasing measuring devices: Pr1-Pr4, Pru1-Pru4, C1, h1, C2, h2, Pra, Prb, operating according to the cyclograms shown in Figs. 2, 3, 4, 5, 6 and 7 [4, 5] for one typical cycle with period $t_1 = 30,000$ s, and being controlled by MTGS: St1-St9, S1-S9. The basic initial data required for the calculations are presented in Tables 1 and 2.

The coordinates of the centers of the heat-releasing devices. Central MTGS on the plate's side $x = 0$: St1, St2, St3, St4, St5. Central MTGS on the plate's side $x = R_1$: S1, S2, S3, S4, S5. Diagonal MTGS on the plate's side $x = 0$: St6, St7, St8, St9. Diagonal MTGS on the plate's side $x = R_1$: S6, S7, S8, S9. Heat-releasing

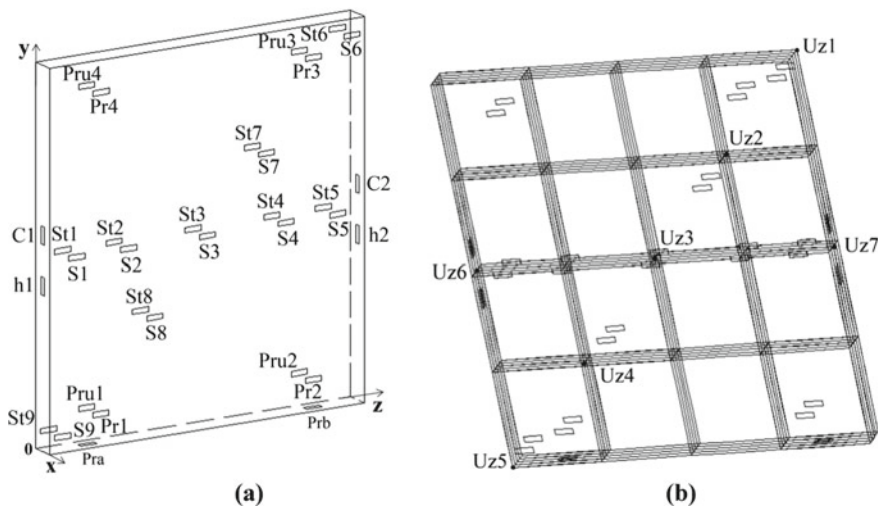


Fig. 1 Carrying framework: **a** Arrangement of heat-releasing devices **b** Arrangement of control points

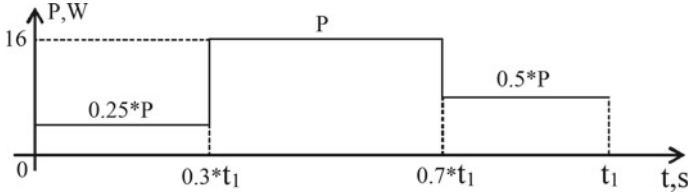


Fig. 2 Cyclogram of changing in heat-releasing power of devices Pr1-Pr4

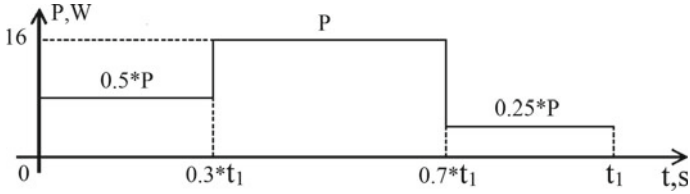


Fig. 3 Cyclogram of changing in heat-releasing power of devices Pru1-Pru4

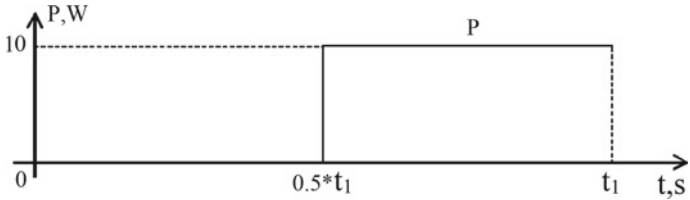


Fig. 4 Cyclogram of changing in heat-releasing power of devices Pra-Prb

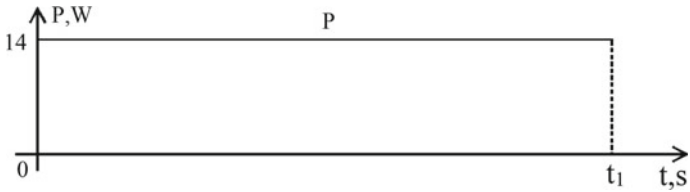


Fig. 5 Cyclogram of changing in heat-releasing power of devices C1, C2

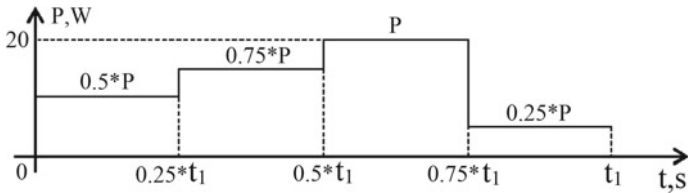


Fig. 6 Cyclogram of changing in heat-releasing power of devices h1

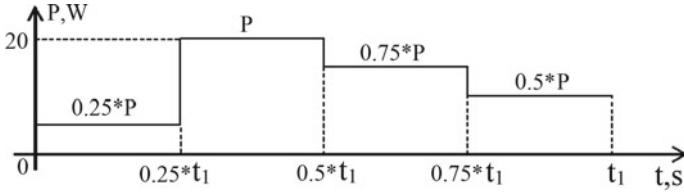


Fig. 7 Cyclogram of changing in heat-releasing power of devices h2

Table 1 Basic parameters

<i>Geometry dimensions of the framework</i>	
R ₁ dimensions of the plate along X axis, m	0.15
R ₂ dimensions of the plate along Y axis, m	2.15
R ₃ dimensions of the plate along Z axis, m	1.97
<i>Thermophysical characteristics</i>	
Specific heat capacity <i>c</i> , J/(kg·°C)	1480
Material density ρ , kg/m ³	1440
Thermal conductivity λ , W/(m·°C)	2.3
Heat-transfer coefficient from body surface to environment α , W/(m ² ·°C)	0.7488
<i>Additional information</i>	
Environment temperature T_{sred} , °C	20
Initial temperature of the plate T_{pl}^0 , °C	40
Dimensions of the seat for heat sources (S), m × m	0.03, 0.1
Biot number <i>Bi</i>	0.7

Table 2 Nominal power of heat-releasing measuring devices

Arrangement	Device	Power, W
Edge YZ, $x = 0, x = R_1$	Pr1–Pr4, Pru1–Pru4	16
Edge XZ, $y = 0$	Pra	10
	Prb	10
Edge XY, $z = 0, z = R_3$	C1, C2	14
	h1, h2	20

measuring devices on the plate’s side $x = 0$: Pru1, Pru2, Pru3, Pru4. Heat-releasing measuring devices on the plate’s side $x = R_1$: Pr1, Pr2, Pr3, Pr4. Heat-releasing measuring devices on the plate’s side $y = 0$: Pra, Prb. Heat-releasing measuring devices on the plate’s side $z = 0$: h1, C1. Heat-releasing measuring devices on the plate’s side $z = R_3$: h2, C2.

The temperature field $\theta_{pl}(l_x, l_y, l_z, \phi)$ of the plate is described by the three-dimensional thermal conductivity equation [6–10]:

$$\frac{\partial \theta_{pl}(l_x, l_y, l_z, \phi)}{\partial \phi} = \frac{\partial^2 \theta_{pl}(l_x, l_y, l_z, \phi)}{\partial l_x^2} + \frac{\partial^2 \theta_{pl}(l_x, l_y, l_z, \phi)}{\partial l_y^2} + \frac{\partial^2 \theta_{pl}(l_x, l_y, l_z, \phi)}{\partial l_z^2},$$

$$0 < l_x < R_1 \cdot R_2^{-1}, \quad 0 < l_y < 1, \quad 0 < l_z < R_3 \cdot R_2^{-1}, \quad \phi \in (0; \infty), \quad (1)$$

by relative units: $y \cdot R_2^{-1} = l_y$, $x \cdot R_2^{-1} = l_x$, $z \cdot R_2^{-1} = l_z$, wherein $\phi = \frac{at}{R_2^2}$ —Fourier number (« non-dimensional time »), $a = \frac{\lambda}{c\rho}$ —thermal diffusivity, $\theta_{pl}(l_x, l_y, l_z, \phi) = (T_{pl}(x, y, z, t) - T^*) \cdot T^{*-1}$, $T^* = T_{sred} = const$ —basic

temperature, °C.

Initial condition:

$$\theta_{pl}(l_x, l_y, l_z, 0) = (T_{pl}^0 - T^*) \cdot T^{*-1}, \quad (2)$$

wherein $T_{pl}^0 = const$ —initial temperature of the plate, °C.

Boundary conditions:

$$\left. \frac{\partial \theta_{pl}(l_x, l_y, l_z, \phi)}{\partial l_x} \right|_{l_x=0} = Q_{pl}^{lx0}(l_y, l_z, \phi), \quad (3)$$

$$\left. \frac{\partial \theta_{pl}(l_x, l_y, l_z, \phi)}{\partial l_x} \right|_{l_x=R_1 \cdot R_2^{-1}} = Q_{pl}^{lx1}(l_y, l_z, \phi), \quad (4)$$

$$\left. \frac{\partial \theta_{pl}(l_x, l_y, l_z, \phi)}{\partial l_y} \right|_{l_y=0} = Q_{pl}^{ly0}(l_x, l_z, \phi), \quad (5)$$

$$\left. \frac{\partial \theta_{pl}(l_x, l_y, l_z, \phi)}{\partial l_y} \right|_{l_y=1} = Q_{pl}^{ly1}(l_x, l_z, \phi), \quad (6)$$

$$\left. \frac{\partial \theta_{pl}(l_x, l_y, l_z, \phi)}{\partial l_z} \right|_{l_z=0} = Q_{pl}^{lz0}(l_x, l_y, \phi), \quad (7)$$

$$\left. \frac{\partial \theta_{pl}(l_x, l_y, l_z, \phi)}{\partial l_z} \right|_{l_z=R_3 \cdot R_2^{-1}} = Q_{pl}^{lz1}(l_x, l_y, \phi). \quad (8)$$

Here $\theta_{pl}^{lx0}(l_y, l_z, \phi)$, $\theta_{pl}^{lx1}(l_y, l_z, \phi)$, $\theta_{pl}^{ly0}(l_x, l_z, \phi)$, $\theta_{pl}^{ly1}(l_x, l_z, \phi)$, $\theta_{pl}^{lz0}(l_x, l_y, \phi)$, $\theta_{pl}^{lz1}(l_x, l_y, \phi)$ —summarized heat flow on the corresponding edges of the framework:

$$Q_{pl}^{lx0}(l_y, l_z, \phi) = q_p(\phi) - \sum_{i=1}^N q^i \cdot V_{lx0}^i(l_y, l_z), \quad (9)$$

$$Q_{pl}^{lx1}(l_y, l_z, \phi) = -q_p(\phi) + \sum_{i=1}^N q_{lx1}^i \cdot V_{lx1}^i(l_y, l_z), \quad (10)$$

$$Q_{pl}^{ly0}(l_x, l_z, \phi) = q_p(\phi) - \sum_{i=1}^M q_{ly0}^i \cdot V_{ly0}^i(l_x, l_z), \quad (11)$$

$$Q_{pl}^{ly1}(l_x, l_z, \phi) = -q_p(\phi) + \sum_{i=1}^M q_{ly1}^i \cdot V_{ly1}^i(l_x, l_z), \quad (12)$$

$$Q_{pl}^{lz0}(l_x, l_y, \phi) = q_p(\phi) - \sum_{i=1}^K q_{lz0}^i \cdot V_{lz0}^i(l_x, l_y), \quad (13)$$

$$Q_{pl}^{lz1}(l_x, l_y, \phi) = -q_p(\phi) + \sum_{i=1}^K q_{lz1}^i \cdot V_{lz1}^i(l_x, l_y). \quad (14)$$

$q_p(\phi)$ —flows of heat losses from the surface, which are assumed to be the same on all surfaces of the plate; q_{lx0}^i, q_{lx1}^i —flows from the heat sources arranged on the edges $l_x = 0$ and $l_x = R_1 \cdot R_2^{-1}$ accordingly, q_{ly0}^i, q_{ly1}^i —flows from the heat sources arranged on the edges $l_y = 0$ and $l_y = 1$ accordingly, q_{lz0}^i, q_{lz1}^i —flows from the heat sources arranged on the edges $l_z = 0$ and $l_z = R_3 \cdot R_2^{-1}$ accordingly, wherein the intensity of flows from the heat sources is defined as a ratio of heat emission power P of the corresponding device to its area S of contact with the plate surface $q^i = P \cdot S^{-1}$; $V_{lx0}^i(l_y, l_z), V_{lx1}^i(l_y, l_z)$ —functions determining the location of the devices on the edges $l_x = 0$ and $l_x = R_1 \cdot R_2^{-1}$ accordingly, $V_{ly0}^i(l_x, l_z), V_{ly1}^i(l_x, l_z)$ —functions determining the location of the devices on the edges $l_y = 0$ and $l_y = 1$ accordingly, $V_{lz0}^i(l_x, l_y), V_{lz1}^i(l_x, l_y)$ —functions determining the location of the devices on the edges $l_z = 0$ and $l_z = R_3 \cdot R_2^{-1}$ accordingly.

The temperature distribution in the plate is determined by solving auxiliary three-dimensional boundary value problem (1)–(8) according to the following algorithm:

1. Solving $\theta_{pl}(l_x, l_y, l_z, \phi)$ three-dimensional boundary value problem (1)–(8) is considered as the product of $\theta_{pl}(l_x, \phi)$, $\theta_{pl}(l_y, \phi)$ and $\theta_{pl}(l_z, \phi)$:

$$\theta_{pl}(l_x, l_y, l_z, \phi) = \theta_{pl}(l_x, \phi) \cdot \theta_{pl}(l_y, \phi) \cdot \theta_{pl}(l_z, \phi)$$

solving the corresponding boundary value problems [11, 12] under condition $q_{lx}^i = 0, q_{ly}^i = 0, q_{lz}^i = 0$, influence thereof is reflected by the summation of said solving and corresponding solving of three-dimensional boundary value problem with the boundary condition of the second kind (BC-2).

2. The convective nature of the heat exchange of the plate with the environment (BC-3) is reflected by the equivalent model for BC-2.

Figure 8 shows proposed in the paper [13] structural representation of one-dimensional third boundary value problem BC-3 for $\theta_{pl}^0 = 0$ by transfer functions

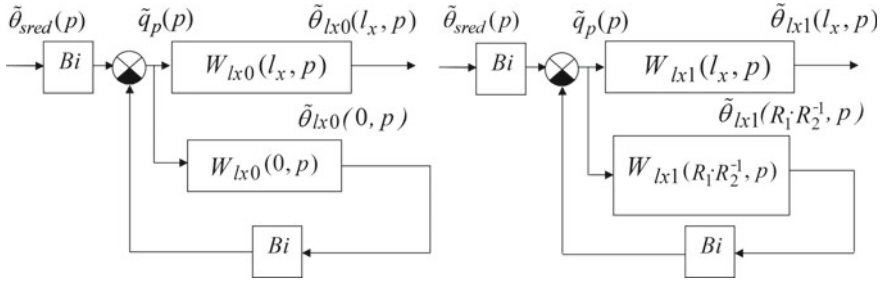


Fig. 8 The framework of one-dimensional auxiliary boundary value problem $\theta_{pl}(l_x, \phi)$ by the Laplace transforms $\tilde{\theta}_{pl}(l_x, p)$

BC-2 $W_{lx0}(l_x, p)$, $W_{lx1}(l_x, p)$ accordingly for the one $l_x = 0$ and for the other $l_x = R_1 \cdot R_2^{-1}$ side of the plate.

Here $Bi = \alpha \cdot R_2 \cdot \lambda^{-1}$ —Biot number. In the current example $\theta_{sred}(\phi) = (T_{sred}(t) - T^*) \cdot T^{*-1} = 0$.

The corresponding transforms $\theta_{pl}(l_y, p)$, $\theta_{pl}(l_z, p)$ of temperature distributions $\theta_{pl}(l_y, \phi)$, $\theta_{pl}(l_z, \phi)$ is determined in the same way.

3. The thermal effect from the heat-releasing devices and MTGS is determined independently, and then taken into account in the general problem (1)–(8) by summation of the corresponding components of the temperature field.

3 Interaction with the Environment

One-dimensional boundary value problems with BC-2 for $\theta_{pl}(l_x, \phi)$, $\theta_{pl}(l_y, \phi)$, $\theta_{pl}(l_z, \phi)$ used in the scheme (Fig. 8) are the following:

$$\begin{cases} \frac{\partial \theta_{pl}(l_x, \phi)}{\partial \phi} = \frac{\partial^2 \theta_{pl}(l_x, \phi)}{\partial l_x^2}, & 0 < l_x < R_1 \cdot R_2^{-1}, \phi \in (0; \infty), \\ \theta_{pl}(l_x, 0) = \theta_{pl}^0, & 0 \leq l_x \leq R_1 \cdot R_2^{-1}, \phi \in (0; \infty), \\ \left. \frac{\partial \theta_{pl}(l_x, \phi)}{\partial l_x} \right|_{l_x=0} = q_p(\phi), & \left. \frac{\partial \theta_{pl}(l_x, \phi)}{\partial l_x} \right|_{l_x=R_1 \cdot R_2^{-1}} = -q_p(\phi). \end{cases} \quad (15)$$

$$\begin{cases} \frac{\partial \theta_{pl}(l_y, \phi)}{\partial \phi} = \frac{\partial^2 \theta_{pl}(l_y, \phi)}{\partial l_y^2}, & 0 < l_y < 1, \phi \in (0; \infty), \\ \theta_{pl}(l_y, 0) = \theta_{pl}^0, & 0 \leq l_y \leq 1, \phi \in (0; \infty), \\ \left. \frac{\partial \theta_{pl}(l_y, \phi)}{\partial l_y} \right|_{l_y=0} = q_p(\phi), & \left. \frac{\partial \theta_{pl}(l_y, \phi)}{\partial l_y} \right|_{l_y=1} = -q_p(\phi). \end{cases} \quad (16)$$

$$\begin{cases} \frac{\partial \theta_{pl}(l_z, \phi)}{\partial \phi} = \frac{\partial^2 \theta_{pl}(l_z, \phi)}{\partial l_z^2}, & 0 < l_z < R_3 \cdot R_2^{-1}, \phi \in (0; \infty), \\ \theta_{pl}(l_z, 0) = \theta_{pl}^0, & 0 \leq l_z \leq R_3 \cdot R_2^{-1}, \phi \in (0; \infty), \\ \left. \frac{\partial \theta_{pl}(l_z, \phi)}{\partial l_z} \right|_{l_z=0} = q_p(\phi), & \left. \frac{\partial \theta_{pl}(l_z, \phi)}{\partial l_z} \right|_{l_z=R_3 \cdot R_2^{-1}} = -q_p(\phi). \end{cases} \quad (17)$$

In order to solve said boundary value problems a finite integral transformations method is applied [13]:

$$\bar{\theta}_{pl}(\mu_n, \tau) = \int_0^{R_1 \cdot R_2^{-1}} \theta_{pl}(l_x, \phi) \varphi_n(\mu_n, l_x) r(l_x) dl_x, \quad (18)$$

$$\bar{\theta}_{pl}(\psi_m, \tau) = \int_0^1 \theta_{pl}(l_y, \phi) \varphi_m(\psi_m, l_y) r(l_y) dl_y, \quad (19)$$

$$\bar{\theta}_{pl}(\gamma_k, \tau) = \int_0^{R_3 \cdot R_2^{-1}} \theta_{pl}(l_z, \phi) \varphi_k(\gamma_k, l_z) r(l_z) dl_z, \quad (20)$$

wherein $\bar{\theta}_{pl}(\mu_n, \psi_m, \gamma_k, \tau)$ —transform of the original function; r —weight function (according to current problems $r = 1$); μ_n, ψ_m, γ_k —proper numbers:

$$\begin{aligned} \mu_n &= \frac{\pi n R_2}{R_1}, \quad n = 0, 1, 2, \dots; \quad \psi_m = \pi m, \quad m = 0, 1, 2, \dots; \\ \gamma_k &= \frac{\pi k R_2}{R_3}, \quad k = 0, 1, 2, \dots \end{aligned}$$

The normalized system of proper functions in one-dimensional problems has the form:

$$\begin{aligned} \varphi_n(\mu_n, l_x) &= \frac{1}{E_n} \varphi_n^*(\mu_n, l_x) = \frac{1}{E_n} \cos(\pi n \frac{R_2 l_x}{R_1}), \quad n = 0, 1, 2, \dots, \\ \varphi_m(\psi_m, l_y) &= \frac{1}{E_m} \varphi_m^*(\psi_m, l_y) = \frac{1}{E_m} \cos(\pi m l_y), \quad m = 0, 1, 2, \dots, \\ \varphi_k(\gamma_k, l_z) &= \frac{1}{E_k} \varphi_k^*(\gamma_k, l_z) = \frac{1}{E_k} \cos(\pi k \frac{R_2 l_z}{R_3}), \quad k = 0, 1, 2, \dots, \end{aligned}$$

Normalizing constants:

$$\begin{aligned} E_n &= \sqrt{\int_0^{R_1 \cdot R_2^{-1}} [\varphi_n^*(\mu_n, l_x)]^2 r(l_x) dl_x} = \begin{cases} \sqrt{R_1 \cdot R_2^{-1}}, & n = 0 \\ \sqrt{R_1 \cdot (2R_2)^{-1}}, & n = 1, 2, 3 \dots \end{cases}, \\ E_m &= \begin{cases} 1, & m = 0 \\ \sqrt{0.5}, & m = 1, 2, 3 \dots \end{cases}, \quad E_k = \begin{cases} \sqrt{R_3 \cdot R_2^{-1}}, & k = 0 \\ \sqrt{R_3 \cdot (2R_2)^{-1}}, & k = 1, 2, 3 \dots \end{cases}. \end{aligned}$$

Solving the boundary value problems (15)–(17) for BC-2 $\theta_{pl}(l_x, \phi)$, $\theta_{pl}(l_y, \phi)$, $\theta_{pl}(l_z, \phi)$ is the following:

$$\begin{aligned} \theta_{pl}(l_x, \phi) &= \sum_{n=0}^{\infty} \varphi(\mu_n, l_x) \int_0^{\phi} R(\mu_n, \tau) G_n^*(\mu_n, \phi - \tau) d\tau \\ &+ \sum_{n=0}^{\infty} \varphi(\mu_n, l_x) \int_0^{R_1 \cdot R_2^{-1}} \theta_{pl}^0 G_n^*(\mu_n, \phi) \varphi(\mu_n, \xi_{lx}) d\xi_{lx} \end{aligned} \quad (21)$$

$$\begin{aligned} \theta_{pl}(l_y, \phi) &= \sum_{m=0}^{\infty} \varphi(\psi_m, l_y) \int_0^{\phi} R(\psi_m, \tau) G_m^*(\psi_m, \phi - \tau) d\tau \\ &+ \sum_{m=0}^{\infty} \varphi(\psi_m, l_y) \int_0^1 \theta_{pl}^0 G_m^*(\psi_m, \phi) \varphi(\psi_m, \xi_{ly}) d\xi_{ly} \end{aligned} \quad (22)$$

$$\begin{aligned} \theta_{pl}(l_z, \phi) &= \sum_{k=0}^{\infty} \varphi(\gamma_k, l_z) \int_0^{\phi} R(\gamma_k, \tau) G_k^*(\gamma_k, \phi - \tau) d\tau \\ &+ \sum_{k=0}^{\infty} \varphi(\gamma_k, l_z) \int_0^{R_3 \cdot R_2^{-1}} \theta_{pl}^0 G_k^*(\gamma_k, \phi) \varphi(\gamma_k, \xi_{lz}) d\xi_{lz} \end{aligned} \quad (23)$$

wherein $R(\mu_n, \phi) = R_1(\mu_n, \phi) - R_0(\mu_n, \phi)$, $R(\psi_m, \phi) = R_1(\psi_m, \phi) - R_0(\psi_m, \phi)$, $R(\gamma_k, \phi) = R_1(\gamma_k, \phi) - R_0(\gamma_k, \phi)$ —functions determined by the boundary conditions: $R_0(\mu_n, \phi) = q_p(\phi) \varphi_n(\mu_n, 0)$, $n = 0, 1, 2, 3 \dots$,

$$R_0(\psi_m, \phi) = q_p(\phi) \varphi_m(\psi_m, 0), \quad m = 0, 1, 2, 3 \dots,$$

$$R_0(\gamma_k, \phi) = q_p(\phi) \varphi_k(\gamma_k, 0), \quad k = 0, 1, 2, 3 \dots,$$

$R_1(\mu_n, \phi) = -q_p(\phi) \varphi_n(\mu_n, R_1 \cdot R_2^{-1})$, $R_1(\psi_m, \phi) = -q_p(\phi) \varphi_m(\psi_m, 1)$, $R_1(\gamma_k, \phi) = -q_p(\phi) \varphi_k(\gamma_k, R_3 \cdot R_2^{-1})$. G_n^* , G_m^* , G_k^* —time components of the Green's function:

$$G_n^*(\mu_n, \phi) = e(-\mu_n^2 \phi) = e(-R_2^2 \pi^2 n^2 (R_1^2)^{-1} \phi), \quad n = 0, 1, 2 \dots, \quad (24)$$

$$G_m^*(\psi_m, \phi) = e(-\psi_m^2 \phi) = e(-\pi^2 m^2 \phi), \quad m = 0, 1, 2 \dots, \quad (25)$$

$$G_k^*(\gamma_k, \phi) = e(-\gamma_k^2 \phi) = e(-R_2^2 \pi^2 k^2 (R_3^2)^{-1} \phi), \quad k = 0, 1, 2 \dots, \quad (26)$$

Transfer functions (TF) used in the scheme (Fig. 8) for one-dimensional boundary value problem with BC-2 along l_x, l_y, l_z and being the Laplace transforms of the corresponding Green's functions have the following form:

$$W_{l_x}(l_x, p) = R_2 \cdot (R_1 p)^{-1} + 2R_2 \cdot R_1^{-1} \sum_{n=1}^{\infty} \cos(\pi n R_2 l_x \cdot R_1^{-1}) \\ \times \cos(\pi n R_2 \xi_{l_x} R_1^{-1}) R_1^2 (R_2^2 \pi^2 n^2)^{-1} (R_1^2 (R_2^2 \pi^2 n^2)^{-1} p + 1)^{-1} \quad (27)$$

$$W_{l_y}(l_y, p) = p^{-1} + 2 \sum_{m=1}^{\infty} \cos(\pi m l_y) \cos(\pi m \xi_{l_y}) \\ \times (\pi^2 m^2)^{-1} ((\pi^2 m^2)^{-1} p + 1)^{-1} \quad (28)$$

$$W_{l_z}(l_z, p) = R_2 \cdot (R_3 p)^{-1} + 2R_2 R_3^{-1} \sum_{k=1}^{\infty} \cos(\pi k R_2 l_z R_3^{-1}) \\ \times \cos(\pi k R_2 \xi_{l_z} R_3^{-1}) R_3^2 (R_2^2 \pi^2 k^2)^{-1} (R_3^2 (R_2^2 \pi^2 k^2)^{-1} p + 1)^{-1} \quad (29)$$

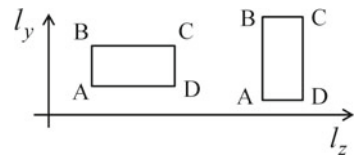
wherein ξ —corresponding spatial coordinate of the heat source arrangement, said heat source is considered as a control (disturbing) action. A design model for solving additional boundary value problems (15)–(17) under the condition $q_{l_x}^i = 0$, $q_{l_y}^i = 0$, $q_{l_z}^i = 0$ may be created by dependencies (27)–(29) within using the scheme according to Fig. 8 in the MATLAB software.

4 Temperature Effect from the Heat Sources

The areas of contact of the heat sources with the plate surfaces $l_x = 0$, $l_x = R_1 \cdot R_2^{-1}$ along the corresponding coordinates are designated in Fig. 9: $A_{l_x 0}(0, A_{l_x 0}^y, A_{l_x 0}^z)$, $B_{l_x 0}(0, B_{l_x 0}^y, B_{l_x 0}^z)$, $C_{l_x 0}(0, C_{l_x 0}^y, C_{l_x 0}^z)$, $D_{l_x 0}(0, D_{l_x 0}^y, D_{l_x 0}^z)$; $A_{l_x 1}(R_1 \cdot R_2^{-1}, A_{l_x 1}^y, A_{l_x 1}^z)$, $B_{l_x 1}(R_1 \cdot R_2^{-1}, B_{l_x 1}^y, B_{l_x 1}^z)$, $C_{l_x 1}(R_1 \cdot R_2^{-1}, C_{l_x 1}^y, C_{l_x 1}^z)$, $D_{l_x 1}(R_1 \cdot R_2^{-1}, D_{l_x 1}^y, D_{l_x 1}^z)$.

The boundary value problem for the temperature component $\theta_{ist}(l_x, l_y, l_z, \phi)$ of the heat sources effect is as follows:

Fig. 9 General designation of the heat sources coordinates when l_x fixed



$$\begin{aligned} \frac{\partial \theta_{ist}(l_x, l_y, l_z, \phi)}{\partial \phi} &= \frac{\partial^2 \theta_{ist}(l_x, l_y, l_z, \phi)}{\partial l_x^2} + \frac{\partial^2 \theta_{ist}(l_x, l_y, l_z, \phi)}{\partial l_y^2} \\ &+ \frac{\partial^2 \theta_{ist}(l_x, l_y, l_z, \phi)}{\partial l_z^2}, 0 \\ &< l_x < \frac{R_1}{R_2}, 0 < l_y < 1, 0 < l_z < \frac{R_3}{R_2}, \phi \in (0; \phi_k). \end{aligned} \quad (30)$$

Initial conditions: $\theta_{ist}(l_x, l_y, l_z, 0) = 0$. Boundary conditions along axis l_x :

$$\left. \frac{\partial \theta_{ist}(l_x, l_y, l_z, \phi)}{\partial l_x} \right|_{l_x=0} = - \sum_{i=0}^{\infty} q_{lx0}^i [1(l_y - A_{lx0}^y) - 1(l_y - B_{lx0}^y)] \cdot [1(l_z - A_{lx0}^z) - 1(l_z - D_{lx0}^z)], \quad (31)$$

$$\left. \frac{\partial \theta_{ist}(l_x, l_y, l_z, \phi)}{\partial l_x} \right|_{l_x=R_1 \cdot R_2^{-1}} = \sum_{i=0}^{\infty} q_{lx1}^i [1(l_y - A_{lx1}^y) - 1(l_y - B_{lx1}^y)] \cdot [1(l_z - A_{lx1}^z) - 1(l_z - D_{lx1}^z)], \quad (32)$$

Boundary conditions along with the coordinates l_y and l_z —formalized similarly. The components of the temperature distribution in the plate under the heat sources effect is determined by the corresponding convolution with the Green's function $G_{ist}(l_x, \xi_{lx}, l_y, \xi_{ly}, l_z, \xi_{lz}, \phi - \tau)$ [14]:

$$\theta_{ist}(l_x, l_y, l_z, \phi) = \theta_{ist}^{lx}(l_x, l_y, l_z, \phi) + \theta_{ist}^{ly}(l_x, l_y, l_z, \phi) + \theta_{ist}^{lz}(l_x, l_y, l_z, \phi), \quad (33)$$

$$\theta_{ist}(l_x, l_y, l_z, \phi) =$$

$$\begin{aligned} &- \sum_{l_x=0}^{\phi_2} \int_{\phi_1}^{D_{lx0}^z} \int_{A_{lx0}^y}^{B_{lx0}^y} \int_{A_{lx0}^z} q_{lx0}^i G_{ist}(l_x, \xi_{lx}, l_y, \xi_{ly}, l_z, \xi_{lz}, \phi - \tau) d\xi_{ly} d\xi_{lz} d\tau \\ &+ \sum_{l_x=R_1 \cdot R_2^{-1}}^{\phi_4} \int_{\phi_3}^{D_{lx1}^z} \int_{A_{lx1}^z}^{B_{lx1}^y} \int_{A_{lx1}^y} q_{lx1}^i G_{ist}(l_x, \xi_{lx}, l_y, \xi_{ly}, l_z, \xi_{lz}, \phi - \tau) d\xi_{ly} d\xi_{lz} d\tau \\ &- \sum_{l_y=0}^{\phi_2} \int_{\phi_1}^{D_{ly0}^x} \int_{A_{ly0}^z}^{B_{ly0}^z} \int_{A_{ly0}^y} q_{ly0}^i G_{ist}(l_x, \xi_{lx}, l_y, \xi_{ly}, l_z, \xi_{lz}, \phi - \tau) d\xi_{lz} d\xi_{lx} d\tau \\ &+ \sum_{l_y=1}^{\phi_4} \int_{\phi_3}^{D_{ly1}^x} \int_{A_{ly1}^z}^{B_{ly1}^z} \int_{A_{ly1}^y} q_{ly1}^i G_{ist}(l_x, \xi_{lx}, l_y, \xi_{ly}, l_z, \xi_{lz}, \phi - \tau) d\xi_{lz} d\xi_{lx} d\tau \\ &- \sum_{l_z=0}^{\phi_2} \int_{\phi_1}^{D_{lz0}^x} \int_{A_{lz0}^z}^{B_{lz0}^y} \int_{A_{lz0}^y} q_{lz0}^i G_{ist}(l_x, \xi_{lx}, l_y, \xi_{ly}, l_z, \xi_{lz}, \phi - \tau) d\xi_{ly} d\xi_{lx} d\tau \end{aligned}$$

$$+ \sum_{l_z=R_3 \cdot R_2^{-1}} \int_{\phi_3}^{\phi_4} \int_{A_{l_z 1}^x}^{D_{l_z 1}^x} \int_{A_{l_z 1}^y}^{B_{l_z 1}^y} q_{l_z 1}^i G_{ist}(l_x, \xi_{lx}, l_y, \xi_{ly}, l_z, \xi_{lz}, \phi - \tau) d\xi_{ly} d\xi_{lx} d\tau. \quad (34)$$

wherein

$$\begin{aligned} G_{ist}(l_x, \xi_{lx}, l_y, \xi_{ly}, l_z, \xi_{lz}, \phi - \tau) &= \sum_{n=0}^{\infty} G_n^*(\mu_n, \phi - \tau) \varphi_n(\mu_n, l_x) \\ &\times \varphi_n(\mu_n, \xi_{lx}) r(\xi_{lx}) \cdot \sum_{m=0}^{\infty} G_m^*(\psi_m, \phi - \tau) \varphi_m(\psi_m, l_y) \\ &\times \varphi_m(\psi_m, \xi_{ly}) r(\xi_{ly}) \sum_{k=0}^{\infty} G_k^*(\gamma_k, \phi - \tau) \varphi_k(\gamma_k, l_z) \\ &\times \varphi_k(\gamma_k, \xi_{lz}) r(\xi_{lz}). \end{aligned}$$

5 Result of Modeling

The mathematical model created in the MATLAB software on the basis of the obtained relations [15, 16] allows us to carry out the approximate synthesis of the controller, analysis of the corresponding control system stability and etc. A finite—element numerical modeling in the ANSYS software [17–19] is applied to problem solving more precisely.

We consider here the task of stabilizing the temperature in the critical cross-section of the carrying framework of the autonomous object (Fig. 1b) along the line from Uz1 to Uz5 by controlling the diagonal MTGS St6, St7, St3, St8, St9 on the one side of the prism and S6, S7, S3, S8, S9 on the other side thereof. The results of modeling the reaction of the temperature distribution in the carrying framework to the effect of the heat sources during $t = 30,000$ s in the ANSYS software are reflected in Fig. 10.

Figure 10b shows the temperature fields of the prism under the effect of diagonal MTGS St6, S6, St9, S9 with the power of 8 W.

The temperature graphs of the corresponding cross-section line are presented in Fig. 11, wherein the vertical axis T_{pl} , °C represents temperature values, and the horizontal axis D, m represents a diagonal cross-section from Uz1 to Uz5.

The results of the operation of the automatic temperature stabilization system in the critical node Uz1 being critical for providing the dimensional stabilization along the line of cross-section from Uz1 to Uz5 are subject to consideration. The closest heat sources influence Uz1 in a most substantial way: from the measuring devices in nodes Pr3, Pru3 being controlled by MTGS St6, S6, as well as the convective heat exchange with the environment.

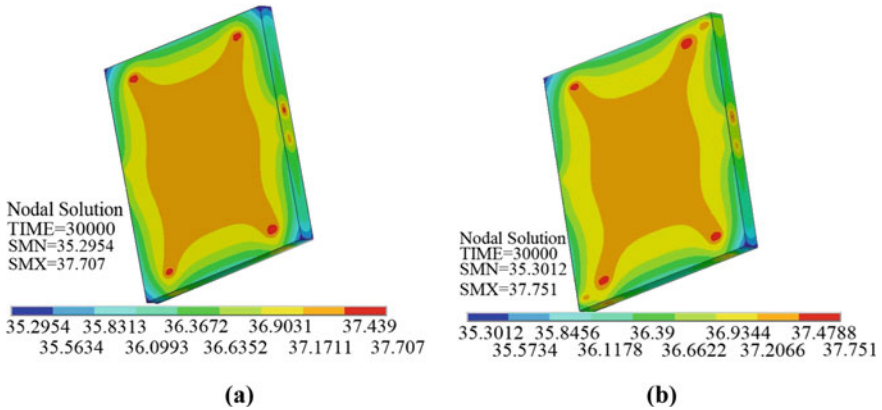


Fig. 10 Finite-element modeling of the carrying framework temperature in the Ansys software ($t = 30,000$): **a** Without MTGS effect **b** When diagonal MTGS effect, wherein MTGS arranged along the line from Uz1 to Uz5

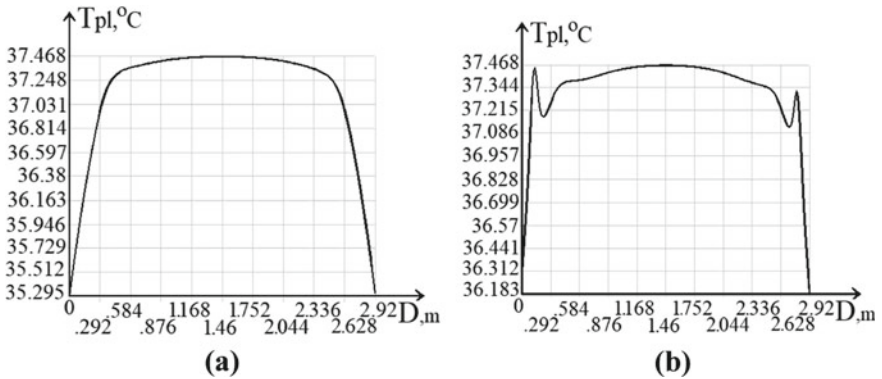


Fig. 11 Graphs of temperature distribution for $t = 30,000$ s: **a** Along diagonal cross section from Uz1 to Uz5 without MTGS **b** Along diagonal cross section from Uz1 to Uz5 when MTGS effect

The algorithm of control of MTGS St6 and S6 effecting on the point of control Uz1 is implemented by the proportional—integral (PI) law of control (Figs. 12, 13).

There is an automatically formed the changing in the power of MTGS St6 and S6 in deviation from the average value of the MTGS power at the PI-controller output.

6 Conclusions

There have been presented an argument for the problem of automatic stabilization of temperature distribution in the carrying framework of the autonomous object as

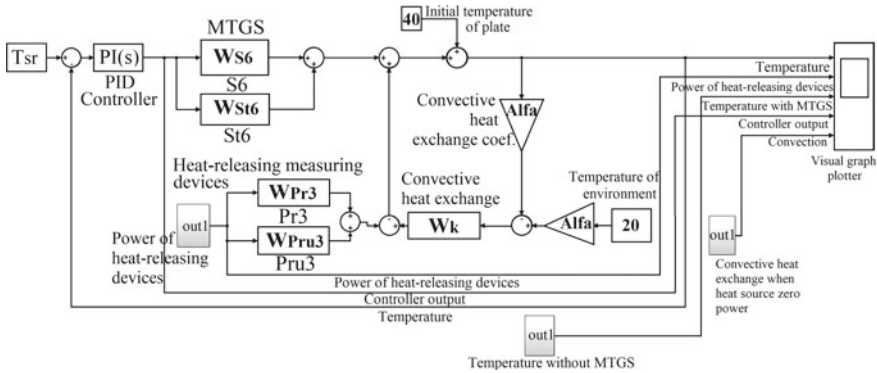


Fig. 12 Scheme of modeling a temperature control system of the critical node of the carrying framework in the MATLAB software: Tsr—the predetermined temperature in the node Uz1, Alfa—the unit of determination of the heat exchange coefficient, α ; WS6, WSt6, WPr3, WPr3, Pr3, Pru3 and convective heat exchange effect, PID Controller—unit of modelling PI-controller (without derivative term)

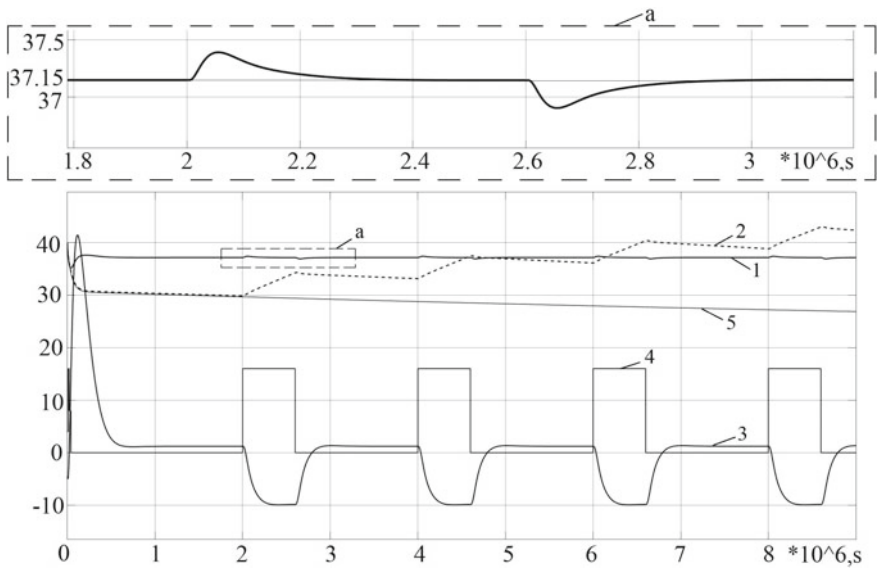


Fig. 13 Result of modeling the automatic temperature stabilization system in the node in the MATLAB software: 1 Temperature in the node Uz1 under the automatic control, °C; 2 Temperature in the node Uz1 without control, °C; 3 Power of MTGS generated at the PI-controller output (control for MTGS), W; 4 Cyclogram of changing in heat-releasing power of the measuring devices, W; 5 Convictional heat losses, °C; a Portion of temperature distribution under the automatic control, °C

the effective means for decreasing the temperature component in the error of the information-measuring system arranged on the said framework.

There has been provided a method of mathematical modeling of the temperature distribution in the carrying frameworks of autonomous objects, said method comprises approximate mathematical modeling in the MATLAB software and more precise modeling in the ANSYS software.

By analytical structural-parametric identification, there have been obtained the transfer functions of the temperature distribution in the carrying framework for implementation in an approximate mathematical model in MATLAB software and controller synthesis.

Modeling of the automatic temperature stabilization system in the node of the critical cross-section of the supporting framework has confirmed its high efficiency.

Acknowledgements The present research has been carried out due to support of the Russian Foundation for Basic Research (project No. 20-08-00240)

References

1. Livshits, M.Y., Derevyanov, M.Y., Kopytin, S.A.: Distributed optimal control of technological thermophysics objects. In Proceedings of the 4th All-Russian Multiconference on Management Problems, vol. 2, pp. 99–102. Taganrog, TTI YUFU (2011)
2. Livshits, M.Y., Derevyanov, M.Y., Davydov, A.N., Kopytin, S.A.: Stabilization of temperature field of autonomous objects carrying frameworks. In: Proceedings of the 9th All-Russian Scientific Conference with International Participation. Mathematical Modeling and Boundary Value Problems, No. 3, pp. 47–52. Samara (2013)
3. Livshits, M.Y., Borodulin, B.B., Nenashev, A.V., Savelieva, Yu.O.: Distributed control of temperature regimes of autonomous objects structural elements. Management and modeling issues in complex systems. In: Proceedings of the XXI International Conference, vol.1, pp. 349–352. Samara, OOO Ofort (2019)
4. Livshits, M.Y., Borodulin, B.B.: Comparative analysis of optimal temperature distributions in the responsible sections of load bearing structures. International youth scientific conference on heat and mass transfer in the thermal control system of technical and technological energy devices, HMTTSC 2017. MATEC WEB OF CONFERENCES. Tomsk, EDP Sciences (2017)
5. Livshits, M.Y., Borodulin, B.B.: Optimization of temperature distributions in critical sections of carrying structures. Proceedings of the Seventh Russian National Conference on Heat Exchange, vol. 3, pp. 148–151 Moscow, Publishing House MEI (2018)
6. Butkovskiy, A.G.: Characteristics of systems with distributed parameters: reference guide, Moscow, The main edition of the physical and mathematical literature of the publishing house Nauka, 224 p. (1979)
7. Savelieva, Yu.O.: The question of realization of math modeling of systems with distributed parameters. *Sovremennye nauchnye issledovaniya i razrabotki*. Moscow, Science CenterOlimp, No. 9 (26), pp. 350–352 (2018)
8. Livshits, M.Y.: Quasi-optimal space-time distributed control of heat and mass transfer processes. XIII All-Russian governance meeting. Moscow, VSPU-(2019)
9. Livshits, M.Y.: System optimization of processes of heat and mass transfer of process thermal physics. Mathematical methods in technique and technology MMTT-29. In: Proceedings of the XXIX International Conference, pp. 104–114. Saratov, Yuri Gagarin State Technical University of Saratov (2016)

10. Kartashov, E.M.: Analytical methods in the thermal conductivity theory of solids: study guide, revised edition, No. 3, 550 p. Moscow, Higher school (2001)
11. Lykov, A.V.: The thermal conductivity theory: manual for thermal engineering specialties of universities, 600 p. Higher school, Moscow (1967). (In Russian)
12. Rapoport, E.Y.: Software controllability of linear multidimensional systems with distributed parameters. In: Proceedings of the Russian Academy of Sciences. Management system theory, Moscow, Russian Academy of Sciences, No 2, 22. (2015) (In Russian)
13. Rapoport, E.Y.: Structural modeling of objects and control systems with distributed parameters: study guide, 299 p. Moscow, Higher School (2003)
14. Polyanin, A.D.: Manual of linear equations of mathematical physics, 576 p. FIZMATLIT, Moscow (2001)
15. MATLAB: Introduction into modern optimization methods of control systems. <https://www.mathworks.com/matlabcentral/fileexchange/53032-interactive-link-between-matlab-and-ansys> Accessed 15 Apr 2020
16. MathWorks: Nick. Interactive link between MATLAB and ANSYS <https://www.mathworks.com/matlabcentral/fileexchange/53032-interactive-link-between-matlab-and-ansys> Accessed 15 Apr 2020
17. Kaplun, A.B., Morozov, E.M., Olfereva, M.A.: ANSYS for engineers: practitioner guide, 272 p. Editorial URSS, Moscow (2003)
18. Basov, K.A.: ANSYS: user reference, 640 p. DMK Press, Moscow (2005)
19. ANSYS Users FORUM: Modeling heat exchange processes by using the ANSYS finite element analysis software/ Guidance material. https://cae-club.ru/sites/default/files/users/files/13/metodika_dlya_zadach_teploobmena_v_ansys_mechanical_apdl.pdf Accessed 9 Jan 2020

Minimum Defect Spline Multiwavelets and Parallel Computing for Big Data Compressing in Cyber-Physical Systems



Boris Shumilov 

Abstract The author’s vision of the problems of mathematical modeling of cyber-physical systems in transport as a three-level hierarchical structure, including environmental sensors at the lower level, data processing centers (DPC) at the middle level, and a single data storage center for developing management decisions at the upper level is considered. Prospects for big data compressing based on Haar-like multiwavelets of zero degree splines are explored. In contrast to the use of wavelet transforms based on Hermitian spline-multiwavelets, the proposed approach does not require the calculation of approximate values of derivatives. On the other hand, the parallelization effect is not rigidly related to the degree of a spline. This can lead to a significant acceleration of calculations due to parallel processing of the measured values by several (instead of one) filters. The results of numerical experiments are given in comparison with the known analogs. The presented algorithm can be used in the planning of road repairs, in the analysis of road accidents, in the processing of applications of road users, etc.

Keywords Cyber-physical systems · Big data compressing · Zero degree splines · Haar-like multiwavelets · Parallel computing

1 Introduction

The implementation of plans to create “smart cities” as one of the most important areas of the digital economy requires the priority development of transport infrastructure, ensuring the movement of people and goods within the city and adjacent territories [1]. Safe operation and maximum throughput of the resulting cyber-physical system are possible provided that a diagnostic technology is created for transport infrastructure facilities, including video-based road conditions [2]. The totality of such devices forms a heterogeneous distributed system of artificial intelligence [3], which should be enriched by some hierarchical structure, which would provide the

B. Shumilov (✉)

Tomsk State University of Architecture and Building, 2 Solyanaya, Tomsk 634003, Russia
e-mail: sbm05@yandex.ru

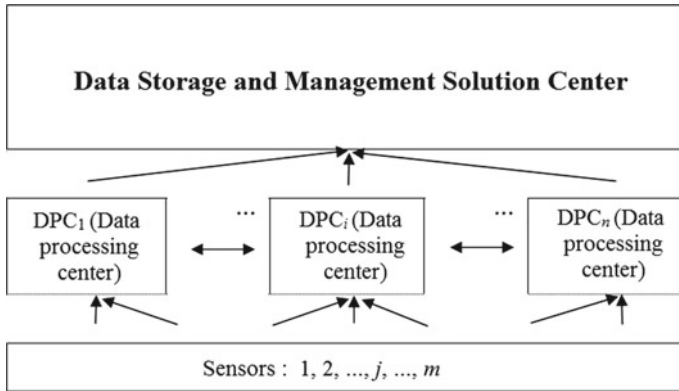


Fig. 1 Block diagram of a cyber-physical urban traffic control system

distribution of tasks between devices, their interaction with the environment, and the exchange of information under fundamental goals and settings (Fig. 1). This implies the existence of protocols [4] for their joint work at the lower level of interaction, as well as protocols for sharing in data processing centers (DPC) at the mid-level and further for transfer to a single data center and development of management decisions at the upper level to form a global cyber-physical urban traffic management system as part of the concept of creating “smart cities”. It refers to the enormous amount of structured, semi-structured, and unstructured data [5] that are exponentially generated by high-performance applications in many domains: view data [6], factor analysis, to mention a few. The difficulties are tremendously growing as applied to mobile cyber-physical applications [7] and supporting Internet services [8] with unmanned autonomous systems [9], as a result of which it is necessary to use the multi-core capabilities of modern processors to parallelize computations [10].

The apparatus of wavelets been introduced by Grossman and Morlet in the mid-80s of the last century in connection with the analysis of the properties of seismic and acoustic signals [11] became the best in compression of non-stationary signals providing a significant advantage over Fourier transform, since, in contrast to wavelets, the basic Fourier functions (sines and cosines) do not decay at infinity.

The basis for constructing wavelets is the presence of a set of embedded approximating spaces $\dots V_{j-1}, V_j, V_{j+1} \dots$ such that each basis function in V_{j-1} can be expressed as a linear combination of basic functions in V_j . In particular, splines—smooth functions glued from pieces of polynomials of degree m on an embedded sequence of grids—have this property. A spline defect is a difference between the degree m and the smoothness of gluing adjacent pieces, and it is equal to the number of basic functions for each node. For example, step functions, broken lines, and simple cubic splines of smoothness C^2 have a defect 1. Hermitian splines of odd degree m have a defect $(m+1)/2$. The use of the wavelet basis at the stage of processing allows revealing the spectral properties of the approximation spline.

From the classical literature on the theory of wavelets, it is known that spline wavelets of the first defect can be built on minimal support $[0, 2m+1]$ —a rather large length. Boundary wavelets have even larger supports. The reduction of supports is achieved by the construction of Hermitian spline multi-wavelets [12–14]. The advantage of multi-wavelets in comparison with scalar wavelets is that [15], under certain conditions, the wavelet expansion relations are split into separate relations for the wavelet coefficients of zero (for function), first (for 1st derivative), second (for 2nd derivative of multiwavelets of the fifth degree), third (for the 3rd derivative of multiwavelets of the seventh degree) and further orders. In particular, for wavelet transform of Hermite splines of the fifth degree, splitting into three simultaneously solvable systems is achieved, of which one is three-diagonal with strict diagonal dominance and two other four-diagonal systems with dominant central diagonals [16]. Similar construction for the case of multiwavelets of the 7th degree leads to a parallel solution of four five-diagonal systems with strict diagonal dominance [17]. That is, the degree of parallelism increases with an increase in the spline defect.

This work aims to build new types of multi-tiered multiwavelets based on minimal defect splines and justify the optimization and parallelization of computational wavelet transform algorithms to solve problems of processing numerical information. The relevance of the work is because in most practical situations only point values of functions are given. In this case, when using wavelet transforms based on Hermitian spline multi-wavelets, we will have to calculate the approximate values of the derivatives necessary for Hermitian interpolation of the table-defined functions, using, for example, regularized numerical differentiation schemes. The transition to multi-wavelets based on basic splines of the minimum defect of several successive levels of thinning of the grid of measured values of the function can lead, if the idea of splitting is successfully realized, to a significant acceleration of calculations due to parallel processing of the measured values by several (instead of one) filters. At the same time, the depth of each filter (the number of successive decimation levels involved in constructing the filters) is not of fundamental importance, which leads, in the limit, to the possibility of a one-step procedure for calculating simultaneously all wavelet decomposition coefficients at all decimation levels instead of reusing the same filters at each successive level of thinning.

2 Zero Degree Spline Multiwavelets

2.1 Haar Wavelets and Parallel Computing

This applies, in particular, to Haar wavelets proposed by the Hungarian mathematician Alfred Haar back in 1909. Haar wavelets are orthogonal, have a compact support, are well localized in space, but are not smooth, because approximating functions for them are zero-order splines that are discontinuous at nodes. Haar transform is used to compress images, mainly color and black and white with smooth transitions. This

type of compression has been known for a long time and directly proceeds from the idea of using coherence of regions. The compression ratio is set and varies between 5 and 100. When you try to set a larger coefficient on sharp boundaries, especially those that run diagonally, a “staircase effect” appears—steps of different brightness with a size of several pixels.

In Haar basis at this level j , there exist 2^j scaling functions and 2^j wavelets. At the same time, the necessary refinement (synthesis) matrices that describe how it is possible to obtain the coefficients of two scaling functions from V_j and two wavelets from W_j using four coefficients of scaling functions from V_{j+1} are of the form:

$$A^2 = \frac{1}{\sqrt{2}} \begin{bmatrix} 1 & 1 & 0 & 0 \\ 0 & 0 & 1 & 1 \end{bmatrix}, \quad B^2 = \frac{1}{\sqrt{2}} \begin{bmatrix} 1 & -1 & 0 & 0 \\ 0 & 0 & 1 & -1 \end{bmatrix}.$$

Let there be a one-dimensional discrete input signal S . Each pair of neighboring elements is associated with two numbers:

$$a_i = \frac{S_{2i} + S_{2i+1}}{\sqrt{2}}, \quad b_i = \frac{S_{2i} - S_{2i+1}}{\sqrt{2}}.$$

Repeating this operation for all elements of the original signal, the output receives two signals, one of which is a coarsened version of the input signal— a_i , and the second contains the detailed information necessary to restore the original signal— b_i . Similarly, the Haar transform can be applied to the received signal a_i , etc.

Consider an example of Haar transformation of a one-dimensional signal of length 16. Let the incoming signal be represented as a string of 16 pixel brightness values (S): (220, 211, 212, 218, 217, 214, 210, 202, 194, 185, 186, 192, 191, 188, 184, 176). After applying Haar transformation, the following two sequences are obtained a_i : (304.763, 304.056, 304.763, 291.328, 267.993, 267.286, 267.993, 254.558) and b_i : (6.364, -4.243, 2.121, 5.657, 6.364, -4.243, 2.121, 5.657). It is worth noting that the values b_i are quite close to 0. Repeating the operation, as applied to the sequence a_i , we obtain a_i' : (430.5, 421.5, 378.5, 369.5), b_i' : (0.5, 9.5, 0.5, 9.5) and further: (602.455, 528.916) (6.364, 6.364), (800) (52).

Using Haar transform as an example, the structure of a discrete wavelet transform of a signal is visible. At each step of the conversion, the signal splits into two components: approximation with a coarser resolution and detailed information. The inverse transformation is performed following the formulas:

$$S_{2i} = \frac{a_i + b_i}{\sqrt{2}}, \quad S_{2i+1} = \frac{a_i - b_i}{\sqrt{2}}.$$

And in this case, it is permissible to annul the wavelet coefficients that are small in absolute value by making the least error in the sense of the least-squares method. For example, for a threshold value <6 , we get 8 non-zero coefficients in the remainder, and the graphical representation of the result has the form (Fig. 2a).

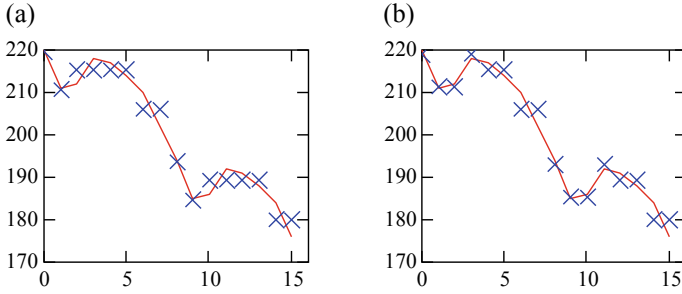


Fig. 2 The solid line is the image of a one-dimensional signal of length 16, the crosses are the restored coefficients of the spline of the 0th degree for conversion (in parentheses are the number of nonzero coefficients): **a** Haar (8); **b** Walsh-Hadamard (7)

It is easy to see that the two components of Haar transformation are calculated independently, so the computational process splits into two threads. In the case of a multi-wavelet interpretation of Haar basis, the scaling functions relate to two consecutive grid nodes, and each tetrad of successive signal values is subjected to transformation by the refinement matrix (synthesis)

$$\frac{1}{\sqrt{2}} \begin{bmatrix} 1 & 1 & 0 & 0 \\ 0 & 0 & 1 & 1 \\ 1 & -1 & 0 & 0 \\ 0 & 0 & 1 & -1 \end{bmatrix}.$$

The corresponding decomposition (analysis) matrices, which are inverse to the matrix presented above, are simply the result of transposition (a consequence of the orthogonality of the basic functions) and, therefore, are also sparse:

$$\frac{1}{\sqrt{2}} \begin{bmatrix} 1 & 0 & 1 & 0 \\ 1 & 0 & -1 & 0 \\ 0 & 1 & 0 & 1 \\ 0 & 1 & 0 & -1 \end{bmatrix}.$$

The next step along the path of parallelizing computations is to switch to the recursive representation of Haar transform [12]. Combine the two successive steps of Haar transformation to receive for each tetrad of neighboring elements one average value and three detailing coefficients under the refinement matrix:

$$\frac{1}{2} \begin{bmatrix} 1 & 1 & 1 & 1 \\ 1 & 1 & -1 & -1 \\ \sqrt{2} & -\sqrt{2} & 0 & 0 \\ 0 & 0 & \sqrt{2} & -\sqrt{2} \end{bmatrix}.$$

All four components of the resulting transformation are calculated independently, so the computational process splits into four threads. In this case, the total number of steps in the computational process decreases exactly two times. The three newly obtained detailing functions, corresponding to the three lower lines of the given system, are tied to one node and therefore can also be called multi-wavelets. In the same place [12], it was proposed as an exercise to bring recursion to an 8-tuple multiwavelet transform and even to a 16-tuple one. Unfortunately, the prospects of this approach to parallelizing computations were not indicated, and therefore, each time it has to be reinvented [18].

2.2 Haar Wavelet Packets and Walsh-Hadamard Transform

There is another way to construct a multiwavelet decomposition of step functions associated with the definition of so-called wavelet packets [12]. In this case, Haar transform is applied not only to the sequence a_i but also to the wavelet coefficients themselves b_i , to obtain Walsh-Hadamard transform as a result:

$$\frac{1}{2} \begin{bmatrix} 1 & 1 & 1 & 1 \\ 1 & 1 & -1 & -1 \\ 1 & -1 & 1 & -1 \\ 1 & -1 & -1 & 1 \end{bmatrix}.$$

Other unitary transformations [19], found by arbitrary rearrangement of rows and columns, can be proposed, but the Walsh-Hadamard transform looks best because it is symmetric. In any case, the found coefficients differ only by permutation. In particular, after applying Walsh-Hadamard transform to the previous signal of length 16, the following sequences are again obtained a_i' : (430.5, 421.5, 378.5, 369.5), b_i' : (0.5, 9.5, 0.5, 9.5) and two more sequences: (1.5, 5.5, 1.5, 5.5), (7.5, -2.5, 7.5, -2.5). Repeating the operation, as applied to the sequence a_i' , we obtain the numbers: (800) (52) (9) (0). For the same threshold value <6 , we obtain 7 non-zero coefficients in the remainder, and the graphical representation of the result has the form (Fig. 2b).

According to the authors [12], the obtained approximation is good, but not excellent. Besides, the total number of computational operations is greater. In our opinion, all this is redeemed by the absence of the square root extraction operation and the uniform loading of computing cores in parallel.

2.3 Use of Orthogonal Wavelets with Compact Support and With Scaling Coefficient N

Another way to construct multi-wavelets for minimum defect splines is to use wavelets with a scaling factor of $N = 4$. According to the theory [20, 21], the refinement matrix describing how to obtain coefficients of the scaling function from V_j and three wavelets from W_j using four coefficients scaling functions from V_{j+2} , has the form:

$$\frac{1}{6} \begin{bmatrix} 3 & 3 & 3 & 3 \\ 3\sqrt{2} & -3\sqrt{2} & 0 & 0 \\ \sqrt{6} & \sqrt{6} & -2\sqrt{6} & 0 \\ \sqrt{3} & \sqrt{3} & \sqrt{3} & -3\sqrt{3} \end{bmatrix}.$$

After applying the presented transformation to a signal of length 16, the same sequence is obtained a_i' : (430.5, 421.5, 378.5, 369.5) and three more sequences: (6.364, 2.121, 6.364, 2.121) and (2.858, 4.491, 2.858, 4.491), (-3.175, 10.104, -3.175, 10.104). At the same time, calculations are rather laborious due to a large number of square roots, and the savings in the number of computational operations are not so great as in the multiwavelet form of Haar transform. Repeating the operation, as applied to the sequence a_i' , we obtain the numbers: (800) (6.364) (38.784) (35.218). For the same threshold value <6 , we obtain 8 non-zero coefficients in the remainder, and the graphical representation of the result obtained has the form (Fig. 3a).

Thus, the last approach considered looks worse in all possible indicators. Nevertheless, since the matrix of transition to the lowest level of resolution has 16 coefficients in the multi-wavelet version instead of 4 in the classical Haar version, the formulation of the multi-wavelet transformation optimization problem in some parameters does not seem hopeless.

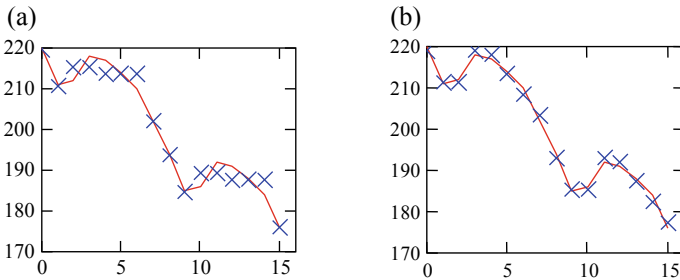


Fig. 3 The solid line is the image of a one-dimensional signal of length 16, the crosses are the restored coefficients of the spline of the 0th degree for conversion (in parentheses are the number of nonzero coefficients): **a** in [20] (8); **b** slant (7)

3 Use of Orthogonality to Polynomials of Higher Degree

One such interesting option for optimizing a multi-wavelet transform is an attempt to find Haar-like multi-wavelets based on the orthogonality property to polynomials of degree higher than the spline degree. In literature, the property of orthogonality for polynomials is usually called the property of zero moments. Previously, only scalar wavelets were used, and, for example, such properties as supports compactness, orthogonality, symmetry, zero moments, and other characteristics important in signal processing cannot be present in a scalar wavelet at the same time. A multi-wavelet-based system can have all of them at once. This means that multi-wavelets can provide perfect reconstruction (due to orthogonality), good efficiency at the signal boundaries (due to symmetry), and a high approximation order (due to the large number of zero moments) so that they can act when processing signals and fields better than scalar ones.

It is said that a wavelet $\psi(x)$ is orthogonal to polynomials of order n if the integral $\int \psi(x)x^k dx$ is identically zero for $k = 0, \dots, n - 1$, but not for $k = n$. Wavelets orthogonal to polynomials of a higher degree are often desirable in applications where numerical approximations of smooth operators are required.

The requirement of orthogonality to polynomials can sometimes be an excessive restriction. There is not a single wavelet basis (except for Haar basis), which simultaneously has compact support and is orthogonal and symmetric. But its drawback is that it is orthogonal only to zero degree polynomials. Therefore, if we want to obtain wavelets with compact support and high accuracy, we need to sacrifice the orthogonality of the basic functions. However, such damage is not always “painful”: for example, in some cases we can build a multi-scale analysis in which wavelets with this resolution are orthogonal to each other, and at the same time, they are orthogonal to higher polynomials.

Recall that for the case of splines of degree zero (step functions), the scaling function $\phi(x)$ with the unit value of the integral

$$\int_{-\infty}^{\infty} \phi(x) dx = 1,$$

which determines the rough approximation of a signal, is constant:

$$\phi(x) = \begin{cases} 1, & 0 \leq x < 1, \\ 0, & x \notin [0, 1). \end{cases}$$

The mother wavelet function $\psi(x)$ [22] with a zero value of the first three moments,

$$\int_{-\infty}^{\infty} \psi(x) x^k dx = 0, \quad k = 0, 1, 2,$$

which determines signal details, is defined as follows:

$$\psi(x) = \begin{cases} 1, & 0 \leq x < 1/4, \\ -3, & 1/4 \leq x < 1/2, \\ 3, & 1/2 \leq x < 3/4, \\ -1, & 3/4 \leq x < 1, \\ 0, & x \notin [0, 1). \end{cases}$$

Unfortunately, the inverse matrix of the defining system of equations for this wavelet is filled. Therefore, in contrast to the classical case (Haar orthogonal wavelets), the transition to explicitly setting synthesis filter coefficients is not advisable. The process of dividing the coefficients a_i into a rougher version a_i' and refinement coefficients b_i' is more convenient to carry out in the form of a solution of a system of linear equations of dimension $2^j \times 2^j$ [23]. There is known the only way to simplify further the numerical solution by splitting the system into even and odd nodes [14–16], to pass as a result to $2^{j-1} \times 2^{j-1}$ matrix. But this trick only works for splines of an odd degree and wavelets with shifted supports [24–26].

3.1 Slant Matrices

In the case of a multi-wavelet interpretation of the basis obtained, the scaling functions refer to four consecutive grid nodes, two four-point wavelets orthogonal to polynomials of zero degrees and one—first degree, respectively, are determined, and each tetrad of successive signal values is transformed by the refinement matrix (the so-called slant matrix [27])

$$\frac{1}{2} \begin{bmatrix} 1 & 1 & 1 & 1 \\ \frac{3}{\sqrt{5}} & \frac{1}{\sqrt{5}} & -\frac{1}{\sqrt{5}} & -\frac{3}{\sqrt{5}} \\ 1 & -1 & -1 & 1 \\ \frac{1}{\sqrt{5}} & -\frac{3}{\sqrt{5}} & \frac{3}{\sqrt{5}} & -\frac{1}{\sqrt{5}} \end{bmatrix}.$$

The corresponding decomposition (analysis) matrices, which are inverse to the matrix presented above, as in the case of Haar matrices, are simply the result of its transposition (a consequence of the orthogonality of the basic functions).

After applying the slant transformation to a signal of length 16, the same numbers a_i' and new sequences b_i' : (1.118, 10.957, 1.118, 10.957) and (7.5, -2.5, 7.5, -2.5), (1.118, 0.671, 1.118, 0.671) are obtained. Repeating the operation, as applied

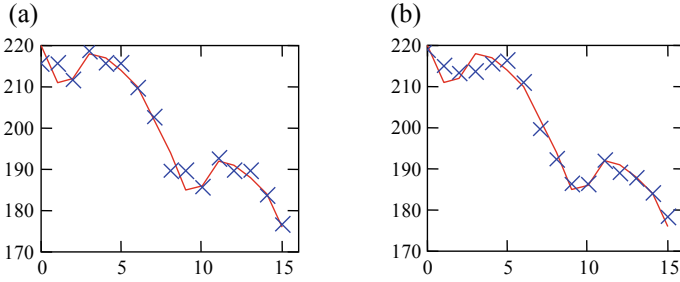


Fig. 4 The solid line is the image of a one-dimensional signal of length 16, the crosses are the restored coefficients of the spline of the 0th degree for the double transform (in parentheses are the number of nonzero coefficients): **a** Walsh-Hadamard (7); **b** slant (6)

to the sequence a_i' , we obtain the numbers: (800) (52.535) (0) (-15.205). For the same threshold value <6 , we obtain 7 non-zero coefficients in the remainder, and the graphical representation of the result has the form (Fig. 3b).

4 Use of Double Transformation

Now we apply Walsh-Hadamard transformation not only to the sequence a_i' , but also to all the multiwavelet coefficients of Walsh-Hadamard decomposition obtained above. Miraculously, most of the coefficients were reset to zero: (800, 10, 7, 5) and three more sequences: (52, 0, 0, 0) and (9, -9, -4, 10), (0, 0, 0, 0). So there is the so-called “lossless” compression effect. If we zero here two coefficients (-4, 5), which are less than 6 in absolute value, then there are also 7 nonzero coefficients, and the reconstructed image is hardly distinguishable from the original (Fig. 4a).

For a slant transformation, similar calculations lead to the values: (800, 50.535, 0, -15.205) and three more sequences: (12.075, -4.4, 0, -8.8) and (5, 4.472, 0, 8.944), (1.789, 0.2, 0, 0.4). If we zero all the coefficients here, which are less than 6 in absolute value, then 6 non-zero coefficients remain, however, in the region of the first signal oscillation, a significant defect of the reconstructed image is observed (Fig. 4b). Note that with the multi-wavelet transformations of Haar and [20], such a “trick” does not work. The compression quality is deteriorating (Figs. 5a, b, and 6a).

5 Experiments With Use a Scaling Factor 8

For a scaling factor of $N = 8$, the calculation of Haar transform splits into eight threads following the matrix

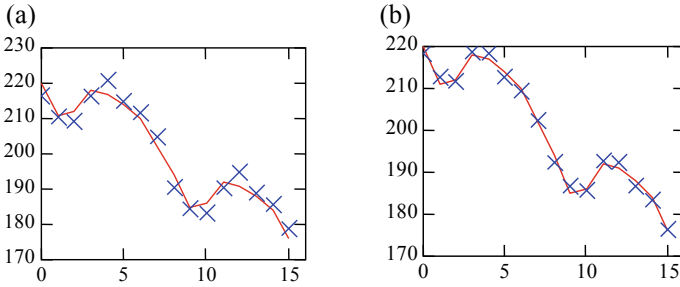


Fig. 5 The solid line is the image of a one-dimensional signal of length 16, the crosses are the restored coefficients of the 0-degree spline for the double conversion of Haar (in brackets are the number of non-zero coefficients): **a** (8); **b** (10)

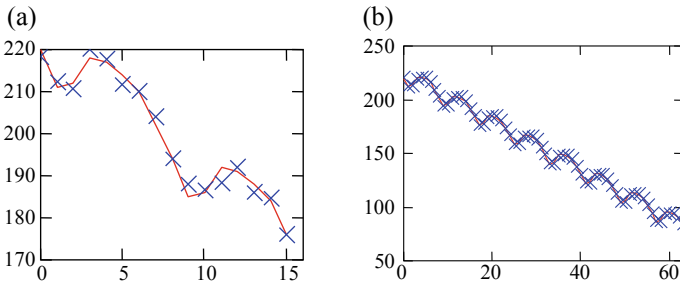


Fig. 6 The solid line is the image of a one-dimensional signal, the crosses are the restored coefficients of the 0-degree spline for the double conversion of (in brackets are the number of non-zero coefficients and the length 16): **a** in [20] (9, 16); **b** Haar (12, 64)

$$\frac{1}{2\sqrt{2}} \begin{bmatrix} 1 & 1 & \sqrt{2} & 0 & 2 & 0 & 0 & 0 \\ 1 & 1 & \sqrt{2} & 0 & -2 & 0 & 0 & 0 \\ 1 & 1 & -\sqrt{2} & 0 & 0 & 2 & 0 & 0 \\ 1 & 1 & -\sqrt{2} & 0 & 0 & -2 & 0 & 0 \\ 1 & -1 & 0 & \sqrt{2} & 0 & 0 & 2 & 0 \\ 1 & -1 & 0 & \sqrt{2} & 0 & 0 & -2 & 0 \\ 1 & -1 & 0 & -\sqrt{2} & 0 & 0 & 0 & 2 \\ 1 & -1 & 0 & -\sqrt{2} & 0 & 0 & 0 & -2 \end{bmatrix}.$$

Therefore, the total number of steps in the computational process decreases exactly four times. For illustration, we will perform a continuous continuation of the signal given above of a length of 16 according to the formulas:

$$S_{i+16} = S_i - 220 + 2S_{15} - S_{14}, \quad i = 0, 1, \dots, 15;$$

$$S_{i+32} = S_i - 220 + 2S_{31} - S_{30}, \quad i = 0, 1, \dots, 31,$$

adding a linear trend to convince: $S_i + i$, $i = 0, 1, \dots, 63$.

Here, Haar double transformation turned out to be slightly better than the single transformation, both in the number of coefficients, which are on modulo >6 (12 instead of 16), and in the quality of the graphical representation of the result obtained after their zeroing (Fig. 6b).

As for the wavelet packets, in this case, the procedure of constructing them has to be repeated 2 times, to obtain Walsh-Hadamard transformation (the essence is the Kronecker product of three Haar matrices [28], which from a computational point of view can be more profitable):

$$\frac{\sqrt{2}}{4} \begin{bmatrix} 1 & 1 & 1 & 1 & 1 & 1 & 1 & 1 \\ 1 & -1 & 1 & -1 & 1 & -1 & 1 & -1 \\ 1 & 1 & -1 & -1 & 1 & 1 & -1 & -1 \\ 1 & -1 & -1 & 1 & 1 & -1 & -1 & 1 \\ 1 & 1 & 1 & 1 & -1 & -1 & -1 & -1 \\ 1 & -1 & 1 & -1 & -1 & 1 & -1 & 1 \\ 1 & 1 & -1 & -1 & -1 & -1 & 1 & 1 \\ 1 & -1 & -1 & 1 & -1 & 1 & 1 & -1 \end{bmatrix}.$$

After the double Walsh-Hadamard transform, most of the obtained coefficients are strictly equal to zero:

$$\begin{bmatrix} 1228 & 10 & 12 & 10 & 2 & -8 & -18 & 20 \\ 72 & 0 & 0 & 0 & 0 & 0 & 0 & 0 \\ 144 & 0 & 0 & 0 & 0 & 0 & 0 & 0 \\ 0 & 0 & 0 & 0 & 0 & 0 & 0 & 0 \\ 288 & 0 & 0 & 0 & 0 & 0 & 0 & 0 \\ 0 & 0 & 0 & 0 & 0 & 0 & 0 & 0 \\ 0 & 0 & 0 & 0 & 0 & 0 & 0 & 0 \\ 0 & 0 & 0 & 0 & 0 & 0 & 0 & 0 \end{bmatrix}.$$

This shows that the Walsh-Hadamard double transformation is exact on linear functions. In Fig. 7a, b presents the results of similar calculations for a quadratic trend $S_i + i^2$, $i = 0, 1, \dots, 63$. Namely, the errors of signal reconstruction using the double Haar and Walsh-Hadamard transforms over a given threshold (>64) are presented. The number of non-zeroed coefficients is indicated in parentheses.

6 Conclusion

There is extensive literature related to Walsh-Hadamard transforms [29] and their generalizations to higher-order orthogonal and biorthogonal spline wavelets [30].

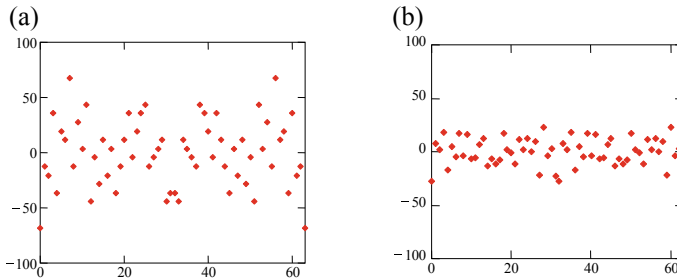


Fig. 7 The error of signal reconstruction using the double transforms **a** Haar (20); **b** Walsh-Hadamard (16) (in parentheses are the numbers of nonzero coefficients)

There is an urgent need for the construction of parallel algorithms for calculating semi-orthogonal spline-multiwavelets of the minimum defect on this basis. In the chapter, the author’s vision of the problem of “Big Data” compressing in cyber-physical systems in transport was presented. Prospects for data compressing algorithms based on a multiwavelet approach that is proposed to be implemented as a program on a mobile device are explored. The presented algorithms can be used in the planning of road repairs, in the analysis of road accidents, in the processing of applications of road users, etc.

Acknowledgments The reported study was funded partially by the Russian Foundation for Basic Research and Administration of Tomsk region according to the research project No. 16-41-700400_r_a.

References

1. Kupriyanovsky, V., Namiot, D., Sinyagov, S.: Cyber-physical systems as a base for digital economy. *Int. J. Open Inform. Technol.* **4**(2). <https://injoit.org/index.php/j1/article/view/266/211> (2016). Accessed 25 Mar 2019
2. Elugachev, P., Shumilov, B.: On the application of the photogrammetric method to the diagnostics of transport infrastructure objects. In: *Cyber-Physical Systems: Industry 4.0 Challenges. Studies in Systems, Decision and Control* 260, 51–62 (2020)
3. Skobelev, P.: Towards autonomous AI systems for resource management: applications in industry and lessons learned. In: *Proceedings of the XVI International Conference on Practical Applications of Agents and Multi-Agent Systems (PAAMS 2018)*. LNAI, vol. 10978, pp. 12–25. Springer (2018). https://doi.org/10.1007/978-3-319-94580-4_2
4. Tsvetkov, V.Y.: Control with the use of cyber-physical systems. *Perspectives of Science & Education. Int. Sci. Electron. J.* **3**(27), 55–60. <https://psejournal.wordpress.com/archive/17/17-03/> (2017). Accessed 25 Mar 2019
5. Rodríguez-Mazahua, L., Rodríguez-Enríquez, C.-A., Sánchez-Cervantes, J.L., Cervantes, J., García-Alcaraz, J.L., Alor-Hernández, G.: A general perspective of Big Data: applications, tools, challenges and trends. *J. Supercomput.* **72**, 3073–3113 (2016)

6. Xiong, N.IN., Shen, Y., Yang, K., Lee, C., Wu, C.: Color sensors and their applications based on real-time color image segmentation for cyber physical systems. *EURASIP J. Image Video Processing*, **23** (2018). <https://doi.org/10.1186/s13640-018-0258-x>
7. Bae, H., White, J., Golparvar-Fard, M., Pan, Y., Sun, Y.: Fast and scalable 3D cyber-physical modeling for high-precision mobile augmented reality systems. *Pers Ubiquit. Comput.* **19**, 1275–1294 (2015). <https://doi.org/10.1007/s00779-015-0892-6>
8. White, J., Clarke, S., Groba, C., Dougherty, B., Thompson, C., Schmidt, D.C.: R&D challenges and solutions for mobile cyber-physical applications and supporting Internet services. *J Internet Serv. Appl.* **1**, 45–56 (2010). <https://doi.org/10.1007/s13174-010-0004-9>
9. Vachtsevanos, G., Lee, B., Oh, S., Balchanos, M.: Resilient Design and Operation of Cyber Physical Systems with Emphasis on Unmanned Autonomous Systems. *Journal of Intelligent&Robotic Systems* **91**, 59–83 (2018). <https://doi.org/10.1007/s10846-018-0881-x>
10. Suh, D., Jeon, K., Chang, S., Kim, J., Kim, J.: Auto-localized multimedia platform based on a modular Cyber Physical System aligned in a two-dimensional grid. *Cluster Comput.* **18**, 1449–1464 (2015). <https://doi.org/10.1007/s10586-015-0479-z>
11. Daubechies, I.: *Ten Lectures on Wavelets* Society for Industrial and Applied Mathematics. University City Science Center, Philadelphia, PA (1992)
12. Strang, G., Nguyen, T.: *Wavelets and Filter Banks*. Wellesley-Cambridge Press, Wellesley, MA (1996)
13. Černá, D., Finěk, V., Plačková, G.: Wavelets of Hermite cubic splines on the interval. In: 38th International Conference on Applications of Mathematics in Engineering and Economics; 8 June 2012–13 June 2012, Sozopol; Bulgaria—AIP Conference Proceedings 1497, pp. 138–143 (2012)
14. Cvejnová, D., Černá, D., Finěk, V.: Wavelets based on Hermite cubic splines. In: International Conference of Numerical Analysis and Applied Mathematics 2015, ICNAAM 2015; Rodos Palace HotelRhodes; Greece; 23 September 2015—29 September 2015; 122034—AIP Conference Proceedings 1738, 100004 (2015)
15. Shumilov, B.M.: An algorithm with splitting of the wavelet transform of hermitian cubic splines *Vestnik Tomskogo gosudarstvennogo universiteta-Matematika i mekhanika-Tomsk state university. J. Mathe. Mech.* **12**, 45–55 (2010)
16. Shumilov, B.M., Kuduev, A.Z.: New type multiwavelets of the fifth degree orthogonal to quintic polynomials *Vestnik Tomskogo gosudarstvennogo universiteta-Upravlenie vychislitel'naja tehnika i informatika-Tomsk state university. J. control Comput. Sci.* **21**(4), 108–116 (2012)
17. Shumilov, B.M.: A splitting algorithm for wavelet transforms of the hermite splines of the seventh degree. *Num. Anal. Appl.* **8**(4), 365–377 (2015)
18. Kopenkov, V.N.: Efficient algorithms of local discrete wavelet transform with Haar-like bases. *Pattern Recognition Image Anal.* **18**(4), 654–661 (2008)
19. Bratteli, O., Jorgensen, P.E.T.: Wavelet filters and infinite-dimensional unitary groups. *AMS/IP Stud. Adv. Math.* **25**, 35–65 (2002)
20. Podkur, P.N., Smolentsev, N.K.: About construction of orthogonal wavelets with compact support and with scaling coefficient N. [arXiv:0705.4150v1](https://arxiv.org/abs/0705.4150v1) [math.FA] 29 May (2007)
21. Smolentsev, N.K.: *Fundamentals of the Theory of Wavelets. Wavelets in MATLAB*. DMK Press, Moscow (2014)
22. Koro, K., Abe, K.: Non-orthogonal spline wavelets for boundary element analysis. *Eng. Anal. With Boundary Elem.* **25**, 149–164 (2001)
23. Stollnitz, E.J., DeRose, T.D., Salesin, D.H.: *Wavelets for Computer Graphics: Theory and Applications*. Morgan Kaufmann Publishers Inc., San Francisco, CA, USA (1996)
24. Shumilov, B.M., Matanov, S.M.: An algorithm with splitting of the wavelet transforms of first degree splines *Vestnik Tomskogo gosudarstvennogo universiteta-Upravlenie vychislitel'naja tehnika i informatika-Tomsk state university. J. control Comput. Sci.* **16**(3), 51–57 (2011)
25. Makarov, A., Makarova, S.: On lazy Faber's type decomposition for linear splines. In: 11th International Conference for Promoting the Application of Mathematics in Technical and Natural Sciences, AMiTaNS 2019; Flamingo Grand HotelAlbena; Bulgaria; 20 June 2019—25 June 2019; 153460—AIP Conference Proceedings 2164, 110006 (2019)

26. Makarova S., Makarov A.: On linear spline wavelets with shifted supports. In: Lecture Notes in Computer Science (including subseries Lecture Notes in Artificial Intelligence and Lecture Notes in Bioinformatics), LNCS, vol. 11974, pp. 430–437 (2020)
27. Ahmed, K., Rao, R.: Orthogonal Transforms for Digital Signal Processing. Springer-Verlag, Berlin-Heidelberg-New York (1975)
28. Malozemov, V.N., Masharskii, S.M.: Generalized wavelet bases related to the discrete Vilenkin-Chrestenson transform. St. Petersburg Mathe. J. **13**(1), 75–106 (2002)
29. Zalmanzon, L.A.: Fourier, Walsh and Haar Transformations and Their Application in Control. Communication and Other Systems. Nauka, Moscow (1989)
30. Farkov, Y.A.: Discrete wavelets and the Vilenkin-Chrestenson transform. Mathe. Notes **89**, 871–884 (2011)

Stress Computation and Reduction by Cyber-Physical Systems Controlling Printed Circuit Board Manufacturing Technology



Igor Kovtun and Vilen Royzman

Abstract The chapter represents theoretical and experimental research aimed at mount stress computation and reduction by cyber-physical systems controlling printed circuit board manufacturing technology. The problem of computation and control of technological and exploring strain transmission between structural elements of printed circuit board assembly was considered. A computational model has been designed for stress estimation in structural elements of the printed circuit board and installed electronic components. The idea of stress reduction by application of cyber-physical systems controlling mount technology has been theoretically substantiated and experimentally verified.

Keywords Cyber-physical systems · Stress · Strain · Printed circuit board · Electronic component · Bend test

1 Introduction

The mounting technology creates an electric connection and provides mechanical support to electronic components on the printed circuit boards (PCB) [1]. Mechanical supports, performed as the solid and fixed grip of two or more leads, cause mechanical interaction between electronic components and PCB substrate through their fixtures—solder joints [2–5]. Fixed supports of the leads, in turn, create conditions for occurrence and transmission of strain and stress in all links of the mechanical chain, which includes PCB substrate, electronic components, contact pads, and leads. Such strain and stress are likely to appear in operational and manufacturing conditions and become the reason for breakages in electric circuits and failures of electronic units [6–10]. Computation and reduction of this stress by application of

I. Kovtun (✉) · V. Royzman
Khmelnysky National University, 11 Istrytutska, Khmelnytsky 290016, Ukraine
e-mail: dr.igorkovtun@gmail.com

V. Royzman
e-mail: royzman@gmail.com

cyber-physical systems controlling printed circuit board manufacturing technology is an urgent task today [11, 12].

2 Mathematical Model of Stress Estimation in the Printed Circuit Board

As much as parts of mechanical system, which connect substrate and components, in particular leads, are assumed to be elastic bodies, their elastic properties, such as elasticity modulus E and linear stiffness k , may be considered in order to estimate the strain transmission effect inside the printed circuit board assembly.

In accordance with Hook’s law [13] for an elastic isotropic body the stiffness is:

$$k = \frac{E \cdot S}{N}, \tag{1}$$

where N —cross-section area; l —length of the body.

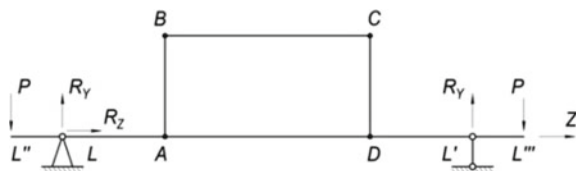
The conjecture was made that reducing the stiffness of the leads will result in the reduction of strain transmission from the PCB substrate to electronic components. This idea can be implemented by controlling mount technology and forming leads by increasing their length l . The theoretical foundation of this conjecture is performed by a mathematical model designed for the relevant calculation scheme.

2.1 Introduction of Calculation Scheme

The calculation scheme of the printed circuit board is introduced by the mechanical system shown in Fig. 1. The introduced system represents the main structure of printed circuit board subassembly, which represents a two-pin electronic component installed on the substrate.

The whole assembly is loaded by the external bending force. Considered forces are likely to appear between PCB and its fixtures while their interaction what brings about a variety of deformations such as tension and bending. Another reason for such forces and deformations in the initial warpage of PCBs, caused by manufacturing

Fig. 1 Planar calculation scheme of two-pin electronic component mounted on printed circuit board



the substrate or mount technologies [14–17], which provoke forces and deformations while straightening PCBs in their installation fixtures.

The calculation scheme was studied by using methods applied in structural mechanics. In terms of structural mechanics, it represents a frame, in particular the planar beam structure, in which members (stiles and rails) are firmly joined (Fig. 1).

In the scheme the edge $L'L'''$ stands for PCB substrate, which rests on two points L and L' representing pinned support (with one degree of freedom) and roller (with two degrees of freedom) support correspondently. PCB is loaded by external forces P applied to points L'' and L''' . These forces produce vertical and horizontal reactions R_Y, R_Z in supports. The edge BC represents the body of the electronic component and edges AB and CD —its leads. The geometric shape $ABCD$ represents the closed-loop in the frame, thus the model is considered to be the frame with the closed-loop inside.

2.2 Equivalent System

The main problem posed for the calculation scheme is to find internal forces and moments of resistance in the electronic components in order to estimate its deformation and strength. In accordance with methods of theoretical mechanics, this model represents the statically indeterminate system, which is impossible to solve by using static equilibrium equations.

The degree of static indeterminacy of the system is found by the formula:

$$n = (n_{ex} + n_{in}) - 3, \quad (2)$$

where n_{ex} —number of external reactions; n_{in} —number of internal reactions, which is calculated as $3 \times K$, where K —number of closed-loops in the frame.

It makes $n = (3 + 3) - 3 = 3$, thus this system has three degrees of static indeterminacy.

Solving the problem was performed by using the force method, which is a general and one of the basic methods for solving statically indeterminate systems. The calculation scheme (Fig. 1) was transformed for more convenient representation (Fig. 2a), in which forces P were substituted by bending moments M , which in the condition of equality of edges $L''L = L'L''' = \Delta z$ is expressed as $M = P \times \Delta z$.

In accordance with the method of forces, the given statically indeterminate system is converted into a geometrically identical statically determinate system by removing additional (extra) joints, which number equals the number of unknown forces. For this reason, the closed-loop structure was broken in the middle point of the edge BC and thus, the basic statically determinate system was obtained (Fig. 2b). On the base of the obtained basic system, the equivalent system (Fig. 2c) was created, in which the removed (broken) joints were substituted by internal forces: X_1 —internal tensile forces; X_2 —internal shear forces; X_3 — internal bending moments.

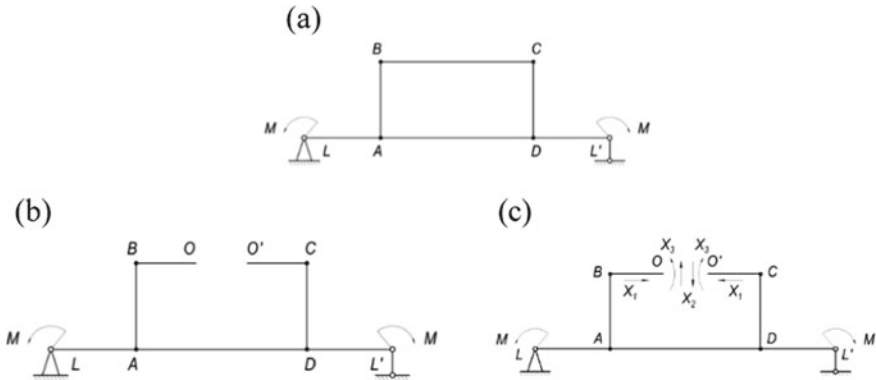


Fig. 2 Calculation schemes: **a** given; **b** basic; **c** equivalent

Conditions of equivalence between basic and given systems are mathematically expressed by canonic equation (3), in accordance with which relative displacements forced by common action of load and unknown force in direction of removed extra joints are to be equal zero. Thus the total displacement in the basic system in direction of removed joint i is expressed as:

$$\delta_i = \delta_{iF} + \sum X_j \cdot \delta_{ij} = 0, \tag{3}$$

where δ_{iF} —displacement in the basic system forced by bending moment M in direction of removed joint i ; δ_{ij} —displacement in the basic system forced by single force X_j in direction of removed joint i .

The number of canonic equations is to be equal to the number of unknown forces. However, since the given system is symmetric the skew-symmetric shear forces X_2 turn to zero and therefore canonic equations are represented by the system of two equations describing displacements in directions of removed joints:

$$\begin{cases} \delta_{1F} + X_1 \cdot \delta_{11} + X_3 \cdot \delta_{13} = 0 \\ \delta_{3F} + X_1 \cdot \delta_{31} + X_3 \cdot \delta_{33} = 0 \end{cases}, \tag{4}$$

Coefficients next to unknown forces and free members of canonic equations are found by using Mohr’s method for all linear members of the system:

$$\delta_{iF} = \sum \int_0^{l_k} \frac{M_k^i M_k^F}{E_k J_k} dl; \quad \delta_{ij} = \sum \int_0^{l_k} \frac{M_k^i M_k^j}{E_k J_k} dl, \tag{5}$$

where k —number of the beam; l_k —length; M_k^i —the internal bending moment in direction of removed joint i ; M_k^F —internal bending moment forced by external bending moment M ; M_k^j —internal bending moment forced by single force X_j ;

E_k and J_k —Young’s modulus and inertia moment of the cross-sectional area correspondently.

In accordance with Maxwell theorem about mutual generalized single displacements, the following expression is true: $\delta_{ij} = \delta_{ji}$.

Represented formulas (5) are obtained with assumptions applied to frame calculations, in accordance with which only bending moments are considered but tensile and shear forces are neglected for their negligible deformations in the basic scheme.

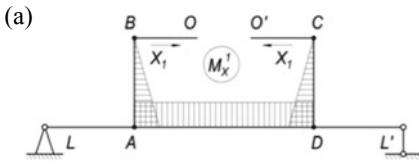
2.3 Internal Forces and Moments of Resistance

The calculation of internal moments of resistance for each member of the system was performed by the method of sections. For symbolic solution the following symbols are used: $AB = CD = a$; $AO = b$; $BO = BO' = b/2$.

The single internal bending moments diagrams in the basic system, in accordance to method of forces, are drawn for alternative application of unknown forces X_j , initially assumed equal to 1: $X_1 = 1$; $X_3 = 1$ (fig. 3a, b), and external bending moment M (fig. 3c).

The area of diagrams calculated for these moments is given in Table 1.

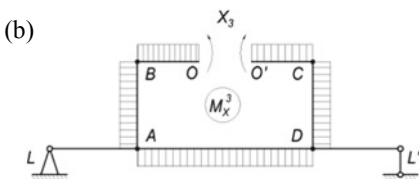
Coefficients next to unknown forces and free members of canonic equations found by using Mohr’s method are:



$$M_0^1 = M_{O'}^1 = M_B^1 = M_C^1 = 0;$$

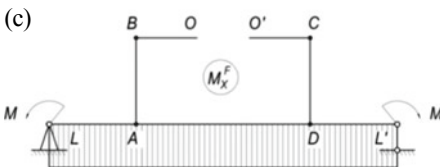
$$M_A^1 = M_D^1 = X_1 \cdot a = a$$

when $X_1 = 1$.



$$M_0^3 = M_{O'}^3 = M_B^3 = M_C^3 = M_A^3 =$$

$$= M_D^3 = X_3 = -1.$$



$$M_L^F = M_{L'}^F = M_A^F = M_D^F = -M$$

Fig. 3 Internal bending moments diagrams in the basic system for the alternative application of a X_1 ; b X_3 ; c M

Table 1 The area of diagrams calculated for internal moments of resistance for all members of the basic calculation scheme

Beam	OB	O'C	AB	CD	AD
Length, l_k	$b/2$	$b/2$	a	a	b
$M_x^1(l)$	0	0	1	1	a
$M_x^3(l)$	- 1	- 1	- 1	- 1	- 1
$M_x^F(l)$	0	0	0	0	- M

$$\begin{aligned}
\delta_{1F} &= \sum \int_0^{l_k} \frac{M_x^1 \cdot M_x^F}{EJ_x} dl = -\frac{Mab}{EJ_x}; & \delta_{11} &= \sum \int_0^{l_k} \frac{M_x^1 \cdot M_x^1}{EJ_x} dl = \frac{2a^3 + 3a^2b}{3EJ_x}; \\
\delta_{3F} &= \sum \int_0^{l_k} \frac{M_x^3 \cdot M_x^F}{EJ_x} dl = \frac{Mb}{EJ_x}; & \delta_{33} &= \sum \int_0^{l_k} \frac{M_x^3 \cdot M_x^3}{EJ_x} dl = \frac{2a + 2b}{EJ_x}; \\
\delta_{13} &= \delta_{31} = \sum \int_0^{l_k} \frac{M_x^1 \cdot M_x^3}{EJ_x} dl = -\frac{a^2 + ab}{EJ_x}.
\end{aligned} \tag{6}$$

The solution of the system of canonic equations (4) was found for symbolic expressions of internal forces and moments of resistance X_1 and X_3 with the purpose to theoretically justify the offered conjecture and reveal the relationship between internal forces in the body of electronic component (members OB and $O'C$) and the length of their leads a . To simplify expressions and conceal the influence of the other function parameters those were assumed constant, and stiffness EJ_x of all beams is assumed the same.

The solution of the system of equations (4) with coefficients (6) resulted in the following expressions:

$$X_3 = \frac{Mab}{a^2 + 4ab - 3b^2}; \tag{7}$$

$$X_1 = \frac{3Mb}{a^2 + 3ba}. \tag{8}$$

The found expressions provide the conclusion that increasing parameter a significantly decreases values of functions X_1 and X_3 .

2.4 Mathematical Model Application

For known values of X_1 and X_3 the equivalent scheme is obtained (Fig. 4), in which internal force factors, stresses, and displacements are identical to those in the given statically indeterminate system.

The designed mathematical model, which provides a computational tool for internal forces of resistance and correspondent strains and stresses in structural elements of printed circuit boards and installed electronic components, can be effectively applied to cyber-physical systems controlling printed circuit board manufacturing technology in order to achieve essential stress reduction and increased reliability.

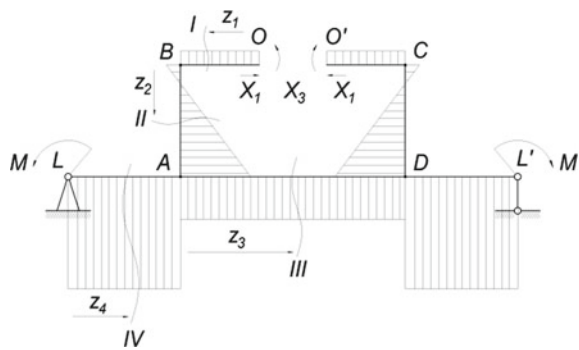
Noteworthy is that bending loads cause linear deformations, which occur along the axis of the beams and are distributed not uniformly across its thickness so that they are tensile on the outer side and compressive on the inner side of the beam [13–18]. The greatest interest is attracted by the case when the body of the electronic component appears on the stretched side of the board, and therefore is subjected to linear tensile deformation.

The stress assessment of such structure can be performed by its maximal value:

$$\sigma_{max} = \frac{M_{max}}{W_{ax}}, \tag{9}$$

where M_{max} —maximal internal bending moment; W_{ax} —axial moment of resistance.

Fig. 4 The total diagram of internal bending moments



$$\begin{aligned} OB, O'C: 0 \leq z_1 \leq b/2; M^I &= -X_3. \\ AB, CD: 0 \leq z_2 \leq a; M^{II} &= X_1 \cdot z_2 - X_3. \\ AD: 0 \leq z_3 \leq b; M^{III} &= X_1 \cdot a - X_3 - M. \\ LA, DL': 0 \leq z_4 \leq a; M^{IV} &= -M. \end{aligned}$$

3 Experimental Verification

3.1 Bend Test

The experimental research was conducted for ceramic resistors OMLT-0,125 installed on PCB by different types of mount technology. The experiments were conducted using a mechanical bend test. Reading strains from resistors were executed by stain gauges MPB-1 attached to their bodies.

The test was conducted for three types of mount technologies: surface mount technology (Fig. 5a); low through-hole technology (Fig. 5b); and proposed – high through-hole technology (Fig. 5c).

In order to provide identical stress and strain condition for resistors mounted on the PCB, the test appliance was created (Fig. 6a). The appliance produces pure bend load onto PCBs [19, 20]. The diagram of moments (Fig. 6b) demonstrates equal

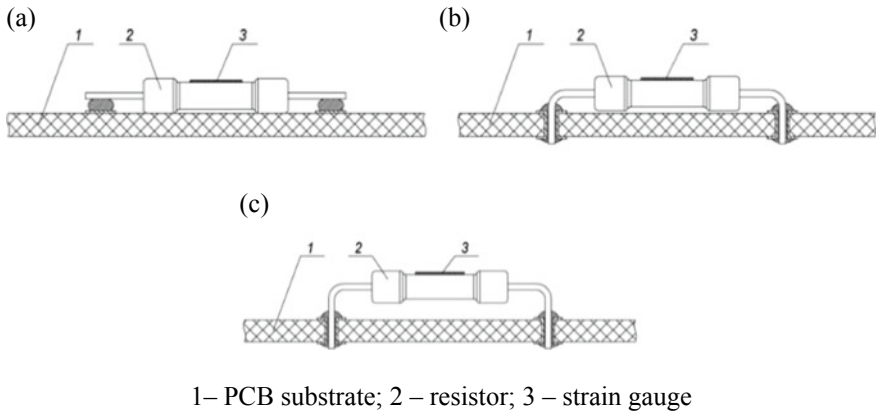


Fig. 5 Types of mount technologies for resistors on PCB: **a** surface mount technology; **b** low through-hole technology; **c** high through-hole technology

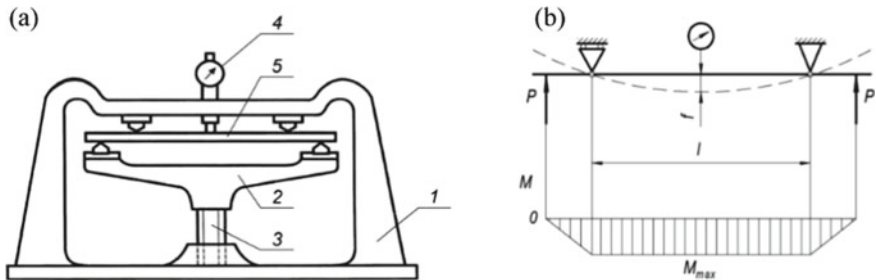


Fig. 6 Pure bend test appliance (a) 1 base; 2 force beam; 3 elevator; 4 indicator; 5 PCB and diagram of bending moments (b)

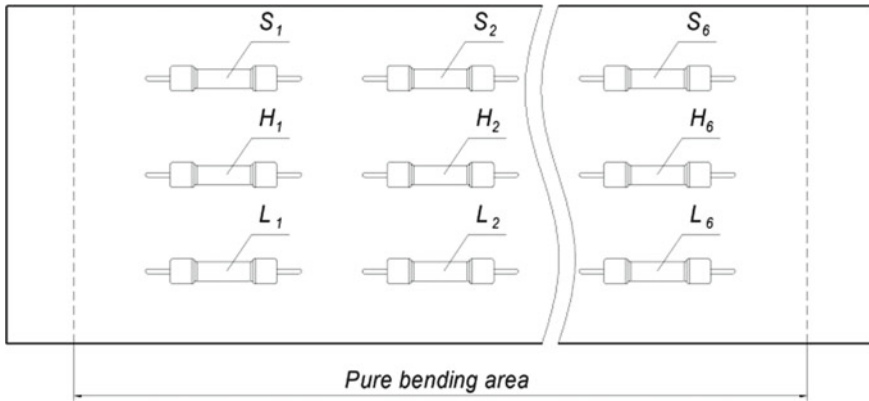


Fig. 7 Resistors layout on the PCB: surface mount technology (S_j); low through-hole technology (L_j) and high through-hole technology (H_j)

load (bending moment) applied to the area between two inner supports—along the segment I.

The trial tests were conducted for PCBs at different loads. 10 mm strain gauges were attached to the tested boards, both in the longitudinal and transverse directions. The deviation in the strain gauge readings did not exceed 5% in both transverse and longitudinal directions. Therewith strain in the transverse direction was actually absent.

For the tests resistors were installed in three rows within the area of PCB subjected to pure bending deformation (Fig. 7). Each of three rows represented specific type of mount technology. Therewith resistors were installed parallel to the longitudinal axis of PCB.

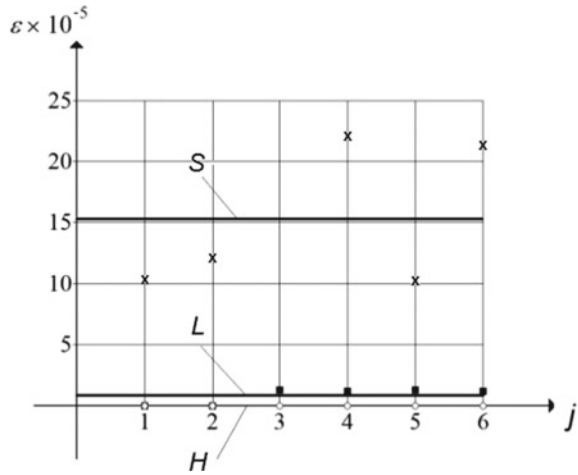
The strain of outer fibers on the PCB is determined by its maximum deflection f , which is, in turn, measured by the clock indicator and executed by the test appliance:

$$\varepsilon = \frac{4h}{l^2} f, \tag{10}$$

where h —thickness of PCB; f —deflection; l —length of pure bend area.

When deflection is produced by the test appliance within $f = 0\text{--}10$ mm, the applied force does not exceed 50 N. Since all resistors were in identical stress and strain conditions the differences in measured values of deformation were determined only by the type of their installation on the PCB, which differed by the length of their leads.

Fig. 8 The tensile strain of resistors (markers) and its mean levels (solid lines) at the maximal deflection of PCB equal to 8 mm; markers: ×—surface mount technology (S); ■—low through-hole technology (L); o—high through-hole technology (H)



3.2 Obtained Results and Discussion

Figure 8 shows the strain gauge data read at the maximal deflection of PCB equal to 8 mm. The highest values of deformation transmitted from PCB to resistors were detected for resistors installed by surface mount technology S_j, and the lowest values were demonstrated by resistors installed by proposed high through-hole technology H_j. Resistors installed by the low through-hole technology L_j represented intermediate strain and stress transmission among the two types described above.

Thus, the results of experimental research have verified mathematical model and proved that modification of mount technology that introduces changes to forming leads with increasing their length provides essential reducing in strain transmission from the printed circuit boards to installed electronic components.

The stress calculation was performed for tested resistors by Hook’s law [13] for elasticity modulus $E = 1 \times 10^5$ MPa. Noteworthy was that at the given deflection stress values transmitted from the printed circuit board to resistors installed by surface mount technology ($\sigma = 9.8 \dots 17.4$ MPa) made about 20% of the ultimate stresses ($\sigma_{ult} = 95 \dots 165$ MPa).

4 Conclusion

The designed mathematical model, which provides a computational tool for internal forces of resistance and correspondent strains and stresses in structural elements of printed circuit boards and installed electronic components, can be effectively applied to cyber-physical systems controlling printed circuit board manufacturing technology in order to achieve essential stress reduction and increased reliability.

Theoretical and experimental research approved the conjecture of the stress reduction in electronic component and also in all structural elements of printed circuit board assembly by application of cyber-physical systems controlling mount technology and forming the length of the mount leads.

Obtained results demonstrate the essential advantage of the proposed mount technology application in comparison with low through-hole technology and surface mount technology. The efficiency test for this technology is produced by the pure bending tests appliance designed to provide identical stress and strain conditions to the tested printed circuit board assemblies.

References

1. Bhunia, S., Tehranipoor, M.: Chapter 4—Printed circuit board (PCB): Design and Test. In: Hardware Security, Chapter 4, pp. 81–105. Elsevier. (2019). <https://doi.org/10.1016/B978-0-12-812477-2.00009-5>
2. Kovtun, I., Boiko, J., Petrashchuk, S.: Nondestructive strength diagnostics of solder joints on printed circuit boards. In: 2017 Proceedings IEEE International Conference on Information and Telecommunication Technologies and Radio Electronics (UkrMiCo), Odessa, 2017, pp. 1-4. (2017). <https://doi.org/10.1109/UkrMiCo.2017.8095401>
3. Tong, J.P.C., Tsung, F., Yen, B.P.C.: A DMAIC approach to printed circuit board quality improvement. *Int. J. Adv. Manuf. Technol.* **23**(7), 523–531 (2004). <https://doi.org/10.1007/s00170-003-1721-z>
4. Samavatian, M., Ilyashenko, L.K., Surendar, A., Maseleno, A., Samavatian, V.: Effects of system design on fatigue life of solder joints in BGA packages under vibration at random frequencies. *J. Electron. Materi.* **47**(11), 6781–6790 (2018). <https://doi.org/10.1007/s1166>
5. Qi, Z., Liu, G.: Precise Control of Elastic Joint Robot Using an Interconnection and Damping Assignment Passivity-Based Approach. *IEEE/ASME Transactions on Mechatronics*, vol. 21, iss. 6, 2728–2736 (2016). <https://doi.org/10.1109/TMECH.2016.2578287>
6. Kovtun, I., Boiko, J., Petrashchuk, S.: Identification of natural frequency and form of oscillation for electronic packages subjected to vibration. In: Proceedings 2018 IEEE 38th International Conference on Electronics and Nanotechnology (ELNANO), Kiev, 2018, pp. 621 – 626. (2018) DOI: <https://doi.org/10.1109/ELNANO.2018.8477492> .
7. Elshabini, A.A., Barlow, F.P., Wang, J.: Electronic packaging: semiconductor packages. In: Reference Module in Materials Science and Materials Engineering. Elsevier (2017). <https://doi.org/10.1016/B978-0-12-803581-8.02048-8>
8. Psota, B., Otáhal, A., Szendiuch, I.: Influence of the PCB attachment on the mechanical properties in modal analysis. In: Proceedings of 2015 European Microelectronics Packaging Conference (EMPC), Friedrichshafen, 2015, pp. 1-4. Available [online]: <https://ieeexplore.ieee.org/document/7390679>.
9. Lall, P., Gupta, P., Goebel, K.: Identification of failure modes in portable electronics subjected to mechanical-shock using supervised learning of damage progression. In: 2011 Proceedings of IEEE 61st Electronic Components and Technology Conference (ECTC), USA, 2011, pp. 1944–1957 (2011). <https://doi.org/10.1109/ECTC.2011.5898783>
10. Viswanadham, P., Singh, P.: Failure Modes and Mechanisms in Electronic Packages. Chapman & Hall, MA, Ed. Boston, Springer (1998). <https://doi.org/10.1007/978-1-4615-6029-6>
11. Royzman, V.: Ways to improve strength reliability of electronics elements and systems. In: Proceedings of IEEE Conference on Modern Problems of Radio Engineering, Telecommunications and Computer Science (IEEE Cat. No.02EX542), Lviv-Slavsko, 2002, pp. 187–190 (2002). <https://doi.org/10.1109/TCSET.2002.1015917>

12. Bushmeleva, K., Avdeuk, O., Uvaysova S., Uvaysova, A.: The system of automated circuit simulation of electronic devices. In: 2019 IEEE International Seminar on Electron Devices Design and Production (SED), Prague, 2019, pp. 1–7. (2019). <https://doi.org/10.1109/SED.2019.8798419>
13. Pisarenko, G.S., Kvitka, O.L., Umanski, E.S.: Strength of materials, 2nd edn, 655 p. Kiev (2004)
14. Jones, R.M.: Buckling of Bars, Plates and Shells. Blacksburg, Bull Ridge Publishing, Virginia, USA (2006)
15. Huang, P.S., Lin, Y.H., Huang, C.Y., Tsai, M.Y., Huang T.C., Liao, M.C.: Warpage and curvature determination of PCB with DIMM socket during reflow process by strain gage measurement. In: Proceedings of 2010 IEEE 5th International Microsystems Packaging Assembly and Circuits Technology Conference, Taipei, 2010, pp. 1–4. (2010). <https://doi.org/10.1109/IMPACT.2010.5699599>
16. Han, L., Voloshin, A.: Statistical analysis for test lands positioning and PCB deformation during electrical testing. *Microelectronics Reliability*, vol. 44, iss. 5, 853–859 (2004). <https://doi.org/10.1016/j.microrel.2003.12.002>
17. Schuerink, G.A., Slomp, M., Wits, W.W., Legtenberg, R., Kappel, E.A.: Modeling printed circuit board curvature in relation to manufacturing process steps. *Procedia CIRP* **9**, 55–60 (2013). <https://doi.org/10.1016/j.procir.2013.06.168>
18. Wong, E.H., Mai, Y.W.: Stresses in solder joints due to the bending deformation of printed circuit boards in microelectronics assemblies. In: *Robust Design of Microelectronics Assemblies against Mechanical Shock, Temperature and Moisture*, pp. 379–409. Elsevier: Woodhead Publishing Series in Electronic and Optical Materials. (2015). <https://doi.org/10.1016/B978-1-84569-528-6.00011-3>
19. Boiko, J., Kovtun, I., Petrashchuk, S.: Vibration transmission in electronic packages having structurally complex design. In: *First Ukraine IEEE international Conference on Electrical and Computer Engineering (UKRCON—2017): Proceedings of a meeting held, 29 May 2 June 2017, Kiev, Ukraine, 2017*, pp. 514–517.I.
20. Kovtun, J., Boiko, S., Petrashchuk, Kałaczyński, T.: Theory and practice of vibration analysis in electronic packages. In: *MATEC Web Conference on 182, 02015* (2018). <https://doi.org/10.1051/mateconf/201818202015>

Geometric Parameters Optimization of Cable-Driven Parallel Robot with a Movable Gripper



Elena V. Gaponenko , Dmitry I. Malyshev , Victoria S. Kuzmina ,
and Larisa A. Rybak 

Abstract The chapter considers the structure of a cable-driven parallel robot for load move in special conditions. This structure is a rigidly fixed frame connected by tensioned ropes to a platform containing an axial movement device. Effective numerical methods and algorithms were developed and tested, which allowed investigating the influence of cable pulling forces on the volume of the operating area and determine the minimum geometric dimensions of the robot that ensure the movement of the output link within the required operating area. In order to implement the proposed methods and algorithms, a software package with the ability to export 3D operating areas in STL format for visualization was developed. The chapter presents the results of mathematical modeling.

Keywords cable-driven parallel robot · Interval analysis · Tensile forces · Algorithm · Geometric parameters

1 Introduction

In recent decades, there has been a growing demand for the use and control of manipulators in various industrial sectors in order to increase productivity, reliability, accuracy, rigidity, and access to the setting inaccessible to humans. Cable-driven parallel robots (CDPR) are of particular interest. They present a special type of kinematic structure, consisting mainly of a work tool connected to a fixed base platform using cables [1–3]. Today, cable robots are successfully used for construction work [4], for measuring the position and orientation of an object [5, 6], for rehabilitation in medicine [7–9], as well as for solving other industrial problems [10]. CDPRs use cables instead of pull-out rods to control the position of the output link. In these mechanisms, the position of the output link is controlled by changing the length of the cables. Cables are usually wound on spools attached to a base and powered by a rotating motor.

E. V. Gaponenko (✉) · D. I. Malyshev · V. S. Kuzmina · L. A. Rybak
Belgorod State Technological University named after V.G. Shukhov, 46 Kostukova, Belgorod
308012, Russia
e-mail: gaponenkobel@gmail.com

CDPRs have such advantages as a large workspace, assembly and disassembly ease, high mobility, heavy load capacity and reset ease. Controlling the length of the cables over a wide range, we can get access to a very large workspace from several tens of centimeters to several tens of meters or more. The use of cables instead of rigid links further reduces weight since the drills do not change position and are fixed to a stable base so that the only moving parts are the cables and the output link. As a result, a robot with higher speed and maneuverability and increased heavy load is obtained. The production costs of CDPRs are significantly lower than those of conventional manipulators. CDPRs are easy to install. Such a manipulator can be assembled using a number of inexpensive winches and cables. In addition, since the motors do not need to be installed close to a moving platform, they are suitable for use in hazardous environments. In addition, their heavy load capacity is relatively high; it is even comparable to construction cranes.

The following authors pay particular attention to the topic of CDPRs: J. B. Isard, M. Michelin, J. P. Merle, K. Gosselin, S. Baradat, and others. Bouchard and Gosselin were engaged in the optimization of the workspace of a CDPR for broadcasting. Thus, in the paper [11], some issues related to inverse kinematics and statics of CDPRs are considered, as well as some limitations typical of workspace. Abbasneyad and the research team developed a planar CDPR for rehabilitation purposes and balancing external forces. J. P. Merle and D. Denis developed the lightweight and mobile cable parallel robot Marionet, which is designed for rescue operations in hard-to-reach places. The article [12] considers the dynamic planning of the 3-DOF trajectory of spatial suspended parallel manipulators. On the basis of the dynamic model of the suspended robot, a set of algebraic inequalities representing the constraints on the cable tension is obtained. During the use of periodic functions in the design of trajectories, it is shown that there are special frequencies, similar to the natural frequencies of pendulum-type systems. These special frequencies can be used in practice to simplify trajectory planning. A prototype of a 3-DOF CDPR was developed in [13]. The proposed approach to trajectory planning can be used to plan dynamic trajectories that go beyond the static workspace of the mechanism, giving new applications and opportunities for CDPRs. The paper [14] considers the dynamic analysis and classification of the workspace based on the general equation of motion of the CDPR and the one-sided properties of cables. Different types of workspaces were qualitatively compared. Zhang and Shang [15] were engaged in planning the trajectory of a three-stage cable robot taking into account dynamic effects. In their work, a geometric approach for trajectory planning was proposed, which can also be applied when the mechanism goes beyond the static equilibrium. The approach proposed by the authors provides an analytical solution that allows for positive and continuous tensions in all control cables. The influence of dynamic behavior of control cables was shown by Du et al. [16], where the authors used a dynamic cable model with variable length to control a mobile platform.

One of the main tasks in CDPR designing is workspace determination, within which the operating body should be located during the technological operations. In order to determine the workspace, the following methods are used: geometric, numerical, discretization methods. One of the existing deterministic methods is the

non-uniform covering method. The cover set is represented by a set of n-dimensional boxes, the boundaries of which are described as:

$$\underline{x}_i \leq x_i \leq \overline{x}_i, i \in 1, n \tag{1}$$

This method can be easily automated and applied to various tasks, including in the field of robotics. The non-uniform covering method used to determine the workspace of some types of parallel robots is considered in [17–19].

The use of the method of non-uniform covering to determine the workspace of a CDPR designed to application in special conditions was discussed earlier in the work [20]. Within the framework of this chapter, we will determine the minimum geometric parameters of a CDPR depending on the required dimensions of the workspace for the performance of technological operations. In addition, we will investigate the influence of cable tension forces on the volume of the workspace for two configurations: with and without axial movement of the output link.

2 Mathematical Model

Let us consider the structure of a CDPR designed for application in special conditions (Fig. 1). The mechanism consists of four columns, four cables, which are connected with one of the ends to the movable platform at points B_1, B_2, B_3, B_4 . The gripping unit with the possibility of axial movement is fixed on the platform. The second ends of the cables passed through the pulleys, designated by points A_1, A_2, A_3, A_4 , installed on the columns, they are fixed on the drums D_1, D_2, D_3, D_4 , respectively. Under the action of the load weight mg , fixed at point C , tensile forces T_1, T_2, T_3, T_4 appear in the cables. The change in the position of the load-attaching point occurs due to the change in the lengths of the cables when the drums rotate with the gear motors M_1, M_2, M_3, M_4 . The gripping unit is a movable platform connected with cables. An output link C is located on the movable platform, which has the ability to axially move h along the Z axis. This mechanism allows objects to be moved in hard-to-reach places with special conditions without human intervention, for example, the

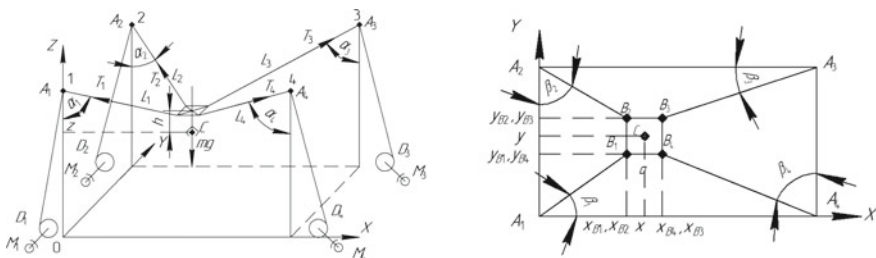


Fig. 1 Cable-driven parallel robot

work with radioactive elements and radiation sources, the work with elements that can irradiate cells, lead to their mutation. They can cause irreparable harm to health. This category also includes work at nuclear, thermal power plants.

Despite many advantages of CDPRs, there are several problems associated with the control of the movement of robot cables. One of the disadvantages is that cables can be pulled but not pushed, resulting in a one-way restriction whereby the cables must always be kept tensed. The positions in which at least one of the cables is loose are special and are not considered in the chapter.

We introduce the limits on the cable tensile forces T_i :

$$T_i := [\underline{T}_i, \overline{T}_i] = \{0 \leq \underline{T}_i \leq T_i \leq \overline{T}_i\}, \quad (2)$$

Let us write down the intervals that describe the ranges of the cosines and sines of the angles α_i and β_i :

$$S_{Ai} := [\underline{S}_{Ai}, \overline{S}_{Ai}] = \{\underline{S}_{Ai} \leq \sin \alpha_i \leq \overline{S}_{Ai}\}, i \in 1, \dots, 4,$$

$$S_{Bi} := [\underline{S}_{Bi}, \overline{S}_{Bi}] = \{\underline{S}_{Bi} \leq \sin \beta_i \leq \overline{S}_{Bi}\}, i \in 1, \dots, 4,$$

$$C_{Ai} := [\underline{C}_{Ai}, \overline{C}_{Ai}] = \{\underline{C}_{Ai} \leq \cos \alpha_i \leq \overline{C}_{Ai}\}, i \in 1, \dots, 4,$$

$$C_{Bi} := [\underline{C}_{Bi}, \overline{C}_{Bi}] = \{\underline{C}_{Bi} \leq \cos \beta_i \leq \overline{C}_{Bi}\}, i \in 1, \dots, 4.$$

The tensile forces in flexible links can be calculated by solving systems of non-linear equations of the form:

$$\begin{cases} T_1 S_{A1} C_{B1} + T_2 S_{A2} S_{B2} - T_3 S_{A3} C_{B3} - T_4 S_{A4} S_{B4} = 0 \\ T_1 S_{A1} S_{B1} - T_2 S_{A2} T_{B2} - T_3 S_{A3} S_{B3} + T_4 S_{A4} C_{B4} = 0 \\ T_1 C_{A1} + T_2 C_{A2} + T_3 C_{A3} + T_4 C_{A4} - mg = 0 \end{cases} \quad (3)$$

where

$$\begin{aligned} C_{Ai} &= \frac{z_{Ai} - Z_{Bi}}{\sqrt{(X_{Bi} - x_{Ai})^2 + (Y_{Bi} - y_{Ai})^2 + (z_{Ai} - Z_{Bi})^2}}, & S_{Ai} &= \\ \frac{\sqrt{(X_{Bi} - x_{Ai})^2 + (Y_{Bi} - y_{Ai})^2}}{\sqrt{(X_{Bi} - x_{Ai})^2 + (Y_{Bi} - y_{Ai})^2 + (z_{Ai} - Z_{Bi})^2}}; & S_{B1} &= \frac{Y_{B1} - y_{A1}}{\sqrt{(X_{B1} - x_{A1})^2 + (Y_{B1} - y_{A1})^2}}; & S_{B2} &= \\ \frac{X_{B2} - x_{A2}}{\sqrt{(X_{B2} - x_{A2})^2 + (Y_{A2} - Y_{B2})^2}}; & S_{B3} &= \frac{Y_{A3} - Y_{B3}}{\sqrt{(X_{A3} - X_{B3})^2 + (Y_{A3} - Y_{B3})^2}}; & S_{B4} &= \frac{X_{A4} - X_{B4}}{\sqrt{(X_{A4} - X_{B4})^2 + (Y_{B4} - Y_{A4})^2}}; \\ C_{B1} &= \frac{X_{B1} - x_{A1}}{\sqrt{(X_{B1} - x_{A1})^2 + (Y_{B1} - y_{A1})^2}}; & C_{B2} &= \frac{Y_{A2} - Y_{B2}}{\sqrt{(X_{B2} - x_{A2})^2 + (Y_{A2} - Y_{B2})^2}}; & C_{B3} &= \\ \frac{X_{A3} - X_{B3}}{\sqrt{(X_{A3} - X_{B3})^2 + (Y_{A3} - Y_{B3})^2}}; & C_{B4} &= \frac{Y_{B4} - y_{A4}}{\sqrt{(X_{A4} - X_{B4})^2 + (Y_{B4} - y_{A4})^2}}. \end{aligned}$$

with $\mathbf{X}_{B1} = \mathbf{X}_{B2} = \mathbf{X}_C - \frac{a}{2}$, $\mathbf{X}_{B3} = \mathbf{X}_{B4} = \mathbf{X}_C + \frac{a}{2}$, $\mathbf{Y}_{B1} = \mathbf{Y}_{B4} = \mathbf{Y}_C - \frac{a}{2}$, $\mathbf{Y}_{B2} = \mathbf{Y}_{B3} = \mathbf{Y}_C + \frac{a}{2}$, $\mathbf{Z}_{Bi} = \mathbf{Z}_C + \mathbf{H}$, где $\mathbf{X}_C := [\underline{X}_C, \overline{X}_C] = \{\underline{X}_C \leq x_c \leq \overline{X}_C\}$, $\mathbf{Y}_C := [\underline{Y}_C, \overline{Y}_C] = \{\underline{Y}_C \leq y_c \leq \overline{Y}_C\}$, $\mathbf{Z}_C := [\underline{Z}_C, \overline{Z}_C] = \{\underline{Z}_C \leq z_c \leq \overline{Z}_C\}$, $\mathbf{H} := [\underline{H}, \overline{H}] = \{\underline{H} \leq h \leq \overline{H}\}$.

The left parts of the system of Eqs. (2) are the functions in the form $g_j, j \in 1, \dots, 3$: $g_1 = T_1 S_{A1} C_{B1} + T_2 S_{A2} S_{B2} - T_3 S_{A3} C_{B3} - T_4 S_{A4} S_{B4}, \dots, g_3 = T_1 C_{A1} + T_2 C_{A2} + T_3 C_{A3} + T_4 C_{A4} - mg$.

The above-mentioned equations allow finding solutions to the system of Eqs. (2) that determine the limitations of the workspace.

3 Analysis of the Effect of Cable Tension Forces.

The approximation algorithm of the set of solutions to systems of nonlinear inequalities for the determination of the workspace is considered in the work [20]. Let us analyze the influence of the cable tensile force ranges on the basis of the obtained algorithm.

We introduce the coefficient k , which is defined as $k = \overline{T_i} / \underline{T_i}$. Let us define the workspace for different values of k in the range from 1, 4 to 10 with an interval 0,1. Let us take the minimum tensile force $\underline{T_i} = 10$ H.

The computational experiment was carried out for the following parameters of the mechanism: $x_{A3} = x_{A4} = y_{A2} = x_{A2} = z_{Ai} = 1000$ mm, $m = 5$ kg.

Two configurations of the cable mechanism were considered: without axial movement of the output link and with movement $h = 100$ mm. The algorithm is implemented in the C++ programming language using the Snowgoose interval analysis library [21], as well as the OpenMP library for the implementation of multi-threaded calculations [18]. The computation time for $k = 5$ without axial movement, approximation accuracy of 4 mm, and using the parallelization of calculations for 8 threads on a personal computer was 3 min. 46 s.

The dependence of the volume of the workspace on the coefficient k is shown in Fig. 2. As can be seen from the figure, the volume of the workspace for the configuration with axial movement of the output link is greater for any k , however, at $k \geq 9.5$ the volume of the workspace is almost equal.

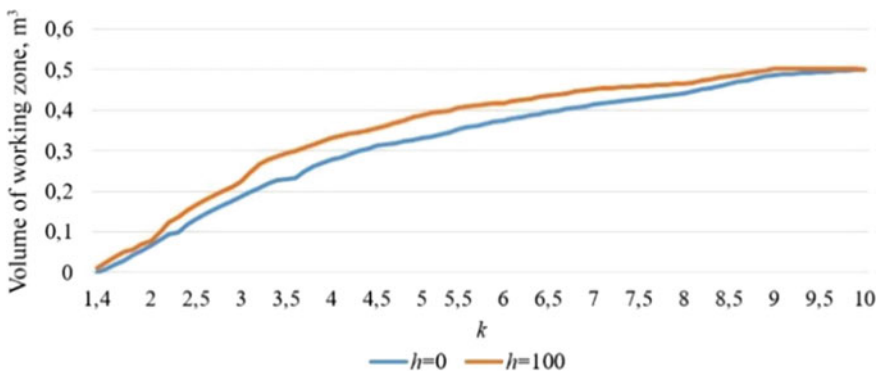


Fig. 2 Volume change of the workspace depending on the coefficient k

In order to evaluate the change in the form of the workspace, the output of the simulation results in STL format was used. Figure 3 shows the workspaces at $k = 3$ (green) and $k = 8$ (blue). Figure 4 shows the change in the workspace at $k = 3$ without axial movement of the output link (green) and with axial movement (blue).

Fig. 3 Workspace at different k values

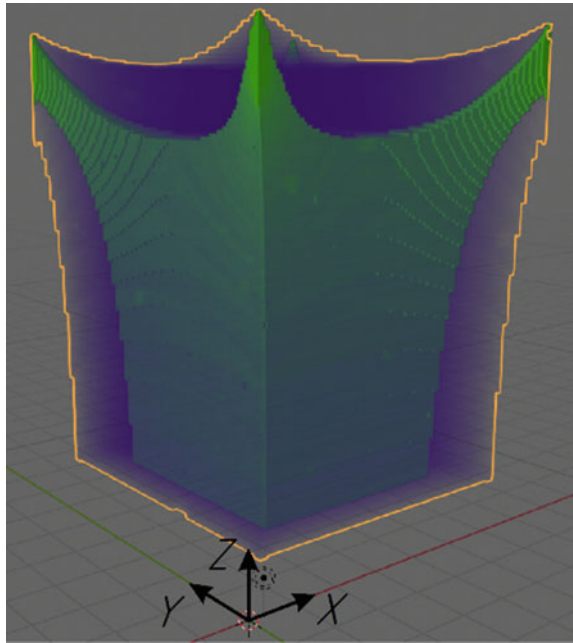
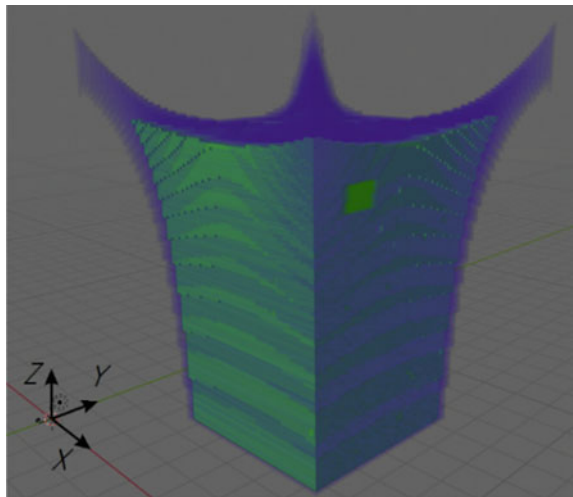


Fig. 4 Increase of workspace due to the axial movement of the output link



4 Geometric Parameters Optimization

Next, we will analyze the optimization of the geometric parameters of the cable mechanism. It includes the selection of the minimum overall dimensions of the CDPR, providing the required dimensions of the workspace. For this, using the methods of interval analysis, we will check whether the system can be solved (3).

In this case, the coordinates correspond to the coordinates of the boundaries' points of the required workspace, the coordinates lie in the interval, the length of which depends on the range of possible location of the required workspace inside the robot along the Z-axis. We synthesize an algorithm for the optimization of geometric parameters using a system of equations written in the general form:

$$\begin{cases} g_i(x) = 0, \\ \dots \\ g_m(x) = 0, \\ a_i \leq x_i \leq b_i, i = 1, \dots, n. \end{cases} \quad (4)$$

The algorithm (Fig. 5) works with two lists of six-dimensional boxes \mathbb{P} (current list), \mathbb{P}_A (cover). Each of the dimensions of the boxes corresponds to the intervals $T_i, i = 1, \dots, 4, \mathbf{Z}'_c$ и H .

The initial box Q , which covers the entire set of solutions X , is determined by the interval limits $a_i \leq x_i \leq b_i, i = 1, \dots, n$. Let us consider any box B . Let $m(B) = \max_{j=1, \dots, m} \min_{x \in B} g_j(x)$ and $M(B) = \max_{j=1, \dots, m} \max_{x \in B} g_j(x)$. If $m(B) > 0$ or $M(B) < 0$, then contains no possible points for system (4). Initially, the overall dimensions of the robot are equal to the dimensions of the required workspace, that is $x_{A3} = x_{\max}^{(w)}, y_{A3} = y_{\max}^{(w)}, z_{A3} = z_{\max}^{(w)}$.

The algorithm works as follows:

1. To set geometric parameters of the required workspace, intervals $H, T_i, i \in 1, \dots, 4$. and approximation accuracy δ .
2. To assign $x_{A3} = x_{\max}^{(w)}, y_{A3} = y_{\max}^{(w)}, z_{A3} = z_{\max}^{(w)}$.
3. The list \mathbb{P}_A is empty, the list \mathbb{P} has only one box Q , including the intervals $T_i, i = 1, \dots, 4, \mathbf{Z}'_c$ and H :
4. To extract from list \mathbb{P} box B .
5. To calculate $m(B)$ and $M(B)$ for points C_l of the surface of the required workspace
6. If $m(B) > 0$ or $M(B) < 0$ at least for C_l , then exclude B and turn to step 9.
7. If $|\mathbf{Z}'_c| < \delta$, then B add to the list \mathbb{P}_A and turn to the list 9.
8. In other cases, B is divided into two equal boxes by \mathbf{Z}'_c . Add these boxes to the end of the list \mathbb{P} , which is $\mathbb{P} := \mathbb{P} \cup \{B_1\} \cup \{B_2\}$.
9. If $\mathbb{P} \neq \emptyset$, then turn to step 4.
10. To extract from the list \mathbb{P}_A box B .
11. To divide B by a uniform $m \times m$ grid by dimensions and H into intervals $T_i^{(p)}$ and $H^{(p)}, p = 1, \dots, m$.

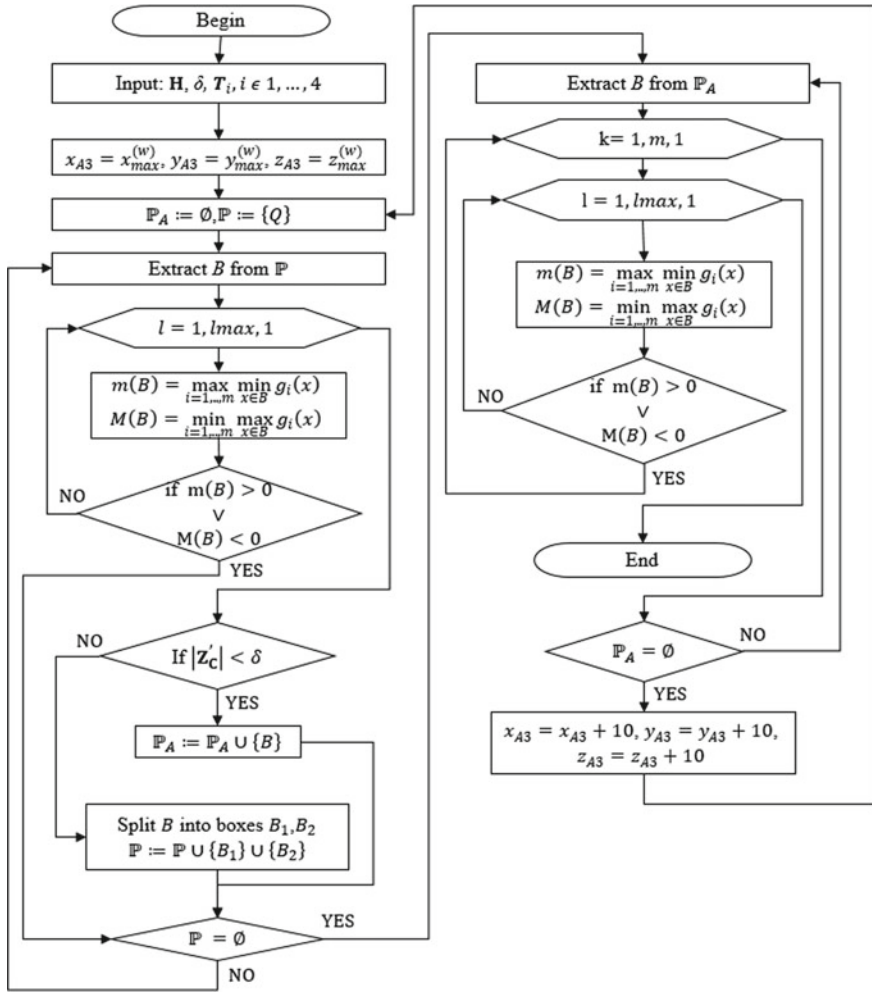


Fig. 5 Algorithm for optimization of the geometric parameters of the cable mechanism

12. To calculate $m(B)$ and $M(B)$ for the points C_l taking into account the intervals $T_i^{(p)}$ and $H^{(p)}$.
13. If $m(B) > 0$ or $M(B) < 0$ at least for one of C_l at all $T_i^{(p)}$ and $H^{(p)}$, then eliminate B and go to step 14. Otherwise, it is necessary to terminate the algorithm.
14. If $P_A \neq \emptyset$, then turn to step 10.
15. Assign $x_{A3} = x_{A3} + 10, y_{A3} = y_{A3} + 10, z_{A3} = z_{A3} + 10$ and turn to step 3.

The simulation was performed for various values of k in the range from 1.5 to 10 with interval 0.1, while $x_{\max}^{(w)} = y_{\max}^{(w)} = z_{\max}^{(w)} = 1000x_{\max}^{(w)} = y_{\max}^{(w)} = z_{\max}^{(w)} = 1000$ mm. Similarly, 2 configurations were considered. The simulation results for some k are given in Table 1.

Table 1 Dependence of the overall dimensions of the robot on the coefficient k

h, mm	Overall dimensions of the robot, mm*10, at the coefficient k										
	1.5	1.6	1.7	1.8	2	2.5	3	3.5	4	4.5	5
0	1473	460	334	306	265	216	192	178	168	162	157
100	1183	396	323	292	257	209	187	174	165	159	154

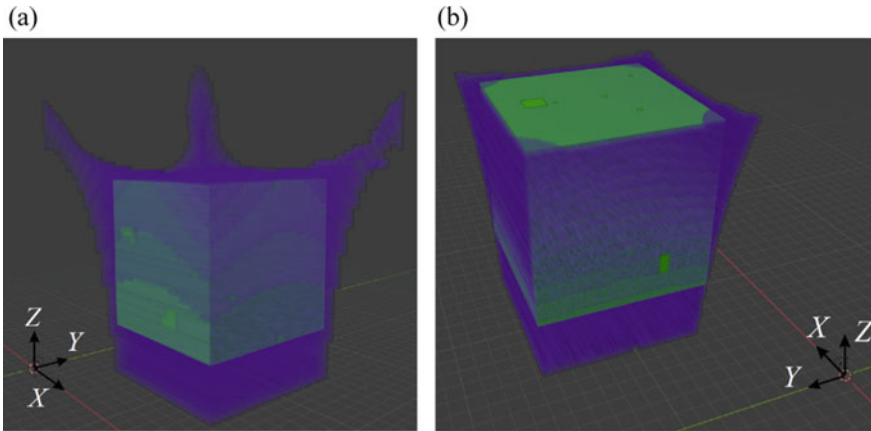


Fig. 6 Workspace for calculated overall dimensions: a) $k = 3$, $h = 100$ mm, $z_{Ai} = 1870$ mm, б) $k = 2,5$, $h = 0$ mm, $z_{Ai} = 2160$ mm

The simulation results were verified checking the entry of the $1000 \times 1000 \times 1000$ mm cube into the workspace of the CDPR with the calculated dimensions (Fig. 6).

5 Conclusion

To conclude, we can state that for the proposed schematic and technical solution of the cable-driven parallel robot, effective numerical methods and algorithms were developed and tested, which allowed determining the minimum geometric parameters of the robot. The results showed that the configuration of the CDPR with the axial movement of the output link allows both increasing the volume of the workspace for the given overall dimensions of the robot, and reducing the overall dimensions for the required workspace during technological operations.

Acknowledgements The reported study was funded by RFBR according to the research projects 18-31-20060.

References

1. Pott, A., Mütterich, H., Kraus, W., Schmidt, V., Miermeister, P., Verl, A.: In: Pott, A., Bruckmann, T. (eds.) *Cable-Driven Parallel Robots*, vol. 12, pp.119–134. Springer, Berlin, Heidelberg (2013)
2. Tavolieri C., Merlet J.P., Ceccarelli, M.: A workspace analysis of a overconstrained cable-based parallel manipulator by using the interval analysis. In: 3rd International Symposium on

- Multibody Systems and Mechatronics, pp. 1–13. School of Engineering, University of San Juan, Argentine (2008)
3. Gaponenko, E.V., Rybak, L.A., Kholoshevskaya, L.R.: Structural analysis and classification of robotic systems with drive mechanisms based on cable elements. *Bull. BSTU Name After V.G. Shukhov*. **9**, 126–136 (2019)
 4. Higuchi, T., Ming, A., Jiang-Yu, J.: Application of multi-dimensional wire crane in construction. In: 5th International Symposium on Robotics in Construction, pp. 661–668. Japan Industrial Robot Association, Japan (1988)
 5. Jeong, J.W., Kim, S.H., Kwak, Y.K., Smith, C.C.: Development of a parallel wire mechanism for measuring position and orientation of a robot end-effector. *Mechatronics* **8**, 845–861 (1998)
 6. Won Jeong, J., Hyun Kim, S., Keun Kwak, Y.: Kinematics and workspace analysis of a parallel wire mechanism for measuring a robot pose. *Mech. Mach. Theory* **34**, 825–841 (1999)
 7. Dovat, L., Lambercy, O., Gassert, R., Maeder, T., Milner, T., Leong, T.C., et al.: A cable-actuated rehabilitation system to train hand function after stroke. *Neural systems and rehabilitation engineering*. *IEEE Trans.* **16**, 582–91 (2008)
 8. Ying, M., Agrawal, S.K.: Design of a cable-driven arm exoskeleton (CAREX) for neural rehabilitation Robotics. *IEEE Trans.* **28**, 922–931 (2012)
 9. Cafolla, D., Russo, M., Carbone, G.: CUBE, a cable-driven device for limb rehabilitation. *J. Bionic. Eng.* **16**(3), 492–502 (2019)
 10. Riechel, A., Bosscher, P., Lipkin, H., EbertUphoff, I.: Cable-driven robots for use in hazardous environments. In: 10th International Topical Meeting Robot Remote System, pp. 310–317. Hazardous Environment, Gainesville (2004)
 11. Roberts, R., Graham, T., Lippitt, T.: On the inverse kinematics, statics, and fault tolerance of cable-suspended robots. *J. Field Robot.* **15**(10), 581–597 (1998)
 12. Merlet, J.P., Daney, D.A.: A portable, modular parallel wire crane for rescue operations. In: IEEE International Conference Robotics and Automation ICRA-2010, pp. 2834–2839. Institute of Electrical and Electronics Engineers Inc., USA (2010)
 13. Gosselin, C.: In: Pott, A., Bruckmann, T. (eds.) *Cable-Driven Parallel Robots*, vol. 12, pp. 3–22. Springer, Berlin, Heidelberg (2013)
 14. Duan, Q.J., Xuechao, D.: Workspace classification and quantification calculations of cable-driven parallel robots. In: *Advances in Mechanical Engineering* 1–9 (2014)
 15. Zhang, N., Shang, W.: Dynamic trajectory planning of a 3-DOF under-constrained cable-driven parallel robot. *Mech. Mach. Theory* **98**, 21–35 (2016)
 16. Du, J., Bao, H., Cui, C., Yang, D.: Dynamic analysis of cable-driven parallel manipulators with time-varying cable lengths. *Finite Elem. Anal. Des.* **48**, 1392–1399 (2012)
 17. Evtushenko, Y., Posypkin, M., Rybak, L., Turkin, A.: Approximating a solution set of nonlinear inequalities. *J. Global Optimization* **7**, 129–145 (2018)
 18. Malyshev, D.I., Posypkin, M.A., Gorchakov, A.Yu., Ignatov, A.D.: Parallel algorithm for approximating the workspace of a robot. *Int. J. Open Informa. Technol.* **7**(1), 1–7 (2019)
 19. Malyshev, D., Posypkin, M., Rybak, L., Usov, A.: Approaches to the determination of the working area of parallel robots and the analysis of their geometric characteristics. *Eng. Trans.* **67**(3), 333–345 (2019)
 20. Rybak, L.A., Gaponenko, E.V., Malyshev, D.I.: Approximation of the workspace of a cable-driven parallel robot with a movable gripper. *Mech. Machine Sci.* **86**, 36–43 (2020)
 21. Posypkin, M., Usov, A.: Implementation and verification of global optimization benchmark problems. *Open Eng.* **7**(1), 470–478 (2017)

Decision Support System for Selecting Designs of Autostereoscopic Displays



Alexander A. Bolshakov and A. V. Klyuchikov

Abstract The architecture of a decision support system for a reasonable choice of the characteristics of autostereoscopic displays is proposed. As a basic set of designs for autostereoscopic displays, the ones developed by the team of authors based on the original patented idea are proposed. It is based on the combined use of reference images using appropriate optical systems. This allows you to significantly reduce the requirements for the speed of information transmission channels, as well as to computers. The main attention is paid to the main modules of the decision support system, which is a hybrid expert system. A description is given of the interconnection in the form of an adjacency matrix between characteristics that affect the quality of the generated output volumetric image. The values of the coefficients of the influence of characteristics on the output image are described. A scheme has been developed for determining user and design characteristics of autostereoscopic displays. An example of determining the design characteristics of a given type of autostereoscopic displays using the proposed decision support system is given. It is advisable to use the obtained results in cyber-physical systems for designing systems using volumetric visualization tools.

Keywords Decision support system · Autostereoscopic displays · Three-dimensional image · Optical system · Design

1 Introduction

Based on physiological abilities, a person receives most of the information based on the visual apparatus. Therefore, there is a legitimate trend towards increasing

A. A. Bolshakov (✉)

Peter the Great St. Petersburg Polytechnic University, Polytechnicheskaya, 29, Saint-Petersburg 195251, Russian Federation
e-mail: abolshakov57@gmail.com

A. V. Klyuchikov

Yuri Gagarin State Technical University of Saratov, 77 Politechnicheskaya street, Saratov 410054, Russian Federation
e-mail: krok9407@mail.ru

attention, attractiveness, and informativeness of graphic information. Moreover, the ability to visualize the image in a three-dimensional format is important. Here it is necessary to highlight the volumetric display [1–10], in which the volumetric image is created by volumetric pixels or voxels. The autostereoscopic way of displaying graphical information implies the ability to observe an object from various angles, which is preferred for the observer [11–22]. Based on this, it can be concluded that technologies aimed at reproducing a three-dimensional image are currently quite promising.

The team of authors based on the combined use of optical and computer processing proposed [23] developed several autostereoscopic displays that differ in design solutions. The model range of volumetric displays proposed based on an analysis of user needs currently includes 5 modifications.

Below is a brief description of them and examples of the 4th and 5th modifications (Figs. 1 and 2):

- 1 A universal mobile nozzle for creating a three-dimensional display without moving parts using multilayer inclined projecting faces.
- 2 A universal mobile nozzle for creating a three-dimensional display without moving parts using parallax barriers and a video sequence from a set of interlaced stereo pairs.
- 3 Volumetric display without moving parts using parallax barriers, interlaced stereo pairs projected on the inclined faces of the pyramid.
- 4 Volumetric circular view display with a rotating working area and an array of projectors (Fig. 1).
- 5 Volumetric display without moving parts using a horizontal stereo pair and an optical system from a lens necklace (Fig. 2).

Fig. 1 Type 4 display

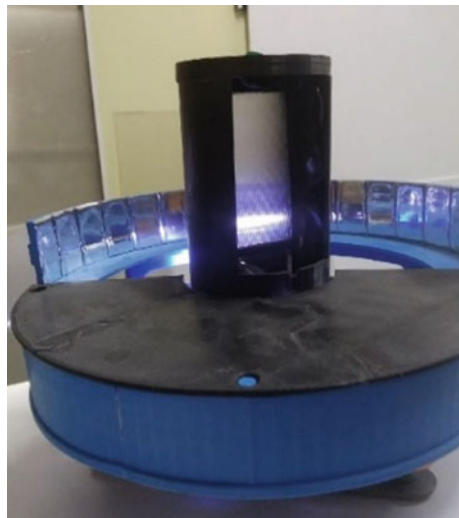


Fig. 2 Type 5 display



In the proposed model range, the above-combined principle of forming a three-dimensional image is used, which is described by the following scheme [24] (Fig. 3).

Under this scheme, a composite image P' is formed from the primary images P by the output device. At the same time, for the correct connection of the composite image elements, synchronization is necessary. Next, we get an image Q , which is synchronized both in time and in space. This image is transmitted to the optical system to form the resulting volumetric image Y . This image is perceived directly by the observer in the form of image Y' . In this case, it is necessary to take into account its psychophysiological features Z .

According to the scheme in Fig. 3, the set of characteristics of two-dimensional images in a certain way affects the final volumetric image. The values of the input and output variables of the system are determined based on these characteristics. It is necessary to take into account certain restrictions that are caused by the use of various technical devices. Moreover, restrictions affect the final volumetric image and also determine the quality of the human perception of the volumetric image.

To solve this so-called direct problem associated with determining the values of Y' from the given characteristics of the input image X and the parameters of the

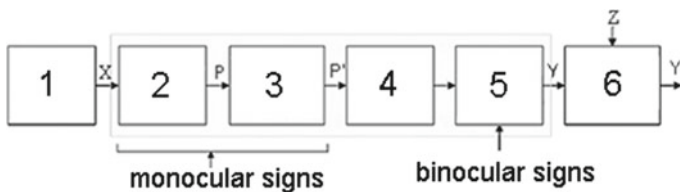


Fig. 3 The sequence of transformations of the original image when forming a three-dimensional image. 1 original image of objects 3D models, 2 Processing formation of primary images, 3 transferring images to input devices, 4 image sync, 5 image transfer to the optical system, 6 formed volumetric image

procedure for generating a three-dimensional image perceived by the observer, we proposed an appropriate mathematical model based on the use of status functions [25].

When designing an autostereoscopic display from the proposed model range and possible others, it is necessary to solve the so-called inverse problem. In this case, according to the required characteristics of the output volumetric image, it is necessary to determine the values of the variables that describe the input image and the process of forming the volumetric image using the devices used that implement the process in Fig. 3. In the general case, inverse problems are known to be incorrectly posed. This is true in our case since the uniqueness and existence of a solution cannot be guaranteed.

This article is devoted to the solution to this urgent scientific and technical problem.

2 Setting Goals and Objectives of the Study

The quality of the output volumetric image and the level of its perception by a person depends on the quality of the input image, the internal structure of the autostereoscopic display, and individual perception. Therefore, it is important to determine the permissible set of values of the input variables of the system and the requirements for the weekend, using the information on the user's preferences for the quality of the final image or scene.

The study aims to synthesize the characteristics of the parameters of autostereoscopic displays from a given set with the required indicators of the quality of formation of the output volumetric image, taking into account the parameters of the input images and the property of devices that implement the process of forming the volumetric image.

To achieve this goal it is required to solve the following tasks:

- 1 To determine the most informative variables, as well as their interrelation in the formation of volumetric images by displays of a given model series. Highlight the variables used in design and user decision-making processes.
- 2 To develop the architecture of a decision support system for the design of autostereoscopic displays of a given model range.
- 3 To test the proposed solutions for the automation of the process of designing autostereoscopic displays.

The result of the research is a software package to support decision-making by the designer in the design of autostereoscopic displays, as well as for users to select and adjust the characteristics of displays of a given model range.

The proposed decision support system (DSS) should solve the direct and inverse problem in the design of autostereoscopic displays. The direct task is to calculate the values of the output characteristics of the generated volumetric image from the given input. The inverse problem is related to determining the requirements for the

values of the parameters of the input image and the design of the display at given values of the output volumetric images.

Next, we consider the results of solving the problem of determining the most informative variables and parameters that determine the quality of a three-dimensional image.

3 Characterization of Variables and Parameters of the Process of Forming Three-Dimensional Images that Determine the Quality of the Three-Dimensional Image

To achieve the required quality of the volumetric image at the output of the volumetric display, it is necessary, as mentioned above, to solve the complex problem of choosing a technical solution, design features, and also the quality of the input image. Therefore, to automate the process of selecting the required characteristics of volumetric displays, it is advisable to use software that can indicate possible solutions to the problem, while leaving the right to choose the final option to the user and designer.

As a tool for solving the problem, it is proposed to use a decision support system to determine the parameters of volumetric displays, in particular, the composition of the optical system and the values of the quantitative characteristics of individual elements, which in the future will be useful for structural engineers, designers when developing or testing the display design, capable of forming an image of a given quality. Also, the obtained values can be used in software image processing. The generated values for the change in the variables of the reference frames that are proposed by the DSS can directly affect the quantitative and qualitative characteristics of the final image, bringing them closer to the desired value.

To create a DSS, a formalized description of the subject area of volumetric displays was carried out, and procedures for determining the output characteristics of visualization processes were developed. Also, databases of parameters for displays of characteristics of primary images, visualization parameters were formed, and relationships were determined (Table 1).

Quality of output three-dimensional image depends on the degree of technical realization of variable characteristics of an input image by output devices, the possible range of variable variation, as well as value set by a user when setting values of input parameters of image quality.

The optical characteristics of the visual apparatus of a person and the assessment of his level of perception do not affect the technical characteristics of the system and image. However, alterations performed in reverse have a significant effect on optical characteristics (the so-called inverse problem, which is usually the number of incorrect ones).

Table 1 The adjacency matrix of the relationships between the parameters affecting the quality of the generated volumetric image

	Relativity of the sizes	Two-dimensional permission	The parallax of the movement	Rotation of an object	Convergence	Binocular disparity	Volume Image Area Size	...	Three-dimensional permission	Color depth	Updating frequency
Relativity of the sizes	0	1	0	0	0	0	1	...	1	0	0
Two-dimensional permission	0	0	0	0	0	0	0	...	0	0	0
The parallax of the movement	1	1	0	1	0	0	1	...	1	0	1
Rotation of an object	1	1	0	0	0	0	1	...	1	0	1
Shadows	0	1	0	0	0	0	1	...	1	1	0
Prospects	1	1	0	0	0	0	1	...	1	0	0
Occlusion	1	1	1	1	0	0	1	...	1	0	0
Heterogeneity of a form	0	1	0	0	0	0	0	...	1	0	0
Texture gradient	0	1	0	0	0	0	0	...	1	1	0
Convergence	1	0	1	1	0	0	1	...	0	0	1
Binocular disparity	1	0	0	0	0	0	0	...	0	0	1
Volume Image Area Size	0	0	0	0	0	0	0	...	0	0	0
Viewing angle	0	0	0	0	0	0	1	...	0	0	1
Three-dimensional permission	0	1	0	0	0	0	1	...	0	0	0

(continued)

Table 1 (continued)

	Relativity of the sizes	Two-dimensional permission	The parallax of the movement	Rotation of an object	Convergence	Binocular disparity	Volume Image Area Size	...	Three-dimensional permission	Color depth	Updating frequency
Lineature	0	1	0	0	0	0	1	...	0	0	0
Brightness	0	0	0	0	0	0	0	...	0	0	0
Contrast	0	0	0	0	0	0	0	...	0	1	0
Color depth	0	0	0	0	0	0	0	...	0	0	0
Updating frequency	0	0	0	0	0	0	0	...	0	0	0

The perception of the object is also influenced by psychological factors and physiological features of the person. Therefore, another aspect of the development of a three-dimensional imaging technique is the need to test it on different groups of recipients.

Several experiments are proving this aspect, including:

- 1 theory of Gregory's visual sentence [26];
- 2 phenomenon of binocular rivalry [27];
- 3 perception of the essence of the scene according to Castellano and Hendersen;
- 4 cognitive, figurative-structured visual perception (COSV).

In addition to the described, there are specific and currently not identified by medicine psychological factors. Several diseases that affect the human brain and visual apparatus should also be considered:

- 1 astigmatism;
- 2 refraction;
- 3 visual agnosia.

Thus, it is advisable to use a relatively large sample in testing, taking into account the various states of the subjects, both physical and psychological.

Besides, the estimated characteristics of the identified parameters are introduced based on the processing of expert estimates (Table 2).

To use volumetric images in various subject areas in cyber-physical systems [28–32] when constructing a mathematical description of the perception of a volumetric image, it is advisable to use the so-called status functions [25]. The above characteristics are used in the construction of DSS, the architecture of which is described below.

4 Development of the Architecture of a Decision Support System for Building Volumetric Displays

The development of autostereoscopic displays using a combined method and certain technical solutions to achieve preset values of the perceived quality in a volumetric manner is an important scientific and technical task. Therefore, it is advisable to automate the design of a promising lineup of autostereoscopic displays. To do this, it is necessary to develop and apply the required software.

The proposed DSM is necessary for determining the values of the parameters of autostereoscopic displays, as well as the process of forming three-dimensional images based on primary images. This information is very useful for designers in the development of design processes, hardware, and software for the production of autostereoscopic displays with the required values of the quality indicators of the perception of output volumetric images.

Functionally, DSM should be based on a formalized description of the subject area of autostereoscopic displays. Also, procedures should be developed for calculating

Table 2 Weighting factors of the characteristics of the output image

Parameters	Expert						Average factor
	1	2	...	8	9	10	
Relativity of the sizes	0.07	0.02	...	0.02	0.04	0.02	0.04
Two-dimensional permission	0.08	0.02	...	0.07	0.06	0.04	0.05
Parallax of the movement	0.06	0.04	...	0.03	0.06	0.03	0.05
Rotation of an object	0.06	0.04	...	0.04	0.05	0.13	0.05
Shadows	0.04	0.04	...	0.07	0.08	0.07	0.07
Perspective (forward, reverse, panoramic, spherical, air, perceptual)	0.12	0.08	...	0.10	0.1	0.09	0.1
Overlapping Objects (Occlusion)	0.05	0.1	...	0.01	0.01	0.02	0.03
Heterogeneity of a form	0.02	0.08	...	0.06	0.09	0.04	0.06
Texture gradient	0.02	0.05	...	0.08	0.06	0.07	0.07
Convergence	0.04	0.08	...	0.05	0.07	0.08	0.06
Binocular disparity	0.09	0.09	...	0.1	0.1	0.10	0.1
Volume Image Area Size	0.04	0.09	...	0.07	0.07	0.08	0.07
Viewing angle	0.08	0.06	...	0.06	0.04	0.05	0.05
Three-dimensional permission	0.07	0.06	...	0.03	0.02	0.07	0.04
Lineature	0.02	0.02	...	0.05	0.06	0.01	0.04
Brightness	0.02	0.04	...	0.05	0.02	0.01	0.03
Contrast	0.02	0.03	...	0.06	0.02	0.02	0.03
Color depth	0.06	0.04	...	0.04	0.04	0.06	0.04
Workspace Refresh Rate	0.04	0.02	...	0.01	0.01	0.01	0.02
Total	1	1	...	1	1	1	1

the values of the output characteristics during visualization (direct task). Database of characteristics of autostereoscopic displays, parameters of primary images, as well as volumetric visualization is required. Further, modules are required for selecting parameters of autostereoscopic displays to provide the specified quality of volumetric visualization (inverse problem).

In connection with the foregoing, DSM architecture is proposed (see Fig. 4), which includes the necessary components. Among them, information support, which contains the following resources:

- Database (DB) of parameters of autostereoscopic displays;
- Knowledge Base (KB) of the subject area of autostereoscopic displays;
- DB of status functions;
- KB for decision support in the field of autostereoscopic displays;
- DB of visualization parameters;
- DB of characteristics of primary images.

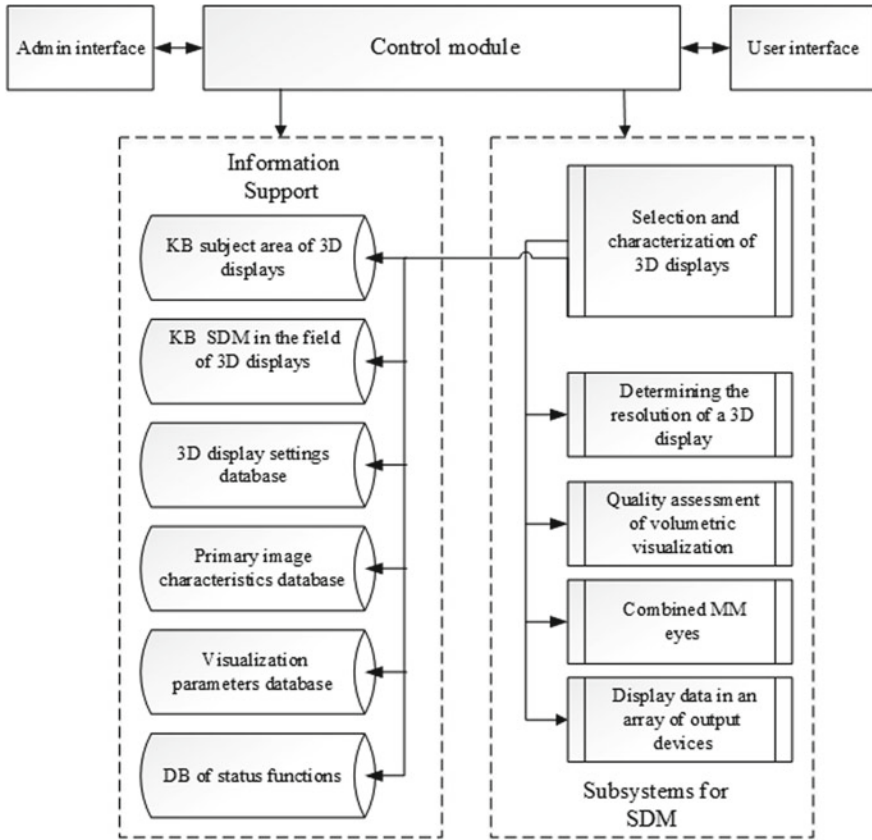


Fig. 4 Architecture DSM for the development of autostereoscopic

- The decision support subsystem for input image and configuration selection includes the following modules):
- type selection from the range of autostereoscopic displays;
- determination of input image parameter values (contrast, brightness, etc.) for autostereoscopic displays of a given model range;
- determination of parameter values that describe the dynamics of images (frame change, resizing, moving, rotating,) for autostereoscopic displays of a given model range;
- determination of the parameter values of the optical and hardware components of autostereoscopic displays;
- output of the resulting information in the form of tables.

The functioning of DSS is carried out under the control of the control module, which organizes the necessary interaction of the modules to support decision-making and information support, as well as two groups of users. These include the administrator and operator, who is the user, or a testing knowledge engineer.

The administrator manages the differentiation of access levels for various categories of users, can enter changes in the source code, algorithm, as well as change and adjust data in the database and database, based on confirmed feedback from the user and experimental data from the engineer.

The user in a step-by-step mode carries out the design process, based on the answers to the questions that determine the most important criteria for the volumetric display and the input image, as a result, the display type, the main parameters of the primary images are determined, and the engineer, in turn, based on the received data, can conduct mathematical modeling of the trace beam or visualize the process of building the image on pre-prepared software, to assess the quality of the resulting three-dimensional image and evaluate the effectiveness of the selection of characteristics performed by DSS. During the operation of the system, the modules (subprograms) are called up to determine the appropriate type of display, to calculate the values of static (brightness, contrast, etc.) characteristics, characteristics that describe the dynamics (rotation, movement, change of frames) on the input image, and also the module for calculating variable values hardware and optical component for displays of the proposed type.

It is proposed to use cloud storage, the level of access to which is also differentiated for different groups, to store the database, database, user survey results, and also the values obtained from the system.

The advantage of such a system is the multidimensionality of the direction of the received data, i.e. access to the results is available to all user groups, which simultaneously allows you to:

- 1 changing the input image by the user;
- 2 creating a display design by a design engineer;
- 3 verification of the effectiveness of the proposed system utilizing mathematical modeling by an engineer-developer;
- 4 editing algorithms and methods for presenting information by a programmer;
- 5 monitoring the functioning of the system by the administrator.

5 Implementation of a Decision Support System for the Design of Autostereoscopic Displays

When implementing the proposed DSS of design, a scheme was developed to identify user and design preferences (requirements). This scheme is implemented in the corresponding module written in the C# programming language. Using this procedure allows you to clearly define the requirements of the designer, user when designing autostereoscopic displays or setting parameters from a given model range of volumetric displays.

To solve the inverse design problem associated with achieving the required quality of the output image based on the selection of the characteristics of the input images, the visualization process, the knowledge of experts is used. Their formalization is carried out based on the production rules “IF THAT”, which is implemented using the Prolog programming language of artificial intelligence.

The following are fragments of the procedure for identifying requirements for the characteristics of autostereoscopic displays using the appropriate module and screenshot of the result.

When functioning DSS first you need to determine the list of questions about the quality of the output image. Based on them, direct or inverse problems are further solved. Questions for increasing information content are presented in a visual form.

So, for example, the second question to the user is about the desired viewing angle from 0 to 360°. Displays of the 1st, 2nd type of the model range are limited by a viewing angle of up to 180° of one projecting plane. A type 3 display can be realized with a viewing angle of 90, 270, or 360°, when selecting one of 3 or 4 projection planes, respectively. Displays of the 4th and 5th type can have any of the possible ranges, however, with an increase in the viewing angle, the overall dimensions of the product significantly increase.

The last question allows the user to determine the diagonal of the screen for building a 3D image with the desired dimensions. You can enter the length, depth, and width of the image in centimeters. To determine the diagonal of the screen, the length and width of the image are sufficient. The diagonal is calculated and then converted to inches and rounded to the nearest whole number to approximate the actual size of the displays. Further, the 11th question also allows you to determine the area of the three-dimensional image, which also introduces some restrictions on the use of a particular type of display. Due to the nature of the optical system, the 4th type display does not allow the image to be formed over 1000 cm³, and the 5th type display is limited to 8000 cm³.

Depending on the list of displays available for playback from the model range, DSS displays information of a recommending nature for the user and developer (Fig. 6) per the operation algorithm (Fig. 5).

The following characteristics are defined for the user:

- brightness level;
- contrast level;
- minimum fps value;
- image resolution.

For a design engineer, a set of characteristics is given below:

- number of lenses;
- LPI value;
- diagonal display;
- number of mirrors.

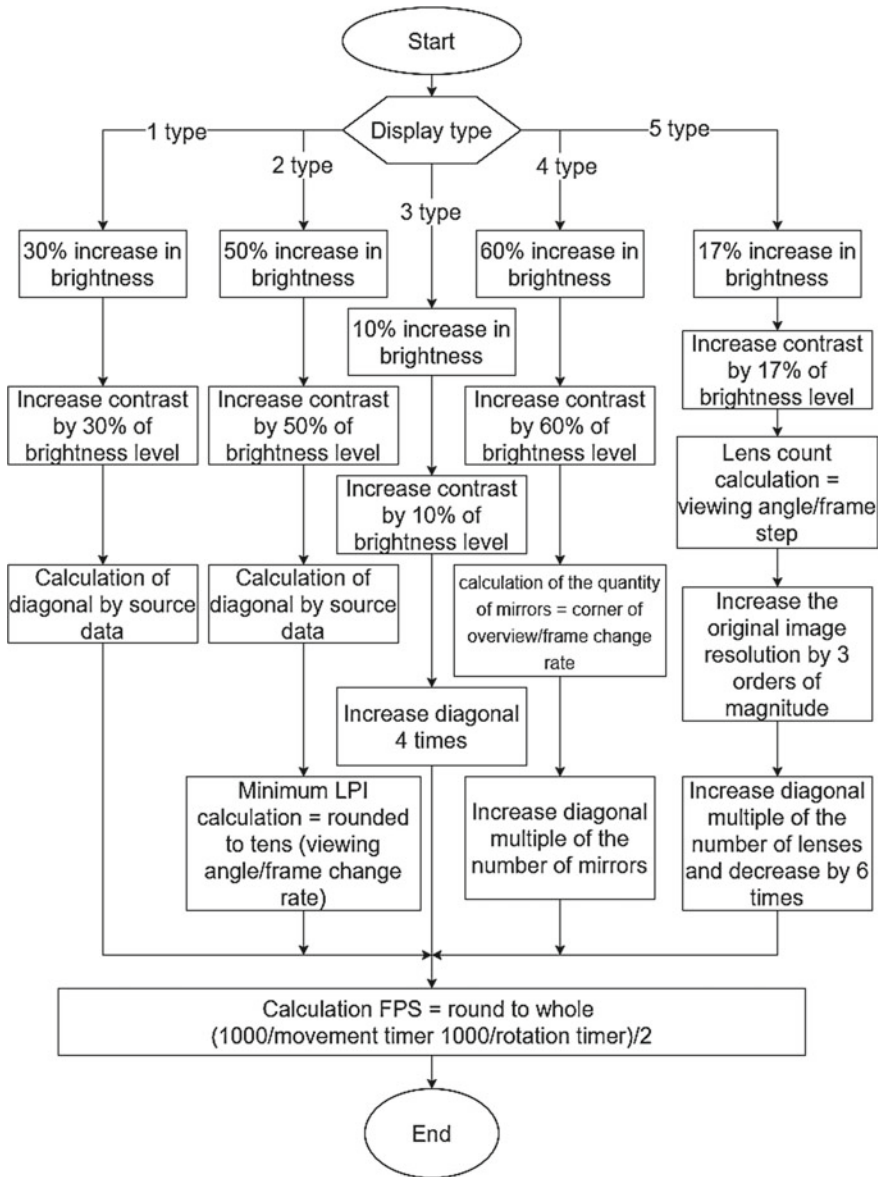


Fig. 5 Algorithm for determining the characteristics of autostereoscopic displays based on user and design requirements

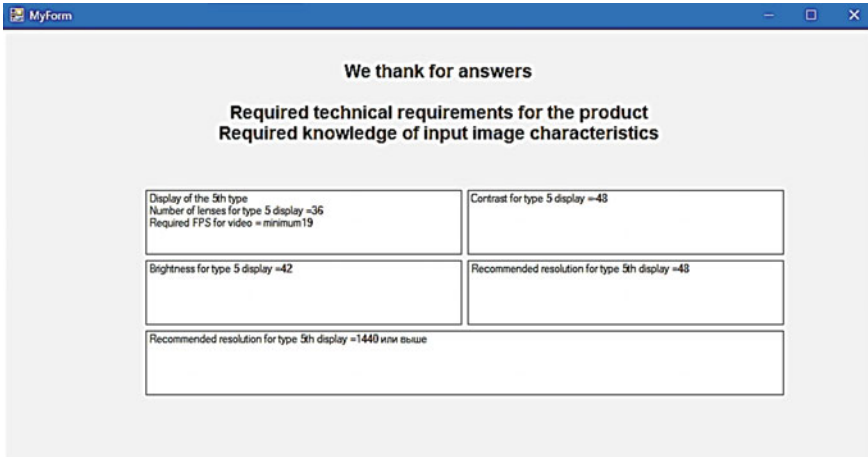


Fig. 6 An example of the result of the work of DSS

6 Conclusion

The article discusses the development of promising auto-stereoscopic displays, allowing them to form three-dimensional images visible from different sides without additional devices (glasses, etc.). The characteristic of the lineup of autostereoscopic displays proposed by the authors is developed based on the patent [23]. To solve decision support, the architecture of the corresponding system is proposed, which allows you to automate the solution of the direct and inverse problems that arise during the design of volumetric displays and their use. A description of the developed algorithm for determining the values of the characteristics of the designed autostereoscopic display from the proposed model range is given. An example of testing an algorithm implemented in the C# programming language is presented. To solve direct and inverse problems in the proposed hybrid expert decision support system, formalization of expert knowledge using the Prolog artificial intelligence programming language is proposed. It is advisable to use the obtained results in cyber-physical systems for designing systems using volumetric visualization tools.

Acknowledgements This work was financially supported by the Innovation Promotion Fund in the framework of Contract No. 1995GS1/26878 of 07/05/2017.

In preparing the article, we used the results obtained during the implementation of a project supported by the RFBR grant No. 20-010-00465.

References

1. Barry, G.B., Adam, J.S.: *Volumetric Three-dimensional Display Systems*, p. 330. Wiley, NY (2013)
2. Fattal, D., Peng, P., Tran, T.V.S., Fiorentino, M., Brug, J., Beausoleil, R.G.: A multi-directional backlight for a wide-angle, glasses-free three-dimensional display. *Nature*, **3**(495), 348–351 (2013)
3. UA Patent No 218.016.2E37 of 17 February 2018 MPK G02B 27/22, H04N 13/00 (2018)
4. Smalley, D., Poon, T.-C., Gao, Y., Kvalve, J., Qaderi K.: Volumetric displays: turning 3-D inside-out. *Optics Photon. News*, **6** (2018).
5. Smalley, D.E., et al.: A photophoretic-trap volumetric display. *Nature*, **553**(486) (2018).
6. Kumagai, K., Hasegawa, S., Hayasaki, Y.: Volumetric bubble display. *Optica* **4**, 298–302 (2017)
7. Samigulova, E.K.: Study-ing an aerial perspective in art school. Sections: Moscow art academy and fine arts (2016)
8. Ochiai, Y., Kumagai, K., Hoshi, T., Rekimoto, J., Hasegawa, S., Hayasaki, Y., Lights, F.: Femtoseconds: aerial and volumetric graphics rendered by focused femtosecond laser combined with computational holographic fields. ArXiv Preprint: Submitted to ACM Transactions on Graphics via Acceptance with major revision in ACM SIGGRAPH (2015)
9. Hyeonseung, Y., KyeoReh, L., Jongchan, P., YongKeun, P.: Ultrahigh-definition dynamic 3D holographic display by active control of volume speckle fields. *Nature Photon.* **11**, 186–192 (2017)
10. Wang, L., Kruk, S., Tang, X., Li, T., Kravchenko, I., Neshev, D.N., Kivshar, Y.S.: Greyscale transparent metasurface holograms. *Optica* **3**(12) (2016)
11. Jones, A., Unger, J., Nagano, K., et al.: An Automultiscopic Projector Array for Interactive Digital Humans. ACM Press, SIGGRAPH (2015)
12. Hua, H., Javidi, B.: A 3D integral imaging optical see-through head-mounted display. *Optics Express*. **22**(11) (2014). <https://doi.org/10.1364/OE.22.013484>
13. Nagano, K., Jones, A. et al.: An Autostereoscopic Projector Array Optimized for 3D Facial Display. In: SIGGRAPH 2013 Emerging Technologies (2013)
14. Lens, S. H., Sung-min, J., Byung-joo, L., Hyung-ki, H., Hyun-ho, S.: 3D displays based on a LTPS 2.4" VGA LCD panel attached with lenticular. Mobile First published: 05 July 2012 (2012). <https://doi.org/10.1889/1.3069639>
15. Nagano, K., Jones, A., Unger, J. et al.: An Automultiscopic Projector Array for Interactive Digital Humans. SIGGRAPH ACM Press (2015)
16. Ito, K., Kikuchi, H., Sakurai H., Kobayashi, I., Yasunaga, H., Mori, H., Tokuyama, K., Ishikawa, H., Hayasaka, K.: 360-degree autostereoscopic display. ACM SIGGRAPH Emerging Technical (2010)
17. Graham, J., Woodgate, J. H.: Late-news poster: high efficiency reconfigurable 2D/3D autostereoscopic display. (2012). <https://doi.org/10.1889/1.1832295>
18. Jones, A., Unger, J., Nagano, K., Busch, J., Yu, X., Peng, H.-Y., Alexander O., Bolas, M., Debevec, P.: An Automultiscopic Projector Array for Interactive Digital Humans. Siggraph 2015. ACM Press (2015)
19. Hideyuki, S., Masami, Y., Takafumi, K., Michio, O., Miho, K.: Autostereoscopic Display Based on Enhanced Integral Photography Using Overlaid Multiple Projectors (2012). <https://doi.org/10.1889/1.3256853>
20. Barnum, P.C., Narasimhan, S.G., Kanade, T.: A Multi-Layered Display with Water Drops. ACM Transactions on Graphics (SIGGRAPH) (2010)
21. Tunable, L., Crystal, L., Yung-Yuan, K., Yan-Pean H., Kai-Xian, Yang., Paul, C.-P., Chi-Chung, T., Chi-Neng, M.: An auto-stereoscopic 3D display using. (2012). <https://doi.org/10.1889/1.3256482>
22. Robert, B., John, S.: Directional backlight lightguide considerations for full resolution autostereoscopic 3D displays (2012). <https://doi.org/10.1889/1.3500410>

23. Bol'shakov, A.A., Nikonov, A.V. Volumetric display and method for forming three-dimensional images (19) RU (11) 2526901 (13) C1 Application: 2013103443/28, 01/25/2013; Published: 08/27/2014; Bull. Number 21 (2013)
24. Bolshakov, A.A., Grepechuk, Y.N., Klyuchikov, A.V., Sgibnev, A.A.: A Model of the Optical System of the Interdisp Display In: International Conference on Actual Problems of Electron Devices Engineering, APEDE. art. no. 8542354, pp. 63–70. (2018). <https://doi.org/10.1109/APEDE.2018.8542354>. ISBN: 978–153864332–7
25. Veshneva, I.V., Chistyakova, T.B., Bolshakov, A.A.: The status functions method for processing and interpretation of the measurement data of interactions in the educational environment. SPIIRAS Proc 6(49), 144–166 (2016). <https://doi.org/10.15622/sp.49.8>. ISSN:20789181
26. Getnet, E.: Factors Affecting Instructional Leaders Perception Towards Educational Media Utilization in Classroom. Teaching Anchor Academic Publishing (2015). ISBN-10: 3954894386 ISBN-13: 978–3954894383
27. Blake, R., O'Shea, R.P.: Binocular rivalry. Reference Module in Neuroscience and Biobehavioral Psychology (2017).
28. Orlov, S., Girin, R.: Intelligent technologies in the diagnostics using object's visual Images. In: Cyber-Physical Systems: Industry 4.0 Challenges. Studies in Systems, Decision and Control, vol. 259. Studies in Systems, Decision and Control, pp. 301–312. Springer Nature Switzerland AG 2020. (2020). <https://doi.org/10.1007/978-3-030-32579-4>. ISSN 2198–4182 ISSN 2198–4190 (electronic) ISBN 978–3–030–32578–7 ISBN 978–3–030–32579–4 (eBook)
29. Suyatinov, S.I.: Conceptual approach to building a digital twin of the production system. IN Cyber-Physical Systems: Industry 4.0 Challenges. Studies in Systems, Decision and Control, vol. 259. Studies in Systems, Decision and Control, pp. 279–290. Springer Nature Switzerland AG (2020). <https://doi.org/10.1007/978-3-030-32579-4>. ISSN 2198–4182 ISSN 2198–4190 (electronic) ISBN 978–3–030–32578–7 ISBN 978–3–030–32579–4 (eBook)
30. Stepanov, M., Musatov, V., Egorov, I., Pchelintzeva, P., Stepanov, A.: Cyber-physical control system of hardware-software complex of anthropomorphous robot: architecture and models. In: Cyber-Physical Systems: Industry 4.0 Challenges. Studies in Systems, Decision and Control. vol. 259. Studies in Systems, Decision and Control, Springer Nature Switzerland AG 2020. pp. 13–24 (2020). <https://doi.org/10.1007/978-3-030-32579-4>. ISSN 2198–4182 ISSN 2198–4190 (electronic) ISBN 978–3–030–32578–7 ISBN 978–3–030–32579–4 (eBook)
31. Moshev, E., Meshalkin, V., Romashkin, M.: Development of models and algorithms for intellectual support of life cycle of chemical production equipment. Cyber-Physical Systems: Industry 4.0 Challenges. Studies in Systems, Decision and Control, vol. 259. Studies in Systems, Decision and Control, pp. 153–156. Springer Nature Switzerland AG (2020). <https://doi.org/10.1007/978-3-030-32579-4>. ISSN 2198–4182 ISSN 2198–4190 (electronic) ISBN 978–3–030–32578–7 ISBN 978–3–030–32579–4 (eBook)
32. Meshalkin, V., Puchkov, A., Dli, M., Lobaneva, Y.: Deep Neural networks application in models with complex technological objects. Cyber-physical Systems: industry 4.0 Challenges. In: Studies in Systems, Decision and Control, vol. 259. Studies in Systems, Decision and Control, pp. 291–300. Springer Nature Switzerland AG (2020). <https://doi.org/10.1007/978-3-030-32579-4>. ISSN 2198–4182 ISSN 2198–4190 (electronic) ISBN 978–3–030–32578–7 ISBN 978–3–030–32579–4 (eBook)

The Rotor Speed Controlling Possibilities of a Promising Wind-Driven Power Plant Using Several Variable Elements of Its Geometry



Vladimir Kostyukov, Mikhail Medvedev, Dmitry Pavlenko, Andrey Mayevsky, and Nikolay Poluyanovich

Abstract The stabilization of the rotor speed of a promising vertically axial wind-driven power plant is considered. It is proposed to use the aerodynamic method of stabilizing the rotor rotation angular speed by controlling the positions of two variable structural elements of the installation in the question relative to its stator. The controller synthesis technique by the rotor rotation angular speed is considered. A controller feature is the presence of two control channels with one state variable. Based on the second-order control error equation, the desired control law of the angular rotor speed is obtained. The synthesized control system was simulated with various input data. It is shown that the constructed controller is able to effectively counter the influence of wind disturbances in a wide range of deviations of the current speed from the desired frequency for a given target value.

Keywords Vortex type wind-driven power plant · Aerodynamic torque · Regulation error equation · Reduced disturbance observers · Rotation frequency stabilization

1 Introduction

Currently, there is a large group of facilities, stationary-based and mobile, including robotic systems, in need of auxiliary autonomous energy sources.

V. Kostyukov (✉) · M. Medvedev · D. Pavlenko · A. Mayevsky · N. Poluyanovich
Southern Federal University, Shevchenko, Taganrog 347922, Russia
e-mail: wkost-einheit@yandex.ru

M. Medvedev
e-mail: medvmihal@gmail.com

D. Pavlenko
e-mail: dmitrij.pawlencko@yandex.ru

A. Mayevsky
e-mail: maevskiy_andrey@mail.ru

N. Poluyanovich
e-mail: nik1-58@mail.ru

For example, many international companies are developing and implementing alternative energy sources on marine surface platforms to reduce their total fuel consumption is carried out by [1, 2].

One of the approaches that allow economically tangible (more than 10%) to reduce the consumption of conventional fuel is the use of a complex power plant (CPP), consisting of a wind-driven power plant (WP) and a solar power plant.

The key problems, in this case, are: (1) to choose a WP type, suitable for installation on a stationary/mobile platform as a CPP element; (2) the development of the CPP electromechanical control system, allowing to optimize its operation according to the criterion of maximum power generated under severe restrictions imposed by the safety requirements and reliability of operation of all carrier systems [3].

Complex power plants can be used as source elements that are part of a distributed electric network, providing a controlled transfer of energy from such sources to consumers—load elements. This transmission occurs under conditions of these elements perturbations, various external influences on the network, and, as a result, various modes of its operation, including emergency ones. For stability and robustness of the control system of such distributed power system, strict restrictions must be imposed not only on the upper level of this control, which is responsible for the correct assessment of the characteristic electrical quantities of the system and control of the key state variables of the sources, receivers and transmission lines themselves [4]. Big demands must be made on the local control systems of source elements. The last requirements are reduced, firstly, to coordinated work with the upper level of control and, secondly, to sufficiently accurate stabilization of the characteristic output values of these sources in accordance with the specified current operating mode of the entire system.

This chapter discusses the problem of vertically axial WP rotor angular speed stabilization due to the regulation of the aerodynamic properties of this plant.

Such regulation in the general case can be carried out using variable geometry elements (VGE) of WP construction [5–7].

A variable geometry element of the horizontally axial WP construction, as a rule, is the total angle of their blades installation. A striking example here is a 600 kW guided modernized research turbine (CART2) operated by the National Renewable Energy Laboratory (NREL), pc. Colorado. The rotor speed controller of this WP takes into account both turbulent wind disturbances and significant parametric uncertainties of the rotor motion model with a maximum value of 20% [5]. These uncertainties are caused, first of all, by the blades considerable flexibility of modern WP, as well as by the mass variability and inertia characteristics of the rotor, generator, and the corresponding error in their estimation, which increase with increasing diameter of the rotor. The paper [6] analyzes a much simpler controller that controls the specified CART2 plant for a number of modes with almost the same quality of work.

However, VGE using for vertically axial WP is currently very limited. Since, for example, the use of a wind wheel for this WP type with an adjustable angle of rotation relative to a certain axis will lead to more complex and much less predictable changes than in the case of a change in the overall pitch of the propeller of a horizontally axial WP. The reason for this is that the theory of the screw is much more studied

than the aerodynamics of the corresponding rotors used for vertically axial plants. Nevertheless, we know publications where a controlled change in the aerodynamic properties of the vertically axial vortex type WP is considered by using a VGE located on the stator part of the installation [7].

For the vertically axial WP, aerodynamic control of rotor speed at the present stage of drive mechanisms development, as well as theoretical and computational dynamics of continuous media, is added to the existing electrical control. At the same time, controlling the aerodynamic properties of such WP can significantly reduce the requirements for a number of system elements for electric control of the generator frequency and amplitude, such as a rectifier, battery, inverter [8]. This becomes possible due to a significant reduction in the changes range in the speed and amplitude of the output signal of the WP generator through such aerodynamic regulation.

The development of precision mechanics, including actuator drives of WP elements and the technology for manufacturing precision parts together with an increase in the efficiency and aerodynamic analysis depth of the processes occurring during WP operation, can eventually make the method of angular speed aerodynamic regulation the main for some WP types, or, at least by back up the existing stabilization method. The consequence of this development is the appearance in the future of two WP classes.

Installations can be attributed to the first, the design of which will allow more efficient control of the angular speed using VGE. For example, for WP with high rated power, appropriate expensive equipment for electrical control is required. However, if there are sufficiently fast-acting VGE for some of them, it will become possible to completely eliminate a number of elements of the specified equipment.

The second class will include WP, the design of which will not allow the introduction of effective control using VGE. This may be due to the complexity of aerodynamic regulation by such VGE, which can lead, especially for low power plants, to the inefficiency of aerodynamic regulation according to the price/quality criterion.

For a number of WP with an increased demand for output characteristics and operation reliability, both stabilization methods can be applied.

In the present work, the vertically axial vortex type WP with one VGE is taken as a basis ([3, 7, 8]). The necessity of introducing an additional variable geometry element for the possibility of the rotor angular speed controlling in a wider dynamic range of wind loads is substantiated, and the corresponding modernized plant design is proposed. Next, the controller of this control system is considered.

2 The Design and Operation Principle of the Original WP

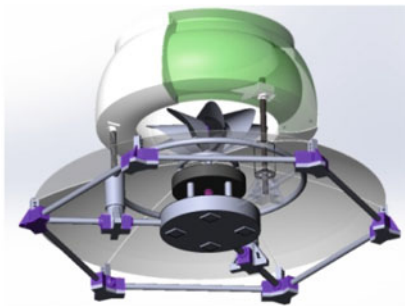
The wind-driven power plant, which is taken as the basis [3, 7], contains a moving part - a rotor with blades, as well as a doubly connected part of the structure - a stator. The latter includes a bell, which is a vertical channel with the possibility of

air passing inside it - a bell, and a lower guide structure made in the form of a cone-shaped rotation figure. The stator as a whole is axisymmetric with the rotor part of the structure, and the rotor is slightly buried in the socket (see Fig. 1a).

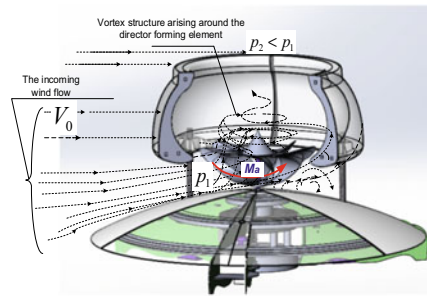
The operation of a vortex type wind-driven power plant is based on the principle of useful aerodynamic interference between the static and rotor parts of the plant [7, 9–13], as well as the use of special-shaped rotor blades that effectively perceive both horizontal and vertical ascending flows [7, 13]. The vortex resulting from the rotor rotation is concentrated inside the diffuser and over its upper part. The formed areas of reduced pressure cause the additional traction effect, which increases the rotor rotation moment. The vortex structure arising above the rotor additionally energizes the rotor, being in dynamic equilibrium with it (see Fig. 1b).

A possible application of considered WP [7] as a part of the complex power plant small-displacement boats are shown in Fig. 1c., and as a part of the recharge station for unmanned aerial vehicles, in Fig. 1d.

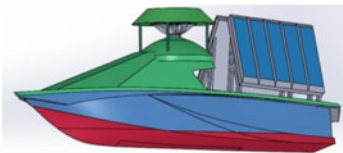
In works [3, 7], the aerodynamic advantages of such a plant are shown, both in terms of the generated power and in terms of minimizing the noise level, in comparison with analogs [13–19]. The design of this plant was obtained as a result



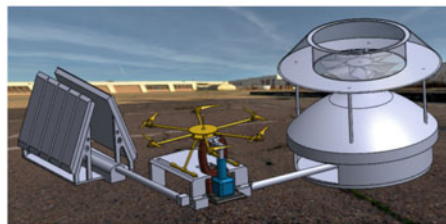
a) a three-dimensional model of the developed vortex type WP



b) the principle of WP (considered in [7]) operation



c) the using of the developed WP in the complex power plants for autonomous supply of boats



d) the possibility of using the developed WP as a part of the recharge station for unmanned aerial vehicles

Fig. 1 General view, the principle of the operation and some areas of the application of the developed WP

of aerodynamic optimization according to the criterion of maximum torque on the WP rotor shaft.

3 A Need for Modernization of the Aerodynamic Control System of WP Rotor Angular Speed

Consider the problem of the rotor rotational speed controlling of a vertically axial vortex type WP, described above (see Fig. 1a).

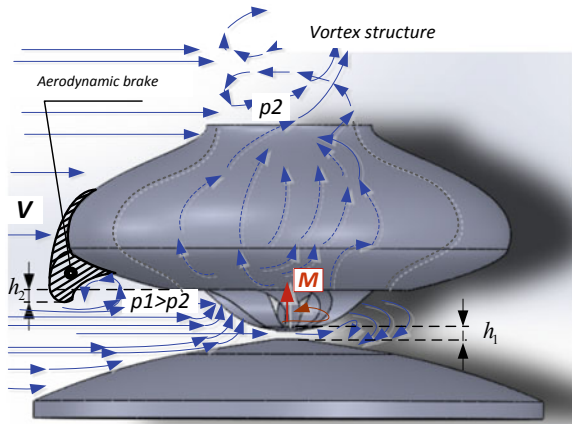
The position of the lower movable part of the stator, characterized by the h magnitude, can vary vertically relative to the rotor (see Fig. 1b). Therefore, this part of the stator is a variable element of WP geometry [3, 7]. The deviation of the position of this element leads to a change in the aerodynamic properties of the plant. By adjusting the value h depending on the wind load, which is within certain limits, it is possible to stabilize the rotor angular speed ω , if the dependence of the rotor aerodynamic torque on the wind speed, angular speed, and on h [7] is known.

However, ω stabilization in the entire range of wind loads using the value h considered in [7] is not possible, since the dynamic range of the change in the rotor aerodynamic torque due to the change in value h is not sufficient to achieve this goal.

In this chapter, we consider a system for controlling the rotor angular speed ω using two variable geometry elements of the plant design: the lower guide structure and the aerodynamic brake flap. The combined use of these two VGEs makes it possible to increase the dynamic range in terms of the rotor aerodynamic torque so that it becomes possible to adjust ω for any average value of the wind load and arbitrary amplitude of the wind disturbance in a certain range of rates of change of this disturbance over time.

Figure 2 shows the principle of vortex type WP operation with an additional element on the construction—an aerodynamic brake flap (ABF). Such flap regulates

Fig. 2 To an explanation of the operation principle of a modernized WP



the effective cross-section of the incident wind flow interaction with the rotor in the range of values from the maximum—when the flap does not overlap the incident flow at all, to almost zero—when the flow is almost completely blocked, as a result of which the rotor rotation is slowed down. At the same time, it also generates significant turbulence, which complicates the aerodynamic analysis and its accuracy. To compensate for the inaccuracy of determining the moment on the rotor shaft at various ABF positions relative to the stator bell, a torque perturbation observer on the rotor shaft can be introduced into the developed control system. Thus, the proposed plant contains two VGEs, which are characterized by values h_1 and h_2 .

4 Synthesis of a Controller of a Modernized Vortex Type WP with Two VGEs

Let's perform a synthesis of the proposed WP controller. For such synthesis, it is necessary, first of all, to have a dependence $\omega_0 = f_0(V_0)$ of the steady-state value of the angular speed ω_0 on the unperturbed uniform wind flow speed V_0 .

In the general case, the target value of the rotor rotation speed ω_g differs from ω_0 that corresponding to the current average wind speed V_0 without taking into account possible wind disturbances, therefore, ACS with the VGE must not only fend off these disturbances but also fend off the difference $V_{0g} - V_0$, where $V_{0g} = f_0^{-1}(\omega_g)$, f_0^{-1} —function inverse to f_0 . Thus, it is necessary to fend off the difference $\Delta V(t) = V(t) - V_{0g}$ between the full free wind speed $V(t)$ and the desired value V_{0g} ; we will proceed from the following exponential law of change in the speed of the incoming airflow during gusts of wind:

$$V(t) = V^*(t) = V_0 + A_V [1 - \exp(\alpha_V t)] \quad (1)$$

where A_V —wind amplitude, α_V —coefficient of the exponential growth of a wind gust. This law is in good agreement with the case when the wind speed is tuned from one steady-state value to another without noticeable oscillations.

Now it is necessary to determine to what extent the difference $\Delta V(t)$ can vary in order to control the angular speed with a given quality.

We establish the required quality of the regulation process with the given parameters of the transient process $\Delta T'_p$ and degree of overshoot $\eta_\omega = \Delta\omega_{\max}/\omega_g$ relative to the permissible $\Delta\omega_g$ deviation from the nominal target value ω_g . For example, let $\Delta\omega_g = 0,05\omega_g$, $\Delta T'_p = 15$, $\eta_\omega = 50\%$. Next, find out which range of the difference $V(t) - V_{0g}$ the control system considered in [7] is capable of stabilizing the angular speed ω with specified quality parameters. The analysis shows that such stabilization by means of VGE of the lower guide structure of the considered vortex type WP is possible at $|V(t) - V_{0g}|_{\max}/V_{0g} \leq \delta_{1V \max} = 0,3$. Here the case is admissible when $V(t) < V_{0g}$, if the nominal dependence $V_{0g} = f_0^{-1}(\omega_g)$ is obtained for the normal intermediate position of the lower guide structure. Its deviation up from the indicated

normal position, i.e. a decrease in the parameter h_1 (see Figs. 1b and 2) leads to an increase in the rotor torque, and a downward deviation leads to its decrease [3, 7].

The introduction of an additional VGE—ABF leads, as mentioned above, to the expansion of the upper limit of the allowable range in speed $V(t)$, therefore, in the end, the dynamic range of the flow rate regulation for the developed ACS is:

$$-\delta_{V1\max} V_{0g} \leq V(t) - V_{0g} \leq V_{kr} \quad (2)$$

where V_{kr} —the maximum allowable wind speed for the integrity of WP construction and its functioning in normal mode; this speed, as a rule, is obviously greater than the upper limit $V_{n,\max}$ of installation operating speed range.

Let the equation of WP controlled object is given, which is an equation of the rotational motion of its rotor with an angular speed ω :

$$J \frac{d\omega}{dt} = M(V, \omega, h_1, h_2) + M_c(\omega) \quad (3)$$

V —the wind speed, changes of which in this problem represent external disturbance; h_1, h_2 —two VGEs control values determining their current position relative to the bell stator; J —the rotor inertia reduced moment; $M(V, \omega, h_1, h_2)$ and $M_c(\omega)$ —useful aerodynamic torque on the rotor and load torque, determined by the following empirical dependencies [7]:

$$M(V, \omega, h_1, h_2) = V \left[a_1 + a_2 (V - \tilde{V}) \right] f_u(h) \quad (4)$$

$$M_c(\omega) = -b\omega \quad (5)$$

$$f_u(h_1, h_2) = f_{u1}(h_1) f_{u2}(h_2), \quad (6)$$

$$f_{u1}(h_1) = \begin{cases} a_3 h^{-1} + a_4, & \text{at } h \in [h_{1\inf}, h_{1\sup}]; \\ h_{1\inf}, & \text{at } h < h_{1\inf}; \\ h_{1\sup}, & \text{at } h > h_{1\sup}. \end{cases} \quad (7)$$

The additional aerodynamic analysis showed that the function of the influence of the second VGE on the rotor torque can be approximated exponentially:

$$f_{u2}(h_2) = \{[\exp(1 - h_2/h_{2kr}) - 1]/(\exp(1) - 1), \text{ } npu \text{ } h_2 \leq h_{2kr} \quad (8)$$

where $a_1, a_2, a_3, a_4, b, \tilde{V}$ —constant coefficients, $h_{1\inf}, h_{1\sup}$ —lower and upper boundary limit values of the control quantity h_1 , determined by WP design features, h_{2kr} —the upper limit value of h_2 . The cases of the control variables values exit h_1, h_2 from the admissible ranges and the corresponding cutoffs considered in

(6) and (7) are necessary only for the correct programming of the corresponding computational problem infinite differences.

For numerical aerodynamic calculations, the Ansys Fluent software package was used; in this case, methods for analyzing unsteady flows in rotating domains based on the approximation of moving grids implemented in this software product were used. For the correctness of the results obtained, two turbulence models were used: $k - \varepsilon$ - and RNG $k - \varepsilon$, the use of which in each particular calculation depended on the Reynolds number.

The indicated methods are widely used in studies devoted to the aerodynamics of modern vertically axial WP [15, 16, 19–22]. In particular, in [19], the authors analyzed the twist effect of Dorier type WP turbine blades, and in [21], the possibilities of increasing the aerodynamic quality of the same type blade by using hollows of a special shape on its profile were considered. Article [22] is devoted to the study and modeling of the process of starting a vertically axial WP.

Note that, based on the equation of state (3), the above static dependence $\omega_0 = f_0(V_0)$ can be found, if Eq. (3) is solved sequentially for a number of values of the speed of the unperturbed flow V_0 and, in the limit, the corresponding steady-state values ω_0 are obtained. Figure 3a shows the time dependencies of the rotor angular speeds for wind speeds $V_0 = 2, 5, 10$ m/s, tending to the indicated steady-state values; Fig. 3b shows the corresponding dependence $\omega_0 = f_0(V_0)$.

The actuators of two VGEs will be approximated by first-order aperiodic links [23], i.e. using equations:

$$q_{1,2} \frac{dh_{1,2}(t)}{dt} + r_{1,2}h(t) = f_{1,2}^*(t) \tag{9}$$

where $q_{1,2}$ and $r_{1,2}$ —constant coefficients, $f_{1,2}^*(t) = q_{1,2}\dot{h}_{1,2}^*(t) + r_{1,2}h_{1,2}^*(t)$ and here the first lower indices correspond to the actuator of the first VGE, and the second to the second VGE. The solution of Eqs. (9) in the general case has the form [24]:

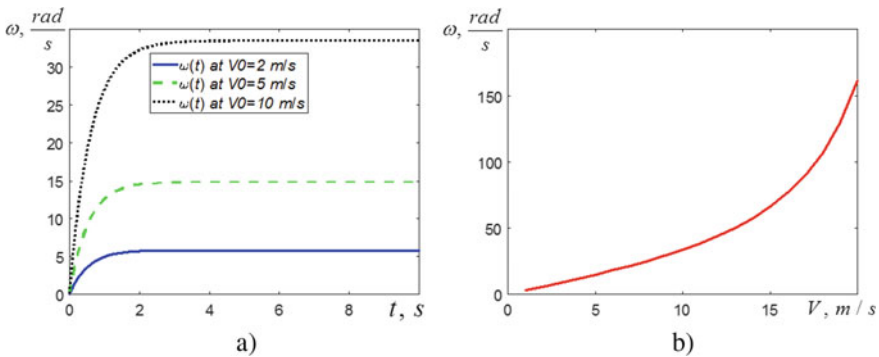


Fig. 3 To the definition of static dependence $\omega_0 = f_0(V_0)$

$$\begin{aligned}
h_{1,2}(t) &= (1/q_{1,2})e^{-(r_{1,2}/q_{1,2})t} \left[\int_0^t e^{(r_{1,2}/q_{1,2})t} f_{1,2}^*(t) dt + q_{1,2} h_{1,2;0} \right] \\
&= h_{1,2}^*(t) + [h_{1,2;0} - h_{1,2}^*(0)] \exp[-(r_{1,2}/q_{1,2})t], \quad (10)
\end{aligned}$$

where $h_{1,2;0} = h_{1,2}(0)$ —set initial values of control actions $h_{1,2}$.

In the synthesis of the desired controller, we will proceed from the following error equation [23]:

$$\frac{d^2\varepsilon}{dt^2} + A \frac{d\varepsilon}{dt} + B\varepsilon = 0 \quad (11)$$

where $\varepsilon = \omega_g - \omega$ —regulation error; ω_g —angular speed target value ω ; A , B —some constant coefficients that determine the nature of the transition process in terms of angular frequency, in particular, the setting time of this process and the degree of its overshoot.

A feature of the synthesized control system is the presence of two control channels with one state variable to be regulated. In addition, these channels are distinguished as follows. The use of the lower guiding structure for regulation, as shown by aerodynamic analysis [3, 7], does not introduce significant turbulent fluctuations in the flow in the rotor vicinity, however, the use of the aerodynamic brake introduces significant turbulence, which can reduce the quality of control due to the impossibility of accurately accounting for them. Therefore, the ABF use is justified only in high deviation modes $V(t) - V_{0g}$, when the dynamic range of torque changes on the rotor shaft due to the displacement from the normal position of the first VGE, the lower guide structure, is not enough to solve the problem. Therefore, the simultaneous use of two VGEs at once on the same regulation cycle is impractical. Based on (2), we introduce the following rule of switching between modes of using two VGEs:

if $|V(t) - V_{0g}| \leq \delta_{V1 \max} V_{0g}$, then only VGE 1 is used;

if $V(t) - V_{0g} > \delta_{V1 \max} V_{0g}$, then only VGE 2 is used;

if $V(t) - V_{0g} < -\delta_{V1 \max} V_{0g}$, then aerodynamic regulation is not possible with the help of VGE data, and ω stabilization is carried out only by electric means.

In this case, based on the equation of state (3) and the error Eq. (11), the following expressions can be obtained:

$$\frac{1}{J} \left(M'_V \dot{V} + (M'_\omega + M'_{c,\omega}) \dot{\omega} + M'_{h_{1,2}} \dot{h}_{1,2} \right) + \frac{A}{J} (M + M_c) + B\omega = f(t), \quad (12)$$

where $f(t) = \ddot{\omega}_g + A\dot{\omega}_g + B\omega_g$, M'_v , M'_ω , —corresponding partial derivatives of the moment $M(V, \omega, h_1, h_2)$ by V , ω ; $M'_{c\omega} = dM_c/d\omega$; $M'_{h_{1,2}}$ —partial derivatives with respect to the first and second control variables:

$$M'_{h_1} = -V a_3 \left[a_1 + a_2 (V - \tilde{V}) \omega \right] h_1^{-2} f_{u2}(h_2) \quad (13)$$

$$M'_{h_2} = -(V/h_{2kr}) \left[a_1 + a_2 (V - \tilde{V}) \omega \right] f_{u1}(h_1) \exp(-h_2/h_{2kr}) \quad (14)$$

If we express the $\dot{h}_{1,2}$ derivatives from (12) and add Eq. (3), then the desired system of equations with respect to the state variable ω and two control variables h_1, h_2 takes the form:

$$\begin{cases} \frac{d\omega}{dt} = [M(V, \omega, h_1, h_2) + M_c(\omega)]/J; \\ \frac{dh_1^*}{dt} = \begin{cases} \frac{1}{M'_{h_1}} \{BJ\varepsilon - F(V, \dot{V}, \omega, h_1^*, h_2^*)\}, & \text{if } G \equiv |V(t) - V_{0g}| \leq \delta_{V1} \max V_{0g}, \\ 0, & \text{otherwise}; \end{cases} \\ \frac{dh_2^*}{dt} = \begin{cases} 0, & \text{if } G, \\ \frac{1}{M'_{h_2}} \{BJ\varepsilon - F(V, \dot{V}, \omega, h_1^*, h_2^*)\}, & \text{otherwise.} \end{cases} \end{cases} \quad (15)$$

Here h_1^*, h_2^* characterize the values of control quantities without taking into account the inertia of their actuators; and function $F(V, \dot{V}, \omega, h^*)$ defined by the expression:

$$\begin{aligned} F(V, \dot{V}, \omega, h_1^*, h_1^*) &= [a_1 + a_2\omega(2V - \tilde{V})] f_u(h_1^*, h_1^*) \dot{V} + \\ &+ \frac{1}{J} [a_2V(V - \tilde{V}) f_u(h_1^*, h_1^*) + AJ - b] (M + M_c) \end{aligned} \quad (16)$$

If we take into account the inertia of VGE triggering according to (10), then we obtain the following estimates for the desired control quantities:

$$h_{1,2}(t) = \begin{cases} \tilde{h}_{1,2}(t), & \text{at } \tilde{h}_{1,2}(t) \in [h_{1,2;\text{inf}}; h_{1,2;\text{sup}}], \\ h_{1,2;\text{inf}}, & \text{at } \tilde{h}_{1,2}(t) < h_{1,2;\text{inf}}; \\ h_{1,2;\text{sup}}, & \text{otherwise.} \end{cases} \quad (17)$$

where $h_{2;\text{inf}} = 0$; $h_{2;\text{sup}} = h_{2;kr}$, values $\tilde{h}_{1,2}(t)$ defined by the expressions:

$$\tilde{h}_{1,2}(t) \equiv h_{1,2}^*(t) + [h_{1,2;0} - h_{1,2}^*(0)] \exp[-r_{1,2}t/q_{1,2}] \quad (18)$$

To compensate for the inaccuracy of the moment determining on the rotor shaft at various ABF positions relative to the stator bell, we introduce the corresponding observer of the rotor torque perturbation into the developed control system. Let us describe the synthesis process of a reduced observer according to a well-known technique [23, 25, 26].

The adjusted equation of WP rotor state taking into account the unaccounted disturbances on the moment

$$J \frac{d\omega}{dt} = M(V, \omega, h_1, h_2) + M_c(\omega) + \Delta M(\delta M, \Delta\omega, \Delta V, \Delta A) \quad (19)$$

where δM —the structural representation error of the moment dependence on the right-hand side of (3) on all variables and parameters (the error of the form of the function M); $\Delta\omega$, ΔV —scalar errors in estimating the angular speed and the module of the flow speed vector at the entrance to WP sensors; ΔA —vector value of the error of estimation of all parameters included in the above dependencies (3)–(9).

Let's introduce the error of perturbation estimation ΔM :

$$\varepsilon_M = \Delta M - \Delta \tilde{M} \quad (20)$$

where the disturbance assessment $\Delta \tilde{M}$ of ΔM images in the form:

$$\Delta \tilde{M} = S(\omega) + z \quad (21)$$

Here $S(\omega)$ —not yet defined smooth function of a variable ω , and Z —the desired function of time, which will go into the general system of equations and will determine the properties and work of the synthesized observer.

Require that the estimation error ε_M satisfy a first-order differential equation:

$$\dot{\varepsilon}_M + a_M \varepsilon_M = 0, \quad (22)$$

where a_M —positive constant characterizing the speed of the observer.

We will first consider a constant perturbation ΔM . It is easy to see that if you impose a restriction on a function $S(\omega)$:

$$dS(\omega)/d\omega = a_M J \quad (23)$$

then from Eqs. (20)–(23) immediately follows the equation of the observer in the approximation of constant perturbation ΔM :

$$\dot{z} = -a_M [M(V, \omega, h_1, h_2) + M_c(\omega) + a_M J \omega + z] \quad (24)$$

According to the Eqs. (21) и (23), disturbance assessment $\Delta \tilde{M}$ can be represented as:

$$\Delta \tilde{M}(\omega, z) = a_M J \omega + z \quad (25)$$

Then the controller, including the torque perturbation observer constructed here, is characterized by the following system of equations:

$$\begin{cases} \dot{\omega} = [M(V, \omega, h_1, h_2) + M_c(\omega) + \Delta M]/J; \\ \dot{h}_1^* = \begin{cases} \frac{1}{M'_{h_1}} \{BJ\varepsilon - \tilde{F}(V, \dot{V}, \omega, h_1^*, h_2^*)\}, & \text{if } G \equiv |V(t) - V_{0g}| \leq \delta_{V1} \max V_{0g}, \\ 0, & \text{otherwise;} \end{cases} \\ \dot{h}_2^* = \begin{cases} 0, & \text{if } G, \\ \frac{1}{M'_{h_2}} \{BJ\varepsilon - \tilde{F}(V, \dot{V}, \omega, h_1^*, h_2^*)\}, & \text{otherwise,} \end{cases} \\ \dot{z} = -a_M[M(V, \omega, h_1, h_2) + M_c(\omega) + a_M J \omega + z], \end{cases} \quad (26)$$

where

$$\begin{aligned} \tilde{F}(V, \dot{V}, \omega, h_1^*, h_2^*) &= F(V, \dot{V}, \omega, h_1^*, h_2^*) \\ &+ \frac{1}{J} [a_2 V(V - \tilde{V}) f_u(h_1^*, h_1^*) + AJ - b] \Delta \tilde{M}. \end{aligned} \quad (27)$$

The last three equations of the system (26) indicate that the law of the control variables change $h_{1,2}^*$ includes an estimate of the moment from (25).

Then the resulting control system using two VGEs will include Eq. (19), the observer Eq. (24), and the last two equations in (15).

The functional diagram of the stabilization system of the rotor angular speed is shown in Fig. 4.

The master device generates the target law of the rotation angular speed $\omega_g(t)$ changing taking into account the current and voltage at the load and the target setting values of the operator about the required nature of the power supply of this load. Further, based on ω_g an output ω' of the rotor angular speed ω meter (encoder), an error signal is generated $\varepsilon = \omega_g - \omega' \approx \omega_g - \omega$, which arrives at the controller. The latter also receives a signal z from the rotor moment perturbations observer; this observer works according to the last equation in (26). The controller generates control signals $h_1^*(t), h_2^*(t)$ for two WP variable geometry elements under consideration in accordance with the second and third equations of the system (26). These signals are fed to the corresponding actuators, which change the position of two VGEs, thereby fending off changes in wind speed in order to stabilize the angular speed ω .

5 Modeling the Operation of the Synthesized Controller

Consider the results of modeling the synthesized controller of the rotor rotation angular speed.

Figure 5a shows the time dependence of the angular speed at a constant component of the wind speed $V_0 = 5$ m/s, target rated rotor frequency $\omega_g = 3\pi$ rad/s and various amplitudes A_v of this disturbance: $A_v = 1$ m/s, 2 m/s, 2,5 m/s, 3,35 m/s, for

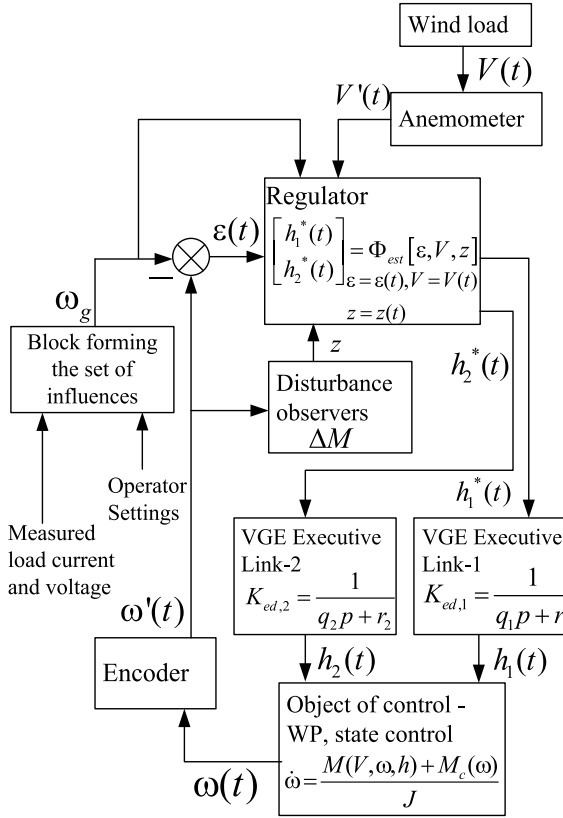


Fig. 4 The functional diagram of the stabilization system of the rotor angular speed

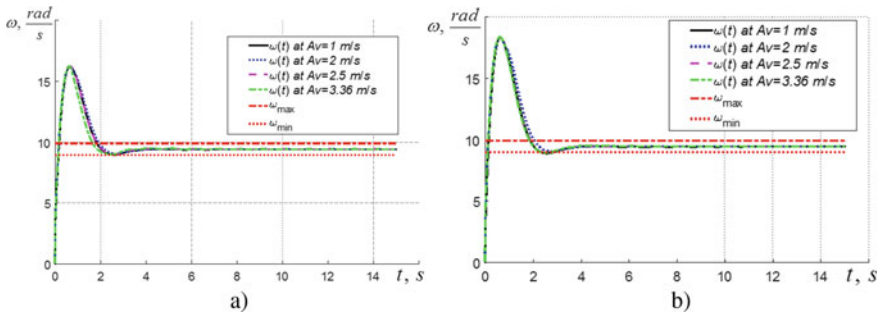


Fig. 5 Dependences of the angular speed on time at $V_0 = 5 \text{ m/s}$, $\omega_g = 3\pi \text{ rad/s}^\infty$ and various amplitudes of perturbations A_v : a) excluding torque perturbation observer; b) given this observer in the approximation $\Delta M = \text{const} = 1 \text{ Nm}$ at $a_H = 3 \text{ s}$

a controller with a system of Eqs. (15) without taking into account the observer of perturbations of the torque.

Other parameter values:

$a_1 = 0.0716$, $a_2 = 1.704 \cdot 10^{-4}$, $a_3 = 0.202$, $a_4 = 0.692$, $b = 0.0019$, $\alpha_V = -0, 1 s^{-1}$, $h_{2kr} = 0.3 m$; actuator transient convergence parameters IG-1,2: $p_{1,2}/q_{1,2} = 5 s^{-1}$. Figures 6a and 7a show the time dependences of control

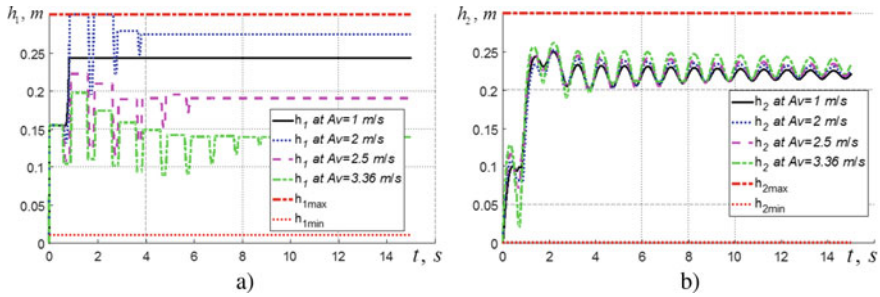
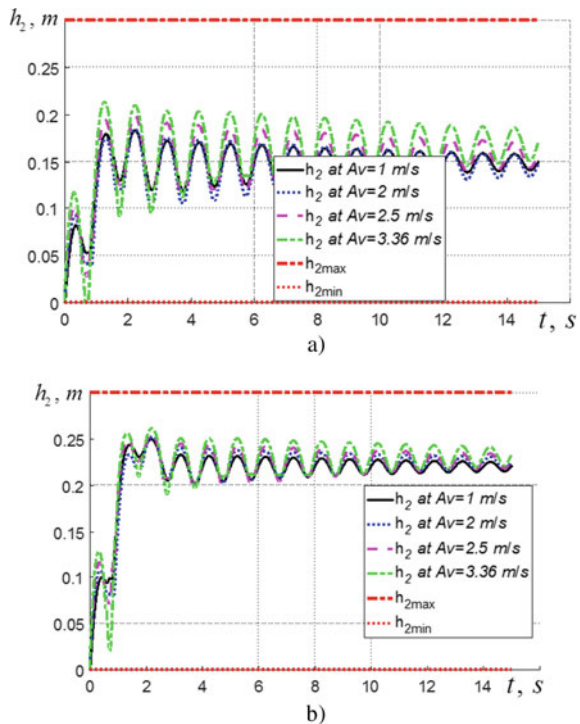


Fig. 6 Dependencies of the control quantity h_1 VGE-1 on time at $V_0 = 5 m/s$, $\omega_g = 3\pi rad/s$ and various amplitudes A_v perturbations: **a** excluding torque perturbation observer; **b** given this observer in the approximation $\Delta M = const = 1Nm$ at $a_H = 3s$

Fig. 7 Dependencies of the control quantity h_2 VGE -2 on time at $V_0 = 5 m/s$, $\omega_g = 3\pi rad/s$ and various amplitudes A_v perturbations excluding torque perturbation observer; **b** given this observer in the approximation $\Delta M = const = 1Nm$ at $a_H = 3s$



variables $h_1(t)$ for VGE-1 (b) and $h_2(t)$ for VGE -2 (c) corresponding to the above values of the amplitudes A_v perturbations.

Figure 5a shows that the angular speed enters the allowable corridor for less than 15 s with an overshoot of less than 50% for all considered A_v values, which corresponds to the initial data on the quality of regulation $\Delta\omega_g = 0, 05\omega_g, \Delta T'_p = 15s, \eta_\omega = 50\%$

From the dependences shown in Figs. 6a, 7a, it follows that, at the initial moment or within about a tenth of a second, the control system transfers the first IEG in a step $h_2 = 0.152$ m, after which this IEG ceases to be used by the control system, since condition G introduced in (15), after such a jump, it ceases to be fulfilled. Further control is carried out using the second IEG—aerodynamic brake flap.

Figures 5b, 6b, 7b shows similar relationships to Figs. 5a, 6a, 7a, only for a controller with a system of Eqs. (26), which includes an observer in the constant perturbation approximation, in this simulation with the value $\Delta M = const = 1Nm$; observer speed set equal $a_H = 3s$.

A comparison of the graphs shown in Figs. 5a, 6a, 7a with the corresponding graphs presented in Figs. 5b, 6b, 7b shows that the introduction of an additional constant unmeasured disturbance to the right side of the equation of the state $\Delta M = 1Nm$ can be effectively counterbalanced using a reduced observer with preservation of the transition time process and a slight increase in the degree of overshoot—by 10%. Note that with the considered dynamics of the wind load changes and the value of the specified test unmeasured increment of the moment, the timing diagram of the controlled value of the first IEG remains unchanged when the disturbance is introduced.

$\delta_{V1\max} = 0, 3$. Thus, the designed controller is capable of effectively counteracting the influence of wind disturbances in a wide range of the current speed deviations from desired for a given frequency target value, and arbitrary excesses of the current wind speed over the desired speed V_{0g} are permissible since the aerodynamic brake flap is able to vary the torque on the shaft up to a complete stop rotor. On the other hand, the lower limit of the wind speed acceptable for the considered control system is given by the first condition in (2), which is determined by the dynamic range of regulation according to the first VGE: $-\delta_{V1\max} V_{0g} \leq V(t) - V_{0g}$, in this case $\delta_{V1\max} = 0, 3$.

Therefore, the proposed speed controller of WP rotor, changing the position of WP construction control elements depending on the measured speed of the wind disturbance, can increase efficiency and reliability of the plant work as well as the quality of electric power generated by it.

Such aerodynamic speed control at the current stage of development of precision mechanics, actuators of WP components actuators, and manufacturing technology of precision parts can work in conjunction with conventional methods of electrical stabilization of the generator frequency. Such joint work significantly reduces the quality requirements of the corresponding electrical equipment by reducing the dynamic range of the generator frequency control by preliminary aerodynamic speed control of the wind-driven power plant rotor speed.

6 Conclusion

In the chapter, the controller that stabilizes the rotor rotational speed of a vortex type wind-driven power plant using two variable elements of its geometry was synthesized. Based on the reduced observers, an additional loop for estimating rotor torque disturbances in the approximation of the constancy of these disturbances was introduced.

This controller is able to maintain the value of the rotor angular speed in a sufficiently small permissible corridor (not more than 5%) with wind disturbances limited from above only by structural strength requirements imposed on the installation elements. This is achieved by introducing an additional control element—the aerodynamic brake flap.

The application of the proposed method for WP rotor speed controlling will significantly increase the control system adaptability of its output characteristics; significantly expand the dynamic range of torque control on the wind-driven power plant rotor, as well as increase the robustness of these characteristics to the external wind and internal structural parametric disturbances.

The use of vertically axial vortex type WP with the rotor speed aerodynamic control discussed in this chapter as part of complex power plants can significantly increase the efficiency of the latter.

References

1. Innovative Technologies & Solutions for Sustainable Shipping. Eco Marine Power. <https://www.ecomarinepower.com/en/about-us> Accessed 26 Oct 2018
2. Ocius Technology Limited (Australia). <https://ocius.com.au/> Accessed 26 Oct 2018
3. Kostyukov, V.A., Medvedev, M.Yu., Poluyanovich, N.K., Dubygo, M.N.: Features of electromechanical control of a complex power plant with a vortex-type wind-conversion device. In: *Cyber-Physical Systems: Advances in Design & Modelling*, pp. 221–219. Springer Nature Switzerland AG 2020 (2019)
4. Omorov, T.T., Takyrbashev, B.K.: Identification of the state of the distribution electric network in automation systems for metering and energy management. *Mechatronics, Automation, Control* **17**(10), 651–656 (2016)
5. Wright, A.D., Balas, M.J.: Design of State-Space-Based Control Algorithms for Wind Turbine Speed Regulation. *J. Sol. Energy Eng.* **125**(4), 386–395 (2003)
6. Ravikumar, N.V.A., Saraswathi, G.: Robust controller design for speed regulation of a flexible wind turbine. *Endorsed Transactions on Energy Web* **6**, 1–10 (2019)
7. Kostjukov, V.A., Medvedev, M.Y., Poluyanovich, N.K., Dubyago, M.N., Bulanovich, D.I., Pavlenko, D.D.: Control law synthesis of the wind-driven power-plant with variable geometry. *EAI Endorsed Transactions on Energy Web*, 125–130 (2019)
8. Kostjukov, V.A., Shevchenko, V.A.: Features of the complex power unit for mobile robotic. In: *ICCM-2018*, pp. 86–92 (2018)
9. Baniotopoulos, C.C., Borri, C., Stathopoulos, T.: *Environmental Wind Engineering and Design of Wind Energy Structures*, 358 p. CISM International Centre for Mechanical Sciences, Springer. ISBN:3709109523 (2011)
10. Pinto, T.: *Electricity Markets with Growing Levels of Renewable Generation: Structure, Operation, Agent-Based Modeling and New Projects*, 640p. Springer, Heidelberg (2018)

11. Gasch, R.: *Wind Power Plants Fundamentals, Design, Construction and Operation*, Second Edition, 567 p. Springer ISBN:3642229379, 978-3-642-22937-4 (2012)
12. Hau, E.: *Wind Turbines—2013 Fundamentals, Technologies, Application, Economics*, third, translated edition, 879 p. Springer. ISBN: 978-3-642-27151-9 (2013)
13. Haskin, L.Ya.: Aerodynamics of a wind wheel with a fairing and an output device. In: *Scientific notes TsAGI*, vol. 24, No. 4 (1993)
14. Wróżyński, R., Sojka, M., Pyszny, K.: The application of GIS and 3D graphic software to visual impact assessment of wind turbines. *Renewable Energy*, **96**, Part A, 625–635 (2016)
15. Li, Q., Murata, J., Endo, M., Maeda, T., Kamada, Y.: Experimental and numerical investigation of the effect of turbulent inflow on a Horizontal Axis Wind Turbine (part II: Wake characteristics). *Energy*, **113**, 1304–1315 (2016)
16. Heo, Y.G., Choi, N.J., Choi, K.H., Ji, H.S., Kim, K.C.: CFD study on aerodynamic power output of a 110 kW building augmented wind turbine. *Energy and Buildings* **129**, 162–173 (2016)
17. Mikhnenkov, L.V.: Planetary type wind power plant. *Scientific Bulletin of MSTU*, No. 125 (2008)
18. Liu, W.: Design and kinetic analysis of wind turbine blade-hub-tower coupled system. *Renewable Energy* **94**, 547–557 (2016)
19. Gorelov, D.N.: Energy characteristics of the Darier rotor (review), pp. 325–333. Publishing House of the Siberian Branch of the Russian Academy of Sciences (2010)
20. Biswas, A., Gupta, R.: Unsteady aerodynamics of a twist bladed H-Darrieus rotor in low Reynolds number flow. *J. Renew Sustain Energy*, **6** (2014). <https://doi.org/10.1063/1.4878995>
21. Sobhani, E., Ghaffari, M., Maghrebi, M.J.: Numerical investigation of dimple effects on darrieus vertical axis wind tur-bine. *Energy* **133**, 231–241 (2017)
22. Beri, H., Yao, Y.: Numerical simulation of unsteady flow to show self-starting of vertical axis wind turbine using flu-ent. *J. Appl. Sci.* **11**, 962–970 (2011)
23. Pshikhopov, V.K., Medvedev, M.Y.: Assessment and management in complex dynamic systems, 295 p. M.: Fizmat-lit. ISSN 978-5-9221-1176 (2009)
24. Matveev, N.M.: *Integration methods of ordinary differential equations*, 555 p. M: Publishing house Higher School (1967)
25. Pshikhopov, V.Kh., Medvedev, M.Yu., Gaiduk, A.R., Neudorf, R.A., Belyaev, V.E., Fedorenko, R.V., Kostyukov, V.A., Krukhmalev, V.A.: Positional-trajectory control system for a robotic aeronautic plate-form: control algorithms. *Mechatronics, Automation and Control*, no. **7**, 13–20 (2013)
26. Pshikhopov, V.Kh., Medvedev, M.Yu.: Assessment algorithms in the control system of an autonomous robotic air-ship. *Izvestiya SFU. Tech. Sc.* **2**(139), 200–207 (2013)

Repair Program Formation on the Basis of the Technical Condition Classifiers



Ruslan Voropai, Ivan Shcherbatov, Vladimir Agibalov, and Mikhail Belov

Abstract A classifier that provides a technical diagnosis of complex equipment is proposed. Predicting the remaining life of the equipment is implemented to determine the time of diagnosis and inclusion of equipment in the repair program. The procedure for forming a repair program based on the forecast value of the remaining resource and financial losses associated with equipment failure is described.

Keywords Diagnostics · Technical condition · Forecasting · Remaining life · Repair

1 Introduction

The main purpose of technical diagnostics is to identify and evaluate the deviation of the current state of the unit from the normal on the basis of measuring information [1]. This information can come from sensors [2], as well as be qualitative (described linguistically in natural language) and relate to expert knowledge [3]. The results of technical diagnostics are used for predicting the technical condition in order to plan measures to maintain the equipment in the proper technical condition [4].

In the present study, it is accepted that the object state is determined by the vector of $S = (s_1, \dots, s_m)$, where m —the total number of diagnostic parameters (a set of parameters of the diagnosed object sufficient to make a diagnosis with a given accuracy). Deviation of the identified state from the normal one (accepted as such

R. Voropai

Technische Universität Ilmenau, 29 Ehrenbergstraße, 98693 Ilmenau, Germany

e-mail: ruslan.voropai@tu-ilmenau.de

I. Shcherbatov (✉) · V. Agibalov · M. Belov

Moscow Power Engineering Institute, 14 Krasnokazarmennaya, Moscow 111250, Russia

e-mail: ShcherbatovIA@mpei.ru

V. Agibalov

e-mail: vovaagibalovv@gmail.com

M. Belov

e-mail: mikle49@yandex.ru

taking into account a number of assumptions) characterizes the technical state of the diagnosed object (specific equipment unit) at the current moment [5].

The magnitude of the deviation (often referred to as a simple error) can be not only a characteristic of the type of emergency situation, such as a failure but also the basis for finding the reasons that led to it (based on expert information accumulated during the operation of the equipment).

The error can be the cause of failure (self-recovery failure)—a state in which the object either returns to the working state itself for a long period of time with the unimportant help of the operator, or the cause of sustainable failure, at which the object requires restoration—repair to return to the working state.

Based on the value of the error, the type of possible failure and its veracity are evaluated, and the reasons leading to the error are searched for. To implement this approach, it is necessary to have expert knowledge that would allow correlating the type of possible failure and the reasons that led to its occurrence. In addition, the probability of occurrence of the specified emergency situation should be assessed. Often, the researcher does not have statistical data that would allow estimating the probability of failure of this or that type (brand) of equipment.

The process of state vector formation is individual for each piece of equipment and is determined by its internal properties. Traditionally several methods are used to determine the magnitude of deviation: analysis of signal models [6]; analysis of system model response; classification; cause-and-effect networks.

When using signal models, the measuring information (signal) is presented in the form of a time series (signal values measured at certain intervals of time) and is divided into four components: trend (describes continuous regular changes of the average level), periodic (repeated at equal intervals of time fluctuations of the measured value), stochastic (the influence of random variables) and pattern (arise and characterize specific modes, situations, and perturbations) [7].

Of greatest interest is the template component, it is described by a curve, which has a unique appearance and allows to identify the moment of occurrence of a particular state (for example, malfunction) and determine from this the cause of its occurrence.

Another effective way to identify the technical state of equipment is classification [8]. The classifier allows calculating the “distance” of the current state to each class and selecting the closest one. Classifiers can be a deterministic, statistical, fuzzy, or neural network [9].

Analysis of system model response consists in its comparison with the measured state vector. The model is an ideal digital copy of an object and characterizes its functioning in a normal state. The deviation of model output from the measured state vector is a source of information for diagnosis. Such models can be synthesized for different modes, thus increasing the accuracy of technical state determination [10].

In addition, cause-effect networks (error trees) can be used to determine the error [11]. Such a network usually consists of three layers: symptoms (quantitative (measured) and qualitative (expert estimates) indicators), events (intermediate symptoms, the set of which determines a specific error, and therefore not a proper technical state), errors (the result of determining the technical state of the diagnosed object). Links between layer elements are formalized using rules of the type

“IF..., THAT...” (logical in case of quantitative information and productive in case of qualitative indicators).

2 Equipment Condition Classifier

Thus, the task of diagnostics, in general, can be formulated in the following way.

$$\forall S \exists K : d = K(S), \tag{1}$$

This means that for any vector of state S [characterized by a set of diagnostic signs (s_1, \dots, s_m)] there is such a classifier that a diagnosis can be made $d_i \in D, i = \overline{1, N}$, where D —a limited set of N equipment diagnoses. The availability of a classifier is a mandatory condition for implementation of the system for evaluation of the actual technical condition of equipment and the formation of repair programs based on it.

In accordance with the methodology proposed in [12] it is necessary to determine the basic (immediately after the installation of equipment, different from the passport, which characterizes the “ideal” state of a particular unit of equipment at the time of start-up) and the actual characteristics of the equipment (at any other time, which requires setting the diagnose). The difference between basic and actual characteristics is a measure of the current technical state of the equipment and is used to clarify the causes of a particular emergency situation.

The basic characteristics are removed for a certain number of modes (set for each type of equipment separately). The type of actual characteristics indicates the presence of a specific symptom and is necessary for making the diagnosis. If it is not possible to remove such characteristics, passport data can be used [13]. The use of pass-port data thus affects the accuracy of estimation of technical structure and quality of the statement of a diagnosis.

The classifier of diagnoses itself is implemented in tabular form (Table 1). Table 1 contains the following designations: $>$ (the current characteristic is larger than the allowable deviation limit values of the base or passport characteristics), $<$ (the current characteristic is smaller than the allowable deviation limit values of the base or passport characteristics), \in (the current characteristic belongs to a set of allowable deviation limit values of the base or passport characteristics). In addition, there may be signs $\geq, \leq, =$ (if the corresponding inequality limit or the exact value of the diagnostic parameter included in the classifier can be strictly estimated).

Table 1 Equipment condition classifier

Diagnosis number	s_1	...	s_m
1	$>$...	$<$
...
N	\in	...	\in

In this case, the classifier is a simple rule of the form IF s_j AND ... AND s_m , THAT $d =$. It allows not only to diagnose a unit of equipment but also to determine the reasons for its occurrence if there is expert knowledge to do so.

The presence of uncertainty, which is caused by the lack of precise knowledge about the limits of change of the diagnostic parameter, provided that production rules can be obtained, reflecting the process of human reasoning of the expert in making the diagnosis leads to the fact that for making the diagnosis can be used fuzzy production rules [14] and the algorithm of fuzzy conclusion (eg, Mamdani). Such an approach will allow us to obtain a value that determines the proximity of the current situation in the object to possible diagnoses.

3 Time to Send Equipment for Repair

Choosing the time for repair of a particular piece of equipment is a very urgent and complex task [15]. On the one hand, one should not allow the failure of a piece of equipment, and on the other hand, too early withdrawal into repair, because the equipment could still function for a certain period of time. This means that it is necessary to choose a point in time when the equipment is still functioning, but its condition is close to a critical one (in this condition the equipment fails and fails).

The decision to put a particular piece of equipment into the repair (to include it into the repair program) is made on the basis of the calculation of the residual operating time τ_{oct} based on the following condition:

$$\begin{cases} \tau_{oct} > 0, r = 1 \\ \tau_{oct} \leq 0, r = 0, d_i \in D \end{cases} \quad (2)$$

To forecast τ_{oct} , a regression model is built (based on pre-processed measurements of diagnostic parameters [16]). The algorithm, which implements diagnosis on the basis of calculation of τ_{oct} , can be presented in the following way.

Step 1. Input data for calculation τ_{oct} .

Step 2. Calculate the τ_{oct} .

Step 3. If the condition $\tau_{oct} > 0$ is met at the forecast time, then conclude that the unit is operable and put the value $r = 1$.

Otherwise, proceed to step 7.

Step 4. output the values of r .

Step 5. output the calculated value of τ_{oct} , as an additional characteristic, which characterizes the time of equipment operation in the current technical condition until the moment of its failure and failure.

Step 6. Move on to step 11.

Step 7. Make a conclusion that the unit of equipment is not working and put the value $r = 0$.

Step 8. Using the classifier obtained from Table 1, perform the classification operation, and diagnose $d_i \in D$.

Step 9. Output the values τ_{oct}, r .

Step 10. Print the value $d_i \in D$.

Step 11. Algorithm stop.

The diagnosis of a unit of equipment $d_i \in D$ obtained from the synthesized algorithm serves as an additional characteristic. By using $d_i \in D$ the causes of its occurrence can be obtained (if there is additional expert knowledge about the presence of such a bond), thus reducing the labor intensity in planning repairs and forming the repair program.

Let us consider the solution of the assigned problem of diagnostics and the formation of a repair program for partially defective equipment that continues to function, but is outside the normative quality [17].

Such equipment is subject to repair, however in case of limited financial resources, and also a considerable quantity of units of the equipment is a partially defective condition, it is necessary to repair at first those units which risk breakage and the cost of repair will be the greatest among a presented set of units of the equipment.

4 The Repair Program Formation

The formation of the repair program should be based on a certain criterion [18]. The restrictions imposed on the criterion are due to the fact that not all the equipment can be repaired, as there is only a certain amount of financial resources that can be spent on repairs and bringing the equipment into the proper technical condition [19].

The moment of failure j -th unit of equipment can be determined using residual life. Therefore, it is suggested to use negative operating time as the first criterion: $R_j = |\tau_{oct,j}|$ for the j -th unit.

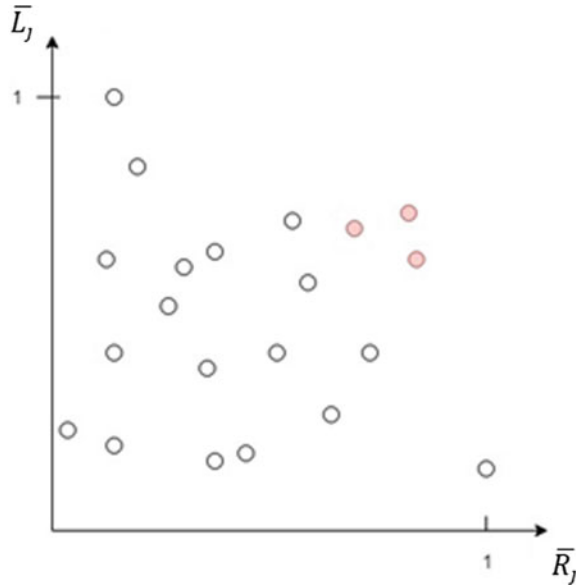
The second criterion to be used in evaluating the items of equipment of candidates for inclusion in the repair program is the total financial loss L . These losses are caused by equipment failure (the cost of repairing the equipment itself, the cost of repairing equipment that may fail due to functional relationship, as well as losses caused by forced downtime).

To analyze the value, it is necessary to standardize $\overline{R}_j = R_j / \max(R_j)$ and $\overline{L}_j = L_j / \max(L_j)$. The geometrical interpretation of the equipment located in the plane of normalized criteria is shown in Fig. 1.

If you put all units of equipment on a plot with R and L axes, you can identify many units with maximum aggregate risk, i.e. many units optimal for repair—points marked in red.

Using two criteria \overline{R}_j and \overline{L}_j it is possible to rank partially defective pieces of equipment according to the degree of expediency of repair and their proper technical condition. This is done using the criterion $I_j = \overline{R}_j + \overline{L}_j$. The higher the value of

Fig. 1 Equipment in the plane of normalized criteria



criterion I , the higher the expediency of repair, which means that a piece of equipment should get into the formed repair program with a higher probability.

Let $\{x_1, \dots, x_l, \dots, x_n\}$, $l = \overline{1, n}$, where n the total number of pieces of equipment—a set of ordered in descending order criterion I units of equipment. Let's denote c_j —the cost of repair i -th unit of equipment and C_r^{\max} —the maximum allowable cost of the repair program (funds allocated for the repair of the equipment). Then the repair program will include only those h units, for which the condition is fulfilled:

$$\sum_{l=1}^h c_l \leq C_r^{\max}, \tag{3}$$

5 Example of the Approach Applying

Let's show an example of a calculation using the described sequence of steps and the synthesized algorithm. The input data for the calculation were taken from [12]. The object of diagnosis is a pump unit NM-10000–210 (used to transport oil through the main oil pipelines, with flow rates up to 10,000 m³/hr).

The proposed approach is implemented as a corresponding software in the programming language R [20].

As a result of the analysis, the classifier is obtained, presented in Table 2 (software implementation of the classifier in R language is shown in Fig. 2).

The current state is determined on the basis of calculation $\tau_{oct} = (\hat{\eta}_{npe\partial} - a_1)/b_1 - \tau$, where $\hat{\eta}_{npe\partial}$ corresponds to the lower boundary of the passport value of pumping unit efficiency, a_1, b_1 —coefficients of regression equation used for calculation of relative efficiency value (trend) $\hat{\eta}_{i,p} = a_1 + b_1 \tau_i$ (τ_i —operating time, [hr]).

Table 2 shows the relative head $Q = Q_{np}/Q_{max}$, pressure H , power N и efficiency η .

The work of the classifier was tested on simulated values of actual and passport characteristics. As a result of the check, all diagnoses and their absence are determined without errors, there are no unidentified conditions and no diagnoses made.

Table 2 Equipment condition classifier for pumping unit NM-10000–210

Diagnosis number	Q, %	H	N	η
1	$\in [0:100]$	<	<	\geq
2, 6	$\in [0:50]$	<	\in	<
3	$\in [0:100]$	\in	>	<
4	$\in [0:100]$	>	>	\geq
5	$\in [0:50]$	\in	\in	<
2, 5, 6, 8	$\in [50:100]$	<	\in	<
7	$\in [0:100]$	<	>	<
8	$\in [0:30]$	>	\in	\geq
8	$\in [30:50]$	<	\in	\geq
9	$\in [0:100]$	>	\in	<

```

160 - Classifier <- function(Q,H,H1,Hu,N,N1,Nu,KPD,KPD1) {
161   Diagn <- "Diagnosis is not found"
162
163   if (H<H1 & N<N1 & KPD>=KPD1) Diagn <- "Diagnosis №1"
164
165   if (between(Q,0,50) & H<H1 & between(N,N1,Nu) & KPD<KPD1) Diagn <- "Diagnosis №2, 6"
166
167   if (between(H,H1,Hu) & N>Nu & KPD<KPD1) Diagn <- "Diagnosis №3"
168
169   if (H>Hu & N>Nu & KPD>=KPD1) Diagn <- "Diagnosis №4"
170
171   if (between(Q,0,50) & between(H,H1,Hu) & between(N,N1,Nu) & KPD<KPD1) Diagn <- "Diagnosis №5"
172
173   if (between(Q,50,100) & H<H1 & between(N,N1,Nu) & KPD<KPD1) Diagn <- "Diagnosis №2, 5, 6, 8"
174
175   if (H<H1 & N>Nu & KPD<KPD1) Diagn <- "Diagnosis №7"
176
177   if (between(Q,0,30) & H>Hu & between(N,N1,Nu) & KPD>=KPD1) Diagn <- "Diagnosis №8"
178
179   if (between(Q,30,50) & H<H1 & between(N,N1,Nu) & KPD>=KPD1) Diagn <- "Diagnosis №8"
180
181   if (H>Hu & between(N,N1,Nu) & KPD<KPD1) Diagn <- "Diagnosis №9"
182
183   Diagn
184 }

```

Fig. 2 The classifier in R programming language

Table 3 Passport characteristics from [12]

Mode	H, м	N, κB _T /ч	η, %
Mode 1	250	6051	85.9
Mode 2	218	6416	90.3

Table 4 Passport characteristics obtained using the proposed approach

Mode	H, м	N, κB _T /ч	η, %
Mode 1	248	6045	85.8
Mode 2	219	6411	90.2

Two modes of operation of the equipment participated in the diagnostics (Tables 3–4, values are given in [12]).

The residual resource was also predicted using the data provided in [12] (Table 5).

As a result of calculations, the value of 675 h of residual time was obtained (in [12] this value is 668 h, which indicates a high accuracy of forecasting).

As a result of diagnostics of both modes in [12] the diagnosis №7 (frail-dimensional leakages through the impeller seal and end seals, passes the check valve) is advanced. A similar diagnosis was obtained using the synthesized classifier (example in Fig. 3).

To test the synthesized method of equipment ranking according to the degree of expediency of its inclusion into the repair program, the following array of criteria values was obtained (for convenience and clarity, the graphical interpretation in Fig. 4 is given), calculated in accordance with the above sequence of steps to obtain and predict the residual resource of the equipment.

Table 5 Results of the relative head measurements and the pumping unit efficiency

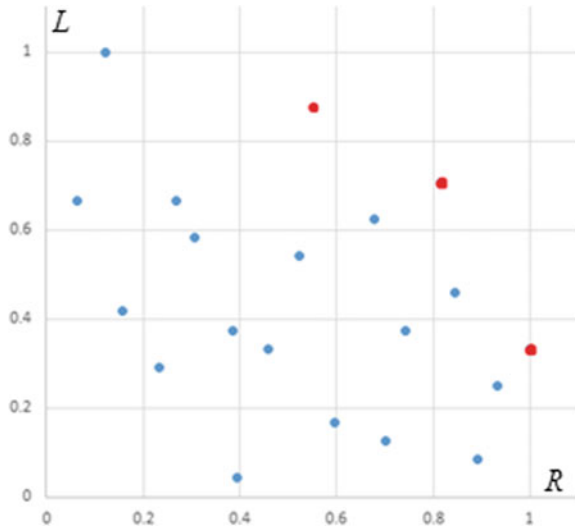
Measurement	1	2	3	4	5	6	7
\hat{H}	0.73	0.78	0.74	0.64	0.66	0.71	0.62
$\hat{\eta}$	1.003	1.001	1.000	1.000	0.998	0.999	0.999

```

Console Terminal x
C:/Users/Ruslan/Desktop/Studium/Russ_Master/R_scripts/
>
> #Results
> Stationarity
[1] TRUE
> Homogeneity
[1] TRUE
> Diagnosis
[1] "Diagnosis №7"
>
    
```

Fig. 3 Example of a diagnosis

Fig. 4 Graphical interpretation of the equipment ranking results and completing the repair program



The red color indicates those units of equipment, for which it is expedient to include in the repair program and transfer to the repair. Taking into account the available financial resources, the repair program may be limited, but it must necessarily include those items of equipment that are identified in the described way.

6 Conclusion

The sequence of calculations offered in work is a basis of a subsystem of support of acceptance at the formation of the repair programs, based on the forecasting of a residual resource and an estimation of an actual condition of the equipment of different functions. The decision of a problem of reception of the diagnosis for the equipment will allow forming the repair program more precisely as provides reception of the information on the reason for possible failure. The implemented software can be built, for example, into EAM-systems [21] to increase their efficiency.

References

1. Wang J., Zhang W., Shi Y., Duan S., Liu J. Industrial Big Data Analytics: Challenges, Methodologies, and Applications. <https://arxiv.org/ftp/arxiv/papers/1807/1807.01016.pdf>. Accessed 21 Apr 2019
2. Czichos, H.: Technical diagnostics: principles, methods, and applications. NCSLI Measure **9**, 32–40 (2014). <https://doi.org/10.1080/19315775.2014.11721681>

3. Protalinskiy, O., Andryushin, A., Shcherbatov, I., Khanova, A.A., Urazaliev, N.: Strategic Decision Support in the Process of Manufacturing Systems Management. 1–4 (2018). <https://doi.org/10.1109/MLSD.2018.8551760>.
4. Alexandrov, O.I.: Sampling of the plan of repairs of the main equipment in the electrical power system. *Energetika*. In: Proceedings of CIS Higher Education Institutions and Power Engineering Associations, 60, 320–333 (2017). <https://doi.org/10.21122/1029-7448-2017-60-4-320-333>
5. Paunescu, I., Paunescu, P., Velicu, S.: Decision support in maintenance activity by using modern techniques for equipment condition monitoring. *MATEC Web Conf.* **112**, 09001 (2017). <https://doi.org/10.1051/mateconf/201711209001>
6. Candy, J.: *Signal Processing: Model Based Approach* (1986)
7. Romberg T.M., Black J.L., Ledwidge T.J.: *Signal Processing for Industrial Diagnostics*. Wiley (1996)
8. Kravchuk, N.: Investigation of intelligent classification of current technical condition of the gas turbine engine. *Technol Audit Prod Reser.* **1** (2015). <https://doi.org/10.15587/2312-8372.2015.38073>
9. Andryushin, A., Arakelyan, E., Shcherbatov, I., Kosoy, A., Dolbikova, N.: Application of neural network technologies in power engineering. *J. Phys. Conf. Series* **1370**, 012054 (2019). <https://doi.org/10.1088/1742-6596/1370/1/012054>
10. Isermann, R.: *Fault Diagnosis Systems An Introduction from Fault Detection to Fault Tolerance*. SERBIULA (sistema Librum 2.0) (2006)
11. Ibrahim, A., Kacianka, S., Pretschner, A., Hartsell, C., Karsai, G.: *Practical Causal Models for Cyber-Physical Systems* (2019) https://doi.org/10.1007/978-3-030-20652-9_14
12. Belkin A.P., Stepanov O.A.: *Diagnostics of Heat and Power Equipment*, 240 p. M.: Lan (2018)
13. Borodin, V., Andryushin, A., Protalinsky, O., Khanova, A.A.: Multiexpert Planning System for Repair Programs of Power-Generating Equipment, 1–5 (2019). <https://doi.org/10.1109/MLSD.2019.8911105>
14. Gayme, D., Menon, S., Ball, C., Mukavetz, D., Nwadiogbu, E.: Fault diagnosis in gas turbine engines using fuzzy logic. **4**(4), 3756–3762 (2003). <https://doi.org/10.1109/ICSMC.2003.1244473>
15. Akinyemi, O.: Development of equipment maintenance strategy for critical equipment. *Pacific J. Sci. Technol.* **11**, 328–342 (2010)
16. Andryushin, A., Shcherbatov, I., Dolbikova, N., Kuznetsova, A., Tsurikov, G.: *Outlier Detection in Predictive Analytics for Energy Equipment* (2020). https://doi.org/10.1007/978-3-030-32579-4_15
17. Yashchura A.I.: *System of Maintenance and Repair of Power Equipment*, 504 p. Handbook. – M.: publishing house of the NTS ENAS (2006)
18. Protalinsky, O., Shcherbatov, I., Stepanov, P.: Identification of the actual state and entity availability forecasting in power engineering using neural-network technologies. *J. Phys. Conf. Series* **891**, 012289 (2017). <https://doi.org/10.1088/1742-6596/891/1/012289>
19. Baskakova, N.T., Sidoruk, I.L.: Optimization repair costs in terms of the theory of constraints with using RCM technology. *Aktualnyye problemy sovremennoy nauki, tekhniki i obrazovaniya* **2**(1), 207–211 (2014)
20. Widemann, B.T.y., Bolz, C.F., Grelck, C.: *The Functional Programming Language R and the Paradigm of Dynamic Scientific Programming*. 182–197 (2013). https://doi.org/10.1007/978-3-642-40447-4_12
21. Srinivasan, V.: *Sustaining Manufacturing Assets Through Smarter Utilization of Information and Communication Technologies*, 478–482 (2009). <https://doi.org/10.1109/COASE.2009.5234087>

Cyber-Physical Systems in Chemical Industry

Computer Modeling System for Energy- and Resource-Saving Control of Multi-Assortment Polymeric Film Production



Tamara Chistyakova  and Andrey Polosin 

Abstract The chapter describes the questions of developing the flexible computer modeling system that allows us to realize the synthesis of mathematical models of hardware flexible extrusion processes for energy- and resource-saving control of large-capacity, multi-assortment production of polymeric films. The problem of energy- and resource-saving control, which is solved at each transition of the production to a new type of film, is to determine parameters of the extruder configuration and operating mode, ensuring the given extrudate quality when meeting the requirements for throughput and energy consumption. The library of mathematical models is the core of the system. It includes structural models of extruder elements for calculating the geometric parameters of extruders of various configurations and functional models of physical processes in the element channels. Static models for calculating throughput, energy consumption, extrudate quality indices (mixing degree, solid fraction, thermal destruction index), and dynamic models for calculating residence time in the extruder are synthesized based on the physical process models in the element channels. The structural synthesis of the models is based on a cell approach to modeling processes in partitioned apparatuses. Setting up the system is carried out using a data bank of production methods and types of films, parameters of extruders, polymer properties. A two-stage iterative algorithm is used to solve the control problem: the extruder configuration is formed in the external cycle, the extruder operating parameters, which ensure the required extrudate quality with given throughput, energy consumption, are determined in the internal cycle. Testing according to data of the polyvinyl chloride and polyethylene film productions in plants of Russia and Germany has confirmed the operability of the system and the possibility of its using as an adviser to operators.

T. Chistyakova (✉) · A. Polosin
Saint Petersburg State Institute of Technology (Technical University),
Moskovsky Prospekt 26, St. Petersburg 190013, Russia
e-mail: nov@technolog.edu.ru

A. Polosin
e-mail: polosin-1976@sapr.tti-gti.ru

Keywords Mathematical modeling · Software package · Energy- and resource-saving control · Polymeric film production · Extruders with variable configurations

1 Introduction

Extrusion (cast, blown) and calendering are the main methods of the high-tech polymeric film (PF) industrial production for foodstuff and medicine packaging. The high demand for packaging materials and a multitude of packaged product types define the high-capacity multi-assortment character of extrusion and calender PF production. Thus, just one of the leading international corporations producing PF, Klöckner Pentaplast, produces 250 thousand tons of PF on 35 extrusion lines, as well as 400 thousand tons of rigid PF with a polyvinyl chloride (PVC) base on 41 calender lines per year. Packaging PF differs in its composition (in particular, the types of film-forming polymers, with PVC, polyethylene terephthalate, polypropylene, and varied density polyethylene being key among them). It is characterized by a large range of potential thickness (from 0.025 to 1.65 mm) and width (up to 6200 mm) of a sheet of film, as well as strict quality requirements (its appearance, color). Certain PF defects are most unacceptable. These include black specks, destruction strips, the inclusion of unmelted polymer, defects such as « fish-eye » (gels), and « orange peel » , as well as deviation from the required color. The difficulty in PF production control lies in a large number of parameters for the raw materials, equipment, production mode, product quality, and their numerous interrelationships [1]. For example, calender PF production is characterized by more than 100 parameters and 800 interrelationships between them. Therefore, the main innovative trend of the development of international high-technology production of the polymer industry within the framework of the Industry 4.0 concept is the creation and application of cyber-physical systems for effective control of PF production processes based on the integration of methods and technologies of computer modeling of physical processes and mining of big production data on process parameters and quality indices of semi-products and target products [2–4].

Regardless of the PF production method, the extrusion process is the key stage, which is implemented using extruders of various types and is defined by equipment flexibility (the possibility of implementing numerous screw configurations so as to produce multi-assortment PF). Extrusion includes physical processes successively following one another in the channels of the screw or screws: the heating and melting of solid polymer, heating, mixing, and molding of melt [5]. The goal is to prepare a homogenous plastic mass (extrudate) from which the PF can then be produced. The extrudate temperature, level of homogeneity, and color coordinates (hue, saturation, lightness) in large part define the most important PF consumer characteristics: the number of black points, inclusions of unmelted polymer, gels per given area of PF, and color coordinates. Extrusion PF production leads to PF thickness being dependent on the extrudate output rate, that is, on the throughput of the extruder. At the same

time, only visual quality control is performed on the production line. As a result, the operators make control decisions based on a subjective judgment of extrudate quality, their own experience, and an experimentally determined set of production rules. Given the multi-assortment production conditions, this leads to errors, which lead to financial losses, resulting from an increase in defective PF, loss of resources spent on its production, an increase in time spent the line change-over, and, as a result, a decrease in throughput and increase in energy consumption.

Thus, it is relevant to develop the flexible computer modeling system (CMS) for the synthesis of mathematical models (MM) for extrusion processes, such that they can be configured for the PF type, its production method, the type and configuration of the extruder. This would enable calculating the extrudate quality characteristics, the throughput, and energy consumption of the process, and solve the problems of energy- and resource-saving control of multi-assortment extrusion and calender PF productions.

2 Controlled Object Characteristics. Energy- and Resource-Saving Control Problem Statement

The formalized description of PF production as a controlled object (CO) is presented in Fig. 1. The extruder type T_{extrud} , diameter D , and length L of the extruder's screw are determined according to the production method M_{prod} , the type of film-forming polymer T_{polym} , and the throughput G_0 and energy consumption E^{max} requirements for the line. Extruders differ in the number of screws q and the way they move: single-screw extruders E_1 (the screw simply rotates at screw speed N), reciprocating extruders E_2 (the screw rotates and also performs oscillating motion with an amplitude S_0), twin-screw extruders with co-rotating screws (E_3) or counter-rotating screws (E_4). The screw configuration C_{scr} consists of N_e elements of various types T_e^j . The element types are determined by the type of extruder. Thus, screws of an E_1 extruder, generally, consist of elements with continuous flights and cylindrical (SC) or conical (SP) core (SP-elements are used in the melting zone). Extruders of type E_2 , as a rule, have conveying elements (EZ), kneading elements (KE), and elements with a restriction ring (ST, used in the degassing zone) [6]. The extruder is assembled with a molding head of type T_{head} , the selection of which depends on the production method M_{prod} . Equipment flexibility enables us to have not only parametric control of the extruder (by changing the extrusion mode) but also structural control (by changing the screw configuration C_{scr} when reconfiguring production to a new PF type T_{film} , which is itself dependent on the polymer type T_{polym} and quality requirements Q_{film0}). Extrusion mode is switched with the help of main CA U_b : speeds of feed screw N_h and main screw N , barrel heating zone temperatures T_{bk} , $k = 1 \dots n_T$. The output parameters Y_{extrus} are dependent on this extrusion mode. They include extruder throughput G and energy consumption E , which determine corresponding line characteristics, average residence time (ART) of polymer in extruder

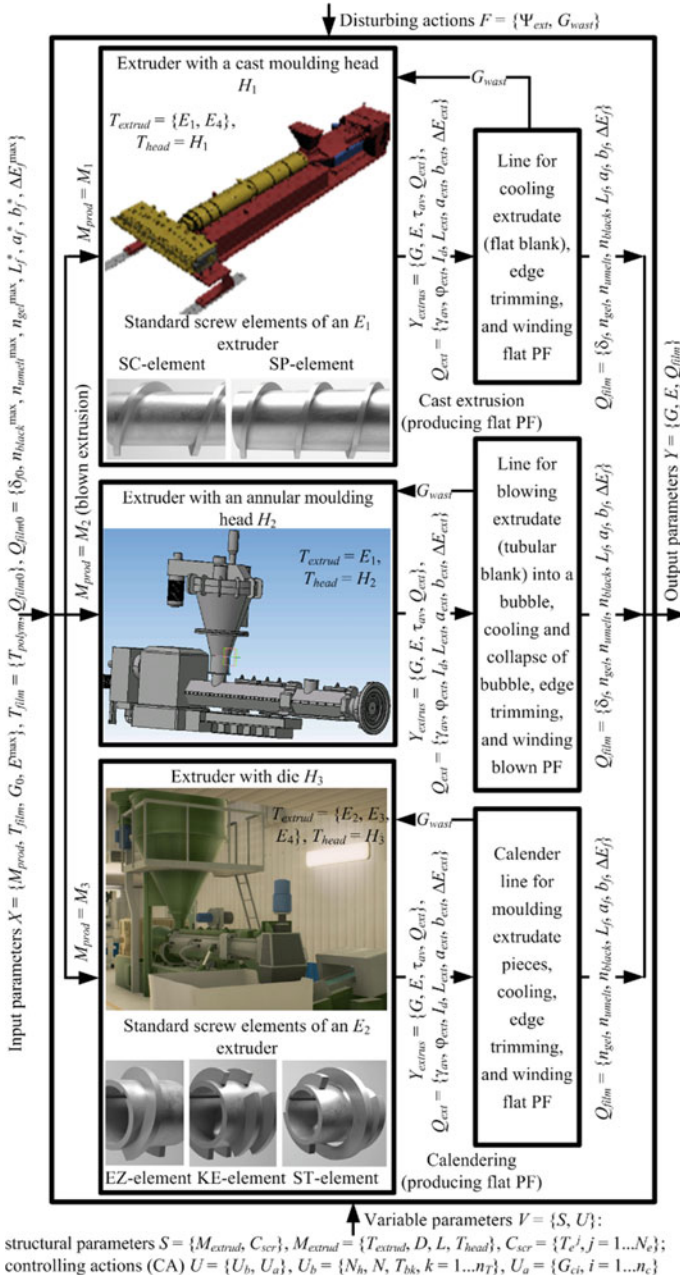


Fig. 1 Formalized description of PF production as CO

τ_{av} and extrudate quality indices Q_{ext} (average mixing degree γ_{av} , a solid fraction φ_{ext} , thermal destruction index I_d).

Film thickness δ_f is dependent on throughput (if $M_{prod} = M_1 \vee M_2$). Raising a solid fraction above a certain upper bound φ_{ext}^{max} indicates the presence of unmelted particles n_{umelt} in PF. Other extrudate quality indices (γ_{av} , I_d) determine corresponding PF quality indices Q_{film} – number of gels n_{gel} and black points n_{black} .

During the production of a colored film, feeding wasted supplies back in the extruder (shredded PF sheet trim) at a flow rate G_{wast} and oscillation in the extrudate supply Ψ_{ext} within the feeding trough of calender lead to a deviation of the PF color coordinates L_f , a_f , b_f from the required values L_f^* , a_f^* , b_f^* due to a deviation in the extrudate color coordinates L_{ext} , a_{ext} , b_{ext} . This color coordinate drift ΔE_f passes a preset upper bound ΔE_f^{max} , which requires correction via additional CA U_a : flow rates of liquid colorants fed into an extruder, G_{ci} , $i = 1 \dots n_c$.

The analysis of the CO allowed us to formulate the problems of PF production control during line change-over and during active production.

The control problem during change-over of the line, which is implementing the production method M_{prod} , to a new task $Y_0 = \{T_{film}, G_0, E^{max}\}$ consists of selecting extruder brand M_{extrud} , forming its screw configuration C_{scr} and admissible values for main CA $U_b^* \in [U_b^{min}; U_b^{max}]$, which ensure the maintenance of quality indices $\gamma_{av} \geq \gamma^{min}$, $\varphi_{ext} \leq \varphi_{ext}^{max}$, $I_d \leq I_d^{max}$, that ensure compliance with the restrictions on the number of PF defects ($n_{gel} \leq n_{gel}^{max}$, $n_{umelt} \leq n_{umelt}^{max}$, $n_{black} \leq n_{black}^{max}$), while maintaining line requirements $G \geq G_0$, $E \leq E^{max}$. Here, γ^{min} and I_d^{max} are the boundary values for extrudate quality, which depend on requirements for their corresponding PF defects.

Control problems while in active production (with the presence of disturbing actions G_{wast} and Ψ_{ext}), consisting of determination (depending on the current extruder throughput G) of flow rates G_{ci}^* , $i = 1 \dots n_c$, so as to ensure fulfillment of extrudate color deviation $\Delta E_{ext} \leq \Delta E_{ext}^{max} \pm \Delta_{max}$ requirements, have been defined in prior work [7]. Here ΔE_{ext}^{max} is the limit deviation of the extrudate color from the standard, determined depending on the PF color requirement (ΔE_f^{max}), Δ_{max} is color measurement error.

Due to the incompleteness of the information regarding the extrusion process state parameters and extrudate quality indicators attainable with CO, solving multi-assortment PF production control problems requires using MM, which enables us to provide a comprehensive evaluation of extrudate quality, extruder throughput, and energy consumption in response to the CA.

3 Library of Mathematical Models for Extrusion Processes

In order to take into account the variety of extruder types and their equipment flexibility, the multitude of polymer types, as well as the complex diagram of motion, melting, and heat exchange within the screw channel, a complex modeling method

has been proposed. It is based on a MM library of extrusion processes, rules, and an algorithm for the structural and parametric synthesis of the control model.

The analysis of MMs of extrusion processes described in literature has shown that they are constructed on the basis of conservation laws of physical substances and include the equations of balances of mass, forces, and energy for solid phase and melt, a rheological equation of state of melt and also the equation of an interphase material and heat balance (for the description of melting) [8]. Different melting mechanisms are modeled: contiguous solids melting (melting of continuous solid phase – solid bed) in extruders of type E_1 [9–13]; dispersed solids melting (melting of dispersed solid phase) in extruders of types E_2 – E_4 [5, 14–16]. Models allow us to calculate the melting zone length, profiles of width (concentration of solid particles for dispersed solids melting) and temperature of the solid phase, fields of flow velocities, stresses of viscous friction inflows, pressure, and temperatures of melt. The scope created by MM generally is limited to a research of patterns of processes of a heat mass transfer of polymers in extruders of separate types with classical geometry of the screw [17], in separate functional zones of the channel of the screw (solid polymer conveying [18], melting, melt conveying [19–22]) or in channels of separate elements of modular screws [23]. Results of modeling allow obtaining information necessary for the design of extruders, but not for quality control of the extrudate. Approaches to assessment of ART in extruders of different types are based on application as separate standard hydrodynamic models (for example, one-parameter axial dispersion model [24]), and the difficult combined models of the structure of the flows. These models are constructed on the basis of standard hydrodynamic models (plug flow reactor model, continuous stirred tank reactor model, tanks-in-series model) including the introduction of recirculating flows modeling melt leakages [25, 26]. Standard models describe extruder zones with the different mechanisms and intensity of mixing [27]. However, MMs do not allow to give a complex assessment of the quality of the extrudate, throughput, and energy consumption of extruders in dependence on CA for different types of polymers taking into account the difficult construction of extruders and main patterns of the extrusion process.

Performed analysis has allowed us to develop a MM library. It includes: basic MMs, describing polymer motion, melting, and mixing in the screw channel, and enabling us to calculate distributions of melt flow velocities v_x^j , v_z^j and shear rates $\dot{\gamma}_{xy}^j$, $\dot{\gamma}_{zx}^j$, $\dot{\gamma}_{zy}^j$, as well as distributions of polymer phase pressure P^j and temperature T^j ;

MMs of melt flows in gaps of various kinds (radial, side, calender) and axial cuts in element flights to calculate corresponding leakage flow rates Q_δ^j , Q_s^j , Q_r^j , Q_c^j ;

MMs for calculating melt viscosity η^j ;

MMs for calculating densities of heat fluxes given heat exchange between the melt and the barrel q_{bk}^j , as well as the melt and the screw q_{scr}^j ;

MMs of melt flow in extruder heads of various types for calculating melt-pressure drop;

Ideal hydrodynamic models, describing flow structure in the channels of the screw sections of various types (dependent on element types of which the sections are compiled);

MMs for calculating extrudate quality indices Q_{ext} .

The structure of the basic MM, describing shear flow in the channel of the j -th screw element, takes the form:

$$\int_0^{H^j} v_x^j dy = \dot{Q}_\delta^j + \dot{Q}_c^j, \quad (1)$$

$$z_f^j \left[(2-q)W^j \int_0^{H^j} v_z^j dy + (q-1) \int_0^W \int_0^{H^j} v_z^j dy dx \right] \\ = (2-q)Q^j - (q-1)(2Q_s^j + Q_r^j), \quad (2)$$

$$Q^j = q^{-1}Q + (Q_\delta^j + Q_c^j) + (q-1)(2Q_s^j + Q_r^j), \quad (3)$$

$$\frac{\partial P^j}{\partial x} = \frac{\partial}{\partial y}(\eta^j \dot{\gamma}_{xy}^j), \quad \frac{\partial P^j}{\partial z} = (q-1) \frac{\partial}{\partial x}(\eta^j \dot{\gamma}_{zx}^j) + \frac{\partial}{\partial y}(\eta^j \dot{\gamma}_{zy}^j), \\ \frac{\partial P^j}{\partial z} = (q-1) \frac{\partial}{\partial x}(\eta^j \dot{\gamma}_{zx}^j) + \frac{\partial}{\partial y}(\eta^j \dot{\gamma}_{zy}^j) \quad (4)$$

$$\rho c_P v_z^j \frac{\partial T^j}{\partial z} = \lambda \frac{\partial^2 T^j}{\partial y^2} + \eta^j \left[(\dot{\gamma}_{xy}^j)^2 + (q-1)(\dot{\gamma}_{zx}^j)^2 + (\dot{\gamma}_{zy}^j)^2 \right], \quad (5)$$

$$P^j|_{z=z^{j-1}} = P_{out}^{j-1}, \quad T^j|_{z=z^{j-1}} = T_{out}^{j-1}, \quad (6)$$

$$v_x^j|_{y=0} = 0, \quad v_x^j|_{y=H^j} = \varphi_1(q, D, N, S_0, \Phi_{osc}) \quad (7)$$

$$v_z^j|_{x=0} = v_z^j|_{x=W^j} = v_z^j|_{y=0} = \varphi_2(q, D, N), \quad v_z^j|_{y=H^j} = \varphi_3(q, D, N, S_0, \Phi_{osc}), \quad (8)$$

$$-\lambda \partial T^j / \partial y|_{y=0} = q_{scr}^j(T_{scr}, T^j), \quad -\lambda \partial T^j / \partial y|_{y=H^j} = q_{bk}^j(T_{bk}, T^j), \quad (9)$$

where x, y, z are coordinates along the width W^j , height H^j and length of the channel (m); z_f^j is number of flights; Q^j is the flow rate through the element (m^3/s); Q is flow rate through the extruder with the head (equivalent to throughput, m^3/s); ρ, c_P, λ are melt density (kg/m^3), specific heat ($J/(kg \cdot ^\circ C)$), thermal conductivity ($W/(m \cdot ^\circ C)$); z^{j-1} is channel entrance coordinate (m); $P_{out}^{j-1}, T_{out}^{j-1}$ are pressure (Pa) and temperature ($^\circ C$) at channel exit of the $(j-1)$ -th element; Φ_{osc} is screw oscillation phase in a type E_2 extruder (rad); T_{scr} is screw temperature ($^\circ C$).

In the process of synthesizing MM of extrusion, the MM (1)–(9) is assembled with MMs for calculating the leakage flow rates, viscosity, densities of external heat

fluxes, selected depending on extruder type, screw element type, polymer type, and extrusion heat mode [28, 29]. The used rheological model takes the form:

$$\eta^j = \mu^j(T^j) \left[(\dot{\gamma}_{xy}^j)^2 + (q - 1)(\dot{\gamma}_{zx}^j)^2 + (\dot{\gamma}_{zy}^j)^2 \right]^{(n-1)/2}, \quad (10)$$

where μ^j is consistency index, taking into account the influence of the volume fraction of solid polymer particles in the melt (for dispersed solids melting) and temperature on viscosity ($\text{Pa}\cdot\text{s}^n$); n is the power law index.

The dependence of μ^j on the fraction of solid particles is described by the Maron–Pierce equation [16]. In order to describe its dependence on temperature, the Williams–Landel–Ferry equation and Reynolds equation (depending on the polymer type and process temperature range) are used [30].

In accordance with the presented screw configuration, the formed MMs for polymer motion, melting, and mixing in the channels of the screw elements of various types are assembled. The conditions for the MM conjugation defined by (6) are satisfied when assembling MM. The created MM for polymer motion, melting, and mixing in the channel of a modular screw is integrated with the MM for melt flow in the extruder head, selected depending on the head type [29]. As a result, MM is created for calculating the polymer phase state parameters ($v_x, v_z, \dot{\gamma}_{xy}, \dot{\gamma}_{zx}, \dot{\gamma}_{zy}, P, T, \eta$), throughput G , and energy consumption E of the extruder.

The end of the melting zone is defined by a condition when the fraction of solid phase (the solid bed width carried to the width of the channel at contiguous solids melting or a fraction of solid particles in the melt at dispersed solids melting) becomes less maximum permissible φ_{ext}^{max} [28]. The corresponding value of a fraction of solid phase defines the maintenance of a solid phase in the extrudate φ_{ext} .

In order to evaluate ART τ_{av} , upon which quality indices γ_{av}, I_d are dependent, dynamic MM of the extruder is synthesized (see Fig. 2). The MM consists of standard hydrodynamic models, covered by recycling, taking into account the leakages and oscillation [26, 28].

Various standard models (plug flow reactor model, continuous stirred tank reactor model, tanks-in-series model) describe the structure of flows in sections of various

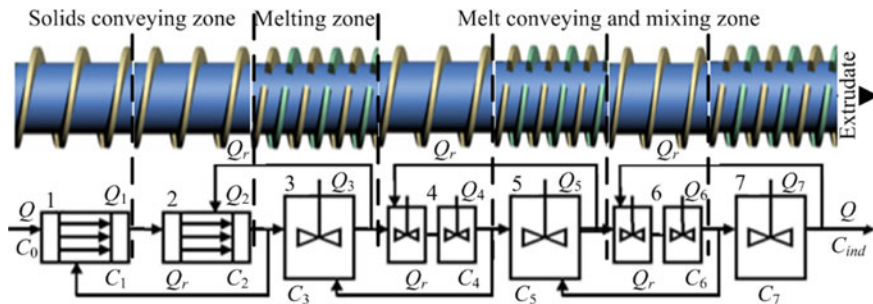


Fig. 2 Example of a structural scheme of a dynamic MM for ART evaluation

types. For example, in the extruder of type E_2 the section consisted of KE-elements is described by a continuous stirred tank reactor model and the section consisted of EZ-elements is described by a tanks-in-series model. The C-shaped chambers in extruders of types E_3 and E_4 are described by the continuous stirred tank reactor model. Distribution of tracer output concentration C_{ind} over time is calculated given pulse disturbance in the composition of the input flow C_0 . It depends on the polymer flow rates Q_l and tracer concentrations $C_l, l = 1 \dots N_s$ (in the example in Fig. 2 $N_s = 7$) in the screw sections, as well as the recycling flow rates Q_r . ART τ_{av} is calculated using a C -curve and the method of moments.

The mixing degree γ_{av} and the thermal destruction index I_d are calculated using the shear rates, temperature, and ART. The mixing degree is determined as the average shear strain accumulated by the polymer. The thermal destruction index is determined as a mapping of the dependence of the destruction degree on time given some temperature-time mode in the extruder, on the dependence derived experimentally for the specific polymer type given isothermal conditions. Regression MMs attained by data processing of active production experiments are used for evaluating the color coordinates of extrudate $L_{ext}, a_{ext}, b_{ext}$, and the CIELab model is used for calculating the color deviation of the extrudate ΔE_{ext} [31, 32].

The MMs has been evaluated by comparing the calculated and measured values of extrudate temperature, throughput and ART for extruders of various types (E_1 – E_4) and configurations (C_{scr}), using corresponding heads (H_1 – H_3), during the processing PVC, polystyrene, polypropylene, and low density polyethylene (LDPE). The adequacy of the models has been confirmed by checking the data with Fisher's criterion and mean squared deviation which does not exceed 3% for the temperature and 10% for the ART.

4 Software Package of Model Synthesis for Extrusion Control and Results of Its Testing

CMS is implemented in the form of a flexible software package. It includes modules for selecting extruder brand M_{extrud} (depending on the production method M_{prod} and parameters of task Y_0), the formation of the extruder's screw configuration C_{scr} , structural synthesis, and parametric setup of the MM for calculating extrusion process output parameters Y_{extrus} (within the procedural ranges of CA) and visualization of the modeling results. The information ware of the package includes a databank of PF production parameters, a rule base for extruder model selection, a rule base for placement and assembly of 3D models for screw elements, and a rule base for extrusion process MM synthesis. The databank includes databases of PF production methods and geometric parameters of extruders, screw elements, and extruder heads. It also includes databases of PF types, quality requirements for extrudate and PF, properties of film-forming polymers, and procedural ranges of CA. The visualization module enables presenting the results in the form of 3D models for screws of formed

configurations, 3D graphs of polymer phase state parameter distribution along the screw channel, 3D graphs of the dependence of extrudate quality indicators, extruder throughput, and energy consumption on the CA, trends of extrusion process output parameters.

The synthesized MM of the extrusion process allows us to solve the investigation problem of CA influence on extrudate quality indices Q_{ext} and the determination problem of CA U_b on the extruder of configuration C_{scr} ensuring given quality at the implementation of requirements to throughput G and energy consumption E . A two-stage iterative algorithm is used to solve the energy- and resource-saving control problem: the extruder's screw configuration C_{scr} is formed in the external cycle, the CA U_b , which ensures the required extrudate quality with given throughput and energy consumption, are determined in the internal cycle.

The software package has been tested using data from calender lines producing flat PF with PVC as the core constituent (the extruders of types E_2 and E_4) and extrusion lines producing blown PF with LDPE as the core constituent (the extruders of type E_1) at plants in Russia and Germany. Testing has confirmed its operability for the solution of control problems of multi-assortment PF productions, both during the change-over mode and during active production. Examples of the software package work results are presented in Fig. 3.

5 Conclusion

The flexible CMS has been developed that allows us to select the extruder brand for a given production method, type of PF, production line throughput, and energy consumption requirements. CMS also allows us based on the synthesized MM of extrusion process to determine the configuration of screw/screws and CA on the extruder, which ensures the specified extrudate quality characteristics (which guarantees the specified consumer characteristics of PF) when meeting the production line performance requirements.

The test results have confirmed the operability of CMS and the possibility of its use as part of industrial cyber-physical systems for efficient energy- and resource-saving control of the extrusion stage at multi-assortment productions of flat and blown PFs in the mode of operator's adviser. CMS was introduced into pilot operation at plants for the production of multi-assortment PF for packaging pharmaceuticals and food products in Russia (Klößner Pentaplast Rus LLC) and Germany (Klößner Pentaplast Europe GmbH and Co. KG).

The application of CMS within the framework of the Industry 4.0 concept allows us to ensure the specified quality of the extrudate, and therefore the quality of PF, reduce defects and energy consumption of the extrusion process, reduce the time spent the production line change-over by determination of rational screw configuration and CA values on the extruder, which help prevent abnormal situations associated with impaired extrudate quality.

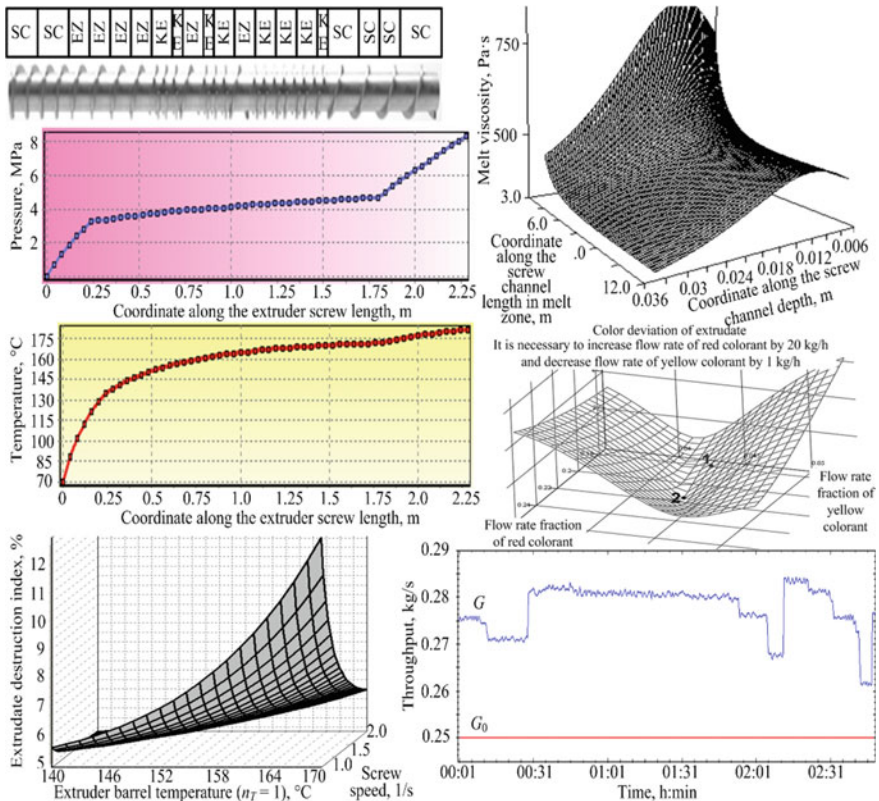


Fig. 3 3D model of the screw and calculated characteristics of the process in the extruder of type E_2

Acknowledgements The chapter is based on the results of the research project “Computational intelligence for analysis and control of complex industrial processes” supported by DAAD (Project ID 57483001).

References

- Gartner, H., Schnabel, A., Kohlert, C.: Control systems for calenders – from mixer to take-off. *Kunststoffe Plast Europe* **87**(6), 24–27 (1997)
- Kohlert, M., Hissmann, O.: Applied Industry 4.0 in the polymer film industry – practical results. In: *Proceedings of the 16th TAPPI European PLACE Conference*, pp. 191–198. TAPPI Press, Basel (2017)
- Chistyakova, T., Teterin, M., Razygraev, A., Kohlert, C.: Intellectual analysis system of big industrial data for quality management of polymer films. In: Cheng, L., Liu, Q., Ronzhin, A. (eds.) *Advances in Neural Networks 2016, LNCS*, vol. 9719, pp. 565–572. Springer, Cham (2016)

4. Chistyakova, T.B., Kleinert, F., Teterin, M.A.: Big data analysis in film production. In: Kravets, A.G., Bolshakov, A.A., Shcherbakov, M.V. (eds.) *Cyber-Physical Systems: Advances in Design and Modelling 2019*, SSDC, vol. 259, pp. 229–236. Springer, Cham (2020)
5. Rauwendaal, C.: *Polymer Extrusion*, 5th edn. Carl Hanser, Munich (2014)
6. White, J.L., Potente, H. (eds.): *Screw Extrusion: Science and Technology*. Carl Hanser, Munich (2003)
7. Chistyakova, T.B., Polosin, A.N.: Computer modeling system of industrial extruders with adjustable configuration for polymeric film quality control. In: *Proceedings of 2017 IEEE II International Conference on Control in Technical Systems (CTS)*, pp. 47–50. Saint Petersburg Electrotechnical University “LETI”, St. Petersburg (2017)
8. Wilczyński, K., Nastaj, A., Lewandowski, A., Wilczyński, K.J.: Multipurpose computer model for screw processing of plastics. *Polymer-Plastics Technol. Eng.* **51**(6), 626–633 (2012)
9. Shapiro, J., Halmos, A.L., Pearson, J.R.A.: Melting in single screw extruders Part 1: the mathematical model. *Polymer* **17**(10), 905–918 (1976)
10. Basov, N.I., Volodin, I.N., Kazankov, Y.V., Pervushin, V.E.: Hydrodynamics and heat exchange in melting in the screw channel of an extruder. *Theor. Found. Chem. Eng.* **17**(1), 61–67 (1983)
11. Elbirli, B., Lindt, J.T., Gottgetreu, S.R., Baba, S.M.: Mathematical modeling of melting of polymers in a single-screw extruder. *Polym. Eng. Sci.* **24**(12), 988–999 (1984)
12. Pervadchuk, V.P., Trufanova, N.M., Yankov, V.I.: Mathematical model and numerical analysis of heat-transfer processes associated with the melting of polymers in plasticating extruders. *J. Eng. Phys.* **48**(1), 60–64 (1985)
13. Lee, K.Y., Han, C.D.: Analysis of the performance of plasticating single-screw extruders with a new concept of solid-bed deformation. *Polym. Eng. Sci.* **30**(11), 665–676 (1990)
14. Potente, H., Melish, U.: Theoretical and experimental investigations of the melting of pellets in co-rotating twin-screw extruders. *Int. Polym. Proc.* **11**(2), 101–108 (1996)
15. Zhu, L., Narh, K.A., Geng, X.: Modeling of particle-dispersed melting mechanism and its application in co-rotating twin-screw extrusion. *J. Polym. Sci. Part B: Polym. Phys.* **39**(20), 2461–2468 (2001)
16. Vergnes, B., Souveton, G., Delacour, M.L., Ainsler, A.: Experimental and theoretical study of polymer melting in a co-rotating twin-screw extruder. *Int. Polym. Proc.* **16**(4), 351–362 (2001)
17. Thibault, F., Tanguy, P.A., Blouin, D.: A numerical model for single screw extrusion with poly(vinyl chloride) (PVC) resins. *Polym. Eng. Sci.* **34**(18), 1377–1386 (1994)
18. Tadmor, Z., Broyer, E.: Solids conveying in screw extruders Part II: non isothermal model. *Polym. Eng. Sci.* **12**(5), 378–386 (1972)
19. White, J.L., Chen, Z.: Simulation of non-isothermal flow in modular co-rotating twin screw extrusion. *Polym. Eng. Sci.* **34**(3), 229–237 (1994)
20. Chiruvella, R.V., Jaluria, Y., Sernas, V.: Extrusion of non-newtonian fluids in a single-screw extruder with pressure back flow. *Polym. Eng. Sci.* **36**(3), 358–367 (1996)
21. Lyu, M.-Y., White, J.L.: Simulation of non-isothermal flow in a modular Buss kneader and comparison with experiment. *Int. Polym. Proc.* **12**(2), 104–109 (1997)
22. Monchatre, B., Raveyre, C., Carrot, C.: Influence of the melt viscosity and operating conditions on the degree of filling, pressure, temperature, and residence time in a co kneader. *Polym. Eng. Sci.* **58**(2), 133–141 (2018)
23. Mehranpour, M., Nazokdast, H., Dabir, B.: Computational study of velocity field in the KE element of a modular ko-kneader with CFD method. *Int. Polym. Proc.* **18**(4), 330–337 (2003)
24. Todd, D.B.: Residence time distribution in twin-screw extruders. *Polym. Eng. Sci.* **15**(6), 437–443 (1975)
25. Puaux, J.P., Bozga, G., Ainsler, A.: Residence time distribution in a co-rotating twin-screw extruder. *Chem. Eng. Sci.* **55**(9), 1641–1651 (2000)
26. Hoppe, S., Detrez, C., Pla, F.: Modeling of a cokneader for the manufacturing of composite materials having absorbent properties at ultra-high-frequency waves. Part 1: modeling of flow from residence time distribution investigations. *Polym. Eng. Sci.* **42**(4), 771–780 (2002)
27. Monchatre, B., Raveyre, C., Carrot, C.: Residence time distributions in a co-kneader: a chemical engineering approach. *Polym. Eng. Sci.* **55**(6), 1237–1245 (2015)

28. Chistyakova, T.B., Polosin, A.N.: Mathematical models and software package for extrusion control at flexible multi-assortment productions of polymeric materials. *Bullet. South Ural State Univer. Series: Math. Modell. Program. Comput. Softw.* **12**(4), 5–28 (2019)
29. Polosin, A.N., Chistyakova, T.B.: The mathematical models and program complex for synthesis of reciprocating extruders with adjustable configurations. *J. Phys.: Conf. Ser.* **1202**(1), 012007 (2019)
30. Covas, J.A., Agassant, J.F., Diogo, A.C., Vlachopoulos, J., Walters, K. (eds.): *Rheological Fundamentals of Polymer Processing*. Springer, Dordrecht (1995)
31. Chistyakova, T.B., Razygrayev, A.S., Polosin, A.N., Araztaganova, A.M.: Joint innovative IT projects in the field of production of polymeric sheet materials. In: *Proceedings of the 2016 IEEE V Forum “Strategic Partnership of Universities and Enterprises of Hi-Tech Branches (Science. Education. Innovations)”*, pp. 61–64. Saint Petersburg Electrotechnical University “LETI”, St. Petersburg (2016)
32. McDonald, R. (ed.): *Color Physics for Industry*, 2nd edn. Society of Dyers and Colourists, Bradford (1997)

Models and Algorithms for Selecting Safety Valves for Petroleum Industries



A. V. Nikolin and E. R. Moshev

Abstract The chapter deals with the problem of automatic determination of the design and technological characteristics of safety valves. The normative-technical and scientific-technical literature devoted to the object of research was analyzed. It is shown that in the literature, there are no models and algorithms that allow automating the process of defining the above-mentioned characteristics. The functional model of determining safety valve characteristics as an organizational and technological process is presented. Production models of knowledge representation and also heuristic-computing algorithms for choosing the required characteristics are developed. The models and algorithms enable creating the problem-oriented cyber-physical system which will define the design and technological characteristics of safety valves in an automated mode.

Keywords Safety valve · Effective seat area · Critical flow · Overpressure · Functional model · Production model · Heuristic-computing algorithm · Cyber-physical system

1 Introduction

To prevent accidents in petrochemical industries, safety valves (SV) are installed on process equipment, including pipelines. These are fittings designed for emergency relief of operating pressure if it exceeds the amount allowed by the technological regulations. The process of determining the SV characteristics that meet the requirements of industrial safety rules is a complex engineering task [1], the results of which depend on the chemical composition, pressure, temperature, and volume of the working medium, as well as the parameters and type of the technological process

A. V. Nikolin (✉) · E. R. Moshev
Perm National Research Polytechnic University, Komsomolsky Prospekt 29, Perm 614990, Russia
e-mail: aletrof@mail.ru

E. R. Moshev
e-mail: erm@pstu.ru

that occurs in a particular unit of equipment. According to the above, the implementation of this process can be lengthy and require not only routine operations of retrieval and processing of technological and regulatory data but also procedures for making intelligent decisions [2, 3]. It is possible to simplify and speed up the determination of SV characteristics if you create and apply special software - a problem-oriented cyber-physical system (CPS) [4–7]. However, the analysis of scientific and technical literature did not reveal models [8–13] and algorithms [14, 15] that could be used for the specified CPS development. Based on the above, the purpose of this study was to create models and algorithms that allow you to automate the process of determining the SV characteristics.

To achieve this goal, the following tasks were formulated:

- analyze the process of determining the SV characteristics as an object of computerization;
- develop a functional model (FM) for determining the SV characteristics as an organizational and technological process;
- develop algorithms to automate SV selection; and
- develop models for the representation of knowledge and data about SVs that will automate the process of determining their characteristics.

2 The Process of Determining the Safety Valves Characteristics as an Object of Computerization

The analysis of normative and technical documentation and scientific and technical literature established that the process of determining the SV characteristics consists of four main stages: calculation of the critical flow rate of the working medium, calculation of the SV effective seat area, SV brand selection, and SV quantity calculation. Moreover, the first and second stages are the most difficult in terms of computerization. This is due to the fact that the critical flow rate of the working medium has complex relationships with the parameters of a particular technological process and its hardware design, and it involves engineering calculations requiring good knowledge of chemical technology. The procedure for determining the SV effective seat area contains not only the data retrieval and processing operations, but also the procedures for making intelligent decisions, as was mentioned above. At the same time, there are dependencies between the SV and the working medium characteristics, which in most cases are discrete. Analysis of the procedures for determining the SV characteristics showed that a significant part of them can be formalized using the theory of artificial intelligence [2, 3], which allows their automation.

3 Development of a Functional Model for Determining the Safety Valves Characteristics

As a result of the analysis of knowledge about the subject of research performed using the system approach [16, 17], a logical-information model was developed that formalizes the solution to the problem of choosing the SV as an organizational and technological process. The model is described following the methodology of structural analysis and design SADT (Structured Analysis and Design Technique) (Fig. 1). The SADT methodology [18, 19] was chosen because it is often used in the development of complex systems and in many cases it is considered an integral component of CALS technologies [20, 21]. In the Russian Federation, it is also widely known as the functional modeling methodology.

The developed FM differs in applying a system approach and taking into account the complex relationships between the various stages of determining the SV characteristics, as well as in connection with data- and knowledge bases, which allows automating the implementation of the above steps while ensuring high-speed information exchange. As an example of FM detailing, the decomposition of block A2 (Fig. 2) of diagram A0 is presented, which shows the relationships between various functions of the procedure for calculating the SV effective seat area, as well as data- and knowledge bases.

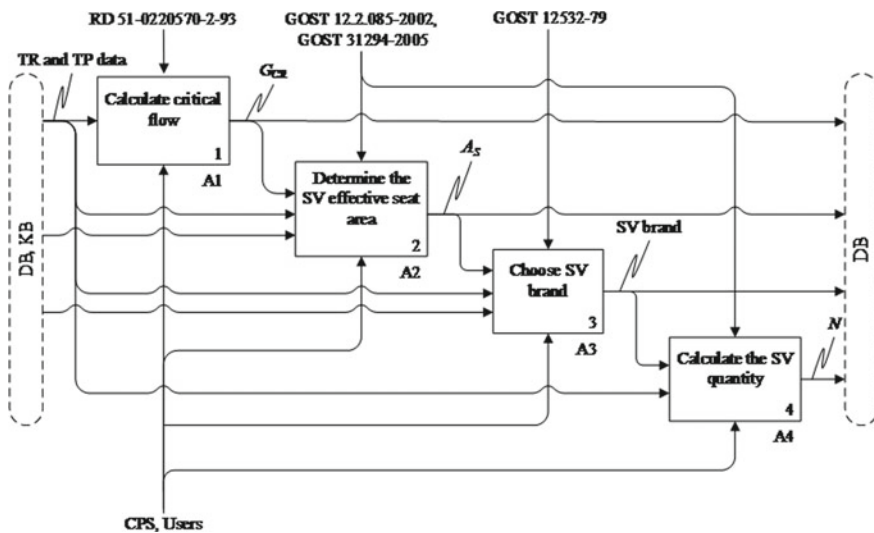


Fig. 1 Diagram A0 of the functional model for determining the safety valves characteristics: TR—technological regulations; TP—technical passport of the vessel; G_{CR} —critical flow rate of the working medium; A_S —the SV effective seat area; N —SV quantity; DB—database; KB—knowledge base

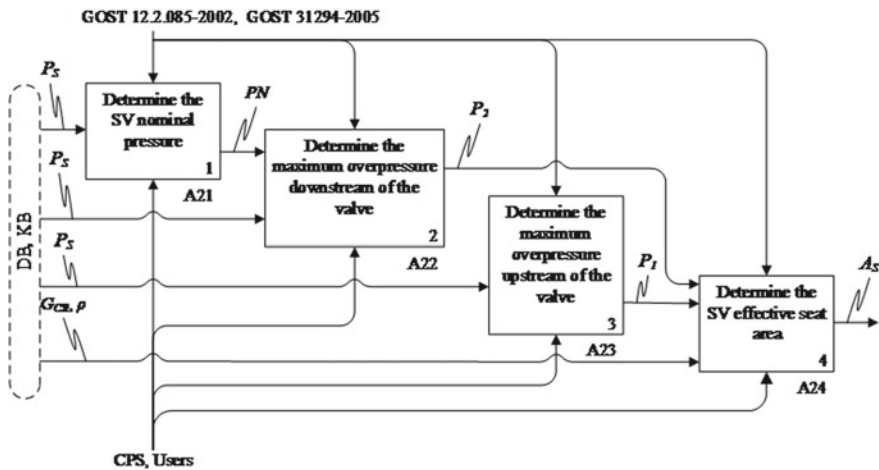


Fig. 2 Decomposition of block A2 of diagram A0: P_S is valve setting pressure; PN is the SV nominal pressure; P_2 is the highest overpressure downstream of the valve (overpressure downstream of the valve in the position of its full opening); P_1 is the highest overpressure upstream of the valve (overpressure upstream of the valve equal to the pressure of full opening); ρ is the density of steam, gas or liquid upstream of the valve

4 Development of Algorithms to Automate the Safety Valves Characterization

As a mechanism for implementing the functions indicated in the FM blocks, the corresponding heuristic-computational algorithms were developed. An example of an algorithm that automates the execution of blocks A21 and A22 is shown in Fig. 3. This algorithm formalizes the process of determining the following SV characteristics: nominal pressure PN ; the highest overpressure downstream of the valve P_2 and the possible nominal diameter values of the outlet pipe D_{NOUT} . Using a given initial characteristic of the setting pressure P_S and production models of knowledge representation (Table 1), the algorithm automates computational and intelligent decision-making procedures for determining SV characteristics as required by normative and technical documentation.

An example of the heuristic-computational algorithm that automates the execution of block A24 is shown in Fig. 4.

The following designations are used in the algorithm (Fig. 4): β is pressure ratio; β_{CR} is a critical pressure ratio; B_1, B_2, B_3 are coefficients for determining the effective seat area for gases and water vapor; k is the adiabatic index; R_{SP} is gas constant.

The developed algorithm formalizes the process of determining the effective seat area of a spring safety valve. Using the specified initial characteristics of the working medium (P_2, G_{CR}, ρ) and production models for the knowledge representation, the algorithm automates computational and intelligent decision-making procedures

Fig. 3 Block diagram of a heuristic-computational algorithm for determining the SV characteristics: nominal pressure PN ; the highest overpressure downstream of the valve P_2 ; possible nominal pressure values of the outlet pipe DN_{OUT}

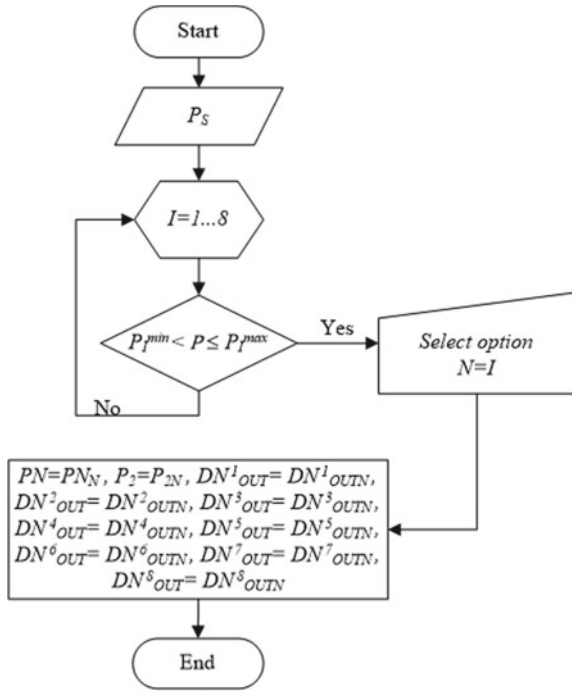


Table 1 Production model for representing valve performance knowledge

Setting pressure P_S kgf/cm ²		Valve nominal pressure PN, kgf/cm ²	P_2 , kgf/cm ²	Nominal diameter of the outlet pipe DN_{OUT} , mm								
min	max			80	100	150	200	300	350	400	–	
0.5	6	6	2.5	80	100	150	200	300	350	400	–	
>6	16	16	6	25	40	65	80	100	150	200	300	
>16	40	40	16	25	40	65	80	100	150	200	300	
>40	63	63	25	25	40	65	80	100	150	–	–	
>63	100	100	40	25	40	65	80	100	150	–	–	
>100	160	160	40	15	25	40	65	80	100	–	–	
>160	250	250	40	15	25	40	65	80	–	–	–	
>250	320	320	40	15	25	32	40	–	–	–	–	
>320	400	400	40	15	25	40	65	–	–	–	–	
Applicability conditions		Required specifications										

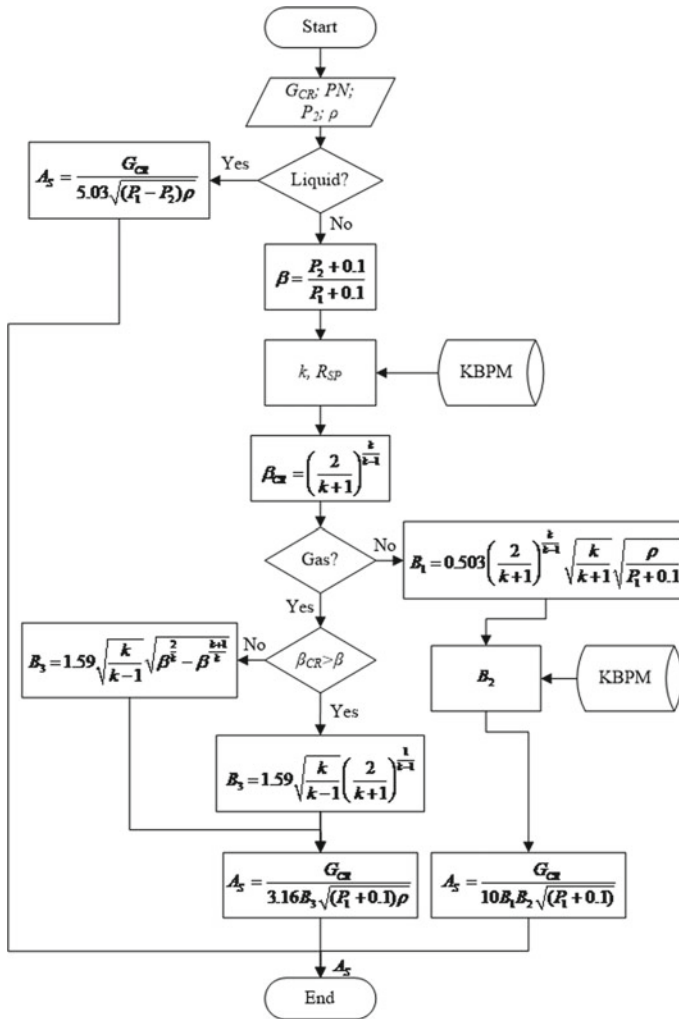


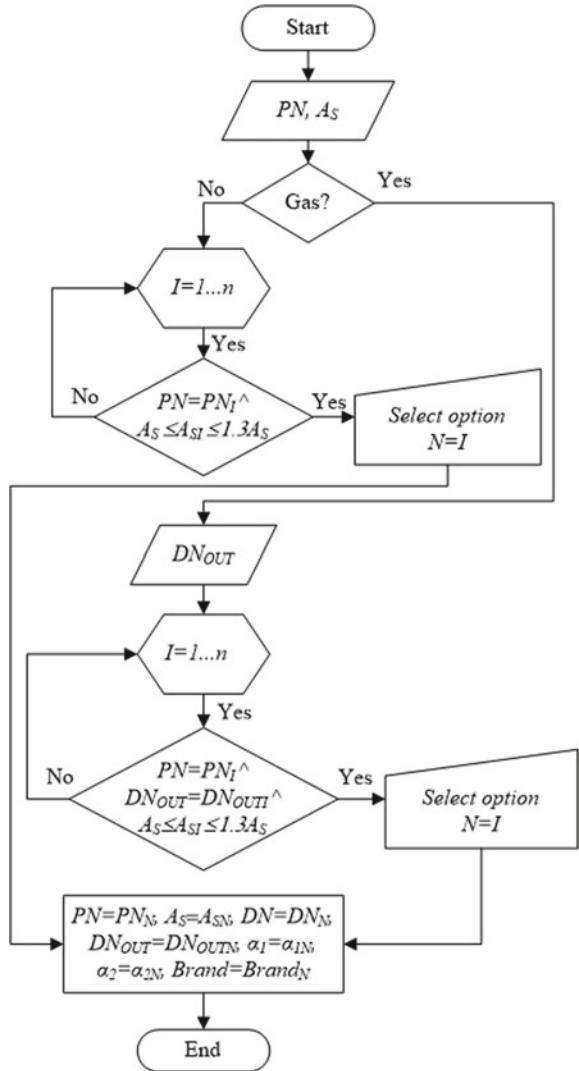
Fig. 4 Block diagram of a heuristic-computational algorithm for determining the effective seat area of a safety valve

for determining the SV effective seat area as required by regulatory and technical documentation.

An example of the algorithm that automates the execution of block A3 is shown in Fig. 5.

With the help of the specified initial parameters (PN, DNOUT, AS) and the database, the algorithm (Fig. 5) allows you to automate computational and intelligent decision-making procedures for selecting SVs as required by regulatory and technical documentation.

Fig. 5 The block diagram of the SV brand selection algorithm



5 Development of Models for the Representation of Knowledge and Data on the Rules for Determining SV

To ensure the automated operation of the algorithm for determining the effective seat area, production models for representing knowledge used in the methods of the theory of artificial intelligence were created [5, 7]: of valve characteristics, of B2 coefficient, and gas characteristics.

Table 2 Production model for B_2 coefficient knowledge representation

β	k	B_2	β	k	B_2	β	k	B_2
0.5	1.1	1	0.577	1.1	1	0.7	1.1	0.965
0.5	1.135	1	0.577	1.135	1	0.7	1.135	0.955
0.5	1.310	1	0.577	1.310	0.99	0.7	1.310	0.945
0.5	1.4	1	0.577	1.4	0.99	0.7	1.4	0.93
0.528	1.1	1	0.586	1.1	1	0.8	1.1	0.855
0.528	1.135	1	0.586	1.135	0.98	0.8	1.135	0.85
0.528	1.310	1	0.586	1.310	0.99	0.8	1.310	0.83
0.528	1.4	1	0.586	1.4	0.99	0.8	1.4	0.82
0.545	1.1	1	0.6	1.1	0.99	0.9	1.1	0.655
0.545	1.135	1	0.6	1.135	0.957	0.9	1.135	0.65
0.545	1.310	1	0.6	1.310	0.975	0.9	1.310	0.628
0.545	1.4	0.99	0.6	1.4	0.99	0.9	1.4	0.62
Applicability conditions			Applicability conditions			Applicability conditions		

An example of a production model for the valve’s characteristics is given in Table 1. This model formalizes the regulatory relationship between the setting pressure (of the safety valve) PS on the one hand and the SV characteristics (PN, P2, DNOU—the SV outlet pipe nominal diameter) on the other hand.

An example of a production model for the coefficient B_2 is shown in Table 2. This model takes into account the correlation between the B_2 coefficient on the one hand and the adiabatic index k as well as the pressure ratio β (the ratio of the highest overpressure downstream of the valve to the highest overpressure upstream of the valve) on the other.

An example of a production model for the characteristics of gases is presented in Table 3. The model establishes a mutual relationship between the type of gas on the one hand and its gas constant R_{SP} , as well as the adiabatic exponent k on the other. The adiabatic index k is necessary for calculating the critical ratio of pressures (β_{CR}), coefficients B_1 and B_3 as well as for determining the B_2 coefficient.

6 Conclusion

Thus, as a result of this study, using the analysis of regulatory and technical documentation and scientific and technical literature, as well as a system approach to the process of determining the SVs characteristics, the following were developed:

- A functional model for the selection of safety valves as an organizational and technological process, characterized by applying a system approach and taking into account the complex relationships between the various stages of determining

Table 3 Production model for gas characteristics knowledge representation

Gas	Adiabatic index k	Gas constant R_{SP} , kgf·m/(kg·°C)
Nitrogen	1.4	30.25
Butane	1.10	14.60
Hydrogen	1.41	420.00
Methane	1.30	52.6
Carbon oxide	1.40	30.25
Propane	1.14	19.25
Hydrogen sulfide	1.30	24.90
Ethane	1.22	28.2
Ethylene	1.24	30.23
Applicability conditions	Required specifications	

the SV characteristics, as well as by connecting to databases and knowledge, which allows automating the procedure for selecting the SV and providing high speed of information exchange.

- Heuristic-computational algorithms, which, with the help of predetermined initial process characteristics and production models of knowledge representation, enable automated computational and intelligent decision-making procedures for determining SV characteristics as required by regulatory and technical documentation.
- Production models for representing knowledge of the valves and gases characteristics, ensuring the operation of algorithms for calculating and selecting SV characteristics, which formalize regulatory relationships between process parameters on the one hand and SV characteristics on the other.

The developed models and algorithms will make it possible to create a CPS, the use of which will reduce the duration of the data retrieval and processing procedures, as well as the number of subjective errors, which will increase the quality of determining the structural and technological characteristics of SVs, and, consequently, the industrial safety and economic efficiency of petrochemical plants in general.

References

1. Horlacher, H.-B., Helbig, U. (Hrsg.): Rohrleitungsplanung–Grundsätze, Vorschriften, Regelwerke. Rohrleitungen 1, pp. 35–43. Springer Reference Technik.C. (2016)
2. Wu, D., Olson, D.L., Dolgui, A.: Artificial intelligence in engineering risk analytics. Eng. Appl. Artif. Intell. **65**, 433–435 (2017)
3. Russell, S.J., Norvig, P.: Artificial Intelligence: A Modern Approach, 3rd edn. Prentice Hall, New Jersey (2010)

4. Buldakova, T.I., Suyatinov, S.I.: Assessment of the state of production system components for digital twins technology. In: Kravets, A., Bolshakov, A., Shcherbakov, M. (eds.) *Cyber-Physical Systems: Advances in Design and Modelling*. Studies in Systems, Decision and Control, vol. 259. Springer, Cham (2020)
5. Stepanov, M., Musatov, V., Egorov, I., Pchelintzeva, S., Stepanov, A.: Cyber-physical control system of hardware-software complex of anthropomorphous robot: architecture and models. In: Kravets, A., Bolshakov, A., Shcherbakov, M. (eds.) *Cyber-Physical Systems: Advances in Design and Modelling*. Studies in Systems, Decision and Control, vol. 259. Springer, Cham (2020)
6. Alekseev, A.P.: Conceptual approach to designing efficient cyber-physical systems in the presence of uncertainty. In: Kravets, A., Bolshakov, A., Shcherbakov, M. (eds.) *Cyber-Physical Systems: Advances in Design and Modelling*. Studies in Systems, Decision and Control, vol. 259. Springer, Cham (2020)
7. Moshev, E., Meshalkin, V., Romashkin, M.: Development of models and algorithms for intellectual support of life cycle of chemical production equipment. In: Kravets, A., Bolshakov, A., Shcherbakov, M. (eds.) *Cyber-Physical Systems: Advances in Design and Modelling*. Studies in Systems, Decision and Control, vol. 259. Springer, Cham (2020)
8. Guo, F., Zou, F., Liu, J., Wang Z.: Working mode in aircraft manufacturing based on digital coordination model. *Int. J. Adv. Manuf. Technol.* **98**, 1547-1571. Springer, Cham (2018). <http://dx.doi.org/10.1007/s00170-018-2048-0>
9. Kim, H., Han, S.: Interactive 3D building modeling method using panoramic image sequences and digital map. *Multimedia Tools Appl.* **77**(20), 27387-27404. Springer, Cham (2018). <http://dx.doi.org/10.1007/s11042-018-5926-4>
10. Cheng, J., Liu, Z., Yu, X., Feng, Q., Zeng, X.: Research on dynamic modeling and electromagnetic force centering of piston/piston rod system for labyrinth piston compressor. *Proc. Inst. Mech. Eng. Part I: J. Syst. Control Eng.* **230**(8), 786-798 (2016)
11. Comelli, M., Gourgand, M., Lemoine, D.: A review of tactical planning models. *J. Syst. Sci. Syst. Eng.* **17**(2), 204-229 (2008)
12. Moshev, E.R., Romashkin, M.A.: Development of a conceptual model of a piston compressor for automating the information support of dynamic equipment. *Chemical and Petroleum Engineering*. vol. 49(9-10), pp. 679-685. Springer, Cham (2014). <http://dx.doi.org/10.1007/s10556-014-9818-9>
13. Elena, Nenni M.: A Cost model for integrated logistic support activities. *Adv. Oper. Res.* **2013**, 1-6 (2013)
14. Menshikov, V., Meshalkin, V., Obratsov, A.: Heuristic algorithms for 3D optimal chemical plant layout design. In: *Proceedings of 19th International Congress of Chemical and Process Engineering (CHISA-2010)*, vol. 4, pp. 1425. Prague (2010)
15. Lu, J., Zhu, Q., Wu, Q.: A novel data clustering algorithm using heuristic rules based on k-nearest neighbors' chain. *Eng. Appl. Artif. Intell.* **72**, 213-227 (2018)
16. Bertoni, M., Bertoni, A., Isaksson, O.: A value-driven concept selection method for early system design. *J. Syst. Sci. Syst. Eng.* **27**(1), 46-77 (2018)
17. Martin, P., Kolesár, J.: Logistic support and computer aided acquisition. *J. Logistics Manage.* **1**, 1-5 (2012)
18. Bogomolov, B.B., Bykov, E.D., Men'shikov, V.V. et al.: Organizational and technological modeling of chemical process systems. *Theor Found Chem Eng* **51**, 238-246 (2017). <https://doi.org/10.1134/S0040579517010043>

19. Marca, D.A.: SADT/IDEF0 for Augmenting UML, Agile and Usability Engineering Methods. In: Escalona, M.J., Cordeiro, J., Shishkov, B. (eds.) *Software and Data Technologies. ICSoft 2011. Communications in Computer and Information Science*, vol. 303. Springer, Berlin, Heidelberg (2013)
20. Meshalkin, V.P., Moshev, E.R.: Modes of functioning of the automated system “Pipeline” with integrated logistical support of pipelines and vessels of industrial enterprises. *J. Mach. Manuf. Reliab.* **44**(7), 580–592 (2015)
21. Moshev, E.R., Meshalkin, V.P.: Computer-based logistics support system for the maintenance of chemical plant equipment. *Theor. Found. Chem. Eng.* **48**(6), 855–863 (2014)

Development of a Cyber-Physical Subsystem for Support and Decision Making of Managing Oil Production and Transportation Processes Under Uncertainty Conditions



Artur Sagdatullin  and Gennady Degtyarev

Abstract In the chapter, features of data gathering, interpretation, and modeling are investigated. A model has been developed for the intellectual support of the management of oil production and transportation processes under conditions of uncertainty based on the results of the analysis of oil production equipment. The existing data model for individual oil field facilities is analyzed. An algorithm for the operation of a neural network model is proposed to predict an important characteristic of an object—profitability. The algorithm is improved based on the optimization block, which performs the role of classifying and identifying features in existing data based on the p-criterion. The proposed system algorithms are designed to make decisions when performing various types of operations in the field. The proposed decision support subsystem for managing oil production and transportation processes under conditions of uncertainty has shown the efficiency of profitability prediction at the level of 73.5%.

Keywords Oil field · Production well · Neural network model · Architecture · Information system · Profitability · Optimization

1 Introduction

Cyber-physical systems are playing an increasingly important role in the management of technological processes such as transportation and oil preparation. So, the algorithms used to model and predict the behavior of a real object, for example, neural networks, fuzzy logic, and their various variations, can have a significant positive impact on the nature, performance, and profitability of the processes in the oil industry. The use of digital modeling technologies in the oil industry allows us to solve many complex problems. For example, digital models are used to predict risks, automate production, and optimize waterflooding systems and field conditions [1–10]. Among the existing developments, it should be noted systems are

A. Sagdatullin (✉) · G. Degtyarev
Kazan National Research Technical University named after A. N. Tupolev—KAI, K.
Marx St. 10, Kazan 420111, Russia
e-mail: saturn-s5@mail.ru

based on models of neural networks, probabilistic methods, and fuzzy logic [11–20]. The development of systems will further improve the efficiency and productivity of technological processes for the extraction and transportation of petroleum products. However, in the context of the increasing complexity of the methods for producing and developing fields, which is primarily associated with a significant water cut of the produced products and various factors affecting the physicochemical structure of the oil, significant uncertainties are beginning to appear that accompany the process of extraction and transportation of oil and oil products. These uncertainties can be associated with changes in physical or chemical properties, temperature fluctuations, as well as changes in equipment operating modes. As a result, existing systems for managing industrial oil production facilities can operate in areas that depart from the nominal ones, which leads to energy losses and unproductive expenses. Under existing conditions, it is proposed to use cyber-physical subsystems [12, 13, 15, 18, 20], which can analyze non-linear processes, as well as multidimensional data models. In this chapter, questions will be raised regarding the development of a particular subsystem of cyber-physical systems, which represents the integration of computational processes and data on a real physical system. Thus, it is urgent to develop an integrated cyber-physical system consisting of computing units and real data on the physical process with the continuous receipt and use of current and accumulated information to optimize the management processes for oil, gas, and water production and transportation facilities.

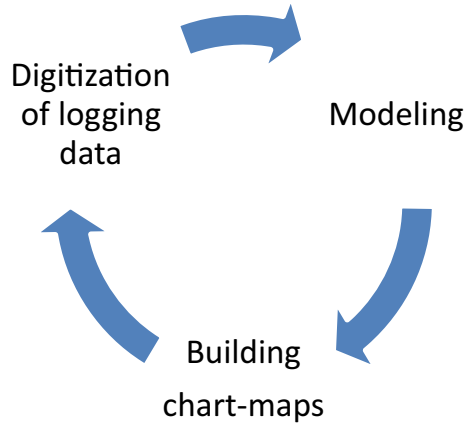
Formulation of the problem. To develop an intelligent decision support subsystem for managing oil production and transportation processes in the face of uncertainty, as well as analyze its operation, the following tasks need to be solved:

1. Description of existing and developing methods and models for predicting mining characteristics of downhole equipment.
2. The construction of a model describing the dependence of the reduced production characteristics over time.
3. Interpretation of the results and analysis of the developed algorithms.

2 Description of Existing and Developing Methods and Models for Predicting the Production Characteristics of Downhole Equipment

One of the main ways to support the management of oil production and transportation processes in the face of uncertainty is the development of geological models. Model development is based on the collection of information about the object, such as field tests, geological and geophysical studies of the reservoir and wells. Modeling allows you to reflect the dynamics of production, to predict certain measures to increase the efficiency of development, to calculate many of their options, and choose the most profitable. An analysis [21] of the creation of such models showed that the main stages of their creation are: digitization of logging data, correlation, interpretation

Fig. 1 The process of creating a geological model



of geological data, modeling, obtaining results, and plotting maps, which can be reflected in the following graph (Fig. 1).

It is possible to note the features of the method that affect the accuracy of forecasting and development efficiency as a whole: the difficulty of obtaining relevant information about objects and technological processes, the “discontinuous” nature of the data, the costs of obtaining and updating the database, as well as a significant time gap between measurements.

One of the promising methods that can improve the quality of existing models is artificial neural networks.

3 Building a Model Describing the Dependence of the Reduced Production Characteristics Over Time

Among the well-known methods for solving problems, the development of a cyber-physical subsystem based on artificial neural networks (ANN) was chosen [11–13, 15, 18, 19, 25], which will be used to refine and adjust the models used in oil production. The scientific novelty of the proposed cyber-physical decision support subsystem for managing oil production and transportation processes in the face of uncertainty is that in a model based on neural network methods, coefficients are adjusted that reflect:

- water cut of injected liquid;
- technological modes;
- work of injection wells.

Based on the adjusted parameters, the neural network corrects the weight coefficients, which allows us to predict various options and technological modes of operation of the wells.

For example, consider the task of multivariate analysis of information about a field and objects located on the surface (Fig. 2). The information is a model of the various characteristics given, reflecting the dynamics of the oil well production, and their performance characteristics for one area.

The model consists of 30 columns characterizing various parameters of the down-hole equipment, as well as 1000 rows - parameter values with a display period of one hour. The dependence for the presented values (from 24 to 29 wells) in time can be represented in the form (Fig. 3).

	0	1	2	3	4	5	6	7	8	9	10	11
0	1.0	2.314246	3.769363	5.075229	3.686145	6.779463	4.983996	3.190300	3.329130	2.793481	5.198414	3.142064
1	0.0	0.008046	1.874479	2.290018	0.645221	3.260678	2.026647	1.733029	0.684999	0.719652	2.264911	1.347627
2	1.0	1.267164	1.224649	1.754363	1.733204	2.252532	1.823014	0.970453	1.519227	1.209469	1.833326	1.117737
3	1.0	2.927081	5.258729	7.018861	4.829159	9.428980	6.834051	4.489528	4.388430	3.720570	7.167928	4.326858
4	1.0	1.849879	6.350670	8.131473	4.080473	11.223620	7.586863	5.637773	3.868648	3.505956	8.184153	4.908447

Fig. 2 A model of the given characteristics reflecting the dynamics of production for various wells of the same area

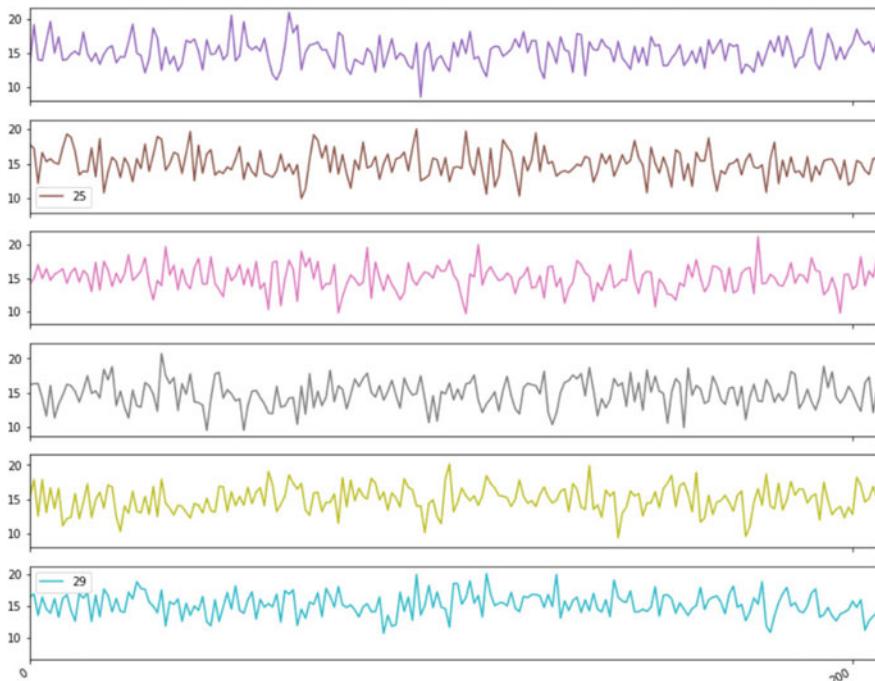


Fig. 3 Dependence of reduced production characteristics for the presented values (from 24 to 29 wells) over time

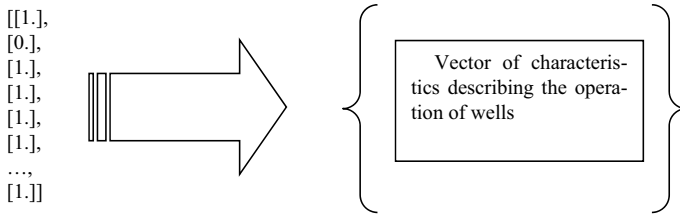


Fig. 4 The vector of initial input data, where units reflect the fact that the object is profitable and zeros are unprofitable

The main essence of the problem is to determine the profitability of a mechanized object for further operation, which determines the following column vector with a size of (1000×1) (Fig. 4):

The given dependence of the studied production characteristics for $24 \div 29$ parameters is presented for an interval of ~ 210 h. Now the task of constructing a model is reduced to displaying the predicted values of the variables through the range of probability density functions of the possible values of the studied characteristics. So, the values of time t and parameters $\zeta(t)$ of a random process $x(t)$ are discrete, which allows us to consider the process as a discrete process with a multidimensional distribution function [22–25]:

$$F_{(\zeta_1, \dots, \zeta_n)}(t_1, \dots, t_j) = \sum_{i,j} P (\zeta_1 = \zeta_{1i}, \dots, \zeta_n = \zeta_{ij}),$$

where $\zeta_1, \dots, \zeta_{ij}$ —are the values of the discrete set.

The joint probability distribution density:

$$F(\zeta_1, \zeta_2, \dots, \zeta_n) = \int_{-\infty}^{\zeta_1} \int_{-\infty}^{\zeta_2} \dots \int_{-\infty}^{\zeta_n} f(\zeta_1, \zeta_2, \dots, \zeta_n) d\zeta_1, d\zeta_2, \dots, d\zeta_n,$$

The distribution densities of individual random variables $\times 0 \dots \times 29$ can be obtained by differentiating the equations for each of the parameters:

$$\left\{ \begin{array}{l} \int_{-\infty}^{+\infty} f(\zeta_1, \zeta_2, \dots, \zeta_n) d\zeta_2 = f_1(\zeta_1) \\ \int_{-\infty}^{+\infty} f(\zeta_1, \zeta_2, \dots, \zeta_n) d\zeta_3 = f_1(\zeta_2) \\ \dots\dots\dots \\ \int_{-\infty}^{+\infty} f(\zeta_1, \zeta_2, \dots, \zeta_n) d\zeta_{n+1} = f_n(\zeta_n) \end{array} \right.$$

Based on these equations, it becomes possible to interpret the problem being solved through a probability function that includes an estimate of the probability density of a random variable from the set of data predicted based on the developed models [12]. The software algorithm is presented in Fig. 5, the work of which begins with the collection of information (block 1). Data acquisition unit 2 automatically downloads the incoming information and performs a preliminary analysis for the

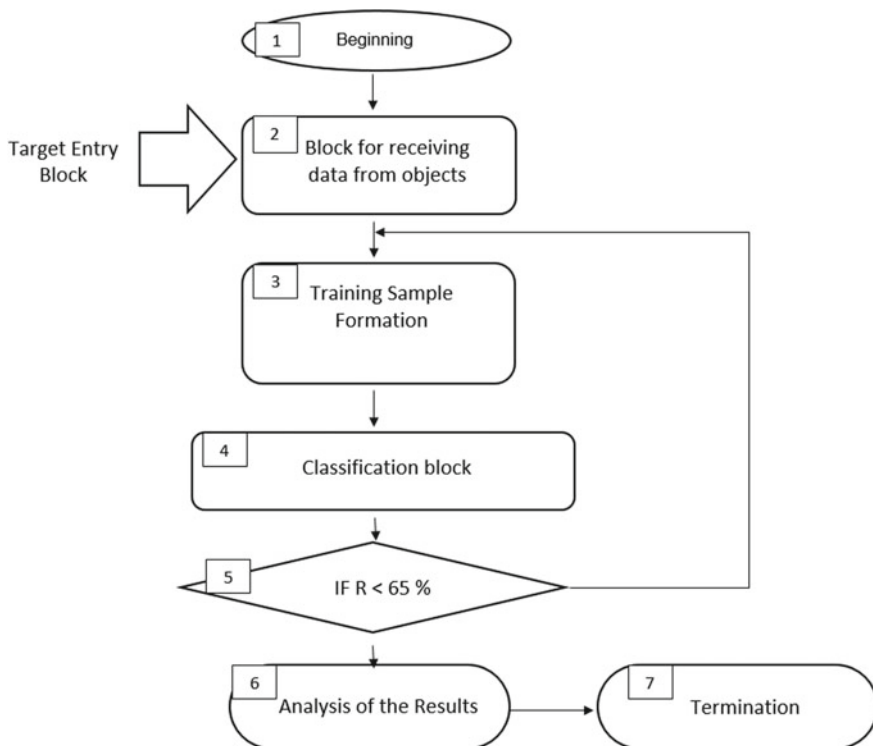


Fig. 5 The block diagram of the algorithm

lack of data. The incoming information is represented by an array containing 1000 rows, reflecting the hours of operation of the equipment, as well as 30 columns - its characteristics. Also, this block receives input data based on which the model will be trained. The initial data are presented by categories – “0” or “unprofitable”, and also “1” – “profitable”.

All categorical information after block 2 is separated from the main data block and the algorithm forms a separate vector. Further, the separated ones are divided into test and training ones in block 3 and block 4, classification is performed, which is about 50 training epochs of the resulting neural network model. In block 5, a comparison is made with a given criterion for the quality of the model (the predictive ability of the developed model should be at least 65%), and in block 6, the results are analyzed and interpreted.

An analysis of the results of the obtained model showed that the ability of the cyber-physical subsystem to predict the profitability of existing equipment is 68%. On sufficiently unstructured data and taking into account uncertainties, this is a pretty good result. However, it is possible to improve the cyber-physical subsystem model without significantly changing its overall structure. To improve the operation of the algorithm, a new structure is proposed, the feature of which is the presence of a block for selecting important characteristics (Fig. 6). The block of a selection of important

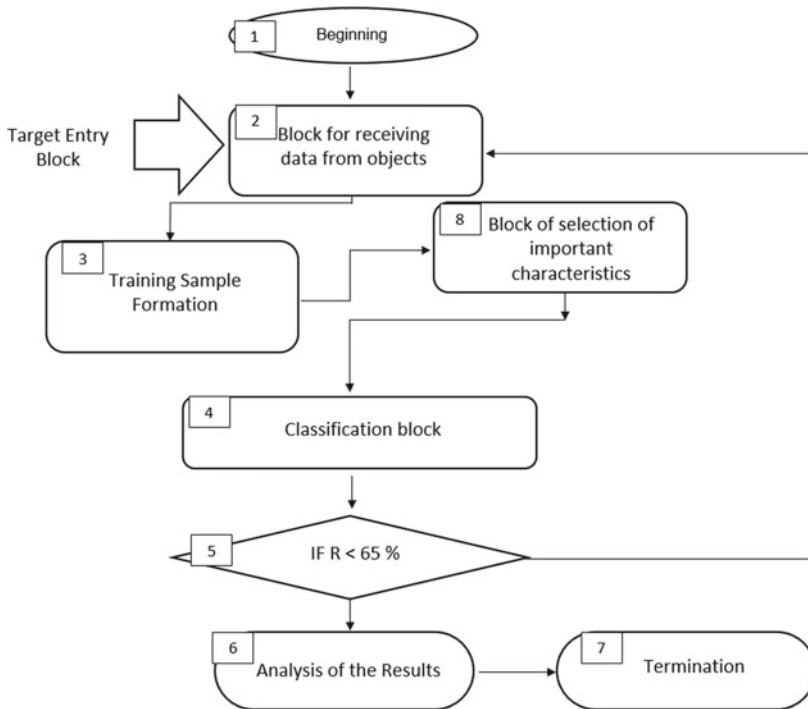


Fig. 6 The block diagram of the improved algorithm

characteristics 8 is responsible for the selection of important characteristics of the data that have the greatest impact. The basis of the algorithm is the p-test and the null hypothesis, showing the probability that there is no reason to take into account the data and the relationships between the measured values. The P-test allows us to determine the probability that if the null hypothesis is true, then statistical observations will be higher or equal to a given value. In the experiment, the statistic value is 0.05.

4 Interpretation of Results and Analysis of Developed Algorithms

The result showed that the data presented have two of the most important characteristics (Fig. 7).

The graphs visualize the characteristics selected for block 8, where “nor” is an unprofitable object, and “ren” is a cost-effective object.

The result of the cyber-physical subsystem algorithm showed that the ability to predict the block has increased and amounts to 73.5%.

Conclusions. The analysis of the existing approach to the development of the cyber-physical subsystem model showed that the difficulty of obtaining relevant data on objects and technological processes, the discontinuous nature of the data, the costs of obtaining and updating the database, and the significant time gap between the data obtained reduce the accuracy of the model and its predictive characteristics.

The study of the obtained source data showed that the information obtained is an unstructured model with various reduced characteristics that reflect the dynamics of oil well production, the characteristics of their work for one area, and the model itself is multidimensional. The search for a method for studying the dependence of the reduced characteristics of the production of the presented values in time has shown that a cyber-physical subsystem based on the work of neural network models

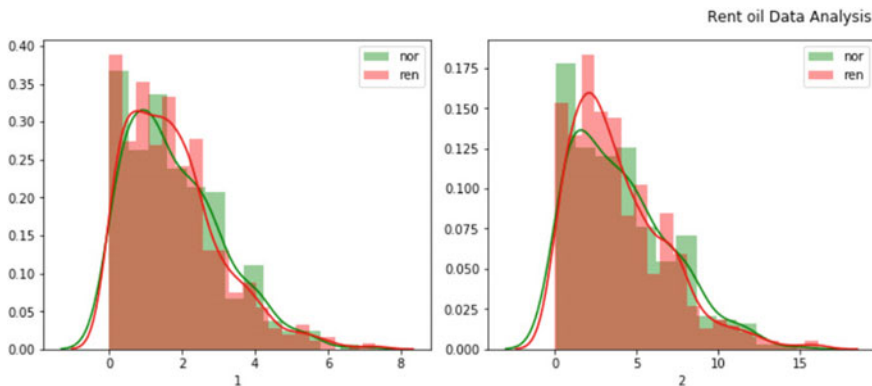


Fig. 7 Characteristics selected for block 8 parameters

can be effectively used to analyze unstructured data, it can successfully analyze non-linear data and identify the operation of wells. A model of the cyber-physical subsystem created based on the program's operation algorithm, including 30 columns characterizing various parameters of the downhole equipment and 1000 rows of parameter values with a display period of one hour, making it possible to increase the ability to forecast the profitability of existing equipment from 68 to 73.5%.

5 Conclusion

Thus, the objects of oil production of the oil field are investigated in the work. The proposed model of the cyber-physical subsystem of the intellectual support for controlling the processes of oil production and transportation in the face of uncertainty is intended to make decisions in the development of fields and determine a workable fund. An algorithm has been developed to determine the profitability of an individual well. The ability to predict the profitability of the well, according to the data obtained under uncertainty, is 73.5%. According to the developed algorithms and the architecture of the intellectual system, the blocks and algorithms for improving the operation of the system are created, necessary to improve the quality and predictive capabilities of the software.

References

1. Shah, N., Mishra, P.: Oil production optimization: a mathematical model. *J. Petrol Explor. Prod. Technol.* **3**, 37–42 (2013). <https://doi.org/10.1007/s13202-012-0040-z>
2. Dake, L.P.: The practice of reservoir engineering, revised edition, developments in petroleum science. Elsevier, London (2004)
3. Sagdatullin, A.M.: Development of mathematical model and technological process flow diagram of delivery of reagent in initial treatment of oil production of wells in separator tanks. *Chem. Pet. Eng.* **55**, 884–887 (2020). <https://doi.org/10.1007/s10556-020-00708-9>
4. Vajk, I., Hetthéssy, J., Bars, R.: In: Control Theory for Automation—Advanced Techniques. Springer Handbook of Automation. pp. 173–198 (2009) https://doi.org/10.1007/978-3-540-78831-7_10
5. Ossai, C.I.: Modified spatio-temporal neural networks for failure risk prognosis and status forecasting of permanent downhole pressure gauge. *J. Petroleum Sci. Eng.* **184**, 106496 (2020)
6. Sagdatullin, A.: In: Development of an Intelligent Control System Based on a Fuzzy Logic Controller for Multidimensional Control of a Pumping Station. *Advances in Intelligent Systems and Computing*. vol. 1127 AISC, pp. 76–85. (2020)
7. Epelle, E.I., Gerogiorgis, D.I.: Mixed-integer nonlinear programming (MINLP) for production optimisation of naturally flowing and artificial lift wells with routing constraints. *Chem. Eng. Res. Des.* **152**, 134–148 (2019)
8. Sagdatullin, A.M.: Development of a start-up model of a submersible electric motor when the electric centrifugal pump is installed and set to operating mode. In: Proceedings of 1st International Conference on Control Systems, Mathematical Modelling, Automation and Energy Efficiency, SUMMA, 8947544, pp. 456–460 (2019)

9. Li, K., Xu, W., Han, Y.: A hybrid modeling method for interval time prediction of the intermittent pumping well based on IBSO-KELM. *Measurement* **151**, 107214 (2020)
10. Gonzalez, D., Stanko, M., Hoffmann, A.: Decision support method for early-phase design of offshore hydrocarbon fields using model-based optimization. *J. Petroleum Explor. Prod. Technol.* <https://doi.org/10.1007/s13202-019-00817-z>
11. Yang, B., et al.: Production optimization for water flooding in fractured-vuggy carbonate reservoir—from laboratory physical model to reservoir operation. *J. Petrol. Sci. Eng.* **184**, 106520 (2020). <https://doi.org/10.1007/s13202-019-00817-z>
12. Mamudu, A., Khan, F., Zendeheboudi, S., Adedigba, S.: Dynamic risk assessment of reservoir production using data-driven probabilistic approach. *J. Petroleum Sci. Eng.* **184**, 106486 (2020). <https://doi.org/10.1016/j.petrol.2019.106486>
13. Andryushin, A., Shcherbatov, I., Dolbikova, N., Kuznetsova, A., Tsurikov, G.: Outlier detection in predictive analytics for energy equipment. In: *Cyber-Physical Systems: Advances in Design and Modelling. Studies in Systems, Decision and Control.* vol. 259, pp. 193–203. (2019)
14. Monteiro, D.D. et al.: Using data analytics to quantify the impact of production test uncertainty on oilflow rate forecast. *Oil and Gas Sci. Technol.–Rev. IFP Energ. Nouvelles* **75**, 7 (2020). <https://doi.org/10.2516/ogst/2019065>
15. Xiaofeng, Li.: Application of fuzzy mathematics evaluation method in prediction of comprehensive efficiency of low efficiency oil wells. *IOP Conf. Ser.: Earth Environ. Sci.* **384**, 01201 (2019). <https://doi.org/10.1088/1755-1315/384/1/012012>
16. Song, X., Liu, Y., Xue, L., Wang, J., Zhang, J., Wang, J., Jiang, L., Cheng, Z.: Time-series well performance prediction based on long short-term memory (LSTM) neural network model. *J. Petroleum Sci. Eng.* **186**, 106682 (2020). <https://doi.org/10.1016/j.petrol.2019.106682>
17. Schiozer, D.J. et al.: Oil and Gas Science and Technology–Rev. IFP Energies nouvelles **74**, 46 (2019). <https://doi.org/10.2516/ogst/2019019>
18. Wei, L., Wei, D.L., Jianwei, G.: Predictive model for water absorption in sublayers using a Joint Distribution Adaption based XGBoost transfer learning method. *J. Petroleum Sci. Eng.* **188**, 106937 (2020). <https://doi.org/10.1016/j.petrol.2020.106937>
19. Moshev, E., Meshalkin, V., Romashkin, M.: Development of models and algorithms for intellectual support of life cycle of chemical production equipment. In: Kravets, A., Bolshakov, A., Shcherbakov, M. (eds.) *Cyber-Physical Systems: Advances in Design and Modelling. Studies in Systems, Decision and Control*, vol. 259, pp. 153–165. (2019). https://doi.org/10.1007/978-3-030-32579-4_12
20. Yang, Renfeng, et al.: The injectivity variation prediction model for water flooding oilfields sustainable development. *Energy* **189**, 116317 (2019). <https://doi.org/10.1016/j.energy.2019.116317>
21. Liu, W., Liu, W.D., Gu, J.: Forecasting oil production using ensemble empirical model decomposition based Long Short-Term Memory neural network. *J. Petroleum Sci. Eng.* **189**, 107013 (2020). <https://doi.org/10.1016/j.petrol.2020.107013>
22. Wriggers, P., Kultsova, M., Kapysh, A., Kultsov, A., Zhukova, I.: Intelligent decision support system for river floodplain management. In: *Knowledge-Based Software Engineering. JCKBSE 2014. Communications in Computer and Information Science.* vol. 466, pp. 195–213 (2014). https://doi.org/10.1007/978-3-319-11854-3_18
23. Sagdatullin, A.: Improving automation control systems and advantages of the new fuzzy logic approach to object real-time process operation. In: *2019 1st International Conference on Control Systems, Mathematical Modelling, Automation and Energy Efficiency (SUMMA)*, vol. 8947538, pp. 256–260 (2019). <https://doi.org/10.1109/summa48161.2019.8947544>
24. Korolov, L., Sinai, Y.: *In: Theory of Probability and Random Processes.* Springer, Berlin, Heidelberg, Corr., 2nd printing (2012). <https://doi.org/10.1007/978-3-540-68829-7>
25. Shcherbakov, M.V., Glotov, A.V., Cheremisinov, S.V.: Proactive and predictive maintenance of cyber-physical systems. In: *Cyber-Physical Systems: Advances in Design and Modelling. Studies in Systems, Decision and Control.* vol. 259, pp. 263–278. (2019). https://doi.org/10.1007/978-3-030-32579-4_21

Modeling of Vacuum Overhead System for Amine Mixtures Separation Unit



Eduard Osipov , Eduard Telyakov, and Daniel Bugembe 

Abstract The analysis of indicators of the distillation units for the separation of mixtures that operate at close values of the residual pressure of the top is considered. To reduce the cost of conducting vacuum pumps, it was proposed to replace individual vacuum pumps with a liquid ring vacuum pump. Using the Unisim software, the calculated models of the column and the vacuum overhead system were synthesized, as well as a feasibility study of the proposed solutions.

Keywords Vacuum overhead systems · Liquid ring vacuum pumps · Steam jet pumps · Separation of mixtures of ethanolamine · Universal modeling programs

Abbreviation

CCC	Chemically contaminating condensate
MEA	Monoethanolamine
DEA	Diethanolamine
TEA	Triethanolamine
LRVP	Liquid ring vacuum pump
SEP	Steam ejector pump
VOS	Vacuum overhead system
UMP	Universal modeling program
P	Pressure mm Hg
T	Temperature °C
V	System volume, m ³
B, C	Coefficients depending on the pressure inside the evacuated system
W	The amount of sucked air, kg/h

E. Osipov (✉) · E. Telyakov · D. Bugembe
Kazan National Research Technological University, 68 Karl Marx Street, Kazan 420015, Russia
e-mail: eduardvosipov@gmail.com

E. Telyakov
e-mail: tesh1939@mail.ru

D. Bugembe
e-mail: danielsmurts@gmail.com

Indices

*	Calculated values
N	Initial
K	Is finite normal standardized
sl	Service liquid

1 Introduction

Currently, when designing complex technological objects, the methods of cyber-physical modeling are actively applied, which allows you to virtually simulate a real technological object, reduce the design time and improve the quality of the proposed design solutions [1]. However, when modeling such objects, the question of the adequacy of the developed mathematical model and its “connection” with the real object must be carefully worked out, otherwise, the results will be unreliable.

In addition, during the stages of studying the properties of the object and the optimal conditions for its operation, it is necessary to determine the range of variation of the input process variables, which must coincide with the conditions in which the modeling object will be operated.

This chapter discusses the problem of reconstructing a vacuum system in distillation columns of the process for the production of ethanol-ammonia hydroxyethylation ammonia using water as a catalyst. Due to the low thermal stability of the components to be separated, as well as to the rather stringent requirements for the products obtained, the rectification process is carried out under vacuum, while the residual pressure reaches 5 mmHg. It is advisable to carry out the solution to this problem using computer facilities and specialized software systems designed for modeling complex chemical-technological systems.

2 Structural Analysis of the Considered Production Facility

To create an adequate cyber-physical model, it is necessary to conduct a structural analysis of the studied object [2]. At the production facility in question, the separation of the amine mixture into the target products is carried out in three distillation columns- K-40, K-56, and K-92, equipped with four-stage Steam Jet pumps, the working medium of which is medium-pressure water vapor. The structural diagram of the production facility in question is presented in Fig. 1.

In the pipe space of the SJP intermediate capacitors, “cooled” circulating water is supplied, and condensate and non-condensed gases are discharged from the annular space. Thus, during the operation of SJP, the following energy resources are consumed—water vapor and recycled water. Since the working fluid and the pumped

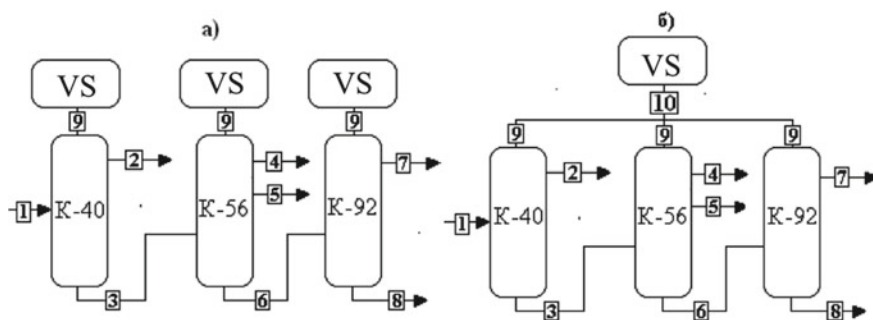


Fig. 1 Structural diagrams of the existing **a** and proposed **b** blocks. Streams: 1—the bottom product of column 29; 2—MEA stream; 3—DEA brand B; 4—MEA + water; 5—DEA brand A; 6—TEA; 7—TEA brand A; 8—the remainder; 9—gas flow to the VS from the columns; 10—total flow to the VS

medium containing ethanol-amines are displaced in the ejector, the condensate leaving the SJP can be considered as chemically contaminated.

Based on all of the above, it can be concluded that concerning the production facility under consideration, the SJP is obsolete and non-environmentally friendly, so replacing it with a modern energy-efficient and environmentally friendly VOS is an urgent task. When assessing the feasibility study of the proposed solution to improve the existing VOS, it is necessary to take into account the costs of the enterprise for the production of steam and circulating water, as well as for utilization of the CCC. Prices for these resources are presented in Table 1 [3].

Based on the experience of carrying out such works [4–6], the most optimal solution for the reconstruction of existing VOSs is to replace SJPs with a single VOS, based on the Liquid Ring Vacuum Pump, for all the columns. The proposed block diagram is shown in Fig. 1b.

To determine the layout of the proposed VOS, it is necessary to calculate the flow rate and composition of the mixture supplied to the suction of the vacuum pump, that is, determine the load on the VOS. This load will be determined by the condensation conditions in the annular space of the “tail capacitors”, which depend on the operating conditions of the installation. The parameters that determine the effectiveness of the condensation of the medium are the temperature and pressure in the annulus, which are not directly measured and not controlled at the facility. Therefore, these tuning

Table 1 Energy prices

Resource name	Value	Unit
Water vapor	1070	Rub/Gcal
Circulating water	1.5	Rub/m ³
Electric power	3	Rub/kW
Cleaning chemically contaminated condensate	11.6	Rub/m ³

parameters of the mathematical model are selected according to the results of the installation survey [6–9].

3 Design Diagrams of the Basic Elements of the Unit

The design scheme of the distillation unit. After the distillation of water and residual ammonia in the K–20 apparatus, the dehydrated stream of ethanolamines is supplied between the second and third sections of the nozzle of the K–40 column and is divided into mono-ethanolamine (distillate) and B grade diethanolamine (bottoms). Non-condensing vapors in the reflux condenser enter the tail condenser, which is cooled by the flow of a refrigerated refrigerant. Those gases that were not condensed in the tail condenser are pumped out by a four-stage steam ejection vacuum pump, which creates a vacuum in the distillation column.

As noted above, the distillation unit was simulated in the Unisim universal modeling program (UMP), in which the design scheme (cyber-physical model) of the columns was synthesized (Fig. 2).

The main task of computer modeling of this process was to determine the composition and flow rate of gases entering the VOS. To calculate the column in the program database, there are various modules of distillation columns, whose inherent mathematical descriptions differ from each other. Based on the recommendations of the program, the Distillation column module was used to calculate the column. For the convergence of the calculation, the following data must be entered into the module specifications: column pressure, differential pressure, the number of theoretical plates, condenser, and cube operating modes.

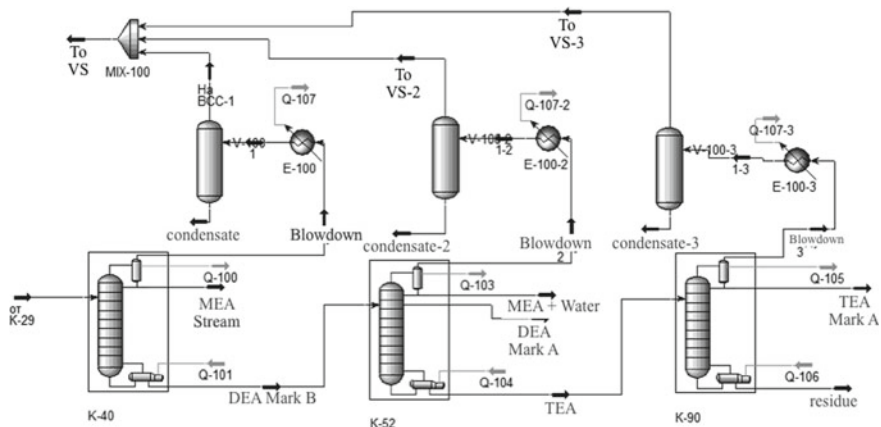


Fig. 2 The design scheme of the block separation of mixtures of amines synthesized in UMP Unisim

The pressure in the column was set based on production data. Since the capabilities of the module allow you to enter the parameters of contact devices, and the database contains the geometric and mass transfer characteristics of various nozzles, the type of nozzle was set in the module, and the efficiency and pressure drop in the column were calculated by the program. Tail capacitors were set by Separator and Cooler modules, in which final temperatures of heat carriers were set. It was this module that formed the flow going to the VOS.

Next, the bottom residue of the K-40 column enters the K-52 column, which is designed to produce grade A diethanolamine, which is removed from the unit by side distillation. Vapors of water, MEA, and DEA from the top of the column are condensed in a reflux condenser and discharged to a collection tank, from which part of the condensate is returned to the type of reflux irrigation. Non-condensing vapor in the reflux condenser enters the "tail" capacitor, which forms the final load on the VOS. The heat required for the rectification process is supplied to a film evaporator heated by steam.

The distillation unit was simulated using the same modules as the K-40 column, except that side sampling, which was set by the sampling plate and mass flow rate, was added to the specification of module 2. Numerical values were set in such a way as to ensure compliance with production values.

The K-92 column is designed to produce grade A triethanolamine with improved performance in appearance from the bottom liquid of the K-56 column. Power is supplied to a distribution plate located between the layers of the nozzle. Heat is supplied through a film evaporator, vapors from the column enter the reflux condenser, condense and drain onto a blank plate. The resulting liquid is partially returned to the column as reflux, and the distillate is removed from the installation.

A comparison of design parameters with production data is presented in Tables 2 and 3.

The calculation data is in concordance with the technological parameters of the column, therefore, we can conclude that the models are adequate and the calculation data is correct as per the studied range.

Table 2 Technological parameters of the column and calculation data for the K-40 column

Stream name	Composition, mass. fraction.				Temperature, °C	Consumption, kg/hr
	Water	MEA	DEA	TEA		
Distillate	0.001–0.2	0.98–0.999	0.009–0.07	–	30–40	900–1340
Distillate*	0.001	0.99	0.009	–	35	1247
Feed	0.0004	0.502	0.317	0.1806	60–100	1900–2700
Feed*	0.00037	0.501	0.313	0.181	90	2554
Bottom residue	0.0001–0.003	0.015–0.037	0.55–0.72	0.39–0.48	141–150	1000–1360
Bottom residue*	–	0.0158	0.621	0.361	142	1285

* denotes simulation data

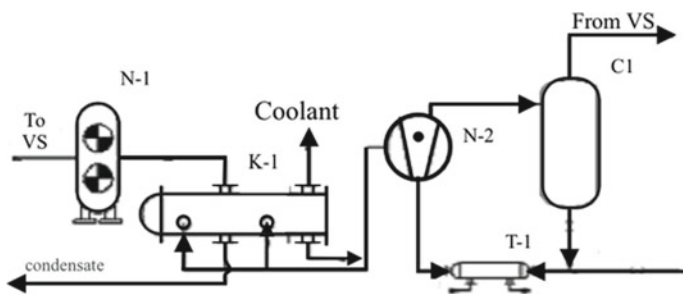
Table 3 Technological parameters of the column and calculation data for the K–56 column

Stream name	Composition, mass. fraction.				Temperature, °C	Consumption, kg/hr
	Water	MEA	DEA	TEA		
Distillate	0.001–0.002	0.29–0.79	0.29–0.79	≤0.0005	70–90	550–750
Distillate*	–	0.11	0.89	–	90	323
Reflux	0.001–0.002	0.29–0.79	0.29–0.79	≤0.0005	60–80	350–650
Reflux*	–	0.11	0.89	–	80	367
Side selection	0.1	0.006–0.01	0.98–0.992	0.001–0.002	140–160	480–660
Side selection*	–	0.0012	0.985	0.014	147	546
Feed	0.001–v0.002	0.018–0.035	0.50–0.72	0.38–0.47	95–v105	800–1100
Feed*	0.001	0.035	0.72	0.244	105	1100
Bottom residue	0.001–0.002	0.001–0.002	0.65–0.9	0.90–0.945	195–205	320–440
Bottom residue*	–	–	0.75	0.925	205	320

* denotes simulation data

The design scheme of VOS (Fig. 3). Existing VOSs are four-stage steam-jet vacuum systems that are installed on each column. Each SJP is designed to pump out 10 kg/h of the mixture (9.5 kg/h of air and 0.5 kg/h of amines) with a residual pressure at the inlet of 1 mmHg. However, according to production data, at the moment, the residual pressure in the vacuum columns is 8–12 mmHg, which indicates that the VOS is currently operated in the zone of significant overload. The most probable reason for this is the mismatch of production conditions with the characteristics of VOS [10].

Measurement of the residual pressure at the suction in the VOS with a standard pressure gauge showed that it is -1 kg/cm^2 (gauge), which indicates a “scale” of the device. Therefore, the assembly of the VOS on the characteristics of the existing SJP can lead to significant errors.

**Fig. 3** Proposed VOS scheme

As noted above, the optimal solution to the problem of reconstructing VOS at this production facility is to replace existing SJPs with a single vacuum-generating system based on the Liquid Ring Vacuum Pump. Since the residual pressure at the inlet of the LRVP is limited by the pressure of saturated vapors of the service fluid, it is advisable to install a pre-drawn vacuum pump in front of the LRVP, which would pre-compress the pumped mixture. Mechanical booster pumps are well suited for this purpose [11].

The pumped-off mixture enters the suction in a mechanical booster pump N-1, is compressed and fed into a shell-and-tube vacuum condenser K-1, into which tube “cold” water is supplied. A part of the water vapor condenses, and the rest of the vapor is sucked into the Liquid Ring Vacuum Pump, where the distillate of the vacuum column is used as a service fluid, which is recycled through a T-1 heat exchanger, into which the “chilled” water is also supplied to the pipe space.

For the right choice of Liquid Ring Vacuum pump, the problem arises of recalculating the passport characteristics of the machine to new operating conditions [10, 11]. Various methods, for example, in [11–17, 19], describe the recalculation of passport characteristics when pumping out dry air or air saturated with water vapor at a temperature of 20 °C, while water is used as a service fluid. Since the composition of the pumped gas contains a large amount of water and amine vapors, and as a service fluid, it is most appropriate to use a distillate of a vacuum column.

In the Unisim software package, there is no LRVP model; therefore, in [18], a cyber-physical study of the processes occurring in the LRVP was carried out, the results of which were integrated into the calculation process scheme.

4 Calculated Study of the Main Units

Since the suction pressure in the VOS was not precisely determined, and the required pressure at the top of the vacuum columns should be no more than 5 mmHg, the required pressure was fixed at the top of the column, and the condensation pressure, based on production data, was taken to be 3 mmHg. An analysis of the characteristics of steam ejection pumps according to the GIPRONEFTEASH catalog [17] shows that the amount of mixture supplied to the suction in each SJP is 11.5 kg/h of the mixture at a pressure of 3 mmHg. Therefore, the flow rate of leakage gases introduced into the column in a separate stream was determined based on the conditions for achieving a flow rate of non-condensable gases equal to 11.5 kg/h. The results of a numerical study are presented in Fig. 4 a–c.

Thus, 0.6 kg/h of atmospheric air enters the K-40 column, 8.7 kg/h of K-56, and 0.8 kg/h to the K-92 column. Since the K-40 and K-92 columns are close in terms of their hardware and technology design, the flow of leaking gases turned out to be almost the same. Column K-56 has an additional lateral selection, therefore, the amount of leaking air is greater.

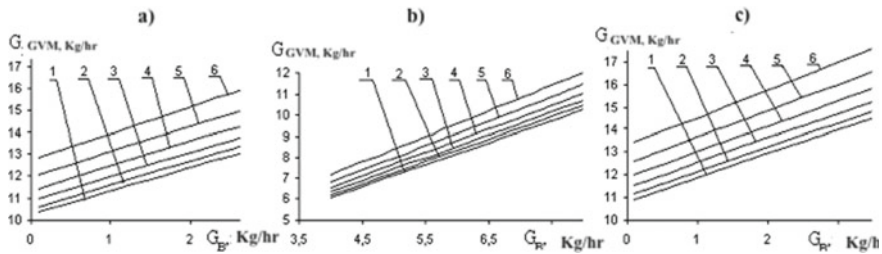


Fig. 4 Dependence of the yield of non-condensed gases on the flowing air for K40 **a**, K-56 **b** and K-92 **c** at various temperatures: 1—at a temperature of 10 °C; 2—at 13 °C; 3—at 16 °C; 4—at 19 °C; 5—at 22 °C; 6—at 25 °C

5 Defining the Arrangement of Reconstructed VOS

Thus, the total load on the VOS will be 9600 m³/hour of the mixture, which will mainly consist of air and water vapor. Despite the fact that it is supposed to use a vacuum column distillate as a service liquid for the liquid ring vacuum pump, the pump will not develop a residual suction pressure below 30 mmHg, therefore, the booster pump must be selected so that the compression ratio of the mixture is at least 10–12.

As the compression ratio increases, the volumetric capacity of the pump decreases. Since these data are a trade secret of manufacturers, for a preliminary assessment, you can take a margin of productivity of about 20–30% and assign a compression ratio of 12 and use these values to determine the required standard sizes of equipment.

The pairing conditions between the upstream booster pump and the LRVP will be determined by the temperature and condensation pressure of the annulus of the K-1 vacuum condenser. Therefore, to determine the size of the capacitor and the condensation conditions of the mixture, a numerical experiment was conducted in which the condensation temperature was changed. The results are shown in Fig. 5.

From the graph, it follows that the minimum load on the VOS will be 300 m³/hour. To pump out such a quantity of medium, LRVP 65320 is suitable, the characteristics of which must be recounted under new conditions. On the computational model, LRVP was modeled per the provisions of [16]. The temperature of the evacuated gas was fixed in the model, and for each specific point of the capacitor characteristic (curves 1–3), the performance of the liquid ring vacuum pump was determined (curves 1'–3'). The points where these curves coincide are the mating points.

Thus, at the accepted condensation temperature in K-1, $t = 20$ °C and $t_{sl} = 18$ °C, the characteristics mate at $P = 30$ mmHg. This means that the pump N-1 must provide compression of the mixture to $P = 30$ mmHg, and the compression ratio will be 10. However, to achieve these conditions, it is necessary to bring the “refrigerated” refrigerant to the VOS, which increases the capital and operating costs for the process of evacuating the system.

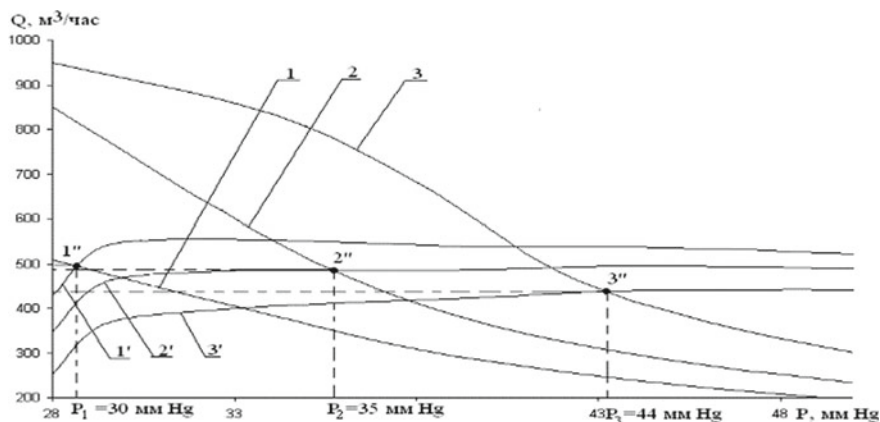


Fig. 5 The output of non-condensed gases from the K-1 condenser and the characteristics of the LRV depending on pressure: curves 1, 2, 3—the output of non-condensed gases at temperatures of 20, 24 and 28 °C, respectively; 1', 2' and 3' are the characteristics of the LRV LPH 56320 at $t_{sl} = 18, 21, \text{ and } 25$ °C, respectively

6 Feasibility Study

To achieve optimal technical and economic indicators, the standard size of the equipment was determined at point 2''. Standard sizes of selected equipment are presented in Table 4.

Total in total for columns K-40, K-56, and K-90: formed: 0.6 m³/h of chemically polluted effluents; 516 kg/h (0.35 Gcal/hr) of medium pressure steam is consumed; circulating water –30 m³/hr.

The economic effect is planned to be obtained by eliminating the use of water vapor, reducing the consumption of recycled water, and eliminating the formation

Table 4 Parameters of the selected equipment

Equipment brand	Parameters
First stage	
Double rotor pump Aerzen Gmb17.15HV	Productivity: 15,685 m ³ /h; drive power –30 kW; working pressure at the suction –3 mmHg
Condenser	
Condenser 600 КВНГ-2-М1/25Г-3-2-У-И	Diameter of the casing –600 mm; the number of moves –2; The length of the pipes is 3 m
Second stage	
LRVP SIHI LPH 65320	Productivity: on dry air –300 m ³ /h; according to working conditions –490 m ³ /hr. Drive power –8 kW

of chemically polluted effluents. The total energy consumption will be 38 kWh of electricity and 3 m³/hr of recycled water. The formation of CCC is absent.

With the accepted operating time of the installation of 8000 h, the costs for the existing VOS will be: steam –2,953,200 rubles/year; recycled water –357,600 rubles/year; electricity is absent; purification of chemically polluted effluents – 55,248 rubles/year. The total cost of the VOS will be 3,366,048 rubles/year.

For the proposed VOS, the costs will be steam—none; recycled water—17,880 rubles/year; electricity—938,144 rubles/year; purification of chemically polluted effluents—none. The total cost of the VOS will be 956,024 rubles/year.

Thus, the economic effect of the introduction will be –2,410,024 rubles/year. Estimated capital expenditures will amount to 10 500 000 rubles. Then the payback period of the project will be 4.35 years.

7 Conclusion

The proposed reconstruction of the VOS unit for the separation of ethanolamines makes it possible to achieve significant savings using inexpensive energy resources, and the use of computer simulation tools can significantly increase the accuracy of calculations and select such standard sizes of equipment at which an acceptable payback period of the project is achieved. This research was funded by the Ministry of Science and Higher Education of the Russian Federation grant number 075-00315-20-01 «Energy saving processes of liquid mixtures separation for the recovery of industrial solvents»

References

1. Monostori, L.: Cyber-physical systems. In: Chatti, S., Tolio, T. (eds.) *The International Academy for Production, CIRP Encyclopedia of Production Engineering*. Springer, Berlin, Heidelberg (2018)
2. Vlasov, S.S., Shumikhin, A.G.: Models and algorithms for fuzzy control system of atmospheric block in atmospheric-and-vacuum distillation unit: design and analysis. *Autom. Remote Control* **73**, 923–935 (2012). (<https://doi.org/10.1134/S0005117912050189>)
3. Osipov, E.V., Telyakov, E.S., Sadykov, K.S.: Optimal design process of a steam jet vacuum system for a hydrocracking unit. *Chem. Petrol Eng.* **52**, 339–343 (2016)
4. Martin G.R., Lines J.R., Golden, S.W: Understand vacuum-system fundamentals. *Hydrocarbon Processing*, October 1994, pp. 1–7
5. Mangal, K.: In: Mangal, K. (ed.) *Liquid Ring Vacuum Pumps Chemical Engineer*. vol. 265. pp. 346–352 (1972)
6. Bannwarth, H.: In: *Liquid Ring Vacuum Pumps, Compressors and Systems*. pp. 487. Gundelfingen, Verlag (2005)
7. Nazarov, A.A., Ponikarov, S.I.: Gas-dynamic and heat-exchange processes in a facility for the vacuum dehydrogenation of hydrocarbons. *Theor. Found. Chem. Eng.* **53**, 515–528 (2019). <https://doi.org/10.1134/S0040579519040250>

8. Moskalev, L.N., Ponikarov, S.I.: Use of a vortex-type contact condenser in absorption of methanol and formaldehyde from a contact gas. *J. Eng. Phys. Thermophy* **89**, 1179–1185 (2016). <https://doi.org/10.1007/s10891-016-1481-x7>. 10; Telyakov E.S., Osipov E.V., Bugembe, D.: Reconstruct a vacuum column injector system using computer modeling–Part 1. In: *Hydrocarbon Processing*. vol. 97. №10. pp. 83–88 (2018)
9. Telyakov, E.S., Osipov, E.V., Bugembe, D.: Reconstruct a vacuum column injector system using computer modeling–Part 2. *Hydrocarbon Processing*. **97**(11), 61–64 (2018)
10. *Steam Jet Vacuum Pumps*. Giproneftemash. M, pp. 129 (1965)
11. *Liquid Ring Vacuum Pumps and Compressors: Technical Details and Fields of Application*, Sterling Fluid Systems Group, Netherlands (2017)
12. Pfeleiderer, C., Die Kresel, P.: VDI.-Verlag, pp. 327. Springer, Berlin (1955)
13. Grabow, G.: Determination of the internal shape of a ring of fluid in the liquid ring vacuum pumps and compressors. In: Grabow, G. (eds.). vol. 1. pp. 32–40. *Pumpen und Verdichtez* (1962)
14. Kamei, W.: Experiments on the fluid friction of a rotating disc with blades. In: Kamei, W. (ed.) *Bulletin of JSME*, vol. 5, № 17, pp. 49–57 (1962)
15. Kearton, W.J.: The influence of the number of impeller blades on the pressure generated in a centrifugal compressor and on its general performance. In: Kearton, W.J. (ed.) *Proceedings of the Institute of Mechanical Engineers*. vol. 124. pp. 481–568 (1933)
16. Linsi, U.: Experiments on radial compressors of turbocharges. *Brown Boveri Rev.* **52**(3), 161–170 (1965)
17. Prager, R.: Operational conditions and application field of liquid machines. In: *Proceedings 3rd conference fluid mechanics and fluid mach.* pp. 469–475. Budapesht (1969)
18. Osipov, É.V., Telyakov, É.S., Latypov, R.M., et al.: Influence of heat and mass exchange in a liquid ring vacuum pump on its working characteristics. *J. Eng. Phys. Thermophy* **92**, 1055–1063 (2019). <https://doi.org/10.1007/s10891-019-02020-7>
19. Aviso, K.B., Dominic, F.: (ed.): *Chemical engineering process simulation*. *Process Integr. Optim. Sustain* **2**, 301 (2018). <https://doi.org/10.1007/s41660-018-0056-z>

A Model of Rotational Mixing of Loose Environment on the Platform of Cyber-Physical Systems



A. B. Kapranova , D. D. Bahaeva , D. V. Stenko, and I. I. Verloka 

Abstract Based on the energy method, a stochastic model of the process of rotational mixing of the loose environment at the first stage of the mixer-compactor with a conveyor belt on the platform of cyber-physical systems is proposed taking into account the physicomachanical properties of the components being mixed. Analytical expressions are obtained for the differential functions of the distribution of the number of particles of loose components according to their scattering angle during the formation of rarefied streams above the conveyor belt during the operation of one row of elastic blades fixed in tangent planes to the surface of a cylindrical drum. The described elements of the cyber-physical system are required to create a theoretical base for the engineering method for calculating the parameters of the mixer-compactor.

Keywords Cyber-Physical system · Mixer-Compactor · Loose materials · Mixture · Elastic shoulder blades · Distribution functions · Parameters

1 Introduction

Current trends in the development of chemical technologies in the field of processing of loose components reflect the need to organize appropriate technological processes in the absence of contradictions between their two main characteristics - energy efficiency and intensity [1]. The growing needs of the food, chemical, pharmaceutical, construction, and other sectors of the national economy for homogeneous loose

A. B. Kapranova (✉) · D. D. Bahaeva · D. V. Stenko · I. I. Verloka
Yaroslavl State Technical University, Moskovskiy Prospect, 88, Yaroslavl 150023, Russia
e-mail: kapranova_anna@mail.ru

D. D. Bahaeva
e-mail: bakhaevadd@mail.ru

D. V. Stenko
e-mail: dvs3d@yandex.ru

I. I. Verloka
e-mail: ivdean@inbox.ru

mixtures with specified mechanical properties and regulated requirements for the porosity index confirm the urgency of developing new equipment for these purposes. In this regard, the combination of several technological operations [2] or, as a special case, their execution in sequential mode [3], but in the working volume of one device, becomes a priority in the design of mixing and compactor equipment to obtain a deaerated homogeneous mixture of solid dispersed materials with a given volume ratio of components. There is a need to take into account the influence of many factors that can adversely affect the final product of the production of the loose mixture, including the effect of segregation [4], the properties of aerability and adhesion, the ratio of the particle-size distribution of the components, etc. [5–7]. One of the ways to combat the undesirable effect of segregation during the preparation of granular mixtures may be to organize the process of mixing particles of components in rarefied streams [8, 9]. Providing designers with appropriate dependencies of the main indicators of mixing, as one of the processes within the framework of one technological chain, on the set of its design and operating parameters suggest the development of a theoretical base from the perspective of a cyber-physical system [10]. The aim of the work is to develop a stochastic description of the process of formation of rarefied flows at the stage of rotational mixing during the organization of further combining this operation with compaction of the obtained granular mixture on a conveyor belt on a cyber-physical platform. The latter includes the formation of a set of independent parameters of the specified mixing process.

2 Features of the Construction of Mixing Models During the Operation of the Mixer-Compactor of Loose Materials with a Conveyor Belt

The difficulties of mathematical modeling of the process of mixing particles of granular components are associated, first of all, with the multifactorial nature of the tasks solved in this case [11], which is reflected in the choice of the main approach to the description of this technological operation and attention to the creation of an appropriate cyber-physical platform. Despite the wide range of available mixing models from deterministic descriptions [5–7, 12] to stochastic models [1, 13–15] and their various modifications with combination elements, in this case, it is advisable to use the second one to obtain information on particle distribution according to a given process characteristic. In addition, the probabilistic nature of particle motion in rarefied flows of granular materials determines a specific method of mathematical description for the selected modeling approach, in particular, it is proposed to use the energy method [16], which allows one to take into account the basic physical and mechanical characteristics of loose materials and the features of motion -partition of their constituent particles. Thus, the interest in studying the process of rotational mixing from the standpoint of the cyber-physical system has all the bases. The use of conveyor belts in apparatus for processing solid dispersed environment [17] allows

you to successfully combine a number of technological operations within the same working volume [3]. Such an organization allows for continuous operation of the designed equipment, for example, in the production of dry construction mixtures using movable rigid perforated ridges [18], mixing powders on the conveyor with fixed separating plates [19], or even without mixing organs due to vibration effects [20], etc.

In this case, one of the methods for organizing rarefied flows from layers of loose components on a movable belt is to use rotary drive devices in the form of drums with elastic blades [21], symmetrically mounted above the conveyor at an angle to the direction of movement of the belt. The vertical screen to the horizontal working surface of the conveyor serves as an additional mixing device and the sealing roller with holes for removing air on the other side of the vertical screen functions as a deaerator. The organization of the process of formation of rarefied flows depends on the choice of the configuration of the elastic elements and the method of their fastening on the mixing drum [8–10, 21], for example, there are: a radial arrangement of thin cylindrical bills [1], screw winding of flexible elements [9], meetings arrangement of screw coils for brush elements [8, 10], etc. In this case, the surfaces of rectangular elastic blades are fixed in tangent planes to the cylindrical surfaces of each mixing drum located above the conveyor belt. At the same time, the installation of these elastic blades is carried out in rows with alternating directions of their location along the axis of symmetry of the cylindrical mixing drums. Such fastening of the elastic blades ensures the scattering of particles in different directions of the mixed components fed by a conveyor belt into the gap of these drums in the form of layers. The stochastic description using the energy method [16] of the process of forming rarefied streams of loose components over a conveyor at the stage of rotational mixing using one row of rectangular elastic blades fixed in this way is the main task of this study.

The concept of a mechanical mixer of two loose components with continuous operation proposed in [10] can be adapted to the case of rotational mixing with a set of information variables, set $z(t) = \{x(t), y(t), a, b\}$ total number. The following notation is accepted here.: $a = \{a_{j_1} = cont\}$, $j_1 = \overline{1}, u_1$ —design parameters for threads «1» and «2»; b —set of operational parameters; $x(t) = \{x_i(t)\}$, $i = \overline{1}, 2$ and $y(t) = \{x_1(t), x_2(t), V_C\}$ —respectively, the sets of input and output parameters of the studied process, where V_C —mixture heterogeneity coefficient. Splitting information variables into two categories (basic z_m —calculated from the proposed model and designed z_p —remaining in this division) suggest the choice of the following two sets from the last category. The first one relates to a set of regulated parameters z_{pr} , the number of which determines the number of degrees of freedom of the mixing process, and the second to optimizing parameters z_{po} . However, the formulation of the multifactor task of optimizing the process of mixing loose solids in some cases can be replaced by a more simplified task of finding effective ranges for changing the desired parameters using the generated analytical base.

For example, an analysis of the modeled differential functions of the distribution of the number of particles of loose components according to the selected process

characteristic allows us to identify such effective limits for the change of design and operating parameters so that the condition for achieving the specified quality of the mixture formulated in [8–10] is fulfilled. We clarify that for the considered rotational mixing of loose components on a conveyor belt, the following sets of parameters can be distinguished: $x = \{Q_{Vi}, n_{Vi}\}$, $y = \{Q_{Vi}, n_{Vi}, V_C^{tech}, \Delta V_C\}$, $b = \{\omega, h_0, h_L\}$, where Q_{Vi} —component volumetric consumption $i = 1, 2$; n_{Vi} —their volume fractions, V_C^{tech} —regulatory values of the coefficient of heterogeneity, ΔV_C —absolute parameter errors V_C^{tech} , ω —angular rotation speed of the drum, h_0 —clearance height drum-tape, h_L —the height of the layers of loose materials supplied by the conveyor to the specified gap. In this set a determined by the values of the following design parameters: length and width of the conveyor belt; radius r_b and drum width; length l_b and width of elastic blades, number of blades n in one row, and the number of these rows on the cylindrical surface of the mixing drum, etc. In this presentation, we restrict ourselves only to the main set $a = \{r_b, l_b, n\}$.

3 Analysis of the Peculiarities of the Movement of the Elastic Blades of the Mixing Drum When Scattering Particles of Loose Materials

Consider the movement of elastic blades long— l_b , making up the one-row bill, which is fixed in the manner described above on a rotating with an angular velocity ω in mixing drum. Let the radius of the drum be r_b , the distance between the drum and horizontal conveyor belt— h_0 , the number of deformed bills within a quarter of the angle of rotation of the drum— n_b . To describe the movement of the endpoints of the elastic blades M_j , $j = \overline{1, n_b}$ after leaving the gap between the drum and the conveyor, we introduce two Cartesian coordinate systems with parallel axes Oxy , $O_1x_1y_1$ in the transverse plane of the cross-section of the drum. The first center O lies on the axis of rotation of the mixing device, the coordinates of the second center $O_1(x_{O_1}; y_{O_1})$ in system Oxy respectively equal $x_{O_1} = r_b \sin \alpha_0$, $y_{O_1} = r_b \cos \alpha_0$ in direction axes Ox , O_1x_1 vertically down and perpendicular to the tape, where $\alpha_0 = 2\pi/n$ —the angle between attachment points K_s, K_{s+1} , $j = 1, \dots, s, s+1, \dots, n_b$ adjacent elastic blades on the surface of the drum, n —total number of blades of one row.

We connect the polar coordinate system (r, θ) with axe O_1x_1 when counting counterclockwise the polar angle θ . We introduce the equation of motion of the endpoints of the elastic blades M_j , $j = \overline{1, n_b}$ in polar coordinates in the form of a spiral of Archimedes $r_a(\theta)$, assuming that for the initial position of the blade deformed in the gap, the number $j = 1$ the coordinates of the points are respectively equal: $K_1(r_b; 0)$ in system Oxy and $M_1(x_{1M_1}; y_{1M_1}) = M_1(h_0 + r_b(1 - \cos \alpha_0); 0)$ in system $O_1x_1y_1$. Moreover, it is assumed that the position of the point M_δ , $j = 1, \dots, n_b$, δ, \dots, n for the reconstructed blade is the endpoint of the specified spiral, in particular, let $M_\delta(x_{M_\delta}; y_{M_\delta}) = M_\delta(-r_b; -l_b)$. Then the equation of the spiral of Archimedes is given by the expression

$$r_a(\theta) = A + B\theta \tag{1}$$

where are the notation $A = h_0 + r_b(1 - \cos\alpha_0)$, $B = \{ (r_b + l_b)^2 + [r_b(1 + \cos\alpha_0)]^2 \}^{1/2} - A / \theta_\delta$, $\theta_\delta = \pi + \arctg\{ (r_b + l_b) / [r_b(1 + \cos\alpha_0)] \}$. Point position M_j , $j = \overline{1, n_b}$ in the polar system is determined by the following equation for an arbitrary point M on the spiral of Archimedes (1)

$$r_{M_j}(\theta) = r_M(\theta) = r_a(\theta)\cos[3\beta(\theta)/2] + \{ (2r_a(\theta)\cos[3\beta(\theta)/2])^2 - 4[r_a(\theta)]^2 - r_b^2 \}^{1/2} / 2, \tag{2}$$

where angle $\beta(\theta) = \arctg[B/r_a(\theta)]$ is the angle between the polar normal to the tangent spiral at the point $M = M_j$ and radius vector $\overrightarrow{O_1M_j} = \vec{r}_a(\theta_{M_j})$. Note that the approximation is accepted for the connection between the angles $\beta(\theta) \approx 2\beta'(\theta)$, where β' - the angle between the same polar normal and radius vector $\overrightarrow{OM_j} = \vec{r}_{M_j}$. In view of the Eqs. (1), (2) analyzed the movement of particles of two loose components ($i = 1, 2$), which are scattered by deformable elastic blades from layers stacked on top of each other $h_L = \sum_{v=1}^2 h_{Lv}$ on a movable tape that fills the gap between the mixing drum and the specified conveyor. Let the average diameter of spherical particles with a density ρ_{Ti} taking into account the number of fractions n_v defined by the expression $d_{Ti} = \sum_{v=1}^{n_v} d_{Tiv} n_v$. Particle speed $V_{r\theta i}$ for each loose component ($i = 1, 2$) with the described movement at the moment of separation from the end of the deformed elastic blade in the polar coordinate system is given by

$$V_{r\theta i}(r_M(\theta), \theta) = \omega r_M(\theta) / \cos\{\arctg[B/r_a(\theta)]\}. \tag{3}$$

Then the two components of kinetic energy (E_{1i} for translational movement of a particle with mass together with its center of mass in a projection onto the transverse plane of the mixing drum and E_{2i} for the rotational motion of a particle relative to this center, taking into account the values of the random component of the angular momentum L_i and axial moment of inertia I_i calculated by the Formulas

$$E_{1i} = m_i [V_{r\theta i}(r_M(\theta), \theta)]^2 / 2 = (\pi/12) \rho_{Ti} \omega^2 d_{Ti}^3 [r_M(\theta) / \cos\{\arctg[B/r_a(\theta)]\}]^2, \tag{4}$$

$$E_{2i} = L_i^2 / (2I_i) = (5\pi/6) \rho_{Ti} \omega^2 d_{Ti} [r_M(\theta)]^4. \tag{5}$$

Note that the energy of the elastic interaction of each particle with a flexible blade when scattering loose materials is determined by the work of the elastic forces of the corresponding beat with an empirical angular coefficient of its stiffness k_u

$$E_{3i} = k_u \theta_i^2 / 2 \approx k_u \theta^2 / 2. \tag{6}$$

So, the energy of each particle $E_i = \sum_{\nu=1}^3 E_{\nu i}$ in the described movement when scattering from an elastic blade equal to the sum of its three components according to the expressions (4)–(6)

$$E_i = a_i d_{Ti} \omega^2 \left\{ d_{Ti}^2 + 10 p_{30} \frac{(c_0 + c_1 \theta)^4}{c_0^2 [(p_0 + p_1 \theta)^2 + p_{20}^2]} \right\} \frac{(c_0 + c_1 \theta)^4}{c_0^2 [(p_0 + p_1 \theta)^2 + p_{20}^2]} + \frac{k_u \theta^2}{2} \quad (7)$$

where

$$\begin{aligned} a_i &= \pi \rho_{Ti} / 12, \quad c_0 = k_0 + k_1, \\ c_1 &= \{3k_2 / (2A^3) + k_0 k_4 B / A + A^3 B [2k_4 (k_0^2 - A^2) + k_3] / (8k_1)\} / k_4, \\ p_0 &= \cos\{(1/2) \arctg[B/A]\}, \quad p_1 = (B^2 / 2k_4) \sin\{(1/2) \arctg[B/A]\}, \\ p_{20} &= [p_0(1 - p_0)]^{1/2}, \quad p_{30} = (p_0^2 + p_{20}^2)^2, \quad k_0 = A \cos\{(3/2) \arctg[B/A]\}, \\ k_2 &= B^2 \sin\{(3/2) \arctg[B/A]\}, \quad k_3 = (3/2) A B \sin\{3 \arctg[B/A]\}, \\ k_4 &= A^2 + B^2. \end{aligned}$$

4 Description of the Use of the Energy Method in Stochastic Modeling of Rotational Mixing from the Perspective of a Cyber-Physical System

To further simulate the process of formation of rarefied flows of two loose materials mixed by a rotary device, it is proposed to use the energy method [16], which allows one to take into account the energy form of the stochastic particle motion in the form (7) within the framework of the stochastic approach. Considering the indicated technological operation as a random process of a homogeneous, continuous, stationary, Gaussian type, we apply the formalism of the Markov process for the states of the macrosystem of particles of each component without an influx of energy from outside. Then, in the absence of macro-fluctuations of these macrosystems associated with particle collisions, we consider that in the resulting flows there is insignificant cross-motion of one flow in another, and the particle displacements of both formed flows are co-directed. In this approximation, the Ornstein–Uhlenbeck formalism [16] is valid with the solution of the Fokker–Planck equation in the energy representation for the stationary case with respect to the distribution function of the number of particles in the following form

$$\phi_i = A_i \exp(-E_i / E_{0i}) \quad (8)$$

where is the normalization constant A_i is found from the condition $\int_{\Psi_i} \phi_i d\Psi_i = 1$ with the introduction of the phase volume element $d\Psi_i = dv_{xi}dv_{yi} \equiv dv_x dv_y$ or $d\Psi = dv_x dv_y = -\omega^2 r dr d\theta$ in the approximation of the simultaneous interaction of an elastic element with particles of each component. Here, the choice of phase variables is explained by the application of the expression for the stochastic energy of a single particle of the component ($i = 1, 2$) in the form (7). Due to (8), the decrease in the number of particles dN_i component $i = 1, 2$ in elementary volume $d\Psi$ is given by the formula [16]

$$dN_i = A_i \exp(-E_i/E_{0i}) d\Psi. \tag{9}$$

Expressions (8), (9) contain the energy parameter E_{0i} , whose physical meaning is determined by the energy of the stochastic motion of particles at the moment of the beginning of stochastization of the states of the macrosystem ($i = 1, 2$). Expressions (8), (9) make it possible to determine the desired expression for the differential distribution function of the number of particles of the component $i = 1, 2$ by the distinguished feature of the process under study, for example, by the scattering angle, which in this case coincides with the polar angular coordinate θ

$$f_i(\theta) = (1/N_i) dN_i/d\theta. \tag{10}$$

Then, taking into account expressions (7)–(9) for the energy of stochastic motion of particles of each loose material E_i and exponential law for the number of these particles dN_i in elementary volume $d\Psi$ we obtain the desired dependence

$$\begin{aligned} f_i(\theta) = & Q_i \{ [H_1(\theta)]^2 + p_{20}^2 \}^{1/2} \{ \exp[-k_u \theta^2/E_{0i}] \} \\ & \times \left[\operatorname{erf} \left(\lambda_{2i} [H_2(\theta)]^2 \{ [H_1(\theta)]^2 + p_{20}^2 \}^{-1/2} \right) - \operatorname{erf} \left(\lambda_{2i} \{ [H_1(\theta)]^2 + p_{20}^2 \}^{-1/2} \right) \right] \\ & / \{ \exp[-10(\lambda_{1i} + k_u \theta^2/E_{0i})] - \exp(-\lambda_{1i}) \} \end{aligned} \tag{11}$$

where $Q_i = [c_0/(16c_1)] [\pi k_u/(E_{0i} g_{1i} g_{1i})]^{1/2}$, $H_1(\theta) = p_0 + p_1 \theta$, $H_2(\theta) = c_0 + c_1 \theta$, $\lambda_{2i} = (3/2c_0^2) [k_u g_{1i} g_{2i}/(E_{0i})]^{1/2}$, $\lambda_{1i} = k_u g_{1i} g_{2i}/[E_{0i} (2p_0^2 + p_{20}^2)]$.

The value of the energy parameter E_{0i} determined from the balance equation for the total particle energies of each macrosystem ($i = 1, 2$): when capturing particles of a component $i = 1, 2$ the ends of the flexible elements from the gap of the drum-tape (E_{Ci}) and when disseminating these particles with specified bills (E_{Di}) in the field of changes in the polar angular coordinate $\theta \in [\theta_{0i}; \theta_{1i}]$. Then, taking into account the effect of mixing the components, we have

$$\sum_{i=1}^2 E_{Ci} = \sum_{i=1}^2 E_{Di}. \tag{12}$$

When taking into account the different thicknesses of the layers of loose materials on the conveyor belt ($h_{Li} = h_L/2$), as well as the nature of the movement of the endpoints of the elastic blades M_j , $j = \overline{1, n_b}$ in polar coordinates (1), (2) and when averaging the particle velocity $V_{r\theta i}$ mass m_i for each loose component ($i = 1, 2$) by the polar angular coordinate in the region $\theta \in [0; \alpha_0]$ the Eq. (12) relatively E_{0i} takes the form

$$\sum_{i=1}^2 N_i m_i \left\{ h_0^2/2 + \alpha_0^{-1} \int_0^{\alpha_0} [r_M(\theta)]^4 / \{ [H_1(\theta)]^2 + p_{20}^2 \} d\theta \right\} + \sum_{i=1}^2 A_i \int_{\theta_{0i}}^{\theta_{1i}} d\theta \int_{r_{Li}}^{r_M(\theta)} E_i \exp(-E_i/E_{0i}) r dr = 0r_{Li} \quad (13)$$

where $r_{L1} = h_0 + r_b(1 - \cos\alpha_0)$, $r_{L2} = r_{L1} - h_L/2$ at appropriate values θ_{1i} .

5 Results of Modeling

Let us consider an illustration of the proposed stochastic model of the process of forming rarefied flows of loose components at the stage of rotational mixing using one row of rectangular elastic blades fixed in tangent planes to the cylindrical surface of the mixing drum located above the conveyor belt. Let the technological operation of mixing natural sand be carried out State Standard (GOST) 8736–93 at $i = 1$ ($\rho_{T1} = 1.525 \times 10^3$ kg/m³; $d_{T1} = 1.5 \times 10^{-4}$ m) and semolina GOST 7022–97 at $i = 2$ ($\rho_{T2} = 1.440 \times 10^3$ kg/m³; $d_{T2} = 4.0 \times 10^{-4}$ m). The choice of these loose materials is associated with the need to replace some toxic compounds with model mixtures with similar physical and mechanical properties, in particular, provided that the densities of the constituent substances are comparable. We give the main values of the parameters of the formed cyber-physical platform of the process under study: а) $r_b = 3.0 \times 10^{-2}$ m; $l_b = 4.5 \times 10^{-2}$ m; $n = 8$ for the design of the mixer at the preliminary stage of operation of the apparatus of the mixer-compactor loose environment with a conveyor belt; б) $h_0 = 3.0 \times 10^{-2}$ m; $h_L = 3.0 \times 10^{-2}$ m; $\omega = (41 - 53)$ s⁻¹ for operating modes of the designed equipment.

According to the stochastic modeling of the rotational mixing process under study using expression (11), families of curves are constructed for the dependences of the differential distribution function of the number of particles of each component $f_1(\theta)$ and $f_2(\theta)$ by polar angular coordinate θ respectively in Fig. 1a and b.

The values of the energy parameters calculated according to (13) E_{0i} presented in Table 1.

An analysis of the results shows that at the initial angles of rotation of the elastic blades, the loose discharge of loose materials occurs (see the characteristic first bursts in charts 1–3, Fig. 1a, b), in particular, more than half of component 1, when the flexible elements are maximally deformed after the drum-tape leaves the gap. At the same time, for both components there remains a tendency to further remove the

Fig. 1 Dependence $f_i(\theta)$:
a—natural sand GOST 8736-93 ($i = 1$);
b—semolina GOST 7022-97 ($i = 2$); $\omega = 41.9 \text{ s}^{-1}$ (1);
 $\omega = 47.1 \text{ s}^{-1}$ (2); $\omega = 52.4 \text{ s}^{-1}$ (3)

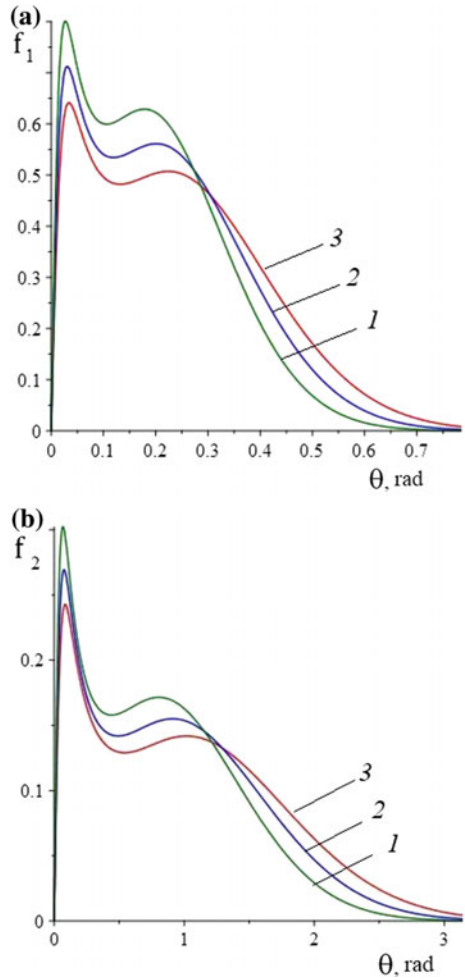


Table 1 Model features

Loose material name, brand	Drum rotational speed $\omega, \text{ s}^{-1}$	Energy parameter $E_{0i}, \times 10^{-5} \text{ J}$
Natural sand GOST 8736-93	41.9	3.312
	47.1	4.193
	52.4	5.176
Semolina GOST 7022-97	41.9	59.320
	47.1	75.080
	52.4	92.690

remaining particles during the restoration of the shape of the elastic scapula (see the second bursts in the graphs indicated above). In addition, the dispersion for component 2 is more pronounced than for component 1, for example, the dispersion range for semolina is about 1.5 times longer than for sand. This fact indicates that, for given structural and operational parameters, the particles of component 2 scatter at a faster rate than component 1, which is explained by the physicomachanical features of the loose materials under consideration. Smaller particles of natural sand ($d_{T2}/d_{T1} = 2.7$), but heavier ($\rho_{T2}/\rho_{T1} = 0.94$) than semolina particles, due to which they bounce at a smaller angle from the surfaces of elastic blades. However, a simple change in the angular velocity of rotation of the mixing drum in the selected range (41–45) s⁻¹ does not change this picture, which confirms the conclusions made in [8–10] about the need for additional research of other factors that significantly affect the process of formation of rarefied flows in a rotational way. For example, as was shown in [8–10], these factors include the degree of deformation of flexible elements in the gaps with the drum, which is characterized by the ratio of the beat length to the height of the gap. In addition, the result of the work of only one row of elastic blades is considered.

6 Conclusion

The above remarks on the obtained simulation results lead to the need to expand the set of studied design parameters when forming a cyber-physical platform to develop an engineering method for calculating the designed mixer-compactor.

The revealed characteristic tendency to scatter the main number of particles at small rotation angles of the mixing drum for both components is the basis for obtaining the conditions for the effective mixing of loose components. This requires such adjustment of the ranges of the set of process parameters that affect the formation of the cyber-physical system in order to ensure the convergence of extreme angular values for the polar coordinate θ of the mixed components. For example, this indicated approach is actually observed ($\theta < 0.19$ rad) when comparing the first bursts in graph 3 (Fig. 1a) and graph 3 (Fig. 1b), plotted with the same maximum value of the angular velocity of the drum from the selected parameter variation range ω .

Thus, the stochastic modeling of the process of forming rarefied flows of loose components at the stage of rotational mixing using one row of rectangular elastic blades fixed in tangent planes to the cylindrical surface of the mixing drum located above the conveyor belt showed the possibility of applying the energy method.

The resulting analytical dependences for the differential distribution functions of the number of particles of each component along the polar angular coordinate allow:

- identify the main factors of analysis necessary for the analysis of the efficiency of the mixing process;

- expand the parameters of the process under study involved in the formation of the platform of its cyber-physical system;
- to predict the behavior of loose components during their rotational mixing in order to create conditions for effective mixing when analyzing the attainability of the criterion for the convergence of extreme angular values of the polar coordinate for mixed loose components;
- taking into account the above facts, confirm the feasibility of using a mixing device in the form of a drum with elastic blades fixed on the conveyor belt using this method by evaluating the quality criterion of the obtained loose mixture, for example, by calculating its heterogeneity coefficient.

References

1. Kafarov, V.V., Dorokhov, I.N., Arutyunov, S.Yu.: In: System Analysis of Processes of Chemical Engineering. pp. 440. Science, Moscow (1985)
2. Kapranova, A.B.: Stochastic model of parallel or sequential processes of deaeration and mixing of granular media using the operation of a centrifugal device as an example. Theoretical Foundations Chem. Eng. **53**(2), 292–304 (2018)
3. Kapranova, A.B., Zaitzev, A.I., Kuz'min I.O.: Studying the porosity of powders under pressure compaction in deaeration mixers. Theor. Found. Chem. Eng. **49**(4), 436–446 (2015)
4. Bauman, I., Curic, D., Boban, M.: Mixing of solids in different mixing devices. Sadhana **33**(6), 721–731 (2008). <https://doi.org/10.1007/s12046-008-0030-5>
5. Makarov, Yu. I.: In: Devices for Mixing Loose Materials, pp. 216. Mechanical Engineering, Moscow (1973)
6. Kim, V.S., Skachkov, V.V.: In: Dispersion and Mixing in Production Processes and Processing of Plastics. pp. 240. Chemistry, Moscow (1988)
7. Satomo, I.: Solids mixing. Puranto Kogaku. **10**(5), 63–69 (1972)
8. Kapranova, A.B., Verloka, I.I.: Stochastic description of the formation of flows of particulate components in apparatuses with brush elements. Theor. Found. Chem. Eng. **52**(6), 1004–1018 (2018). <https://doi.org/10.1134/S0040579518050330>
9. Kapranova, A.B., Bakin, M.N., Verloka, I.I.: Simulation of the quality criterion of a mixture in a drum-belt apparatus. Chem. Petrol. Eng. **54**(5), 287–297 (2018). <https://doi.org/10.1007/s10556-018-0477-0>
10. Kapranova, A.B., Verloka, I.I., Bahaeva, D.D.: About preparation of the analytical platform for creation of a cyber-physical system of industrial mixture of loose components. In: Cyber-Physical Systems: Advances in Design and Modelling. Studies in Systems, Decision and Control. **259**, 81–91 (2020). https://doi.org/10.1007/978-3-030-32579-4_7
11. Shaul, S., Rabinovich, E., Kalman, H.: Generalized flow regime diagram of fluidized beds based on the height to bed diameter ratio. Powder Technol. **228**, 264–271 (2012)
12. Lai, F.S.: The convective mixing process and striated mixture. J. Powder Loose Solids Technol. **38** (1978)
13. Leonchik, B.I., Mayakin, V.P.: Measurements in dispersed flows. pp. 248. Energy, Moscow (1985)
14. Dehling, H.G., Gottschalk, T., Hoffmann, A.C.: In: Stochastic Modeling in Process Technology. pp. 279. Elsevier Science, London (2007)
15. Almendros-Ibanez, J.A., Sobrino, C., de Vega, M., Santana, D.: A new model for ejected particle velocity from erupting bubbles in 2-D fluidized beds. Chem. Eng. Sci. **61**, 5981–5990 (2016)

16. Klimontovich, Y. L.: In: *Turbulent Motion and the Structure of Chaos: A New Approach to the Statistical Theory of Open Systems*, pp. 328. LENAND, Moscow (2014)
17. Kaye, B.H.: *Mixing of Powders*. In: Fayed, M.E., Otten, L. (eds.) *Handbook of Powder Science and Technology*. Boston (1997). https://doi.org/10.1007/978-1-4615-6373-0_11
18. Trofimov, V.I., Lebedev V.E.: Utility Model Patent 2325993 Russian Federation, IPC B 28 C 5/36. A device for preparing a dry building mixture. Publ. 07.20.10, Bull. No. 20 (2010)
19. Garthus, D.R.: Utility Model Patent 4591275 USA, IPC B 28 C 5/36. Apparatus for mixing pulverulent material on a conveyor belt. Publ. 05.27.1986 (1986)
20. Pershin, V.F., Baryshnikova, S.V., Kalyapin D.K., Osipov A.A.: Utility Model Patent: 2242273 Russian Federation, IPC B 01 F 3/18. A method of preparing multicomponent mixtures and a device for its implementation. Publ. 12.20.04 (2004)
21. Lebedev, A.E., Vatagin, A.A., Borisovsky, M.E., Romanova, M.N., Badaeva, N.V., Sheronina, I.S.: Utility Model Patent: 2624698 Russian Federation, B01F3/ 18. Unit for mixing and compaction of loose materials. Publ. 07.05.2017 (2017)

Cyber-Physical Systems for New Materials Design

Computer System of Visual Modeling in Design and Research of Processes of Carbon Nanocluster Compounds Synthesis



Dmitriy Petrov , Tamara Chistyakova , and Nikolay Charykov 

Abstract The chapter presents a flexible, customizable to the material and technical base of an industrial enterprise, a multi-component man-machine visual simulation system of potentially dangerous, complex in the control of production processes for the synthesis of carbon nanocluster compounds with the prediction of their qualitative characteristics in simulated conditions close to real ones. The task of visual modeling in the design and study of processes of synthesis of carbon nanocluster compounds is formulated. The architecture of the visual modeling system is presented, which includes a database of characteristics of design and control objects, a database of rules and restrictions for the layout of reactor sections and assembly of extraction plants, a database of situational knowledge to support the training of control and production personnel, mathematical support for calculating the qualitative characteristics of the synthesis processes of carbon nanocluster compounds, software including dialog interfaces of the administrator, immersive interfaces of the designer and researcher. The results of functional testing and pilot operation of the visual modeling system in the tasks of decision support in the design and research of technological processes on the example of the model of the reactor section of the industrial enterprise and fullerene C₆₀ are presented.

Keywords Visual modeling · Manufacturing process · Design and research · Immersive space · Carbon nanocluster compounds

D. Petrov (✉) · T. Chistyakova · N. Charykov
State Institute of Technology (Technical University), 26, Moskovskiy Prospekt, Saint-Petersburg
190013, Russia
e-mail: petrov.dmitry@technolog.edu.ru

T. Chistyakova
e-mail: nov@technolog.edu.ru

N. Charykov
e-mail: ncharykov@yandex.ru

1 Introduction

One of the popular trends of the fourth industrial revolution is the development and introduction of digital twins that contribute to the rapid growth of digitalization of production processes in order to optimize their economic and quality indicators, including during the reconfiguration of production lines, as well as increase production safety [1, 2].

The modern market of high-tech interactive tools, graphics libraries, high-performance technical support, and progressive programming languages contributes to the rapid development of the cyber physics system industry [3, 4, 5].

The need for digital transformation and intellectualization of industry is justified by its complexity associated with increased requirements for quality and competitiveness of products. Innovative approaches to the integrated assessment of enterprise activity are being developed [6], as well as methods to support decision-making in industrial cyber-physical systems [7] and flexible product lifecycle control [8]. Construction industry [9], transport sector [10], oil industry [11], high-tech production facilities [12] are characterized by rapid development of intelligent computer simulators [13–16]. One of the most important tasks of computer simulators is ensuring the quality of remote training of personnel, on-the-job [17].

This chapter describes the components of a man-machine visual simulation system as a means to improve quality and reduce the risks of complex, potentially dangerous production through human synergy, as a decision-maker in design and control, with the proposed computer system.

2 Design Object Description

2.1 *Historical Information and Market Analysis of Carbon Nano Industry*

With the hypothesis of the existence of a stable allotropic carbon modification, physicist E. Osawa (Japan) in 1970 predicted the discovery of closed carbon clusters experimentally obtained in 1985 by scientists Richard Smalley and Robert Kerl (USA) and Harold Croto (UK) with laser irradiation of graphite [18]. Open compounds are called “fullerenes” by the name of the American architect Buckminster Fuller, designing the domes of his buildings with pentagons and hexagons similar in structure to fullerenes molecules.

Currently, the carbon nano industry accounts for 10% of the total nanomaterials market \approx \$100 billion. The main interest in the development of the carbon nano industry is associated with the high demand for fullerenes and their derivatives both for the purpose of studying their unique structures and for the synthesis of materials with fundamentally new physical and chemical properties. Fullerenes can be used as modifiers to create materials with specified parameters. Regional exporters offer

fullerene products of high purity C_{60} at a price of \$86 per gram, C_{70} at a price of \$223 per gram, which is several times more expensive than the gold of a similar mass.

2.2 The Life Cycle of Carbon Nanocluster Compounds

Synthesis of carbon nanocluster compounds belongs to the class of energy-intensive multistage processes, which have special requirements for reactor sites and extraction sites of target components. The life cycle phases of fullerene products covered by the proposed computer visual simulation system are shown in Fig. 1.

The symbols adopted in Fig. 1 are described in detail in item 2.3 Formalized description.

At the stage of the design of production premises, special attention is paid to the presence of a high-voltage network, water main, ventilation system, fire, and explosion safety of the room.

The most productive method of synthesis of carbon nanocluster compounds is considered an electric arc. Graphite electrodes are burned in a plasma reactor in the medium of inert gas of low pressure. Obtained nano dispersed powder (fullerene carbon soot) by the flow of circulating inert gas is taken from reactor to soot collector [19].

Complexity in process control is due to thermodynamic instability of plasma and increased risk of reactor depressurization. The synthesis of fullerene carbon soot is potentially dangerous to humans because the process takes place at a high temperature in a cooled reactor filled with a harmful inert gas. From the circulation circuit of inert gas during its depressurization, emissions of nano dispersed fullerene carbon soot, which causes damage to respiratory organs, are possible.

Fullerene soot is a carrier of the end product, mainly fullerenes C_{60} and C_{70} . At the next stage, the end product is extracted from fullerene carbon soot, to which production is tuned [20]. When extracting the desired product, rotary vacuum evaporators or Soxhlet extractors are used. Complex combined devices combining extraction, evaporation, and drying can be used.

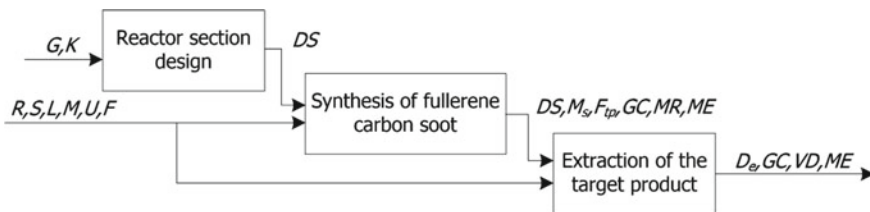


Fig. 1 Fullerene product lifecycle stages

2.3 Formalized Description

We introduce a formalized description of the design and modeling of the process of synthesis of carbon nanocluster structures in the following vector form. $Y=f(X,U,F)$, $X\{G,K,R,S,L,M\}$, $U\{U_A, L_E, G_C, G_G, \nu_M, W_H, \tau_1, \tau_2\}$, $F\{\xi_1, \xi_2, \xi_3\}$, $Y\{DS,Q\}$. X —an initial data vector including components: G —regulatory documents in the field of construction, fire safety, ergonomics and labor protection of personnel and drawings of production facilities (premises and equipment), $K\{H,E\}$ —characteristics of production facilities, where H —room characteristics, E —characteristics of the equipment. $H\{Ph_1^s, Ph_2^s, \dots, Ph_{cps}^s; Ph_1^m, Ph_2^m, \dots, Ph_{cpm}^m, H_h, W_h, L_h\}$, where Ph_i^s —singlet characteristic (voltage, type of current (direct or alternating), water pressure in the line, etc.), $i \in [1;cps]$, cps —number of singlet characteristics of the room. Ph_j^m —integral characteristic, $j \in [1;cpm]$, cpm —number of integral characteristics of the room. H_h, W_h, L_h —height, width, and length of the room. $E\{E_1, E_2, \dots, E_{ce}\}$ —equipment in the room where $E_p\{PE_1, PE_2, \dots, PE_{cpe}, H_e, W_e, L_e\}$ —characteristics of the p -th equipment, $p \in [1;ce]$, ce —number of equipment in the room, cpe —number of characteristics of p -th equipment, H_e, W_e, L_e —height, width, and length of the equipment. $R\{R_1, R_2, R_3, R_4, R_5\}$ —system of design and operational rules and requirements. $R_1\{RCM_1, RCM_2, \dots, RCM_{cpm}\}$, $R_2\{\{D(E_1, E_2), D(E_3, E_2), \dots, D(E_{ce}, E_2), D(H, E_2)\}, \dots, \{D(E_1, E_{ce}), D(E_2, E_{ce}), \dots, D(E_{ce}, E_{ce-1}), D(H, E_{ce})\}, \{D(E_1, H), D(E_2, H), \dots, D(E_{ce}, H)\}\}$, $R_3\{U_A^{\min}, U_A^{\max}, L_E^{\min}, L_E^{\max}, G_C^{\min}, G_C^{\max}, G_G^{\min}, G_G^{\max}, \nu_M^{\min}, \nu_M^{\max}\}$. R_1 —rules for comparing integral characteristics. RCM_j —the rule of comparison of the integral characteristic of the room Ph_j^m with the equipment of the same name ($>$, $<$, \geq , \leq , $=$). R_2 —matrix of spatial constraints. $D(E_{p1}, E_{p2})$ —distance requirement between $p1$ -th equipment and $p2$ -th equipment, maximum—at $p1 > p2$ and minimum—at $p1 < p2$, at the same time, $p1 \neq p2$, $D(H, E_p)$ —requirement for maximum distance between room walls and p -th equipment, $D(E_p, H)$ —the requirement for minimum distance between room walls and p -th equipment. R_3 —requirements to safety and operability of equipment in the form of operating ranges by arc voltage $[U_A^{\min}, U_A^{\max}]$, interelectrode distance $[L_E^{\min}, L_E^{\max}]$, refrigerant volumetric flow rate $[G_C^{\min}, G_C^{\max}]$, volume flow rate of inert gas circulation $[G_G^{\min}, G_G^{\max}]$, anode feed rate to reactor $[\nu_M^{\min}, \nu_M^{\max}]$. $R_4\{GC_{max}, MR_{max}, VD_{max}, ME_{max}\}$ —operational and economic restrictions, where GC_{max} —maximum volumetric flow rate of coolant during the synthesis of fullerene carbon soot and extraction $\tau_1 + \tau_2$, MR_{max} —the maximum mass of consumable graphite rods over time τ_1 , VD_{max} —the maximum volume of consumable solvent during extraction τ_2 , ME_{max} —maximum power consumption for total synthesis time $\tau_1 + \tau_2$. $R_5\{m_s^R, F_{tp}^R, D_e^R\}$ —requirements for qualitative indicators of the process, where m_s^R —required mass of fullerene carbon soot, F_{tp}^R —required content of synthesized target product in the mass of fullerene carbon soot, D_e^R —required degree of extraction of the end product. $S\{S_1, S_2, \dots, S_{cs}\}$ —material and energy flows of the process, cs —number of flows. $S_f\{S_T, SC_1, SC_2, \dots, SC_{csc}\}$ —characteristics of

the f -th flow, where S_T —the type of flow (inert gas, coolant, graphite rod, extractant, etc.), SC_w —characteristic of the f -th flow (density, heat capacity, viscosity, purity, etc.), $w \in [1; csc]$, csc —number of the f -th flow characteristics, $f \in [1; cs]$. $L\{NS, RSN, REC\}$ —situational knowledge of the research object in the form of a production-frame model, where $NS\{NS_1, NS_2, \dots, NS_{nsn}\}$ —possible emergency situations, $RSN\{RSN_1^{NS_i}, RSN_2^{NS_i}, \dots, RSN_{rsnn}^{NS_i}\}$ —causes of emergency situations NS_i , where $RSN_k^{NS_i}\{P, [P_{\min}; P_{\max}], v_{\max}, RM\}$, P —characteristic—initiator of the cause of the emergency situation, $[P_{\min}; P_{\max}]$ —its range of identification of an emergency situation, v_{\max} —the limit rate of characteristic change, RM —text of the message to the operator. $REC\{REC_1^{RSN_k^{NS_i}}, REC_2^{RSN_k^{NS_i}}, \dots, REC_{recn}^{RSN_k^{NS_i}}\}$ —recommendations to the researcher to eliminate the cause $RSN_k^{NS_i}$ of emergency situation NS_i . $REC_j^{RSN_k^{NS_i}}\{WR, RCM\}$, where WR —priority of the recommendation, RCM —text of the recommendation to the operator, $j \in [1; recn]$. nsn —number of possible abnormal situations in the simulated process, $i \in [1; nsn]$, $rsnn$ —number of causes of emergency situation NS_i , $recn$ —number of recommendations to the researcher to eliminate the cause $RSN_k^{NS_i}$ of the emergency situation NS_i , $k \in [1; rsnn]$. $M:Q=f(X, U, F)$ —system of algebraic and differential equations for calculation of qualitative-integral indices Q of the simulated process [21]. U —a variable characteristics vector of a manufacturing process comprising U_A —electric arc voltage, L_E —interelectrode distance, G_C —volumetric flow rate of coolant, G_G —volume flow rate of inert gas circulation, v_M —anode feed rate to reactor, W_H —extractant heater power, τ_1 —fullerene carbon soot synthesis time, τ_2 —the time of extraction of the target product. F —a vector of uncontrolled disturbances of the external environment, including ξ_1 —errors in the construction of the 3D room and equipment models, ξ_2 —heterogeneity of material flow properties, ξ_3 —voltage differences in the electrical network. Y —a vector of qualitative-integral indicators, including DS —pre-design specification for manufacturing room sketch, $Q\{M_s, F_{tp}, D_e, GC, MR, VD, ME\}$ —qualitative and integral indicators of the process, where M_s —the mass of carbon soot synthesized during τ_1 , F_{tp} —the content of target product in carbon soot mass, D_e —degree of extraction of the end product, GC —volumetric flow rate of coolant during the synthesis of fullerene carbon soot $\tau_1 + \tau_2$, MR —weight of spent graphite rods in time τ_1 , VD —the volume of solvent consumed during extraction τ_2 , ME —energy consumption during synthesis $\tau_1 + \tau_2$.

3 Project Objective and Task Setting

At SPbSIT (TU) (St. Petersburg), the Faculty of Chemistry of Substances and Materials laid the foundation for research on innovative multi-stage complex in the control of the synthesis processes of carbon nanocluster compounds. In 2014, the Department of Automated Design and Control Systems, with the support of the Infrastructure and Educational Programs Fund, together with scientists of the Faculty of

Chemistry of Substances and Materials, initiated an interdisciplinary comprehensive project to create a flexible, customizable to technological regulations and the material and technical base of the intelligent simulator complex of the technological process of fullerene synthesis [21]. The software package is implemented and used in the training process. The implementation of the idea of creating a digital twin of the carbon nano-industry to support the life cycle control of fullerene products expanded the functionality of the current software complex by including additional components—the visual designer of the reactor sites for the synthesis of carbon nanocluster compounds and the virtual fullerene extraction site.

The relevance and practical significance of the project are justified by the need to solve the complex problem of designing and studying the processes of synthesis of fullerene compounds, which contributes to:

1. Support decision-making in design activities during the initial design phase of an industrial facility [22];
2. Minimization of risks of equipment breakdown and loss of expensive raw materials in preparation of control and production personnel on the simulation-situational production model [21].
3. Forecasting of quality indicators of the production process at the specified material and technical base and technical regulations of production.

We formulate the goal of creation and implementation of the proposed computer system of visual modeling: ensuring the quality of organization of production of carbon nanocluster compounds with minimization of costs and risks of design and control errors of the chemical-technological process with the prediction of quality characteristics and economic indicators affecting the cost of production.

Setting a complex task of visual design and investigation of the process of synthesis of carbon nanocluster compounds: for a given vector of input parameters X :

- using the dialog mode, visual designer, and 3D models of the room and equipment, in accordance with the system of design and operational rules and requirements R , prepare a 3D model of the reactor area with the specification DS for it;
- varying the characteristics of U in the safety ranges R_3 performing virtual synthesis of the target product taking into account the accepted operational and economic restrictions R_4 and in accordance with the requirements for quality indicators of the process R_5 .

Thus, the complex task of designing and researching the processes of synthesis of fullerene compounds covers the product life cycle from the design of a model of a production site to the calculation of qualitative and integral indicators Q , which allows you to correct not only the design solution during the construction of an industrial facility but also the values of varying characteristics in order to obtain the best quality indicators of R_5 . Subsequently, targeted products become more accessible to consumers, and the enterprise becomes more competitive.

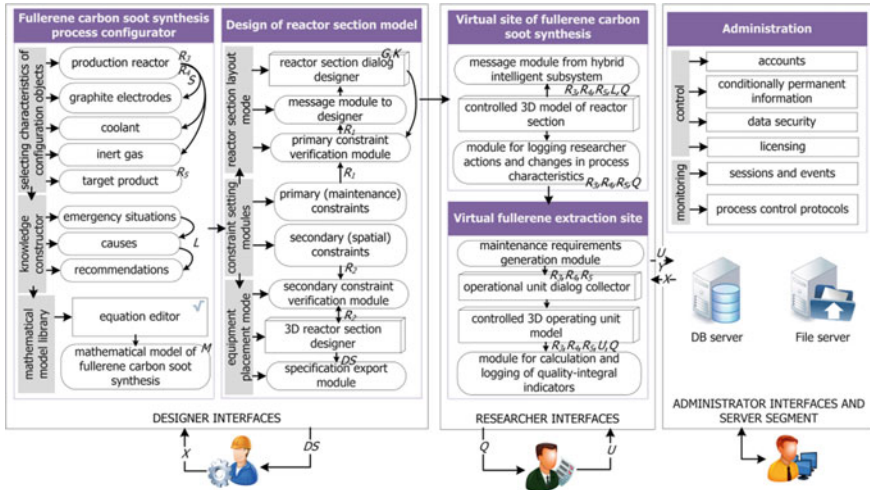


Fig. 2 The architecture of the computer system for processes of carbon nanocluster compounds synthesis visual modeling

4 Visual Simulation Architecture

The architecture of the computer visual modeling system (Fig. 2) includes the dialog and virtual graphical interfaces of the designer, researcher (operator), administrator interface, and server segment. The client-server architecture of the system is two-level.

The main stages of design and research of processes of synthesis of carbon nanocluster compounds are presented in Table 1.

As a result, when the production cycle is successfully completed in simulated production conditions close to the real ones, the resulting qualitative-integral characteristics Q make a decision to adjust the initial data X and the variable characteristics U .

5 Trial Operation

The system is multi-user with a centralized relational database of characteristics and 3D models of premises H and equipment E , material resources S , systems of equations of mathematical model M , situational knowledge L , rules, requirements and limitations R , qualitative-integral indicators of the process Q , as well as users, sessions, events, and protocols.

Pilot operation of the system of visual modeling of the processes of synthesis of carbon nanocluster compounds was carried out on the basis of the Department of

Table 1 Stages of the solution of the problem of visual design and research of processes of synthesis of carbon nanocluster compounds

Stage description	Data sources
1. Entering reference data E, H, S	G
2. Configuring simulated fullerene carbon soot synthesis process online with restriction entry R_1, R_3, R_4, R_5 , situational knowledge L , and systems of equations M	E, S
3. Develop scaled equipment E models and space H models in the selected 3D graphics editor.	G, K
4. In the dialog, select the K equipment models to be placed in the H room model based on the R_1 . Considering G enter spatial constraints R_2	G, R_1
5. Placement of equipment models E in the virtual space of the reactor section H in accordance with spatial limitations R_2	R_2
6. Operator, varying $U_A, L_E, G_C, G_G, v_M, \tau_I$, in the 3D environment of the reactor site model, performs virtual synthesis of fullerene carbon soot with characteristics M_s, F_{tp}, GC, MR, ME , according to regulations R_3, R_4, R_5	$E, H, S, R_3, R_4, R_5, U$
7. With the obtained mass of fullerene carbon soot by varying G_C, W_H, τ_2 , the process of target product extraction is simulated with the calculation of quality-integral indicators D_e, GC, VD, ME	$E, S, R_3, R_4, R_5, m_s, F_{tp}, U$
8. Studying the protocol of virtual synthesis of fullerene, comparing R_4 and R_5 with Q with a decision on the techno-cost-effectiveness of the process conducted	

Automated Design and Control Systems in the educational process with the involvement of undergraduates in chemical areas of training—18.04.01 “Chemical Technology” and 18.04.02 “Energy and Resource Saving Processes in Chemical Technology, Petrochemistry and Biotechnology”.

As initial data, the characteristics of the reactor section of the industrial enterprise “Closed Joint-Stock Company” Innovations of Leningrad Institutes and Enterprises”, St. Petersburg and the reactor section with an industrial reactor of the Kretschmer design [19] were used. Material resources: technical water as a refrigerant, inert gas—helium, graphite rods of a high degree of purification. Fullerene C_{60} is used as a target product.

Three-dimensional graphics editor selected to develop 3D equipment models “Autodesk 3ds Max”. Scaled equipment and space models are obtained. In the configurator dialog, you have entered reference data for designing the manufacturing process model.

The knowledge designer introduces situational knowledge frames. Frame example of situational knowledge: NS_1 : Electric arc break. $RSN_1^{NS_1}$ {Ta, [0;300], 100, “Electrode fracture, massive protuberance”}, $REC_1^{RSN_1^{NS_1}}$ {1, “Turn off electrode voltage, shut off inert gas and coolant”}, $REC_2^{RSN_1^{NS_1}}$ {2, “Replace electrode”}. $RSN_2^{NS_1}$

$\{L_E, [0.1;10], 0.3, \text{“Failure of inter-electrode distance ACS”}\}, REC_1^{RSN_2^{NS_1}} \{1, \text{“Turn off electrode voltage, shut off inert gas and coolant”}\}, REC_2^{RSN_2^{NS_1}} \{2, \text{“Eliminate malfunction of inter-electrode distance ACS”}\}.$

Among the process parameters for tracking their values by the researcher are direct ones corresponding to the vector of varying characteristics U and indirect ones calculated by model (for example, arc temperature T_a , coolant temperature, inert gas pressure).

A semi-empirical system of equations is introduced as a mathematical model, reflecting the dependence of safety and operability characteristics and qualitative-integral parameters of the simulated process on technical, operational, and variable characteristics of the process [21].

When generating the characteristics of the room, rules for comparing the integral characteristics of the R_I are introduced. The integral characteristics are: the power of the power grid, volume airflow rate of plenum-exhaust ventilation, light flux power of lighting devices. The singlet characteristics of the room are: electrical voltage, water pressure in the main, temperature, and humidity of the environment.

Taking into account G, R_2 spatial constraints are formulated and introduced into the matrix. The requirements of safety standards, ergonomics, and speed of personnel, requirements of safety and operability of equipment and tools of instrumentation were taken into account.

The design of the reactor section with regard to spatial limitations is carried out using the 3D designer (Fig. 3). The designer, using visual positioning tools with regard to the matrix of spatial constraints R_2 places equipment models in the model space of the reactor section.

The 3D designer tracks collisions and collisions, which imposes additional spatial constraints. It is not excluded that the equipment cannot be placed according to the spatial constraint matrix R_2 . In this case, the R_2 is corrected, the designer continues the placement until the equipment in the parcel model assumes the position according to R_2 .

In the designed reactor area, the process of synthesis of fullerene carbon soot is simulated (Fig. 4).

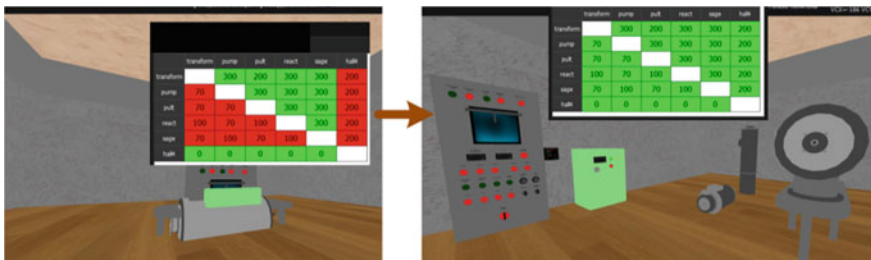


Fig. 3 Space and equipment models in the 3D designer before placement (left) and after placement according to spatial constraints R_2 (right). If the distance is R_2 , the matrix element changes color from red to green



Fig. 4 Fragments of virtual reactor site operator interface for fullerene carbon soot synthesis

With the observance of the accepted ranges of safety and operability of the equipment R_3 and operational and economic restrictions of R_4 the operator, varying characteristics of U makes the synthesis of fullerene soot of the required weight m_s^R with the required weight of the target product F_{tp}^R . Incorrect or untimely action of the operator, as well as setting a variable characteristic outside its safety range increases the risk of an emergency, as well as reduces the main qualitative indicator of the process—the content of fullerene C_{60} in the soot.

The operator assembles the extraction plant before the extraction. The criterion constraints when assembling an extraction plant are $D_e^R, VD_{max}, ME_{max}$. In addition, the geometric characteristics of the parts of the extraction plant (a type of the bottom of the flask, slips) are taken into account, as well as calculated by the solubility of the extracted target product, the selected extractant, and the requirement D_e^R bulb working volume. After assembly of the extraction plant, the operator, including the heater and the coolant supply, initiates the fullerene C_{60} extraction process (Fig. 5).

After the completion of the simulation of the production cycle, the following results were obtained: the mass of the synthesized carbon soot $M_s = 0.9$ kg, fullerene content in it $C_{60} F_{tp} = 14.8\%$, mass of fullerene in the soot $m_{tp} = M_s \cdot F_{tp}/100 =$

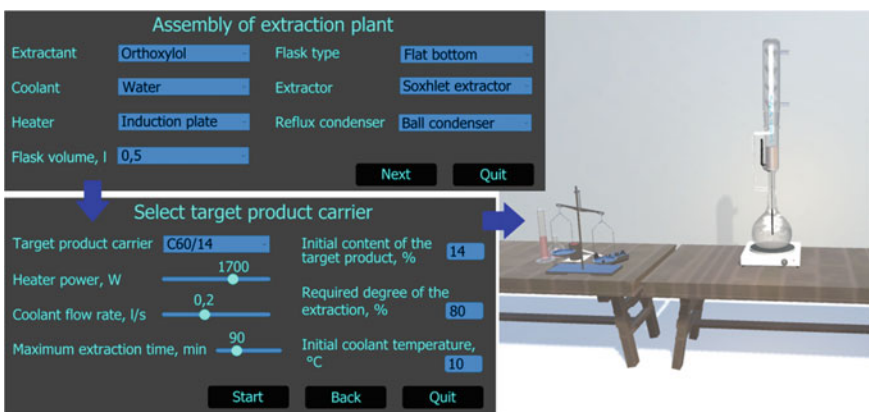


Fig. 5 Operator interface fragments for assembly of extraction plant model and virtual extraction of fullerene

0.133 kg, that is more than the required mass $C_{60} m_{tp}^{R1} = 0.126$ kg than 0.007 kg. The resulting difference is not critical for the first synthesis step. For the second stage of synthesis—extraction, with the required degree of extraction of fullerene $C_{60} D_e^R = 90\%$ and actual $D_e = 87\%$ the weight of fullerene in the extractant was 0.116 kg, which is higher than the required weight $C_{60} m_{tp}^{R2} = m_{tp}^{R1} \cdot D_e^R = 0.126 \cdot 0.9 = 0.113$ kg for 0.003 kg.

The obtained results of the pilot operation make it possible to conclude the applicability of the visual modeling system for design tasks, research of the process of synthesis of carbon nanocluster compounds, as well as the tasks of training control and production personnel in process control in both working and abnormal conditions.

6 Conclusions

It is known that the cost of unadjusted design errors of production facilities at subsequent stages of the product life cycle increases many times. Deviation from the process regulations in the process management not only leads to a decrease in the profitability of the enterprise, but also increases the intensity of wear and tear and the risk of equipment breakdown, and can also pose a potential danger to the health and life of control and production personnel.

The proposed system of visual modeling allows not only to reduce time and errors of design of the production area but also to increase qualitative and integral indicators of the process of synthesis of carbon nanocluster compounds. The obtained computer visual simulation system can be recommended both to enterprises in the field of synthesis of carbon nanocluster structures and scientific and educational centers and to educational institutions that carry out training in educational programs of automated design and control.

The authors express gratitude to all participants in the project for the development and trial operation of a visual simulation system.

The work was carried out on the instructions and with the financial support of the Fund for Infrastructure and Educational Programs “RUSNANO” within the framework of applied research work on the topic “Development of an educational program for advanced training and a training and methodological complex for specialists of chemical and biotechnological enterprises in the field of automated production nanotechnologies”.

Acknowledgements This research was partially supported by the Russian Fund of Basic Research (grant No. 18-08-00143 A).

References

1. Xu, L.D., Li, L., Xu, E.L.: Industry 4.0: state of the art and future trends. *Int. J. Prod. Res.* **56**(8), 2941–2962. Taylor & Francis (2018)
2. Ojra, A.: Revisiting industry 4.0: a new definition. In: *Intelligent systems and computing*, vol. 858, pp. 1156–1162. Swansea University, Swansea (2019)
3. Espejo, R.: Cybernetics of Governance the Cybersyn Project 1971–1973. In: Metcalf, G. S. (ed.) *Social Systems and Design, Translational Systems Sciences Book Series (TSS)*, vol. 1, pp. 71–90. Springer, Japan (2014)
4. Letichevsky, A.A., Letychevskiy, O.O., Skobelev V.G., et al.: Cyber-physical systems. In: *Cybernetics and Systems Analysis*, vol. 53. issue 6, pp. 821–834. Springer, New York (2017)
5. Ragunathan, R., Insup, L., Lui, S, et al.: Cyber-physical systems: the next computing revolution. In: *Design Automation Conference (DAC), 47th ACM/IEEE*, pp. 731–736. IEEE (2010)
6. Veshneva, I.V., Bolshakov, A.A., Fedorova A.E.: Organization of engineering education for the development of cyber-physical systems based on the assessment of competences using status functions. In: Kravets, A., Bolshakov, A., Shcherbakov, M. (eds.) *Cyber-Physical Systems: Industry 4.0 Challenges. Studies in Systems, Decision and Control*, vol. 260, pp. 277–288. Springer, Cham (2020)
7. Kizim, A.V., Kravets, A.G.: Systemological approach to intelligent decision-making support in industrial cyber-physical systems. In: Kravets, A., Bolshakov, A., Shcherbakov, M. (eds.) *Cyber-Physical Systems: Industry 4.0 Challenges. Studies in Systems, Decision and Control*, vol. 260, pp. 167–183. Springer, Cham (2020)
8. Cai, H., Xu, L., Xu, B., et al.: IoT-based configurable information service platform for product lifecycle management. *IEEE Trans. Indus. Info.* **10**(2), 1558–1567. IEEE (2014)
9. Cai, P.: Simulation-enabled vocational training for heavy crane operations. In: *Simulation and Serious Games for Education*, pp. 47–59. Springer, Singapore (2017)
10. Staroverova, N.A., Shustrova, M.L., Satdarov, M.R.: Development of a cyber-physical system for the specialized on-track machine operators training. In: Kravets, A., Bolshakov, A., Shcherbakov, M. (eds.) *Cyber-Physical Systems: Industry 4.0 Challenges. Studies in Systems, Decision and Control*, vol. 260, pp. 315–325. Springer, Cham (2020)
11. Chistyakova, T.B., Furaev, D.N.: A computer system for training of specialists in design of industrial facilities for petrochemistry and oil processing. In: *Proceedings of 2018 17th Russian Scientific and Practical Conference on Planning and Teaching Engineering Staff for the Industrial and Economic Complex of the Region, PTES*, vol. 17, pp. 92–94. IEEE (2018)
12. Glotova, T., Deev, M., Krevskiy, I., et al.: Models of supporting continuing education of specialists for high-tech sector. In: Kravets, A. et al. (eds.) *Joint Conference on Knowledge-Based Software Engineering 2014, CCIS*, vol. 466, pp. 100–112. Springer, Switzerland (2014)
13. Dozortsev, V.M.: Virtual reality technologies in technological process operator training. In: *Automation in Industry*, vol. 6, pp. 42–50. LLC publishing house “InfoAvtomatizatsiya” (2018)
14. Balamuralithara, B., Woods, P.C.: Virtual laboratories in engineering education: the simulation lab and remote lab. In: *Computer Applications in Engineering Education*, vol. 17, no 1, pp. 108–118. Wiley Periodicals, Inc., USA (2009)
15. Finogeev, A.G., Maslov, V.A., Finogeev, A.A.: Architecture of virtual learning environment with support for wireless access to information resources. In: *Distance and Virtual Learning*, vol. 6, pp. 76–97. SGU, Moscow (2010)
16. Finogeev, A.G., Fionova L.R.: Elaboration of automated systems for development of professional competence. *Res. J. Appl. Sci.* **10**, 7–11. ARPJ Journals, Ipswich (2015)
17. Glotova, T.V., Deev, M.V., Krevskiy, I.G.: Individualized learning trajectories using distance education technologies. In: Kravets, A., Shcherbakov, M., Kultsova, M., Shabalina, O. (eds.) *Creativity in Intelligent Technologies and Data Science. Communications in Computer and Information Science*, vol. 535, pp. 778–792. Springer, Cham (2015)
18. Kratchmer, W., Lamb, L.D., Fostiropoulos, K., Huffman, D.R.: Solid C₆₀: a new form of carbon. In: *Nature*, vol. 347, pp. 354–359. Nature Publishing Group, Great Britain (1990)

19. Alekseyev, N.I., Charykov, N.A.: Mechanism of selection of perfect fullerenes in arc synthesis. *Russian J. Phys. Chem. A Focus Chem.* **82**, 2182–2190. Pleiades Publishing Ltd (2008)
20. Tsetkova, L.V., Keskinov, V.A., Charykov, N.A. et al.: Extraction of fullerene mixture from fullerene soot with organic solvents. *Russian J. General Chem.* **81**(5), 920–926. Springer, Russia, Moscow (2011)
21. Chistyakova, T.B., Petrov, D.N.: The mathematical model and program complex for support of management synthesis of carbon nanostructures process. *J. Phys. Conf. Ser.* **803**(1), 205–217. IOP Publishing, UK (2018). (In Russian)
22. Chistyakova, T.B., Furaev, D.N., Zashchirinskiy, S.V.: Computer-aided design systems for 3D models of industrial plants In: *Automation in Industry*, no 9, pp. 9–12. LLC Publishing house “InfoAvtomatizatsiya” (2018)

Intellectual System of the Life Cycle of Packaging Materials Characteristic Analysis



Tamara Chistyakova, Aleksandr Razygraev , and Christian Kohlert

Abstract The article considers an intelligent system for analyzing the life cycle characteristics of packaging materials, which allows, at given requirements for packaging materials, to evaluate the complex of properties of packaging materials, to calculate specific and generalized criteria for evaluating packaging materials, and to provide the user with the opportunity to choose the most suitable packaging material based on the results. The life cycle of packaging includes the following main stages: production of raw materials for packaging, production of packaging, recycling, and disposal of packaging. Each stage of the packaging life cycle includes its own set of qualitative and quantitative characteristics. The developed system is open, flexible, and built using modern client-server technologies, including a library of customizable criteria, a database of rules for selecting packages, databases of life cycle stages, packages, packaging materials, and characteristics of packaging materials. The system has an ergonomic interface and includes modules for entering package selection requirements, a module for evaluating package life cycle characteristics, a module for calculating package selection criteria, a module for changing expert data, a module for displaying comparison results in the form of various graphs and nomograms. The system is tested on the example of comparative analysis of the process of manufacturing packages, which may include: polyvinylchloride, polypropylene, polystyrene, low-pressure polyethylene, high-pressure polyethylene, polyethylene terephthalate, glass, paper, cardboard, white tin, aluminum. The developed intelligent system can be used for a comprehensive assessment of the life cycle of the production of packaging materials taking into account environmental safety, consumer, and economic characteristics.

T. Chistyakova (✉) · A. Razygraev
Saint-Petersburg State Institute of Technology (Technical University), 26 Moscow Avenue,
Saint-Petersburg 190013, Russia
e-mail: chistb@mail.ru

A. Razygraev
e-mail: rozaa@yandex.ru

C. Kohlert
Kohlert-Consulting, Rotsteinerstraße 14, 56414 Oberahr, Germany
e-mail: info@kohlert-consulting.com

Keywords Intelligent system · Packaging · Life cycle assessment

1 Introduction

Packaging plays an important role in promoting the product to the market, so preliminary studies of various packaging parameters, including environmental ones, will avoid errors and help manufacturers position their products correctly [1–3].

The history of packaging began with the use of natural materials, and then fabric, ceramics, glass, wood, tin, paper, cardboard, plastic appeared. Packages of different combinations of packaging material have now been widely used to benefit from the individual characteristics of each material [2, 3].

The life cycle of packaging includes the following main stages: production of raw materials for packaging, production of packaging, recycling (transition to the production stage), and disposal of packaging.

Figure 1 shows an example of the life cycle of packaging materials using polyvinylchloride (PVC) as an example. Each stage of the packaging life cycle is comparable to its own set of indicators, which can change over time due to social trends and scientific and technological progress. For example, the following characteristics [4–8] can be considered at the stage of packaging production:

- environmental characteristics of packaging materials, which take into account aspects of the use of natural resources in production, namely the parameters: the amount of energy consumed, the amount of air required for production, the amount of water required for production, the amount of waste produced, the amount of water consumed, the amount of oil consumed.
- consumer characteristics of packaging materials imply the physical properties of packaging materials important to the customer: water permeability, vapor

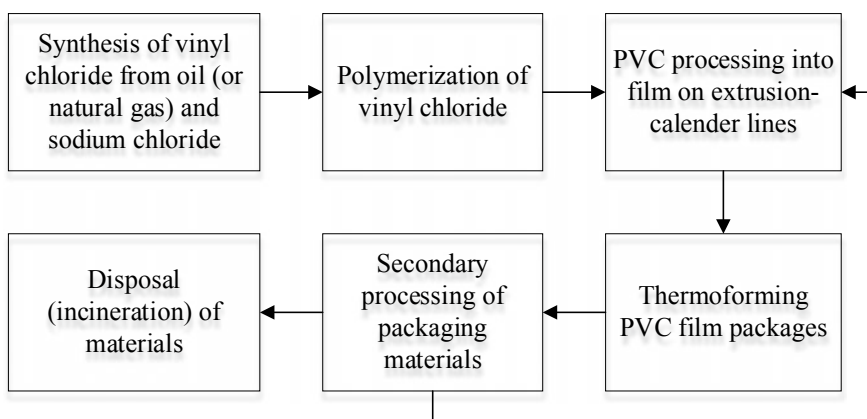


Fig. 1 Packaging product life cycle (PVC example)

permeability, density, heat resistance, elasticity, the maximum temperature of use, minimum temperature of use, surface tension, energy for the manufacturing process, forming depth, printing capability, antistatic, photosensitivity, stiffness, tensile strength, impact resistance.

- economic characteristics of packaging materials imply economic effect from the production of packaging material and include parameters: raw material cost, packaging production costs, income from packaging production.

In developed industrial countries, the ratio of economic and consumer characteristics is constant, that is, packaging with better consumer properties is expensive and vice versa. The principle of rational use of natural resources (environmental characteristics) in the selection of packaging materials has become more and more important since about 2015. Developing countries often overestimate the economic aspect of packages, saving on quality in favor of value without taking into account environmental characteristics [9].

Product Life Cycle Analysis (LCA) [10] is often used to assess natural resource management. This analysis is used to assess the environmental impact of a product associated with all its life cycle stages. At the same time, a life cycle assessment (taking into account the environmental aspect of the impact on the environment of an individual product) and a comparative life cycle assessment (is a comparison of several products with holistic consideration of environmental, consumer, and economic characteristics) are distinguished.

The methodology for life cycle analysis is established in international standards ISO 14040-ISO 1404 [11, 12]. The interpretation of the results of the product life cycle assessment should lead to subsequent improvement of the product, for example, due to the improvement of production technology [13, 14]. Implementation of product improvement solutions often results in product marketing benefits [15].

In view of the above, the task of developing an intelligent system for analyzing the life cycle characteristics of packaging materials has become relevant enabling the assessment of properties and calculation of specific and generalized criteria for the evaluation of packaging materials, according to the specified composition of the compared packaging materials, according to the comparison criteria determined by the product rules in accordance with the specified stage of the life cycle and the scope of application of the packaging, and enable the user to compare the life cycle and select the most appropriate package based on the results.

2 Description of the Developed Intelligent System

Figure 2 shows the architecture of the developed intelligent system for analyzing the life cycle characteristics of packaging materials.

The developed architecture consists of their three main modules [8]:

- the administrator interface (knowledge engineer) is introduced to implement the function of replenishing the rule database and the database with expert data, such

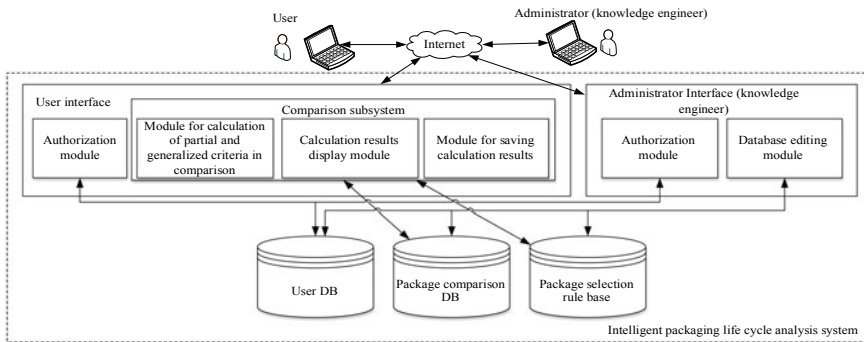


Fig. 2 Packaging materials intelligent life cycle analysis architecture

as: specific values of the characteristics of packaging materials, the number of characteristics used in comparing packaging materials for a given area of application of packaging and a given stage of the life cycle, the values of the weight coefficients of the characteristics (used in calculating the comparison criterion using the method of linear convolution of criteria), and other reference books. This expert data cannot be changed by the user, and some of this data is hidden from the user, for example, specific values of the characteristics of packaging materials. For this purpose, an authorization module is introduced into the interfaces;

- the user interface includes a subsystem for comparing packaging materials, which includes: a module for calculating partial and generalized comparison criteria, a module for displaying the result in the form of tables and nomograms, and a module for storing calculation results;
- information subsystem includes: data describing package comparison modules (scope of comparison packages, name of comparison module, names of compared packages, composition and weight values of packages); data necessary for the calculation of criteria for evaluation of characteristics of packaging materials (specific values of characteristics of packaging materials, weight coefficients used in the calculation of a generalized criterion); rules for the selection of packages determining the composition and weight coefficients of the comparison criteria depending on the application of the compared packages and the stage of the life cycle of the packages; system user data.

Setting the task of evaluation of characteristics of packaging materials: for specified input variables (package life cycle stage A, package application area B, comparison module name S, number of packages in comparison module n, number of packaging materials in comparison module m, array of package names U, array of weight values of packaging materials in package P) and selected using a rule database and a database of variables (an array of packing material K characteristic names; quantity of characteristics of packaging materials s; array of specific values of characteristics of packaging materials Y, array of names of packaging materials M; array of weight coefficients of characteristics W) to form output variables (array of absolute values of

characteristics of packages G; an array of relative values of the environmental characteristics of the Grel packages; an array of aggregated packing indicators by group I) in the form of tables, graphs and nomograms, according to which the user will carry out a comparative life cycle assessment and choose the most suitable packaging.

The algorithm for evaluating the characteristics of packaging materials consists of the following procedures:

- calculation of values of characteristics of packaging materials for compared packages;
- bringing all characteristics to a single scale by calculating the relative values of the characteristics of packaging materials;
- calculation of criteria for evaluation of characteristics of packaging material by linear convolution method [16–18].

The intelligent system database contains specific values for the characteristics of packaging materials and must be recalculated for packages according to their recipe. If the specific values in the database are given in absolute units (for example, for the environmental and economic characteristics of the packaging production stage), then the recalculation is carried out according to the formula:

$$G_{ki} = \sum_{j=1}^m (Y_{kj} \times P_{ij}), \quad (1)$$

where G_{ki} —the array of package characteristic values taking into account package recipe, $k = 1..s, i = 1..n$; Y_{kj} —the array of specific values of packing materials characteristics, $k = 1..s, j = 1..m$; P_{ij} —the array of weight values of packaging materials in package, $i = 1..n, j = 1..m$; n —number of packages in comparison module; m —the number of packaging materials in comparison module; s —the quantity of packing material characteristics.

If the specific values in the database are given in relative units (for example, for consumer characteristics of the packaging production stage, all parameters in points from 0 to 2 relative to polyvinylchloride, in which all values are 1), then the recalculation is carried out according to the formula with averaging:

$$G_{ki} = \sum_{j=1}^m (Y_{kj} \times P_{ij}) / \sum_{j=1}^m P_{ij}. \quad (2)$$

Calculation of relative values of package characteristics is performed by the formula:

$$G_{ki}^{rel} = G_{ki} / \sum_{i=1}^n G_{ki}, \quad (3)$$

where G_{ki}^{rel} —the array of relative values of package characteristics, $k = 1..s, i = 1..n$.

Calculation of the criterion for evaluating the characteristics of packaging material and calculation of linear convolution generalized by the method is made according to the Formula:

$$I_i = \sum_{k=1}^s (G_{ki}^{rel} \times W_k) / \sum_{i=1}^n \sum_{k=1}^s (G_{ki}^{rel} \times W_k), \tag{4}$$

where I_i —vector of generalized packing indicators, $i = 1...n$; W_k —vector of weight coefficients of environmental characteristics, $k = 1...s$.

The package selection rule base is represented by product rules allowing, according to the given name of the package life cycle stage A and the packaging application area B , to form a plurality of characteristics of the packaging materials K and their weights W used in the comparison of packages. Table 1 shows an example of a production rule for comparing food PET packages at the stage of packaging production.

The process of interaction of the user with the developed intelligent system in order to carry out the analysis of characteristics of packaging material includes the following steps:

- creation of a module for comparison of characteristics of packaging materials: generation of a name of the comparison module with the indication of the scope of application of compared packages and stage of the life cycle of packages, the formation of an array of package names, generation of weight values of packaging materials in the package, preservation of the comparison module and its settings;
- calculation of characteristics of packaging materials: calculation of characteristics, the formation of tabular results, generation of nomograms, preservation of results;
- comparison and selection of packages.

An intelligent system for analyzing the life cycle characteristics of packaging materials has been developed using modern client-server technologies. The client part is developed using HTML, CSS, JS, Axios, Vue.js, and Vuetify.js. The server part is designed using NodeJS. The development of the relational database was carried out in the database management system MySQL.

Table 1 Sample product rule

If	So
A = « PRODUCTION OF PACKAGES» AND B = « FOOD PET PACKAGING»	(K ₁ = « AMOUNT OF ENERGY CONSUMED» , W ₁ = « 0.2») AND (K ₂ = « AMOUNT OF CARBON MONOXIDE EMISSION IN PRODUCTION » , W ₂ = « 0.3 » AND (K ₃ = « AMOUNT OF OIL CONSUMED» , W ₃ = «0.4 »)

3 Intelligent System Test Case

Table 2 shows an example of input data for comparing three pharmaceutical packages at the stage of packaging production. Open-source data was used to test the database with specific characteristics of packaging materials [19].

Figure 3 shows an example of comparison results according to Table 2 as a graph of comparison by a group of environmental characteristics of packages. Figure 4 shows an example of comparison results according to Table 2 as a comparison of a generalized graph of the results of the evaluation of the characteristics of packaging materials in the stage of their production. By analyzing the results, the user will be able to choose the most environmentally friendly package (Package 3) or with the best consumer characteristics (Package 1) at the stage of packaging production.

Comprehensive testing of the software complex was carried out on the basis of the data provided by the international corporation Klöckner Pentaplast Europe GmbH & Co. KG characterized by multi-assorted production of packages. The system is tested on the data of the process of production of food and pharmaceutical packages, which may include: polyvinylchloride, polypropylene, polystyrene, low-pressure polyethylene, high-pressure polyethylene, polyethylene terephthalate, glass, paper, cardboard, white tin, aluminum.

Table 2 Composition of compared packages

Material	Package name		
	Package 1	Package 2	Package 3
Polyvinylchloride	5.72 r	0	0
Polypropylene	0	3.8 r	0
Aluminum	7.27 r	7.9 r	15.6 r

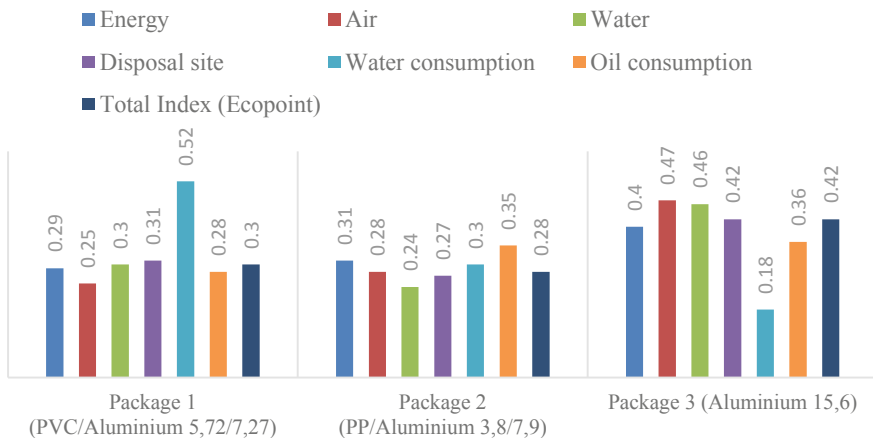


Fig. 3 Schedule of comparison of three pharmaceutical packages at the stage of production by a group of environmental characteristics of packages

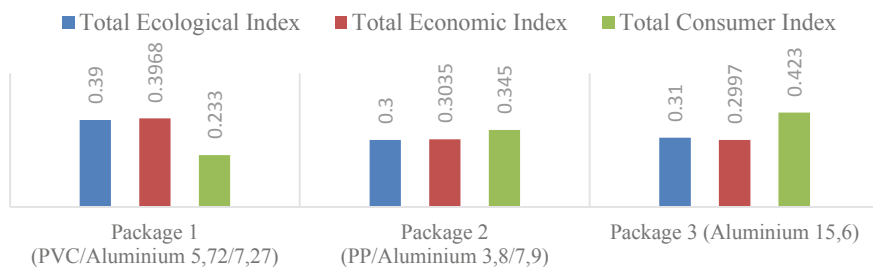


Fig. 4 Schedule of comparison of three pharmaceutical packages at the stage of production by generalized indicators

4 Conclusion

A flexible intelligent system has been developed, customizable to various comparison criteria, types of packaging materials, stages of the life cycle of packages, areas of application of packages, allowing for the specified requirements for packaging materials, to evaluate the characteristics of multi-component packages and provides the user with the opportunity to analyze and select a packaging material based on the results.

Testing of the intelligent system confirmed its operability to solve the problem of analyzing the life cycle characteristics of packaging materials. The developed intelligent system was introduced into experimental and industrial operation at the company for the production of polymer film materials Klöckner Pentaplast Europe GmbH & Co. KG [20].

The developed system can be used by packaging manufacturers to position products in dialogue with buyers, environmentalists, government services, and other stakeholders in a comprehensive assessment of the life cycle of packaging materials production taking into account environmental safety, consumer, and economic characteristics.

References

1. Jung, H.: In: General Characteristics of Packaging Materials for Food System. vol. 624. Academic Press (2014)
2. Meneses, M., Pasqualino, J., Castells, F.: Environmental assessment of the milk life cycle: the effect of packaging selection and the variability of milk production data. *J. Environ. Manage.* **107**, 76-83 (2012). <https://doi.org/10.1016/j.jenvman.2012.04.019>
3. Navajas, A., Bernarte, A., Arzamendi, G., Gandia, L.M.: Ecodesign of PVC packing tape using life cycle assessment. *Int. J. Life Cycle Assessment* **19**, 218-230 (2014). <https://doi.org/10.1007/s11367-013-0621-1>
4. Meshalkin, V.P., Khodchenko, S.M.: The nature and types of engineering of energy- and resource-efficient chemical process systems. *Polymer Sci. Series D* **10**(4), 347-352 (2017). <https://doi.org/10.1134/s1995421217040128>

5. Ciacci, L., Passarini, F., Vassura, I.: The European PVC cycle: In-use stock and flows. *Resour. Conserv. Recycl.* **123**, 108–116 (2017). <https://doi.org/10.1016/j.resconrec.2016.08.008>
6. Janajreh, I., Alshrah, M., Zamzam, S.: Mechanical recycling of PVC plastic waste streams from cable industry: a case study. *Sustain. Cities Soc.* **18**, 13–20 (2015). <https://doi.org/10.1016/j.scs.2015.05.003>
7. Selke, S., Culter, J.D.: *Plastics packaging 3E properties, processing, applications, and regulations*. pp. 487. arl Hanser Verlag GmbH & Co, Munich, Germany (2016)
8. Braun, D.: Recycling of PVC. *Prog. Polym. Sci.* **27**, 2171–2195 (2011). [https://doi.org/10.1016/S0079-6700\(02\)00036-9](https://doi.org/10.1016/S0079-6700(02)00036-9)
9. Kohlert, C.: Nachhaltigkeit von Kunststoffverpackungen—von der Wiege bis zur Bahre. *Sitzungsberichte der Leibniz-Sozietät der Wissenschaften zu Berlin*, vol. 130, pp. 89–98 (2017). <https://leibnizsozietat.de/wp-content/uploads/2017/01/Kohlert.pdf>
10. Silvenius, F., Katajajuuri J., Grönman, K., Soukka, R., Koivupuro, H., Virtanen, Y.: Role of packaging in LCA of food products. In: *Towards Life Cycle Sustainability Management*, Springer, pp. 359–370 (2011). https://doi.org/10.1007/978-94-007-1899-9_35
11. ISO 14040: Environmental management—life cycle assessment—principles and framework. International Organisation for Standardisation, Geneva (2006)
12. ISO 14044: Environmental management—life cycle assessment—requirements and guidelines. International Organization Standardisation, Geneva (2006)
13. Belukhichev, E.V., Sitnikova, V.E., Samuylova, E.O., Uspenskaya, M.V., Martynova, D.V.: Films based on a blend of PVC with copolymer of 3-Hydroxybutyrate with 3-Hydroxyhexanoate. *Polymers* **12**, 270 (2020). <https://doi.org/10.3390/polym12020270>
14. Sin, L.T., Rahmat, A.R., Rahmat, W.A.: *Polylactic Acid—PLA Biopolymer Technology and Application*, pp. 352. William Andrew; Norwich, NY, USA (2012)
15. Hauschild, M.Z.: Life cycle assessment: goal and scope definition. In: Chatti, S., Laperrière, L., Reinhart, G., Tolio, T. (eds.) *The International Academy for Production (eds) CIRP Encyclopedia of Production Engineering*. Springer, Berlin, Heidelberg (2018)
16. Kolbin, V.V.: In: *Decision Making and Programming*. World Scientific Publishing Co, pp. 756 (2003)
17. Razygraev, A.S., Makaruk, R.V., Chistyakova, T.B., Kohlert, C.: Remote computer system for selection of packaging material on ecological parameters. In: *Proceedings 29th International Symposium Mathematical methods in engineering and technology*, pp. 61–64 (2016)
18. Panasenkov R.E., Razygraev A.S., Chistyakova T.B.: Web-application for comparison of ecological characteristics of polymer materials. In: *Proceedings 30th International Symposium “Mathematical Methods in Engineering and Technology*, pp. 53–56 (2017)
19. Nowack, K.: *Aspekte von Verpackungsmaterialien bei Ökoprodukten*. Forschungsinstitut für biologischen Landbau (FiBL), Schweiz (2007). https://orgprints.org/13508/1/Endbericht_Verpackung.pdf
20. Chistyakova T.B., Razygrayev A.S., Polosin A.N., Araztaganova A.M.: Joint innovative it projects in the field of production of polymeric sheet materials. *Institute of Electrical and Electronics Engineers Inc.*, pp. 61–64 (2016). <https://doi.org/10.1109/ivforum.2016.7835855>

Model of Paired and Solitary Influence of Ingredients of Polymer Composition



Ilya V. Germashev , Evgeniya V. Derbisher , Vyacheslav E. Derbisher ,
and Tatyana P. Mashihina

Abstract The problem of calculating the properties of a polymer-modified with a complex of active additives is considered. The proposed approach to solving the problem involves the use of already available information about polymer compositions to create a black-box model and further refine the interaction of composition components based on the laws of the subject area and a gradual transition to the gray box. This work is devoted to creating a black-box model based on two-component interaction and so far does not take into account the complex component. The proposed model also allows you to evaluate the unknown pair influence of the ingredients of the polymer composition from the known single effect of these ingredients. The resulting model has been tested on a specific example. Computations using fuzzy mathematics has been held. Based on the results obtained, a solution to the task is suggested.

Keywords Polymer composition · Active additive · Property · Fuzzy numbers · Decision making

1 Introduction

Composite materials (composites) are multicomponent systems, today it is one of the most filled scientific and technical niches. However, the number of developments related to the creation of new materials in this category is constantly growing, since it is here where it is expected to obtain significant results for technology and economics. Managing the properties and overall quality of composites during their design and development is a multicriteria problem solved by experimental and model methods. Moreover, in this category, special mixtures are distinguished by composite mixtures

I. V. Germashev (✉) · T. P. Mashihina
Volgograd State University, Volgograd, Russia
e-mail: germashev@volsu.ru

E. V. Derbisher · V. E. Derbisher
Volgograd State Technical University, Volgograd, Russia

created on the basis of high molecular weight compounds—polymers, which can be either organic or inorganic in nature [3, 21].

It will not be superfluous to note that at present high-molecular compounds as individual substances are practically not processed today but are used to prepare technological mixtures, and the main tool for regulating the properties of the final material is, so to speak, a game with ingredients. Moreover, the use of active additives to solve technical problems for various materials is quite broad [13]. For the ingredient control of the properties of polymeric materials in the presence of a base high molecular weight matrix, various active and inactive fillers, modifying, and non-modifying additives are widely used. This is especially true for multi-ingredient (more than two) polymer compositions (PCs) and materials produced on their basis. At the same time, the goals are directed, efficient, economical regulation and optimization of both the composition of the system “polymer matrix (up to 100%) + filler (0–95%) + additives (0–45%)” and its processing technology, as well as a wide range of operational characteristics [1, 5, 18, 20].

In terms of theory, there is a need to solve the multifactor task of optimizing PCs, which is essentially fuzzy [4, 6, 8, 9, 11, 17], today it is based on the dependency platform “composition—property—quality—application” and provides reasonable (better quantitatively) selection of a certain amount and quality of ingredients with the necessary technical functions. Today’s sets of ingredients are presented very widely today, so the result is ambiguous solutions that are unlikely to be unambiguous in the future.

Another theoretical prerequisite for this topic is that raw PCs (in other words, mixtures), abstracting from the specific content, must be considered as complex chemical-technological systems (CTS), in which the composition, physicochemical state of the system (PC and the interaction between the ingredients and the polymer matrix individually and in combination), depend not only on their nature of the elements of the system but also on the technological processes of their processing and are difficult to theoretically multifactor modeling and on this basis of identification and forecasting [10, 14]. Here, the research tool is system analysis methods and, in particular, modeling. And given the similarity of the structural models of materials of natural and artificial origin from the point of view of chemical composition and degree of ordering in the polymer structure [16], we can talk about the prospects for describing natural phenomena.

Turning specifically to the subject matter of this chapter, we have that the materials obtained on the basis of PCs also fall into this circle, being extremely complex heterogeneous systems that can be divided according to prevailing views according to processing technology and structural features [3, 21] about the following groups:

- fiber filled;
- dispersed filled;
- with interpenetrating structures of continuous phases;
- mixed;
- voluminous (“3D”);
- layered (“2D”).

Given the special modern scientific, technical, and consumer interest in nanotechnology, we separately distinguish PCs of the composition “polymer matrix—additive (filler)”, which uses 2D and 3D nanoparticles—graphene, carbon nanotubes, and similar filler ingredients. They make it possible to obtain PCs with a number of unique properties [2]. Other technologies also make it possible to control fiber geometry [12] or nanoparticle reinforcement [15].

In this chapter, fillers are not considered in detail—their range is relatively limited, and there is an extensive and detailed set of theoretical and practical developments on that part [19]. Another thing is supplements. Today, their diversity, offered by the chemical industry and underdevelopment, is very large and constantly growing. Widely represented, for example, super concentrates (2–5% of the mass of the polymer matrix). However, at the same time, the number of problems associated with their properties and the properties of the PC as a system object is growing.

Enlarged additives for PCs located on the production market can be divided into two classes: technological (processing) and modifying (functional), associated with the operation of the polymer product. We note the main most common purposes of their use in a PC (the most relevant for modern conditions are indicated in bold):

- generation and satisfaction of new needs of society;
- technology optimization;
- giving specific effects;
- extension of durability (weather resistance, water resistance, frost resistance, crack resistance, fatigue, chemical resistance, etc.);
- increase fire resistance;
- expansion of the intervals of physical and mechanical characteristics;
- expansion of technical and ergonomic functions;
- regulation of shrinkage;
- improvement of surface properties;
- improvement of environmental friendliness;
- improvement of aesthetic properties;
- acceleration of drying and a set of standardized properties;
- saving resources.

The most important types of additives (without details) are presented in Table 1.

The formation of a complete and current formulation, taking into account the goals and properties listed above, has a peculiar feature that, for example, the virtual (pre-design) composition of a PC, like the real one, is also a multicomponent and multifactor complex, often intelligent, system with uncertain the number and quality of communications, which is incomplete and requires engineering support in the technology for the implementation of the full algorithm “PC design—practice” through further design and experimental work. This, in addition to the above, maybe the definition of additional conditions, the nature of co-ingredients, their concentration, technological and operational characteristics, etc.

We give a tabular example (Table 2) showing only a partial variety of PC ingredients (mainly of polymer nature in modern technologies).

Table 1 Types of additives in PC

No	Type of additive	Content, mass % to the polymer matrix
1	Retardants	0–3.0
2	Antiseptics	0–2.0
3	Antistatics	0–3.0
4	Inhibitors	0–2.0
5	Dyes (pigments)	0–2.0
6	Hardeners	0–10.0
7	Plasticizers	0–45.0
7	Rheological	0–3.0
8	Greases	0–2.0
9	Stabilizers	0.1–5.0

Table 2 Additives in polymer composites

Type of additive	Technical function	Active substance
Polyolefins	Ethylene propylene copolymer, ethylene propylene diene vinyl copolymer, ethylene–vinyl acrylate copolymer	Polyolefins
Polypropylene	Ethylene propylene divinyl copolymer, terephthalic ether, ethylene methyl acrylate, polybutadiene	Polypropylene
Polystyrene, styrene plastics	A copolymer of butadiene and styrene, a copolymer of ethylene, butadiene, and styrene	Polystyrene
Polyamides	Methyl disulfide, methyl acrylonitrile copolymer, ethylene, butadiene, and styrene copolymer, grafted copolymers methyl acrylonitrile	Polyamides
Polyesters	Acrylates, polyethylene glycidyl dimethacrylate	Polyesters
Polycarbonate	A copolymer of methyl methacrylate, butadiene, and styrene, ABC (PS/ABC mixture)	Polycarbonate
Polyphenylene sulfide	Polyethylene glycidyl dimethacrylate	Polyphenylene sulfide
Anti-blocking	Sticking prevention	Silicic acid, amide waxes
Antioxidant	Thermal oxidation prevention	Phenols, phosphides
Flame retardant	Flammability reduction	Inorganic oxides, hydroxides metals halogen-containing, phosphorus-containing, etc

In connection with the foregoing, we point out that the management of PC properties for the creation of competitive technologies is possible only in a combination of theoretical and empirical methods while taking into account the multicomponent nature of the PC and the variety of technologies for its processing, the following design work vectors are possible:

- pre-experimental heuristic identification of PCs as a system and selection of material properties;
- design of the polymer matrix and the technology for its production (polymerization, polycondensation, modification, crystallization, structuring, etc.).
- the choice of composition and structure by varying the ingredients;
- regulation of the technical functions and concentration of ingredients, taking into account possible environmental damage and the interests of society.

Naturally, such a cumbersome task and its solution must be considered in stages, starting, for example, with a two-component system, which is done in the present work.

In connection with the foregoing, it is clear that there is always a need to develop new accurate methods for predicting and constructing properties of PCs, which will allow us to create qualitatively new materials in the future. Therefore, the possibility of designing effective materials based on adequate models, which make it possible to predict with a high degree of accuracy the properties of newly created composites and not only polymer ones, is important.

2 Formulation of the Problem

Let polymer P be given. Based on this polymer, it is planned to create a composition C in order to provide the best possible values of some m properties Q_1, Q_2, \dots, Q_m . The values of these polymer properties are denoted by x_1, x_2, \dots, x_m , respectively. Here we will assume that the parameters x_j are normalized so that an increase in its value corresponds to an improvement in the corresponding property. Some clarification is required here, which is understood as “best properties”.

When buying polymer products, the consumer pays attention to a number of properties. These properties should meet the expectations of the consumer to the maximum extent, i.e., one of the main requirements for the polymer composition is the user's needs. Another important source of requirements for the properties of the polymer composition is the technological process (for example, the features of the technological process can lead to polymer degradation, then stabilizers will be additionally needed, or softening of the composition may be required in the production process, then plasticizer is required, etc.). Other sources of polymer composition requirements may arise. In any case, a list of requirements for the property values (in our case, their number is indicated by m) of the polymer composition is obtained. Hereinafter, we will consider those values that are least different from property values according to the formulated requirements to be considered the best.

Let polymer composition C consist of a polymer matrix P and ingredients $s_i, i = 1, \dots, n$, where n is the number of ingredients in C . It is required to evaluate how the properties of Q_j for C will change compared to $P, j = 1, \dots, m$. To do this, we construct a mathematical model of the interaction of the components of the composition and obtain a procedure for calculating its properties.

3 Mathematical Model of the Interaction of Components

Denote by x_{ij} the value of the Q_j property of the polymer P after modification with the compound $s_i, i = 1, \dots, n$. Suppose that additives s_i interact in pairs with each other, exerting a cumulative effect on P according to the following scheme (Fig. 1). So s_{i_1} and $s_{i_2} (i_1 \neq i_2 = 1, \dots, n)$ together give the property Q_j the value $x_{i_1 i_2 j}, j = 1, \dots, m$. Then the effect of the additives s_{i_1} and s_{i_2} on P can be expressed by the formula

$$x_{i_1 i_2 j} = a_{i_1 i_2 j} x_j$$

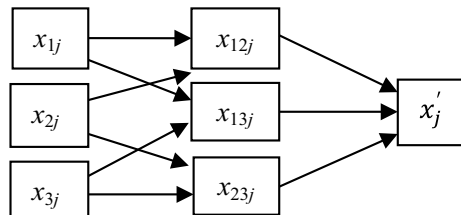
where $i_1 \neq i_2 = 1, \dots, n$ are the numbers of active additives, $a_{i_1 i_2 j}$ is the coefficient of influence of additives s_{i_1} and s_{i_2} on the Q_j property of the polymer composition, $x_{i_1 i_2 j}$ is a manifestation of the Q_j property polymer composition after modification. From that we have

$$\frac{x_{i_1 i_2 j}}{x_j} - 1 = a_{i_1 i_2 j} - 1 = q_{i_1 i_2 j},$$

where $q_{i_1 i_2 j}$ is the reduced coefficient of influence of the additives s_{i_1} and s_{i_2} on the property Q_j of the polymer composition, the feature of which is that when the property worsens, it takes negative values, and with improvement, it takes positive values.

The total effect of the entire complex of additives s_1, s_2, \dots, s_n will be expressed by the ratio

Fig. 1 Example of pairwise interaction of additives for $n = 3$



$$q_j = \frac{x'_j}{x_j} - 1, \tag{1}$$

where q_j is a certain reduced coefficient that describes the combined effect of all n additives on the property $Q_j, j = 1, \dots, m$, resulting in the value x'_j .

For the upper and lower bounds (1) in [8] it is suggested to take

$$q_j \leq \sum_{i_1 < i_2 = 1}^n q_{i_1 i_2 j} = \bar{q}_j, \tag{2}$$

$$q_j \geq \frac{1}{C^n} \sum_{i_1 < i_2 = 1}^n q_{i_1 i_2 j} = q_j, \tag{3}$$

It is believed that additives are selected so as not to impair the properties of the polymer composition, i.e.

$$0 \leq q_j \leq \bar{q}_j.$$

As a result, we obtain that the cumulative effect on the property Q_j is expressed by an odd number

$$\hat{q}_j(x_j) = \exp\left(-\frac{(x_j - \tilde{q}_j)^2}{\delta_j^2} \ln 2\right), \tag{4}$$

where $\tilde{q}_j = (\bar{q}_j + q_j)/2, \delta_j = (\bar{q}_j - q_j)/2, j = 1, \dots, m$.

The overall assessment \hat{q} of the impact of the whole complex of additives is expressed by the formula

$$\hat{q} = \sum_{j=1}^m \alpha_j \hat{q}_j,$$

where $\alpha_j \geq 0$ reflects the importance of the property Q_j in comparison with others and for which the relations

$$\sum_{j=1}^m \alpha_j = 1.$$

4 Computing Experiment

Consider two polymer compositions (Table 3) and evaluate them in terms of compliance with consumer needs.

For this, it is necessary to use the above model and determine how additives interact in pairs with each other and how they affect the corresponding property of the polymer composition (Tables 4 and 5).

Here $j = 1, 2, 3$ means the sustainability of the polymer composition to combustion, oxidation, photodestruction, respectively.

For composition C_1 , according to (2) and (3), we obtain

$$\bar{q}_1 = \sum_{i_1 < i_2 = 1}^3 \bar{q}_{i_1 i_2 1} = 0.4 + 0.05 + 0.02 = 0.47,$$

$$q_1 = \frac{1}{C_3^2} \sum_{i_1 < i_2 = 1}^3 q_{i_1 i_2 1} = \frac{1}{3} (0.2 + 0.02 + 0.01) \approx 0.077,$$

where $\bar{q}_{i_1 i_2 1} = \sup q_{i_1 i_2 1}, q_{i_1 i_2 1} = \inf q_{i_1 i_2 1}$.

Carrying out similar calculations, we obtain the results given in Table 6.

Table 3 Examples of polymer compositions' contents

No	Designation	Polymer, %	Flame retardant (%)	Antioxidant (%)	Light stabilizer (%)
1	C_1	86.8–92.9	6–10	1–2	0.4–0.6
2	C_2	82.1–91.8	7–14	1–3	0.1–0.3

Table 4 The effect of pairs of additives on the polymer composition C_1

j	Designation	Complex of two additives, $i_1 i_2$		
		12	13	23
1	$q_{i_1 i_2 1}$	0.2–0.4	0.02–0.05	0.01–0.02
2	$q_{i_1 i_2 2}$	0.01–0.02	0.3–0.5	0.4–0.7
3	$q_{i_1 i_2 3}$	0.00–0.01	0.1–0.18	0.4–0.7

Table 5 The effect of pairs of additives on the polymer composition C_2

J	Designation	Complex of two additives, $i_1 i_2$		
		12	13	23
1	$q_{i_1 i_2 1}$	0.20–0.35	0.03–0.04	0.02–0.05
2	$q_{i_1 i_2 2}$	0.02–0.06	0.2–0.44	0.2–0.4
3	$q_{i_1 i_2 3}$	0	0.1–0.3	0.4–0.7

Table 6 The results of the calculation of the upper and lower estimates of changes in the properties of the compositions C_1 and C_2

j	C_1		C_2	
	q_j	\bar{q}_j	q_j	\bar{q}_j
1	0.077	0.47	0.083	0.44
2	0.24	1.22	0.14	0.90
3	0.17	0.89	0.17	1.00

According to (4), we obtain the following cumulative effect of the complex are additive on the polymer composition C_1

$$\hat{q}_1(x_1) = \exp\left(-\frac{(x_1 - 0.27)^2}{0.039} \ln 2\right), \hat{q}_2(x_2) = \exp\left(-\frac{(x_2 - 0.73)^2}{0.24} \ln 2\right),$$

$$\hat{q}_3(x_3) = \exp\left(-\frac{(x_3 - 0.53)^2}{0.13} \ln 2\right)$$

and to the composition C_2

$$\hat{q}_1(x_1) = \exp\left(-\frac{(x_1 - 0.26)^2}{0.032} \ln 2\right), \hat{q}_2(x_2) = \exp\left(-\frac{(x_2 - 0.52)^2}{0.14} \ln 2\right),$$

$$\hat{q}_3(x_3) = \exp\left(-\frac{(x_3 - 0.59)^2}{0.17} \ln 2\right).$$

Further, we assume that the most important thing for the customer is the incom-bustibility of the material and the high resistance to light exposure and put $\alpha_1 = 0.5$, $\alpha_2 = 0.2$, $\alpha_3 = 0.3$ and calculate \hat{q} using the formulas obtained in [7] for the polymer composition C_1

$$\hat{q} = \sum_{j=1}^3 \alpha_j \hat{q}_j = \exp\left(-\frac{(x - 0.44)^2}{1.1} \ln 2\right),$$

and to the composition C_2

$$\hat{q} = \sum_{j=1}^3 \alpha_j \hat{q}_j = \exp\left(-\frac{(x - 0.41)^2}{0.93} \ln 2\right).$$

5 The Model with Unknown Interaction of Some Components

Let's review the case when some additives are not known for how they interact with other components, and this introduces an additional factor of uncertainty. Suppose the result of the interaction of additives 2 and 3 is unknown.

We apply the approach described in [8] and estimate the value q_{23j} , $j = 1, 2, 3$. To do this, we need data on the effect of each of additives 2 and 3 separately on polymer compositions, which are given in Tables 7 and 8.

For composition C_1 , according to (2) and (3), we obtain

$$\bar{q}_1 = \sum_{i=2}^3 \bar{q}_{i1} = 0.15 + 0.03 = 0.18,$$

$$q_1 = \frac{1}{2} \sum_{i=2}^3 q_{i1} = \frac{1}{2}(0 + 0.01) = 0.005,$$

where $\bar{q}_{i1} = \sup q_{i1}$, $q_{i1} = \inf q_{i1}$

Carrying out similar calculations, we obtain the results given in Table 9.

According to (4), we obtain the following cumulative effect of the additive 2 and 3 on the polymer composition C_1

$$\hat{q}_{231}(x_1) = \exp\left(-\frac{(x_1 - 0.0925)^2}{0.0875} \ln 2\right), \hat{q}_{232}(x_2) = \exp\left(-\frac{(x_2 - 0.825)^2}{0.475} \ln 2\right),$$

$$\hat{q}_{233}(x_3) = \exp\left(-\frac{(x_3 - 0.85)^2}{0.35} \ln 2\right)$$

Table 7 The effect of additives 2 and 3 on the polymer composition C_1

J	Designation	Number of additives, i	
		2	3
1	q_{i1}	0–0.15	0.01–0.03
2	q_{i2}	0.5–0.8	0.2–0.5
3	q_{i3}	0.4–0.5	0.6–0.7

Table 8 The effect of additives 2 and 3 on the polymer composition C_2

J	Designation	Number of additives, i	
		2	3
1	q_{i1}	0.03–0.06	0.01–0.04
2	q_{i2}	0.2–0.4	0.3–0.4
3	q_{i3}	0.6–0.8	0.3–0.5

Table 9 The results of the calculation of the upper and lower estimates of changes in the properties of the compositions C_1 and C_2

j	C_1		C_2	
	q_j	\bar{q}_j	q_j	\bar{q}_j
1	0.005	0.18	0.02	0.10
2	0.35	1.30	0.25	0.80
3	0.50	1.20	0.45	1.30

Table 10 Real estimates of the effect of the complex of additives 2 and 3 on polymer compositions C_1 and C_2

J	Designation	Composition	
		C_1	C_2
1	q_{231}	0.005–0.17	0.02–0.1
2	q_{232}	0.35–1.3	0.25–0.8
3	q_{233}	0.5–1.2	0.45–1.3

and to the composition C_2

$$\hat{q}_{231}(x_1) = \exp\left(-\frac{(x_1 - 0.06)^2}{0.04} \ln 2\right), \hat{q}_{232}(x_2) = \exp\left(-\frac{(x_2 - 0.525)^2}{0.275} \ln 2\right),$$

$$\hat{q}_{233}(x_3) = \exp\left(-\frac{(x_3 - 0.875)^2}{0.425} \ln 2\right).$$

Fuzzy estimates were obtained for unknown parameters $q_{23j}, j = 1, 2, 3$. In order to use the computational model proposed above, it is necessary to defuzzification these estimates. As real values of the parameters $q_{23j}, j = 1, 2, 3$, we take a range of values at which the value of the membership function does not exceed 0.5. The obtained values are presented in Table 10.

Now there is all the necessary information and, repeating the calculations given in paragraph 4, we obtain a similar result, adjusted for the approximate values of the complex effect of additives 2 and 3 on polymer compositions.

6 Conclusion

It should be noted that the results obtained are oriented only on a specific consumer. Nevertheless, the proposed model allows us to evaluate polymer compositions and make an informed choice. In the above example—this is composition C_1 .

The proposed approach to solving the problem involves using the already available information about polymer compositions to create a black-box model and further clarify the interaction of the composition components based on the laws of the subject

area and a gradual transition to the gray box. The approach used here allows us to identify the direction of research in the subject area to refine and refine the model.

Acknowledgements The reported research was funded by the Russian Foundation for Basic Research and the government of the Volgograd region, grant no. 18-48-340011.



References

1. Akhnazarova, S.L., Kafarov, V.V.: Methods for optimizing an experiment in chemical technology. Higher school, Moscow (1985)
2. Behdinin, K., Moradi-Dastjerdi, R., Safaei, B., Qin, Z., Chu, F., Hui, D.: Graphene and CNT impact on heat transfer response of nanocomposite cylinders. *Nanotechnol. Rev.* **9**(1), 41–52 (2020)
3. Bobryshev, A.N., Erofeev, V.T., Kozomazov, V.N.: Polymer composite materials. Publishing house ASV, Moscow (2013)
4. Chandra, P.H., Kalavathy, S.M.S.T., Jayaseeli, A.M.I., Karoline, J.P.: Mechanism of fuzzy ARMS on chemical reaction. *Adv. In Intell. Syst. Comput.* **424**, 43–53 (2016)
5. Egilis, F.M.: Efficiency of industrial stabilizers polypropylene. *Ductile Masses* (12), 41 (1987)
6. Emami, M.R.S.: Fuzzy logic applications in chemical processes. *J. Math. Comput. Sci.* **1**(4), 339–348 (2010)
7. Germashev, I.V., Derbisher, E.V., Derbisher, V.E., Kulikova, NYu.: Convergence of series of fuzzy numbers with unimodal membership function. *Math. Phys. Comput. Simul.* **21**(1), 11–17 (2018)
8. Germashev, I.V., Derbisher E.V., Mashihina T.P.: Evaluation of the properties of the polymer composition using a fuzzy analysis of the formulation. In: 2019 International Multi-Conference on Industrial Engineering and Modern Technologies, FarEastCon 2019. IEEE (2019)
9. Germashev, I.V., Derbisher, V.E., Orlova, S.A.: Evaluation of activity of the fireproofing compounds in elastomer compositions by means of fuzzy sets. *Kauch. Rezina* **6**, 15–17 (2001)
10. Germashev, I.V., Derbisher, V.E., Vasil'ev, P.M.: Prediction of the activity of low-molecular organics in polymer compounds using probabilistic methods. *Theor. Found. Chem. Eng.* **32**(5), 514–517 (1998)
11. González-González, D.S., Praga-Alejo, R.J., Cantú-Sifuentes, M.: A non-linear fuzzy degradation model for estimating reliability of a polymeric coating. *Appl. Math. Model.* **40**(2), 1387–1401 (2016)
12. Ivanov, M.V., Dibrov, G.A., Loyko, A.V., Varezhkin, A.V., Kagramanov, G.G.: Techniques to manage geometry characteristics of hollow-fiber membranes. *Theor. Found. Chem. Eng.* **50**(3), 316–324 (2016)
13. Jeong, S., Jeong, H., Jang, S., Lee, D., Kim, H.: Reduction of the maximum step height on a package substrate by the optimization of slurry chemical additives. *Int. J. Precis. Eng. Manuf.* **20**(6), 905–913 (2019)
14. Khidhir, B.A., Al-Oqaiel, W., Kareem, P.M.: Prediction models by response surface methodology for turning operation. *Am. J. Model. Optim.* **3**(1), 1–6 (2015)
15. Nikfar, N., Esfandiari, M., Shahnazari, M.R., Mojtahedi, N., Zare, Y.: The reinforcing and characteristics of interphase as the polymer chains adsorbed on the nanoparticles in polymer nanocomposites. *Colloid Polym. Sci.* **295**(10), 2001–2010 (2017)
16. Porter, D., Vollrath, F., Shao, Z.: Predicting the mechanical properties of spider silk as a model nanostructured polymer. *Eur. Phys. J. E* **16**(2), 199–206 (2005)
17. Reza, Z.A., Mehdi, R.: Fuzzy optimization approach for the synthesis of polyesters and their nanocomposites in in-situ polycondensation reactors. *Ind. Eng. Chem. Res.* **56**(39), 11245–11256 (2017)

18. Sadgova, N.S.: Prediction of electrical and strength properties of polymeric materials. Scientific forum: technical and physics and mathematics: collection of articles. In: XIX International Scientific and Practical Conference, vol. 9(19), pp. 25–29. Publishing house “MTSNO”, Moscow (2018)
19. Samsudin, S.S., Majid, M.S.A., Ridzuan, M.J.M., Osman, A.F.: Thermal polymer composites of hybrid fillers. IOP conference series: materials science and engineering. In: 6th International Conference on Applications and Design in Mechanical Engineering 2019, ICADME 2019, vol. 670, issue 1, 2. Institute of Physics Publishing (2019)
20. Startsev, O.V., Anikhovskaya, L.I., Litvinov, A.A., Krotov, A.S.: Increasing the reliability of predicting the properties of polymer composites in hygrothermal aging. Dokl. Chem. **428**(1), 228–232 (2009)
21. Kerber, M.L.: Technology of polymer processing. Physical and chemical processes: publishing house for universities edited, 2nd edn. Yurayt Publishing House, Moscow (2018)

The Indirect Methods of Conversion Monitoring Throughout Polymerization Processes in Bulk



Yuri P. Yulenets , Armen R. Avetisian, Roman Yu. Kulishenko, and Andrey V. Markov 

Abstract Two methods of monitoring the conversion throughout the polymerization process in bulk (polymerization of isoprene as an example) are considered. Both techniques are built so to define the conversion in the terms of indirect running parameters of polymerization process in molx i.e. the reactor with a thin fixed bed of the reaction mixture. The first of these parameters is the temperature of the bed top, and also the wall reactor temperature. Due to the second technique to check-out the conversion in real-time it's enough to control and analyze the bed top temperature bound up to conversion with rigorous dependence.

Keywords Conversion monitoring · Polymerization in bulk · Indirect methods

1 Introduction

Bulk polymerization is carried out itself in monomer medium in the presence of catalyst or starters. The absence of diluents provides the maximum purity of the final product and excludes the necessity of apparatuses for their recycling. Due to the maximum concentration of the monomer in bulk polymerization, there are achieved the maximum rate and, often, maximum conversion—i.e. the degree of polymerization. However, polymerization in bulk being widely used when producing homopolymers and copolymers has no application in the production of diene rubbers. This point of the matter is explained by the higher viscosity of the reaction mixture, a situation that excludes the use of any mixing devices, and also hindered heat removal in conditions of the very high rate of the polymerization process.

Y. P. Yulenets (✉) · R. Yu. Kulishenko · A. V. Markov
Saint-Petersburg State Institute of Technology (Technical University),
26, Moskovski ave., St. Petersburg 190013, Russia
e-mail: yyp2807@mail.ru

A. R. Avetisian
Federal State Unitary Enterprise S.V. Lebedev Institute of Synthetic Rubber,
1, Gapsalskaya st., St. Petersburg 198035, Russia

Physical and chemical principles to obtain *cis*-1,4-polyisoprene using bulk polymerization of isoprene in the presence of various catalytic systems are of wide publication [1–6]. As for engineering facilities of the bulk polymerization process, the significant advantages belong to apparatuses with a fixed thin bed of the reaction mixture [7–14].

In apparatuses of this type, the problem of heat removal may be solved in a simple, by comparison, way. An additional gain they give to an efficient thermal mode that may be easily attained. Structurally the most simple instrumentation for the bulk polymerization process is a reactor (polymerization mold) as a cylinder of a large diameter and a small height—i.e. the disc. However, a certain difficulty to introduce in practice the innovative technology of rubber production, and, in particular, to implement the automatic control of the polymerization process, in the absence of continuous conversion monitoring technique. Actually, monitoring the conversion with the help of dielectric principle [2, 15, 16] (through variation of dielectric constant and dielectric loss tangent of monomer and polymer) in question is not applicable therefore dielectric properties of isoprene (the nonpolar liquid) and polyisoprene (the dielectric of high—quality) are extremely close: $\varepsilon_1 \approx \varepsilon_2 = 2.1$; $\text{tg}\delta_1 \approx \text{tg}\delta_2 = 0.005 \div 0.006$ [17, 18]. The ultrasonic technique based on monitoring the conversion via polymer viscosity is efficient only as a batch (-operated) technique [19–21].

From the viewpoint of the possibility of operation control and automation, the engineering processes are divided into controllable, conditionally controllable, and also difficultly controllable ones. Up today bulk polymerization is considered as difficultly controllable or at best as conditionally controllable processes. Both suggest that quality production verification in particular the conversion monitoring is performed with the help of batch-operated analytical facilities. As a result, there is no means to create the working capacity automatic quality control systems.

The present study is dedicated to working out the indirect methods of monitoring conversion via the current parameters of the polymerization process (isoprene polymerization in bulk as an example).

2 Methodology

Let us suppose that the heat conductivity of the reactor wall or, otherwise, the wall of the polymerization mold is infinitely large. The heat exchange is considered to proceed in the reaction bulk via the mechanism of heat conductivity. In addition, let's suppose that the reaction constant depends on temperature according to the Arrhenius equation and that the pre-exponential factor z does not depend on temperature. A mathematical model based on the named assumptions is as follows [8]:

$$c_p \rho \frac{\partial T}{\partial \tau} = \lambda \frac{\partial^2 T}{\partial x^2} + Qz \exp\left(-\frac{E}{RT}\right)(1 - U)[M]_0 \quad (1)$$

$$\frac{\partial U}{\partial \tau} = z \exp\left(-\frac{E}{RT}\right)(1 - U) \quad (2)$$

with the boundary conditions:

$$-\lambda \frac{\partial T}{\partial x} \Big|_{x=x_0} = \alpha(T|_{x=x_0} - T_R), \quad \frac{\partial T}{\partial x} \Big|_{x=0} = 0, \\ T|_{\tau=0} = T_0, \quad U|_{\tau=0} = 0. \quad (3)$$

where E is the activation energy of polymerization factor; R is the universal gas constant; T is the local temperature of the reaction mixture; T_0 is the initial temperature of the reaction mixture; T_R is the temperature of the coolant (water) in the reactor jacket; x is the current in height coordinate; x_0 is the height of the reaction-mixture bed; c_p , ρ , and λ are the specific heat capacity, density, and heat—conductivity coefficient of the reaction mixture; Q is the specific heat of polymerization; α is the heat emission (from water to reactor wall) coefficient; τ is the time; U is the conversion (the degree of conversion of the monomer into the polymer): $U = ([M]_0 - [M])/[M]_0$, and $[M]_0$ and $[M]$ are the initial and current concentration of isoprene in the reaction mixture.

Set of Eqs. (1)–(3) was solved numerically at the following factors of the reaction mixture (isoprene—a catalytic system based on neodymium bis-(2-ethylhexyl) phosphate [Nd]) and kinetic parameters: $c_p = 2.25$ kJ/(kg·K), $\rho = 680$ kg/m³, $\lambda = 0.13$ W/(m·K), $Q = 74.8$ kJ/mol, $R = 8.314$ J/(mol·K), $z = 1.209$ 1/s, $E = 20.67$ kJ/mol, $[C_5H_8] = [M]_0 = 10$ kmol/m³, $[Nd] = 2 \cdot 10^{-4}$ kmol/m³. The heat emission coefficient is calculated proceeding from the condition that heat be freely able to conduct away from the reactor volume (the reactor diameter is $D = 0.3$ m and $x_0 = 3$ mm): $\alpha = 1500$ W/(m²·K); the rate of water flow in the reactor jacket: $G_R = 0.26 \cdot 10^{-3}$ m³/s.

The works [10, 12] show that the maximum efficiency of the disk-shaped apparatus for bulk polymerization of isoprene up to final conversion $U_{fin} = 0.9$ is achieved in the bed height $x_0 = 3$ mm. Table 1 illustrates this fact while analyzing the relative reactor productivity L as a function of bed height h , whereupon $h = x_0$.

The relative reactor productivity is defined as follows:

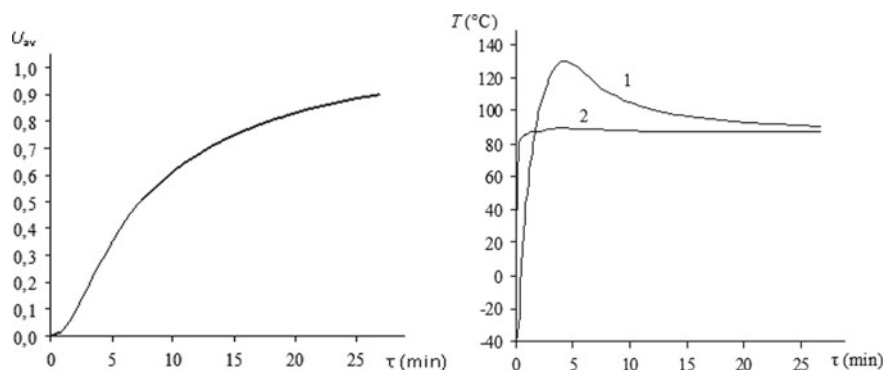
$$L = \frac{G_h}{G_0} = \frac{h\tau_0}{h_0\tau},$$

where G_0 is the reactor productivity at the minimum bed height ($h_0 = 2$ mm); G_h is the reactor productivity at a bed height h ; τ_0 —is the polymerization time at the minimum bed height; formulae to calculate the reactor productivity has the form:

$$G = \frac{hS\rho U_{fin}}{\tau},$$

Table 1 The productivity of disk-shaped reactor for bulk polymerization of isoprene in beds of different heights ($T_0 = -40$ °C, $U_{fin} = 0.9$)

Parameter	Height of the bed h (mm)				
	2	3	4	5	6
Reactor wall temperature T_w (°C)	107	87	69	51	35
Maximum polymerization temperature T_{max} , (°C)	129.0	129.0	129.0	129.0	127.7
Polymerization time τ , min	20.4	26.7	36.0	49.7	68.7
Relative reactor productivity L	1.0	1.15	1.11	1.03	0.89

**Fig. 1** Dependences of (1) the bed—top temperature, T_T , (2) the temperature of the reactor wall, T_w , and average conversion of the monomer, U_{av} , on time during the bulk polymerization of isoprene in a disc reactor ($x_0 = 3$ mm) of $T_0 = -40$ °C, $T_{max} = 130$ °C, $T_R = 87$ °C, $\alpha = 1500$ W/(m²·K)

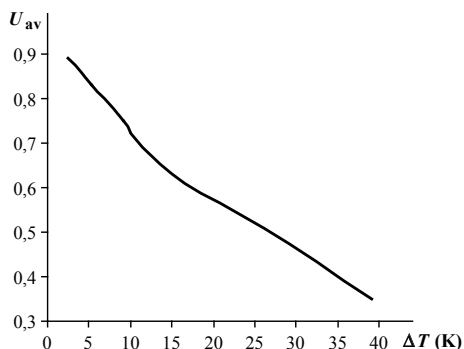
where S —is the reactor base area; ρ —is the density of the reactor mixture.

Figure 1 shows the dependences of (1) the bed-top temperature, T_T , (2) the temperature of the reactor wall, $T_w(\tau) = T(\tau, x_0)$, and average conversion of the monomer, U_{av} , on time.

3 Results and Discussion

The maximum achieved value of T_T is determined by the fraction of the monomer that has reached by this time. When the maximum is passed, the reaction-mixture temperature T_T falls sharply and then tends toward a constant value: the reactor-wall temperature T_w . The tendency of T_T variation is specified because the process of fast exhaustion («burning») of the monomer is predominant under the process of progressing release of heat caused by the exothermic polymerization reaction. The

Fig. 2 Monitoring the conversion in a disc reactor ($x_0 = 3$ mm) during isoprene polymerization process in bulk according to technique 1—a calibration curve



reactor-wall temperature T_w (see curve 2 in Fig. 1) even after a short time from the beginning is of constant value close to the coolant temperature T_R .

While considering curves in Fig. 1 it follows a method of continuous monitoring of the conversion (technique 1) based on the estimation of the indirect process characteristics—the temperature T_T and the temperature T_w . With the help of their current difference, there are determined a dependence: $U_{av} = f(T_T - T_w)$.

Figure 2 illustrates an example of technique 1 run-up. Temperature measurements and recordings were fulfilled with the help of the IR-thermometer Testo 845 and automatic controller—tester TRM-202.

Technique 1 demonstrates an adequate accuracy in particularly at the final time interval of the polymerization process: the error of conversion definition is not more than 5%. But it needs in dial layout of the dependence $U_{av} = f(T_T - T_w)$, an individual one for each reactor design, depended on the height of the reaction—mixture bed as are the heat exchange conditions between the reactor wall and the coolant. With a connection to indicated let us regard the second method of conversion monitoring.

In the assumption that the reactor wall temperature is constant: this condition may be realized under the conditions of the correct option of the temperature and the flow mode of coolant in the reactor jacket, the mathematical model of polymerization process corresponds to Eqs. (1) and (2) but with new boundaries:

$$c_p \rho \frac{\partial T}{\partial \tau} = \lambda \frac{\partial^2 T}{\partial x^2} + Qz \exp\left(-\frac{E}{RT}\right)(1-U)[M]_0 \quad (4)$$

$$\frac{\partial U}{\partial \tau} = z \exp\left(-\frac{E}{RT}\right)(1-U) \quad (5)$$

$$-\lambda \frac{\partial T}{\partial x} \Big|_{x=x_0} = \alpha(T|_{x=x_0} - T_R), \quad \frac{\partial T}{\partial x} \Big|_{x=0} = 0,$$

$$T|_{\tau=0} = T_0, \quad U|_{\tau=0} = 0. \quad (6)$$

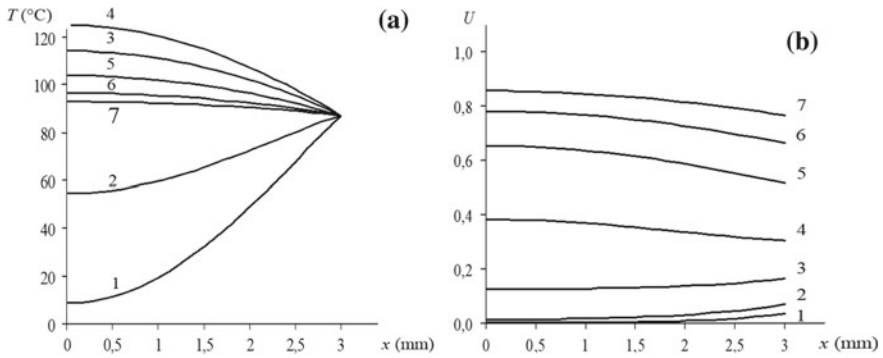


Fig. 3 Profiles of **a** temperature and **b** monomer conversion during the bulk polymerization of isoprene in a disc reactor ($x_0 = 3$ mm, $T_0 = -40$ °C, $T_w = 87$ °C) at $\tau =$ (1) 0.5, (2) 1, (3) 2.5, (4) 5, (5) 10, (6) 15, and (7) 20 min

The set of Eqs. (4) and (5) with conditions (6) were calculated numerically at the factors of the reaction mixture and kinetic parameters as before.

Figure 3 shows the bed height distribution of temperature and conversion at various times. It is noticeable that the distribution of conversion is close to uniform during full time. The temperature profiles proportional at the beginning straighten in the second half of the polymerization process. Weak current in height coordinate dependence of local temperature gives a possibility to consider reactor mode with a thin fixed bed close to isothermal one. Then $T(x) = T$, and Eq. (5) is analytically tractable:

$$U(\tau, T) = 1 - \exp\left[-z\tau \exp\left(-\frac{E}{RT}\right)\right]. \quad (7)$$

According to expounded, conversion monitoring technique, i.e.—technique 2, incorporates calculation of conversion in real-time by Eq. (7) rest on the data of current temperature measuring at an arbitrary position of the reaction—mixture bed. An example of technique 2 run-ups in comparison with a primary standard (introduction of ethanol as a stopper, periodical taking the samples outside the reactor, monitoring the conversion with the help of gravimetric analysis [22]) is given in Fig. 4.

Temperature measurements, i.e. $T_\tau(\tau)$, and calculation of conversion in real-time were fulfilled using IR-thermometer Testo 845 and computer.

Technique 2 demonstrates a (high-) precision accuracy of conversion monitoring at major times corresponding to a deep degree of polymerization that is of prime importance when you need to control the process in polymerization molds.

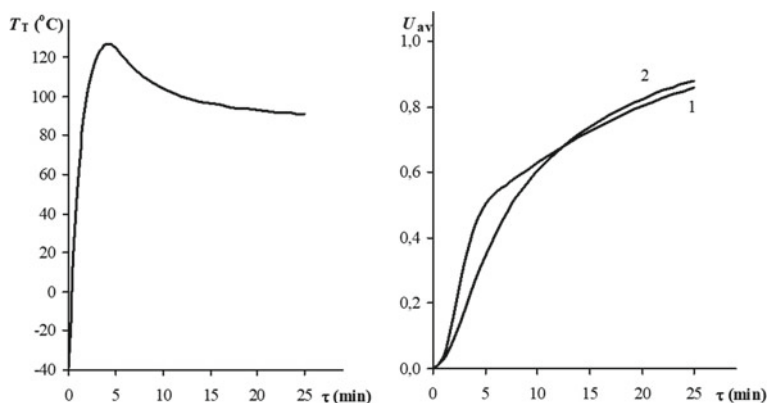


Fig. 4 Monitoring the conversion in a disc reactor during the bulk polymerization of isoprene according to technique 2 ($T_0 = -40^\circ\text{C}$, $T_w = 87^\circ\text{C}$, $x_0 = 3\text{ mm}$): 1—technique 2; 2—a primary standard technique

4 Conclusions

The considered techniques are referred to as indirect methods of process characteristic check-up. General for both techniques is the definition of conversion by the means of the composite experimental and also calculated manner, based on continuous monitoring of the polymerization process in apparatus with a thin fixed bed reaction-mixture. The best advantage both techniques demonstrate at the final time stage of polymerization.

Moreover, in contrast to technique 1, technique 2 is not required in the dial layout of conversion dependence on measured in the reactor and therefore deflected its thermal features characteristics of the polymerization process. According to technique 2, the calculation of conversion is carried out in real-time with the help of the strict analytical dependence conversion against the temperature of the reaction mixture, the latter being measured at an arbitrary bed position.

The proposed techniques, both, make it possible to transform the conditionally controllable or even the difficultly controllable polymerization process at the type of controllable one.

Indeed, in accordance with technique 1 and also with technique 2 the time required to form the controlling signal in the terms of conversion is significantly less than the period during that it might be accomplished the irreversible transformation of monomer.

As a whole, the proposed techniques may be suitable for continuous conversion monitoring in different catalytic bulk polymerization processes.

References

1. Harper, C.A.: Handbook of Plastics, Elastomers, and Composites, 884 p. Mc. Graw-Hill, N.Y., (2002). ISBN 9780071460682
2. Averko-Antonovich, L.A., Averko-Antonovich, Ju.O., Davletbaeva, I.M., Kirpichnikov, P.A.: Chemistry and technology of synthetic rubber, 357 p. Kolos S (2008)
3. Kissin, Y.V.: Isospecific polymerization of olefins—with heterogeneous Ziegler-Natta catalysts, p. 439. Springer, New York (1985)
4. Mark, J.E., Eрман, B., Roland, M.: The Science and Technology of Rubber. Elsevier (2013)
5. Mingaleev, V.Z., Ionova, I.A., Zakharov, V.P.: Polymerization of butadiene and isoprene in the presence of titanium catalytic system under ultrasonic irradiation. Polym. Sci. Ser. B. **53**(7–8), 375–384 (2011)
6. Nuyken, O.: Neodymium Based Ziegler Catalysts: Fundamental Chemistry: 204 Advances in Polymer Science, p. 297. Springer, Berlin Heidelberg (2006)
7. Patent RF 2563844. Sposob polimerizacii izoprena v masse v maloobjomnyh jachejkah (2015). Bjul. No. 6. 5s. [RF patent 2563844. Method of isoprene polymerization in bulk in low-volume cells. 2015. Bul. No. 6. 5p.]
8. Elfimov, V.V., Markov, A.V., Yulenets, Yu.P.: Bulk polymerization of isoprene in apparatuses with a fixed bed of the reaction mixture. Polym. Sci. Ser. B. **58**(3), 284–291 (2016). <https://doi.org/10.1134/s1560090416030052>
9. Samsonov, A.G., Yulenets, Yu.P., Elfimov, V.V., et al. An apparatus for isoprene polymerization in bulk, Patent RU No 2617411 (2017)
10. Elfimov, V.V.: Optimum conditions for the bulk polymerization of isoprene. Int. Polym. Sci. Technol. **43**(12), 31–34 (2016)
11. Elfimov, V.V., Yulenets, Yu.P., Markov, A.V., Elfimov, P.V., Avetisjan, A.R.: Matematicheskaja model' processa polimerizacii izoprena v masse Kauchuk i rezina, vol. 4, S.38–41 (2015)
12. Elfimov, V.V., Yulenets, Yu.P., Markov, A.V.: Isoprene bulk polymerization in experienced conditions. Izvestia S.-Peterb. Gos. Technol. Inst. (Technical Univ.) **37**(63), 47–50 (2016)
13. Avetisyan, A.R., Yulenets, Yu.P., Markov, A.V.: Automated system for controlling the process of isoprene polymerization in bulk. Instrum. Syst. Manage. Control Diagn. **4**, 1–6 (2017)
14. Markov, A.V., Elfimov, V.V., Yulenets, Yu.P.: Optimizing the isoprene bulk polymerization process by selecting the mode with incomplete monomer conversion, Russia, vol. 7, pp. 31–34, May–June 2017 (Digests 30th intern. conf., Russia, S.-Peterb., 2017) (In Russian)
15. Bugrov, A.V.: High-frequency capacitive converters and instruments for quality control. Machine building, Moscow (1982)
16. Markov, A.V., Yulenets, Y.P.: Multifunctional control of the process variables in the thermal-electric facility for high-frequency dielectric heating. Russian Electric. Eng. **78**, 7, 390–394 (2007)
17. Tinga, W.R., Nelson, S.O.: Dielectric Properties of materials for microwave processing—tabulated. J. Microw. Power **8**(1), 23–65. <https://doi.org/10.1080/00222739.1973.11689017>
18. Grigoriev, I.S.: Physical values. Handbook. Inergoatomizdat, Moscow (1991)
19. Kulakov, M.V.: Technological measurements and devices for chemical production, 423 p. Alyans (2008)
20. Khvostov, A.A.: Acoustic method of quality control of polymer solutions with variable disturbance parameters. Control Syst. Inform. Technol. **1–2**(35), 300–303 (2009)
21. Franco, E., Adamowski, C., Buiocchi, C.: Ultrasonic viscosity measurement using the shear-wave reflection coefficient with a novel signal process technique. IEEE Trans. Ultrasonics Ferroelect. Freq. Control **57**, 1133–1138 (2010). <https://doi.org/10.1109/TUFFC.2010.1524>
22. Wolfson, S.A.: The basics of creating a technological process for obtaining polymers. Chemistry 148–150 (1987)

Deformation and Filtration Characteristics of a Leather Semi-Finished Product



Shavkat Khurramov, Farkhad Khalturaev, and Feruza Kurbanova

Abstract The results of the study of deformation and filtration properties of a leather semi-finished product after chrome tanning are presented. The analytical dependencies of compressive load on compression (recovery) strain and moisture content of a leather semi-finished product are obtained. The empirical dependencies of hydraulic gradient on filtration rates are determined for various compression ratios of the leather semi-finished product. It was revealed that with an increase in compressive load and moisture content of the leather semi-finished product, the compressive deformation increases. At that, the shoulder section is subject to the greatest deformation, then follows the belly section, and the least deformation is observed in the butt section. A linear relationship has been established between the hydraulic gradient and the rate of moisture filtration through the leather semi-finished product in the directions perpendicular and parallel to its surface.

Keywords Semi-finished leather product · Strain properties · Filtration properties · Mathematical models of leather filtration properties · Mathematical models of leather strain patterns

S. Khurramov (✉) · F. Khalturaev · F. Kurbanova
Academy of Sciences of the Republic of Uzbekistan Institute of Mechanics and Seismic Stability of Structures Named M.T. Urazbaev, 33 Dormon Yoli, Tashkent 100125, Uzbekistan
e-mail: shavkat-xurramov59@mail.ru

F. Khalturaev
e-mail: fedya-spets@mail.ru

F. Kurbanova
e-mail: ladykurbanova@mail.ru

1 Introduction

An important and crucial place in the technology of leather mechanical processing occupies the water squeezing from a leather semi-finished product, performed mainly by rollers.

A theoretical description of the process of rolling the fibrous material is one of the most difficult tasks in modern mechanics. The problem is to find a joint solution to two tasks: the first one is the contact interaction in two-roll modules (the contact task); the second task is the moisture filtration in a deformable inhomogeneous porous medium (the hydrodynamic problem) [1]. The leather squeeze by rollers is poorly understood. One of the reasons for this is the lack of analytical dependencies describing the deformation and filtration characteristics of the leather semi-finished product [2].

At present, there are a lot of publications devoted to the physic mechanical properties of finished leather [3–7]. However, only a few are devoted to the study of deformation properties of a leather semi-finished product after chrome tanning. In [8, 9], graphical characteristics of deformation properties of a leather semi-finished product after chrome tanning under compression were given. In [10, 11], the “strain–stress” dependences of chrome-tanned leather under compression were established. Experimental data (in the form of tables, graphs) and conclusions available in [8–11] are insufficient to describe the strained nature of a leather semi-finished product by mathematical formulas. In [12], the strain behavior of a leather semi-finished product after tanning under compression and recovery was specified by rheological dependencies based on Maxwell and Kelvin models. In [13], as a result of analysis of experimental studies of the stress–strain curves of a leather semi-finished product after tanning under compression, it was recommended to divide each curve into four regions described by different formulas: the first and the last ones—by linear dependencies, the second and the third ones—by power dependencies.

In [14, 15], devoted to the strain properties of a leather semi-finished product, a “strain–stress” dependence was given by the formula $\varepsilon = A Q^n$, where ε —is the strain; Q —is the stress; A, n —are the empirical coefficients. The authors of [14] suggested that $A = 0.103W + 1.44$, for leather upper shoes, where W —is the leather moisture content. In [15], a formula of the following form was given.

$$\varepsilon(\sigma, \tau, W) = a(0,47\sigma^{0.243} + 0.275\tau^{0.05} - 0.273)\left(\frac{W}{73}\right)^{2.31} + b$$

for a leather semi-finished product after chrome tanning, where τ —is the time of load impact.

It can be concluded that at present there is no correct mathematical model for the strain in a leather semi-finished product after chrome tanning under compression.

To simulate the processes of contact interaction, the strain models of the “stress–strain” type of the leather semi-finished product are necessary, that is, the dependencies of the form $\sigma = \sigma(\varepsilon)$ [2]. An empirical dependence was given in [16] by formula $\sigma = a + b\varepsilon + c\varepsilon^2 + d\varepsilon^3$, where a, b, c, d —are the coefficients characterizing the topographic features of the leather semi-finished product, recommended for use in the study of the roll squeezing of the leather semi-finished product under vertical feed.

The main thing in the study of filtration of capillary-porous materials is the study of the relationship between hydrostatic pressure and the rate of fluid filtration. The practice presented in research papers [17–21] in the field of filtration of capillary-porous materials has established some patterns connecting the rate of filtered fluid and the effective hydrostatic pressure. However, there is no data on the change in the rate of moisture filtration through the leather semi-finished product as a function of the hydraulic gradient.

Thus, at present, there are no mathematical models for the deformation and filtration of a leather semi-finished product after chrome tanning under compression (and recovery) to be used in solving contact and hydrodynamic problems of the squeezing process by rolls.

Based on the analysis of publications, two tasks were posed: the first—modeling the strain pattern of the leather semi-finished product under compression and recovery; the second task is the simulation of the filtration properties of the leather semi-finished product.

2 Experimental Studies

2.1 *Study of Deformation Properties of a Leather Semi-Finished Product*

In the theory of contact interaction in two-roll modules, the most important is the problem of determining analytical equations that reflect the shapes of the roll contact curves. The shape of the roll contact curves is judged by the change in material layer thickness along the roll contact zone. Some researchers believe that the strain of a material layer caused by the rolls at each point in time occurs in the radial direction to the roll axis, others think that it occurs in the vertical direction to the layer surface [2]. Therefore the strain in the leather semi-finished product is investigated in a vertical direction to its surface and in the radial direction to the roll axis.

To obtain the initial data of the quantitative value of compression and recovery strain in the leather semi-finished product based on the values of compression stress and initial moisture content of the leather semi-finished product, the following installation was used; its scheme is shown in Fig. 1.

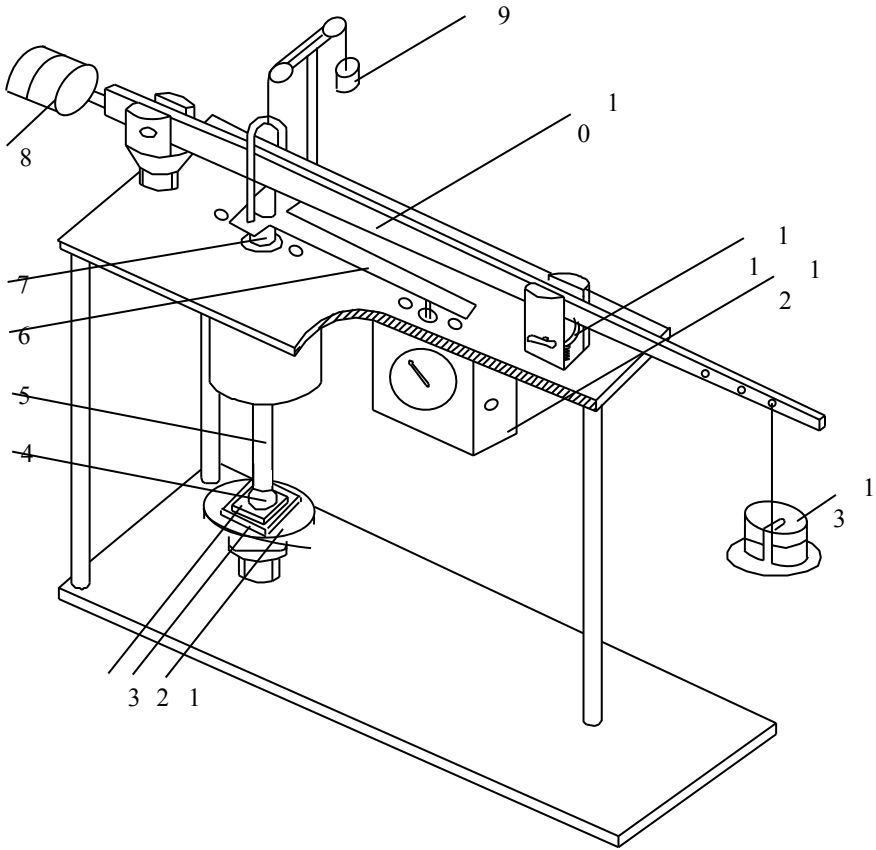


Fig. 1 Installation to study the strain pattern of a leather semi-finished product

The operation principle of the installation: using a counterweight 8, lever 10 is installed in a horizontal position and fixed by stop 11. A hemispherical head 7 abuts against lever 10. A stamp (stamp I) 2 with the test sample 3 is placed on the center of support 1, during rotation of which a gap is formed between the sample and the head (head I) 4, equal to the measured thickness of the test sample. In tests, two sets of stamps and heads were used. The first set is designed to study the strain in a leather semi-finished product in a direction of its vertical surface, and the second—in a direction radial to the roll axis. The necessary compressive load is created by selecting the load mass 13 and its location on the lever 10. The cam mechanism 11 lowers, allowing a smooth lowering of the lever 10, which, through the head 7 presses the rod 5, which moving down, compresses the sample 3 with the head 4 having a surface area of 1cm². After a set time, the compressive load is removed by lifting the cam mechanism 11. Then the sample 3 begins to recover the strain and moves rod 5 in the opposite direction. In this case, sample 3 is under the force

0.001 MPa caused by load 9. The compression and recovery strain of sample 2 is measured using indicator 11 through a T-shaped plate 5.

Samples were cut from selected leather semi-finished products in three topographic sections—a shoulder, belly, and butt. Based on the methodology for leather testing under compression, 60×60 mm² samples were prepared from each leather semi-finished product and divided into groups.

In the tests, the following values were taken: load on the sample from 2 to 10 MPa; the moisture content of the leather semi-finished product from 0.8 to 1.0 (from 60 to 75%, respectively); time of compression load impact—1 min.

2.2 Study of Filtration Properties of a Leather Semi-Finished Product

A characteristic feature of filtration during squeezing is the significant compression of the leather semi-finished product during the moisture movement in its pores.

Depending on the degree of compression of the material, its filtration characteristics also change. In this regard, we studied moisture filtration through a leather semi-finished product at various degrees of compression.

The installation (Fig. 2), on which the tests were carried out, consists of three parts: a filtration device I, a press II, and a device for water supply III.

The main part of the filtration device I is a base 2—a massive hollow container, in the upper part of which, on the ring collar, metal grill 4, rubber ring 23, inside which the test sample 5 is, metal grill 6 and piston 21 are consecutively placed. On the side of base 2, pipe 3 is fixed, and tube 22, from which water is drained into glass 24.

In the filtering apparatus I, grill 4, sample 5, and grill 6 are designed to test the water filtration through a leather semi-finished product in a direction perpendicular to its surface. When studying the water filtration through the leather semi-finished product in a direction parallel to its surface, grill 4, sample 5, and grill 6 are replaced by a grill 4', a sample 5', and a grill 6', respectively.

The operation principle of the installation: the filtration device I is installed on frame 1. The rod 7 of the press II abuts against piston recess 21. Using extension cord 8 and indicator 20, the required strain value of sample 6 is set and fixed by the lock nut of extension cord 8. A branch pipe 11 of device III is connected to hose 3. Water is poured into cylinder 16 through funnel 14 until it appears in tube 15. When the cylinder is filled with water, valve 12 closes, and piston 13 is lowered until it comes into contact with water. The necessary pressure is created using load 9 and opens valve 12. Hydraulic pressure is determined by pressure gauge 17, and the piston displacement is measured using ruler 19 through rod 18 and plug 10.

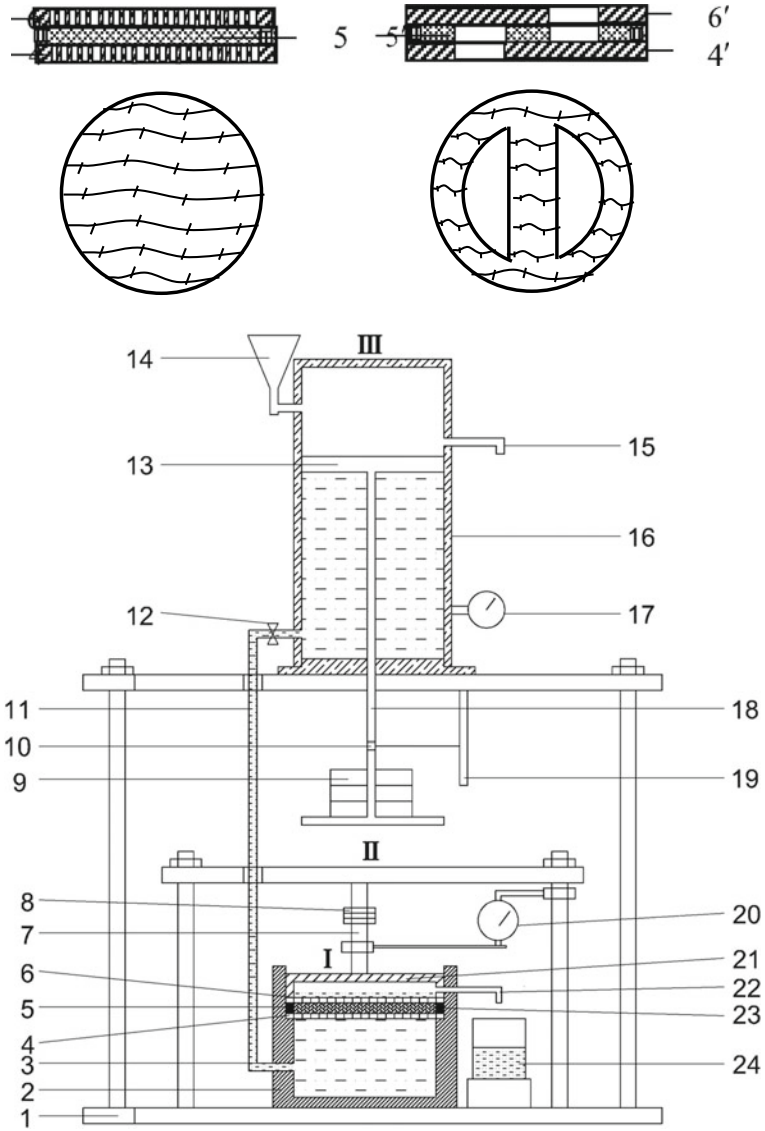


Fig. 2 Installation to test the leather semi-finished product filtration

When studying the water filtration through a leather semi-finished product in the direction perpendicular to its surface, the samples of size 10 cm² (of diameter 35.7 mm) were prepared, and in parallel direction—as shown in Fig. 2. These samples were cut and completed using the method of asymmetric fringe from bovine leather semi-finished products, processed according to the technology of chrome leather production after chrome tanning and laying. A fluid used for chrome tanning of a leather semi-finished product was taken as a filtering fluid.

The relative strain of the leather semi-finished product in the tests varied from 0.314 to 0.593, and the pressure on the cylinder was 0.05–2.13 MPa. Piston displacement and hydrostatic gradient were measured after 5, 10, 20, 40, and 60 s.

Moisture filtration rates through the leather semi-finished product in the directions parallel and perpendicular to its surface and the hydraulic gradient in these directions were calculated from formulas given in [22]:

$$v_x = \frac{1}{5} \sum_{i=1}^5 v_{xi} = \frac{1}{5} \sum_{i=1}^5 \frac{g_i}{F_x t_i}, v_y = \frac{1}{5} \sum_{i=1}^5 v_{yi} = \frac{1}{5} \sum_{i=1}^5 \frac{g_i}{F_y t_i},$$

$$I_x = \frac{1}{5l_1} \sum_{i=1}^5 \left(\frac{\gamma}{\gamma_B} \sigma_y - \frac{S_i - S_{i-1}}{2} \right), I_y = \frac{1}{5l_2} \sum_{i=1}^5 \left(\frac{\gamma}{\gamma_B} \sigma_y - \frac{S_i - S_{i-1}}{2} \right),$$

where v_x, v_y —are the filtration rates, cm/s; I_x, I_y —are the hydraulic gradients; F_x, F_y —are the areas by which the filtration occurs, cm²; t_i —is the filtration duration, s; l_1 —is the length of filtration path equal to the length of the sample jumper, 5', cm; l_2 —is the sample thickness after compression in the press II , cm; σ_y —is the pressure on the cylinder, cm of water column; γ —is the density of water g/cm³; γ_B —is the density of the filtered moisture, equal at a temperature of 20° to 1.035, at 40° to 1.020, at 60° to 1.010, g/cm³; S_i —is the piston path in time t_i cm; g_i —is the amount of water filtered through the leather semi-finished product in time t_i , determined by formula $g_i = \frac{\pi(d_y^2 - d_i^2)}{4} (S_i - S_{i-1})$, $S_0 = 0$, cm³, here d_y, d_i —are the diameters of the rod and cylinder, cm.

3 Mathematical Processing of Experimental Results

As a result of experiments, the data were obtained showing the relative compression and recovery strain of the leather semi-finished product depending on the magnitude of compressive load and humidity (Figs. 3, 4 and 5).

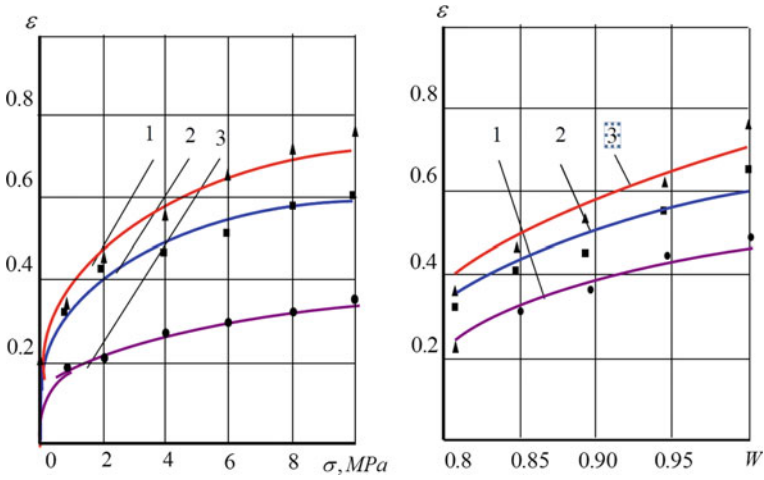


Fig. 3 Dependences of compression strain ε of the butt section on compressive load σ ($1 - W = 1$; $2 - W = 0.94$; $3 - W = 0.82$) and moisture content W ($1 - \sigma = 10$ MPa; $\sigma = 6$ MPa; $\sigma = 2$ MPa)

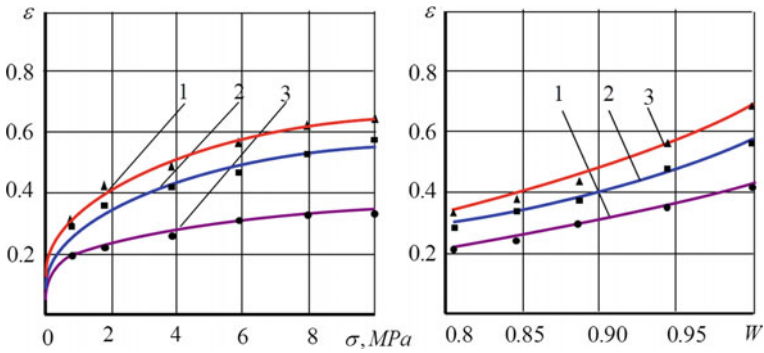


Fig. 4 Dependences of recovery strain ε of the belly section on compressive load σ ($1 - W = 1$; $2 - W = 0.94$; $3 - W = 0.82$) and moisture content W ($1 - \sigma = 10$ MPa; $\sigma = 6$ MPa; $\sigma = 2$ MPa)

The obtained experimental data were approximated by empirical formulas showing the dependence of compressive load on compression (recovery) strain and load and moisture content of the leather semi-finished product:

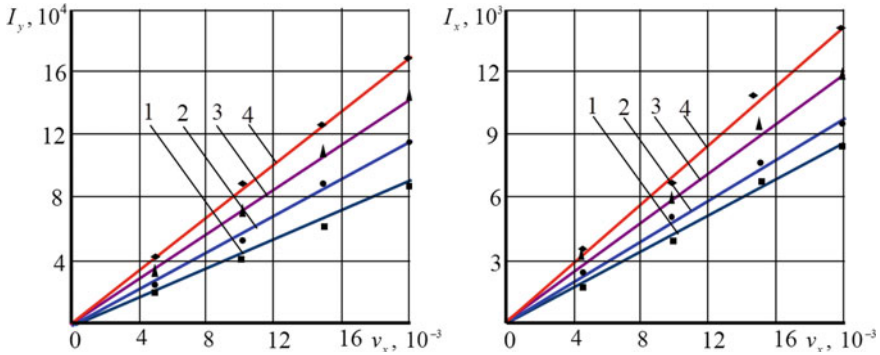


Fig. 5 Dependence of hydraulic gradients on moisture filtration rate through a leather semi-finished product, with various degrees of compression: a $\epsilon = 0.593$; b $\epsilon = 0.5$; c $\epsilon = 0.407$; d $\epsilon = 0.314$

- under compression

$$\sigma = 25.28 \cdot \left(\frac{\epsilon - b}{a}\right)^{3.73} \cdot W^{-14.74}; \tag{1}$$

- under recovery

$$\sigma = 51.80 \cdot \left(\frac{\epsilon - b}{a}\right)^{3.55} \cdot W^{-11.88}, \tag{2}$$

where a and b —are the coefficients characterizing the topographic features of the leather semi-finished product given in Table 1.

The coefficients of empirical Formulas (1) and (2) were determined by the least-squares method [23, 24].

The empirical dependences of compressive load on the compression (recovery) strain and the moisture content of the leather semi-finished product after chrome tanning in the vertical direction to the roll axis were obtained in a similar way:

Table 1 Coefficients for topographic features

Coefficient	Topographic sections	Compression	Recovery
a	Butt	1	1
	Belly	0.96	1.040
	Shoulder	0.94	1.051
b	Butt	0	0
	Belly	0.012	0.011
	Shoulder	0.018	0.019

Table 2 Coefficients for topographic features after chrome tanning

Coefficient	Topographic sections	Compression	Recovery
<i>a</i>	Butt	1	1
	Belly	0.97	1.018
	Shoulder	0.96	1.021
<i>b</i>	Butt	0	0
	Belly	0.013	0.014
	Shoulder	0.016	0.016

- under compression

$$\sigma = 40.2 \cdot \left(\frac{\varepsilon - b}{a} \right)^{3.12} \cdot W^{-15.44}; \quad (3)$$

- under recovery:

$$\sigma = 81.8 \cdot \left(\frac{\varepsilon - b}{a} \right)^{3.88} \cdot W^{-12.45}, \quad (4)$$

coefficients *a* and *b* are given in Table 2.

The graphs of dependencies of moisture filtration rate through a leather semi-finished product on a hydraulic gradient are shown in Fig. 5.

When summarizing the obtained dependences and graphs, empirical formulas are found that describe the filtration properties of the leather semi-finished product in directions perpendicular and parallel to its surface:

$$I_y = (a_1 \varepsilon + b_1) v_y, \quad (5)$$

$$I_x = (a_2 \varepsilon + b_2) v_x, \quad (6)$$

where ε —is the relative strain of the leather semi-finished product.

The coefficients from formulas (1) and (2), equal to $a_1 = 147 \cdot 10^5$, $b_1 = 8 \cdot 10^4$, $a_1 = 132 \cdot 10^4$, $b_2 = -19 \cdot 10^3$, were determined by the least-squares method.

An analysis of the curves plotted according to Formulas (1)–(6) shows that they are in good agreement with the experimental curves. The degrees of reliability and approximation accuracy of experimental data were estimated by the correlation and variation coefficients [23]. The approximation accuracy indices for these formulas are quite satisfactory, and the reliability indices are high. So, for example: the coefficients of variation and correlation in Formula (1), at $W = 1.0$ (at moisture content 75%) are

0.0013 and 0.995, respectively and at $\sigma = 6 \text{ MPa} - 0.011$ and 1.005 , respectively; in formula (5), at $\varepsilon = 0.5$ (at relative strain 50%) they are 0.01 and 0.99, respectively, and at $v_x = 10^{-4} \text{ cm/s} - 0.033$ and 0.97 , respectively). Therefore, we can assume that Formulas (1)–(6) well describe the deformation and filtration properties of the leather semi-finished product. This confirms the reliability of the developed mathematical models. So, they can be used in solving the contact and hydrodynamic problems of the leather squeezing process by rolls.

4 Conclusions

When analyzing the obtained experimental data and graphs characterizing the deformation properties of the leather semi-finished product under compression and recovery, the following aspects were revealed:

- with an increase in compressive load, the compression strain increases, and the maximum compressive strain of a butt section at a moisture content of 75% is reached under the load of 10 MPa;
- the lower the moisture content of the leather semi-finished product, the less its strain. So, for example, under a compressive load of 6 MPa, the relative compressive strain of a butt section at a moisture content of 60% is 0.326, at a moisture content of 65%—0.432, at a moisture content of 70%—0.563 and a moisture content of 75%—0.684, and the relative recovery strains in these cases are 0.304, 0.401 0.502 and 0.573, respectively;
- the compression and recovery strain curves with increasing impact time of compressive load increase sharply, then the growth slows down, and they asymptotically approach a straight line parallel to the abscissa axis;
- other conditions being equal, the greatest strains are observed in the shoulder section, then in the belly, and the last ones—in the butt section.
- there are linear dependencies between the hydraulic gradient and the rate of moisture filtration through the leather semi-finished product in the directions perpendicular and parallel to its surface.

References

1. Bakhadirov, G., Tsoy, G., Nabiev, A., Umarov, A.: Experiments on moisture squeezing from a leather semi-finished product. *Int. J. Recent Technol. Eng. (IJRTE)*. vol. 8 issue 5, January 2020 E6125018520/2020©BEIESP <https://doi.org/10.35940/ijrte.E6125.018520>.
2. Khurramov, Sh.R.: On the theory of contact interaction in two-roll modules. *Bulletin Univ. Technol. Light Ind.* **3**, 8–13 (2019) (in Russian)
3. Ward, A.G.: The mechanical properties of leather. *Chem. Rheol. Acta* **13**, 103–112 (1974). <https://doi.org/10.1007/BF01526892ID:95953151>
4. Li, Z., Paudecerf, D., Yang, J.: Mechanical behavior of natural cow Leather in tension. *Acta Mechanica Solida Sinica* **22**(I), 37–44 (2009)
5. Kozar, O., Mokrousova, O., Wozniak, B.: Deformation characteristics of Leather for shoe upper, filled with natural minerals. *J. Chem. Chem. Eng.* **8**, 47–53 (2014)
6. Kozar, O.P., Mokrousova, O.R., Conoval, V.P., Makuska, R.: Deformation characteristics of genuine Leather, manufactured using natural minerals. In: *Proceedings of the 13th International Conference “Baltic Polymer Symposium” Trakai Lithuania*, vol. 9, pp. 18–21 (2013)
7. Lu, C.K., Latona, N.P., Di Miao, G., Cooke, P.: Milling effects on mechanical behaviors of leather. *JALCA* 102 (2007)
8. Wenge, Y.: The mechanical properties of leather in relation to softness. Thesis posted on 15.12.2014. Leicester.Com.>artictes>The_mechanical_prop
9. Tuckermann, M.M., Pompe, W., Rich, G.: Stress measurements on chrome-tanned Leather. *J. Mater. Sci.* **36**, 1789–1799 (2001)
10. Chuyan, Z., Mladek, M., Kolomaznik, K., Greshak, V.: Influence of pressure on the deforming properties of the treated skin. *Leather* **1**, 26–28 (1984)
11. Chuyan, Z., Mladek, M., Kolomaznik, K.: Determination of material constants necessary for the deformation curve, characteristic of the deformation curve of the test skin under pressure deformations. *Leather*. **2**, 56–57 (1984)
12. Chuyan, Z., Mladek, M., Kolomaznik, K., Greshak, V.: Mathematical characteristic of the deformation curve of the test skin under pressure deformations. *Leather*. **1**, 29–30 (1984)
13. Wenge, Y.: The mechanical properties of leather in relation to softness. A Thesis submitted for the degree of Doctor of Philosophy. University of Leicester, Leicester (1999)
14. Batisene, M.Y., Mayauskene, N.Y.: Leather hardness for shoe upper. *Leather and Footwear Ind.* **9**, 54–55 (1980) (in Russian)
15. Amanov, T.Y., Khurramov, S.R.: Study of the strain pattern of the leather semi-finished product under compression and recovery. *Bulletin Univ. Technol. Light Light Ind.* **2**, 64–69 (1987) (in Russian)
16. Amanov, A., Bakhadirov, G., Amanov, T., Tsoy, G., Nabiyeu, A.: Determination of strain properties of the leather semi-finished product and moisture-removing materials of compression rolls. *J. Mater.* **12**, 3620 (2019)
17. Lindsay, J.D.: Relative flow porosity in fibrous media: measurements and analysis, including dispersion effects. *Tappi J.* **77**(6), 225–239 (1994)
18. Ellis, E.P.: Compressibility and permeability of never dried bleached softwood kraft pulp and its application to the prediction of wet press. Ph.D. Thesis, University of Marine, Orono (1981)
19. Cowan, W.F.: Wet pulp characterization by means of specific surface, specific volume and compressibility. *Pulp Paper Mag. Canada* **71**(9), 63–66 (1970)
20. Lindsay, J.D., Brady, P.H.: Studies of anisotropic permeability with applications to water removal in fibrous webs. Part I.: experimental methods, sheet anisotropy, and relationships to freeness. *Tappi J.* **79**(9), 119–127 (1993)
21. Walstom, P.B.: Conference preprints. In: 44th Appita Annual General Conference, p. A211. Rotarua, New Zealand (1991)

22. Lomtadze, V.D.: Physical and mechanical properties of rocks. Laboratory research methods, p. 328. Sankt-Petersburg (1990) (in Russian)
23. Rabinovich, S.G.: Statistical methods for experimental data processing. In: Evaluating Measurement Accuracy. Springer (2009)
24. Frasser, C.E.: Mathematical methods of experimental data processing and analysis, January (2006). <https://www.researchgate.net/publication/319256581>

Simulation Modeling for Drying Process of Pellets from Apatite-Nephenine Ores Waste



Vladimir Bobkov , Maksim Dli, and Alexandr Fedulov

Abstract The chapter presents a multiscale mathematical model for a complex multilevel drying process of pelletized industrial waste from apatite-nepheline ores. It takes into account the heat-technological specificity of a conveyor-type indurating machine, the intensity of the internal moisture transfer in a pellet, negative phenomena for over moistening of individual levels in a moving dense multilayer pellets mass, and heat carrier gas. This makes it possible to increase energy efficiency by intensifying heat-mass exchange for multilayer drying processes. The study revealed the essential dependence of efficiency for using heat and electric energy from the organization of heat and aerodynamic conditions of thermal treatment for pellets from apatite-nepheline ores waste on the quality of the produced pellets. According to numerous computational experiments, carried out on the developed simulation model, it is shown that when drying a moving multilayer pellets mass in a drying zone of a convey type indurating machine moisture is redistributed along with the height of the multilayer mass, as a result, they are over moistening is observed in some areas.

Keywords Pellets · Indurating conveyor-type machine · Industrial waste · Mathematical modeling · Drying

1 Introduction

In a scheduled operating condition of modern conveyor-type indurating machines operation in the condition of drying zone capillary exchange of moisture in the pellets does not occur isothermally but under conditions of variable pressure gradient and

V. Bobkov (✉) · M. Dli · A. Fedulov
National Research University “Moscow Power Engineering Institute“ (Branch) in Smolensk,
Smolensk 214013, Russia
e-mail: vovabobkoff@mail.ru

M. Dli
e-mail: midli@mail.ru

temperature [1, 2]. Therefore, in conditions of multilayer convective drying, an overmoistening zone is formed on the conveyor of the indurating machine, which has a significantly negative effect on the characteristics of heat and mass transfer [3, 4]. The effect of moisture redistribution along the height of the moving multilayer mass of pelletized solid waste from apatite-nepheline ores of mining and processing plants (pellets) is observed in a conveyor-type indurating machine [5, 6]. The change in the moisture content of the heating carrier gas also plays a significant role [7, 8].

Thermal preparation provides: the requirements for industrial raw materials in addition to enrichment of waste from apatite-nepheline ores dumps; moisture removal, carbonates dissociation; required granulometric composition of raw materials [9–11]. Many factors affecting the properties of raw materials do not allow the formation of a unified criterion for raw materials, and state standard defines only restrictions on a number of parameters and the ranges of their possible variations. Therefore, in cases where the properties of raw materials vary, in order to ensure a high level of efficiency for processing apatite-nepheline ores waste, it is necessary to adapt the operating condition of conveyor-type indurating machines to their properties [12–15]. The coefficient of efficiency for operating indurating machines is within 40%. The organization of the thermal condition for the thermal preparation of pellets from apatite-nepheline ores waste largely determines the efficiency of heat use and the quality of the produced pellets [16, 17].

2 Technological Specificity of a Conveyor-Type Indurating Machine Operation in the Drying Zone

The technological scheme for a conveyor-type indurating machine is quite complicated [18, 19]. Table 1 presents the process procedure indicators for the scheduled operating conditions in the technological drying zone for indurating machines of Russian classification for standards OK (indurating machines of the OK type).

Drying is carried out at 200–400 °C. In the lower levels of the dynamic multilayer pellet mass, and over moistening effect is observed, it is accompanied by deterioration in the gas permeability of the multilayer mass and the decrease in the heat transfer efficiency at subsequent stages. Therefore, at the initial stage of drying the supply of the drying agent for the heat carrier gas is often used from the bottom up, which helps to prevent the deformation of wet pellets located in the lower levels of the dense layer (see Table 1).

From the point of view of the system analysis, the technological process for drying pellets from apatite-nepheline ores waste at the micro-level is a set of processes for removing moisture in an individual pellet, and at the macro level, it is a set of processes for drying pellets in layers and a moving multilayer mass. The operating conditions and the completeness of this complex power engineering process in the moving multilayer pellets mass in the conveyor-type indurating machine determine the quality of their thermal treatment [20].

Table 1 Process procedure indicators for the indurating machine of OK-520/536 type

		Zero chamber	Drying		
			I	II	III
Length, m		4	14	18	10
Square at	m ²	16	56	72	40
Width 4 m	%		10.8	13.9	7.7
Stay time, s					
Average temperature of pellets at the exit, °C		40	95	295	315
Suction velocity, m/s		0.5↓	1.1↑	1.0 ↑	0.65↓
Temperature of the heat carrier above the layer and in the vacuum chamber, °C	maximum	200/50	60/250	80/350	400/300
	average	200/45	50/240	70/340	325/280
	minimum	200/40	40/230	60/330	350/260
Underpressure (–), pressure (+) in the hearth chambers and vacuum chambers, Pa	maximum	– 30/ – 3500	– 50/ + 5500	– 50/45,500	– 50/ – 4000
	average	– 20/ – 3300	– 200/ + 5000	-200/45,000	– 30/ – 3500
	minimum	– 10/ – 3100	-300/44,500	– 300/44,500	– 10/ – 3000
Natural gas consumption, Nm ³ /h					
Resistance of the bed layer and bars, Pa		1000	3100	3300	2300
Number of chambers and a vacuum chamber number, No		1	3	5	2
		1	2–4	5–9	10–11

3 Model of a Localized Front for Moisture Evaporation in a Pellet

In multiscale modeling for a complex multistage process for drying of moving multi-layer pellets mass it is considered at three levels: 1-st level—a model for the drying process of an individual pellet; 2-nd level—a model for the drying process of a vertical multilayer pellets stack; 3-d level—a model for the drying process of a vertical moving multilayer pellets stack.

The multiscale mathematical model for the technological process of drying represents a system of partial differential equations (PDE) [21].

Summarizing the previous studies of the authors [22] for the drying process of an individual spherical pellet, it was found that heat transfer is carried out by heat conduction in the presence of the endothermic effect of heat absorption on the phase transition during evaporation:

$$\rho_m c_m W_g \frac{\partial T_m}{\partial \tau} = x^{-2} \frac{\partial}{\partial x} \left(\lambda x^2 \frac{\partial T_m}{\partial x} \right) - q(\omega), \quad (1)$$

where: T_m —temperature; ρ_m —density; c_m —specific heat; x —coordinate for the pellet radius; λ —the coefficient for the material heat conductivity; τ —time; q —thermal effect of the drying process, it depends on the drying rate ω , initial moisture content u_k and radius r_p for the pellets coming into the drying zone of the indurating machine as well as the physical and chemical composition of the apatite-nepheline ores waste V^T : $q = q(\omega; u_k; r_p; V^T)$.

For the drying process of the vertical multilayer, pellets stack the heat transfer in the gas carrier flow is carried out by the convection in the direction of flow supply and is described by the equation:

$$\rho_g c_g W_g \frac{\partial T_g}{\partial y} = \alpha_V (T_g - T_m)_{x=r_p}, \quad (2)$$

where: T_g —temperature; ρ_g —density; c_g —specific heat; W_g —heat carrier gas velocity; y —coordinate along with the pellets layer height; $\alpha_V = \alpha_V(r_p)$ —volume coefficient of heat transfer in a layer, significantly depends on the pellets radius.

The pressure in the gas flow varies along with the depth of the multilayer mass and is equal to:

$$\frac{\partial P}{\partial y} = \frac{375(1 - \varepsilon_c)^2 W_g \mu_g}{\varepsilon_c^3 r_p^2} + \frac{35(1 - \varepsilon_c) \rho_g W_g^2}{\varepsilon_c^2 r_p}, \quad (3)$$

where: P —pressure, $\varepsilon_c = \varepsilon_c(r_p)$ —the porosity of the multilayer pellets mass; μ_g —dynamic viscosity for the heat carrier gas.

The process of mass transfer between the pellet and gas flow:

$$\rho_g W_g \frac{\partial a_w}{\partial y} = \frac{\beta_w S (P_{VR} - P_V)}{R_V T_g}, \quad (4)$$

$$\rho_m \frac{\partial u}{\partial \tau} = \frac{\beta_w S (P_{VR} - P_V)}{R_V T_g}, \quad (5)$$

where: u —moisture content in the pellet; a_w —moisture content of the heat carrier gas; P_{VR} —moisture vapor pressure on the surface of the pellet; P_V —vapor pressure in the gas; β_w —mass-transfer coefficient; $S = S(r_p)$ —the specific surface of the pellet in the multilayer mass.

The equation for the specific degree of the pellet drying has a form of:

$$\omega = \frac{\partial \gamma}{\partial \tau} = \frac{3 \lambda (t_0 - T_{m*}) \sqrt[3]{\gamma}}{\rho_m u Q_s r_p^2 (\sqrt[3]{\gamma} - 1)}, \quad (6)$$

where γ —relative degree of drying, determined by the movement of the localized evaporation front deep into the pellet, Q_s —specific heat vapor generation, T_{m*} —the temperature of the pellet material on the localized evaporation front, t_0 —the temperature of the wet thermometer.

The initial and boundary conditions for PDE (1–6) describing the drying process of the entire moving multilayer mass of pellets have a form of:

$$\begin{aligned} x = r_p, \quad -\lambda \frac{\partial T_m}{\partial x} &= \alpha_F (T_g - T_m)_{x=r_p}, \\ y = 0, \quad T_g &= T_{g0}, \quad P = P_0, \quad a_w = a_{w0}, \\ \tau = 0, \quad T_m &= T_{m0}, \quad u = u_k \end{aligned}$$

where $\alpha_F = \alpha_F(r_p)$ —heat transfer coefficient from the surface.

For the numerical solution of the equations system (1–6), the authors use the finite difference method with the number of partitions along with the radius of the pellet $i = 1 \dots 50$, along with the height of the multilayer mass $j = 1 \dots 120$, at time $k = 1 \dots 150$. The Eq. (1) in the implicit finite-difference scheme is in the form of:

$$\begin{aligned} \rho_{m i, j}^k c_{m i, j}^k W_g \frac{T_{m i, j}^k - T_{m i, j}^{k-1}}{\Delta \tau} &= \\ = x_i^{-2} \Delta x^{-2} \left[x_{i+1/2}^2 \lambda_{i+1/2, j}^k (T_{m i+1, j}^k - T_{m i, j}^{k-1}) - x_{i-1/2}^2 \lambda_{i-1/2, j}^k (T_{m i, j}^k - T_{m i-1, j}^k) \right] \\ + q_{i, j}^k, \end{aligned} \quad (7)$$

where $\lambda_{i+1/2} = (\lambda_{i+1} + \lambda_i)/2$.

The finite-difference form of the Eq. (2) for the convective heat transfer in gas:

$$\rho_{g j} c_{g j} W_g \frac{T_{g j} - T_{g j-1}}{\Delta y} = \alpha_{V j} (T_{g j} - T_{m l, j}). \quad (8)$$

The finite-difference form of the equation for the gas pressure change along with the layer height (3):

$$\frac{P_j - P_{j-1}}{\Delta y} = \frac{375(1 - \varepsilon_c)^2 W_g \mu_{g j}}{\varepsilon_c^3 r_p^2} + \frac{35(1 - \varepsilon_c) \rho_{g j} W_g^2}{\varepsilon_c^2 r_p}, \quad (9)$$

The finite-difference form of the Eqs. (4 and 5):

$$\rho_{g j} W_g \frac{a_{w j} - a_{w j-1}}{\Delta y} = \frac{\beta_{w j} S (P_{V R j} - P_{V j})}{R_V T_{g j}}, \quad (10)$$

$$\rho_m \frac{u_k - u_{k-1}}{\Delta \tau} = \frac{\beta_{w,j} S (P_{VRj} - P_{Vj})}{R_V T_{g,j}}, \quad (11)$$

For Eq. (6), describing the relative degree for the pellet drying, the difference equation can be presented in the form of:

$$\omega = \frac{\gamma_k - \gamma_{k-1}}{\Delta \tau} = \frac{3 \lambda_{i,j} (t_{0,j} - T_{m^*i,j}) \sqrt[3]{\gamma_k}}{\rho_m u_k Q_s r_p^2 (\sqrt[3]{\gamma_k} - 1)}, \quad (12)$$

As a result, the system of Eqs. (7–12) will have an ordered ribbon-diagonal structure and include more than 2105 equations, the solutions of which were carried out using a computer program in the Borland C++ environment.

The obtained relations (7) allow solving the problem of internal heat transfer in a spherical pellet, and in conjunction with Eqs. (8–12) completely describe the distribution of temperatures and moisture content for pellets and heat carrier gas in a moving dense multilayer mass on a conveyor of the indurating machine.

4 Computational Experiments and Simulation Model Verification

The calculation results of the drying parameters for the OK -3–520/536 indurating machine according to the computer model developed by the authors based on Eqs. (7–12) are in good agreement with its regulatory indicators (determined by the use of least squares method) and qualitatively coincide with numerous empirical dependencies (Fig. 1).

The drying parameters obtained by the computational experiments on the computer simulation model: the relative degree of drying, moisture content, moisture transfer intensity in the pellet, and moisture content in the moving dense multilayer mass are shown in Figs. 2–4. The change for the relative degree of pellets drying γ is presented in Fig. 2, which shows its isolines.

It was found that during multilayer drying, pellets over moistening for more than 13–14% entails their softening, shape change, destruction, and, as a result, deterioration of the gas permeability of the layer. Figure 3 presents the isolines of pellets moisture content in the multilayer mass moving on a conveyor-type indurating machine, the isolines show that in some of the mass levels moreover moistening is observed: at the height of 0.22–0.28 m and the distance of 8–40 m, the pellet humidity is 20–25%.

It has been found that the most intensive process of moistening for the heat carrier gas occurs when the flow is reversed, as a result, the “dry” heat carrier gas (0.013 kg/kg) first enters the less dried and cold levels and, absorbing a certain amount of moisture, passes through already heated areas of the layer where the condensation takes place insignificantly. It is proved by Fig. 4 which shows the isolines for the gas

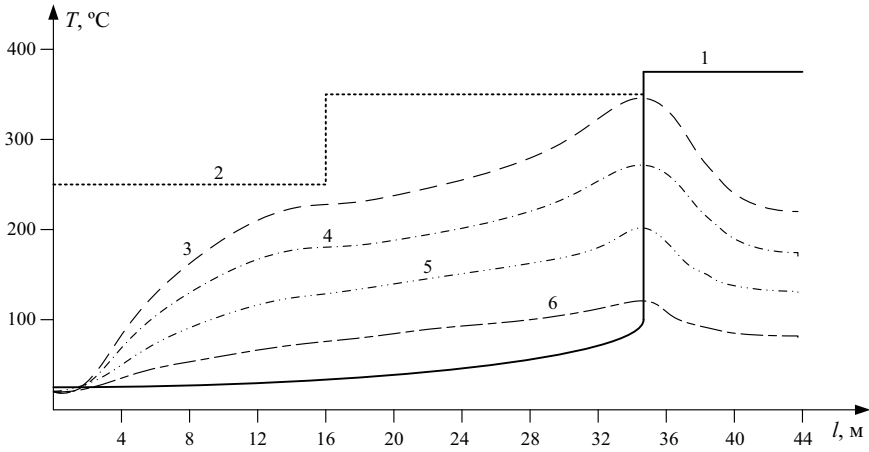


Fig. 1 Gas carrier temperature in a dense multilayer pellets mass in the drying zone of the conveyor-type indurating machine in a scheduled operating condition: a above the multilayer mass; b under the multilayer mass; c–f temperature for the pellets material in various levels of the multilayer mass from top to bottom

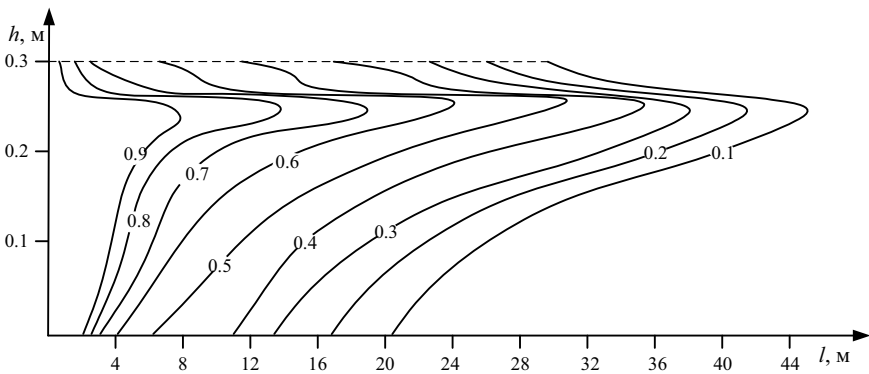


Fig. 2 Parametric family of curves characterizing the relative degree for pellets drying γ in the moving dense multilayer mass in the drying zone of the conveyor-type indurating machine

carrier moisture content in the dynamic multilayer pellets mass. The indicated isolines show that in some areas the heat carrier gas has a moisture content of 0.04–0.07 kg/kg, which is more than the initial value.

Thus, as a result of numerous computational experiments on the developed simulation model, it was shown that when drying a moving multilayer mass of pellets, moisture is redistributed along with the layer height, as a result over moistening is observed in some areas. During the pellets drying process, two types of destruction are possible: cracking and explosive destruction or shock. The beginning of the drying process, characterized by the removal of capillary water, is particularly unfavorable

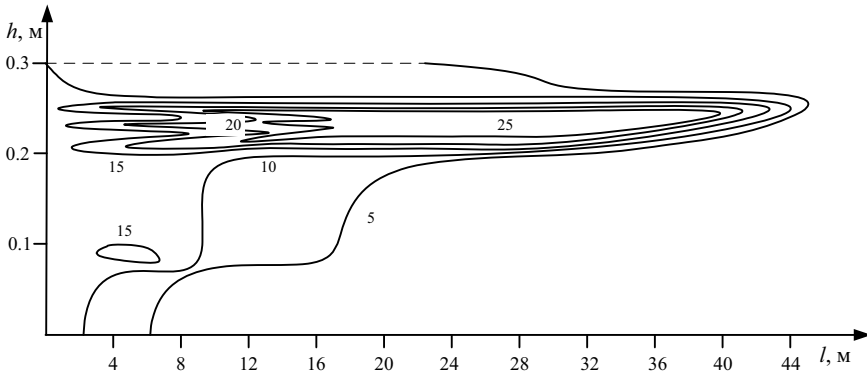


Fig. 3 Parametric family of curves characterizing pellets moisture content u in the moving dense multilayer mass of the drying zone in the conveyor-type indurating machine

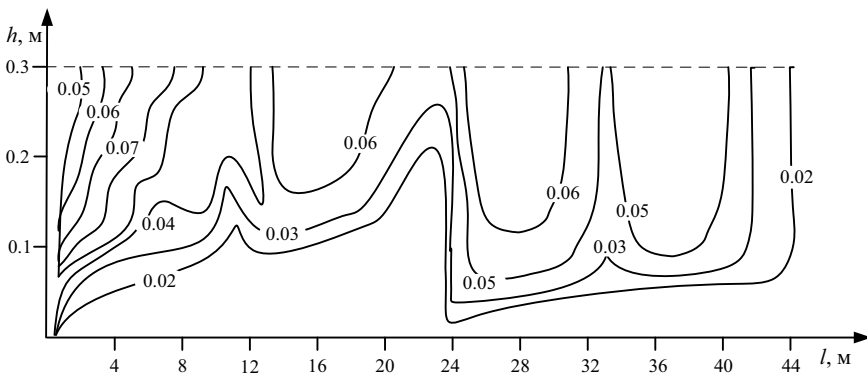


Fig. 4 Parametric family of curves characterizing gas carrier moisture content a_w in the moving dense mass of the conveyor-type indurating machine

and leads to the formation of the cracks since the monolithic of the pellets material is mainly provided by capillary forces [23]. An explosive shock in the pellet sphere is observed in the final drying period of the upper levels in the multilayer pellets mass, therefore, when choosing a multilayer drying condition, it is necessary to take into account the heating rate, the temperature gradient in the pellet, and moisture transfer intensity [23].

The developed multiscale mathematical model for the heat and mass transfer in the layer, describing the internal heat transfer in the pellet and the external one for the temperature field of the heat carrier gas, takes into account nonstationarity and quasi-two-dimensionality. It provides operability in the entire range of thermal and aerodynamic effects; discovers qualitative and quantitative agreement between calculations and experiment; the range of deviations of gas temperatures at the exit

of the multilayer pellets mass does not exceed 47 °C; the error in calculating the average moisture content in the layer is 6%.

Based on the multiscale mathematical model for thermal treatment of pellets from apatite-nepheline ores waste a simulation computer program was developed to analyze the operating conditions of the indurating machine. The program allows visualizing heat, aerodynamic field, and moisture distribution in the dynamic multilayer mass of pellets during the drying process. In the interactive mode, the user-friendly interface makes it possible to control the processes of heat transfer and drying by changing the aerodynamic effects, time by varying the pallet travel speed of the conveyor indurating machine. Using the integrated environment it is possible to analyze the influence of material chemical composition, pellets granulometric composition, bonding additive of the bed on the multilayer mass thermal behavior, drying conditions, pellets strength. Finally, the program is a computer simulator for training operators; due to it, they get skills of controlling the indurating machine. The program uses the ideas of virtual reality, i.e. allows fixing inaccessible areas of the control object, allowing you to monitor the physical condition of the multilayer pellets mass in the drying zone of the conveyor-type indurating machine and make reasonable technical decisions on control parameters.

5 Conclusion

The analysis of technical indicators during the thermal influence on the mass of the multi-layer pellet was carried out taking into account almost all the characteristic features of drying processes on the conveyor-type indurating machine, as well as the pellets radius, the initial moisture content, and the conveyor speed.

Efficient roasting conditions, i.e. the maximum productivity of the conveyor-type indurating machine, processing of pelletized waste from apatite-nepheline ores, at a known height and fractional composition of the backfill are ensured by: heating the layer to the maximum possible temperature at the highest possible speed; keeping the material at this temperature for the time necessary to complete the drying process. This results from the fact that the drying process of the pellets substantially depends on the temperature of the material [24]. The maximum influence on the dense multilayer mass of pellets can be obtained by determining the optimal drying parameters [25].

The analysis of the revealed dependencies and data obtained during computational experiments substantiates that in order to reduce the volume of the over moistening zone, it is necessary to increase the flow rate and temperature of the heat carrier gas, the radius of the pellets, and the porosity of the multilayer pellets mass. We consider that the over moistening of the pellets obtained from apatite-nepheline ores waste of mining and processing plants is proportional to the difference between the initial temperature of the pellet and the equilibrium temperature of the drying process, which is determined by the parameters of the heat carrier gas.

The described model made it possible to automate the decision-making procedure for choosing technological conditions of conveyor-type indurating machines operation to process apatite-nepheline ores waste at mining and processing plants.

Acknowledgements The reported study was funded by RFBR according to the research project No 18-29-24094 MK.

References

1. Butkarev, A.A., Butkarev, A.P., Zhomiruk, P.A., Martynenko, V.V., Grinenko, N.V.; Pellet heating on modernized OK-124 roasting machine. *Steel Transl.* **40**(3), 239–242 (2010)
2. Qing, G., Tian, Y., Zhang, W., Wang, X., Huang, W., Dong, X., Li, M.: Study on application of iron ore fine in pelletizing. *Miner. Metals Mater. Ser. Part F8*, 279–285 (2018)
3. Nayak, N.P., Pal, B.K., Paul, G.P.: Beneficiation of goethite-laterite ore—an alternative. *J. Mines Metals Fuels* **66**(4), 253–255
4. Gan, M., Ji, Z., Fan, X., Lv, W., Zheng, R., Chen, X., Liu, S., Jiang, T.: Preparing high-strength titanium pellets for ironmaking as furnace protector: optimum route for ilmenite oxidation and consolidation. *Powder Technol.* **333**, 385–393 (2018)
5. Sun, H., Bian, M.: Study on energy utilization of high phosphorus oolitic haematite by gas-based shaft furnace reduction and electric furnace smelting process. *Miner. Metals Mater. Ser.* **777–785** (2019)
6. Sahu, S.N., Sharma, K., Barma, S.D., Pradhan, P., Nayak, B.K., Biswal, S.K.: Utilization of low-grade BHQ iron ore by reduction roasting followed by magnetic separation for the production of magnetite-based pellet feed. *Metal. Res. Technol.* **116**(6), 611 (2019)
7. Gan, M., Sun, Y.-F., Fan, X.-H., Ji, Z.-Y., Lv, W.: Preparing high-quality vanadium titanomagnetite pellets for large-scale blast furnaces as ironmaking burden. *Ironmaking Steelmaking* **47**(2), 130–137 (2020)
8. Li, W., Fu, G., Chu, M., Zhu, M.: Effect of porosity of Hongge vanadium titanomagnetite-oxidized pellet on its reduction swelling behavior and mechanism with hydrogen-rich gases. *Powder Technol.* **343**, 194–203 (2019)
9. Wang, Y., Schenk, J., Zhang, J., Liu, Z., Wang, J., Niu, L., Cheng, Q.: Novel sintering indexes to evaluate and correlate the crystal characteristics and compressive strength in magnetite pellets. *Powder Technol.* **362**, 517–526 (2020)
10. Meshalkin, V.P., Bobkov, V.I., Dli, M.I.: Automated decision support system in the energy- and resource-efficiency management of a chemical-energy engineering system for roasting phosphorite pellets. *Theor. Found. Chem. Eng.* **53**(6), 960–966 (2019)
11. Blank, C.E., Parks, R.W., Hinman, N.W.: Chitin: a potential new alternative nitrogen source for the tertiary, algal-based treatment of pulp and paper mill wastewater. *J. Appl. Phycol.* **28**, 2753–2766 (2016)
12. Li, J., An, H.-F., Liu, W.-X., Yang, A.-M., Chu, M.-S.: Effect of basicity on metallurgical properties of magnesium fluxed pellets. *J. Iron. Steel Res. Int.* **27**(3), 239–247 (2020)
13. Meshalkin, V.P., Puchkov, A.Y., Dli, M.I., Bobkov, V.I.: Generalized model for engineering and controlling a complex multistage chemical energotechnological system for processing apatite-nepheline ore wastes. *Theor. Found. Chem. Eng.* **53**(4), 463–471 (2019)
14. Aichmayer, L., Garrido, J., Wang, W., Laumert, B.: Experimental evaluation of a novel solar receiver for a micro gas-turbine based solar dish system in the KTH high-flux solar simulator. *Energy* **159**, 184–195 (2018)
15. Lavrinenko, A.A., Varichev, A.V., Ugarov, A.A., Kozub, A.V., Puzakov, P.V., Bragin, V.V., Bokovikov, B.A., Kuznetsov, A.L.: Innovative heating system in the MOK-1-592 roasting machine. *Steel Transl.* **47**(12), 806–813 (2017)

16. Meshalkin, V., Bobkov, V., Dli, M., Dovi, V.: Optimization of energy and resource efficiency in a multistage drying process of phosphate pellets. *Energies* **12**(17), 3376 (2019). <https://doi.org/10.3390/en12173376>
17. Shvydkii, V.S., Fakhtudinov, A.R., Devyatykh, E.A., Spirin, N.A.: To the mathematical modeling of layered metallurgical furnaces and units *Institution News. Ferrous Metal.* **60**(1), 19–23 (2018)
18. Akberdin, A.A., Kim, A.S., Sultangaziev, R.B.: Planning of numerical and physical experiment in the simulation of technological processes *Institution News. Ferrous Metal.* **61**(9), 737–742 (2018)
19. Shvydkii, V.S., Yaroshenko, Yu.G., Spirin, N.A., Lavrov, V.V.: Mathematical model of roasting process of ore and coal pellets in an indurating machine *Institution News. Ferrous Metal.* **60**(4), 329–335 (2018)
20. Novichikhin, A.V., Shorokhova, A.V.: Control procedures for the step-by-step processing of iron ore mining waste *Institution News. Ferrous Metal.* **60**(7), 565–572 (2018)
21. Kowalska, J., Kowalska, H., Cieślak, B., Derewiaka, D., Lenart, A.: Influence of sucrose substitutes and agglomeration on volatile compounds in powdered cocoa beverages. *J. Food Sci. Technol.* **57**(1), 350–363 (2020)
22. Cui, L., Ba, K., Li, F., Hong, J., Zuo, J.: Life cycle assessment of ultra-low treatment for steel industry sintering flue gas emissions. *Sci. Total Environ.* **725**, 138292 (2020)
23. Hu, S., Li, J., Yang, X., Weng, L., Liu, K.: Improvement on slurry ability and combustion dynamics of low quality coals with ultra-high ash content. *Chem. Eng. Res. Design* **56**, 391–401
24. Bobkov, V.I., Fedulov, A.S., Dli, M.I., Meshalkin, V.P., Morgunova, E.V.: Scientific basis of effective energy resource use and environmentally safe processing of phosphorus-containing manufacturing waste of ore-dressing barrows and processing enterprises. *Clean Tech. Environ. Policy* **20**, 2209–2221 (2018)
25. Chen, Y., Shi, L., Du, J., Zhang, H., Jiao, X.: Preparation and properties of the lightweight thermal insulation wall materials with iron tailings. *J. Build. Mater.* **22**(5), 721–729 (2019)

Optimal Control for Energy and Resource Efficiency in the Drying Process of Pellets from Apatite-Nepheline Ores



Vladimir Bobkov  and Maksim Dli

Abstract The chapter considers the problem of energy and resources efficiency optimization in the drying process of pelletized industrial waste from apatite-nepheline ores as a discrete dynamic programming problem when the discretization for the stay time of pellets in the drying zone of a conveyor-type indurating machine corresponds to the length of individual vacuum chambers. The constraints on the vector of control actions and the state variables of the drying process are taken into account due to the technical feasibilities of the indurating machine and the technological conditions for the drying process. The optimal values, in terms of energy and resource efficiency, for the initial moisture content and the pellets radius, the speed for the conveyor of the indurating machine were identified. The energy and resource-efficient drying conditions for a conveyor-type indurating machine operating with the pelletized waste of apatite-nepheline ores are reasonably obtained, at a known height and fractional composition of the backfill they are provided by: heating the multilayer mass to the maximum possible temperature with the highest possible speed; keeping the material at this temperature for the time necessary to complete the drying process. The obtained results made it possible to automatize the decision making procedure for the selection of a technological operating condition in the chemical and power engineering system of apatite-nepheline ores waste processing at mining and processing plants.

Keywords Optimization · Discrete dynamic programming · Energy and resource efficiency · Drying · Pellets · Indurating machine · Industrial waste

V. Bobkov (✉) · M. Dli
National Research University “Moscow Power Engineering Institute” (Branch) in Smolensk,
Smolensk 214013, Russia
e-mail: vovabobkoff@mail.ru

M. Dli
e-mail: midli@mail.ru

1 Introduction

The implementation of the thermal and aerodynamic conditions of operation in the thermal treatment system of pelletized apatite-nepheline ores waste determines the use efficiency of the heat and electric energy, as well as the quality of the pellets produced. A technical flowsheet of the indurating machine is quite complicated and its operating procedure provides for the specific parameter values in various zones of the indurating machine. But the variation in properties of the initial industrial waste raw material from the dumps of mining and processing plants and the operating conditions of the indurating machine lead to the necessity to changes these conditions [1, 2]. In this case, the deviation from the scheduled operating procedure indicators must not lead to a decrease of the thermal treatment efficiency which is provided by the forecasting based on the multiscale mathematical modeling [3, 4].

Thermal preparation ensures: requirements for the industrial raw material in addition to the enrichment of the waste from apatite-nepheline ores dumps; moisture removal; carbonates dissociation; required granulometric composition of the raw material [5, 6]. Many factors affecting the properties of the raw material do not allow forming a unified criterion for raw materials, and state standards define only constraints according to a number of parameters and the ranges of their possible fluctuations [7, 8]. Therefore, in cases when the raw material properties vary to provide a high level of efficiency for the processing of the apatite-nepheline ores waste, it is necessary to adapt the operating conditions of indurating machines to their properties [9, 10]. The coefficient of efficiency for operating indurating machines is within 40%.

2 Technological Specificity of Pellets Drying on the Conveyor of the Indurating Machine

In the scheduled operating conditions of modern conveyor-type indurating machines in the conditions of the drying zone the capillary exchange of moisture in the pellets does not occur isothermally but under conditions of inconsistent pressure and temperature gradient [11, 12]. Therefore, on the conveyor of the indurating machine in the conditions of the multilayer convection drying and over moistening zone is formed, which significantly negatively affects the characteristics of heat and mass transfer. The effect of moisture redistribution along the height of a moving multilayer mass of pelletized solid waste from apatite-nepheline ores from mining and processing plants (pellets) is observed in a conveyor-type indurating machine [13, 14]. A significant role is also played by the change in the moisture content of the heating carrier gas [15, 16].

The multiscale mathematical model takes into account thermal and engineering peculiarities of the indurating machine, the intensity of the internal moisture transfer in a pellet, and negative processes of the over moistening in the individual levels of

the multilayer pellets mass and the heat carrier gas, that allows increasing energy and resource efficiency by the intensification of heat and mass transfer of the multilayer drying processes [17–20].

The efficiency of the thermal energy use and the quality of the produced pellets largely depend on the organization of the heating condition for the thermal preparation of pellets from apatite-nepheline ores waste [21, 22].

The operating procedure provides for specific parameter values in various zones of the indurating machine. However, changes in the properties of the initial industrial waste raw materials from the dumps of mining and processing plants and the operating condition of the indurating machine lead to the need to change these characteristics. In this case, the deviations from the operating procedure indicators must not lead to the decrease of the thermal processing efficiency, which can be forecasted on the basis of the mathematical modeling [23].

The drying is carried out at 200–400 °C. In the lower levels of the dynamic multilayer pellets mass the effect of over moistening is observed, it is accompanied by the deterioration in the gas permeability of the multilayer mass and the decrease in the heat transfer efficiency in subsequent stages. Therefore, at the initial stage of drying, the supply of the drying agent of the carrier gas is often used from the bottom up, which helps to prevent the deformation of wet pellets located in the lower levels of a dense multilayer mass.

From the point of view of the system analysis, at the micro-level, the technological process for drying of pellets from apatite-nepheline ores waste is a set of moisture removal processes in an individual pellet, and at the macro level, it is a set of processes for drying pellets in layers and a moving multilayer mass. Conditional parameters and the completeness of this complex chemical power engineering process in the moving multilayer pellets mass in the conveyor-type indurating machine define the quality of their thermal treatment.

3 Modeling for the Process of Pellets Drying in the Dense Multilayer Mass

In multiscale modeling for a complex multistage process of drying of moving multilayer pellets mass, it is considered at three levels: 1-st level—a model for the drying process of an individual pellet; 2-nd level—a model for the drying process of a vertical multilayer pellets stack; 3-d level—a model for the drying process of a vertical moving multilayer pellets stack. The developed by the authors [6, 7], a multiscale mathematical model for the technological drying process represents a system of partial differential equations (PDE).

The results of the drying parameters calculations for the indurating machine of OK-3-520/536 type according to the computer model, developed by the authors on the basis of PDE, are in good agreement with its scheduled operating procedure indicators and qualitatively coincide with numerous empirical dependencies. Numerous

computational experiments were carried out, due to the experiments the basic parameters for the drying were obtained: the relative degree of drying, moisture content, moisture transfer intensity in a pellet, and their moisture content in the dynamic multi-layer mass. It was found that during multilayer drying over moistening for pellets of more than 14.5% entails their softening, change in shape, destruction, and, as a result, deterioration of the gas permeability in the layer, and in some areas moreover moistening is observed. For example, at the height of 0.25–0.3 m and the distance of 5–55 m the pellets humidity is 20–25%.

It was revealed that the most intensive process of gas humidification occurs at its reverse feed, as a result of which the “dry” heat carrier gas (0.012 kg/kg) first enters the less dried and cold level of the multilayer mass and, absorbing a certain amount of moisture, passes through the already heated areas where condensation is negligible. This fact is confirmed by the calculation results for the gas moisture content of the mass of the pellet, in the individual areas the heat carrier gas has the moisture content of 0.04–0.07 kg/kg which is more than the initial values.

Thus, as a result of numerous computational experiments on the developed computer model, it is shown that when drying the moving multilayer pellets mass the re-distribution of the moisture is occurred along with the height of the layer, as a result, pellets’ over moistening is observed. During the pellets drying process two types of destructions are possible: cracking and explosive destruction, or shock. The beginning of the drying process, characterized by the removal of capillary water, is particularly unfavorable and leads to the formation of cracks since the monolithicity of the material is mainly provided by capillary forces. An explosive shock in the pellet sphere is observed in the final drying period of the upper levels in the multilayer pellets mass, therefore, when choosing a multilayer drying condition, it is necessary to take into account the heating rate, the temperature gradient in the pellet, and moisture transfer intensity [24].

The multiscale mathematical model for the heat transfer in the layer, describing the internal heat exchange in the pellet and external for the temperature field of the heat carrier gas, takes into account nonstationarity and quasi-two-dimensionality. It provides the operability in the whole range of the thermal action conditions; detects the qualitative and quantitative agreement between calculations and experiment; the range of deviations for gas temperatures at the exit from the multilayer pellets mass does not exceed 50 °C; the calculating error of the average moisture content in the layer is 7%.

On the basis of the multiscale mathematical model for the thermal treatment of pellets from apatite-nephenine ores a computer program to analyze the conditions of the indurating machine operation is developed. The program allows visualizing the thermal, hydrodynamic field and the distribution of moisture in the layer during drying. The user-friendly interface makes it possible to control the heat transfer processes in the layer in the interactive environment, to control drying by changing the hydraulic effect, time by varying the pallets speed. Due to this integrated environment, it is possible to analyze the influence of the chemical composition of the material, the granulometric composition of pellets, bonding additives, bed on the thermal behavior of the dense layer, drying conditions, pellets strength. Finally, the program

is a computer simulator to train operators to control the indurating machine. The program uses the ideas of virtual reality, i.e. it allows monitoring the physical state of the layer and making reasonable engineering decisions on control parameters.

The analysis of technological indicators during thermal effect on the multilayer pellets mass was carried out taking into account practically all characteristic features of the drying process on the conveyor of the indurating machine as well as the pellets radius, initial moisture content, and the conveyor speed.

Effective roasting conditions, i.e. the maximum efficiency of the conveyor-type indurating machine, working with the pelletized waste of apatite-nepheline ores, at a known height and fractional composition of the backfill is ensured by: heating the layer to the maximum possible temperature at the highest possible speed; keeping the material at this temperature for the time necessary to complete the drying process. This follows from the fact that the drying process of the pellets depends significantly on the material temperature. The maximum effect on the dense multilayer pellets' mass can be obtained by determining the optimal drying parameters [25].

The analysis of the revealed dependencies and data obtained during computational experiments substantiates that it is necessary to increase the flow rate and temperature of the heat carrier gas, the radius of the pellets, and the porosity of the multilayer pellets mass to reduce the volume of the over moistening zone. We consider, that over moistening of pellets produced from apatite-nepheline ores of mining and processing plants is in proportion to the difference between the initial temperature of the pellet and the equilibrium temperature of the drying process, which is determined by the parameters of the heat carrier gas.

4 Optimal Control for the Energy Efficiency of the Drying Process

The models for interconnected processes of drying in the conveyor-type indurating machine, developed by the authors, allow optimizing in terms of the energy and resource efficiency according to the generalized criterion for the energy and resource efficiency (CE) ($C \Phi = \Phi(u_{in}; r_p; V_{len}) E$) the dehydration process of pelletized waste from apatite-nepheline ores during drying and they allow intensifying the process of raw material thermal preparation for its final processing in the ore thermal furnaces, where u_{in} —initial moisture content of the pellets entering the drying zone of the indurating machine, r_p —their radius, V_{len} —conveyor speed. The models also allow forming the control variables: carrier gas temperature and its feed rate, vector $X(T_{g0}; G_g)$, to prevent pellets destruction on the basis of the control for the flow of water vapor filtered through its dried layer, the temperature of the heat carrier gas at the outlet $T_{gh} \leq T_{gh}^{MAX}$, heat rate $\partial T_m / \partial \tau \leq \Delta_1 T_m^{MAX}$ and gradient $\partial T_m / \partial x \leq \Delta_2 T_m^{MAX}$ for the temperature in the pellet, moisture content $u \leq u^{MAX}$ and moisture transfer $I \leq I^{MAX}$.

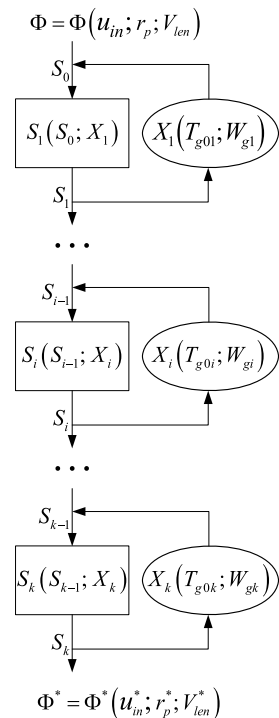
Due to the engineering features of the indurating machine, constraints are imposed on vector X of the control variables: rate $0 \leq W_g \leq W_g^{MAX}$ and temperature $T_{g0}^{MIN} \leq T_{g0} \leq T_{g0}^{MAX}$ of the fed heat carrier gas. The vector for the variables of the drying process state has the form of $S(T_m; \partial T_m / \partial x; \partial T_m / \partial \tau; T_{gh}; u; I; \gamma; r_p)$.

We consider the problem of optimization for the drying process as a problem of discrete dynamic programming (DP) at time discretization for the pellet stay in the drying zone into k equal stages each of which corresponds to the length of the vacuum chamber Δl , for time intervals $\Delta \tau$.

Each vector S_i of the subsequent state for the variables of the drying process is determined by its previous condition S_{i-1} and the vector of the control variables $X_i(T_{g0i}; W_{gi})$ in accordance with the system of PDE (Fig. 1).

A particular criterion for the efficiency (CE) at each stage i is Φ_i —a function of variables for the drying process state at the previous step $i-1$ and solution X_i , made at this stage $\Phi_i = \Phi(X_i; S_{i-1}) = c_h Q_h(T_{g0i}) + c_{el} Q_{el}(W_{gi})$, where Q_h —the quantity of the thermal energy during fuel combustion spent to heat the heat carrier gas flow to the temperature T_{g0i} , Q_{el} —the quantity of the electric energy spent on the heat carrier gas flow with the rate W_{gi} in i -th vacuum chamber, c_h, c_{el} —the cost of heat and electric energy.

Fig. 1 The scheme for the problem statement of optimization for the generalized criterion of the energy and resource efficiency in the multistage technological drying process as a problem of discrete dynamic programming



The general CE for the multistage drying process Φ is an adaptive separable function of quotients Φ_i throughout the drying zone ($i = 1 \dots k$)

$$\min_{X_i} \Phi = \min_{X_i} \sum_{i=1}^k \Phi_i(X_i; S_{i-1})$$

In accordance with Bellman’s principle of optimality for dynamic programming problems, CE can be written through CE of k-th element of decomposition and for the first $k - 1$ elements:

$$\min_{X_i} \Phi = \min \left\{ \Phi_k(X_k; S_{k-1}) + \sum_{i=1}^{k-1} \Phi_i(X_i; S_{i-1}) \right\} \tag{1}$$

In expression (1) the value of the augend $\Phi_k(X_k; S_{k-1})$ is changed only due to the discrete optimizing vector at the last k-th stage $X_k(T_{g0k}; W_{gk})$, and the value of the addend $\sum_{i=1}^{k-1} \Phi_i(X_i; S_{i-1})$ is minimized when the control or optimizing vectors $X_i(T_{g0i}; W_{gi})$ are changed, where $i = 1, 2, \dots, k - 1$.

The operation of finding the optimal solution for the DP problem consists of reverse and direct sweep procedures. The reverse sweep starts with the last k-th stage of the multistage drying process (Fig. 1). The constrained minimum for CE Φ_k^* will be defined by the formula: $\Phi_k^*(S_{k-1}) = \min_{X_k} \Phi_k(S_{k-1}, X_k^*)$, where X_k^* —conditional optimal control at the last stage $i = k$.

CE value at the stage $i = k - 1$ is equal to:

$$\Phi_{k-1}(S_{k-2}) = \Phi_{k-1}(S_{k-2}, X_{k-1}) + \Phi_k^*(S_{k-1}) \tag{2}$$

The vector of state variables S_{k-1} is included in (2), therefore, to continue the search for the optimal solution, it is necessary to determine how the vector of output state variables changes under the influence of the control vector X_{k-1} at the $(k - 1)$ -th stage: $S_{k-1} = S_{k-1}(S_{k-2}; X_{k-1})$.

The constrained minimum for CE at the $k - 1$ -th stage is equal to:

$$\Phi_{k-1}^*(S_{k-2}) = \min_{X_{k-1}} \{ \Phi_{k-1}(S_{k-2}, X_{k-1}) + \Phi_k^*(\varphi_{k-1}(S_{k-2}, X_{k-1})) \}$$

Having determined the constrained minimum $\Phi_{k-1}^*(S_{k-2})$ and the values of the conditional optimizing vector proceed to stage $k - 2$, etc.

For the i -th stage ($k - i + 1$ the stage from the end), Bellman’s equation is written:

$$\Phi_i^*(S_{i-1}) = \min_{X_i} \{ \Phi_i(S_{i-1}, X_i) + \Phi_{i+1}^*(S_i(S_{i-1}, X_i)) \} \tag{3}$$

Solving Bellman's Eq. (3) in sequence, at each stage i from k to 1 , the values of minima for CE $\Phi_k^* \rightarrow \Phi_{k-1}^* \rightarrow \Phi_{k-2}^* \rightarrow \dots \rightarrow \Phi_2^* \rightarrow \Phi_1^*$ and the values for conditional optimal vectors $X_k^* \rightarrow X_{k-1}^* \rightarrow X_{k-2}^* \rightarrow \dots \rightarrow X_2^* \rightarrow X_1^*$, corresponding to the reverse sweep procedure are obtained. Then, using the known initial value for the vector of state variables S_0 , the subsequent vector of state variables S_1 is determined with a minimum of CE— Φ_1 and the optimal value for vector X_1 and so on for i from 1 to k . For the direct sweep procedure, finding the optimal value for control variables T_{g0i} and W_{gi} at each i -th stage of the chemical power engineering process decomposition, the sequence of vector variables of control values $\left\{ X_i(T_{g0i}; W_{gi}) \right\}_{i=1}^k$, which determine the optimal drying condition for the indurating machine in the moving multilayer pellets mass throughout the drying zone of the indurating machine, is obtained.

At each i -th stage the value of particular CE— Φ_i represents a function of two variables $\Phi_i(T_{g0i}; W_{gi})$, for this function the optimal value for the vector of control variables $X_i^*(T_{g0i}^*; W_{gi}^*)$ is determined by Nelder–Mead method (polytope method).

The constraints fulfillment for control variables are the rate $W_{gi} \leq W_{gi}^{MAX}$ and temperature $T_{g0i} \leq T_{g0i}^{MAX}$ of the heat carrier gas at the inlet of the pellets layer is achieved by introducing “barrier” functions into the function $\Phi_i(T_{g0i}; W_{gi})$. This is the hardest constrain as it provides mathematically correct and physically feasible solutions to the DPE system.

The search for a minimum of particular CE $\Phi_i(T_{g0i}; W_{gi})$ when fulfilling the constrain conditions for state variables is carried out by the penalty function method of the “cut-off square” type.

5 Conclusion

Thus, the optimal values of the initial moisture content and pellets radius, the speed for the conveyor of the indurating machine were found in terms of energy and resource efficiency, and the thermal and aerodynamic conditions for the energy and resource efficiency of the conveyor-type indurating machine operation was determined.

The analysis of the revealed dependencies and data obtained in computational experiments substantiates that it is necessary to increase the flow rate and temperature of the heat carrier gas, the radius of the pellets, and the porosity of the multilayer pellets mass in order to reduce the volume of the over moistening zone. We suggest, that the over moistening of pellets produced from apatite-nepheline ores of mining and processing plants is proportional to the difference between the initial temperature of the pellet and the equilibrium temperature of the drying process, which is determined by the parameters of the heat carrier gas.

Acknowledgements The reported study was funded by RFBR according to the research project No 18-29-24094 MK.

References

1. Shvydkii, V.S., Fakhitudinov, A.R., Devyatykh, E.A., Spirin, N.A.: To the mathematical modeling of layered metallurgical furnaces and units institution news. *Ferrous Metal*. **60**(1), 19–23 (2018)
2. Akberdin, A.A., Kim, A.S., Sultangaziev, R.B.: Planning of numerical and physical experiment in the simulation of technological processes institution news. *Ferrous Metal*. **61**(9), 737–742 (2018)
3. Shvydkii, V.S., Yaroshenko, Yu.G., Spirin, N.A., Lavrov, V.V.: Mathematical model of roasting process of ore and coal pellets in a indurating machine. *Institution News. Ferrous Metallurgy*. **60**(4), 329–335 (2018)
4. Novichikhin, A.V., Shorokhova, A.V.: Control procedures for the step-by-step processing of iron ore mining waste institution news. *Ferrous Metal*. **60**(7), 565–572 (2018)
5. Lavrinenko, A.A., Varichev, A.V., Ugarov, A.A., Kozub, A.V., Puzakov, P.V., Bragin, V.V., Bokovikov, B.A., Kuznetsov, A.L.: Innovative heating system in the MOK-1-592 roasting machine. *Steel Transl.* **47**(12), 806–813 (2017)
6. Meshalkin, V., Bobkov, V., Dli, M., Dovi, V.: Optimization of energy and resource efficiency in a multistage drying process of phosphate pellets. *Energies* **12**(17), 3376 (2019). <https://doi.org/10.3390/en12173376>
7. Meshalkin, V.P., Bobkov, V.I., Dli, M.I., Belozerskii, A.Y., Men'shova, I.I.: Optimizing the energy efficiency of a local process of multistage drying of a moving mass of phosphorite pellets. *Doklady Chem.* **486**(1), 144–148 (2019)
8. Aichmayer, L., Garrido, J., Wang, W., Laumert, B.: Experimental evaluation of a novel solar receiver for a micro gas-turbine based solar dish system in the KTH high-flux solar simulator. *Energy* **159**, 184–195 (2018)
9. Li, J., An, H.-F., Liu, W.-X., Yang, A.-M., Chu, M.-S.: Effect of basicity on metallurgical properties of magnesium fluxed pellets. *J. Iron. Steel Res. Int.* **27**(3), 239–247 (2020)
10. Meshalkin, V.P., Puchkov, A.Y., Dli, M.I., Bobkov, V.I.: Generalized model for engineering and controlling a complex multistage chemical energotechnological system for processing apatite-nepheline ore wastes. *Theor. Found. Chem. Eng.* **53**(4), 463–471 (2019)
11. Meshalkin, V.P., Bobkov, V.I., Dli, M.I.: Automated decision support system in the energy- and resource-efficiency management of a chemical-energy engineering system for roasting phosphorite pellets. *Theor. Found. Chem. Eng.* **53**(6), 960–966 (2019)
12. Blank, C.E., Parks, R.W., Hinman, N.W.: Chitin: a potential new alternative nitrogen source for the tertiary, algal-based treatment of pulp and paper mill wastewater. *J. Appl. Phycol.* **28**, 2753–2766 (2016)
13. Wang, Y., Schenk, J., Zhang, J., Liu, Z., Wang, J., Niu, L., Cheng, Q.: Novel sintering indexes to evaluate and correlate the crystal characteristics and compressive strength in magnetite pellets. *Powder Technol.* **362**, 517–526 (2020)
14. Li, W., Fu, G., Chu, M., Zhu, M.: Effect of porosity of Hongge vanadium titanomagnetite-oxidized pellet on its reduction swelling behavior and mechanism with hydrogen-rich gases. *Powder Technol.* **343**, 194–203 (2019)
15. Gan, M., Sun, Y.-F., Fan, X.-H., Ji, Z.-Y., Lv, W.: Preparing high-quality vanadium titanomagnetite pellets for large-scale blast furnaces as ironmaking burden. *Ironmaking Steelmaking* **47**(2), 130–137 (2020)
16. Sahu, S.N., Sharma, K., Barma, S.D., Pradhan, P., Nayak, B.K., Biswal, S.K.: Utilization of low-grade BHQ iron ore by reduction roasting followed by magnetic separation for the production of magnetite-based pellet feed. *Metal. Res. Technol.* **116**(6), 611 (2019)
17. Sun, H., Bian, M.: Study on energy utilization of high phosphorus oolitic haematite by gas-based shaft furnace reduction and electric furnace smelting process. *Minerals Metals Mater. Ser.* 777–785 (2019)
18. Gan, M., Ji, Z., Fan, X., Lv, W., Zheng, R., Chen, X., Liu, S., Jiang, T.: Preparing high-strength titanium pellets for ironmaking as furnace protector: Optimum route for ilmenite oxidation and consolidation. *Powder Technol.* **333**, 385–393 (2018)

19. Nayak, N.P., Pal, B.K., Paul, G.P.: Beneficiation of goethite-laterite ore—an alternative. *J. Mines Metals Fuels* **66**(4), 253–255 (2018)
20. Qing, G., Tian, Y., Zhang, W., Wang, X., Huang, W., Dong, X., Li, M.: Study on application of iron ore fine in pelletizing. *Minerals Metals Mater. Ser. Part F8*, 279–285 (2018)
21. Bobkov, V.I., Fedulov, A.S., Dli, M.I., Meshalkin, V.P., Morgunova, E.V.: Scientific basis of effective energy resource use and environmentally safe processing of phosphorus-containing manufacturing waste of ore-dressing barrows and processing enterprises. *Clean Tech. Environ. Policy* **20**, 2209–2221 (2018)
22. Brooke, K.M., Baker, L.A., Boyer, T.H.: Total value of phosphorus recovery. *Environ. Sci. Tech.* **50**, 6606–6620 (2016)
23. Butkarev, A.A., Butkarev, A.P., Zhomiruk, P.A., Martynenko, V.V., Grinenko, N.V.: Pellet heating on modernized OK-124 roasting machine. *Steel Trans.* Vol. 40, pp. 239–242 (2010)
24. Bustillo, R.M.: *Mineral Resources: From Exploration to Sustainability Assessment* (2018). Springer Nature, Cham, Switzerland, pp. 96–128
25. Butkarev, A.A., Butkarev, A.P.: Reversible pellet-cooling system at roasting machines. *Steel Trans.* **35**, 1–3 (2005)

Cyber-Physical Systems and Industrial Applications in Energetics

Life Cycle Management of Power Grid Companies' Equipment



Oleg Protalinskiy , Aleksandr Shvedov, and Anna Khanova 

Abstract The chapter describes the formalization of a task of the life cycle management of a power grid company. During the life cycle of electrical grid equipment operation, it is possible to reveal the period in which total expenses for equipment repair in the future will exceed its complete replacement by the new equipment with similar parameters. Estimated functions of replacement of equipment are obtained taking into account the previously performed emergency and scheduled repair, payment of compensation for damage to consumers, the discounting coefficient, and the residual book value of the equipment. A software product for life cycle management of electrical grid equipment has been developed, which provides cost-saving when considering the long-term perspective of electrical grid equipment operation.

Keywords Condition index · Electrical grid equipment · Maintenance · Repair · Replacement function · Life cycle

1 Introduction

A high percentage of power grid companies' equipment has a service life that exceeds or is close to the standard service life [1]. A funding gap of repair and investment programs leads to a situation when cost planning for equipment repair is made only for the near future without taking into account efficiency of complete replacement of equipment in conditions of increase in the cost of repair of old equipment and increase in payments for compensation of damage to consumers. Modern enterprise

O. Protalinskiy (✉)

Moscow Power Engineering Institute, Krasnokazarmenaya street, 14, Moscow 111250, Russia
e-mail: protalinskiy@gmail.com

A. Shvedov · A. Khanova

Astrakhan State Technical University, Tatishcheva street 16, Astrakhan 414056, Russia
e-mail: sashokin-1596@mail.ru

A. Khanova

e-mail: akhanova@mail.ru

productive asset management systems (PAMS) accumulate historical data on equipment repairs during its life cycle, the analysis of which makes it possible to establish a period in which the total cost of repairing obsolete equipment in the future will exceed the cost of replacing it with new similar equipment, along with its technical support.

Alekseev et al. [2–4] and others devoted their papers to the problems of increase of organizational and economic efficiency of maintenance and replacement of production facilities, management of equipment life cycle. Despite the extensive research base, the existing models of equipment assessment, planning of repair, and replacement of equipment are based on a personalized approach (requires information about each piece of equipment, which is very expensive in terms of time and financial resources) and assessment of physical and chemical, operational factors affecting the condition of the equipment [5]. There are no models that take into account the interrelation of economic impacts and the residual operation life of the equipment and allow using minimum initial information to assess the integral state of the equipment of the enterprise and the costs necessary for its repair. The results of the analysis and modeling will allow providing the increase of efficiency of the life cycle management process for power grid companies' equipment in the conditions of implementation of the concept Industry 4.0 [6, 7].

2 System Analysis of the Life Cycle Management Process for Power Grid Companies' Equipment

During the life cycle of electrical grid equipment, maintenance and restoration of its performance are carried out. According to STO (Company standard) 34.01–24–002–2018, the following types of repairs are allocated:

- Current repair is a repair carried out to ensure or restore the normal operation of the product, it consists of replacement and (or) restoration of individual parts (GOST 18,322–2016);
- Mid-life repair is a repair carried out for normal operation and partial restoration of the product life with the replacement or restoration of components of a limited range and control of the technical condition of the components, carried out in the volume established in the standards and technical documentation;
- Overhaul is a repair carried out to restore normal operation and full or close to full restoration of the product life with the replacement or restoration of any of its parts, including key parts;
- Unscheduled repair is a repair, the performance of which is not provided for in the annual (monthly) repair schedule agreed with the subject of operational-dispatching office. Unscheduled repairs are carried out to eliminate the consequences of malfunctions or defects affecting normal and safe operation, as well as the results of integrity monitoring;

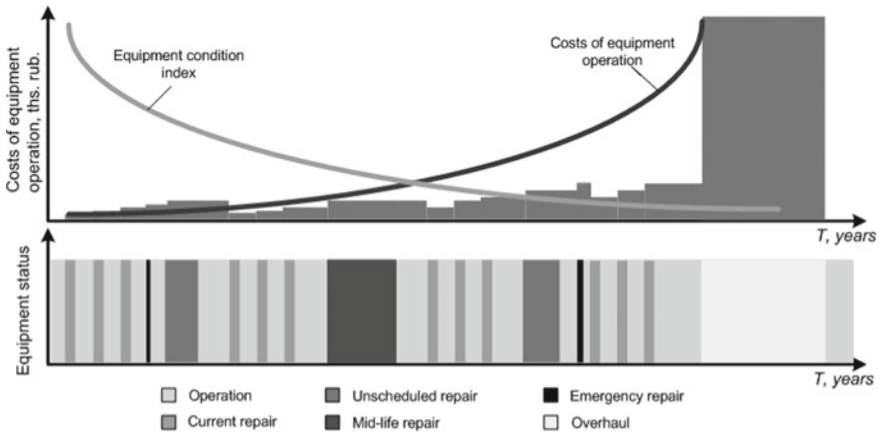


Fig. 1 Life cycle cost allocation for equipment repair

- Emergency repair is the elimination of sustained fault to the equipment, which occurred as a result of disturbance (accident).

The most expensive are overhauls and emergency repairs. A multi-year maintenance and repair plan (MRO) is drawn up for scheduled work. The annual MRO plan is formed every year on the basis of the multi-year plan. The equipment is included in the multi-year plan in accordance with the frequency of repairs for each type, taking into account the priority of the most expensive (in descending order—overhaul, mid-life, current, etc.) [8]. With each new repair (apart from overhauls), the condition of the equipment becomes worse compared to the design parameters, and the cost of repairs is higher. At some point, future repairs are not profitable and a complete replacement of the equipment will be an economically feasible solution (Fig. 1). Before forming a multi-year plan, it is necessary to analyze the feasibility of its complete replacement [9].

In order to draw up an MRO plan in accordance with the frequency of work and a prioritized list, equipment for repair is selected. The prioritized list is a list of equipment recommended for repair, ranked according to the set of indicators: condition index, consequences of failure, probability of failure. The Condition Index is a conventional indicator of the electrical grid equipment condition, which is calculated on the basis of static and dynamic parameters of the main unit and its defects. The Condition Index is based on an integrated assessment of a set of more than two hundred equipment specifications. The process of calculating the Condition Index indicator is labor-intensive and the result does not always reflect the real condition of the equipment due to unreliable or incomplete initial technical data [10].

The received MRO plan based on technical characteristics often includes equipment with overestimated indicators of its condition relative to the actual ones, which leads to excessive repair costs. The chapter proposes a new approach to life cycle management of power grid companies' equipment, based on additional analysis of

the MRO plan and identification of equipment that is more cost-effective to replace with new equipment.

In order to determine the efficiency of the complete replacement of the main unit, it is necessary to analyze the past period costs and calculate future ones [11]. After obtaining data on possible long-term equipment costs, it is necessary to make a comparative analysis with the costs incurred by the power grid company for the complete replacement of new equipment and its further maintenance for the same period [12].

Information support of equipment life cycle management process is distinguished by semantic heterogeneity: the set of groups and brands of equipment, mismatch, and inconsistency of the equipment description levels, parameters, defects, measured characteristics and parameters dimensions of the equipment, as well as of the terminology used [13]. There are differences in the interpretation of these types of data by individual systems that is why solving the problem of semantic interpretation of data when transferring them from one control system to another one becomes a priority in order to ensure the data-level systems integration [14–17]. Ontologies are used to solve such problems in information systems [5] (Fig. 2).

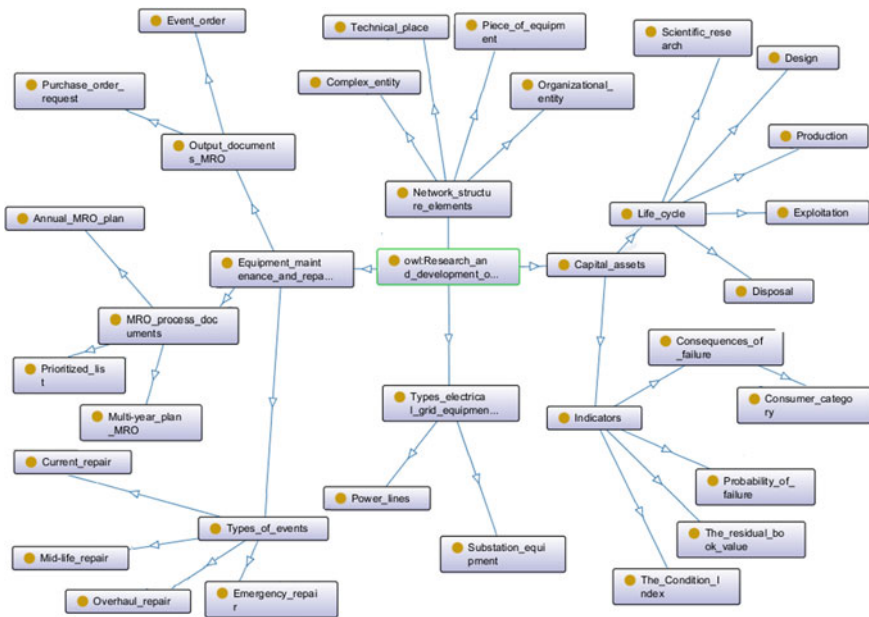
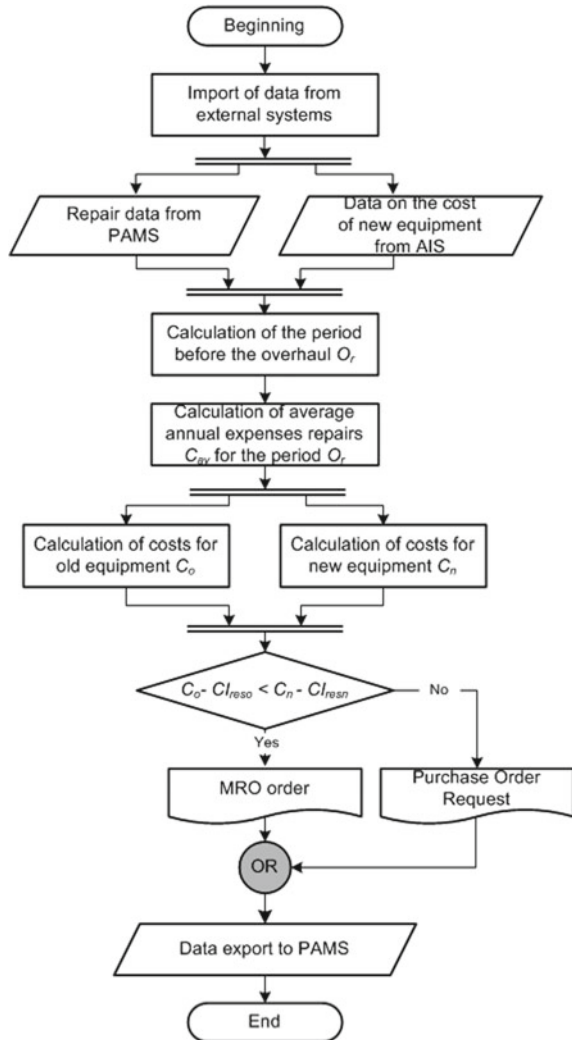


Fig. 2 The ontological model

3 The Procedure of Life Cycle Management of Power Grid Companies' Equipment Based on Economic Indicators

Decision making at the management of equipment life cycle [18] of the power grid companies is based on monitoring of the change of the level of condition of the equipment depending on expenses for repair service and directed on the definition of optimum peri-od of replacement for a group of the homogeneous equipment of the power grid company (Fig. 3).

Fig. 3 Decision-making algorithm for life cycle management of power grid companies' equipment based on economic indicators



In order to make an equipment maintenance plan, we offer a methodology that allows you to perform the following actions based on data on repairs of equipment of a certain brand:

1. Import historical data from external systems, including data on equipment repairs from PAMS and data on the cost of new equipment (or analog) from the accounting information system (AIS).
2. Calculate the Estimated Overhaul Period of O_r , Including Unscheduled Overhauls for Each Brand of Equipment:

$$O_r = \frac{\sum_{i=1}^n (Q_{1i} - Q_{2i})}{n}, \quad (1)$$

where Q_{1i} is the date of the last repair of the i -th piece of equipment of a certain brand, $i = \overline{1, n}$; Q_{2i} is the date of the penultimate repair or commissioning of the i -th piece of equipment of a certain brand, $i = \overline{1, n}$; n is the number of pieces of equipment of a certain brand.

3. Calculate the average annual repair costs for a certain brand of equipment:

$$C_{av} = \frac{\sum_{i=1}^n \left(\sum_{j=1}^t (C_{nij} - IN_{ij}) / t \right)}{n}, \quad (2)$$

where C_{nij} are annual maintenance costs of the i -th piece of equipment in the j -th year, $i = \overline{1, n}$, $j = \overline{1, t}$; IN_{ij} is a consumer compensation for i -th piece of equipment in j -th year, $i = \overline{1, n}$, $j = \overline{1, t}$; t is a period, for which equipment costs are recorded (number of years); n is a number of recorded pieces of equipment of a certain brand. Cumulative costs of both scheduled repairs and emergency repairs are taken into account when developing the model. In the event of an accident, consumers are also compensated for damages.

4. Calculate the cost of old equipment C_o is taking into account the scheduled work before the overhaul and its cost:

$$C_o = \sum_{j=1}^t (C_{av_j} \cdot D_j), \quad (3)$$

where C_o are cost during period t for old equipment; D_j is the discounting coefficient in j -th year, $j = \overline{1, t}$:

$$D_j = (1 - r)^j, \quad (4)$$

where r is an estimated rate; j is the year number, $j = \overline{1, t}$. The estimated rate is calculated by the Fisher equation:

$$r = r_0 + i + r_0 \cdot i, \quad (5)$$

where r_0 is the current key interest rate of the Central Bank of the Russian Federation; i is a forecast inflation rate.

5. Calculate the costs of buying new equipment C_n , taking into account the cost of new equipment and its scheduled maintenance until the period of overhaul O_r ,

$$C_n = CI_n - ((C_e + C_{sc}) \cdot D), \quad (6)$$

where CI_n is a capital investment in the equipment, C_{sc} is a scheduled repair, C_e are emergency repair costs per year:

$$C_e = (C_t + IN) \cdot u, \quad (7)$$

where C_e is emergency repair costs, C_t are 1 repair costs, IN is a consumer indemnity, u is a piece of equipment failure rate;

$$C_{sc} = \sum_{j=1}^t C_j, \quad (8)$$

where C_{sc} is a scheduled repair, C_j are scheduled repair costs in j -th year, $j = \overline{1, t}$.

It is proposed to calculate the costs of support of the old and installation of new equipment annually when drawing up a multi-year maintenance and repair program so that the equipment can be excluded from it in the purchase acts or investment programs. A sign of exclusion from the repair program of the equipment is the following attitude:

$$C_o - CI_{reso} < C_n - CI_{resn}, \quad (9)$$

where CI_{reso} is a residual value of old equipment; CI_{resn} is a residual value of new equipment.

6. Compare the cost of maintaining and repairing the old C_o equipment with the cost of buying new C_n and maintaining it considering the residual book value.
7. As a result, recommend the creation of an MRO Order or a Purchase Order Request document (Fig. 3).
8. Export data to PAMS [19, 20].

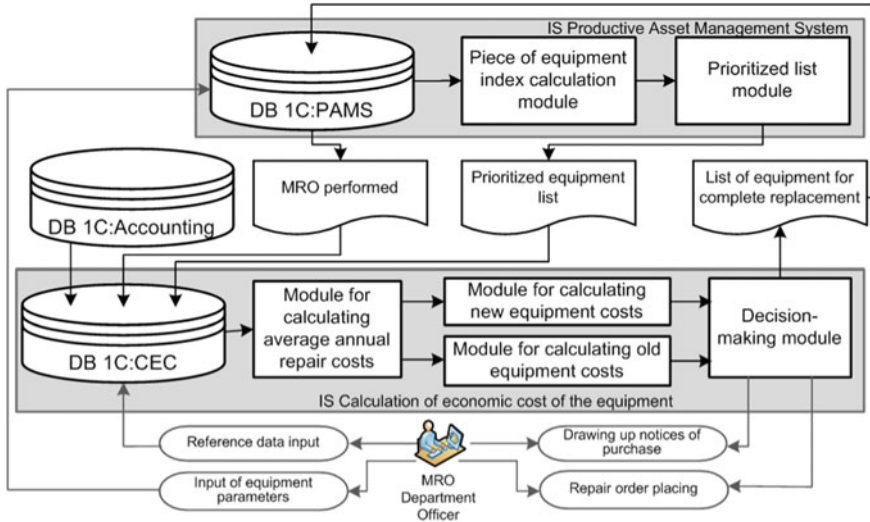


Fig. 4 Structure of the decision-making support system for life cycle management of power grid companies' equipment based on economic indicators

4 Structure of the Decision-Making Support System “Calculation of Economic Cost of the Equipment”

The algorithm of decision-making during life cycle management of the equipment of the power grid companies on the basis of economic indicators (Fig. 3) is implemented as a decision-making support system “Calculation of economic cost of the equipment” (CEC) which structure is given on Fig. 4.

Accounting for the economic activity of the power grid company based on 1C: Productive Asset Management System 8. That is why 1C: Enterprise 8.3 software product was chosen as the development environment, which allowed to integrate 1C: CEC with a line of already developed applications, while the cost of implementation is much lower than the acquisition and implementation of the software product developed in another environment.

5 Conclusion

The procedure of life cycle management of power grid companies' equipment based on economic indicators is proposed, which will improve the technical condition of power grid companies' equipment and increase the efficiency of repair programs for the entire life of the equipment. A decision-making algorithm for life cycle management of power grid companies' equipment based on economic indicators is developed.

1C: CEC solves the problem of inefficient use of resources during technical inspections and repairs of equipment of power grid companies, allows parallel analysis of data from existing information systems, to build mathematical functions, and to obtain results for future periods.

References

1. Protalinskiy, O., Andryushin, A., Shcherbatov, I., Khanova, A., Urazaliev, N.: Strategic decision support in the process of manufacturing systems management. In: Proc. Eleventh International Conference "Management of Large-Scale System Development" (MLSD, Moscow, 2018), pp. 1–4 (2018). <https://doi.org/10.1109/MLSD.2018.8551760>
2. Alekseeva, A.I.: Comprehensive economic analysis of economic activities. KnoRus, Moscow (in Russian) (2009)
3. Belikova, T.N.: Accounting and the reporting from zero to balance. Piter, St.Petersburg (in Russian) (2007)
4. Andreev, D.A.: Modern problems of operation and technical re-equipment of a single national electric network. *Electricity* **6**, 3–9 (2007). (in Russian)
5. Protalinskiy, O., Savchenko, N., Khanova, A.: Data mining integration of power grid companies enterprise asset management. In: Kravets, A., Bolshakov, A., Shcherbakov, M. (eds.), *Cyber-Physical Systems: Industry 4.0 Challenges*. Studies in Systems, Decision and Control, vol. 260 (2020). Springer, Cham. https://doi.org/10.1007/978-3-030-32648-7_4
6. Lee, E.A.: Cyber physical systems: design challenges. In: Proc. 11th IEEE International Symposium on Object Oriented Real-Time Distributed Computing, Orlando, FL, 6 May 2008
7. Lu, Y.: Industry 4.0: a survey on technologies, applications and open research issues. *Journal of Industrial Information Integration* **6**, 1–10 (2017). <https://doi.org/10.1016/j.jii.2017.04.005>
8. Vanin, A.S., Valyanski, A.V., Nasyrov, R.R., et al.: Quality monitoring of electrical power to evaluate the operational reliability of power equipment and active–adaptive voltage control in distribution power grids. *Russian Electr. Eng.* **87**, 452–456 (2016). <https://doi.org/10.3103/S1068371216080101>
9. Jorge, R.S., Hawkins, T.R., Hertwich, E.G.: Life cycle assessment of electricity transmission and distribution—part 1: power lines and cables. *Int. J. Life Cycle Assess* **17**, 9–15 (2012). <https://doi.org/10.1007/s11367-011-0335-1>
10. Gurinovich, V.D., Yanchenko, Y.A.: Development and introduction of information technologies for supporting the management of maintenance and repairs at nuclear power stations. *Therm. Eng.* **58**, 390 (2011). <https://doi.org/10.1134/S0040601511050077>
11. Paklin, N.B., Oreshkov, V.I.: Business analytics: from data to knowledge. Piter, St.Petersburg (in Russian) (2010)
12. Eltyshv, D.K., Kostygov, A.M.: Intelligent diagnostic control and management of the condition of electrotechnical equipment. *Russian Electr. Eng.* **90**, 741–746 (2019). <https://doi.org/10.3103/S1068371219110038>
13. Protalinsky, O.M., Khanova, A.A., Shcherbatov, I.A., Protalinsky, I.O., Kladov, O.N., Urazaliev, N.S., Stepanov, P.V.: Ontology of maintenance management process in an electric grid company. *Bulletin Moscow Energy Inst.* **6**, 110–119 (2018) (in Russian). <https://doi.org/10.24160/1993-6982-2018-6-110-119>
14. Tolk, A.: Truth, trust, and turing—implications for modeling and simulation. In: Tolk, A. ed., *Ontology, Epistemology, and Teleology for Modeling and Simulation*. Intelligent Systems Reference Library, vol. 44, pp. 1–26 (2012)
15. Sithithanasakul, S., Choosri, N.: Using ontology to enhance requirement engineering in agile software process. In: Proc. 10th International Conference on Software, Knowledge, Information Management & Applications (2016). IEEE, Chengdu. <https://doi.org/10.1109/skima.2016.7916218>

16. Suarez-Figueroa, M.C., Gomez-Perez, A., Motta, E., Gangemi, A. (eds.): *Ontology Engineering in a Networked World*. Springer, Heidelberg (2012). <https://doi.org/10.1007/978-3-642-24794-1>
17. Gangemi, A., Catenacci, C., Ciaramita, M., Lehmann, J.: Modelling ontology evaluation and validation. In: *The Semantic Web: Research and Applications*, vol. 4011 (2006). Springer, Berlin, Heidelberg. https://doi.org/10.1007/11762256_13
18. Meng, K., Qian, X., Lou, P. et al.: Smart recovery decision-making of used industrial equipment for sustainable manufacturing: belt lifter case study. *J. Intell. Manuf.* **31**, 183–197 (2020). <https://doi.org/10.1007/s10845-018-1439-2>
19. Bobyr' M.V., Titov V.S. & Nasser A.A. : Automation of the cutting-speed control process based on soft fuzzy logic computing. *Journal of Machinery Manufacture and Reliability* **44**, 633–641 (2015). <https://doi.org/10.3103/S1052618815070067>
20. Makarch'yan, V.A., Chernyaev, A.N., Andryushin, A.V., et al.: A software system used for load distribution at a combined heat and power plant with the complex mix of the equipment and complex schemes of heat and electric power supply. *Therm. Eng.* **60**, 374–380 (2013). <https://doi.org/10.1134/S0040601513050078>

Developing an Energy Provider's Knowledge Base of Flow Charts



V. A. Borodin, Oleg Protalinskiy, and Anna Khanova

Abstract The chapter discusses the problem of scheduling a repair program using flow charts in major energy providers. A knowledge base has been developed determining relationships between defects and flow charts, equipment unit factor types have been considered. The knowledge base allowed systematizing information about defects and flow charts, speeded up the compilation of a repair program, and reduced the number of errors.

Keywords Energy providers · Knowledge base · Flow charts

1 Introduction

Maintenance and repair of equipment is an important task for energy providers. Timely scheduling repairs, managing, and coordinating the operations of repair teams is an especially important task for major energy providers. To cope with it, it is necessary to systematize the scheduling process and establish the regulatory documents for work performance. Such a document is a flow chart containing the data on the cost of works aimed at elimination of the equipment defects, the number of materials, necessity of using machines and mechanisms, workforce skill level, and staff. The flow charts are assigned to a repair team for the elimination of a set of defects within a particular work type. Document “GOST 18,322-2016. Equipment maintenance and repair system. Terms and definitions” [1] determine three types of scheduled repair—current, mid-life, and overhaul repair.

V. A. Borodin (✉) · A. Khanova
Astrakhan State Technical University, ul. Tatischeva 16, 414025 Astrakhan, Russia
e-mail: vitkt@yandex.ru

A. Khanova
e-mail: akhanova@mail.ru

O. Protalinskiy
Moscow Power Engineering Institute, ul. Krasnokazarmennaya 14, Moscow 111250, Russia
e-mail: protalinskiy@gmail.com

The current repair is carried out to eliminate minor malfunctions and does not stipulate the equipment disassembly. To carry out the current repair, a short-time equipment shut-down may be required. The mid-life repair is aimed at maintaining the operability of the most important equipment items. The most large-scale repair type is the overhaul repair—complete equipment disassembly may be required for it. To schedule a repair at the energy provider plant, information about defects is collected, then a flow chart is matched with each defect. A document describing a set of defects and flow charts to eliminate them is called a repair program.

However, scheduling is associated with some problems at major energy providers. A large number of equipment units, defects, and flow charts may slow down the scheduling process significantly. The high complexity of scheduling can result in compliance with the actual scope of works with the scheduled one. It reduced the accuracy of the repair budget planning for an energy provider and may result in economic losses. To solve these problems, a flow chart knowledge database [2–11] has been developed. It enables harmonizing the work with regulatory documents, reduces scheduling time, and the number of errors [12–14].

2 Knowledge Base Model

As a rule, a flow chart (Fig. 1) comprises the following sections: general data, work organization and technology, operational inspection during operations, occupational safety and health, environmental protection, fire safety, and drawings (figures, sketches) [15].

The general data section (Fig. 2) includes the operation type, team composition (profession, grade, number of people, rights of the persons responsible for operating safety, etc.). Time standards are determined in this section in accordance with the existing unified standards and rates for civil construction, installation, and repair and construction works. This section regulates tools, appliances, and accessories required for work performance, the basic specifications are detailed, types, grades, purpose, and quantity of jiggings, tools, process (operation) accessories for a group or a team. Also, the general section contains information about materials, their scopes are determined based on the working documentation with due allowance for the existing consumption rates. This flow chart section contains a description of mechanisms necessary for the work performance, also protective equipment, work conditions, etc. are detailed.

The work organization and technology section (Fig. 3) contains: descriptive part of the work performance with references to the appended drawings, diagrams; process flow, post, electrical level, the number of operation performers, and their rights of security officers.

The operational inspection section (Fig. 4) includes the incoming inspection of design and process documentation which stipulates checking for compliance with the requirements specification, its complete set, legality, and completeness, availability of the source data for the process execution, the list of works, structures, and

Fig. 1 Flow chart structure

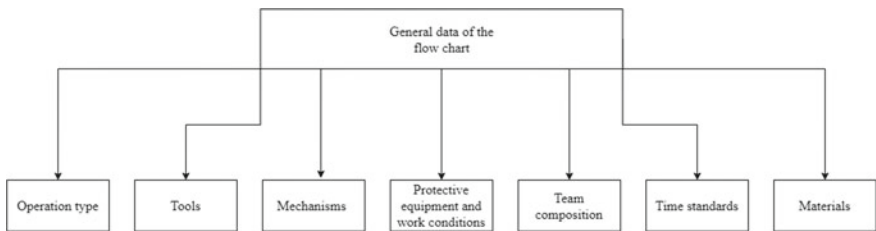
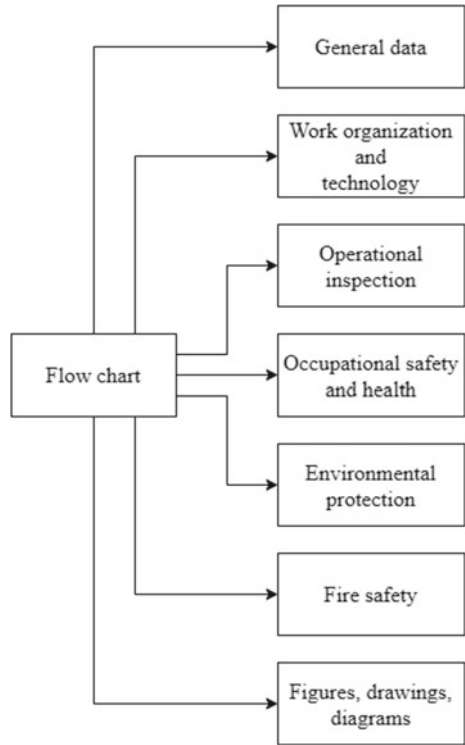


Fig. 2 General data of the flow chart

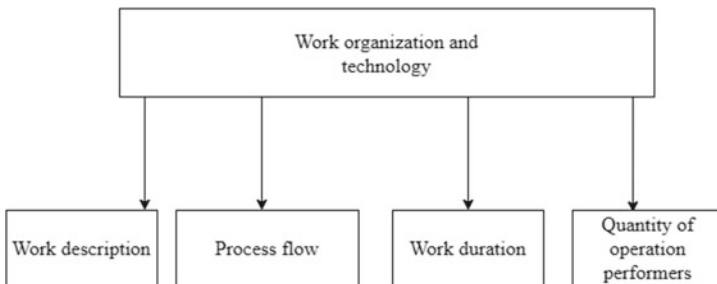
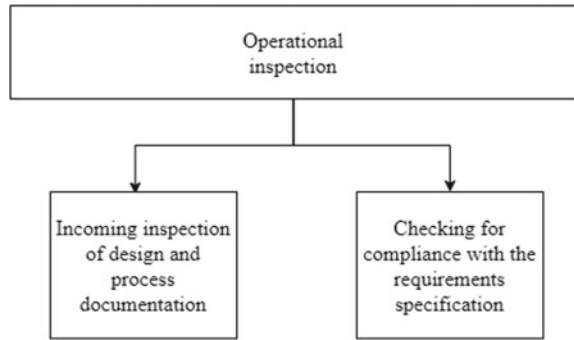


Fig. 3 Work organization and technology

Fig. 4 Operational inspection



equipment, their performance indices. For each of the monitored processes, a table shall be prepared where permissible values and inspection methods are stated for each monitored parameter.

The occupational safety section contains health and safety solutions adopted for the particular process, safe work practices, safe machine operation rules, jiggling, safe hot work performance, protection equipment application methods, measures for restriction of hazardous load handling zones.

The environmental protection section prescribes the activities for the environmentally safe operation of mechanisms, assurance of green planting preservation. Also, noise, dust, and hazardous emission limitation measures are determined, and activities for collection, disposal, and recycling of waste are described.

A flow chart section related to fire safety regulates the combustible material storage process, equipping the work zone with fire-fighting means, rules of carrying out the fire hazardous works. Any necessary drawings may be appended to the flow chart—work execution diagram, hoisting device referencing diagrams, specifications of mechanisms, etc.

The work program contains the flow chart name and code. A special code and a respective measurement group (a component of an equipment unit) are used for the description of defects in work programs. For example, one and the same problem may be related to different equipment units, which supposes different solutions.

In addition to the defect codes and the flow chart, the work program contains information about the equipment brand, equipment unit code, activity type, order number, scheduled (or actual) work performance data, and the attribute of the necessity of executing the flow chart.

$$Ord = \{EqMark, Eq, Wt, Dt, Tcs, Dfs, Sts\} \quad (1)$$

where *EqMark* is the equipment brand, *Eq* is the equipment unit, *Wt* is the work type (current, mid-life or overhaul repair), *Dt* is order completion date, *Tcs* is a set of flow charts, *Dfs* is a set of defects. *Sts* is a set of attributes of mandatory execution of the flow chart. The work program consists of multiple such orders (Fig. 5).

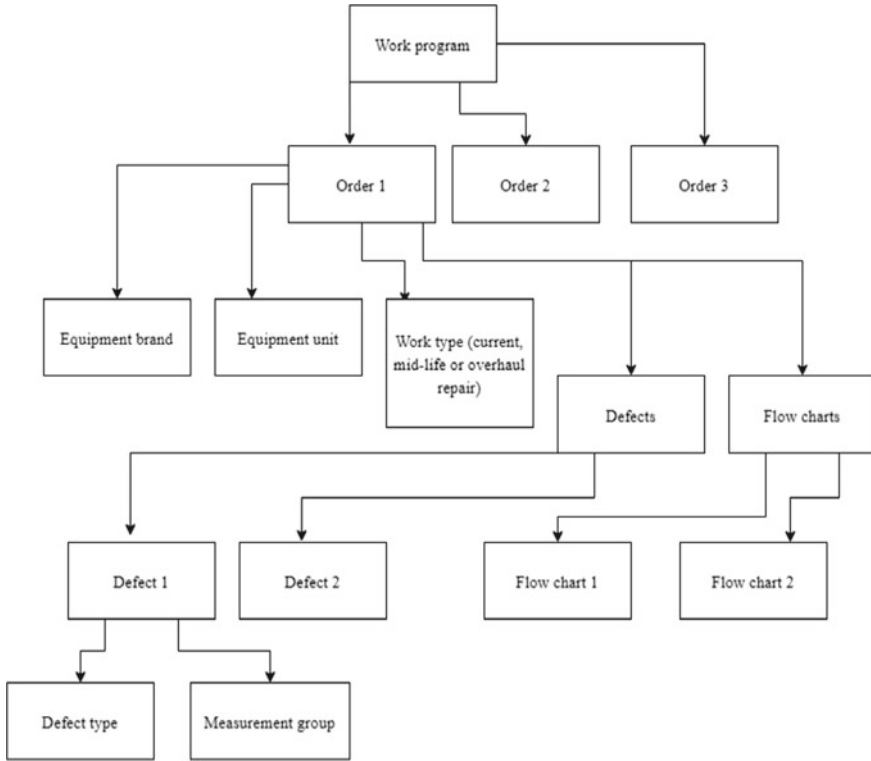


Fig. 5 Work program structure

When the actual data is filled in, the flow chart set may appear to be non-matching with the source data. Thus, it becomes necessary to distinguish such entries so that to obtain correct information about flow charts on defects. Factors are introduced for this purpose. Factors reflect the peculiarities of the equipment, for example, the installation method. These peculiarities do not influence the list of defects, but it is the necessary information for the team to carry out additional works which could remain unaccounted during scheduling. Notification of the knowledge base user about possible factors may preclude errors in the compilation of the plan of works.

Entries are stored in the following form in the knowledge base:

$$Rcd = \{EqMark, Fcts, Wt, Tcs, Dfs, Sts\} \tag{2}$$

where *EqMark* is the equipment brand, *Fcts* is a set of factors, *Wt* is a type of works, *Tcs* is a multitude of flow charts, *Dfs* is a multitude of defects, *Sts* is a set of attributes of mandatory execution of the flow chart.

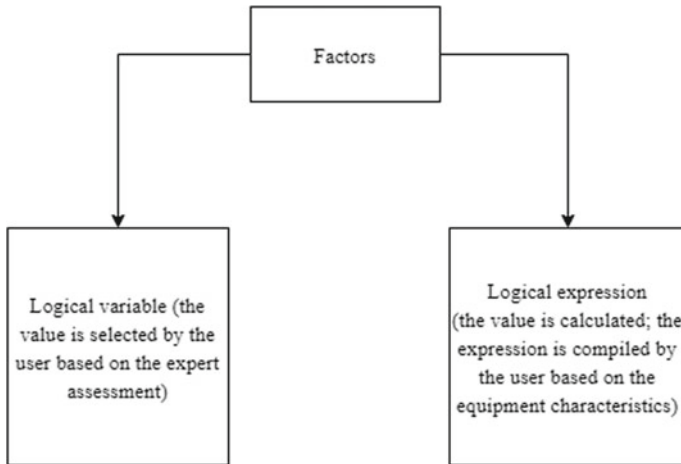


Fig. 6 Types of factors

A different set of factors should be specified for conflicting knowledge base entries. The factors may be specified as logical variables and logical expressions (Fig. 6).

The variable factor value is specified by the user for each conflicting sample. For the expression factor, the user may add some characteristics (for example, service life or the current state) to the equipment brand—real, integral numbers, or a line—and make the factor computable based on such attributes.

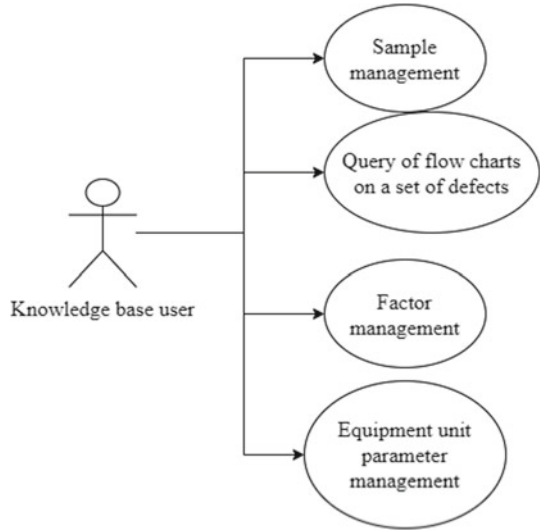
3 Adding Knowledge and Searching

The flow chart knowledge base contains information in the form of samples [2] and supposes several operation modes: adding new samples, modifying the current samples, querying flow charts based on a set of defects, factor operations, changing user parameters of equipment units (Fig. 7).

When adding samples, it is necessary to take into account possible conflicts between the current knowledge and the knowledge being added:

1. The input of a new sample.
2. If the sample is unique, then the transition to Clause 8 is executed.
3. A new filter creation subroutine call.
4. If the subroutine is completed normally, then the transition to Clause 8 is executed.
5. If the user determines one of the conflicting samples as outdated, then transition to step 6 is executed, otherwise to Step 7.
6. An outdated sample is deleted. If a new sample was selected as an outdated one, then the addition is completed, otherwise, the transition to Clause 8 is executed.

Fig. 7 Knowledge base applications



7. The existing conflicting samples are flagged as outdated, but they are not removed from the knowledge base.
8. Adding a new sample to the knowledge base.

The uniqueness of a sample is determined by the uniqueness of a set of defects, work type, equipment brand, and parameters of an equipment unit for the particular set of flow charts:

$$EqS(S_1.S_2) = Dfs_1 = Dfs_2 \ \&\&EqMark_1 = EqMark_2 \ \&\&Wt_1 = Wt_2 \ \&\&EqPrms_1 = EqPrms_2 \quad (3)$$

An algorithm for the creation of a new factor supposes the possibility of creating a logical variable or a condition:

1. The user enters a new factor name
2. If the user selects creating a simple filter, then transition to Clause 3 is executed, otherwise to Clause 4.
3. The user specifies differing logical values of the factor for conflicting samples. Transition to Clause 5.
4. The user inputs a logical expression consisting of parameters of an equipment unit. If the conflicting samples are divided into 2 groups by a condition, then transition to Clause 5 is executed, otherwise, the repeated input of the condition or the subroutine exit is executed.
5. Completion of the factor addition.

The query of flow charts on a set of defects supposes an exact sample or search of the closest sample in the base:

1. Data input from a sample
2. Search of an exact sample match, if a matching sample is found, then transition to Clause 13 is executed.
3. If the knowledge base entries do not contain samples containing at least one of the specified defects, then the system returns an empty solution. Transition to Clause 13.
4. If there are entries matching in terms of a set of defects, equipment brand, and some factors, but some factors are not specified for the query, then transition to Clause 5 is executed, otherwise to Clause 6.
5. The user is prompted to specify the value of non-specified factors so that to determine the query to one of the entries. If the user cannot specify the values, then the first entry is selected. Transition to Clause 13.
6. If there are entries matching in terms of defects and equipment brand, but conflicting in terms of factors, then the search of the closet sample is carried out among all entries with the same equipment brand and defects. Transition to Clause 13, otherwise to Clause 7.
7. A search of the closest sample is carried out among entries with the same equipment brand, first of all by defects, then by factors.
8. Hamming distance [16, 17] to the closest sample is calculated by factors and defects— d_{eq} .
9. A search of the closest sample is carried out among entries with other equipment brands similar to Clause 7.
10. Hamming distance to such a sample is calculated by factors and defects— d_{al} .
11. If $d_{al} \geq d_{eq}$, then the closest sample is selected among entries with the same equipment brand, the transition is executed to Clause 13.
12. If $d_{eq} - d_{al} < k_d$, then one should select the closest sample among entries with other equipment brands, otherwise a sample with the same equipment brand should be selected.
13. The user acquires a set of flow charts by the specified defects and the equipment unit.
14. If required, the user amends the obtained solution and adds an entry according to the new knowledge addition algorithm.

The search for an exact match is carried out by the equipment brand, a set of defects and factors. For Clause 4 the exact match is necessary for terms of the equipment brand, set of defects, and factors specified in the query; some factors may be missing. In Clauses 6, 7, and 9 the search of the closest sample is carried out using Hamming distance. Parameter k_d is set by the user.

4 Conclusion

The developed knowledge base allowed systematizing information about defects and flow charts, speeded up the compilation of a repair program, and reduced the number

of errors. Using the base as a component of an intelligent decision-making support system may result in further scheduling process enhancement. Such an approach can be used for accounting flow charts in other industries [13, 18–20].

References

1. Equipment maintenance and repair system. Terms and definitions. GOST 18322-2016 (2017). <https://docs.cntd.ru/document/1200144954>. Accessed 1 June 2020 (in Russian)
2. Stefik, M.: Introduction to knowledge systems. Elsevier (2014)
3. Giarratano, J.C., Riley, G.: Expert systems: principles and programming. Brooks/Cole Publishing Co (1989)
4. Jackson, P.: Introduction to expert systems (1998). Addison-Wesley Longman Publishing Co. Inc.
5. Schreiber, A.T. et al.: Knowledge engineering and management: the Common KADS methodology (2000). MIT press
6. James, G., et al.: An introduction to statistical learning. Springer, New York (2013)
7. Izvercian, M., Ivascu, L., Miclea, S.: An expert system for enterprise risk assessment. In: Proceeding of International Conference on Economics, Business and Management, Kuala Lumpur (2010)
8. Waterman, D.: A guide to expert systems (1986)
9. Liebowitz, J. (ed.): The handbook of applied expert systems. CRC Press (1997)
10. Frangopoulos, C. (ed.): Exergy, Energy System Analysis and Optimization-Volume III: Artificial Intelligence and Expert Systems in Energy Systems Analysis Sustainability Considerations in the Modeling of Energy Systems, vol. 3, EOLSS Publications. (2009)
11. Krishnamoorthy, C.S., Rajeev, S.: Artificial intelligence and expert systems for engineers (1996). CRC press
12. Sazykin, V.G.: Классификация экспертных систем в электроэнергетике. (Classification of expert systems in electric power industry). *Elektrichestvo* **4** (1993)
13. Carayannis, G.: Artificial intelligence and expert systems in the steel industry. *JOM* **45**(10), 43–51 (1993)
14. Denisov, M., Kizim, A., Kamaev, V., Davydova, S., Matohina, A.: Solution on decision support in determining of repair actions using fuzzy logic and agent system. Springer, Cham (2014)
15. Procedural guidelines for development of flow charts and HVL maintenance and repair method statement. PJSC UES FGC (2014). https://www.fsk-ees.ru/upload/docs/STO_56947007-29.240.55.168-2014.pdf. Accessed 1 June 2020 (in Russian)
16. Choi, S.S., Cha, S.H., Tappert, C.C.: A survey of binary similarity and distance measures. *J. Syst. Cybern. Inform.* **8**(1), 43–48 (2010)
17. Adriaans, P., Zantinge, D.: Data Mining. Addison Wesley Longman Ltd., Harlow, England (1996)
18. Guo, Y., Lu, Y., He, X., Zhang, T.: Research and Design of Expert System Based on Oil-Gas Field Energy Saving Information Platform. Springer, Cham (2019)
19. Leonov, E.A., Averchenkov, V.I., AVerchenkov, A.V., Kazakov, Y.M., Leonov, Y.A.: Architecture and self-learning concept of knowledge-based systems by use monitoring of internet network (2014). Springer, Cham
20. Yurin, A., Berman, A., Nikolaychuk, O., Dorodnykh, N.: Knowledge Base Engineering for Industrial Safety Expertise. Springer, Cham (2019)

A Method for Change Detection in Operating of Power Generating Equipment



I. D. Kazakov , N. L. Shcherbakova , E. S. Rayushkin ,
and Maxim V. Shcherbakov 

Abstract The chapter discusses the issue of energy generation system reliability in terms of cyber-physical system management. Authors present a method for change-points detecting in the operation of energy generation cyber-physical systems based on electricity-generating process data. A benchmark approach for the task is a sequence (or pipeline) of steps enhancing results from the basic 3-sigma rules approach through comparing real generation data with a baseline of operation (standard of performance). The core of the proposed method is a DBSCAN algorithm which outperforms a benchmark. Advanced heuristic rules for disturbance detection help experts to develop appropriate activities for efficient asset performance management. Use cases show benefits of the proposed method both for synthetic and real data.

Keywords Cyber-physical systems · Outlier · Power generating equipment · Change-point · 3-sigma rules · DBSCAN algorithm

1 Introduction

Electricity is one of the main human resources on which all other structural divisions of the state depend. Companies generating electricity must avoid blackouts and supply this resource without break. Also, monitoring the generation process is crucial for identifying and correcting all causes of possible malfunctions. Solutions are based on local power plants and autonomous power supply sources that generate

I. D. Kazakov (✉) · N. L. Shcherbakova · E. S. Rayushkin · M. V. Shcherbakov
Volgograd State Technical University, Volgograd 400005, Russia
e-mail: igorkazakov1997@gmail.com

N. L. Shcherbakova
e-mail: natalia.shchrbakova@gmail.com

E. S. Rayushkin
e-mail: J.Rayushkin@gmail.com

M. V. Shcherbakov
e-mail: maxim.shcherbakov@vstu.ru

electrical and thermal energy directly at the facility or in its vicinity using various types of fuel [1].

Cyber-physical systems are systems that interact with multiple sensors and sensors that monitor the physical state of the system [2–6]. The operation of the generating equipment is monitored by many sensors reading main parameters that determine the general condition of the equipment and its components. The data obtained from the sensors of cyber-physical systems are used for a more complete description of the observed object and more rational control of the processes occurring in it. With the help of some of the main parameters of power generating equipment (PGE), it is possible to predict the pre-failure state of equipment [7, 8]. These parameters include the generated active power, ambient temperature, rotation frequency, etc. There is a performance standard for each generating equipment, which determines the relationship between these parameters, for example, the generated active power on the ambient temperature [9]. The general rule of the standard, which is described above, is that as the ambient temperature rises, the maximum active power generated decreases and vice versa. Tracking the change in temperature and temperature-dependent power, one can judge a general violation of the process of generating electricity—change-points.

The contribution of the chapter is a method for change-points detecting in the operation of energy generation cyber-physical systems based on electricity-generating process data. The main finding is in using the DBSCAN algorithm based on heuristic rules for clustering time series describing energy-generating processes.

2 Background

Statistical change-points detection methods can be divided into a posteriori (detecting change-points with a delay in the accumulation of process data) and sequential (detecting change-points while the process is running). A posteriori methods collect all process data and analyze it for abrupt changes. Based on this, a conclusion is drawn about how the process took place. This method detects false change-points less often than sequential ones. Sequential methods analyze the process each time the state of the characteristics is updated (new data arrives). The analysis is performed on all available historical data obtained at the previous stages of observation. Based on this information, either a decision is made about the presence of change-points or the continuation of observations. The main characteristics of sequential change-points detection methods are the meantime between adjacent false alarms and the meantime lag when change-points are detected.

The problem of detecting a change in the distribution in a sequence of random variables is well studied. To solve this problem, the methods of moving average, exponential smoothing, cumulative sums are used. To date, some methods have also been developed for detecting the moments of change-points of random processes with dependent values. Autoregressive processes are often used as models of the observed processes, which allow a good approximation of the correlation function with a

small number of parameters. In many cases, the problem of detecting the moment of change-points of random processes turns out to be closely related to the problem of estimating the parameters of these processes. The methods of least squares, maximum likelihood, stochastic approximation are used to estimate unknown parameters of autoregressive processes [10, 11].

To determine the change-points of the process, it is necessary to identify the data outliers from the sensors [12–15]. A single outlier is most likely a sensor failure, multiple outliers on one sensor for a certain time or on several sensors simultaneously signal the onset of a process change-points [16–19]. Change-points detection methods and further data cleaning are also used for PGE [20–22], which reduces the risk of failure of generating equipment. DBSCAN (Density-based spatial clustering of applications with noise), or density-based spatial clustering of applications, is an unattended machine learning algorithm that allows you to classify sensor data and detect noise. The noise obtained as a result of the operation of the algorithm are data outliers and serve as the basis for determining these points, as change-points in the generation process [23–25]. The main disadvantage of the methods for detecting change-points is false-positive alarms (false alarm), based on which it is possible to draw an incorrect conclusion about the state of PGE.

3 A Method for Change-Detection

To reduce the number of false positives and the number of missing facts of changes in the main parameters of the system, the intervention of experts is required and, therefore, the time for analyzing the data obtained after the calculation increases. To minimize the time of an expert’s work to determine the cause of the process change-points and develop a strategy of actions for the repair of cyber-physical energy generation systems, the chapter proposes a method for identifying the change-points. Figure 1 shows the scheme of the proposed method. The basic approach used for change detection is a sequence of steps that improve the results of the 3-sigma approach by adding initial operating conditions and comparing the actual generation data with the performance standard. The proposed method is based on the DBSCAN algorithm based on heuristic rules, and the statistical approach for determining outliers is compared with an approach that uses the DBSCAN algorithm to reduce the number of false positives.

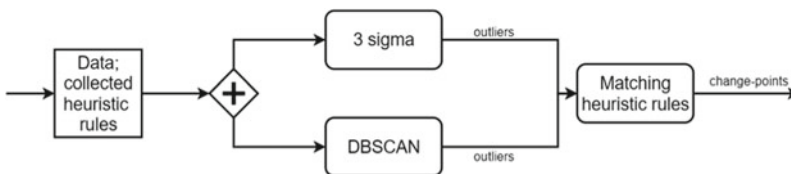


Fig. 1 Schematic representation of the method for detecting change-points

This chapter uses data on the operation of gas generating equipment on the example of a gas turbine unit (hereinafter referred to as GTU). The method and approaches considered in this work may differ, depending on the generating equipment, in terms of the set of input data and initial conditions. The data for work is synthetic data of one turbine operating cycle according to the parameters of the active power of the turbine, the ambient temperature, the turbine rotation speed with 4 explicit emissions introduced, to test the efficiency of the methods, 8 h, 2 measurements per minute, 960 points; real gas turbine data for detecting false alarms, 24 h, 2 measurements per minute, 1440 points.

3.1 Statement of the Problem of Detecting Change-Points

Change-points problems form part of the statistics of random processes associated with conclusions about their characteristics based on the analysis of their implementation. Let the observed random process $\xi = (\xi_t)_{t \geq 0}$ have the structure

$$\xi_t = \begin{cases} \xi_t^\infty, & \text{if } 0 \leq t \leq \theta, \\ \xi_t^0, & \text{if } t \geq \theta, \end{cases} \quad (1)$$

where $\xi^\infty = (\xi_t^\infty)_{t \geq 0}$ and $\xi^0 = (\xi_t^0)_{t \geq 0}$ processes are different in their structure, t —the discrete-time of the process, θ —the moment when the change-points occur. The process ξ^∞ corresponds to a normal state (without change-points) ξ^0 —to an anomalous state (with change-points). As long as the data are consistent with ξ^∞ , continue to observe the process, if the state has changed to ξ^0 —it is required to detect the change, avoiding false positives. An alarm should be raised if, by time θ , there is evidence of change-points.

3.2 Using the 3-sigma Rule to Identify Outliers

The application of the 3-sigma rule for the input data, divided into segments, the length of which is set by the expert, is used to calculate σ —the standard deviation and determine the belonging of the next data point ($X \in \xi_t$) to the interval $[-3\sigma; 3\sigma]$. The minimum amount of data to analyze point X using the 3-sigma rule is 10 points. A graphical representation of data for the analysis of emissions at points X and X + 1 is shown in Fig. 2.

This rule works perfectly provided that the GTU is in a certain operating mode (“off” or “generation”). If the GTU has switched from the “off” mode of operation to the “generation” mode, then the 3-sigma rule detects spurious emissions in the process.

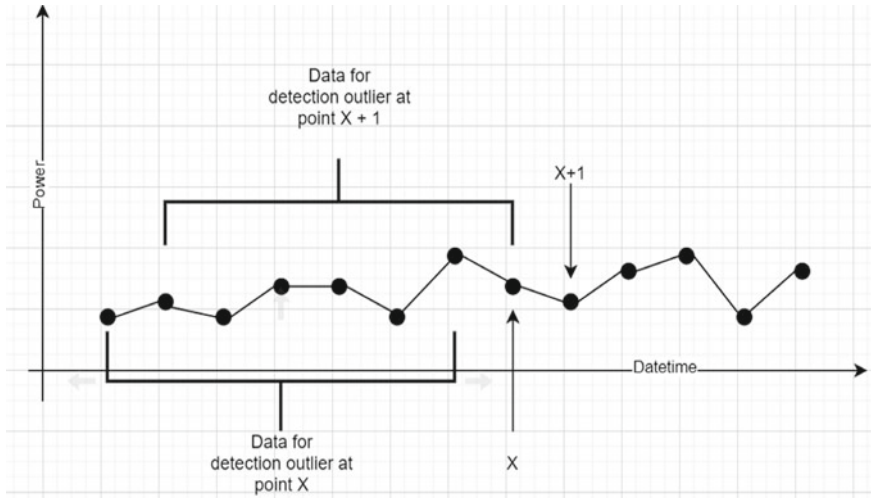


Fig. 2 Presentation of data for analysis of outliers at points X and X + 1 according to the 3-sigma rule

Figure 3 shows the identified outliers in a certain operating mode of the GTU. Outliers are correct. The figure shows the points that the method identified as outliers due to a sharp change in the operating mode of the GTU to “generation”. The change-points when the turbine is switched on in the “generation” mode was determined by experts as false. The process proceeded normally.

The rule of three sigma works with a stable operating mode of the gas turbine. If the operating mode changes, then the rule gives false positives. It is necessary to further research the rule by introducing initial conditions for the input data.

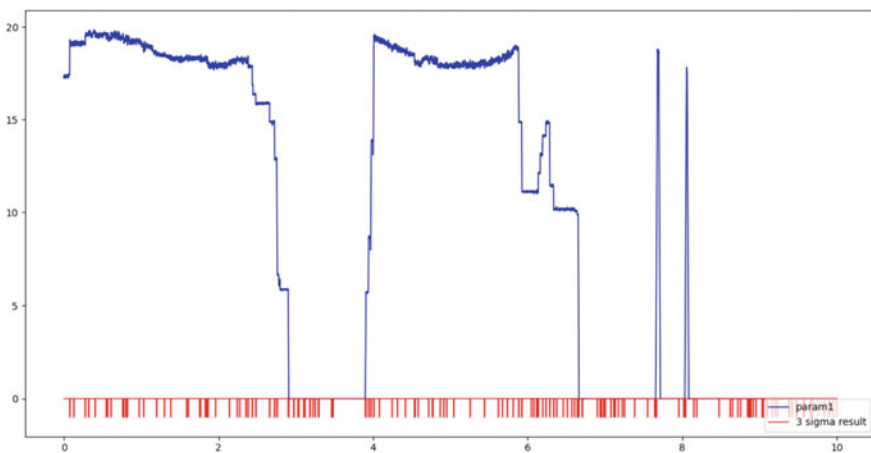


Fig. 3 Results of applying the 3-sigma

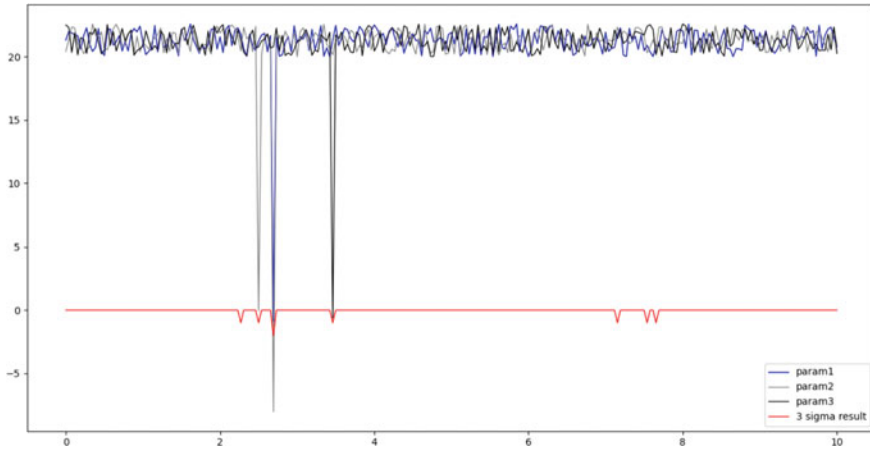


Fig. 4 Results of the introduction of the initial conditions for the 3-sigma rule

3.3 *Introducing Initial Conditions for the 3-Sigma Rule*

Let us introduce the initial conditions that separate the data on the operation mode of the GTU. To do this, it is necessary to monitor the active generated power (AGP) of the GTU. If the AGP at the current moment is strictly greater than zero, then the GTU is in the “generation” mode, otherwise, it is “off”. The 3-sigma rule should only be applied to GTU data that is defined as “generation”.

Figure 4 graphically shows the detection of data outliers using the 3-sigma rule with the introduction of initial conditions. The red graph is the result of applying the rule. A value less than zero on the ordinate means that there is a data outlier at a given time. The introduction of the initial conditions has proven an increase in the accuracy of detecting outliers in the process ξ and a significant reduction in false positives.

3.4 *Identification of Emissions Based on a Comparison of the Main Parameters of GTU with a Performance Standard*

A comparison of the current values of the main parameters of generating equipment with the performance standard allows experts to identify the general state of the GTU operation, provided that the GTU is in the “generation” mode. An example of a performance standard table with synthetic data is shown in Table 1.

As a result of the experiment, an array of data was obtained for the difference in the current state of the GTU with the performance standard. However, the data is not self-sufficient to determine the state of a malfunctioning process without expert

Table 1 Example of a performance standard table

Sensor/Date time	00:00	00:30	01:00	01:30
Ambient temperature	0	10	20	30
Active generated power	15	16	18	20
Fuel pressure	20	21	22	24
Air pressure in the turbine	1	1.2	1.4	1.6
Average exhaust gas temperature	900	1000	1200	1400

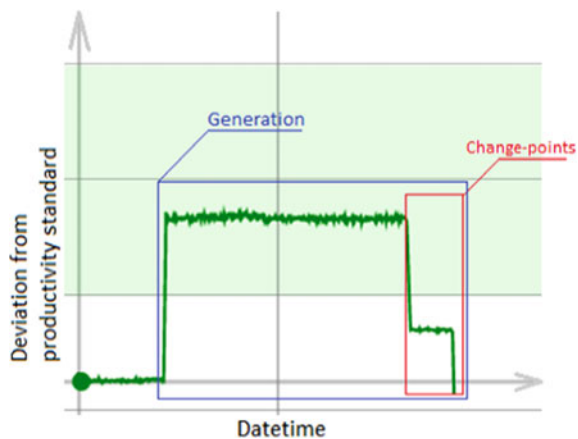
intervention in the process. It is necessary to determine the threshold of difference in values to detect outliers using the method of comparison with the performance standard.

If the data array obtained as a result of comparing the state of the gas turbine with the performance standard is checked for outliers according to the 3-sigma rule, then a new method for identifying outliers can be obtained. This approach reveals a sharp deviation of the generation process from a stable position.

Figure 5 shows synthetic data with added change-points in the process. The approach detects the change-points and provides an employee with information about the beginning of the change-points. Experts analyze the schedule and determine the cause of the process disturbance. In this case, experts did not confirm the change-points. The behavior of synthetic power generation equipment was defined as a planned reduction in power generation.

This approach for detecting emissions is adaptive to the individual properties of each turbine since each turbine has its own generation characteristics and may differ significantly from another turbine of a similar model and series. A sharp deviation from the performance standard is detected, rather than a critical deviation from the standard.

Fig. 5 The result of applying the 3-sigma rule to the method of comparison with the performance standard



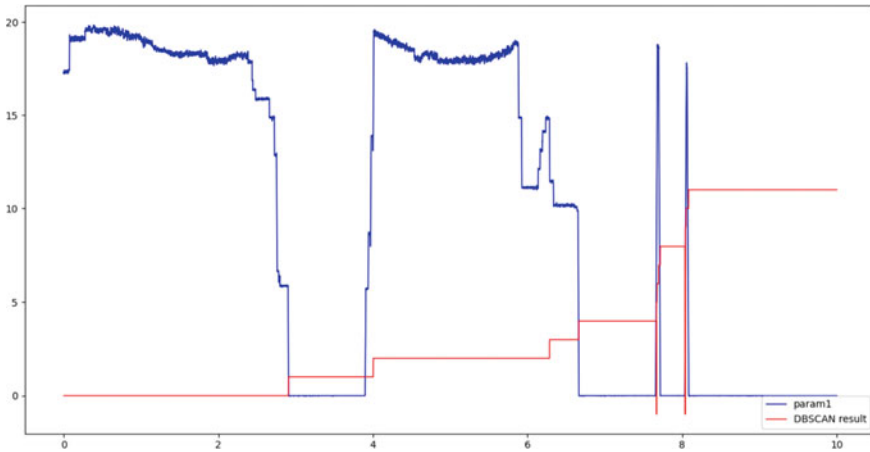


Fig. 6 Using the DBSCAN algorithm on synthetic data of a full working cycle

The approach is self-sufficient and does not require expert intervention. An expert can join the work to determine the causes of emissions and develop an action plan to correct them.

3.5 Applying the DBSCAN Algorithm in the Change-Points Detection Method

The results of applying the DBSCAN algorithm on synthetic data with two added change-points are shown in Fig. 6. Blueline—data on the activity generated power. Redline—data on the cluster number identified by DBSCAN. Model settings: $\text{eps} = 1.5$, $\text{min_samples} = 3$. This model clustered these change-points as noise. The noise cluster number is -1 . After analyzing other main parameters of the generating equipment, it was revealed that this emission occurred at each main parameter.

Figure 7 shows the results of the method of synthetic GTU data in the “generation” mode. No false positives were detected.

3.6 Heuristic Rules for Detecting Change-Points in the Operation of PGE

Identifying outliers in a random process prepares the data for identifying a change-points process. To identify the change-points, you can use the algorithm for identifying heuristic rules based on the calculation of emissions $k_j^o(i)$ (2) for each i -th parameter of the generating equipment, where $(i \in [1, n], n$ is the number of main

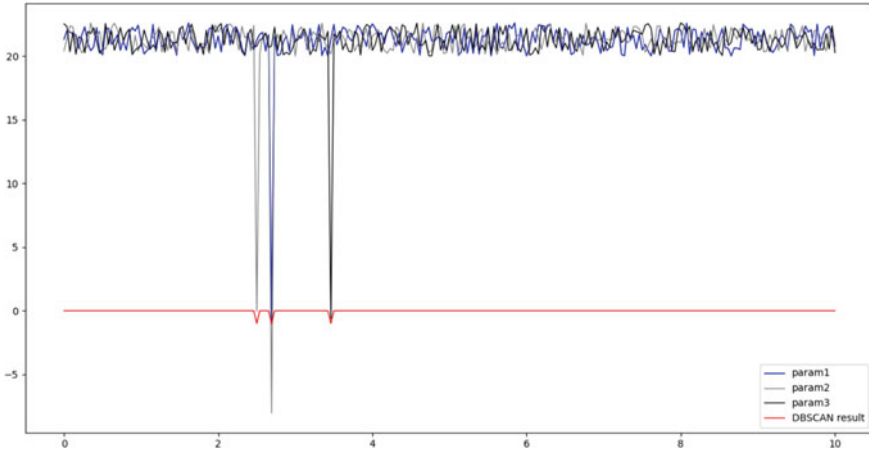


Fig. 7 Using the DBSCAN algorithm on synthetic data of the “generation” mode

generating equipment) in j -th time interval of length ω , where $\omega \in [t_0, t_\theta]$ and $\omega \ll \tau$ (operating time of generating equipment in the “generation” mode); $j \in [1; t_\theta - t_0 - \omega]$.

$$k_j^\omega(i) = \sum_{l=1}^{\omega} x_l, \tag{2}$$

where $x = \begin{cases} 0, & \text{in case of absence outliers at time } l \text{ for parameter } i; \\ -1, & \text{esle.} \end{cases}$

The count of outliers for all the main parameters in the j -th time interval with length ω is calculated by the formula (3):

$$q_j^\omega = \sum_{i=1}^n k_j^\omega(i). \tag{3}$$

For each local maximum from the set of values $Q[q_j^\omega], j \in [1; t_\theta - t_0 - \omega]$, heuristic rule (4) is formed from the sequence $k_j^\omega(i)$ for all the main parameters of the generating equipment (Fig. 8):

$$[k_j^\omega(1), \dots, k_j^\omega(i), \dots, k_j^\omega(n)], \tag{4}$$

These rules are used to proactively identify change-points in the process of generating electricity by generating equipment.

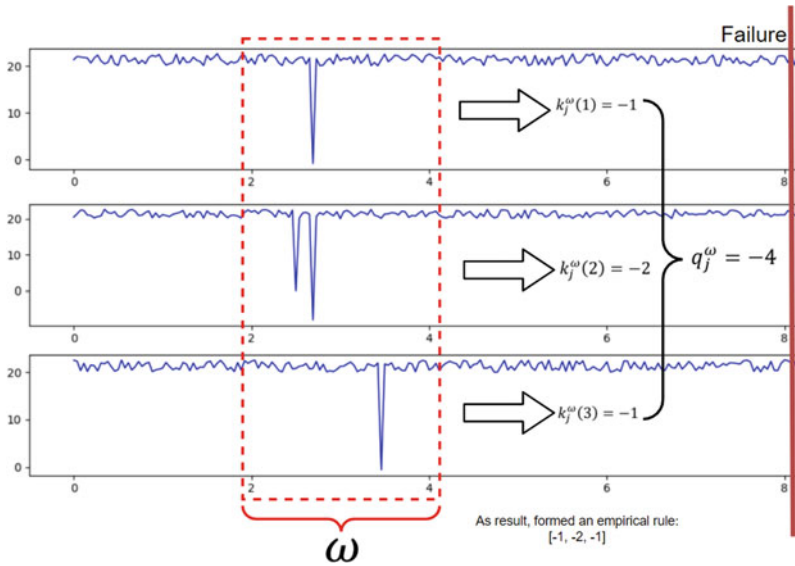


Fig. 8 Graphical representation of the application of heuristic rules to detect change-points

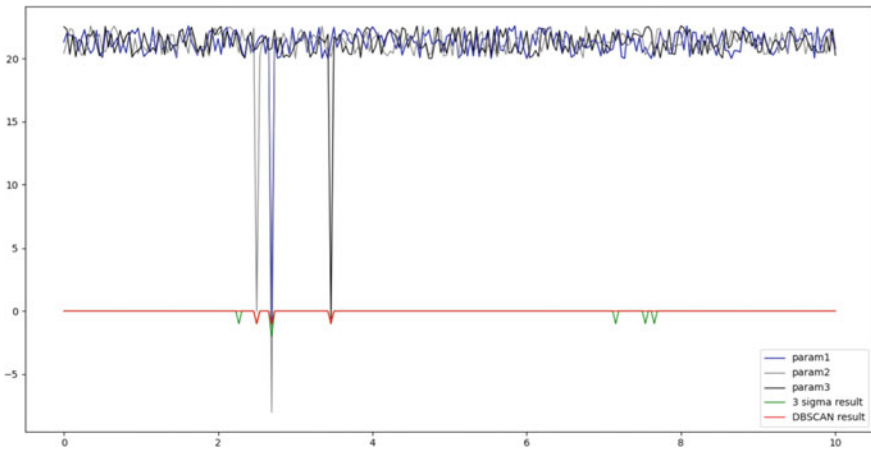


Fig. 9 Comparison of the 3-sigma rule outlier detection methods, taking into account the initial conditions and the performance standard, and the DBSCAN algorithm

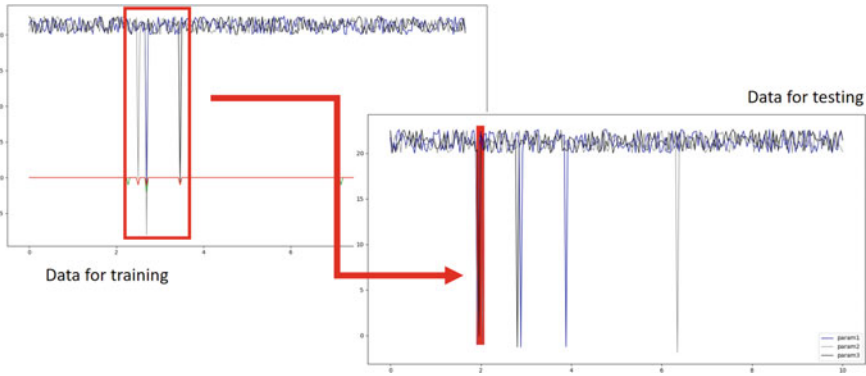


Fig. 10 Search result for signatures similar to heuristic rules

4 Results and Discussion

Comparison of the results of determining the change-points. Figure 9 shows the results of comparing outlier detection methods on synthetic data of a turbine operating in the “generation” mode. There are 3 false positives of the 3-sigma rule-based method. The method based on the use of the DBSCAN algorithm revealed the presence of outliers without false positives.

The heuristic rule-based change-points detection method allows detecting similar outlier signatures with heuristic rules. The detected signatures are a signal for experts that in the near future a change-points may occur, which will lead to equipment failure, and it is necessary to make technical interventions on the equipment to prevent an abnormal situation. An example of identifying a signature similar to a heuristic rule on synthetic data is shown in Fig. 10, where a similar signature is highlighted in red.

The change-points data obtained after applying the conditions allow the experts working with the cyber-physical system to identify the cause of the disturbance most quickly due to the information about the time of the failure and the sensors on which the failures occur. Prompt identification of the cause of the change-points allows you to develop a strategy of actions for repairing equipment in the shortest possible time and with minimal intervention in the process (until the system reaches a critical state).

5 Conclusion

The developed method of the cyber-physical system makes it possible to determine the change-points during the operation of the GTU, provided that the GTU is in the “generation” operating mode. The basic approach to defining change-points is using

a 3-sigma rule with a leverage approach by comparing real generation data with a performance standard. The proposed method is based on the DBSCAN algorithm, which is superior in performance to the basic approach. Advanced heuristics for change-point detection help experts design appropriate actions to efficiently manage GTU performance. This method does not determine the causes of the change-points but allows experts to identify them and determine the necessary actions for the repair of the gas turbine plant.

Acknowledgements The reported study was supported by RFBR research project 19-47-340010

References

1. Shcherbakov, M.V., Glotov, A.V., Cheremisinov, S.V.: Proactive and predictive maintenance of cyber-physical systems. In: Kravets, A., Bolshakov, A., Shcherbakov, M. (eds.) *Cyber-Physical Systems: Advances in Design & Modelling. Studies in Systems, Decision and Control*, vol. 259 (2020). Springer, Cham
2. Jin, R., Deng, X., Chen, X., Zhu, L., Zhang, J.: Dynamic quality-process model in consideration of equipment degradation. *J. Qual. Technol.* **51**(3), 217–229 (2019). <https://doi.org/10.1080/00224065.2018.1541379>
3. Kazakov, I.D., Shcherbakova, N.L., Brebels, A., Shcherbakov, M.V.: Accelerometer data based cyber-physical system for training intensity estimation. In: Kravets, A., Bolshakov, A., Shcherbakov, M. (eds.) *Cyber-Physical Systems: Advances in Design & Modelling. Studies in Systems, Decision and Control*, vol. 259 (2020). Springer, Cham
4. Tran, V.P., Shcherbakov, M., Nguyen, T.A.: Yet another method for heterogeneous data fusion and preprocessing in proactive decision support systems: distributed architecture approach. In: Vishnevskiy, V., Samouylov, K., Kozyrev, D. (eds.) *Distributed Computer and Communication Networks. DCCN 2017. Communications in Computer and Information Science*, vol. 700 (2017). Springer, Cham
5. Tran, V.P., Shcherbakov, M., Sai, V.C.: On-the-fly multiple sources data analysis in AR-based decision support systems. In: Vishnevskiy, V., Kozyrev, D. (eds.) *Distributed Computer and Communication Networks. DCCN 2018. Communications in Computer and Information Science*, vol. 919 (2018). Springer, Cham
6. Shcherbakov, M., Brebels, A., Shcherbakova, N., Kamaev, V., Gerget, O., Devyatykh, D.: Outlier detection and classification in sensor data streams for proactive decision support systems. In: *Conference on Information Technologies in Business and Industry (2016)*; *J. Phys. Conf. Ser.* **803**(1), Tomsk (2017). <https://doi.org/10.1088/1742-6596/803/1/012143>
7. Antoniadou, I., Manson, G., Dervilis, N., Staszewski, W.J., Worden, K.: On damage detection in wind turbine gearboxes using outlier analysis. In: *Proceedings SPIE 8343, Industrial and Commercial Applications of Smart Structures Technologies 2012, 83430N* (29 March 2012). <https://doi.org/10.1117/12.914772>
8. Fung, T., LeDrew, E.: Application of principal components analysis to change detection. *Photogramm. Eng. Remote Sens.* **53**, 1649–1658 (1987)
9. GOST 28842-90: Hydraulic turbines. Full-scale acceptance test methods (ST IEC 41-63, ST IEC 607-78)
10. Vorobeychikov, S.E. Sequential detection of moments of disorder of random processes: abstract of thesis. *Doctors of physical and mathematical sciences: 05.13.16/Tomsk state. un-t, Vorobeichikov S.E. Tomsk*, 30 p. (2000)
11. Brodskii, B.E., Darkhovskii, B.S.: Problems and methods of probabilistic diagnostics. *Avtomat. i telemekh.* **8**, 3–50 (1999); *Autom. Remote Control*, **60**, 8, 1061–1096 (1999)

12. Van Zoest, V.M., Stein, A., Hoek, G.: Outlier Detection in urban air quality sensor networks. *Water Air Soil Pollut.* **229**, 111 (2018). <https://doi.org/10.1007/s11270-018-3756-7>
13. Do Nascimento, R.M., Oening, A.P., Marcilio, D.C., Aoki, A.R., de Paula Rocha, E., Schiochet, J.M.: Outliers' detection and filling algorithms for smart metering centers. *PES T&D* (2012). <https://doi.org/10.1109/tdc.2012.6281659>
14. Zhao, Y., Lehman, B., Ball, R., Mosesian, J., de Palma, J.-F.: Outlier detection rules for fault detection in solar photovoltaic arrays. In: 2013 Twenty-Eighth Annual IEEE Applied Power Electronics Conference and Exposition (APEC) (2013). <https://doi.org/10.1109/apec.2013.6520712>
15. Sanayha, M., Vateekul, P.: Fault detection for circulating water pump using time series forecasting and outlier detection. In: 2017 9th International Conference on Knowledge and Smart Technology (KST) (2017). <https://doi.org/10.1109/kst.2017.7886095>
16. Xie, Y., Siegmund, D.: Sequential multi-sensor change-point detection. In: 2013 Information Theory and Applications Workshop (ITA) (2013). <https://doi.org/10.1109/ita.2013.6502987>
17. Vagnoli, M., Remenye-PreScott, R.: An ensemble-based change-point detection method for identifying unexpected behaviour of railway tunnel infrastructures. *Tunn. Undergr. Space Technol.* **81**, 68–82 (2018). <https://doi.org/10.1016/j.tust.2018.07.013>
18. Culman, C., Aminikhanghahi, S., Cook, J.: Easing power consumption of wearable activity monitoring with change point detection. *Sensors* **20**(1), 310 (2020). <https://doi.org/10.3390/s20010310>
19. Li, J., Tian, Y., Wang, D.: Change-point detection of failure mechanism for electronic devices based on Arrhenius model. *Appl. Math. Model.* **83**, 46–58 (2020). <https://doi.org/10.1016/j.apm.2020.02.011>
20. Shen, X., Fu, X., Zhou, C.: A combined algorithm for cleaning abnormal data of wind turbine power curve based on change point grouping algorithm and quartile algorithm. *IEEE Trans. Sustain. Energy* 1–1 (2018). <https://doi.org/10.1109/tste.2018.2822682>
21. Letzgsus, S.: Change-point detection in wind turbine SCADA data for robust condition monitoring with normal behaviour models. *Wind Energy Sci. Discuss* (2020). <https://doi.org/10.5194/wes-2020-38>
22. Han, S., Qiao, Y., Yan, P., Yan, J., Liu, Y., Li, L.: Wind turbine power curve modeling based on interval extreme probability density for the integration of renewable energies and electric vehicles. *Renew. Energy* (2020). <https://doi.org/10.1016/j.renene.2020.04.097>
23. Celik, M., Dadaser-Celik, F., Dokuz, A.S.: Anomaly detection in temperature data using DBSCAN algorithm. In: 2011 International Symposium on Innovations in Intelligent Systems and Applications (2011). <https://doi.org/10.1109/inista.2011.5946052>
24. Sheridan, K., Puranik, T.G., Mangortey, E., Pinon-Fischer, O.J., Kirby, M., Mavris, D.N.: An application of DBSCAN clustering for flight anomaly detection during the approach phase. *AIAA Scitech 2020 Forum* (2020). <https://doi.org/10.2514/6.2020-1851>
25. Wang, P., Govindarasu, M.: Anomaly detection for power system generation control based on hierarchical DBSCAN. In: 2018 North American Power Symposium (NAPS) (2018). <https://doi.org/10.1109/naps.2018.8600616>

Forecast of the Cost of Electricity and Choice of Voltage Level for the Enterprise



Nikita Ustyugov 

Abstract A solution to the problem of predicting the cost of electricity for an enterprise is proposed, to determine a favorable voltage level. Mathematical models of forecasting with an algorithm for determining the optimal voltage level have been developed, allowing the consumer to independently plan the costs of electric energy (power) and choose an investment-justified technological connection. Variants of application of research results in cyber-physical systems of a smart city are considered. An experimental study was carried out at an operating facility, confirming the practical feasibility and economic efficiency from the application of the forecast of the cost of electricity and technological connection to a cost-effective voltage level. As a result of the experiment, the cost reduction for the purchase of electricity was 12.8%, and the cost of performing the technological connection to the optimal voltage level paid off in 8 months. The study clearly demonstrates the possibility of free-of-charge improvement of the energy efficiency of all energy-consuming facilities (both in Russia and in the world) through the dissemination of information useful to citizens.

Keywords Electricity cost forecast · Voltage level · Mathematical model · Smart city · Cyber-physical systems

1 Introduction

After ensuring a reliable and uninterrupted power supply, the task of the energy service at the enterprise is reduced to the legitimate reduction of electricity costs. Costs can be minimized by reducing the amount of electricity consumed [1]. However, it is difficult to do without reducing the volume of products produced, provided that all energy-saving recommendations are implemented [2, 3].

Many diverse measures allow minimizing the cost of electricity with an unchanged volume of production [4, 5]. Some of them are suitable for all consumers (for example,

N. Ustyugov (✉)

Moscow Power Engineering Institute, Krasnokazarmennaya street, house 14, 111250 Moscow, Russia

e-mail: ustyugovnv@dom.mos.ru

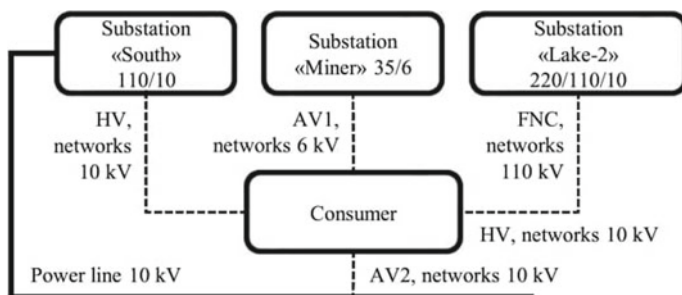


Fig. 1 Types of consumer connection to voltage levels

the choice of voltage level), others are very specific and expensive (for example, energy efficiency and energy management) [5, 6], therefore they can be used only in a limited circle of enterprises [7–9]. Under the voltage level (Fig. 1) we mean the tariff in the calculations of the guaranteeing supplier for services for the transfer of electric energy to the consumer.

2 Methodology Concept

The voltage level for payment of services for the transfer of electric energy and the rate for the maintenance of electric networks are determined by the boundary of balancing equipment [10], which in most cases coincides with the boundary of the site. The higher the voltage level, the lower the rate for payment of technological losses in electric networks [11] (Table 1).

The legislation provides for four tariff voltage levels [12]: 110 kV (and above)—high (HV); 35 kV—middle first (AV1); from 1 to 20 kV—middle second (AV2); 0.4 kV—low (LV). Also, consumers connected to the networks of the Federal Network Company of the Unified Energy System (Rosseti FNC UES) pay for services at the FNC tariff, which is significantly lower than the HV tariff. If a consumer pays

Table 1 The rate for the content of electric networks and the rate for payment of technological losses, taking into account the voltage class for consumers in the Vologda region, the 1st half of 2019

Voltage level	Rate for the maintenance of electric networks rubles/MW * month	Rate for payment of technological losses in electric networks, rubles/MW * h
HV (110 and above)	628,938,42	151,98
AVI (35 kV)	1,267,826,87	338,26
AV2 (from 1 to 20 kV)	1,245,524,41	344,25
LV (0,4 kV)	1,572,394,30	701,19

for transmission services to HV, then he has only one opportunity to reduce the cost of paying for transmission services—to connect to FNC networks, if they are in close proximity. However, the consumer, with rare exceptions, can do this only by building his own 110 kV substation and making investments of about 104 million rubles, which is possible only for super-large enterprises. For this reason, the connection to the wholesale market of electric energy and power (FNC network) will be considered in a separate article.

This chapter discusses the connection options offered in the retail electricity market. If the consumer pays for the transmission services of AV1, AV2, or LV, then it is advisable to analyze the connection to an external electric network. If payments for transmission services are carried out in accordance with the law, then you can switch to a higher voltage level only using the technological connection procedure [13]. If, for example, a consumer is connected to a 110/10 kV substation and pays for transmission services at the AV2 tariff, then you must immediately contact a guaranteeing provider to bring the calculations in accordance with applicable law. In this case, the consumer overpaid significant funds due to an incorrectly determined voltage level and he needs to switch to the voltage level—HV, which allows reducing the cost of transmission services, and as a result, the price of electric energy. By renting the supply lines, the consumer can switch to a lower voltage level.

Therefore, considering the proposals of network organizations for the rental of power supply equipment, it is necessary to assess the risks. The voltage level is determined by connecting to the networks of the network organization. If the consumer is connected to another electric power facility that is not part of the equipment of the network organization, then it is indirectly connected to the networks of the network organization.

Therefore, the voltage level is determined by the points of connection to the networks of the network organization located above. It is possible not to pay for electricity transmission services, but only in two cases: if the consumer and the electricity producer are not connected to an external electric network; if the electricity consumer owns also generating equipment and networks connecting it to the equipment.

3 Problem Statement and Method

Perform a forecast of the cost of electricity for the enterprise with the subsequent selection of the optimal voltage level, which allows reducing the cost of electric energy ($C_e \rightarrow \min$). To carry out the medium-term forecast (from month to year), the minimum initial data are required: the company's electricity consumption and the cost of electricity from the guaranteeing supplier for the previous calendar year. The maximum initial data are power consumption for the entire duration of the installation and the cost of electricity (power) for the period of activity of the supplier. The physical experiment [14] performed on the prototype is the research method: the Gagarinsky road tunnel (ventilation unit No. 1 and No. 2), at the address: Moscow,

the intersection of Leninsky Prospekt and the 3rd transport ring. Prototype electricity consumption from January to December 2018 amounted to—57,272,5 kW, and power consumption—77,9 kW.

Electricity transmission services are provided at uniform tariffs, with division by constituent entities of the Russian Federation (determined on the basis of the connected voltage level), installed (at the customer's choice) in two versions: one-rate and two-rate.

1. To calculate a single-rate tariff (price), it is necessary to build a mathematical model for forecasting the sales allowance (for electric power transmission services) at a high, average first, average second, and low voltage level (rubles/kWh) P_{sa}^h , P_{sa}^{a1} , P_{sa}^{a2} and P_{sa}^l (1–4):

$$P_{sa}^h = \frac{P_{en}^h * \sum_{m,n} W_p^h}{\sum_{m,n} E_p^h} + P_{rtl}^h \quad (1)$$

$$P_{sa}^{a1} = \frac{P_{en}^{a1} * \sum_{m,n} W_p^{a1}}{\sum_{m,n} E_p^{a1}} + P_{rtl}^{a1} \quad (2)$$

$$P_{sa}^{a2} = \frac{P_{en}^{a2} * \sum_{m,n} W_p^{a2}}{\sum_{m,n} E_p^{a2}} + P_{rtl}^{a2} \quad (3)$$

$$P_{sa}^l = \frac{P_{en}^l * \sum_{m,n} W_p^l}{\sum_{m,n} E_p^l} + P_{rtl}^l \quad (4)$$

where: P_{en}^h (P_{en}^{a1} , P_{en}^{a2} , P_{en}^l)—rate for the content of electric networks, rub/kW; W_p^h (W_p^{a1} , W_p^{a2} , W_p^l)—is the total planned power for the consumer (kW) in the n group, the estimated period m; E_p^h (E_p^{a1} , E_p^{a2} , E_p^l)—planned electricity for the consumer, kW; P_{rtl}^h (P_{rtl}^{a1} , P_{rtl}^{a2} , P_{rtl}^l)—the rate for regulatory technological losses, rub/kW.

4 To Calculate the Two-Part Tariff, It is Necessary to Build a Mathematical Forecast Model for Two Rates (Prices).

a. Rates for the maintenance of electric networks for the corresponding voltage levels (rub/kW) P_{en}^h , P_{en}^{a1} , P_{en}^{a2} and P_{en}^l (5–8):

$$P_{en}^h = \frac{\sum_{m,n} V_i^h}{\sum_{m,n} (W_p^h + W_{a1}^h + W_{a2}^h)}, \quad (5)$$

$$P_{en}^{a1} = \frac{\sum_{m,n} V_i^{a1} + (P_{en}^h * \sum_{m,n} W_{a1}^h)}{\sum_{m,n} (W_p^{a1} + W_{a2}^{a1} + W_l^{a1})}, \quad (6)$$

$$P_{en}^{a2} = \frac{\sum_{m,n} V_i^{a2} + (P_{en}^h * \sum_{m,n} W_{a2}^h) + (P_{en}^{a1} * \sum_{m,n} W_{a2}^{a1})}{\sum_{m,n} (W_p^{a2} + W_l^{a1})}, \quad (7)$$

$$P_{en}^l = \frac{\sum_{m,n} V_i^l + (P_{en}^{a1} * \sum_{m,n} W_l^{a1}) + (P_{en}^{a2} * \sum_{m,n} W_l^{a2})}{\sum_{m,n} W_p^l},$$

where: V_i^h (V_i^{a1} , V_i^{a2} , V_i^l)—the total volume of the necessary income of the electric grid company to compensate for reasonable expenses, rubles; W_{a1}^h (W_{a2}^h)—the planned power for the consumer, transformed from a high voltage level to a voltage level of the average first (middle second), kW; W_{a2}^{a1} (W_l^{a1} , W_l^{a2})—the planned power for the consumer, transformed from the first (from the second) voltage level to the second (lower) voltage level, kW.

b. Rates for regulatory technological losses of electricity in the process of transmission to the consumer (rub/kW) P_{rtl}^h , P_{rtl}^{a1} , P_{rtl}^{a2} and P_{rtl}^l (9–12):

$$P_{rtl}^h = \frac{\sum_{m,n} S^h}{\sum_{m,n} (E_p^h + E_{a1}^h + E_{a2}^h)}, \quad (8)$$

$$P_{rtl}^{a1} = \frac{\sum_{m,n} S^{a1}}{\sum_{m,n} (E_p^{a1} + E_{a2}^{a1} + E_l^{a1})}, \quad (9)$$

$$P_{rtl}^{a2} = \frac{\sum_{m,n} S^{a2}}{\sum_{m,n} (E_p^{a2} + E_l^{a2})} \quad (10)$$

$$P_{rtl}^l = \frac{\sum_{m,n} S^l}{\sum_{m,n} E_p^l} \quad (11)$$

where: S^h (S^{a1} , S^{a2} , S^l)—spending associated with losses in the networks of the corresponding voltage level, rub; E_{a1}^h (E_{a2}^h , E_{a2}^{a1} , E_l^{a1} , E_l^{a2})—the planned electricity for the consumer, transformed from a high (from an average first or second) voltage level to an average first (second, lower) voltage level, kW.

The experimental verification of the single-rate tariff was carried out in the third price category (3PC) with the application of the corresponding mathematical model for forecasting the cost of electricity (13–15):

$$C_e^{3pc} = \sum_c \left(P_{j,m,n,h}^{ml,e} * N_h^{pe} \right) + P_{m,n}^{ml,w} * N_m^{pw}, \quad (12)$$

$$P_{j,m,n,h}^{ml,e} = P_{m,h}^{up,e} + P_{j,m}^{sa} + P_m^s + P_{m,n,h}^{sa,e} \quad (13)$$

$$P_{m,n}^{ml,w} = P_m^{up,w} + P_{m,n}^{sa,w} \quad (14)$$

where: $P_{j,m,n,h}^{ml,e}$ —rate for electricity of the maximum level of unregulated prices at the j level of voltage; N_h^{pe} —the planned number of electrical energy per hour h ; $P_{m,n}^{ml,w}$ —rate for the capacity of the marginal level of unregulated prices; N_m^{pw} —the planned number of power consumed during hours of maximum power consumption in the region; $P_{m,h}^{up,e}$ —the weighted average unregulated price of electricity in the wholesale market; $P_{j,m}^{sa}$ —single-rate tariff differentiated by voltage levels; P_m^s —payment for other services; $P_{m,n,h}^{sa,e}$ —sales allowance of the guaranteeing supplier, taken into account in the cost of electricity per hour; $P_m^{up,w}$ —the weighted average unregulated price of power in the wholesale market; $P_{m,n}^{sa,w}$ —the premium of the guaranteeing supplier is taken into account in the cost of capacity.

Verification of the two-part tariff was implemented in the fourth price category (4PC) with a mathematical model for forecasting the cost of electricity (15–17):

$$C_e^{4pc} = \sum_c \left(P_{j,m,n,h}^{ml,e} * N_h^{pe} \right) + P_{m,n}^{ml,w} * N_m^{pw} + P_{j,m}^{en} * N_h^w, \tag{15}$$

$$P_{j,m,n,h}^{ml,e} = P_{m,h}^{up,e} + P_{j,m}^{rtl} + P_m^s + P_{m,n,h}^{sa,e} \tag{16}$$

$$P_{m,n}^{ml,w} = P_m^{up,w} + P_{m,n}^{sa,w} \tag{17}$$

where: $P_{j,m}^{en}$ and $P_{j,m}^{rtl}$ —rates for the maintenance of electric networks and regulatory technological losses; N_h^w —the number of power paid by the consumer according to the average hours of peak load.

The guaranteeing supplier was requested the missing initial data for the previous period (2018) and the mathematical models of the forecast for the next period-2019 were checked (Table 2).

Table 2 Test results for mathematical forecast models, completion date January 2019

Voltage level	Single rate, P/a	Two-part rate	
		P en	P rtl
HV	1,04,853	570,0294	0,043
AVI	1,55,013	902,78,903	0,039
AV2	1,93,461	926,84,878	0,0663
LV	2,93,707	1163,29,581	0,4
		Cost of electricity	
		3 PC, rub	4PC, rub
HV		197,981,50	185,020,22
AVI		226,711,85	212,846,82
AV2		248,731,98	218,934,04
LV		306,141,93	251,251,59

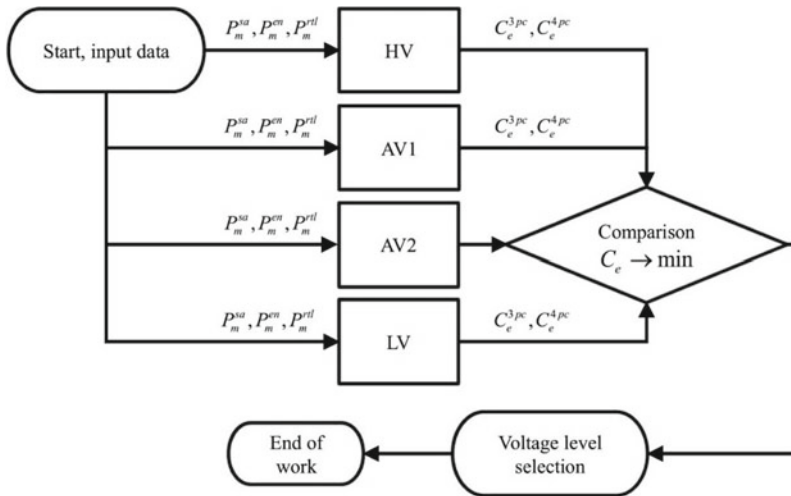


Fig. 2 The algorithm for determining the optimal voltage level

Having received the predicted cost of electricity (per 57272, 5 kW) and power (per 77, 9 kW) for the next period, we proceed to the algorithm for determining the optimal voltage level (Fig. 2).

At the beginning of the algorithm, the input data are input: power consumption for the entire duration of the installation and the cost of electricity and capacity for the period of activity of the guaranteeing supplier (at least one previous year). Further, calculations are made based on the assumption that the consumer has the opportunity to make a technological connection to any voltage level.

The calculation results are compared between different connection options and determined by the most financially profitable.

After choosing a cost-effective consumer voltage level, the amount of investment costs necessary to connect, and the payback period is determined. This will reduce energy costs without expanding the volume of energy consumption.

5 Application of Research Results in the Cyber-Physical Systems of a Smart City

We should look at the object of study more broadly, as one of the components of the general information space of the city, as a component in the Smart City system. Today we can talk not about individual types of information, but about creating a comprehensive program that covers all aspects of our lives. Residents of Moscow are consumers of electronic services: an electronic diary, a Moscow electronic school, an entry to a city polyclinic, an electronic ticket “Troika”, etc. The number of such services in the city is only increasing. Besides, through the “Active Citizen” and the

website of the Mayor of Moscow, citizens help the authorities control the work of the municipal economy and vote on construction projects. With the implementation of the Smart City program, a new stage in the informatization of the city’s urban economy began in 2019. This program has many areas and areas: healthcare, education, security, payments, public procurement, business, innovation, urban digital structure, and new mechanisms for communicating with citizens. Considering that the testing of the electricity consumption forecast was carried out at the housing and communal services object, we will consider the prospects for applying the research results in the selected field.

Information on the consumption of electric energy will be useful at the four levels of the program. The first level is in the section of the housing and communal services (Fig. 3) for analysis and planning of the total volume.

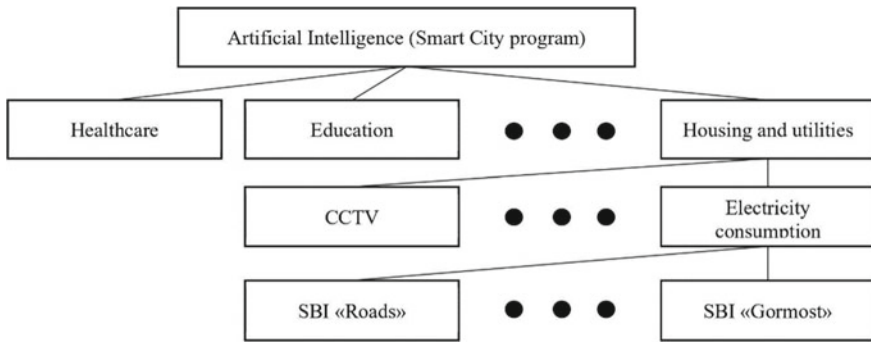


Fig. 3 The place of consumed electric energy in the smart city program

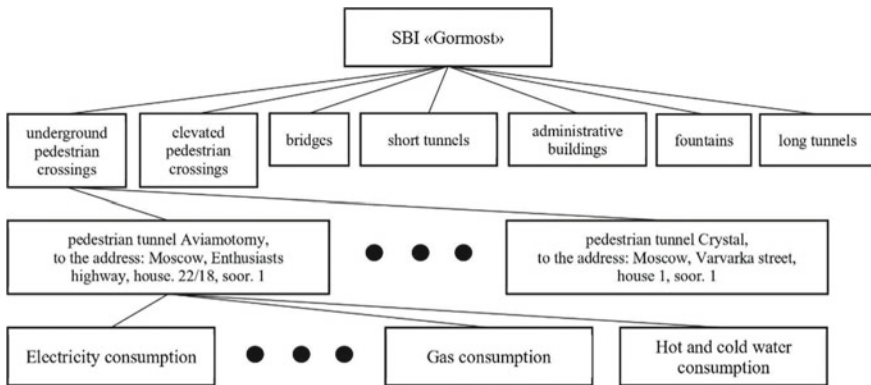


Fig. 4 The place of consumed electric energy in the second, third and fourth levels of the smart city program

The second level is in the section of the Budgetary Institution Gormost, (Fig. 4), as an organizational-technical system [15], for individual control over the institution's consumption.

The third level—in the section, types of engineering structures, as subsystems, for a visual separation of the total number of objects.

The fourth level is in the section the name and address of the engineering structure, as a unit of the organizational and technical system, for monitoring the energy consumption of each object. It is technically possible to collect information about all the energy consumption of an object.

The Smart City program can offer additional information necessary for residents of the city about electricity, heat, gas, water, and wastewater. It will help to keep track of the consumption of communal resources, simplify the payment procedure, and the energy consumption forecast will reduce consumer spending.

Based on the operating automated information and measurement system for commercial metering of electricity (AIMS CEM) and a mathematical model for forecasting the cost of electricity, it is possible to carry out the activities envisaged by the Smart City project in Russia: the creation of a single urban intelligent control center; application of the system of remote accounting of communal resources; introduction of a digital model for managing public utility facilities; reduction of energy consumption in state and municipal institutions.

The results of the research performed can be applied to achieve the goals of the state program “Smart City”, implemented in Moscow: increasing the efficiency of public investments; transparent and centralized city management; organization of sustainable growth in the quality of life of citizens.

Energy consumption visualization based on AIMS CEM can be used in the implementation of the “Smart City—2030” strategy, which poses internal and external digitalization tasks for Muscovites [16]. Moscow should become an innovative city that applies and develops modern digital technologies, artificial intelligence, working with large amounts of data. One of the goals of the strategy: end-to-end city-house management, in which citizens participate. The urban environment, which includes urban development and housing, and communal services, is one of the areas of development. As of 2018, the housing and communal services sector has: an automated collection of readings from metering devices; a unified dispatch center, and a system for monitoring urban transport; government services and services; the portal “Our City”; an automated resource consumption accounting system. According to the development strategy, the housing and communal services sector by 2030 should apply and offer to the townspeople: sensors of the Internet of things for the accounting of resource consumption; unified digital housing and communal services platform, transparent management of supply and consumption.

6 Conclusions

A physical experiment was conducted at the existing facility—the Gagarinsky road tunnel, a forecast was made of the cost of electricity and power for the next period for all voltage levels, a profitable and a feasible one was selected, a technological connection to AV2 (with LV) was made, in 2019 it was received a reduction of electricity costs—12.8% (by 4PC), the estimated payback period coincided with the actual one and amounted to 8 months. The research results were sent to the smart city decision bank [17] for further development, systematization [18–21], and application.

The study showed practical applicability and economic efficiency. On the basis of mathematical models for forecasting the cost of electricity (power), a consumer can independently and free of charge carry out medium-term power consumption planning, choose a favorable voltage level and make investments with an acceptable payback period.

References

1. Bendel, O.: Energiemanagement. <https://wirtschaftslexikon.gabler.de/definition/energiemanagement-53997>. Accessed 16 Mar 2020
2. Energiespeicher—Bedarf, Technologien, Integration. <https://www.springer.com/de/book/9783662488928>. Accessed 16 Mar 2020
3. Validation and Verification of Automated Systems. <https://www.springer.com/de/book/9783030146276> Accessed 16 Mar 2020
4. The Renewable Energy Transition. <https://www.springer.com/de/book/97830302911>. Accessed 16 Mar 2020
5. Mehr Energieeffizienz durch gezielte Anwenderinformationen: Bundesamt für Energie BRE. Schlussbericht 29 Sep. 2010, CH: 2010, 195 p.
6. Akzeptanz und politische Partizipation in der Energietransformation. <https://link.springer.com/book/10.1007/978-3-658-24760-7>. Accessed 16 Mar 2020
7. Wosnitza, F.: FH Aachen, Fachbereich Elektrotechnik und Informatik. Energieeffizienz und Energiemanagement. <https://www.springer.com/de/book/9783834819413>. Accessed 17 Mar 2020
8. IT-gestütztes Ressourcen und Energiemanagement. <https://www.springer.com/de/book/9783642350290>. Accessed 17 Mar 2020
9. Energieeffizienz und Energiemanagement. <https://www.springer.com/de/book/9783834819413>. Accessed 17 Mar 2020
10. Energiemanagement. <https://www.springer.com/de/book/9783658028336>. Accessed 18 Mar 2020
11. Full version of tariffs. <https://www.mosenergosbyt.ru/website/faces/>. Accessed 18 Mar 2020
12. Tariffs for electric power transmission services. <https://www.mosenergo-sbyt.ru/>. Accessed 18 Mar 2020
13. Transmission of electrical energy. <https://www.fsk-ees.ru/>. Accessed 18 Mar 2020
14. Russian energy. <https://minenergo.gov.ru/>. Accessed 18 Mar 2020
15. Balakirev, V.S., Dvoretzky, S.I., Aniskina, N.N.: Mathematical modeling of technological processes: textbook. Allowance; under. ed. Balakireva, V.S. , 352 p. Yaroslavl: Publ. house N.P. Pastukhova (2018)

16. Novikov, D.A.: Cybernetics: the navigator. History of cybernetics, current state, development prospects, 160 p. (Series “Smart Management”). M.: LENAND (2016)
17. The strategy of “Smart City—2030”. https://ict.moscow/docs/Strategy_Smart_City_v5.pdf. Accessed 18 Mar 2020
18. Project No. 526. Forecast of electricity consumption of the enterprise in order to determine the voltage level. <https://russiasmartcity.ru/>. Accessed 18 Mar 2020
19. Andryushin, A., Shcherbatov, I., Dolbikova, N., Kuznetsova, A., Tsurikov, G.: Outlier detection in predictive analytics for energy equipment. In: Studies in Systems, Decision and Control, vol. 259. Springer, 193–203 (2020)
20. Protalinskiy, O., Savchenko, N., Khanova, A.: Data mining integration of power grid companies enterprise, asset management. In: Studies in Systems, Decision and Control, vol. 260. Springer, 39–49 (2020)
21. Korshikova, A.A., Trofimov, A.G.: Predictive model for calculating abnormal functioning power equipment. In: Studies in Systems, Decision and Control, vol. 260. Springer, 249–259 (2020)

Method of Operational Determination of Amplitudes of Odd Harmonics of Voltages and Currents in Power Supply Circuits of Powerful Electrical Installations



P. K. Lange, V. N. Yakimov, E. E. Yaroslavkina, and V. V. Muratova

Abstract This chapter discusses the practical implementation of the method of operational measurement of the amplitude of the odd harmonics of voltage and current in the power circuits of powerful electrical equipment. This method is based on the use of preliminary spline approximation of the analyzed signal samples. The coefficients of the parabolic spline approximation are determined using a sliding approximating digital filter. The signal is sampled over an interval of a half signal period. It is shown that to achieve a small error (about 1%) of the approximation, it is sufficient to use a small number of signal samples (15 ... 20 values). The described method also uses a spline approximation of the sine and cosine components of the 3rd harmonic. The obtained approximation coefficients of signal and harmonic samples are used in the method of the harmonic amplitude determining based on the Fourier integral. It is shown that the proposed method allows us to determine the 3rd harmonic amplitude of a periodic signal with sufficient accuracy for practice. The proposed method has a high speed in connection with the using signal samples only during half period of the signal. It is proposed to use the considered method for early detection of emergency situations of powerful electrical equipment.

Keywords Power supply · Electric network · Odd signal harmonic · Spline approximation · Signal sampling · Binary stochastic quantization · Random noise · Industrial electrical equipment

1 Introduction

Currently, more and more attention is paid to the development of methods and means of measuring the technological parameters of electric networks. In its composition, the electric network contains a combination of powerful power plants [1]. The main purpose of electrical networks is the transmission, conversion, and distribution of electrical energy with a given quality and reliability [2, 3]. This task is carried out

P. K. Lange (✉) · V. N. Yakimov · E. E. Yaroslavkina · V. V. Muratova
Samara State Technical University, Samara, Russia
e-mail: k0046979@yandex.ru

using power supply systems, the normative indicators of which are related to the frequency, amplitude, and shape of voltages and currents. To ensure optimal control of power supply systems and compliance of electric energy with quality standards, it is necessary to determine and control the instantaneous and integral values of voltages and currents [3, 4].

Up-to-date control of the technological parameters of electric networks is associated with the need to measure the characteristics of periodic signals. For harmonic voltage and current signals of a fixed frequency, measuring their parameters does not cause many difficulties. Such measurements can be performed using various existing methods with a high degree of accuracy. However, in actual operating conditions of the electric network, voltage and current signals are distorted due to load changes, the effect of conducted electromagnetic interference, and the occurrence of malfunctions caused by external events [3, 5].

As a result of this, they can differ from the pure sinusoid and will have harmonics that are multiples of the fundamental [3, 6]. In this case, the energy contained in these harmonics can have a destabilizing effect on the electrical equipment. The main effects caused by higher harmonics are the occurrence of extreme currents in high-power circuits at their frequencies due to serial and parallel resonances, a decrease in the quality of generation and transmission of electricity, a decrease in the efficiency of electricity using by the consumer, a reduction in the life of electrical equipment with its subsequent failure [7–16].

The distortion of the harmonic form of voltages and currents is determined by the frequencies and amplitudes of the harmonic components present in them. Among these harmonics, the third is the most significant. The effective value of the current of the third harmonic in the neutral wire can exceed the effective value of the current of the fundamental frequency in the phase wires [17].

In this regard, harmonic analysis of current and voltage signals based on the Fourier transform [18, 19] is an important tool to evaluate the effect of harmonics. Moreover, its discrete analog, the fast Fourier transform (FFT), which is established as the main method of harmonic analysis, is often used at present. The use of FFT allows one to determine the value of each spectral component of current or voltage and to classify subtypes of harmonics. The use of FFT allows one to evaluate each spectral component of current or voltage and to classify subtypes of harmonics [6, 9–11, 20, 21].

In the application to energy systems, harmonic analysis based on the FFT is constantly being developed [22, 23–27]. However, the use of FFT in practice has shown that it is difficult to obtain a sufficiently reliable estimate of the amplitudes of the harmonics amplitude. This is because, in order to ensure the high accuracy of harmonic analysis, it is necessary to determine the frequency of the analyzed signal very accurately. In [28] it was shown that this requires the implementation of high-precision synchronization of the sampling frequency with the frequency of the analyzed signal.

To implement this requirement, it is proposed to use a combined filter with a finite impulse response, the use of a correction coefficient, and also the combination of the FFT method with the least-squares method [23]. The disadvantage of this

approach is the distortion of the shape of the analyzed signal by the filters used, which causes the appearance of an error in harmonic analysis. It should also be noted that a characteristic feature of discrete methods of harmonic analysis is the need to use a significant sample size of signal samples (at least 500 ... 1000 samples) to determine its harmonics values.

Methods and means of monitoring parameters of the quality of electricity in electric networks with high speed (with a measurement time of the order of half the period of the analyzed signal) allow you to determine only the instantaneous and integral characteristics of the signal (average or effective value) [29–31] and are not suitable for evaluating its odd harmonics.

In order to increase the efficiency of electric network control, intelligent sensor networks are used that determine standard parameters such as effective values, power factor, and total harmonic distortion, as well as surges or interruptions in power supply circuits [11, 30–33]. However, to ensure the required effectiveness of such tools, a significant amount of operational data is required for a particular network.

Thus, the urgent task is to increase the efficiency of methods and means of harmonic analysis aimed at determining parameters of the electricity quality in electric networks. In this case, the fast determination of the third harmonic amplitude should be attributed to a separate task of particular importance.

2 Formulation of the Problem

Signals of currents and voltages in industrial applications, as a rule, have symmetrical shape, but may differ from the harmonic form. To quickly determine the amplitude of the 3rd harmonic of a periodic nonharmonic signal, it is proposed to use the approximation of its samples at half the signal period, and then use the obtained approximation coefficients in the method of determining the amplitude of its 3rd harmonic using the classical Fourier integral.

To approximate the samples of the analyzed periodic signal, it is proposed to use a smoothing digital spline filter, which determines the coefficients of the parabolic spline approximation of these values.

3 Theoretical Part

Consider the use of the Fourier integral method to determine the harmonic amplitude of a periodic non-sinusoidal signal.

First of all, we consider the situation of presence in the signal with the industrial (main) frequency of the first and third harmonics (see Fig. 1):

$$x_1(t) = A_1 \sin \omega_1 t \text{ and } x_3(t) = A_3 \sin(3\omega_1 t + \varphi_3),$$

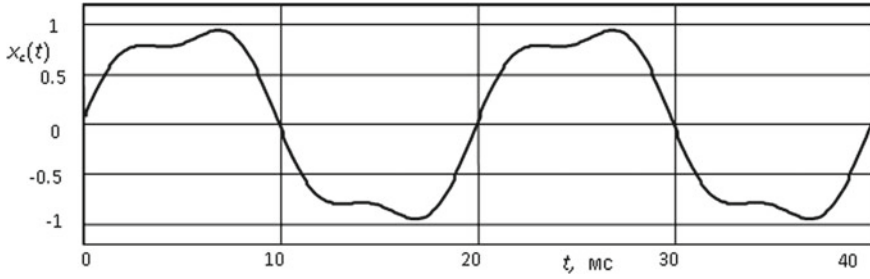


Fig. 1 Diagram signal in the presence of the first and third harmonics

where $\omega_1 = 2\pi f_1$; $A_1 = 1$ and $A_3 = 0, 2$ —relative amplitudes of the first and third harmonics.

Such a signal has the form:

$$x(t) = A_1 \sin \omega_1 t + A_3 \sin(3\omega_1 t + \varphi_3), \tag{1}$$

One of the most common methods in practice for determining the amplitude of the k-th harmonic of a periodic signal is its Fourier transform.

The method is based on the well-known relation [34], which determines the amplitude of A_3 of the 3rd harmonic:

$$|A_3| = \sqrt{A_{3s}^2 + A_{3c}^2}, \tag{2}$$

where A_{3s} , A_{3c} are the sine and cosine components of the Fourier integral defined by the expressions

$$A_{3s} = \frac{2}{T} \int_{-T/2}^{T/2} x_c(t) \cdot \sin(3\omega_1 t) dt, \quad A_{3c} = \frac{2}{T} \int_{-T/2}^{T/2} x_c(t) \cdot \cos(3\omega_1 t) dt, \tag{3}$$

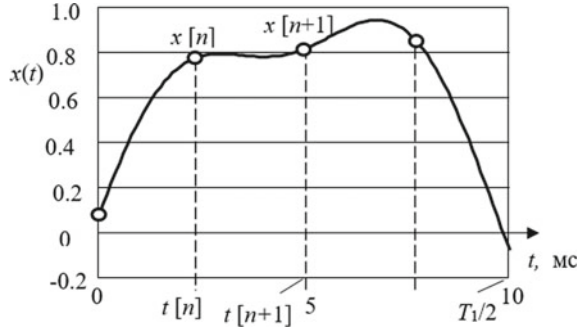
where T is the period of the analyzed signal $x_c(t)$, $\omega = 2\pi/T$ is its angular frequency.

In the case when the signal $x_c(t)$ with the period T_1 (Fig. 2) has a symmetrical shape, in expressions (3) you can use integration in the range $0 \dots T_1/2$, and when determining the amplitude of the 3rd harmonic these expressions take the form

$$A_{3s} = \frac{4}{T} \int_0^{T/2} x_c(t) \cdot \sin(3\omega_1 t) dt, \quad A_{3c} = \frac{4}{T} \int_0^{T/2} x_c(t) \cdot \cos(3\omega_1 t) dt. \tag{4}$$

If the signal is represented by discrete samples, then in this expression the integral is replaced by summation.

Fig. 2 Sampling of the signal at four discrete intervals for half the signal period with 50 Hz frequency



The basis of (3) and (4) is an integral term of the form:

$$S_d = \frac{4}{T} \int_0^{T/2} x_c(t) f_1(t) dt, \tag{5}$$

where $f_1(t)$ is the harmonic function of sin or cos of the corresponding frequency.

Consider the definition S_d using an approximating function: $f_c(t) \approx x_e(t)$.

The transition to the approximating function $f_c(t)$ makes it possible to determine the signal $x_c(t)$ values inside the sampling intervals when it is discretely represented. To approximate the signal $x_c(t)$, we will use spline functions, which are smooth curves that are “stitched” at the boundaries of the approximation intervals together with their several derivatives.

As is known, a parabolic spline function has no discontinuities at the boundaries of the sampling intervals with respect to the zero and first derivatives. Therefore, the use of approximating splines practically does not cause the appearance of higher harmonics in the spectrum of the signal reconstructed using such an approximation.

In addition, a digital filter that implements the approximation algorithm has the property of smoothing the signal, which is subject to additive interference [34]. The coefficients of parabolic and cubic approximating spline functions are defined in [35, 36]. In particular, the algorithm for a five-point parabolic spline approximation has the form:

$$\begin{cases} a_0[n] = 16^{-1}(-x_c[n-2] + 4x_c[n-1] + 10x_c[n] + 4x_c[n+1] - x_c[n+2]); \\ a_1[n] = (8t_d)^{-1}(-x_c[n-2] - 6x_c[n-1] + 6x_c[n+1] - x_c[n+2]); \\ a_2[n] = (16t_d^2)^{-1}(-x_c[n-2] + 7x_c[n-1] - 6x_c[n] - 6x_c[n+1] + 7x_c[n+2] - x_c[n+3]). \end{cases} \tag{6}$$

In (6) $a_0[n]$, $a_1[n]$ and $a_2[n]$ are the values of the coefficients of parabolic approximation in the n th interval, $x_c[n]$ is the signal value at the n -th sampling point, t_d is the signal sampling interval (see Fig. 2).

At the n -th sampling interval, the signal $x(t)$ is approximated by a parabola:

$$f_{2c}(t) = a_2[n]t^2 + a_1[n]t + a_0[n]. \tag{7}$$

Accordingly, in the interval $t \in [0; T/2]$, the signal $x_c(t)$ for m the number of sampling intervals is approximated by the function

$$y_{p5}(t) = \sum_{n=0}^m [a_2[n](t - nt_d)^2 + a_1[n](t - nt_d) + a_0[n]], nt_d < t \leq (n + 1)t_d. \tag{8}$$

The spline approximation of the discrete values of the signal (1) for $m = 10$ on the interval $t \in [0; T/2]$ is shown in Fig. 3.

In Fig. 4 presents a graph of the relative error of this signal spline approximation. As can be seen from the consideration of Fig. 4, the relative error of the spline approximation of ten samples $x[n]$ of the signal (1) does not exceed 1%.

Fig. 3 Spline approximation of the signal (1) samples for $m = 10$

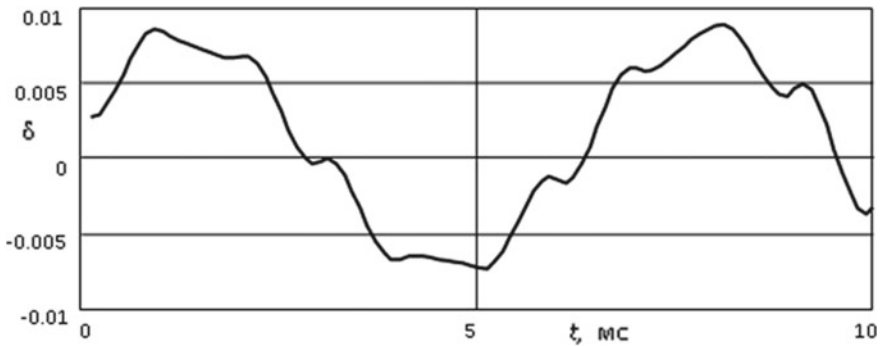
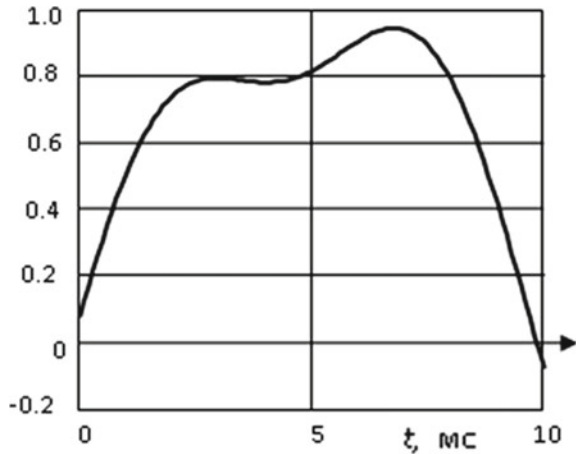


Fig. 4 Relative error of the spline approximation of the signal (1) samples

Similarly, in the same sampling intervals as for signal (1), the functions $\cos 3\omega_1 t$ and $\sin 3\omega_1 t$ the integrands (4) can be approximated by the functions $f_{1c}(t)$ and $f_{1s}(t)$.

In particular, the sine function on the n th sampling interval is approximated by a parabola:

$$f_{1s}(t) = b_2[n]t^2 + b_1[n]t + b_0[n]. \tag{9}$$

In turn, the cosine function is approximated by a parabola:

$$f_{1c}(t) = c_2[n]t^2 + c_1[n]t + c_0[n]. \tag{10}$$

In (9) and (10), the coefficients $b_i[n]$ and $c_i[n]$ are determined using a digital filter algorithm similar to (6).

The spline approximation graphs of the sine and cosine functions on the interval $t \in [0; T/2]$ are shown in Fig. 5.

In Fig. 6 presents a graph of the relative error of the sine function spline approximation. From this graph, it can be seen that this error does not exceed 5%. As you can see, it is significantly larger than the signal $x_c(t)$ approximation error. This is explained by the fact that the frequency of the third harmonic is three times higher than the frequency of the first harmonic of the signal, and, therefore, the period of the third harmonic accounts for only about three intervals of its sampling. In principle, to reduce this error, you can increase the number of sampling intervals.

Consider the method for determining the amplitude of the third harmonic of the signal (1) using the spline approximation of functions $x_c(t)$ and $f_1(t)$ in the main integral expression (4). Parabolic approximations of the signals $x_c(t)$ and $f_1(t)$ in the n th sampling interval are shown ins Fig. 7.

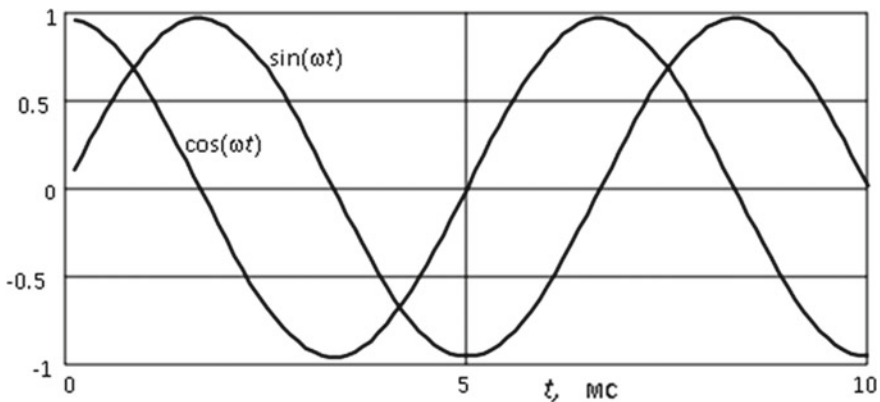


Fig. 5 Relative error of the spline approximation of the signal (1) samples

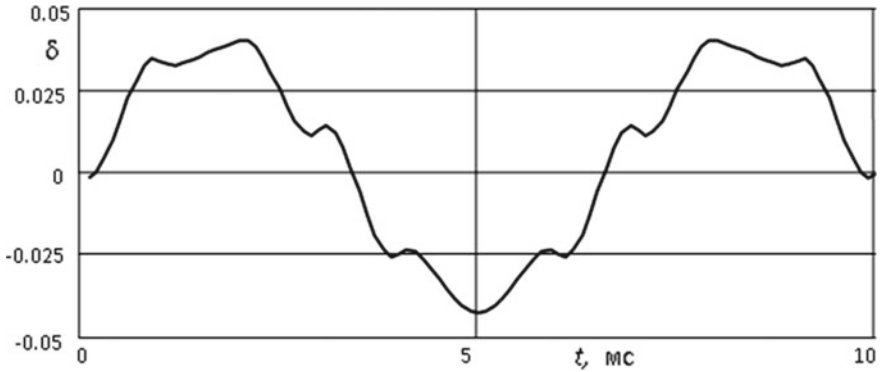
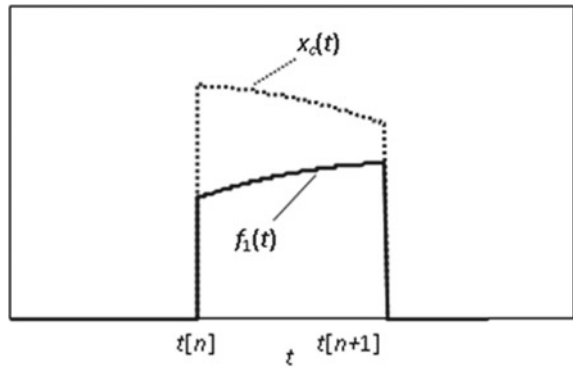


Fig. 6 Graph of the relative error of the sine function spline approximation

Fig. 7 Graph of the relative error of the sine function spline approximation



In this case (4) can be represented as follows:

$$S_d = \frac{4}{T} \sum_{n=0}^m \int_0^{t_d} x_c(t) f_1(t) dt, \tag{11}$$

where m is the number of sampling intervals; $t_d = t[n + 1] - t[n]$ —the length of the approximation interval.

Consider the task of determining the integral term in (5) on the n th sampling interval:

$$S_d[n] = \frac{4}{T} \int_0^{t_d} x_c(t) f_1(t) dt. \tag{12}$$

Substituting in (12) the parabolic functions (9) and (10), we obtain:

$$S_d[n] = \frac{4}{T} \int_0^{t_d} (a_2[n]t^2 + a_1[n]t + a_0[n])(b_2[n]t^2 + b_1[n]t + b_0[n])dt = k \cdot K[n], \quad (13)$$

$$\text{where } K[n] = \left(\begin{array}{l} \frac{a_2[n]b_2[n]}{5}t_d + \frac{a_1[n]b_2[n]+a_2[n]b_1[n]}{4}t_d \\ + \frac{a_2[n]b_0[n]+a_0[n]b_2[n]+a_1[n]b_1[n]}{3}t_d \\ + \frac{a_1[n]b_0[n]+a_0[n]b_1[n]}{2}t_d + a_0[n]b_0[n] \end{array} \right)$$

$$k = \frac{4t_d}{T} = \frac{4t_d}{2mt_d} = \frac{2}{m}.$$

The total integral value (13), determined for half the signal period from its m samples in this interval and representing the approximate value (estimate) of the sine term A'_{3s} in (4), is equal to:

$$A'_{3s} = \sum_{n=1}^m S_d[n] = \frac{2}{m} \sum_{n=1}^m \left(\frac{a_2[n]b_2[n]}{5}t_d^4 + \frac{a_1[n]b_2[n]+a_2[n]b_1[n]}{4}t_d^3 \right. \\ \left. + \frac{a_2[n]b_0[n]+a_0[n]b_2[n]+a_1[n]b_1[n]}{3}t_d^2 + \frac{a_1[n]b_0[n]+a_0[n]b_1[n]}{2}t_d + a_0[n]b_0[n] \right). \quad (14)$$

Similarly, the approximate value (estimate) of the cosine term A'_{3c} in (4) is

$$A'_{3c} = \sum_{n=1}^m S_d[n] = \frac{2}{m} \sum_{n=1}^m \left(\frac{a_2[n]c_2[n]}{5}t_d^4 + \frac{a_1[n]c_2[n]+a_2[n]c_1[n]}{4}t_d^3 \right. \\ \left. + \frac{a_2[n]c_0[n]+a_0[n]c_2[n]+a_1[n]c_1[n]}{3}t_d^2 + \frac{a_1[n]c_0[n]+a_0[n]c_1[n]}{2}t_d + a_0[n]c_0[n] \right). \quad (15)$$

For signal (1), these values turned out to be equal to $A'_{3s} = 0.171$ and $A'_{3c} = 0.071$. According to (2), we determine the amplitude of the signal third harmonic:

$$A'_3 = \sqrt{A'^2_{3s} + A'^2_{3c}} = 0,185. \quad (16)$$

The obtained value (16) differs from the true value $A_3 = 0,2$. This is explained by the presence of an error in the spline approximation of the sine and cosine time functions. In order to compensate for this error in determining the amplitude of the third harmonic, the value (16) should be multiplied by a correction factor:

$$k_3 = A_3/A'_3 = 1,081.$$

Table 1 Dependence of the coefficient k_3 on the number of sampling intervals m

m	8	10	12	15	18	20	22
k_3	1.197	1.081	1.040	1.015	1.008	1.005	1.004

Thus, taking into account the coefficient k_3 , the considered method of spline approximation of the functions included in the Fourier integral allows us to determine the estimate of the third harmonic amplitude without a methodological error:

$$A_3 = k_3 A'_3 = k_3 \sqrt{A'^2_{3s} + A'^2_{3c}}.$$

4 The Results of Experimental Studies

The analysis showed that the coefficient k_3 does not depend on the signal (1) third harmonic amplitude A_3 , nor on its phase φ_3 . It depends only on the number m of discrete intervals at half the analyzed signal period and, with increasing m , approaches unity in view of a decrease in the approximation error of the functions in (9) and (10). The dependence of k_3 on m is given in Table 1.

As can be seen from the consideration of this table, when the number of signal approximation intervals at half its period is more than 15, the error in determining the 3rd harmonic amplitude does not exceed 1%, which is quite enough for its practical evaluation.

This approach can be generalized to determine any other odd harmonics; however, to obtain an estimate of its amplitude with sufficient accuracy, the number of approximation intervals should be increased accordingly.

5 Conclusion

The problem of fast determination an odd harmonic in the analyzed symmetric signal, in particular the third, is solved using the spline approximation of its samples in half a signal period.

The obtained coefficients of the signal spline approximation, as well as the sine and cosine functions of its third harmonic, are used in the Fourier integral, with which the estimate of the value of the third harmonic of the analyzed signal is determined.

In this case, a small error in the harmonic amplitude determining is achieved by using a small number of samples (8 ... 10) of the signal. This approach is efficient because the task is solved after processing the signal samples on an interval within its half period.

Acknowledgements The reported study was funded by RFBR according to the research projects No 19-08-00228-A and No 18-08-00253-A.

References

1. State Standard 19431-84: Power and electrification. Terms and definitions. Collection of standards (2005). Standartinform Publ., Moscow, pp. 66–73
2. State Standard 29322–2014 (IEC 60038:2009) Standard voltages (2015). Standartinform Publ., Moscow, 13 p.
3. State Standard 32144–2013 (EN 50160:2010) Electric energy. In: Electromagnetic Compatibility of Technical Equipment. Power Quality Limits in the Public Power Supply Systems (2014). Standartinform Publ., Moscow, 20 p.
4. State Standard 30331.1–2013 (IEC 60364–1:2005) Low-voltage electrical installations. In: Part 1: Fundamental Principles, Assessment of General Characteristics, Definitions (2014). Standartinform Publ., Moscow, 46 p.
5. State Standard 30804.4.30–2013 (IEC 61000–4–30:2008) Electric energy. In: Electromagnetic Compatibility of Technical Equipment. Power Quality Measurement Methods (2014). Standartinform Publ., Moscow, 58 p.
6. State Standard 30804.4.7–2013 (IEC 61000–4–7:2009) Electromagnetic compatibility of technical equipment. In: General Guide on Harmonics and Interharmonics Measuring Instruments and Measurement for Power Supply Systems and Equipment Connected Thereto (2013). Standartinform Publ., Moscow, 40 p.
7. Saccomanno, F.: *Electric Power Systems: Analysis and Control*, vol. 744 (2003). Wiley-IEEE Press
8. Arrillaga, J., Bradley, D. Bodger, P.: *Power system harmonics* (1985). Chichester etc. Wiley Ltd. XII, 336
9. Arrillaga, J., Watson, N.R.: *Power System Harmonics*, 2nd edn., p. 406. Wiley, Ltd (2003)
10. Wakileh, G.J.: *Power Systems Harmonics: Fundamentals, Analysis and Filter Design*, p. 506. Springer, Berlin Heidelberg, XV (2001)
11. De La Rosa, F.C.: *Harmonics, Power Systems, and Smart Grids*, 2nd edn., p. 278 (2015). CRC Press
12. Zhezhelenko, I.V.: *Higher harmonics in power supply systems of industrial enterprises*, 4th edn., Revised. and add (in Russian) (2000). Moscow, Energoatomizdat, pp. 331–152
13. Shidlovsky, A.K., Zharkin, A.F.: *Higher harmonics in low voltage electrical networks*, p. 209. Naukova Dumka, Kiev (2005)
14. Smirnov, S.S.: *Higher harmonics in high voltage networks* (2010). Novosibirsk, Nauka, p. 327 (in Russian)
15. Pospelov, G.E., Fedin, V.T., Lychev, P.V.: *Electrical Systems and Networks*, p. 720. Minsk, Technoprint (2004)
16. Lykin, A.V.: *Electric Power Systems and Networks*, p. 360. Yurait Publishing House, Moscow (2018)
17. State Standard R 50571.5.52-2011 (IEC 60364-5-52:2009) Low-voltage electrical installations—Part 5-52: Selection and erection of electrical equipment—wiring systems (2013). Standartinform Publ., Moscow, 67 p.
18. Robert, J., Marks, I.I.: *Handbook of Fourier Analysis and its Applications* (2009). Oxford University Press, p. 800
19. Hansen, E.W.: *Fourier Transforms: Principles and Applications* (2014). Wiley, p. 776
20. Xue, H., Yang, R.: A novel algorithm for harmonic measurement in power system. *Proc. IEEE Int. Conf. Power Syst. Technol.* **1**, 438–442 (2002)

21. Yang, J.-Z., Yu, C.-S., Liu, C.-W.: A new method for power signal harmonic analysis. *IEEE Trans. Power Deliv.* **20**(2), 1235–1239 (2005)
22. Chen, X., Zhang, Y.: Detection and analysis of power system harmonics based on FPGA. In: *Proceedings of First International Conference: Wireless Communications and Applications ICWCA (2011)*. Sanya, China, pp. 445–454
23. Heydt, G.T., Fjeld, P.S., Liu, C.C., Pierce, D., Tu, L., Hensley, G.: Applications of the windowed FFT to electric power quality assessment. *IEEE Trans. Power Deliv.* **14**(4), 1411–1416 (1999)
24. Gu, Y.H., Bollen, M.H.J.: Time-frequency and time-scale domain analysis of voltage disturbances. *IEEE Trans. Power Delivery* **15**(4), 1279–1284 (2000)
25. Hidalgo, R.M., Fernandez, J.G., Rivera, R.R., Larrondo, H.A.: A simple adjustable window algorithm to improve FFT measurements. *IEEE Trans. Instrum. Meas.* **51**(1), 31–36 (2002)
26. de Carvalho, J.R., Duque, C.A., Lima, M.A.A., Coury, D.V., Ribeiro, P.F.: A novel DFT-based method for spectral analysis under time-varying frequency conditions. *Electric Power Syst. Res.* **108**, 74–81 (2014)
27. Lange, P.K., Yaroslavkina, E.E., Yakimov, V.N., Kozhevnikova, E.G.: Operative measurement of the effective values of voltage and current in industrial electrical equipment. *Instrum. Syst. Monitor. Control Diagn.* **5**, 1–8 (2019)
28. Lange, P.K., Yaroslavkina, E.E.: Approximation method for determining the pulse signal form and its intensity measurement with an available random noise. *Vestnik of Samara State Technical University. Tech. Sci. Ser.* **2**(62), 99–113 (2019) (in Russian)
29. Wang, X.-H., He, Y.-G.: A new neural network based power system harmonics analysis algorithm with high accuracy. *Power Syst. Technol.* **3**, 72–75 (2005)
30. Morales-Velazquez, L., de Jesus, R., Romero-Troncoso, G.-R., Morinigo-Sotelo, D., Osornio-Rios, R.A.: Smart sensor network for power quality monitoring in electrical installations. *Measurement* **103**, 133–142 (2017)
31. Kruglova, T.N.: Intelligent diagnosis of the electrical equipment technical condition. *Proc. Eng. Int. Conf. Ind. Eng.* **129**, 219–224 (2015)
32. Hamming, R.: *Digital Filters*, p. 224. Prentice Hall inc., Englewood Cliffs, New Jersey (1977)
33. Lange, P.K., Yaroslavkina, E.E.: *Approximation methods and tools for measuring data acquisition* (2017). LAP LAMBERT Academic Publishing, Germany, Düsseldorf, 236 p. (in Russian)
34. Lange, P.K.: Spline approximation of signals discrete samples using digital filtering methods. *J. Samara State Tech. Univ. Ser. Phys. Math. Sci.* **19**, 134–138 (2003)
35. Oran, B.E.: *The Fast Fourier Transform and its Applications*, p. 448. Prentice Hall, Inc. XVI, Englewood Cliffs, New Jersey (1998)
36. Rao, K.R., Kim, D.N., Hwang, J.-J.: *Fast Fourier Transform—Algorithms and Applications*, p. 426. Springer, Netherlands, XVIII (2010)
37. Lange, P.K., Yaroslavkina, E.E., Muratova, V.N.: Methods for quick measurement of integral parameters of a periodic signal. In: *Proceedings of XXI International conf. Problems of Control and Modeling in Complex Systems*, vol. 2 (2019). Samara State Technical University, pp. 149–152

Uncertainty Region Decomposition Approach for Problem of Flexible One-Stage Heat Exchange Network Design



T. V. Lapteva, Nadir Ziyatdinov, Ilya Emelyanov, and D. A. Mitsai

Abstract The solving of system synthesis design problems, including cyber-physical, without taking into account the requirement of system flexibility requires the solution of a discrete–continuous problem of nonlinear programming. To ensure the flexibility of the designed system, it is necessary to take into account possible changes in the conditions of its functioning, which leads to taking into account hard or chance constraints and the integral form of the objective function in the optimization problem. This chapter proposes a method of uncertainty region decomposition for a one-stage heat exchange system design problem, based on partitioning the uncertainty region into subregions of smaller dimension and size. The resulting subregions are selected according to the choice of subsets, including one hot stream and one cold stream, from the set of hot and cold streams. In this case, the resulting subregions are associated only with uncertain parameters related to the change in the properties of flows from the corresponding subset. This will allow us to divide the problem into a set of problems for designing optimal flexible heat transfer subsystems of two flows. In addition, as a result of solving the subproblems, the values of the effectiveness estimates will be obtained, independent of changes of the uncertain parameters. This will allow us to design an optimal efficient one-stage system of heat exchangers by selecting and combining subsystems with the best performance characteristics.

Keywords Technical system synthesis · Optimization under uncertainty · Cyber-physical systems · One-stage heat exchange

T. V. Lapteva (✉) · N. Ziyatdinov · I. Emelyanov · D. A. Mitsai
Kazan National Research Technological University, 68 Karl Marx, Kazan 420015, Russia
e-mail: tanlapteva@yandex.ru

N. Ziyatdinov
e-mail: nnziat@yandex.ru

I. Emelyanov
e-mail: uilyaemelyan@gmail.com

D. A. Mitsai
e-mail: mda189@mail.ru

1 Introduction

Optimum flexible systems design involves providing operations optimality of the designed system with the project requirements satisfaction regardless of the system's functional requirements [1]. Nowadays, operability is impossible to be achieved without the usage of automated control systems, supporting the necessary operating modes of existing systems [2]. It motivates the integration of the cyber-physical system involving the proposed technical or technological systems and the automated control system [3]. This approach is applicable to the majority of the technical and technological systems.

Taking the heat exchanger network as the designed system, we will confine it to the one-stage heat exchange process, where hot and cold streams transfer heat once and no longer participate in the heat transfer. We assume that the problem–solution should give us not only the optimal system topology and the heat-exchanger network size but, moreover, the optimal operating modes to be implemented as the result of the cyber-physical system work. Taking into account the requirements for the designed system flexibility will be implemented by taking into account changes in the operating conditions in the formulation of the problem. To this end the concept of uncertain parameters reflecting external and internal influences on the work of the proposed system [4]. Uncertain parameters change ranges correspond to the system performance conditions changes. The uncertain parameters value range and uncertain parameters themselves form the uncertainty region, where all the system work requirements have to be satisfied.

2 Design Approaches to Optimum Flexible Heat Exchanger Networks

The problem of the optimum flexible heat exchanger network design includes several sub-problems, which should be solved simultaneously. First, sub-problem is the choice of optimum network topology, showing which streams will exchange the heat in heat exchanger networks with the necessity of additional heating and cooling. The second sub-problem is the definition of the optimal construction parameters of the heat exchangers and the optimal flow rate for the additional heating and cooling streams. Both sub-problems must be solved regarding the uncertainty of the initial information in the problem formulation.

Among the modern methods of optimum heat exchanger networks (OHENs) synthesis problem solving the following groups of methods should be underlined. The first group includes the thermodynamic analysis methods of pinch analysis methods [5], heuristical [6, 7], and evolutionary methods [8]. This group of methods is actively developing and implementing in solving the OHENs synthesis under uncertainty problems, but these methods do not include the economic expenditures of the proposed systems. Therefore, such methods are not able to guarantee the designed

system flexibility regarding the economic criteria. A detailed overview of the thermodynamic analysis methods can be found [9]. The second group is based on nonlinear programming methods [10]. Here we can highlight the integration methods of OHENs synthesis [11]. These methods are based on the mixed-integer nonlinear problem (MINLP). They are difficult to implement and often involve multi-extremal problems solving. The development of these methods is commonly used for heat exchanger network synthesis under uncertainty [12].

In the second group, we must highlight the one-stage and multi-stage heat exchanger networks synthesis problem-solving techniques developing by Ziyatdinov's group [13, 14]. The authors did not use discrete–continuous programming methods but proposed the decomposition of the initial problem into two layers. At the lower level is solving the problem of the design of the optimum heat exchanger subsystems, called simple blocks (SB), are solving for all pairs of hot and cold streams [14]. The solution to problems is proposed according to the economic criterion regarding reduced capital and operating costs. Economic criteria values that shown as performance estimates at the upper level are calculating for the SB [14]. The OHENs structure design is proposing at the upper level. The system is constructed from the chosen SBs, ensuring the fulfillment of the requirements of the specified streams temperatures and the minimum total costs. The SB choice is based on the assignment problem-solving. The authors of the article have confirmed the approach efficiency just as for the one-stage heat exchange process, so for the multi-stage heat exchange process. However, these methods are not taking into account the initial information uncertainty in the problem statement.

Considering OHENs synthesis under uncertainty problems solving methods, we have to mention that these methods are solving the problem based on the multi-level procedure [12, 15]. At the upper level, there is generating OHENs structure at some point in the uncertainty region, which is usually nominal. Here is solved the mixed discrete–continuous nonlinear optimization. At the lower level, the proposed system flexibility index is calculated [16]. If the system is not flexible, so the new construction parameters and system structure are selected. The algorithm finds points from the uncertainty region, where the design requirements for the proposed system are tested [17]. This approach guarantees to obtain the flexible OHEN at the found uncertainty region but is not ensuring the system flexibility at the specified region. Other approaches include the flexibility requirement into the OHENs synthesis problem as the constraint on the value of flexibility function [18]. Flexibility function value calculation is related to the multi-extremal nondifferential optimization problem-solving. As the result, we have OHENs structure synthesis problem solving for a set of points from the uncertainty region at one level, while on the other, lower level, there the specified structure heat exchanger network design problem is solved as a one-stage or two-stage optimization problem [15]. The observed methods are extremely complex and computationally expensive. Moreover, solving of these problems related to the multi-extremality problem.

We have to mention, that in the theory of the system's design under uncertainty, the probabilistic constraints usage is actively developing [19]. With the low risk, probabilistic constraints usage drives the system to a lower cost. However, in the

OHENs synthesis problems solving area this type of constraint is not taking into account. It can be related to the high-level computational complexity of constraints [20].

In this chapter, we propose the method for decomposition of uncertainty region to solve the problem of flexible cyber-physical system synthesis based on the one-stage OHEN. The proposed method allows us to associate OHENs synthesis problems solving methods (from [13]) with methods for solving the technical system design under uncertainty problem, proposed in [21, 22]. We will get the method for solving of flexible one-stage OHEN synthesis problem.

3 The Proposed Uncertainty Region Decomposition Method Considering

We consider the problem of the one-stage OHENs under uncertainty design. Let heat exchange between N hot streams and N cold streams must be executed. For case hot streams numbers are less, it will be increased to N by the steam streams, for cold streams—by the cold water streams. Considering the uncertain parameters, stream parameters, composition, and their flowrate changes may be used. Moreover, heat transfer determines parameters that have to be used. In the case of the one-stage heat exchange process, no more than two streams exchange the heat to each other in one unit. Therefore, the proposed system will involve N heat exchangers.

Let us denote the uncertain parameters set for one of the hot streams as $\theta_i^{j,h}$, where $j = 1, \dots, N$ —hot stream number, $i = 1, \dots, n_j$ —parameter number of stream with number j , h —hot stream. Let's denote uncertain parameter set for cold stream, with $\theta_i^{q,c}$, $q = 1, \dots, N$ —hot stream number, $i = 1, \dots, m_q$ —parameter number of stream with number q , c —cold stream. Let us denote heat exchanger uncertain parameters with $\theta_i^{r,he}$, $r = 1, \dots, N$ —unit number, $i = 1, \dots, k_r$ —parameter number of unit with number r , he —heat exchanger identification.

Let's assume those uncertain parameters uncorrelated and distributes by Gaussian law. Each of the uncertain parameters during the operation of the system can change in the range

$$\bar{\theta}_i^{j,h} \leq \theta_i^{j,h} \leq \bar{\theta}_i^{j,h}, i = 1, \dots, P_j, \bar{\theta}_i^{q,c} \leq \theta_i^{q,c} \leq \bar{\theta}_i^{q,c}, i = 1, \dots, M_q \quad (1)$$

$$\bar{\theta}_i^{r,he} \leq \theta_i^{r,he} \leq \bar{\theta}_i^{r,he}, i = 1, \dots, L_r, q = 1, \dots, N, j = 1, \dots, N, r = 1, \dots, N. \quad (2)$$

The ranges indicated in (1) and (2) form the uncertain region Ω . The obtained uncertain region Ω has the dimension

$$R = \sum_{j=1}^N (P_j + M_j + K_j). \quad (3)$$

Using the well-known methods of OHEN design under uncertainty problem solving it is necessary to rest on all the Ω regions on every layer. This involves serious computational expenses.

Let's assume we solved the problem. As a result of the OHEN design under uncertainty problem solving we will have a system of N SBs. Every SB has uncertain parameters set, related to the apparatuses and streams involved in SB. As we have the one-stage heat exchange process, so the set of uncertain parameters related to one SB is not related to the other SBs in the designed OHEN. Therefore, we can decompose the initial uncertainty region Ω on the subregions related to certain SBs. We will have N subregions of the form

$$\Omega_s = \Omega_h^s \cup \Omega_c^s \cup \Omega_{he}^s, s = 1, \dots, N, \quad (4)$$

$$\Omega_h^s = \{\theta_i^{j_s, h} : \bar{\theta}_i^{j_s, h} \leq \theta_i^{j_s, h} \leq \bar{\bar{\theta}}_i^{j_s, h}, i = 1, \dots, H_{j_s}\}, \quad (5)$$

$$\Omega_c^s = \{\theta_i^{q_s, c} : \bar{\theta}_i^{q_s, c} \leq \theta_i^{q_s, c} \leq \bar{\bar{\theta}}_i^{q_s, c}, i = 1, \dots, M_{q_s}\}, \quad (6)$$

$$\Omega_{he}^s = \{\theta_i^{r_s, he} : \bar{\theta}_i^{r_s, he} \leq \theta_i^{r_s, he} \leq \bar{\bar{\theta}}_i^{r_s, he}, i = 1, \dots, K_{r_s}\}, \quad (7)$$

where j_s, q_s —are numbers of hot and cold streams, involved into s -th SB, therefore, r_s —number of the heat exchanger, involved into s -th SB.

It is obvious, that the following expression is true

$$\Omega_s \subset \Omega, s = 1, \dots, N. \quad (8)$$

Moreover, it is easily seen that the following expression is false

$$\bigcup_{s=1}^N \Omega_s = \Omega. \quad (9)$$

Denote the number of uncertain parameters falling within the region of Ω_s as n_s . Now, it is obvious that

$$n_s = H_{j_s} + M_{q_s} + K_{r_s}. \quad (10)$$

Hereinafter, for simplicity, we will denote parameter change intervals that belong to the Ω_s region as $\theta_i^L \leq \theta_i \leq \theta_i^U, i = 1, \dots, n_s$. It is obvious, interval boundaries have the form

$$\theta_i^L = \bar{\theta}_i^{j_s, h}, \theta_i^U = \bar{\bar{\theta}}_i^{j_s, h}, i = 1, \dots, H_{j_s}, \theta_i^L = \bar{\theta}_i^{q_s, c}, \theta_i^U = \bar{\bar{\theta}}_i^{q_s, c}, i = H_{j_s} + 1, \dots, M_{q_s}, \quad (11)$$

$$\theta_i^L = \bar{\theta}_i^{r_s, he}, \theta_i^U = \bar{\bar{\theta}}_i^{r_s, he}, i = H_{j_s} + M_{q_s} + 1, \dots, K_{r_s} \quad (12)$$

The proposed decomposition of the uncertainty region fits the decomposition method from [13] well.

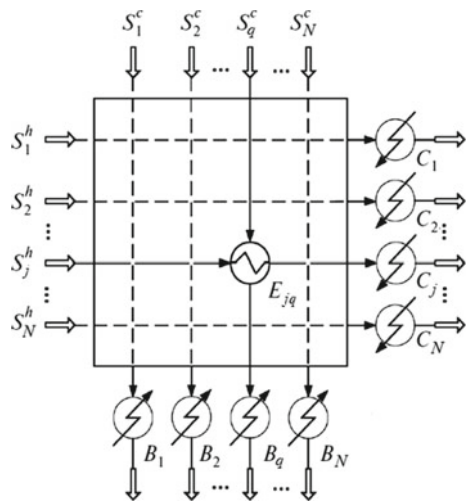
4 Formalization of Solved Problems

Let's consider the problems that are solved at the lower level in approach [13] under uncertainty. While the one-stage OHEN designing this approach involves building the superstructure of the form that can be seen in Fig. 1 (v. [13]). This superstructure includes the possibility of streams after aftercooling and streams to finish warming to the required temperatures. The superstructure is associated with the matrix of size $N \times N$. The rows of the matrix correspond to the hot streams of the heat exchange process, while the columns to the cold streams of the heat exchange process. At the intersection of the j -th row and q -th column of the matrix we have the efficiency estimation value of the optimum SB, ensuring the cooling of j -th hot stream and warming of the q -th cold stream to the required temperatures.

It is obvious, that for optimum SB design under uncertainty we have to ensure the corresponding subregion of the uncertainty region. Such a subregion will include uncertain parameters corresponding to the j -th hot stream and the q -th cold stream.

The solving of the optimum SB design under uncertainty can be proposed by the one-stage or two-stage optimization problem [23]. The effective methods for solving such problems are applied to the design of optimum technological processes under chance constraints as proposed in [21, 22]. The advantage of methods proposed in [22] is the fact that problem-solving gives not only the units' construction parameters values of the system but also the system operating parameters values that must be set to keep system flexibility.

Fig. 1 Superstructure of the one-stage heat exchange system



In the case of a one-stage optimization problem, we assume that during the operation of the system, it is impossible to obtain accurate values of uncertain parameters at any specific time. In this case, we assume that the system must work in an invariant state. In case, the cyber-physical system allows us to obtain the accurate values of uncertain parameters at any specific time—there we considering the two-stage optimization problem. In that case, the problem’s solving will give us the functional dependence that allows us to determine the optimal system operating mode, depending on the values of uncertain parameters.

One-stage optimization problem, corresponding to the optimum s -th SB design under uncertainty, $s = 1, \dots, N^2$, have the form of

$$F_s = \min_{d,z} E[f_s(d, z, \theta)] \tag{13}$$

$$\Pr\{h_v^s(d, z, \theta) \leq 0\} \geq \alpha_v, v = 1, \dots, p_2, \tag{14}$$

where

$$E[f_s(d, z, \theta)] = \int_{\tilde{\Omega}_s} f_s(d, z, \theta) d\theta, \tag{15}$$

$$\tilde{\Omega}_s = \{\theta \in \Omega_s, \varphi_l^s(d, z, \theta) = 0, l = 1, \dots, p_1\}. \tag{16}$$

In (14) we have $h_v^s(d, z, \theta)$, $v = 1, \dots, p_2$,—as the constraints of the problem, reflecting the requirements to SB work. They include the stream temperature requirements at the output of SB and the requirements for the heat exchange process. These constraints (14) represent the requirements of the flexibility of the designing SB at the uncertainty region Ω_s with the specified probability level. In (16) $\varphi_l^s(d, z(\theta), \theta) = 0$, $l = 1, \dots, p_1$, are the set of equations of the mathematical model of SB.

To calculate (13) we will use the approximation, proposed in [22] and involving uncertainty region partitioning by subregions R_q , $q = 1, \dots, Q$,

$$E_{ap}[f_s(d, z, \theta)] = \sum_{q=1}^Q (a_q f_s(d, z, \theta^q) + \sum_{i=1}^{n_s} \partial f_s(d, z, \theta^q) / \partial \theta_i (E_q[\theta_i] - a_q \theta_i^q)), \tag{17}$$

$$\theta^q \in R_q, a_q = \int_{R_q} \rho(\theta) d\theta = \prod_{i=1}^{n_s} [\Phi(\tilde{\theta}_i^{U,q}) - \Phi(\tilde{\theta}_i^{L,q})], \tag{18}$$

$$E_q[\theta_i] = \prod_{r=1}^{i-1} [\Phi(\tilde{\theta}_r^{U,q}) - \Phi(\tilde{\theta}_r^{L,q})] \prod_{r=i+1}^{n_s} [\Phi(\tilde{\theta}_r^{U,q}) - \Phi(\tilde{\theta}_r^{L,q})] \int_{\tilde{\theta}_i^{L,q}}^{\tilde{\theta}_i^{U,q}} \theta_i \rho(\theta_i) d\theta_i, \tag{19}$$

$$\tilde{\theta}_i^{L,q} = (\theta_i^{L,q} - \mu_i)/\sigma_i, \tilde{\theta}_i^{U,q} = (\theta_i^{U,q} - \mu_i)/\sigma_i,$$

where $\Phi(\xi)$ —distribution function $N(0; 1)$ of the random variable ξ , μ_i , $(\sigma_i)^2$ —mean and the variance of the parameter θ_i .

We will calculate (14) basing on the approximation of the probability constraints as deterministic constraints, as proposed in [21]. One constrain (14) here replaced by two constraints

$$\sum_{l=1}^{P_j} \left(\prod_{i=1}^{n_s-1} [\Phi(\tilde{\theta}_r^{U,v,l}) - \Phi(\tilde{\theta}_r^{L,v,l})] \cdot I_{n_{\theta},v,l} \right) \geq \alpha_v, \tag{20}$$

$$h_v(d, z, \bar{\theta}_1^{v,l}, \dots, \bar{\theta}_{n_s-1}^{v,l}, y_{v,l}) = 0, v = 1, \dots, p_2, l = 1, \dots, P_v, \tag{21}$$

where $\tilde{\theta}_i^{L,v,l} = (\theta_i^{L,v,l} - \mu_i)/\sigma_i$, $\tilde{\theta}_i^{U,v,l} = (\theta_i^{U,v,l} - \mu_i)/\sigma_i$, $\theta_i^{L,v,l}$, $\theta_i^{U,v,l}$ —boundaries of region $R_{v,l}$, $l = 1, \dots, P_v$, subdivided from region Ω_s for the increasing of approximation accuracy of constraints (14), $i = 1, \dots, n_s$, $v = 1, \dots, p_2$, $\bar{\theta}_i^{v,l} = 0.5(\theta_i^{L,v,l} + \theta_i^{U,v,l})$, $i = 1, \dots, n_s - 1$. One-dimension integral $I_{n_s,v,l}$ calculated by formulae

$$I_{n_s,v,l} = \begin{cases} \Phi((y_{v,l} - \mu_{n_s})/\sigma_{n_s}) - \Phi(\tilde{\theta}_{n_s}^{L,v,l}), & \partial h_v(d, z, \theta) / \partial \theta_{n_s} \geq 0, \\ \Phi(\tilde{\theta}_{n_s}^{U,v,l}) - \Phi((y_{v,l} - \mu_{n_s})/\sigma_{n_s}), & \partial h_v(d, z, \theta) / \partial \theta_{n_s} \leq 0, \end{cases}$$

where $y_{v,l}$ — n_s -th uncertain parameter value at which (21) is satisfied.

We have got the sequence of the problems which calculate the problem (13) and (14) estimation in the form of the nonlinear programming problem

$$\bar{F}_s^{(k)} = \min_{d,z,y_{v,l}} E_{ap}[f_s(d, z, \theta)] \tag{22}$$

$$h_v(d, z, \bar{\theta}_1^{v,l}, \dots, \bar{\theta}_{n_s-1}^{v,l}, y_{v,l}) = 0, v = 1, \dots, p_2, l = 1, \dots, P_v,$$

$$\sum_{l=1}^{P_j} \left(\prod_{i=1}^{n_s-1} [\Phi(\tilde{\theta}_r^{U,v,l}) - \Phi(\tilde{\theta}_r^{L,v,l})] \cdot I_{n_{\theta},v,l} \right) \geq \alpha_v. \tag{23}$$

To clarify estimation (22) and (23) the uncertain region partition procedure proposed in [21].

It is obvious that the solution of the (13) and (14) will give us the efficiency estimation value of SB of number s , $s = 1, \dots, N^2$, under the uncertainty. We have to mention that solving the problem (13) and (14) will give us the value F_s , independent from the uncertain parameters. It will correspond to some element of the estimation matrix of the place at the intersection of j_s -th row and q_s -th column. Having calculated the efficiency estimations $F_{j,q}$, $j = 1, \dots, N$, $q = 1, \dots, N$, for every N^2 elements of

the estimation matrix, we will have the initial information for the construction of the structure of the designing cyber-physical system. Since the estimations in the matrix do not depend on uncertain parameters, the solution of the problem can be carried out on the basis of the usual assignment problem, as suggested in [13]. The task will take the form

$$\min_{z_{jq}} \sum_{j=1}^N \sum_{q=1}^N F_{jq} z_{jq} \tag{24}$$

$$\sum_{j=1}^N z_{jq} = 1, \sum_{q=1}^N z_{jq} = 1, z_{jq} = \{0; 1\}. \tag{25}$$

The problem (24) and (25) is the discrete-linear programming problem, for which there were developed efficient methods to solve [24]. As a result of the problem (24) and (25) solving will be the values of the variables z_{jq} , from which we will obtain the required system structure.

5 Computational Experiment

Let us consider OHEN for the one-stage heat exchange process, where 2 hot streams, $j = 1; 2$, and 2 to cold streams, $j = 3; 4$ are taking part. As the uncertain parameters, we will have the stream temperatures and mass flow rate. The uncertainty region will be defined as the set of intervals $\theta_{i,j}^N - \Delta_{i,j} \leq \theta_{i,j}^N \leq \theta_{i,j}^N + \Delta_{i,j}$ as is shown in Table 1.

As the optimum SB criterion with the number s , we will take the total costs, including reduced capital and operating costs. Capital costs including the main heat exchanger costs $c_1(A_E^s)^{0.75}$, where hot and cold streams exchange heat, cooler costs $c_1(A_C^s)^{0.75}$, and heater costs $c_1(A_H^s)^{0.75}$. Cooler and heater intended for the hot stream aftercooling and cold stream finish warming. Operation costs involve cold water cost

Table 1 Uncertainty region characteristics

Stream	Uncertainty parameter	μ_i	Δ_j
1	Temperature	82.86	0.83
	Mass flow rate	10,317.51	309.53
2	Temperature	124.08	1.24
	Mass flow rate	15,591.89	467.76
3	Temperature	18	0.18
	Mass flow rate	35,550	1066.5
4	Temperature	30	0.3
	Массовый расход	105,835.2	3175.06

$c_3 F_w^s$ and steam cost $c_2 F_{st}^s$. Criteria has the form

$$c_1((A_E^s)^{0.75} + (A_H^s)^{0.75} + (A_C^s)^{0.75}) + c_2 F_{st}^s + c_3 F_w^s, \quad (26)$$

where c_1, c_2, c_3 —cost coefficients, A_E^s, A_H^s, A_C^s —heat exchanger area for main heat exchanger, heater and cooler, F_{st}^s, F_w^s —steam and water flow rate, respectively.

The problem search variables are heat exchanger areas A_E^s, A_H^s, A_C^s and utility rates F_{st}^s, F_w^s .

As problem constrains used following:

the requirement for the temperature of the cold stream leaving the SB

$$\Pr\{T^{C,out} \geq T^{C,min}\} \geq \alpha_1, \quad (27)$$

the requirement for the temperature of the hot stream leaving the SB

$$\Pr\{T^{H,out} \geq T^{H,max}\} \geq \alpha_2, \quad (28)$$

the requirement for the temperature difference between the hot flow at the entrance to the main heat exchanger and the cold flow at the exit from it

$$\Pr\{T^{H,in} - T^{C,out} \geq 5\} \geq \alpha_3, \quad (29)$$

the requirement for the temperature difference between the hot flow at the outlet of the main heat exchanger and the cold flow at the inlet

$$\Pr\{T^{H,out} - T^{C,in} \geq 5\} \geq \alpha_4. \quad (30)$$

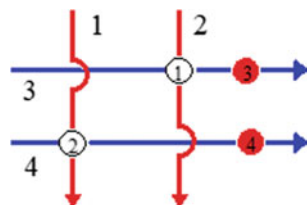
Probability levels are equal to $\alpha_1 = \alpha_2 = 0.95, \alpha_3 = \alpha_4 = 1$.

For problem-solving it is necessary to calculate the efficiency estimations for the four SBs. At the first SB we have 1st and 3rd streams exchanging the heat, streams 1st and 4th at the second SB, 2nd and 3rd streams at the third SB, and the 2nd and 4th on the fourth one. For every SB there will be specified the subregion of the total uncertainty region, including only the uncertain parameters corresponding to the specific SB. It is obvious, that the set of uncertainty regions of each SB will give summarizing less uncertainty region. It became real by the decomposition of the main solving problems to the problems of the design of the particular SBs.

As the result of problem (16) and (17) solving for each SB we have the following estimations: 30.685—for the first SB, 47.138—for the second SB, 40.954—for the third SB, and 73.052—for the fourth. The solution to the problem (24) and (25) gave us the superstructure shown in Fig. 2.

The figure shows that the optimal heat transfer is between 2 and 3 streams, as well as between 1 and 4 streams. It can be seen that heaters 3 and 4 were required for cold flows.

Fig. 2 The optimal structure of the flexible one-stage heat exchange network



6 Conclusion

In this work, there were proposed the method of the uncertainty region decomposition for the one-stage heat exchange network design under uncertainty problem. The combination of the approaches of OHENs synthesis methods without uncertainty [13] with approaches of system design under uncertainty methods [19, 20] allowed us to dispose of the discrete–continuous nature of the problem of the OHENs structure design. Coordination of the decomposition of the uncertainty region and the superstructure of a one-stage heat exchange network made it possible to solve the problems of OHENs design under uncertainty using uncertainty regions of lower dimension and size. The resulting solution gives us the optimal structure of the OHEN, the construction parameters of units included in the OHEN, and the OHEN operation modes, which guarantee OHEN flexibility. The inclusion of the resulting system in the cyber-physical system will allow maintaining the found operating modes in changing operating conditions and ensuring the operability of the existing system.

Acknowledgements The research at Kazan National Research Technological University was supported by the Ministry of Science and Higher Education of the Russian Federation grant “Energy and Resource-Saving Processes for Separation of Liquid Mixtures for the Separation of Industrial Solvents”.

References

- Hollermann, D.E., Goerigk, M., Hoffrogge, D.F., et al.: Flexible here-and-now decisions for two-stage multi-objective optimization: method and application to energy system design selection. *Optim. Eng.* **2020**, 1–27 (2020)
- Michailidis, M.G., Valavanis, K.P., Rutherford, M.: *Nonlinear Control of Fixed-Wing UAVs with Time-Varying and Unstructured Uncertainties*, 119 p. Springer International Publishing (2020)
- Wolf, W.: Cyber-physical Systems. In: *Computer*, No. 3(42), pp. 88–89 (2009)
- Alekseev, A.P., Kravets, A., Bolshakov, A., Shcherbakov, M.: Conceptual approach to designing efficient cyber-physical systems in the presence of uncertainty. *Cyber-Phys. Syst.: Adv. Des. Modell.* **259**, 69–80 (2020)
- Townsend, D.W., Linnhoff, B.: Heat and power networks in process design. Part II. Design procedure for equipment selection and process matching. *AIChE J.* **29**, 748–771 (1983)
- Linnhoff, B., Hindmarsh, E.: The pinch design method of heat exchanger networks. *Chem. Eng. Sci.* **38**, 745–763 (1983)

7. Couper, J.R., Penney, W.R., Fair, J.R., Walas, S.M.: *Chemical Process Equipment: Selection and Design*, 2nd edn., p. 8701. Elsevier. Gulf Professional Publishing, Oxford (2005)
8. Ponton, J.W., Donaldson, R.A.B.: A fast method for the synthesis of heat exchanger networks. *Chem. Eng. Sci.* **29**(12), 2375–2377 (1974)
9. Klemeš, J.J., Varbanov, P.S., Walmsley, T.G., Jia, X.: New directions in the implementation of Pinch Methodology PM. *Renew. Sustain. Energy Rev.* **98**, 439–468 (2018)
10. Biegler, L.T.: *Nonlinear Programming: Concepts, Algorithms, and Applications to Chemical Processes*, p. 399. SIAM, Philadelphia, PA (2010)
11. Yee, T.F., Grossmann, I.E.: Optimization models for heat integration—II. Heat exchanger network synthesis. *Comput. Chem. Eng.* **14**, 1165–1184 (1990)
12. Novak, P.Z., Kravanja, Z.: (2015) A methodology for the synthesis of heat exchanger networks having large numbers of uncertain parameters. *Energy* **92**, 373–382 (2015)
13. Ostrovskii, G.M., Ziyatdinov, N.N., Emel'yanov, I.I.: Designing a heat-exchange system upon the reconstruction and synthesis of optimal systems of distillation columns. *Theor. Found. Chem. Eng.* **50**, 178–187 (2016)
14. Ostrovskii, G.M., Ziyatdinov, N.N., Emelyanov, I.I.: Synthesis of optimal systems of simple distillation columns with heat recovery. *Doklady Chem.* **1**(461), 89–92 (2015)
15. Zheng, K., Lou, H.H., Wang, J., Cheng, F.: A method for flexible heat exchanger network design under severe operation uncertainty. *Chem. Eng. Technol.* **36**, 757–765 (2013)
16. Zirngast, K., Kravanja, Z., Novak Pintarič, Z.: A robust decomposition methodology for synthesis of flexible processes with many uncertainty parameters—Application to HEN Synthesis. *Chem. Biochem. Eng. Q.* **32**(4), 401–411 (2018)
17. Li, J., Du, J., Zhao, Z., Yao, P.: Structure and area optimization of flexible heat exchanger networks. *Ind. Eng. Chem. Res.* **53**, 11779–11793 (2014)
18. Halemane, K.P., Grossmann, I.E.: Optimal process design under uncertainty. *AIChE J.* **29**, 425–433 (1983)
19. Bernardo, F.P.: Model analysis and optimization under uncertainty using thinned cubature formulae. *Comput. Chem. Eng.* **92**, 133–142 (2016)
20. Küçükyavuz, S.: On mixing sets arising in chance-constrained programming. *Math. Program.* **1–2**(132), 31–56 (2012)
21. Lapteva, T.V., Silvestrova, A.S., Ziatdinov, N.N.: An approach to solve the power and resource-intensive process design problem in a one-stage optimization problem form. *IOP Conference Series: Earth Environ. Sci.* **288**, 012102 p (2019)
22. Ostrovsky, G.M., Ziyatdinov, N.N., Lapteva, T.V.: Optimization problem with normally distributed uncertain parameters. *AIChE J.* **7**(59), 2471–2484 (2013)
23. Kämmerling, N., Kurtz, J.: Oracle-based algorithms for binary two-stage robust optimization. *Comput Optim Appl* **2020**, 1–24 (2020)
24. Fenyo, S.: *Modern Mathematical Methods in Technology*, Vol. 17, 1st ed, 334 p. North Holland (1975)

Optimal Heat Integration of Large-Scale Cyber-Physical Oil Refining Systems



Alina Ryzhova, Ilya Emelyanov, Nadir Ziyatdinov,
and Zufar Khalirakhmanov

Abstract The issues of joint thermal integration of an interconnected facilities system of an oil refinery characterized by different energy levels are considered. An evaluation of the integrative thermodynamic effect when organizing large-scale heat recovery in distributed heat exchange networks is given. The method of making administrative decisions for cyber-physical systems of technological processes with the aim of optimal design of heat exchange networks is presented.

Keywords Cyber-physical systems · Oil refinery · Heat integration · Pinch analysis · Synthesis of an optimal heat exchange system · Decomposition approach · Isomerization process · Hydrocracking · CDU/VDU

1 Introduction

A modern oil refinery is a complex cyber-physical chemical-technological system that meets «Industry 4.0» standards. This means that the modern refinery is characterized by fully automated, vertically and horizontally integrated digital production, controlled by intelligent systems in real-time in constant interaction with the external environment [1]. The quality of management of such systems at the manufacturing execution system level, aimed at obtaining oil products of a given quantity and specified quality at minimum operating costs, including energy, is largely determined by the technological perfection of the designed facilities. Thus, the search for reserves to improve the energy efficiency of refinery through the heat integration of process

A. Ryzhova (✉) · I. Emelyanov · N. Ziyatdinov · Z. Khalirakhmanov
Kazan National Research Technological University, 6 Universitetskaya, Kazan 420111, Russia
e-mail: alinagainullina0@yandex.ru

I. Emelyanov
e-mail: ilyaemelyan@gmail.com

N. Ziyatdinov
e-mail: nzizat@yandex.ru

Z. Khalirakhmanov
e-mail: zufar.kh@mail.ru

flows and the maximum use of secondary fuel and energy resources, as well as design methods aimed at the synthesis of optimal heat exchange systems, is relevant. The relevance is also confirmed by the thermodynamic imperfection of technological processes that consume significantly more energy than theoretically needed. According to [2] only 30–35% of the received heat energy is used at a refinery, while the rest of the energy (including low-grade) becomes non-recuperative. It leaves the system along with cooling water or air, released into the atmosphere with the flue gases of the process furnaces, dissipated into the environment in the form of heat given off by the hot surfaces of the equipment.

Oil refinery consists of units for the preparation of raw materials, preliminary distillation, and refabrication of oil fractions and mixing components of petroleum oil interconnected by technological flows. The issues of increasing the energy efficiency of individual refineries based on heat integration are considered in many works of Russian and foreign authors. In [2, 3] methods for the synthesis of heat exchange systems for the entire refinery were proposed. Articles [4, 5] describe a pinch analysis of the process flow system of crude and vacuum distillation unit (CDU/VDU) that proposes a project for the reconstruction of a heat exchange system. However, the issues related to the joint heat integration of the facilities that are part of the refinery are not studied sufficiently at the time [6]. Given that the technological facilities in the refinery are operating at different energy levels, the organization of heat exchange between them is of undoubted interest. In this case, high-temperature units can be a source of thermal energy, while subsystems located at a lower energy level are energy consumers. The heat exchange system (Fig. 1) is organized with the involvement of external auxiliary hot and cold heat-transfer agents circulating in the circuit between the complex of plants. The excess heat of each facility can be directed to the block of multi-threaded steam generators to compensate for the lack of heat in systems characterized by a lower energy level [3]. The coordinating module of the complex

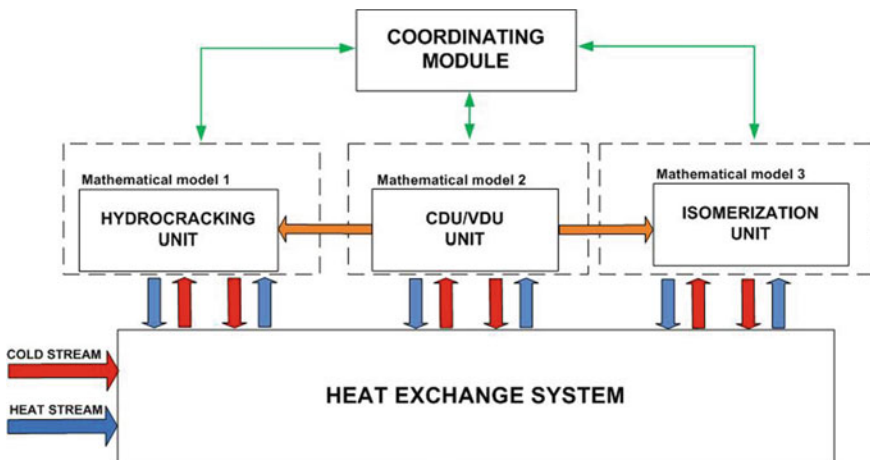


Fig. 1 Energy distribution scheme in a system of interconnected units

monitors energy consumption in subsystems and distributes spare energy according to predicted demands.

The key issue in the design of a system of energetically coupled units is the choice of a synthesis method for a heat exchange system (HES). Synthesis of optimal HES on an industrial scale is complicated by the computational complexity of the problem being solved, related to the large dimension of the search space and the combinatorial nature of the problem. Solving problems of large-scale integration of technological processes requires the development of effective methods for the synthesis of optimal heat exchange systems, ensuring the global minimum of the multi-extreme optimization problem with minimal time costs.

Heat integration methods are based on three approaches: heuristic [6], thermodynamic [7], and mathematical programming [8]. Heuristic rules are distinguished by their simplicity, but they give only an approximate solution, which is often contradictory, and in some cases, significantly different from the optimal one. The thermodynamic approach makes it possible to obtain thermodynamically optimal solutions based on the pinch method [7], as well as a method based on estimating the minimum entropy production [9]. It gives good results but does not fully take into account the economic aspects of the task. These deficiencies can be addressed with mathematical programming techniques. Thus, the optimal HES synthesis problem takes the form of a mixed-integer nonlinear programming problem [10–14], which can be formalized on the basis of a superstructure containing a large number of potential schemes of heat exchange systems. These methods allow one to achieve better economic results but are characterized by high computational costs. One of the ways to reduce the complexity of this problem is its structural or target decomposition based on a transportation model [13, 14], or a model with median points [15]. However, the heuristic nature of this approach narrows the search domain of the synthesis problem, while the computational complexity of algorithms being used to solve nonlinear programming problem further makes it difficult to use the approach for large-scale problems.

2 Problem Statement and Research Methodology

To solve the optimal HES synthesis problem, we will conduct a thermodynamic analysis of the interconnected units system to determine the energy reserves of the refinery. An effective method to evaluate the potential to increase the energy efficiency of technological systems is pinch analysis. The paper inspects the primary (CDU/VDU) and secondary oil refining units (isomerization unit (IU) и hydrocracking unit (HU)) for one of the largest oil refineries in the Russian Federation as objects of research.

Computer models of the considered facilities were developed in Aspen HYSYS software using rigorous mathematical models of technological equipment. They were used to evaluate the energy potential and the expediency of the existing heat exchange system. Based on the data on the parameters of technological flows obtained as a result of calculating a computer model of CDU/VDU, isomerization, and hydrocracking

units, composite curves of hot and cold flows were plotted. They are shown in Table 1. The minimum allowable temperature difference was set to 10 °C. This value was selected considering the structural features of heat exchangers and the features of the process under study. As a result of the conducted pinch analysis, one can observe a large overlap zone of composite curves characterizing the maximum possible amount of recuperated energy (Fig. 2). The size of this zone is a prerequisite for solving the problem of optimal heat integration of technological flows.

Figure 2 shows composite curves of hot and cold flows for a complex of interconnected units of the refinery (CIUR) constructed to estimate energy reserves for the integration of all three plants.

Table 1 shows that the integrative thermodynamic effect obtained in the form of the difference between the maximum possible amount of recuperated energy for a complex of interconnected units of refinery and the actual total energy consumption is 156.01 MW or 17.8 M USD/year. The difference between the maximum possible

Table 1 Comparative analysis of the results

Index name	CDU/VDU	IU	HU	Sum	CIUR
The actual amount of supplied heat (MW)	134.3	47.3	46	227.6	
The actual amount of withdrawn heat (MW)	90.7	51.7	142.2	284.6	
The actual amount of recuperated heat (MW)	132.4	10.5	190.8	333.7	
Maximum possible amount of supplied energy (MW)	78.9	41.5	0	120.4	69.5
Maximum possible amount of withdrawn energy (MW)	37.3	45.9	96.4	179.6	126.6
Maximum possible amount of recuperated energy (MW)	185.8	16.3	236.8	438.9	489.7

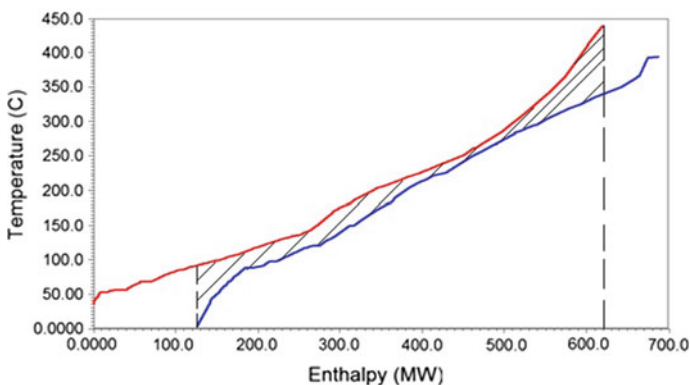


Fig. 2 Composite curves on the temperature-enthalpy diagram for the complex of interconnected units of the refinery

amount of recuperated energy for a complex of interconnected units and for each unit individually is 50.83 MW, which is 5.8 M USD /year.

To solve the optimal HES synthesis problem, we have developed a large-scale heat integration method based on the assignment problem and the decompositional principle of fixation of variables [16, 17]. However, this method does not take into account cases when flows split. The paper proposes a new method that removes this limitation.

Consider the problem statement of optimal HES synthesis. There are M^h hot flows S_i^h , ($i = 1, \dots, M^h$) and M^c cold flows S_j^c , ($j = 1, \dots, M^c$), having flow rates F_i^h , F_j^c , and initial temperatures $T_i^{h,in}$, $T_j^{c,in}$, respectively. For each hot flow ΔQ_i^h is the amount of heat to cool it down to a given temperature $T_i^{h,out}$. Likewise for each cold flow ΔQ_j^c is the amount of heat to heat it to a given temperature $T_j^{c,out}$. The goal is to find values of search parameters and HES structure for hot and cold flows that provide the minimum value of total reduced capital and operating costs Φ . This HES contains recuperative heat exchangers, coolers, and heaters. Thus the search parameters are values of heat exchange surface areas of recuperative heat exchangers A_{ij} , heaters A_j , and coolers A_i , flow rates of cold heat-transfer agents F_i^{cu} in coolers and hot heat-transfer agents F_j^{hu} in heaters.

The solution to the HES synthesis problem is based on the results of pinch analysis. First, we divide composite curves into enthalpy intervals. Each interval (i.e. it's beginning and end) is determined by flex points of the composite curve. One can determine sets of hot and cold integrable flows on each enthalpy interval, the heat exchange of which is possible using a structure with a parallel transfer of the amount of heat by each hot flow to all cold flows in the considered interval. With known values of the initial and final temperatures of each enthalpy interval, the amount of heat taken from the i -th hot and transferred to the j -th cold flow can be determined using the heat balance equation. We denote these values for the amount of heat as $\Delta Q_{i,p}^h$, $\Delta Q_{j,q}^c$, respectively. Next, we represent $\Delta Q_{i,p}^h, \Delta Q_{j,q}^c$ in the form of multiplication $\beta_{i,p}^h \Delta Q_i^h, \beta_{j,q}^c \Delta Q_j^c$, respectively, where $\beta_{i,p}^h, \beta_{j,q}^c$ are the coefficients of thermal loads distribution at the stages of HES, which meet the following conditions:

$$\sum_{p=1}^K \beta_{i,p}^h = 1, i = 1, \dots, M^h, \quad \sum_{q=1}^K \beta_{j,q}^c = 1, j = 1, \dots, M^c. \quad (1)$$

Then we create a heat exchange superstructure that takes into account both the possible heat exchange within each interval and the transfer of heat into adjacent intervals. To build the structure of the heat exchange unit for each interval we put the flow dividers $D_{i,p}^h$ and $D_{j,q}^c$ on the input of i -th hot and j -th cold flows, respectively. Thus i -th hot flow S_i^h will be split into $L_{i,p}^h$ of elementary flows $S_{i,p}^h$ ($I_i^p = 1, \dots, L_{i,p}^h$) and j -th cold flow S_j^c will be split into $L_{j,q}^c$ of elementary flows $S_{j,q}^c$ ($I_j^q = 1, \dots, L_{j,q}^c$), respectively. Flow rates $F_{i,p}^h, F_{j,q}^c$ of flows $S_{i,p}^h$ and $S_{j,q}^c$ will be equal to $\alpha_{i,p}^h F_i^h, \alpha_{j,q}^c F_j^c$, respectively, where $\alpha_{i,p}^h, \alpha_{j,q}^c$ are split coefficients, that meet the following conditions:

$$\sum_{l_i^p=1}^{L_{i,p}^h} \alpha_{l_i^p}^h = 1, \quad i = 1, \dots, M^h, \quad \sum_{l_j^q=1}^{L_{j,q}^c} \alpha_{l_j^q}^c = 1, \quad j = 1, \dots, M^c. \quad (2)$$

The amount of heat energy $\Delta Q_{l_i^p}^h, \Delta Q_{l_j^q}^c$ transferred from hot to cold elementary flows $S_{l_i^p}^h$ and $S_{l_j^q}^c$ is equal to $\alpha_{l_i^p}^h \Delta Q_{i,p}^h, \alpha_{l_j^q}^c \Delta Q_{j,q}^c$ on considered intervals, respectively.

The found coefficients $\alpha_{l_i^p}^h, \alpha_{l_j^q}^c$ and $\beta_{i,p}^h, \beta_{j,q}^c$ for elementary flows will be used as initial values of search variables of HES on a superstructure optimization problem. Considering all the above, this superstructure will take the form given in Fig. 3.

We will break down the problem into two subproblems using the principle of fixation of variables [18]. The first one is to determine the optimal structure of multistage HES with fixed values of the coefficients $\alpha_{l_i^p}^h, \alpha_{l_j^q}^c, \beta_{i,p}^h, \beta_{j,q}^c$. The second

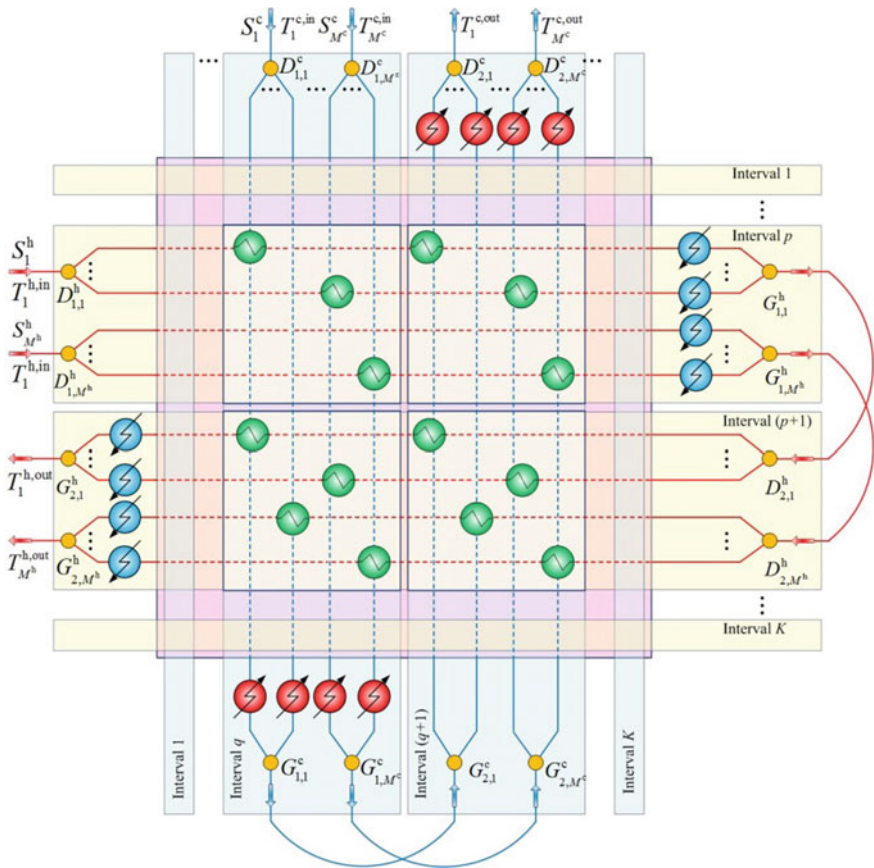
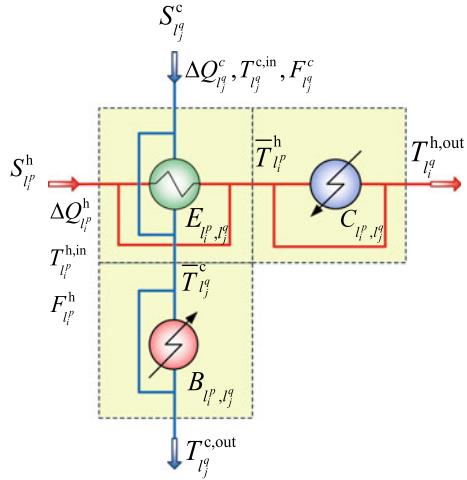


Fig. 3 Superstructure of the heat exchange system

Fig. 4 EBHES superstructure



subproblem is to find new values of these coefficients for a given structure that provide a lower value of the optimization criterion.

The problem of finding the optimal structure of HES can be reduced to finding the minimum criterion value for the total reduced capital and operating costs for heat transfer of all possible matching for the pairs of l_i^p -th hot and l_j^q -th cold flows. For this, we take superstructure from the HES superstructure that includes all possible options for organizing heat transfer of two elementary flows (Fig. 4).

This new structure is called the elementary blocks of the heat exchange system (EBHES) [16]. It consists of a recuperative heat exchanger $E_{l_i^p, l_j^q}$, cooler $C_{l_i^p, l_j^q}$ and heater $B_{l_i^p, l_j^q}$.

The problem of finding the minimum costs for the organization of EBHES is formalized in the form of Eqs. (3)–(12). It is a nonlinear mathematical programming problem that has effective solution methods. Note that its solution does not require large computational costs due to the small dimensionality.

$$f_{l_i^p, l_j^q}^{\text{opt}} \rightarrow \min_{A_{l_i^p, l_j^q}^{\text{he}}, A_{l_i^p, l_j^q}^{\text{col}}, A_{l_i^p, l_j^q}^{\text{reb}}, F_{l_i^p, l_j^q}^{\text{cu}}, F_{l_i^p, l_j^q}^{\text{hu}}} f_{l_i^p, l_j^q} \tag{3}$$

optimization criterion:

$$\begin{aligned} f_{l_i^p, l_j^q} = & \left(\tilde{m}_1^{\text{col}} + \tilde{m}_2^{\text{col}} \left(A_{l_i^p, l_j^q}^{\text{col}} \right)^{\gamma^{\text{col}}} + \hat{m}^{\text{col}} F_{l_i^p, l_j^q}^{\text{cu}} \right) \\ & + \left(\tilde{m}_1^{\text{reb}} + \tilde{m}_2^{\text{reb}} \left(A_{l_i^p, l_j^q}^{\text{reb}} \right)^{\gamma^{\text{reb}}} + \hat{m}^{\text{reb}} F_{l_i^p, l_j^q}^{\text{hu}} \right) \\ & + \left(\tilde{m}_1^{\text{he}} + \tilde{m}_2^{\text{he}} \left(A_{l_i^p, l_j^q}^{\text{he}} \right)^{\gamma^{\text{he}}} \right), \end{aligned} \tag{4}$$

equations of mathematical models for recuperative heat exchangers, coolers, and heaters, respectively:

$$\begin{aligned} \varphi^{\text{he}}(\overline{T}_{l_i^p, l_j^q}^{\text{h}}, \overline{T}_{l_i^p, l_j^q}^{\text{c}}, T_{l_i^p}^{\text{h, in}}, T_{l_j^q}^{\text{c, in}}, A_{l_i^p, l_j^q}^{\text{he}}, F_{l_i^p}^{\text{h}}, F_{l_j^q}^{\text{c}}, \\ U_{l_i^p, l_j^q}, c_{l_j^q}^{\text{c}}, c_{l_i^p}^{\text{h}}) = 0, \end{aligned} \quad (5)$$

$$\begin{aligned} \varphi^{\text{col}}(\overline{T}_{l_i^p, l_j^q}^{\text{h}}, T_{l_i^p}^{\text{h, out}}, T^{\text{cu, in}}, T^{\text{cu, out}}, A_{l_i^p, l_j^q}^{\text{col}}, F_{l_i^p}^{\text{h}}, F_{l_j^q}^{\text{cu}}, \\ U_{l_i^p, l_j^q}, c^{\text{cu}}, c_{l_i^p}^{\text{h}}) = 0, \end{aligned} \quad (6)$$

$$\begin{aligned} \varphi^{\text{reb}}(\overline{T}_{l_i^p, l_j^q}^{\text{c}}, T_{l_j^q}^{\text{c, out}}, T^{\text{hu, in}}, T^{\text{hu, out}}, A_{l_i^p, l_j^q}^{\text{reb}}, F_{l_j^q}^{\text{c}}, F_{l_i^p}^{\text{hu}}, \\ U_{l_i^p, l_j^q}, c_{l_j^q}^{\text{c}}, c^{\text{hu}}) = 0, \end{aligned} \quad (7)$$

constraints on the physical feasibility of the heat transfer process:

$$T_{l_i^p}^{\text{h, in}} - \overline{T}_{l_i^p, l_j^q}^{\text{c}} \geq \Delta T_{\text{min}}, \quad \overline{T}_{l_i^p, l_j^q}^{\text{h}} - T_{l_j^q}^{\text{c, out}} \geq \Delta T_{\text{min}}, \quad (8)$$

$$T^{\text{hu, out}} - \overline{T}_{l_i^p, l_j^q}^{\text{c}} \geq \Delta T_{\text{min}}, \quad T^{\text{hu, in}} - T_{l_j^q}^{\text{c, out}} \geq \Delta T_{\text{min}}, \quad (9)$$

$$T_{l_i^p}^{\text{h, out}} - T^{\text{cu, in}} \geq \Delta T_{\text{min}}, \quad \overline{T}_{l_i^p, l_j^q}^{\text{h}} - T^{\text{cu, out}} \geq \Delta T_{\text{min}}. \quad (10)$$

$$\Delta Q_{l_i^p, l_j^q}^{\text{he}} > 0, \quad \Delta Q_{l_i^p, l_j^q}^{\text{col}} > 0, \quad \Delta Q_{l_i^p, l_j^q}^{\text{reb}} > 0. \quad (11)$$

U —heat transfer coefficient; c —specific isobar heat capacity; $\tilde{m}_1^{\text{he}}, \tilde{m}_2^{\text{he}}, \tilde{m}_1^{\text{col}}, \tilde{m}_2^{\text{col}}, \tilde{m}_1^{\text{reb}}, \tilde{m}_2^{\text{reb}}, \gamma^{\text{he}}, \gamma^{\text{col}}, \gamma^{\text{reb}}, \hat{m}^{\text{col}}, \hat{m}^{\text{reb}}$ —price and correlation coefficients; ΔT_{min} —minimum allowable temperature difference.

We can formalize the problem of finding optimal HES structure based on derived economic estimates $f_{l_i^p, l_j^q}^{\text{opt}}$. To do this we introduce a binary variable $z_{l_i^p, l_j^q}$ that determines the presence or absence of EBHES in the synthesized HES. Thus the problem of finding optimal HES structure is reduced to a linear discrete programming problem (also known as «assignment problem»). It takes the form:

$$\Phi \rightarrow \min \sum_{z_{l_i^p, l_j^q}} \sum_{i=1}^{M^h} \sum_{p=1}^K \sum_{j=1}^{M^c} \sum_{q=1}^K \sum_{l_j^q=1}^{L_{j,q}^c} \sum_{l_i^p=1}^{L_{i,p}^h} f_{l_i^p, l_j^q}^{\text{opt}} z_{l_i^p, l_j^q}, \quad (12)$$

$$\sum_{i=1}^{M^h} \sum_{p=1}^K \sum_{l_i^p=1}^{L_{i,p}^h} z_{l_i^p, l_j^q} = 1, \quad \sum_{j=1}^{M^c} \sum_{q=1}^K \sum_{l_j^q=1}^{L_{j,q}^c} z_{l_i^p, l_j^q}^{(k)} = 1. \quad (13)$$

However, the resulting HES structure is optimal only for the fixed values of variables $\alpha_{l_p^p}^h, \alpha_{l_q^q}^c, \beta_{i,p}^h, \beta_{j,q}^c$. We define new approximations of these variables by optimizing the graph whose structure was obtained in the first step. So, based on this, we propose the following iterative algorithm:

Step 1. Put the iteration number $k = 1$. Set the initial approximations of the coefficients $\alpha_{l_p^p}^{h,(k)}, \alpha_{l_q^q}^{c,(k)}, \beta_{i,p}^{h,(k)}, \beta_{j,q}^{c,(k)}$.

Step 2. Solve the problem (3) for all the EBHES.

Step 3. Solve «assignment problem» (12) and (13).

Step 4. By solving the nonlinear mathematical programming problem (14), find the optimal regime for HES with a fixed structure, taking into account the fulfillment of constraints (5)–(11).

$$\min_{F_{l_p^p, l_q^q}^{cu}, F_{l_p^p, l_q^q}^{hu}, F_{l_p^p, l_q^q}^c, F_{l_p^p, l_q^q}^h, A_{l_p^p, l_q^q}^{hc}, A_{l_p^p, l_q^q}^{reb}, A_{l_p^p, l_q^q}^{col}} \Phi^{(k)}, \forall (l_i^p, l_j^q) \in Z^{(k)}, \tag{14}$$

where $Z^{(k)}$ is the set of pairs of elementary flows whose EBHES are included in the HES structure at the current iteration.

Step 5. If $(|\Phi^{(k)} - \Phi^{(k-1)}| < \xi)$, then stop, else put $k = k + 1$ and go to step 6.

Step 6. Determine new approximations for split coefficients of flows:

$$\beta_{i,p}^{h,(k)} = \frac{\Delta Q_{i,p}^{h,(k-1)}}{\Delta Q_i^h}, \beta_{j,q}^{c,(k)} = \frac{\Delta Q_{j,q}^{c,(k-1)}}{\Delta Q_j^c},$$

$$\alpha_{l_p^p}^h = \frac{F_{l_p^p}^{h,(k-1)}}{F_i^h}, \alpha_{l_q^q}^c = \frac{F_{l_q^q}^{c,(k-1)}}{F_j^c}, \tag{15}$$

and go to step 2.

3 Interpretation and Discussion of Research Results

This algorithm was tested on a model that includes two hot and two cold flows. Initial data is given in Table 2.

HES graph obtained using the proposed method is shown in Fig. 5.

Table 2 Initial and final temperatures, amount of heat taken from hot flows and transferred to cold technological flows

Hot flow	$T_i^{h,in}$ (K)	$T_i^{h,out}$ (K)	ΔH_i^h (kW)	Cold flow	$T_j^{c,in}$ (K)	$T_j^{c,out}$ (K)	ΔH_j^c (kW)
H1	430	380	2000	C1	410	411	4000
H2	425	424	3000	C2	390	420	900

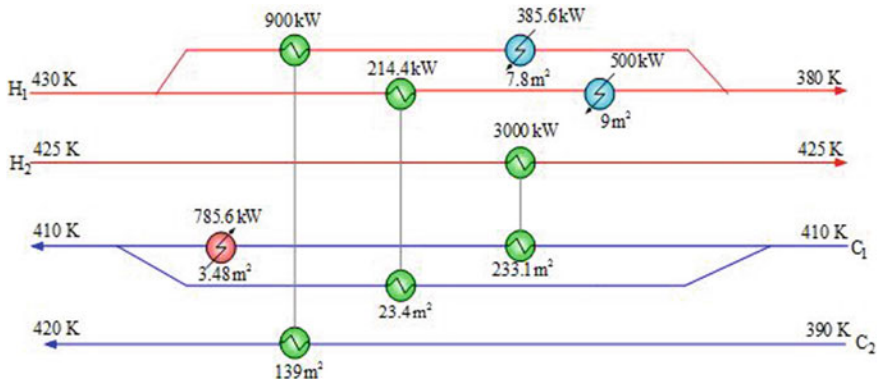


Fig. 5 HES graph obtained using the proposed method

An analysis of the obtained results showed that the structure of the heat exchange system shown in Fig. 5 is characterized by a lower value of the economic criterion (116.87 USD/year) in comparison with the structure obtained using the SYNHEAT program (166.95 USD/year) [19, 20]. Note that the calculated value of the criterion is 30% less than that found using the integrated approach to the HES synthesis of the considered example.

4 Conclusion

The conducted thermodynamic analysis of the oil refinery showed the low efficiency of the existing heat exchange system, which is explained by the use of units with air coolers, irrational costs for the utilization of low-potential energy, which can be redirected for the initial heating of the input flows of the system. A pinch analysis for a complex of interconnected units has shown the promise of solving the optimal heat integration problem for a complex of refinery units. For this, a new algorithmic method for the synthesis of optimal multistage heat exchange networks with the separation of material and heat flows is proposed, which makes it possible to minimize the computational and time costs for solving large scale problems.

Acknowledgements The research at Kazan National Research Technological University was supported by the Ministry of Science and Higher Education of the Russian Federation grant “Energy and Resource-Saving Processes for Separation of Liquid Mixtures for the Separation of Industrial Solvents”.

References

1. Zhong, R.Y., Xu, X., Klotz, E., Stephen, T.: Newman intelligent manufacturing in the context of Industry 4.0: a review. *Engineering* **3**, pp. 616–630 (2017)
2. Lisitsyn, N.V., Krivospitskii, A.N., Kuzichkin, N.V.: Optimum control of a crude oil processing Plant. *Theor. Found. Chem. Eng.* **3**(36), 273–278 (2002)
3. Song, R., Wang, Y., Panu, M., El-Halwagi, M., Feng, X.: Improved targeting procedure to determine the indirect interplant heat integration with parallel connection pattern among three plants. *Ind. Eng. Chem. Res.* **5**(57), 1569–1580 (2018)
4. Tovazhnyanskii, L.L., Kapustenko, P.A., Ul'Ev, L.M., Boldyrev, S.A., Arsen'Eva, O.P., Tarnovskii, M.V. Thermal process integration in the AVDU A12/2 crude distillation unit during winter operation. *Theor. Found. Chem. Eng.* **6**(43), 906
5. Bagajewicz, M., Valitinson, G., Nguen Thanh, D.: Retrofit of crude units preheating trains: mathematical programming versus pinch technology. *Ind. Eng. Chem. Res.* 2013, V.52, analysis (PA) and mathematical programming (MP). *Curr. Opin. Chem. Eng.* **4**2, 14913–14926 (2013)
6. Klemeš, J.J., Varbanov, P.S., Walmsley, T.G., Jia, X.: New direction in the implementation of Pinch Methodology. *Renew. Sustain. Energy Rev.* **98**, 439–468 (2018)
7. Linnhoff, B., Flower, J.R.: Synthesis of heat exchanger networks. I. Systematic generation of energy optimal networks. *AIChE* 1978, **24**, 633–642 (1987)
8. Biegler, L.T., Grossmann, I.E., Westerberg, A.W.: *Systematic Methods of Chemical Process Design*. Prentice Hall PTR, New Jersey (1997)
9. Tsirlin, A.M., Akhremenkov, A.A., Grigorevskii, I.N.: Minimal irreversibility and optimal distributions of heat transfer surface area and heat load in heat transfer systems. *Theor. Found. Chem. Eng.* **2**(42), 203–210
10. Biegler, L.T.: *Nonlinear Programming: Concepts, Algorithms, and Applications to Chemical Processes*, (2010). Philadelphia: Society for Industrial, Applied Mathematics, and Mathematical Optimization Society (2010)
11. Grossmann, I.E., Yeomans, H., Kravanja, Z.A.: Rigorous disjunctive optimization model for simultaneous flowsheet optimization and heat integration. *Comput. Chem. Eng.* **22**(Suppl.), S157–S164 (1998)
12. Yee, T.F., Grossmann, I.E.: Optimization models for heat integration – II. Heat exchanger network synthesis. *Comput. Chem. Eng.* **14**, 1165–1184 (1990)
13. Cerda, J., Westerberg, A.W.: Synthesizing heat exchanger networks having restricted stream/stream matches using transportation problem formulation. *Chem. Eng. Sci.* **38**(10), 1723–1740 (1983)
14. Cerda, J., Westerberg, A.W., Mason, D., Linnhoff, B.: Minimum utility usage in heat exchanger network synthesis. *Chem. Eng. Sci.* **38**(3), 373–387 (1983)
15. Papoulias, S.A., Grossmann, I.E.: A structural optimization approach in process synthesis II. Heat recovery networks. *Comput. Chem. Eng.* **7**(6), 707–721
16. Ziyatdinov, N.N., Ostrovskii, G.M., Emel'yanov, I.I.: Designing a heat–exchange system upon the reconstruction and synthesis of optimal systems of distillation columns. *Theor. Found. Chem. Eng.* **2**(50), 178 (2016)
17. Ziyatdinov, N.N., Emel'yanov, I.I., Lapteva, T.V., Ryzhova, A.A., Ignat'ev, A.N.: Method of automated synthesis of optimal heat exchange network (HEN) based on the principle of fixation of variables. *Theor. Found. Chem. Eng.* **2**(54), 258 (2020)
18. Ostrovsky, G., Brusilovsky, A.: On decomposition optimization methods of complex chemical-technological systems. *Comput. Chem. Eng.* **32**(12), 1527 (1977)
19. Ziyatdinov, N.N., Emel'yanov, I.I., Tuen, L.Q.: Method for the synthesis of optimum multistage heat exchange networks. *Theor. Found. Chem. Eng.* **6**(52), 614 (2018)
20. Yee, T.F.: Simultaneous optimization models for heat integration—II. Synthesis of heat exchanger networks. *Comput. Chem. Eng.* **10**(14), 1165 (1990)

Predictive Systems for the Well Drilling Operations



O. V. Zhdaneev , K. N. Frolov , and Y. A. Petrakov 

Abstract The article outlines the potential for the development of predictive systems for the drilling operations, as well as the main criteria that will determine technical requirements for research and development in these areas. Operational drilling efficiency improvements would include a whole range of options from developing solutions to decrease non-productive time (NPT) (e.g. by selecting optimum drilling parameters) to equipment performance analysis in order to predict equipment failures. The key areas where digital prediction systems could be implemented are the following: remote monitoring of drilling operations; predictive rig maintenance and repair system; predictive NPT recording and analysis system; geosteering, geomechanics, and petrophysics soft-ware; drilling failures prediction and prevention during drilling oil and gas wells; automated drilling system; and well-targeting technology system. The standalone software packages are to be combined into one automated and adaptive decision-making system based on physical and mathematical models of well construction and rock conditions. The presented study summarized a minimum number of models necessary for the operation of a predictive drilling system. The practical implementation of digital solutions in drilling is analyzed through the main approaches used in the development of predictive analytics algorithms. The basic assumptions for all algorithms are formulated to ensure the limitations of the developed model. Also, technical requirements are formulated for a uniform data collection and storage system that is the foundation of the predictive analytics block.

Keywords Oil and gas well drilling · Prediction system · Drilling decision making system · Big data · Artificial intelligence · Industrial IoT (internet of things)

O. V. Zhdaneev (✉) · K. N. Frolov
Technology Development Center for the Energy and Fuel Complex of Russian Energy Agency of Ministry of Energy of the Russian Federation, Moscow, Russia
e-mail: Zhdaneev@rosenergo.gov.ru

Y. A. Petrakov
Geonaft (Zyfra Group), Moscow, Russia

1 Introduction

Today a typical well drilling process often is driven by a single person—a drilling engineer who is fully responsible for the end result: a well drilled in time and according to the good plan. This may be an employee of the drilling contractor (in case of the turn-key contract type), the general contractor, the license holder (the case of the day-rate wells), or the engineering service contractor (both turnkey and day-rate contract).

The range of good data obtained during and known prior to drilling are:

- Drilling torque, standpipe pressure, and other surface measurements—a total of 20 parameters—measured and transmitted by the Drilling Data Management System (DDMS). The persons responsible for gathering and transmitting the data are the electronics engineer or/and the geophysicists.
- Downhole measurements, i.e. measure while drilling (MWD) and logging while drilling (LWD) information gathering. The amount of data transmitted from the downhole is discretionary and depends on the capabilities of the communication channel. L/MWD engineer is in charge of this set of operations.
- Drilling mud parameters, mostly measured manually by the mud engineer; several properties such as mud weight (MW) could be measured by the DDMS sensors.
- Cuttings are collected by mud logging engineer in some cases alongside with wellsite geologist. The cuttings analysis report is then distributed to involved parties.
- Running hours, failures, threshold loads, and downtime due to critical failures of mechanical, power, and electronic surface equipment are recorded by the mechanic and power/electronic engineers. In some cases, additional information may be provided by a solids control mechanic, top drive system mechanic.
- The rig manager and company man are responsible for the driller's and rig crew's activities, coordination of all parties presented on site.
- Real-time downhole geological data gathering is the geologist or the geosteering engineer (for the horizontal section of the well) responsibility.
- The geology data from the previous coring and logging operations, drilling parameters embedded in the Drilling Pro-gram, wellbore stability, and hydraulics calculations are pre-pared before spud.

These specialists quite often utilize different software and process control systems that are not emerged into a single platform [1], not fully synchronized in a timely fashion (sometimes the system is just a pencil and a pad).

Obviously, a single person cannot exercise full control using all this real-time data coming all at once. The responsibility and authority to make decisions are split between different engineers. Quite often to make the only right decision, each of these engineers de-pends on the data from other colleagues. It is also to be noted that in drilling, due to technological specifics of at surface and down-hole operation and, above all, due to geological conditions, a successful end result (the producing well) depends on timely action when every minute or, oftentimes, every second count.

The unleashed opportunity to radically increase drilling efficiency is timely decision making based on analysis of a large volume of disjointed data together with the output of an automated prediction system.

2 Machine Learning in Drilling

A well is drilled in several stages, each involving recurrent macro processes that may be broken down into individual operations. An ongoing process in the well is determined by a combination of certain parameters and conditions. The engineer receives data on these conditions from different sources. Besides seeing what is happening at that given time, he receives daily reports from all parties involved in the drilling process. The sum total of this information forms the large picture of the drilling process. Assessment using analytical tools may help predict the failure of certain risks and prevent undesirable events. This is where big data analysis could assist [2]. For example, drilling mechanics data is transmitted, as a rule, every second. There may be more than 100 channels, including data from MWD and surface equipment. With the average well drilling time measured in weeks or months, the total amount of information received is indeed the so-called Big Data [3].

The main challenge for using machine learning in drilling is two-fold:

1. Feeding AI algorithms with all available information as possessed by the engineer in charge and other involved parties. Authenticity and completeness of data is the key challenge.
2. Obtaining a tool that will supply the user with anticipated decisions to increase operational efficiency and reduce drilling and geology-related risks.
3. Successful results of drilling a well depend on implementation technology and systems that can be fairly extensively controlled by humans, but also control of the less predictable and manageable geological factors. Predicting the behavior of certain drilling technology in a given field may be difficult as various factors come into play, e.g. tectonic faults, lithological or stratigraphic heterogeneity, etc.

Quite often the drilling engineer does not immediately recognize changes in the process. The objective of using machine learning is to anticipate things that a human may miss or is unable to detect. In the case of the latter, applying the mathematical approach can assist in solving the problem.

Exemplified on one well, the number of factors affecting drilling efficiency may be divided, on the first level, as follows: drilling mode; operation parameters and reliability of surface process systems of the rig; well profile; well and casing design; BHA; drill string; drilling mud parameters; geological specifics; human factor across the whole process of control and supervision of good drilling.

Each of these may be split on the second level of detail. For example, the good profile includes: well type: vertical, directional or horizontal; actual dogleg severity; vertical and measured well depth, length of a given section.

This example may be used to show how each listed parameter affects the “outcome” of each operation, e.g. tripping. In a vertical, well tripping may be conducted in a quick manner and without particular downhole issues. In a directional well, several problems caused by rapid build-up rates and tortuosity can be met while tripping. For apparent reasons, the length of the section intensifies the difficulties described. Cuttings may have a critical impact on drilling directional and horizontal wells if not sufficiently removed from the wellbore.

This exemplifies just one of the tens of blocks that characterize well drilling; they, in turn, depend on other blocks. All this makes the prediction of certain events very difficult and seemingly requires permanent human control.

3 Main Areas of Implementation of Digital Predictive Solutions

Seven worldwide digital technology priorities are applicable to the improvement of drilling rigs and drilling operations: big data, AI (artificial intelligence), industrial IoT, robotic components, wire-less technology, VR (virtual reality), and AR (additional reality), new manufacturing technology. Applied to current good construction time averages, it is projected that the introduction of these technologies can reduce drilling time by at least 20% for a directional well and 30% for a typical horizontal well [4].

This chapter touches upon the main areas of implementation of predictive control systems in drilling. Listed for each are the main specifications that were calculated based on worldwide industry experience and requirements of companies participating in good construction.

3.1 Remote Monitoring of Drilling Operations

Remote monitoring of drilling operations is provided by means of DDMS, integrated into the drilling rig automation process control system. The drilling rig automatic process control system is the system based on a programmable logic controller (PLC system).

DDMS combined with predictive analysis captures the entire range of drilling parameters from the surface and downhole systems: mud logging and drilling parameters, summarizes and transmits them to a server in real-time, saves the data for the entire drilling operation, compares and analyzes it together with key performance indicators from the previous wells on the pad or nearby areas by exchanging information with the data storage/database and informs the personnel about deviations from the average statistical.

DDMS must ensure continuous monitoring and recording of the following measurements while drilling with time and depth reference (max. increment 0.1 m): total depth; bit depth; hook block position; tripping speed; rate of penetration; weight on hook; weight on bit; standpipe pressure; annulus pressure; mud flow in/out of the well; mud temperature in/out of the well; mud weight in/out of the well; mud rheology [5]; fillup mud weight; mud electric conductance in/out of the well; chlorinity in/out of the well; volume of trip tank fluid; volume of suction tank fluid; volume of mud in each storage tank; rotary table torque; rotary table rpms; iron roughneck/rig tong torque; mud pump strokes per minute; drill stand tally when tripping; displacement volume when tripping; stated interval drill-time; bottom-up circulation time; gas content— H_2S ; gas content— CH_4 ; compositional analysis of hydrocarbon gases contained in the drilling mud; total gas content in a drilling mud; nonproductive/productive rig time-referenced records; top drive rpms; top drive max. continuous torque; top drive max breakout/makeup torque; top drive pipe handler position; top drive float position; iBOP position.

3.2 Predictive Rig Maintenance and Repair System (PRMRS)

To minimize costly downtime, an extensive instrumentation package with associated software designed specifically for monitoring the condition of the main drilling equipment is to be installed. Any equipment where a reduction in performance or shut-down of operation can adversely affect the drilling operation should be instrumented. The PRMRS must be integrated into the rig automation and control system.

The system enables tracking equipment condition, record running hours (using sensors), and equipment condition prediction and, accordingly, timely notifications to the crew on the necessity of scheduled maintenance, overhaul, or unscheduled repair by preset parameters, all in real-time, on request and as automatically generated daily and weekly reports.

The system must be built on predictive analysis—timely notification of an imminent threshold event, a pre-emergency condition in the equipment [6, 7]. First and foremost, this system is applicable for automatic tracking of running hours of the following key assemblies and components: tubular, bottom hole assembly, drill line, top drive system, draw works, crown block, iron roughneck, mud pumps, centrifugal pumps, and solids control equipment.

As a result, this system will reduce maintenance costs and increase fail-free operation time of equipment. The goal is to provide a NPT level that will not exceed 0.1% of the total operating time.

3.3 Predictive NPT Recording and Analysis System

An automated system for measurement and analysis of efficiency in performing drilling and well construction operations; includes a defined set of key efficiency indicators to measure and assess the rig's operation efficiency, as well as to reveal "hidden NPT". Actual readings are matched against preset standards, best practices, or standardized times established by the customer. Based on this comparison efficiency of performance of a given operation is calculated.

Over drilling one well, operating algorithms of the system jointly establish the possible number and duration of tripping, depending on the status of all systems and parts involved, maximum possible duration of the run, circulation, etc.

Objectives:

- Excluding the human factor in data processing, analysis, and reporting;
- Revealing "hidden NPT" and assessing the efficiency of current operations;
- Determining the best practices of performing operations for rigs and crews;
- Reduction of the overall well construction time and optimization of operational costs;
- Improvement in coordination, consistency, safety, and efficiency in running all technological processes on the rig.

3.4 Geosteering, Geomechanics, Petrophysics

LWD is gradually replacing traditional cable logging and the issue of real-time data transmission is partially resolved. Here, the future lies with automatic geological well targeting while drilling [8].

It is planned to automatize the following stages of geological targeting: preliminary geosteering modeling and geosteering when drilling. The crucial matter for both stages is determining the formation dip where the dip angle changes and determining the degree of tilt.

Neural networks will resolve the issue of digital selection of formation angle dips. It is the geological targeting engineer who will make the final decision. But there will be a vast list of typical automatic actions.

The degree of tilt must be determined with a minimum difference between the actual curves and the curves obtained through strati-graphic modeling, classic comparison, and modeling of electro-magnetic survey tool response. Preparations during initial model-ling include determining seam structure behavior based on a projection of 3D surfaces onto the horizontal well log. The structure's surface of a stratum is built on previous wells and seismic data. During drilling, the modeled data is compared to the actual logging data gathered within the section.

The initial approach to automatic geological targeting of a well is built on the development of a mechanism for automatic plotting of the geosteering model curves.

This is based on existing markers in the (previously drilled) offset wells and the wells being drilled.

An offset well is chosen from already wells drilled nearby. Results of geophysical logging in the offset well will determine the predicted geological properties of each good section. Then the function of automatic calculation of formation angle dips is applied to selected data. Marker intersection points on the offset well log are superimposed with marker intersection points on the actual well on the path. Cognominal markers in actual and offset wells are determined by string character comparison of marker names with regard to formation behavior angles.

Further automation of geosteering is achieved by the implementation of the DTW (dynamic time warping) algorithm for automatic correlation of logs in the offset and well being drilled. The integration of the algorithm into the digital selection of formation angle dips will enable the creation of a geological model building system for full automation of the drilling process with minimum human input. It is proposed that the automated geomechanical and petrophysical engineering modules be introduced in a fashion similar to the development of the autogeosteering module development.

3.5 Drilling Failures Prediction and Prevention During Drilling Oil and Gas Wells

Drilling failures prediction and prevention system used to generate, optimize and ensure a single working schedule of drilling division (several rigs) or every drilling crew for certain scenario options, developed using an integrated model of work and taking into account risks. The system should provide the coordination and co-operation of various services and agencies in the formation of a single drilling engineering flow chart. Special mathematical methods are used to optimize the operational plan including an adaptive approach based on machine learning algorithms.

The system is collecting, storing, and displaying large amounts of data on a drilling rig: Drilling data; Surface and downhole equipment data; Equipment alarms; Equipment events (for instance up to replacement of mud pump liner); Boundary conditions: drilling modes, surface, and downhole equipment.

It is necessary to have a client application for displaying and analyzing historical data from rig database system with integrated screenshot capability and comment function. This application is installed on one or two driller's position in a drilling control room and two workstations at the pad. Also, it has to prepare customized predefined reports, for instance, standard ones: Trend, Alarm, and Comment reports. External software packages should be able to integrate into the application: drilling equipment preventive and maintenance system; non-productive time recording and analytical system; geo-steering data; data drilling measuring system; geomechanics and petrophysical model.

An optional server must be added on shore to consolidate data and information from multiple Rigs.

3.6 Automated Drilling System

The software is designed to combine the monitoring and control of both main surface and downhole equipment used in drilling. It controls the drilling equipment and systems to operate within adjustable limits—at least 12 (twelve) parameters simultaneously, such as: weight on hook; manifold pressure; bottom hole annulus/pipe pressure; drill string rpm; the rate of penetration; drilling torque; mud weight out of the well; azimuth; inclination; bottom hole temperature; gamma-ray; bottom hole resistivity, etc.

The system gives the following benefits:

- the system allows for a much faster rate of penetration of good sections with different hardness stringers;
- reduced drill bit damage and wear, by means of reducing vibration load which allows lowering meterage costs;
- improved safety due to smoother drilling operations.

3.7 Well Targeting Technology System

Automatic position reference system for RSS on a preset path with adjustment for drilling equipment parameters, geology, mud properties: Inclination; Azimuth; Min. 8 sectors azimuthal survey; GL; IRL; Litho-density GGL; NNL; Sonic log; NML (optional); BHT; String and annular pressure.

The BHA steering software must include geological and technological targeting tools, namely:

- Geosteering [9]—determining a good position in the formation relative to its boundaries, mitigation of geological risks in drilling outside the target section.
- Petrophysics when drilling [10]—establishing formation sections with the best reservoir properties and a good position in these sections.
- Real-time geomechanics [11]—drilling risk management, algorithms for prevention of borehole instability-related emergency, cave-in and lost circulation detection, oil & gas show prevention, and autofrac.
- Well targeting by technological parameters and accident/failure prevention—assessment of the current borehole condition, drilling technology-related risks, statistical analysis of drilling parameters recorded by the autodriller system:
 - Data visualization and storage with time reference;
 - Automatic split by process operations;

- Console with key indicators of the technological status, drilling parameters mnemonics, mud motor tool-face, or RSS position display;
- Calculation of modeled weight and torque curves for different friction factors;
- Borehole condition monitoring by automatic measuring of weights and torque, and superimposed on the calculated curves for different friction factors;
- Conversion of time data into a depth format with user filters for analysis;
- Time versus Depth curve with automated deviation control from plan time.

All of the above must have the following functions. Downloading data both from file and by using WITSML format. Updating the physics-mathematical models with new incoming data. Comparison of projected and actual readings. Signals to users and interacting parts of the system if the actual readings deviate from projected ones, safe limits are breached, or in presence of accumulated or systematic deviations. LWD is gradually replacing traditional cable logging and the issue of real-time data transmission is partially resolved. Here, the future lies with automatic geological well targeting while drilling [8].

3.8 Automated Adaptive Drilling Decision-Making System

A predictive system controlling a drilling rig and the whole drilling process must contain a number of standalone software programs united in one automated and adaptive decision-making system based on a common digital platform. All standalone software programs described in this chapter must be able to operate together following an assigned algorithm as part of the proposed automated and adaptive platform—the drilling decision-making system [12].

Automated implies the ability to make independent decisions, within its frame of reference, without human input.

Adaptive implies the ability to retrain under changing outside influence and adapt to it.

Each dedicated software program must be able to be used both separately, independently from the common platform, and as part of the latter, ceding control over functions dependent on the general technology of good drilling.

The automated and adaptive decision-making system consists of two subsystems (see Fig. 1):

1. Local Integration System. The main control and execution function in the operation of a drilling rig. The local system brings together operator-selected independently operating rig software/systems and assigns a joint operation algorithm by their current readings in automatic or manual mode. A set of algorithms must be predetermined so that only the operator is able to alter algorithms, on his own or on instructions from a remote analytical system;
2. Remote Analytical System. The calculating and analytical function. This system accumulates all data coming from the drilling rig and compares to the data in up-loaded databases from previous wells or neighbor rigs if any.

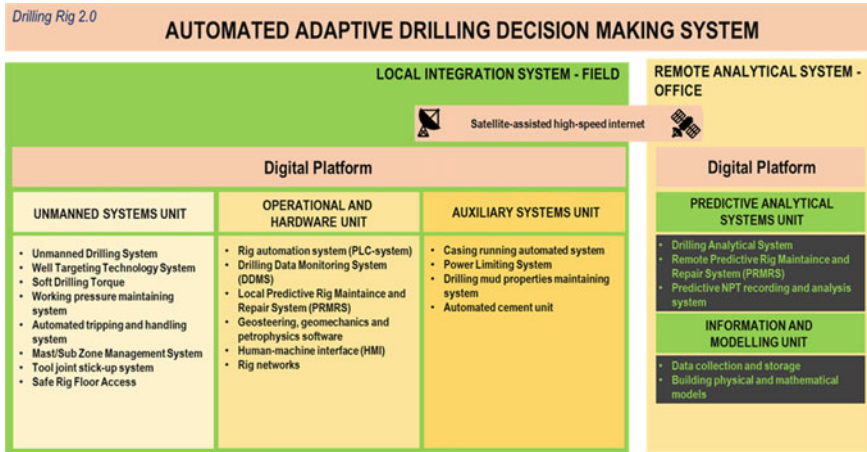


Fig. 1 Automated adaptive drilling decision-making system

Following the results of the analysis, it must issue instructions to alter the initially as-signed algorithms for operation of local subsystems directly on the rig, or make recommendations on changes in the BHA, mud, etc. The algorithm-altering instructions must be verified by operating engineers.

It is important that the operator be able to immediately intervene in the operation of any system or stop the process at any stage of the automatic operation of any rig soft-ware algorithm.

The digital platform provides the basis for the automated and adaptive drilling decision-making system and integrates all standalone rig software programs that enable the operation of surface and downhole process systems. The platform’s purpose is to process, analyze, and visualize the data coming from various engineering software.

The platform must meet the following requirements. Storing geological, technological, and technical project data, as well as data received from each local rig system. Transmit data via modern high-speed protocols. Enable downloads and uploads of data in the system’s internal formats, as well as in all main standards formats of data exchange. Provide a programming interface with the option to install optional outside software. Have the ability to simultaneously use the platform and in-dependent soft-ware by several operators both locally (in the field) and remotely (in the company’s office). Must have a controlled procedure and conditions for user access to objects of the information system. For example, a base case is when the system is operated both by a user and his supervisor, with corresponding sets of rights. Ability to plug in accumulated databases of production, geophysical, and other service companies for exchange of data, and running consequent inclusive analysis.

Ensure security of the system, access is given only to authorized persons; and have the ability to encode and back up repository data. There also must be tools to analyze activities and search for anomalies in user actions. Be able to operate,

run calculations with data from the platform by preset software algorithms, and in manual mode. Enable distributed operation of the predictive analysis software block—local and remote.

4 Practical Implementation

An adaptive and automated digital drilling decision-making system built on machine learning and big data classification and analysis may perform a range of tasks in drilling oil and gas wells.

The task given to the whole machine learning (ML) community by the oil industry in general and drilling in particular include is to increase in efficiency, as in any other technological process. Drilling efficiency may be increased by various improvements in the process. This includes a whole cluster of tasks ranging from developing solutions to reduce non-productive time (e.g. by selecting optimum drilling parameters) to equipment performance analysis in order to predict premature failures and automation of the hand-shake of process control and information systems.

The selection of a method of big data analysis and building predictive models largely depends on accurate wording and clear-cut tasking.

For example, reduction of NPT during drilling may be achieved, among others, by preventing emergencies and complications. When stating such tasks, all possible types of complications to be predicted by the developed algorithm must be determined. Drilling-related complications are to be broken into several groups: Stuck drill and casing string; Borehole stability; Lost circulation; Oil and gas kicks; Complications when drilling in permafrost; BHA and drill string failures; Issues caused by emergency shutdowns of the rig or of any of the primary drilling equipment.

Each group includes several subgroups. There are more than ten main causes for stuck pipe: differential pressure, abnormal formation pressure, highly reactive formations, uncompacted rock, mobile strata, cracked and fractured formations, keyseating, bore-hole geometry, insufficient hole cleaning, junk in the hole, premature cement set, casing string collapse, etc. Any one cause may combine with any or many others simultaneously. Such problems are resolved by finding statistical signs and hidden dependencies between input parameters. The success of such algorithms depends largely on the learning sample size for various scenarios and covering the whole range of situations.

During the course of drilling a reverse task may be formulated, e.g. prediction of success and/or quality of tripping. In this case, the analysis must be made of the whole spread of available information about the well. Tripping is one of the riskiest operations, it is during tripping that borehole conditions deteriorate most often. In such a case, the set of signs for the development of an algorithm must be based not so much on statistical values but rather on the physical principles of the drilling process. Some of the conditions for successful tripping are: good hole cleaning; smooth borehole without ledges; borehole stability, no cavings; sufficient mud weight; BHA type; optimal pipe travel speed.

Each condition requires a certain set of actions to be taken. Good hole cleaning pivots on maintaining high drilling parameters; also, cleaning time greatly affects the volume of transported cuttings and free passage of the string. To ensure a smooth borehole without ledges, equal amounts of rotary and directional drilling must be alternated (if drilling with a downhole motor). A sufficient amount of reaming is required when drilling through hard drilling intervals or if there is a risk of ledges during a change in lithology, which may also cause complications.

As stated above, drilling through heterogeneous rocks directly affects the course of operations. Before the actual drilling, rock properties may only be assessed with a certain allowance for error and after penetration with measurements obtained while drilling. The geology and all related non-uniformities also weigh in significantly on the precision of the developed algorithms. But accounting for geology is a separate and significant type of work.

Search for such engineering and technological dependencies in many ways complicates and draws out the development of predictive algorithms since it is not a purely statistical approach. However, only such systems will show great resilience when scaled.

This exemplifies that, predicting complications is an intricate task to be approached from many directions, adding and not missing important variables. A solution to these problems may not be unattainable—if machine learning and AI are not tasked with it.

4.1 Overview of Approaches Used in the Development of Predictive Analysis Algorithms

Machine learning equips a researcher with a formidable arsenal of means for solving predictive analysis tasks [13]. Information on the choice of various ML algorithms depending on the type and conditions of a task is common knowledge. This section will detail some specifics of applying ML for predictive analysis specifically to the drilling process. For clarity let us review a class of tasks related to the prediction of complications.

In data science, this class of tasks is traditionally associated with the search for anomalies and offers more than ten already developed algorithms [14].

Narrowing down the selection of suitable algorithms is helped by the specifics of predicting complications. As a rule, this class of tasks presents a problem of an extremely low number of real examples of complications. One needs to be ready to operate with no more than a couple of revealed “events”, or whatever is available.

Such scarce statistics makes it difficult to use classic supervised learning [15, 19]. The researcher will also have to abandon deep learning [16, 17] and reinforcement learning [17, 19], concentrating instead on unsupervised [17–19] and semi-supervised learning [19].

It is hard to say beforehand which approach (density, cluster, correlation, etc.) would yield the best result for the given task. In the end, it all boils down to trial and error. Therefore, we will limit ourselves to general recommendations on arranging the process of machine learning.

Traditionally, the very first thing to do is start with the simplest method easily understood by the researcher, gradually moving on to the more complicated. Even if this does not yield a direct result, it helps to study the specifics and regularities of the studied dataset which, undoubtedly, is useful for the application of more complicated ML methods.

Then, whichever way of research is chosen, the account is to be taken of the structure of the data which represents the timing series of drilling mechanics, as well as satellite information on the path, mud properties, etc. As a rule, there are few timing features per se: the number of independent useful channels by timing series rarely exceeds ten (DBTM, DMEA, BPOS, HKLA, TQA, MFIA, SPPA, RPMA, TVT...). By brute force or from the very nature of the task, it will soon become apparent to the researcher that no combination of features at the one-time point in itself may be a sufficient criterion to detect complications—as a longstanding temporal event.

Thus there needs to be established a floating window with an empirically fitted period in which various combinations of features would be collected. Here, the researchers may be helped by packages similar to *tsfresh* [20] that enable mining of thousands of product features including statistical and correlation properties of basic features. A separate and complicated task is the correct reduction of dimensionality and feature extraction.

The main help in distributing features comes from methods of data classification by sections, types of movement, types of operation, stands, etc.

Among the main methods are [21]:

1. Variation in prognosis (prediction of basic-derived features using ARIMA / XGBoost and comparison of predicted results with actual ones);
2. Correlation spike (using correlation factors of individual basic or derived features as standalone features of complication);
3. Density spike (singling out feature distribution density and observing significant changes in the distribution);
4. Non-linear algorithms (violations of non-linear logic).

They all have their advantages and drawbacks, but it is important to remember that, essentially, they all boil down to searching for the correct conversion of features into a dimension where the emergence of a complication may be more or less clearly identified. That is, the output of such a conversion is assumed as a timing series of a generalizing indicator, deviations in which may be interpreted as a probable complication.

4.2 Hybrid Modelling

The methods described in the previous section fall under statistical methods. Such algorithms must lead to a true solution to the problem described. In real life, however, things turn out to be not quite as simple. Blindly generated thousands of features combined with an almost complete absence of a training dataset create a problem of ambiguity in the interpretation of the results obtained.

Indeed, consistent selection and feature extraction by themselves do not prevent ambiguous results due to the inevitable presence of a number of so-called “chimeras”, complicated synthetic features without any physical sense that by chance fit well into a small training sample [22]. They may well include true solutions. But, it is rather difficult to separate them by feel, thus ensuring univocacy. Each iteration of amplification of features requires more and more calculation facilities.

Hybrid modeling is used to overcome the problems described. The essence of hybrid modeling is in the combined use of statistical and physical–mathematical modeling, combined participation of specialized approaches of the subject area, and mathematical big data analysis in problem-solving. The synergy is achieved by iteration exchange of results, continuous two-way communication.

Here, it is crucial to maintain a balance between the statistical and physical component. ML algorithms must not be built on the simple use of rules, physical dependencies of the data domain and record them in an (if/then) system, after which adjusting numerical factors and passing it off for pseudo ML. Experience shows that similar strictly controlled rule systems, in the end, do not stand up to scaling.

It would be more proper to transform physical modeling approaches into directional guidance, a combination of features that, proceeding from the physics of the process, maybe precursors of the events being predicted. This allows a significant narrowing down of the search and quick isolation of the “chimera” branches created by ML. In the same manner, by using just the physical fundamentals of the process, efficient collation of values of some empirical parameters may be made, such as the size of the screen of the floating time window.

Generally, the correct operation of a hybrid model seems to be iterative and must resemble ping-pong, when building physical models with insufficient data is complemented with results of statistical ML modeling, and the obtained calculation results are used as the foundation of a full-scale ML algorithm.

If we take drilling, the simplest example of hybrid modeling may be presented as follows. When assessing bottom hole pressure (BHP) during drilling, physical modeling implies a calculation of pressure losses due to friction in each part of the circulation system and the drill string downhole with consideration to rheological parameters of the mud, as well path and design. An ML algorithm, however, would be based on looking for obvious and hidden dependencies between input parameters (e.g. drilling mechanics, logging) and the output parameter of BHP in a training set. Then, as drilling continues, the algorithm must reconstruct the value of BHP using recorded values of input parameters. Both approaches have obvious drawbacks. Hydraulic calculation during drilling is always complicated by not knowing the exact

values of many input variables, from the exact rheology of the mud at BH to the volume of cuttings transported from the well at each moment in time. Whereas the statistical approach with any size of a training set will always be limited by the completeness and quality of the data based on which the real-time prediction would be made. In this case, the synergy of these two approaches enables complementing the hydraulic calculations with the values of missing parameters assessed statistically and inputting the obtained results into an ML algorithm for further calibration of results.

4.3 Assessment Criteria for ML Solutions

An important aspect of the development of big data analysis algorithms is a quality assessment of the system operation and obtained results when implementing solutions. The criteria, except basic accuracy, are as follows: expansion of assessment, adjust-ability of the model, noise resistance, and interpretability.

To assess the majority of ML solutions, it is absolutely insufficient to know that its accuracy is, say, 94.5%. A combined approach is necessary, including analysis of roc-auc and precision-recall curves, etc. [23, 24]. The solutions must contain setup parameters, the so-called threshold values.

As far as prediction tasks are concerned, it is important to interpret the obtained results correctly. It is important to pay attention to the coordinates of predicted quality curves. For example, an 80% prediction accuracy of a certain event and 7 false responses over a full day mean that, with the average duration of drilling a well and the real number of instances of such events, more than 95% of the signals will be false. Understanding this immediately raises a question of the usefulness of such accuracy in real drilling.

In real life, after the system is implemented in operations, the output data received may contain noise, spikes, and faults in some sections. The resistance of the ML system to various types of problems with input data is yet to be determined. To this end, the model undergoes separate tests, results of which are important to be familiar with in order to have an idea of what to expect in the field.

The next criterion is interpretability. ML algorithms are commonly perceived as a thing of great mystery, i. e. the system works but the principle of operation cannot be explained because the neural network is too complicated. Such an approach is counterproductive. The interpretability of results must be there. Developers of the algorithm must be able to understand the basic operating principles of their ML solution. Even for complicated neural networks, there are many methods of visualization and interpreting the results obtained. Until result interpretation is refined it is wrong to assume the algorithm development is complete; there remains a high probability of ending up with a “pig in a poke”.

Hybrid modeling contributes to the assessment of the authenticity of the results obtained. Due to extremely limited sample scope, with any solution efficiency criterion there always remains a doubt as to the degree of correctness of the algorithm

operation. It would seem that the answer to this question lies only in the collection and testing of the solution in yet new cases. However, besides the quantitative (statistical) confidence there also exists qualitative confidence based on the exposure of the internal physics of the process. Ideally, ML research must reveal some not-so-obvious dependencies. It is such a scientific approach that helps to gain qualitative confidence in the results obtained.

4.4 Data Collection and Storage

Practical implementation of digital solutions in drilling necessitates the establishment of a uniform system that enables collection and storage of historical data, real-time data, and design data for a field, website, neighboring fields, and all company assets:

- Storage of metadata (company name, field name, pad number, well number, etc.);
- Storage of wellsite modeling results (field/cluster/pad/region/basin)—geological, hydrodynamic, petrophysical, geomechanical models);
- Collection and storage of depth data—data on drilling mechanics, logging data, well testing and sampling data, core examination data, and other geological and technical information about the wellsite;
- Collection and storage of time data, namely, real-time drilling mechanics (logging) data, including the main parameters characterizing and describing the drilling process (hook load, hook height, bit depth, BHA, torque, WOB, RT or TD rpms, stand-pipe pressure and BHP, mud in and mud outflow, tank volumes, etc.), as well as historical data;
- Storage of nameplate/reference data, including: type of drilling operations; type of complication/emergency during drilling, bit and drill string diameters and types, lithotypes, mud parameters, etc.;
- Storage of lessons learned data compiled after operations in blocks of predictive analysis & operation control and un-manned drilling;
- Algorithm for converting drilling mechanics data from time to depth based on data from “BH” and “bit depth” channels;
- Filling in the established databases manually by users with corresponding roles, or automatically when setting up access to Customer or contractor databases, or directly from the blocks of predictive analysis & operation control and unmanned drilling;
- Manual filling-in of databases requires a special loader that recognizes the main data formats accepted in the industry (csv, txt, las, ddis et al.);
- Automatic data loading requires loaders (connectors) that take into account the structure of data storage in each specific base, e.g. based on WITSML;
- Authorized users must be able to edit the established databases (including adding new parameter catalogs intended to be accumulated in the established databases).

Besides collection and storage, the system must incorporate algorithms controlling the quality of incoming information.

4.5 *Building Physical and Mathematical Models*

The functioning of the predictive analytics block of the automated and adaptive drilling decision-making system is based on physical and mathematical models of good construction and rock conditions.

Software for building physical and mathematical models should include the following minimum set:

- Loading and visualization of data from the data collection and storage system;
- Tools for working with curves, 2D entities (maps, polygons, surface, projections), and 3D entities (property volumes, seismic data, geological, reservoir simulation, geomechanics models);
- Integrated calculation algorithms for petrophysical proper-ties, such as:
 - Calculation of shale volume based on data from different logs (gamma-ray, spectral gamma-ray, combined neutron-density logs);
 - Calculation of porosity (effective and total) based on density logs, neutron log, acoustic log, cross-plot neutron and density logs, cross-plots neutron, density, and photoelectric factor logs;
 - Calculation of saturation based on the Archie-Dakhnov and dual-water equation;
 - Calculation of permeability based on core equation, taking into account geochemical permeability and well testing and sampling results;
 - Lithology determination based on a set of logging data from different tools;
 - Calculation of reservoir conditions: fluid density, well temperature, well temperature gradient, formation fluid salinity, mud density and resistivity, hydrostatic pressure;
 - Building of volumetric rock models.
- Tools for wireline and LWD data processing (basic and special logging):
 - to build histograms and cross-plots for statistical da-ta evaluation;
 - to splice and coordinate depth curves;
 - to smoothen, interpolate, and despiking curves;
- Integrated algorithms for calculation of stress–strain proper-ties:
 - Calculation of dynamic elastic properties (Yong’s module, Poisson Ratio, Share module, Bulk module);
 - Building a correlation to cross over from dynamic to static properties;
 - Integrated widely accepted dependencies to cross over from dynamic to static properties (Young’s module, Poisson Ratio, Shear module, Bulk module);
 - Ability to write scripts and use user equations;
 - Integrated algorithms to calculate strength property profiles (unconfined compressive strength, tensile strength, friction angle);
 - Building projection of rock strength;

- Integrated algorithms for in-situ state modeling for near-wellbore volume and/or for oilfield/pad/region:
 - Overburden pressure calculation;
 - Pore pressure calculation. Available methods: Eaton methods (based acoustic, resistivity, drilling parameters (D-exp)), Bowers method, Fluid density from reference point or surface above;
 - Horizontal stresses profile calculation based on the poroelastic model for isotropic layers;
 - Horizontal stresses profile calculation based on the poroelastic model for anisotropic layers;
 - Calculation of horizontal stresses with thermal effects;
 - Calculation of horizontal stresses with depletion or injection effects;
- Ability to create user algorithms;
- Algorithms to build geosteering cross-sections (models):
 - Building a geosteering model with thickness changes and pinch-out;
 - Building a geosteering model with tectonic deformations (faults);
 - Geological surface update based on actual data and geosteering models;
 - Interpretation of azimuthal logs for clarification and correct determination of bedding angle;
- Tools to prepare pre-drilling models: geosteering, petro-physical, geomechanics;
- Tools to build drilling and geological risk maps based on geosteering, petro-physics, and geomechanics models:
 - Determination of geological risks of well location in the reservoir;
 - Determination of geomechanics risks:
 - Kick gradient;
 - Breakout gradient;
 - Lost circulation gradient;
 - Breakdown gradient;
 - Fault stability;
 - Sand prediction;
- Software and tools to prepare a good plan, including well-bore trajectory planning, well and BHA design, hydraulic calculations for drilling and cementing, calculation of loads, torques, and drag);
- Algorithms for wellbore trajectory planning include:
 - Design of standard profiles (t, s, j – profiles);
 - Design profiles with stabilization sections;
 - Advanced design methods – exit to the point, keeping intensity, branch-curve-branch;
 - Anti-collision analysis;

- Algorithms to design casings strings, including calculation of the string/annular pressures for oil and gas wells, for vertical and directional wells;
- Algorithms to calculate loads and torques include the following calculations:
 - BH loads that BHA experiences in various operations;
 - Hook load for all operations for different friction factors;
 - Side forces at the bottom;
 - Torque multi-depth road maps and single-depth plots;
 - Drilling string bends (torsions);
 - Buckling limits for all operations;
 - Weight on a bit before buckling;
 - BH loads for casing strings during various operations;
 - Hookloads for casing strings in various operations;
- Hydraulic calculation algorithms include:
 - Calculation of rheological parameters of mud;
 - Pressure losses for all parts of the circulation system (surface, drilling or casing string, downhole tools, bit);
 - Calculation of the circulation pressure, as well as the distribution of pressure over depth during circulation;
 - Optimization of bit hydraulics based on HSI, hydraulic power, and impact force, graphical analysis;
 - ECD roadmaps calculation with wellbore stability gradients from geomechanical calculations and snap-shot chart with distribution over the entire wellbore;
 - Swab and Surge calculation for various speeds;
 - Calculation of the critical flow rate for wellbore cleaning, the concentration of cuttings, the height of the cutting bed;
 - Hydraulics summary of calculations for the run with visualization of each calculation, BHA diagram, and well design;
 - Accounting for effects of temperature and pressure in the well on the rheological mud properties;
- Algorithms for cementing design include:
 - Setting up a cementing program, selection of flu-ids for cementing;
 - Calculation of the casing eccentricity and number of centralizers;
 - Static and circulating pressures during cementing operations;
 - ECD calculation with taking into account the geomechanical model;
 - Flow in and flow out volumes calculation;
 - Calculation of surface cementing pressure;
 - Change in casing load during cementing;
 - Calculation of cement plugs;
 - Two-stage cementing.

5 Conclusion

Machine learning and big data analysis will revolutionize drilling in the next 10 years by creating and developing the predictive control systems of technical and technological (including geological) processes of drilling oil and gas wells [25]. More than 15 companies, JVs, and corporations are already working on creating full-scope or limited unified automated and adaptive decision making systems for drilling [26–28]. At the first stage, they all run into the challenges of time-consuming data gathering, digitizing, completeness and authenticity verifications, checking input data quality, and reconstruction of missing values from drilling systems. This amounts to up to 90% of the total time for the development of technological predictive algorithms.

Creation and gradual implementation of based on machine learning predictive digital solutions, their deep integration into modern drilling rigs, surface and bottom hole process systems automated on different levels will yield the following impact:

- Up to 40% reduction of OPEX for drilling operation;
- 15 to 20% reduction of CAPEX for development of new fields with benign extractable reserves, regardless of the size of the field;
- Labor efficiency will increase by up to 20% of current worldwide average values;
- Reduction of the total number of wells by drilling fishbone wells with extended horizontal sections along with the reduction of average drilling time when developing oil and gas fields;
- Creating up to 10% more new workplaces in the oilfield sector for qualified personnel compare to the total current role of engineers and hands in the industry;
- Environmental impact of surface drilling systems will decrease by an order of magnitude by rational use of drilling materials, prevention of equipment failures, including solids control equipment and drainage systems that would decrease the probability of environmental contamination to a fraction of a percent.

References

1. Zhdaneev, O.V., Lukyanchenko, P.P.: To the problem of the development of the domestic software platform. In: Problems of Economics and Management of Oil and Gas Industry, no. 1, pp. 35–38 (2020). [https://doi.org/10.33285/1999-6942-2020-1\(181\)-35-38](https://doi.org/10.33285/1999-6942-2020-1(181)-35-38)
2. Zhdaneev, O.V., Chubokсарov, V.S.: Technical policy of the oil and gas industry in Russia: tasks and priorities. *Energy Policy* 5(147), 76–91 (2020). https://doi.org/10.46920/2409-5516_2020_5147_76
3. Shah, M.: Big data and the internet of things. In: Japkowicz, N., Stefanowski, J. (eds.) *Big Data Analysis: New Algorithms for a New Society*. Studies in Big Data, vol. 16. Springer, Berlin (2020). https://doi.org/10.1007/978-3-319-26989-4_9
4. Zhdaneev, O.V., Chubokсарov, V.S.: Prospects for industry 4.0 technologies in the fuel and energy complex of Russia. *Energy Policy* 7(149), 16–33 (2020). https://doi.org/10.46920/2409-5516_2020_7149_16

5. Raghuraman, B., Gustavson, G., Van Hal, R., Dressaire, E., Zhdaneev, O.: Extended-range spectroscopic pH measurement using optimized mixtures of dyes. *Appl. Spectroscopy* **60**(12), 1461–1468 (2006). <https://doi.org/10.1366/000370206779321535>
6. Shcherbakov, M.V., Glotov, A.V., Cheremisinov, S.V.: Proactive and predictive maintenance of cyber-physical systems. In: Kravets A., Bolshakov A., Shcherbakov M. (eds.) *Cyber-Physical Systems: Advances in Design & Modelling. Studies in Systems, Decision and Control*, vol. 259. Springer, Berlin (2020). https://doi.org/10.1007/978-3-030-32579-4_21
7. Cuong, S.V., Shcherbakov, M.V.: A predictive maintenance modeling tool implemented as R-package and web-application. In: *Proceedings of the Tenth International Symposium on Information and Communication Technology*. Association for Computing Machinery, New York, NY, USA, pp. 433–440 (2019). <https://doi.org/10.1145/3368926.3369693>
8. Alyaev, S., Suter, E., Brumer, B.R., Hong, A., Luo, X., Fossum, K.: A decision support system for multi-target geo-steering. *J. Petrol. Sci. Eng.* **183**, 2019 (2019). <https://doi.org/10.1016/j.petrol.2019.106381>
9. Stishenko, S., Petrakov, Y., Sabirov, A., Sobolev, A.: Automatic geosteering of wells. In: *SPE Russian Petroleum Technology Conference*. (2018). <https://doi.org/10.2118/191594-18RPTC-MS>
10. Yang, S.: *Fundamentals of Petrophysics*. Springer Geo-Physics (2017). <https://doi.org/10.1007/978-3-662-55029-8>
11. Karev, V., Kovalenko, Y., Ustinov, K.: *Geomechanics of oil and gas wells*. In: *Advances in Oil and Gas Exploration & Production*. Springer, Berlin (2020). <https://doi.org/10.1007/978-3-030-26608-0>
12. Zhdaneev, O.V., Frolov, K.N.: Drilling technology priorities in Russia. *Oil Industry* **5**, 42–48 (2020). <https://doi.org/10.24887/0028-2448-2020-5-42-48>
13. De Togni, R., Restelli, M.: Predictive model for drilling phase duration of oil & gas wells. *Artificial Intelligence and Robotics Laboratory, Politecnico di Milano* (2018). <https://hdl.handle.net/10589/141802>
14. Ge, Z., Song, Z., Ding, S.X., Huang, B.: Data mining and analytics in the process industry: the role of machine learning. *IEEE Access* (2020). <https://doi.org/10.1109/ACCESS.2017.2756872>
15. Saravanan, R., Sujatha, P.: A state of art techniques on machine learning algorithms: a perspective of supervised learning approaches in data classification. In: *Second International Conference on Intelligent Computing and Control Systems (ICICCS)*, Madurai, India, 2018, pp. 945–949 (2018). <https://doi.org/10.1109/ICCONS.2018.8663155>
16. Cao, D., Hender, D., Ariabod, S., James, C., Ben, Y., Lee, M.: The development and application of real-time deep learning models to drive directional drilling efficiency. In: *IADC/SPE International Drilling Conference and Exhibition* (2020). <https://doi.org/10.2118/199584-MS>
17. Pollock, J., Stoecker-Sylvia, Z., Veedu, V., Panchal, N., Elshahawi, H.: Machine learning for improved directional drilling. In: *Offshore Technology Conference* (2018). <https://doi.org/10.4043/28633-MS>
18. Tse, K.C., Chiu, H.-C., Tsang, M.-Y., Li, Y., Lam, E.Y.: Unsupervised learning on scientific ocean drilling datasets from the South China Sea. *Front. Earth Sci.* (2018). <https://doi.org/10.1007/s11707-018-0704-1>
19. Noshi, C.I., Schubert, J.J.: The role of machine learning in drilling operations: a review. In: *SPE/AAPG Eastern Regional Meeting* (2018). <https://doi.org/10.2118/191823-18ERM-MS>
20. Liu, G., Li, L., Zhang, L., Li, Q., Law, S.S.: Sensor faults classification for SHM systems using deep learning-based method with Tsfresh features. *Smart Mater. Struct.* (2020). <https://doi.org/10.1088/1361-665X/ab85a6>
21. Zimek, A., Filzmoser, P.: There and back again: outlier detection between statistical reasoning and data mining algorithms. *Wiley Interdisciplinary Reviews: Data Min. Knowl. Discovery* **8**(6) (2018). <https://doi.org/10.1002/widm.1280>
22. Zimek, A., Schubert, E.: Outlier detection. In: Liu, L., Özsu, M. (eds.) *Encyclopedia of Database Systems*. Springer, New York (2017). https://doi.org/10.1007/978-1-4899-7993-3_80719-1

23. Grau, J., Grosse, I., Keilwagen, J.: (2015) PRROC: Computing and visualizing precision-recall and receiver operating characteristic curves in R. *Bioinformatics* **31**(15), 2595–2597 (2015). <https://doi.org/10.1093/bioinformatics/btv153>
24. Gurina, E., Klyuchnikov, N., Zaytsev, A., Romanenkova, E., Antipova, K., Simon, I., Koroteev, D.: Application of machine learning to accidents detection at directional drilling. *J. Petrol. Sci. Eng.* (2019). <https://doi.org/10.1016/j.petrol.2019.106519>
25. Zhdaneev, O.V., Oleneva, O.N.: (2020) Development of specialized software for Russian oil and gas industry. *GAS Ind. Russia* **7**, 23–29 (2020)
26. Rassenfoss, S.: Drilling automation is the future, but ExxonMobil finds gaps to fill. *J. Petrol. Technol.* 09 March 2020 (2020). <https://pubs.spe.org/en/jpt/jpt-article-detail/?art=6711>
27. Jeffery, C., Creegan, A.: Adaptive drilling application uses AI to enhance on-bottom drilling performance. *J. Petrol. Technol.* 01 August 2020 (2020). <https://pubs.spe.org/en/jpt/jpt-article-detail/?art=7392>
28. Rassenfoss, S.: Man vs. drilling machine can be a productive thing. *J. Petrol. Technol.* 01 February 2020 (2020). <https://pubs.spe.org/en/jpt/jpt-article-detail/?art=6470>

Engineering Education for Cyber-Physical Systems Design

Use of Computer Trainers for Teaching Management Manufacturing Personnel of Chemical Industries



Tamara Chistyakova , Gunter Reinig, and Inna V. Novozhilova 

Abstract The chapter describes the questions of developing the life cycle of intelligent computer trainers that allow teaching modern industrial equipment, training in the control of technological processes on the basis of the Industry 4.0 concept. The advantages of using computer trainers for teaching management manufacturing personnel consist of gaining experience and skills of behavior in emergency situations, a deep understanding of the cause and effect relationships in the facility, quick response to malfunctions, reducing the psychological overload, increasing confidence and self-solving problems of management. Increasing the professional level of the management manufacturing personnel of chemical enterprises allows improving the quality of products, reducing spoilage, and improving the environmental characteristics of industrial production of high-tech industries.

Keywords Distributed control systems · Intelligent technologies · Simulation modeling · Practice-oriented training · Computer trainers

1 Introduction

Intensive development of production technologies dictates the need for the high-quality and timely training of management production personnel of industrial enterprises to master new special professional competencies in the field of design, processing information, and managing complex objects of high-tech industries [1].

T. Chistyakova (✉) · I. V. Novozhilova
Saint-Petersburg State Institute of Technology, 26 Moskovsky prospect, Saint-Petersburg 190013, Russia

e-mail: nov@technolog.edu.ru

I. V. Novozhilova
e-mail: novozhilova@technolog.edu.ru

G. Reinig
Ruhr-Universität Bochum, 150 Universitätsstraße, 44801 Bochum, Germany
e-mail: gunter.reinig@ruhr-uni-bochum.de

Statistical data from J&H Marsh & McLennan, Inc. и Gulf Publishing Holdings, LLC (Hydrocarbon Processing) companies [2] shows that manufacturing enterprises lose up to 20 billion dollars or 5% of annual production volume because of un-planned equipment idle time and low quality of production. According to the results of ARC Advisory Group's research [3] for the global industry, about 80 percent of losses can be prevented, as 40 percent of them are operator errors. The losses, caused by management production personnel's mistakes, lead to a decrease in product quality, unplanned equipment idle time, environmental damage, and other losses comparable in scale with losses from production accidents [4, 5].

The most promising direction for mastering the competence results of training and elimination of qualification deficiencies of managerial production personnel is the development of intelligent computer trainers.

The computer trainers must enable studying of modern industrial equipment, training to control technological processes, based on simulation mathematical models (MM) with 2D and 3D interfaces, as well as virtual reality (Immersive Training) using audio tools to support training.

The advantages of using computer trainers for teaching management manufacturing personnel to consist in gaining experience and skills of behavior in emergency situations, a deep understanding of the cause and effect relationships in the facility, quick response to malfunctions, reducing the psychological overload, increasing confidence and self-solving problems of management [5].

2 Technologies for Computer-Aided Synthesis of Distributed Control Systems and Intelligent Simulators

The solution of these tasks for the implementation of this direction made it possible to develop a unified methodology and technologies for computer-aided synthesis of distributed control systems and intelligent computer training simulators for management production personnel of high-tech industries using modern information and network technologies [6, 7]. Basic architecture types of training systems are represented in Fig. 1.

In Fig. 1 the following notation is used: DCS—Distributed Control System; PLC—Programmable Logic Controller; LAN—Local Area Network; HMI—Human-Machine Interface.

Distributed control system (DCS) is a complex of technical and software solutions for the development of automated process control systems and exhibits a distributed input/output system and decentralization of data processing, as well as deeper integration of code development tools for visualization and management levels.

DCS structure includes three levels. The lowest input/output level contains sensors and actuators. The middle level of the distributed system contains controllers. Controllers are aimed to process obtained data, generate control actions, and transfer

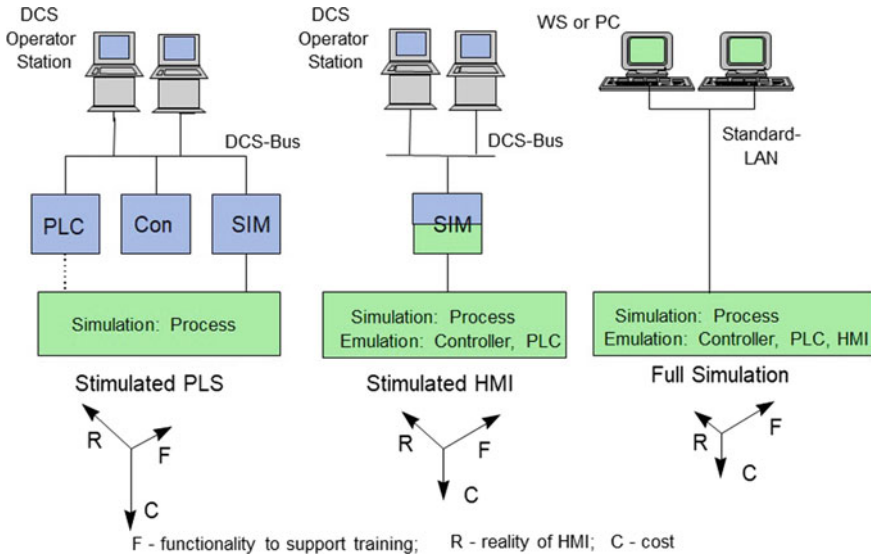


Fig. 1 Architecture of training systems

data to the highest level. The highest level contains database servers and workstations. The workstations provide a human-machine interface for the operator and data communication between the server and programmable logic controller. In the DCS hierarchy separately stands engineer work-station. Software solutions for development and configuration are installed on the work-station.

The solutions are connected to the controllers. Distributed control systems can be developed using programming languages in soft-ware tools such as Matlab, Aspen Dynamics, Hysys, Expert System Shell, Neuro/Fuzzy tools, and complex simulation systems, e.g. Honeywell UNISIM, Aspen OTS Framework, Yokogawa OmegaLand [6, 7].

3 Integrated Dynamic Simulation Environment

The modern direction of evolution of distributed control systems is the development of dynamic simulators. Dynamic simulators are a software tool for the development of an integrated virtual model of industrial enterprise. Systems of this class allow to carry out design and engineering calculations before or during the construction of an industrial enterprise, perform operations on a virtual model, perform visualization and modeling of technological processes according to conditions of the production.

An integrated dynamic simulation environment (Fig. 2) is software that can use simulation function in the stationary mode in addition to dynamic simulation function [8].

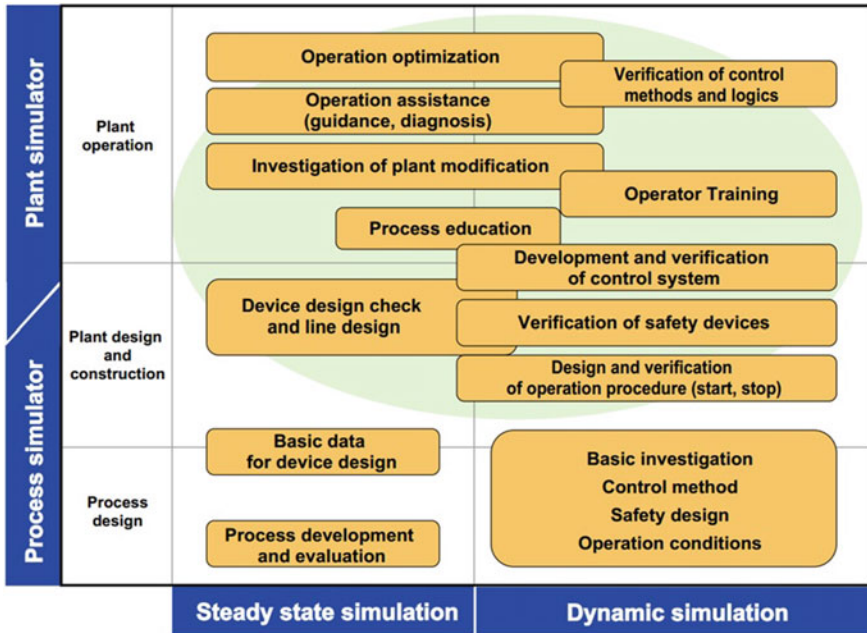


Fig. 2 Use of training systems and computer simulators

The use of dynamic simulation environments and computer simulators exhibits short-term profitability of investments. According to ARC Advisory Group, the world market of computer simulators will grow from \$459 million to \$760 million, with steady growth since the late 1980s.

The cost of an Operator Training System for an oil refinery unit is about \$300,000. At the same time, the cost of engineering costs is about 75% of the total cost of creating a simulator.

Simulators are highly demanded in the study of technology, technological engineering, and engineering of control systems. Effective use of simulators for research of technological processes based on imitation simulation systems and support of control systems, including systems for improved control of technological processes [4].

Modern trends in the development of computer trainers (simulators) based on the concept of Industry 4.0 are: the introduction of cyber-physical systems into production, the use of wireless data transmission, the use of virtual and augmented reality (real objects are supplemented with information superimposed on them) [9], use of additive technologies. Figure 3 shows an example of a HMI realization based on Indus-tries 4.0 [10].

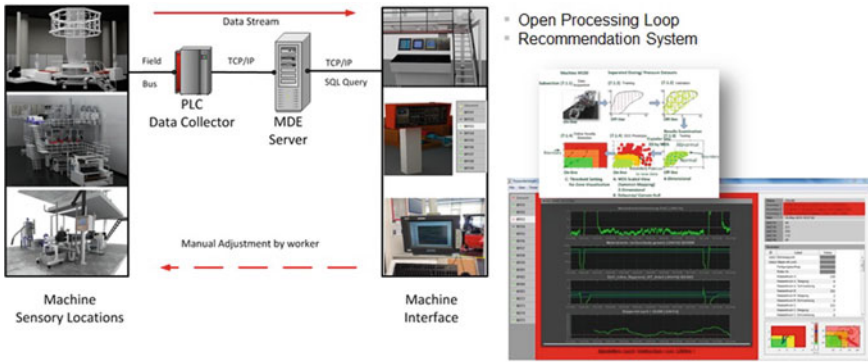


Fig. 3 Example of HMI realization based on Industry 4.0

4 Computer Training Systems Development Lifecycle

The lifecycle of the development of computer training systems includes the following stages [11–13]:

- analysis of qualification deficiencies of specialists in enterprises of high-tech industries and their transformation into special professional competencies; the competencies allow employees to perform their labor functions as part of a new or substantially renewed type of work activity;
- development of the trajectory and forming of the content of training based on unit technology of vocational training, according to the job descriptions and labor functions of the management and production personnel of enterprises;
- development of methods, algorithms, and technologies for the synthesis of training systems, including adaptable imitation modeling subsystems for design and control processes for obtaining high-tech materials of various functional purposes, databases (DB) for raw materials, equipment, technological regulations and parameters, requirements to the quality of materials, a knowledge base of abnormal situations associated with the flows of products;
- approbation of training by the development of computer trainers for management production personnel of processes for obtaining high-technology materials for various functional purposes;
- processing the results (protocols) of training management production personnel based on the use of methods of qualitative and quantitative evaluation of the acquired by trainees special professional competencies, necessary for the performance of their labor functions.

As exploration and simulation object modern production enterprises usually exhibit: different types of production $TP = \{TP1, \dots, TPtp\}$ with wide nomenclature $MP = \{MP1, \dots, MPmp\}$; variety of technological stages $TS = \{TS1, \dots, TSs\}$, equipment $EQ = \{EQ1, \dots, EQeq\}$; possibility to obtain the same product

from different types of raw materials $FS = \{FS1, \dots, FSfs\}$ using variety of recipes $RP = \{RP1, \dots, RPp\}$; strong requirements to quality of half-finished products $IP = \{IP1, \dots, IPip\}$ and finished products $QP = \{QP1, \dots, QPqp\}$; occurring abnormal situations on different production stages $ST = \{ST1, \dots, STst\}$, caused by violation of production quality indicators (causes of flows $RS = \{RS1, \dots, RSrs\}$).

According to the developed methodology of the end-to-end design of training systems [14–23], a formalized description of the object of study is the basis for computer-aided synthesis using the modern information technologies of the core of computer simulators and training systems (Fig. 4).

During the development of the functional structure of the training system, units to perform functions of learning and training are created: the instructor's interface; the learner's interface; the unit for performing computational experiments; the unit for the formation of simulation results; infoware and mathware.

For the training, the instructor has the following options: control of the model; control over the course of training; evaluation of the trainee's actions using the selected model of knowledge control.

The information structure of the trainee interface includes units for the operational management of the structure of the learning object using a dynamically controlled process mimic; control and regulation of process parameters; obtaining explanations, advice, recommendations on management. This structure of the trainee interface allows considering the characteristics of the object of study for various modifications, to obtain profound professional knowledge according to the accumulated experience of experts.

For training to design and control chemical technology processes information models, simulation MMs, and knowledge representation models are used [1, 5].

Information models are implemented in the form of a DBs of geometric models and design parameters of production equipment, technological parameters of processes, characteristics of raw materials, and target products. By dynamic changing the ranges of the corresponding parameters, DBs are set to various structures of the object of study, modes of its functioning, productivity, the composition of raw materials, and product quality.

Thus, developed training systems are adapted for different modifications of the object of study. Therefore, they can be integrated into computer-aided design and control systems for technological enterprises.

Simulation MMs provide active learning during the solution of various training tasks: training for control in emergency situations and while reconfiguration of the production for a new task, raw materials, and productivity, studying the methods and tasks of optimal control, studying the cause-effect relationships in the facility, para-metric synthesis of the object of study and carrying out verification calculations of the developed objects.

Modeling an event (C) includes describing the place of emergence of an event, the moment of system time in the case that there is an event (t), the parameter of the object (V) determining an event, and its threshold restrictions (L).

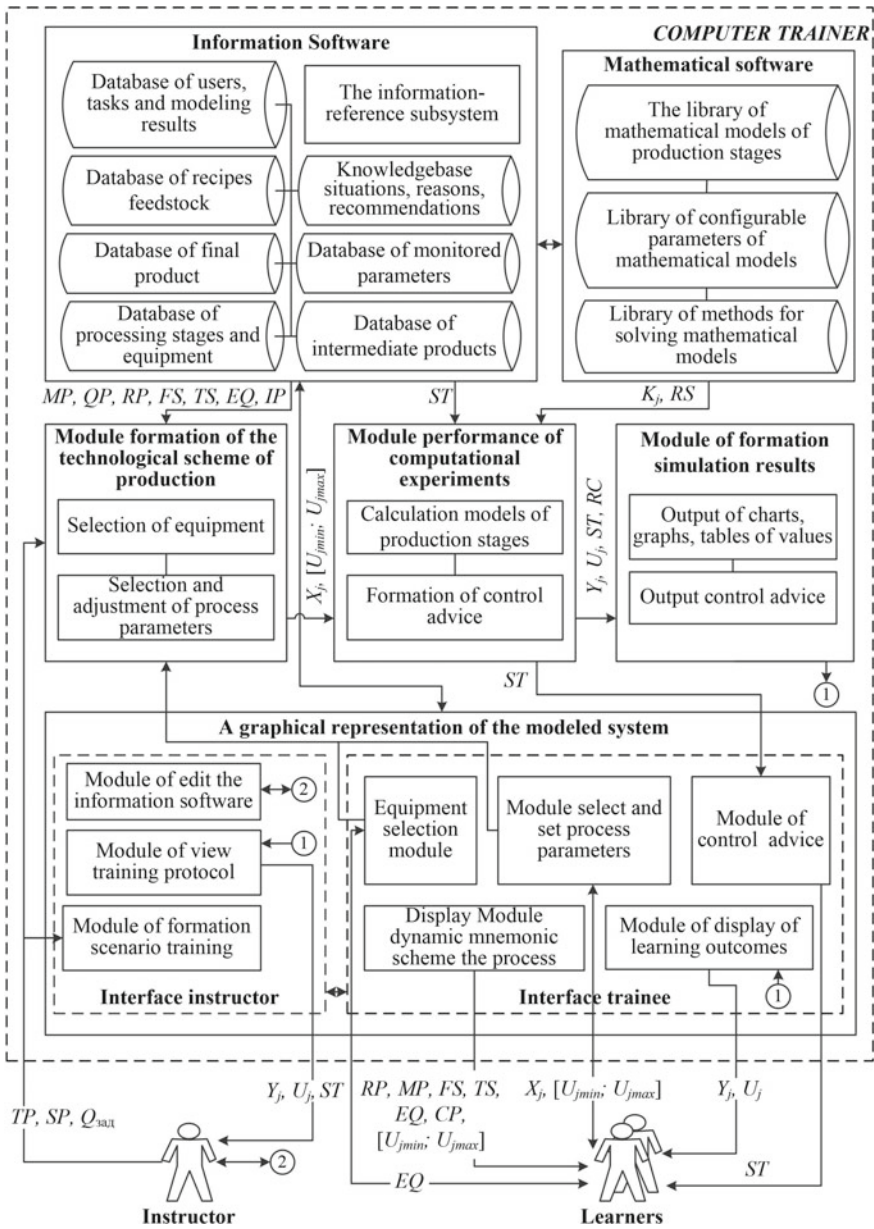


Fig. 4 An example of the computer trainers functional structure

$$C^j = \{t\} \Big|_{V_j \leq V_j^t},$$

where $V = \{X, U, Y\}$ —a vector of technological parameters of the object, respectively: X —entrance, U —managing, Y —outgoing; j —an index of belonging to the place of emergence of an event (to hierarchical level—a stream, a device, a stage, a process). Events (situations) can be simulated in two ways: by means of a set of parameters of information model:

$$M_C^I = \{V, t\} \Big|_{V_j \leq V_j^t};$$

by means of the solution of imitating models:

$$M_C^M = F\{V, K, t\} \Big|_{V_j \leq V_j^t},$$

where K —a vector of coefficients of imitating model.

For the simulation of the causes of violations, the components of the basic model are changed relative to the nominal values. While the simulation of the event, the basic model continues to function, but the priority of the emergency event switches the trainee's attention to the parameters that determine the emergency situation, usually accompanied by sound and light alarms. For some operational and emergency reasons, a stochastic model has been developed. The model provides determination of the probability of a cause, in case of the incompleteness of information.

For studying of expert knowledge, ways to eliminate emergency situations, best practices in the methods of accident-free and effective management and the formation of intellectual advice for the design and control of high-tech products in the training process, models of the representation of non-formalized knowledge about the object of study are integrated into the structure of simulators. To develop computer-aided subsystems of presentation of declarative and procedural knowledge, the tools of object-oriented programming, the shells of expert systems, languages of knowledge representation are used.

The analysis of existing models of knowledge control in different types of training systems made it possible to propose the following methods for determining the level of training of management production personnel: registration of acquired knowledge, assessment of knowledge using a context model, error analysis, method of imposition, generating modeling (computer-aided training is based on the trainee's intentions), mapping the sequence of actions (solution tree, graphs, object state tables).

The manager program is developed to control and organize the training processes using training systems. The program has the following functions: reading settings from a file; setting parameters of object models according to the settings; reading the learning script; display of the state of the learning object on the mimic; recognition and processing of events specified in the training scenario and formed by the trainee and the instructor during the learning process; the output of training results in a protocol log file. As a result of the functioning of the manager program, the instructor

can learn the training results from the training protocol file, examine the tables and graphs of the state of the learning objectives from the stored history of the object, correct the training scenario according to the student's knowledge level.

5 Conclusion

The developed methods and technologies for the design of intelligent computer training systems are used to improve skills and train management production personnel on high-tech technological productions, such as “Mondi Gronau GmbH”, “Maria Soel GmbH – Maria Soel HTF GmbH”, “Kloeckner Pentaplast Europe GmbH & Ko.KG”, “Virial Ltd.”, PAO “Severstal”, CJSC “ILIP”, PAO “Rigel”.

It's important to mention international experience in the development of training programs in the field of computer-aided data processing and control of the production of nanostructured polymer materials using the example of the international corporation “Kloeckner Pentaplast” [11]. The aim of the program is the exploration of new properties of polymer materials, improvement of the technologies for their production and processing, and the introduction of innovative solutions at international enterprises. An example of using computer trainers in the production of polymer films is shown in Fig. 5. The figure shows a 3D model of the calender line, a computer simulator of the position of the calender rolls, and an on-line terminal surface for equipment condition monitoring.

The introduction of intelligent computer simulators in training centers and production showed that the increase in safety and efficiency of high-tech industries was achieved through: improving the characteristics of the control object, improving control systems, improving the professional level of management production personnel.

For modern industrial production, it is actually to improve skills and retrain the management of production personnel to achieve the readiness of specialists to implement their respective professional and labor functions and develop professional competencies that meet the requirements of specific jobs.

Using of computer trainers based on the concept Industrie 4.0 [24, 25] allows to enhance production quality, reduce flows, improve the environmental characteristics of production by enhancing the professional level of management production personnel and approaching their skills to the requirements of professional standards.



Fig. 5 An example of using computer trainers in the production of polymer films

Acknowledgements This research was partially supported by the DAAD (German Academic Exchange Service) on the theme “Computational intelligence for analysis and control of complex industrial processes” (Project-ID: 57483001).

In preparing the chapter, the results of work obtained with the support of the project with the support of the RFBR grant No. 18-08-00143 A were also used.

References

1. Chistyakova, T.B., Novozhilova, I.V.: Intelligence computer simulators for elearning of specialists of innovative industrial enterprises. In: 2016 XIX IEEE International Conference on Soft Computing and Measurements (SCM), pp. 329–332. St. Petersburg (2016). <https://doi.org/10.1109/SCM.2016.7519772>
2. Hydrocarbon Processing. <https://www.hydrocarbonprocessing.com>. Last accessed 20 July 2020
3. Technology Market Research for Industry & Cities ARC Advisory Group. <https://www.arcweb.com>. Last accessed 20 July 2020

4. Dozortsev, V., Agafonov, D., Nazin, V., Novichkov, A., Frolov, A.: Computerized operator training: continued importance, new opportunities, and the human factor. *Autom. Rem. Control* **81**, 935–954 (2020). <https://doi.org/10.1134/S0005117920050124>
5. Dozortsev, V., Nazin, V., Oboznov, A., Mironova, A.: Structural knowledge as an evaluation instrument of trainees progress in learning. In: 2017 IEEE 11th International Conference on Application of Information and Communication Technologies (AICT), Moscow, Russia, 2017, pp. 1–5. <https://doi.org/10.1109/ICAICT.2017.8686943>
6. Reinig G. *Skript Prozessführung – Advanced Process Control*. Ruhr-Universität Bochum (2005)
7. Reinig, G., Winter, P., Linge, V., Nagler, K.: *Training Simulators: Engineering and Use*. Chemical Engineering and Technology (1998)
8. Kamada, Y.: Recent Trends of Dynamic Simulator Applications and Prospects for OmegaLand. Yokogawa Technical Report English Edition, vol. 56. no. 1 (2013)
9. Kohlert, M., König, A.: Advanced multi-sensory process data analysis and on-line evaluation by innovative human-machine-based process monitoring and control for yield optimization in polymer film industry. *Technisches Messen* (2016)
10. Chistyakova, T., Teterin, M., Razygraev, A., Kohlert, C.: Intellectual analysis system of big industrial data for quality management of polymer films. In: *Advances in Neural Networks*. ISSN 2016. 13th International Symposium on Neural Networks Processing [S. l.], pp. 565–572. Springer International Publishing, Berlin (2016)
11. Meshalkin, V.P., Khodchenko, S.M.: The nature and types of engineering of energy- and resource-efficient chemical process systems. *Polym. Sci. Ser. D* **10**, 347 (2017). <https://doi.org/10.1134/S1995421217040128>
12. Makarova, A., Tarasova, N., Meshalkin, V., Kukushkin, I., Kudryavtseva, E., Kantyukov, R., Reshetova, E.: Analysis of the management system in the field of environmental protection of russian chemical companies. *Int. J. Quality Res.* **12**, 43–62 (2018). <https://doi.org/10.18421/IJQR12.01-03>
13. Chistyakova, T.B.: A synthesis of training systems to promote the development of engineering competences. In: Smirnova, E., Clark, R. (eds.) *Handbook of Research on Engineering Education in a Global Context*, pp. 430–442. IGI Global, Hershey, PA (2019). <https://doi.org/10.4018/978-1-5225-3395-5.ch036>
14. Dvoretiskii, D.S., Dvoretiskii, S.I., Polyakov, B.B., Ostrovskii, G.M.: A new approach to the optimal design of industrial chemical-engineering apparatuses. *Theor. Found. Chem. Eng.* **46**(5), 437–445 (2012)
15. Dvoretiskii, D.S., Dvoretiskii, S.I., Ostrovskii, G.M.: Integrated design of power- and resource-saving chemical processes and process control systems: Strategy, methods, and application. *Theor. Found. Chem. Eng.* **42**, 26–36 (2008). <https://doi.org/10.1134/S0040579508010041>
16. Korobiichuk, I., Ladaniuk, A., Ivashchuk, V.: Features of control for multi-assortment technological process. In: Szewczyk, R., Krejsa, J., Nowicki, M., Ostaszewska-Lizewska, A. (eds.) *Mechatronics 2019: Recent Advances Towards Industry 4.0*. MECHATRONICS 2019. *Advances in Intelligent Systems and Computing*, vol 1044. Springer, Cham (2020)
17. Muratova, E.I., Dvoretzky, S.I., Voyakina, E.Y.: Organization of postgraduate students training in the technical field of sciences. In: *International Conference on Interactive Collaborative Learning*, vol. 46(5), pp. 437–445. Kazan, Russia (2013)
18. Veshneva, I., Singatulin, R., Bolshakov, A., Chistyakova, T., Melnikov, L.: Model of formation of the feedback channel within ergatic systems for monitoring of quality of processes of formation of personnel competences. *Int. J. Quality Res.* **9**(3), 495–512 (2015)
19. Patle, D.S., Manca, D., Nazir, S., et al.: Operator training simulators in virtual reality environment for process operators: a review. *Virtual Reality* **23**, 293–311 (2019). <https://doi.org/10.1007/s10055-018-0354-3>
20. Crawley, E.F., Malmqvist, J., Östlund, S., Brodeur, D.R., Edström, K.: *Rethinking Engineering Education*. Springer International Publishing (2014). <https://doi.org/10.1007/978-3-319-05561-9>

21. Rachford, J.: Qualified people—it is a safety and skill set thing. *Trans. Ind. Appl.* **53**(1), 700–708 (2017)
22. Adrian, B., Hinrichsen, S., Nikolenko, A., Meyer, F.: How to combine lean, human factors and digital manufacturing—a teaching concept. In: Nunes, I. (eds.) *Advances in Human Factors and Systems Interaction. AHFE 2019. Advances in Intelligent Systems and Computing*, vol. 959. Springer, Cham (2020)
23. Albinia, M.: Automation of teaching processes on e-learning platforms using recommender systems. In: Bi, Y., Bhatia, R., Kapoor, S. (eds.) *Intelligent Systems and Applications. IntelliSys 2019. Advances in Intelligent Systems and Computing*, vol. 1037. Springer, Cham (2020)
24. Valeyeva, N.S., Kupriyanov, R.V., Valeeva, E., Kraysman, N.V.: Influence of the fourth industrial revolution (Industry 4.0) on the system of the engineering education. In: Auer, M., Hortsch, H., Sethakul, P. (eds.) *The Impact of the 4th Industrial Revolution on Engineering Education. ICL 2019. Advances in Intelligent Systems and Computing*, vol. 1135. Springer, Cham (2020)
25. Tolettini, L., Lehmann, C.: Industry 4.0: New paradigms of value creation for the steel sector. In: Bettiol, M., Di Maria, E., Micelli, S. (eds.) *Knowledge Management and Industry 4.0. Knowledge Management and Organizational Learning*, vol. 9. Springer, Cham (2020)

Higher School Education Quality Forecasting by Regression Analysis Methods



I. M. Kharitonov, E. G. Krushel, O. V. Stepanchenko, and O. O. Privalov

Abstract In addition to the career guidance measures, the computer-aided facilities are proposed to assist secondary school graduates in choosing the appropriate direction of higher school specialty and in the estimation of the perspectives of the future education process achievements. The facilities carried out are based on the multivariate linear regression model with the vector of the independent variables (predictor factors) the components of which consist both of the set of secondary school education results in the disciplines which are essential for successful study at the given specialty as well as of the expert estimation of the high school candidates general ability level. The education quality index is formed as the middle value of the expert estimations assigned by the lecturers for each senior university course student in accordance with the accepted ball scale. An approach efficiency example is presented for the forecasting of the successful study of the computer sciences disciplines. The model identification was carried out based on the predictor factors data (retrospectively) and on the senior course students' education quality existing value. The model adequacy was verified using the data of the students' test group for which the situation of the higher school admission was simulated. The results of the forecasted and existing test group education quality indexes comparison show the model time-invariance and acceptable accuracy. The conclusion of the proposed model suitability for the estimation of the perspectives of the future education process achievements was justified. The ways of further model accuracy increasing are mentioned about namely due to the cluster analysis methods applying.

I. M. Kharitonov (✉) · E. G. Krushel · O. V. Stepanchenko · O. O. Privalov
Kamyshin Technological Institute (Branch) of Volgograd State Technical
University, Kamyshin, Russia
e-mail: wisdom_monk@mail.ru

E. G. Krushel
e-mail: elena-krushel@yandex.ru

O. V. Stepanchenko
e-mail: ovste@mail.ru

O. O. Privalov
e-mail: galva@mail.ru

Keywords Education quality · Predictor factors · Multivariate linear regression · Identification · Model stationary properties · High technology sciences

1 Introduction

The reform of the education system has led to the conversion of Russian universities into a two-level «degree» system of higher education, which allows students to obtain bachelors' and masters' degrees. The main purpose of this reforming is to shift focus on the learning results instead of learning content as well as to recognize the tendencies of the students to choose the future work either in the field of research and design or in the industrial sphere [1, 2].

The main purpose of universities is to form qualified specialists. The results obtained by Russian and foreign scientists show that the formation of a specialist is influenced by a set of factors: the quality of the educational process (teachers' qualifications, availability of modern technical equipment, etc.), personal characteristics of students (readiness to the knowledge perception), and their professional orientation (particularly a creative interest of students to the chosen specialty), etc. [3–5].

The complete accounting of these factors in the educational process is almost impossible due to its high complexity. At the same time, unfortunately, in ordinary universities, we can notice the sharp stratification of the student group by the current learning performance levels. The number of students who do not show any interest in learning sometimes can reach 50% in senior courses of technical universities. It should be noted that this factor can lead to teaching quality reduction because the teacher is forced to adapt the studying discipline complexity to ensure its satisfactory understanding by most students.

One of the reasons for this undesirable feature is as follows. The future education profile being chosen by a school graduate is not always correspond to his real internal interests. In some cases, this choice is influenced by parents, fashion, the promotion of the profession in the media, etc. If this choice is not matching with the indicators of the school training quality as well as with the school graduate internal interests (sometimes these interests are not clear for the graduate himself), then most likely his education at the university will be ineffective.

Since the financing of tuition in a university is calculated based on the actual number of students, teachers are interested in maintaining the students' numerical strength. Therefore, they do not insist on revising the choice of specialty even for poorly performing students (it is very difficult to change the chosen field after 3–4 years of study). As a result—an unloved profession, superficial knowledge, non-prestigious work, low demand in the labor market [6].

Therefore, the important problem is to create computer-aided facilities to help school graduates in the choice of the appropriate direction of university study which will reveal the abilities and internal interests of the graduate in the profession. Naturally, such computer tools are not required for schoolchildren whose interests are already self-determined and supported by real achievements (Olympiads,

scientific efforts, etc.). For a graduate without clear professional orientation, such computer facilities can provide the estimation of his success in future higher education obtaining. Although it is impossible to receive the exact estimation, a school graduate would be able to compare the indicators of the expected education effectiveness between various specialties and make the choice of the study direction at the university more conscious and unemotional [7].

The problem of future academic performance forecast was discussed in [3, 8–15]. The presented work possesses the following elements of newness in compare with the quoted:

1. The problem statement is based on the results of the previously developed modular-competency-based approach [16] which had been carried out to take into account the demands of the modern high education school reform.
2. In accordance with this approach, the study programs of all taught disciplines were divided into a set of modules so that each of them possessed strong internal coupling with relative autonomy from other ones. It made it possible to select the subset of modules the stable residual knowledge of them is necessary for a university graduate to be confident in his own successful future activity accordingly to the social needs in the local labor market. Therefore, the forecasting of academic performance in our work is oriented to namely these modules study while the authors of the quoted works take into account mainly the academic performance averaged across all taught disciplines. Also, the forecast is directed to the students of the senior courses only. It is necessary to notice that the results are not applying to the academic performance of gifted students having good prospects of successful scientific researches and design (unfortunately in ordinary universities such students are rare and so their teaching is carried out individually).
3. The forecasting is based not only on the quantitative results of school educations (middle ball of Unified State Exam [9, 15], a middle grade of secondary-school diploma [10], grades of certain disciplines et al. [14]) but also on the quality information about total suitability of school graduate for the university program mastering (particularly the opinion of the class supervisor).
4. We have refused from the development of the general (universal) model of academic performance forecast in favor of the set of specialty-oriented models taking into account the specific features of the study programs of different study directions. Such features are especially perceptible for universities of the polytechnic profile due to the variety of future activity applications of the graduates' knowledge (the discussed model is oriented namely for this class of universities). In accordance with this remark, the expert estimation of students' study successes is formed by the lecturers of the profiling cathedrals only.
5. The increase of academic performance forecasting effectiveness had been achieved by the detection of the clusters in whole predictors' array taking into account the individual features of each school graduate as well as the influence of external reasons' influence on the school grades values. The account of

school graduate membership in a particular cluster allows increasing the accuracy of prediction of successes in mastering the competencies necessary for future professional activity.

The purpose of the work and problem statement. The purpose of the work is to increase the efficiency of the study direction choice by school graduates and to reduce the risk of their low academic performance during training at the university. In addition to common usual career guidance measures of university specialties' popularization between the schoolchildren, the proposed computer facilities are directed to help school graduate in individual choice of the appropriate direction of study at the university (hereinafter, the term «Forecast» is used as the short name of the proposed computer facilities).

The approach to the problem decision is based on the application of a simulation model that can forecast a school graduate's future university education results. The forecasting algorithm takes into account the set of features of school graduate successes in disciplines correlating with the main disciplines of the chosen study direction. Below the term, «predictor» is used for the components of this set. The proposed model is worked out using the methods of statistical data analysis (in particular, we use the methods of multivariate regression analysis and clustering) [17].

The following particular tasks were considered as the steps of the main problem decision:

1. teaching quality estimation measure choice;
2. choice of components of the predictors set;
3. data acquisition for the statistics of the predictors set;
4. reception of the education quality indexes quantitative estimation for each student from the group chosen for the simulation model identification;
5. simulation model development to be applied in the computer facilities «Forecast» suited for the education quality index prediction of the school graduates with individual predictors sets;
6. simulation model identification as well as its statistical characteristics estimation;
7. prediction of future education efficiency.

The model of the quality education measure dependence from the set of predictors was chosen in the form of the multivariate regression model. For this one, it was determined both the predictors set suitable to the quality training value explanation (being considered below as the dependent (criteria) variable) and also the parameters vector the components of which show the contribution of the corresponding predictor to the value of dependent (criteria) variable [18].

The problem is to determine the dependence between the criteria variable (as the measure of the training process effectiveness), on one hand, and the set of chosen predictors, on the other hand. The details of the initial data reception for the example of a particular education direction are described below in the part «The results of the future education quality prediction».

Information support of the «Forecast» computer facilities was obtained from the data of the senior courses students' education characteristics. The last was applied for the needs of model identification as well as for the verification of the admissibility to consider the model parameters as time-invariant ones (at least approximately). Respectively the whole students' group was divided into two subgroups. Data from the first one (so-called «identification group») were applied for the choice of the predictors set components as well as for the regression model parameters estimation. Data from the second subgroup (so-called «test group») were applied to the verification of the hypothesis about the time invariance of the regression model parameters.

The structure of information support is as follows:

1. $n \times k$ -dimensional array $X_{ID} = \{X_{ID}^{(1)}, X_{ID}^{(2)}, \dots, X_{ID}^{(k)}\}$ of the school quality training characteristics achieved by the identification group students when they had been the schoolchildren (below we use the term «predictors array»). Therein $X_{ID}^{(i)}$ is the n -dimensional vector the, j th component of which $x_{ID_j}^{(i)}$ indicates the value of the i th school quality training characteristic for the j th student; $i = 1, \dots, k, j = 1, \dots, n, n$ —number of students in the identification group. The source of information about the X_{ID} array is the university archive which stores the secondary-school diploma of the students presently passing the university training.
2. $n \times 1$ -dimensional vector of the university training efficiency estimation (below we use the term «education results») Y_{ID} , j th component of which y_{ID_j} shows the expert estimation of the j th student's education successes. y_{ID_j} is determined as the middle value of the individual expert estimates given by each lecturer of the profiling cathedra in the accepted ball scale, $j = 1, \dots, n$.
3. $m \times k$ -dimensional array of predictors X_C with elements $x_{C_j}^{(i)}$, similar to $x_{ID_j}^{(i)}$, and m -dimensional vector («education results») Y_C with elements y_{C_j} , similar to y_{ID_j} , $i = 1, \dots, k, j = 1, \dots, m, m$ is the number of students in the test group.
4. The multivariate linear regression was chosen as the model of dependence of the «education results» vector from the predictor's array. The parameters of the model were determined accordingly to the data about the students' identification group:

$$Y_{ID_estim}(b, a) = b \cdot \text{diag}(E_{n \times n}) + (a^T \cdot X_{ID}^T)^T, \tag{1}$$

5. Formula (1) shows that the «education results» $Y_{ID_estim}(b, a)$ (n -dimensional vector) depend on the scalar parameter b (being interpreted as the «education results» vector value provided zero values of predictors) and k - dimensional vector of the regression parameters. $\text{diag}(E_{n \times n})$ is the diagonal of the $n \times n$ identity matrix used for the dimensionality alignment in (1); T signifies the transposition operation.
6. The parameters $(b, a)^*$ in (1) are determined to minimize the least-squares criterion:

$$(b, a)^* = \arg \min_{b, a} ([Y_{ID} - Y_{ID_estim}(b, a)]^T \cdot [Y_{ID} - Y_{ID_estim}(b, a)]), \quad (2)$$

7. The values $(b, a)^*$ are further applied as parameters (b, a) , in (1) delivering a minimum to the value of the mean square deviation of the «education results» vector Y_{ID} from its estimation $Y_{ID_estim}(b, a)$, being determined accordingly to the predictor's array.

At the same time the values of the regression statistical properties, as well as statistical characteristics of parameters (b, a) are determined (these characteristics are listed below in the illustrative example description).

8. The parameters time independence property in the model (1) is estimated using the data of students' test group predictors provided the parameters (b, a) , corresponding to a minimum of (2). The time independence property index is determined as the average square deviation of the «education results» vector Y_C from its estimation by the model with parameters corresponding to the data of students' identification group.

$$\Delta(b, a) = ([Y_C - Y_{C_estim}(b, a)]^T \cdot [Y_C - Y_{C_estim}(b, a)]) / n, \quad (3)$$

$$Y_{C_estim}(b, a) = b \cdot \text{diag}(E_{n \times n}) + (a^T \cdot X^T)^T, \quad (4)$$

The regression model with parameters (b, a) may be considered as quasi-time invariant if the multiple correlation coefficient between Y_C and the predictor's array X_C remains significant with the chosen significance level although the regression model parameters were determined without using the data Y_C .

The model was worked out in two stages. The 1st stage included the determination of predictors' array components and the estimation of linear multivariate regression model parameters. The predictors' database was filled by the retrospective data about school education characteristics (interpreted as predictors) of the identification group of students presently passing the 3rd education course. The regression model's parameter setting was carried out using the «education results» vector Y_{ID} , assumed to be known. The 2nd phase justified the forecasting possibility of the «education results» vector (naturally unknown at the moment of the university educational direction choice) based on the regression model with the parameters being determined at stage 1. The effectiveness of the proposed approach application was estimated as follows. The forecasted estimate of the «education results» vector $Y_{C_estim}(b, a)$ was carried out for the students' test group without the regression model parameters adjustment in the conditions of the unknown «education results» vector value Y_C . Then the forecasting results $Y_{C_estim}(b, a)$ were compared with true values Y_C for this test group provided by the lecturers. The closeness of $Y_{C_estim}(b, a)$ and Y_C measured by (3) would justify the practical application of the proposed «Forecast» computer facilities.

The results of the learning success forecasting (example). The effectiveness of the proposed facilities is illustrated below relative to the forecasting of the «education

results» vector for the specialty «Computer Science & Control». The identification and control groups of students were selected from the learners of 3rd and 4th courses correspondingly.

The predictors' set includes the following components:

1. group 1 of school training indicators in subjects necessary for mastering the university program (for the direction of "Computer Science & Control" this group includes the school marks in the natural sciences of the secondary-school diploma (algebra, geometry, physics), and also the marks of Unified State Exam of profile mathematics and physics);
2. group 2 of factors characterizing the general level of abilities and working capacities of a school graduate (average mark of secondary-school diploma and the expert estimate of a graduate's abilities made by his supervisor in the chosen scale).

Similar researches carried out for economic specialties [10, 11, 13, 15, 19] had shown the effectiveness of using both the exam marks for particular disciplines and the average mark of secondary-school diploma as the information source for predicting academic performance in a university. The distinction of predictors' components set chosen by us from used in [10, 11] is explainable by the difference between social and technical sciences. Particularly for technical universities the list of school marks being taken into account is narrower than for the humanitarian universities (see group 1). In contrast, the list of predictors in group 2 for technical universities is wider than those for humanitarian ones: for technical universities, it is very important to receive the expert estimate of a graduate's abilities made by his supervisor.

The formation of dependent (criterion) variable Y_{ID} in (2) had preceded the rigorous work of lecturers of profiling cathedra with the taught disciplines the program of study of which was carried out following modern modular-competency-based approach [16]. According to this one the lecturers had selected the modules which should be an important component of an engineer's qualification and therefore the knowledge of them would measure the student's expected readiness for future successive practical activity. Firstly, the scale for the measurement of this readiness was worked out. Each lecturer had appointed 100 balls for the volume of taught discipline knowledge which he considers satisfactory for future engineering successful work. Secondly, each lecturer had estimated the level of each student's success in a corresponding discipline as the part of 100 balls scale. This estimate is considered below an expert one. Notice that this estimation commonly does not coincide with the mark of discipline in the final graduation certificate because it is oriented mainly to engineer's practical needs rather than the discipline theoretical foundations. And finally, the j th component y_{IDj} of the dependent (criteria) variable Y_{ID} which corresponds to each student from the identification group $j = 1, \dots, n$, was determined as the average value of all expert estimates. Such averaging makes the dependent (criteria) variable more objective due to the subjective lecturers' opinions smoothing. The variable Y_C in (3) was formed similarly.

The dependence of Y_{ID} and Y_C from the corresponding predictors' arrays was supposed to be linear.

Since the initial data are given in different scales (the marks for school subjects are of scale 1–5 while the rest predictors were estimated of scale 0–100), all predictors were normalized through reducing to single scale 0.0.1.

The computations carried out for stages 1 and 2 are pointed below.

Stage 1. The determination of predictors' array components and the estimation of linear multivariate regression model parameters provided the model's independent variables are presented by the columns of the predictors' array X_{ID} determined for the identification group of students (Table 1).

Table 1 shows that the predictor x_1 «Expert estimate of a graduate's abilities made by his supervisor» has the highest weight. Small weights of predictors x_4 and x_5 (marks on geometry and physics correspondingly) illustrate the low influence of these disciplines on the forecasting of the studying efficiency at the specialty

Table 1 The results of the regression model's parameters determination (specialty «Computer Science & Control»)

Parameter's designation	Determined value	Confidence bounds of the model's parameters		Comments and parameters interpretation
		Lower	Upper	
b	-0.7	-1.2	-0.1	Value of scalar parameter in (1)
a_1	1.4	0.9	1.8	Weight of predictor x_1 «Expert estimate of a graduate's abilities made by his supervisor»
a_2	-0.4	-1.1	0.3	Weight of predictor x_2 «Middle ball of secondary-school diploma»
a_3	0.4	-0.2	1.0	Weight of predictor x_3 «Mark of algebra in the secondary-school diploma»
a_4	-0.1	-0.6	0.5	Weight of predictor x_4 «Mark of geometry in the secondary-school diploma»
a_5	0.1	-0.4	0.5	Weight of predictor x_5 «Mark of physics in the secondary-school diploma»
a_6	0.2	-0.3	0.7	Weight of predictor x_6 «Mark of physics at Unified State Exam»

«Computer Science & Control»). Maybe this peculiarity reflexes the low application of those disciplines' knowledge by the lecturers of the profiling cathedra in their taught subjects.

It was detected that the standard errors of the regression coefficients are many times less than coefficients themselves therefore the accuracy of their determination may be considered satisfactory.

The significance of each regression coefficient was justified by the procedure of statistical check of hypotheses (we had applied Student criterion with significance level 0.05). Table 1 includes the estimations confidence intervals' bounds for each regression model coefficient as well.

For example, the study success for j th school graduate can be forecasted by following expression with model parameters from Table 1:

$$y(x_j) = -0.7 + 1.4 \cdot x_1 - 0.4 \cdot x_2 + 0.4 \cdot x_3 - 0.1 \cdot x_4 + 0.1 \cdot x_5 + 0.2 \cdot x_6 + 0.1 \cdot x_7 \quad (5)$$

where $y(x_j)$ is the dependent (criterion) variable (ball estimation of the future learning success of school graduate when he would study at high university courses); x_1, \dots, x_7 are his predictors' values with designations from the right column of Table 1.

Expression (5) shows that the forecasting estimate of the students with evident preferences of the school disciplines correlating with the chosen university specialty would be better than possessed by the so-called «round excellent» schoolchild (notice that the estimate forecasts the learning successes on the senior courses of university). Of course, this conclusion does not apply to the gifted school graduate for whom the proposed computer support facilities are needless. We see that the predictors x_2 and x_4 (middle ball of secondary-school diploma and the mark of geometry in the secondary-school diploma correspondingly) are entering in (5) in the inverse linear dependence. The interpretation of such backwardness is following: shifting the attention of the ordinary schoolchildren to the favorite disciplines leads to their better mastering than is available for the schoolchildren paying equal attention to the whole discipline list. We had confirmed this conclusion by the data of not the highest school successes of the best students of the specialty «Computer Science & Control» both from identification and test groups.

Likewise, the use of (5) allows simulating the highest meaning of estimation of the school graduate's future learning success prediction. For this, it is enough to put maximum values to the predictors entering in (5) in the direct linear dependence and to put the values of x_2 and x_4 at minimum levels which are enough to secondary-school diploma achievement. This simulation would be useful for the supervisor of the school graduate class for the recommendations of the rational teaching time distribution. Also, it may be helpful for the university dean's office as well as to the profiling cathedra in the planning of students' group formation and the attraction of junior courses students to the additional training and educational events.

The comparison of the forecasted $Y_{ID_estim}(b, a)$ and realistic Y_{ID} dependent (criterion) functions shows sufficient accuracy of the regression model (Fig. 1).



Fig. 1 Comparison of the forecasted and realistic estimation of the academic performance of the students from the identification group

The information regarding the regression model quality (i.e. regression statistics) [20] is as follows:

1. The normalized multiple correlation coefficient between the independent and dependent variables reflecting the degree of relations between the predictors and dependent (criteria) function turned to be equal 0.87 thereby confirming the significant level of dependence of academic performance from school successes. Naturally, the high value of multiple correlation coefficient (being computed on the same data that were applied for the regression model's identification) cannot prove the model's usefulness (because the subject of interest relates to the period of choice of the future university study direction in the conditions when the forthcoming learning results are principally unknown).
2. The perspectives of the model's useful application in the absence of real data about future learning success estimates (namely this situation constitutes the essence of the discussed problem) were appreciated by the determination coefficient which is determined as the multiple correlation coefficient being squared. The value of the determination coefficient achieved in the discussed example reaches 0.76. Correspondingly to the known interpretation of the determination coefficient, such value means that the worked-out model would correctly show the dependence of expected university study successes from the results of school learning in 76% situations. The achieved value of 76% may be accepted as satisfactory and therefore the regression model may be recommended for forecasting the dependent (criteria) variable.
3. The coefficient of variation (i.e. the ratio of the standard deviation of dependent (criteria) variable to its mean) turned to be 0.26 validating the satisfactory regression model quality.
4. The carried out analysis of variance allowed splitting up the variance of criteria variable for two components. The 1st one can be explainable by the predictors' values while the 2nd one should be considered as random (i.e. independent from the predictors' values). In our case, 75% is related to the explainable variance. Therefore, in most cases, the worked-out model correctly explains the relationship between the predictors and dependent (criteria) variable.



Fig. 2 Comparison of the forecasted and realistic estimation of the academic performance of the students from the test group

Stage 2. The justification of the forecasting possibility of the «education results» vector based on the predictors of test students' groups.

Figure 2 shows the result of testing. We have simulated the applicability of the forecasting of dependent (criteria) function values based on the model with parameters of Table 1 however with the predictors' values corresponding to the test students' group (the students of 4th university course today). The true dependent (criterion) variable values related to this test group were not applied in forecast computation (were applied only for prediction accuracy estimation).

The estimation of the multiple correlation coefficient between the dependent (criterion) function and the set of predictors determined for the test group data is insignificantly different from one determined for the identification group and therefore the usefulness of the proposed approach is indirectly justified.

The model's sensitivity to the initial data uncertainty was determined by the comparison between the results of the identification of model parameters estimated according to the data of the identification group («identification model») and those estimated according to the data of the test group («testing model»). Naturally, the values of coefficients in these two models differ from each other nevertheless the coefficients of the «testing model» lay in the confidence intervals of the «identification model» (Table 2) and vice versa.

The acceptability of the described above predictors' list (basic list) was estimated through the determination coefficients computed for the set of models based on the lists with different predictors (provided that all such lists were chosen as the subsets of the basic list). The results are presented in Table 3. Also, this table illustrates the result of excluding the predictor which its correlation coefficient with the dependent (criterion) variable is the smallest one.

Table 3 shows that excluding the predictor even weakly correlating with the dependent (criterion) function is undesirable since it leads to a notable decrease in the determination coefficient.

The analysis of the statistical characteristics of the worked-out model had shown the significance of both the regression and its parameters. The verification tests which were fulfilled for the specialty «Computer Science & Control» showed that the model

Table 2 The comparison of the «identification» and «testing» models' parameters

Model based on the data of students' identification group				Model based on the data of students' test group			
Parameter's designation	Estimated value	Confidence bounds of the model's parameters		Parameter's designation	Estimated value	Confidence bounds of the model's parameters	
		Lower	Upper			Lower	Верхняя
b	-0.7	-1.2	-0.1	b	-1.0	-1.8	-0.2
a_1	1.4	0.9	1.8	a_1	1.3	0.5	2.0
a_2	-0.4	-1.1	0.3	a_2	-0.4	-2.2	1.4
a_3	0.4	-0.2	1.0	a_3	0.5	-0.7	1.7
a_4	-0.1	-0.6	0.5	a_4	-0.2	-1.0	0.6
a_5	0.1	-0.4	0.5	a_5	0.4	-0.7	1.6
a_6	0.2	-0.3	0.7	a_6	0.4	-0.4	1.1
a_7	0.1	-0.2	0.5	a_7	0.1	-0.4	0.4

Table 3 The determination coefficient value dependence from the list of components of predictors' set

Predictors' set	Determination coefficient
1. Ball of Unified State Exam on the profiling mathematics	0.2582
2. Ball of Unified State Exam on physics	0.0220
3. Middle ball of secondary-school diploma	0.1449
4. Mark of algebra in the secondary-school diploma	0.3110
5. Mark of geometry in the secondary-school diploma	0.1640
6. Mark of physics in the secondary-school diploma	0.2815
7. Expert estimate of a graduate's abilities made by his supervisor	0.7182
8. Predictors of items 2 and 5	0.1676
9. Predictors of items 3 and 6	0.2913
10. Predictors of items 4 and 7	0.7325
11. Predictors of items 1 and 7	0.7369
12. Predictors of items 1, 7 and 6	0.7380
13. Predictors of items 1, 7 and 4	0.7480
14. Predictors of items 1, 7, 4 and 6	0.7480
15. Predictors of items 1, 7, 4 and 3	0.7533
16. Predictors of items 1, 7, 4, 3 and 2	0.7581
17. Predictors of items 1, 0.7, 0.4, 0.3, 0.2 and 6	0.7585
18. Predictors full list	0.7588

was able to predict the future successful university studying with probability not less than 0.75.

Similar models may be carried out for other directions of studying as well. We hope that the estimations of the perspectives of the successful university studying would be useful for school graduates choosing the study direction before the university entrance.

Increasing the effectiveness of studying successful forecasting. Although the current level of the regression model readiness allows the studying successes forecasting the problem of its effectiveness improvement remains to be actual. Therefore, the attraction of other (more sophisticated) multidimensional analysis methods seems to be perspective.

Such perspectives may be detected by the analysis of the disadvantages of the model described above. One of them consists in the poor accounting of the individual character features both of university students and school graduates (for examples, the emotional stress passing Unified State Exam, lack of understanding between certain teachers and schoolchildren, the tendency of marks overstatement sometimes taking place in schools with low teaching level, etc.).

The first almost evident step chosen by us to strengthen the account of the individual features of the university students as well as school graduates was the clustering of the characteristics of the «identification» group of students by certain inner features. We have used the Unweighted Pair-Group Method Using Arithmetic Averages (shortly UPGMA) [21].

The clustering procedure has decoupled the whole group of students who participated in the investigations into 4 subgroups of approximately equal numbers. Subgroup A included the students with an excellent academic performance both at school and at the university. Subgroup B included the students with an excellent academic performance at school but with low successes in the university explainable by their certain personal reasons. Subgroup C included the students with a high level of the middle ball of secondary-school diploma while their school grades in natural sciences were low. Namely, these students possibly had made the mistake of choosing a specialty. And finally, subgroup D united students with insufficient successes of studying as at school as at university (this subgroup can be considered as a kind of clustering random component). As a result, the whole predictors' space was decoupled to 4 clusters corresponding to these students' subgroups data.

The multivariate regression models were carried out for each cluster provided that the models were based on the same predictors' lists and the same interpretation of the dependent (criterion) variables as was described above. The regression statistics estimated for each model separately showed the noticeable growth of the determination coefficients (0.9, 0.83, 0.95, and 0.8 for data of subgroups A, B, C, D correspondingly) in comparison to the determination coefficient (0.76) being determined on the data of all students without clustering. Unfortunately, the information support of the full clustering procedure of school graduates is problematic because of the principal lack of information about their future university successes. Nevertheless, we hope to improve the accuracy of the future successes forecasting due to partial clustering (for example, at least due to separation of the subgroup C school graduates whose

information support is available, and to warn them about the risk of the mistake in future specialty choice).

2 Conclusion and Further Researches Perspectives

1. The computer facilities and the appropriate simulation model are proposed to help school graduates in the choice of the appropriate direction of university study.
2. The example of the model's identification and validation was carried out applicable to specialty "Computer Science & Control". The multivariate regression analysis carried out for the example conditions reflects with the probability 0.75 the linear dependence of the level of successful university studying from the academic performance of the school graduate in the disciplines correlating with the skills and knowledge of the profiling disciplines taught at the senior university courses.
3. The decoupling of students' group into subgroups according to certain inner features was carried out through a cluster analysis method application. Due to the clustering, the prehistory of the school academic performance was partially taken into account resulting in to study forecast accuracy improvement.
4. The nearest direction of our work should be the AI achievements [22, 23] (in particular the artificial neural nets [8, 24]) application. Also, we are planning to validate the multivariate regression models application for the forecasting of successful studying for other university technical specialties.

References

1. Antonova, O.G., Dyl'nova, Z.M.: On the issue of development trends of Russian higher education. *University proceedings. Volga region. Soc. Sci.* **4**(44), 127–135 (2017)
2. Kostyukevich, S.V.: Current tendencies in higher education and its classical values: the relevance of the balance. *Vestnik vysshey shkoly* **4**, 11–19 (2013)
3. Isaeva, E.R., Toussova, O.V., Tishkov, A.V., Shaporov, A.M., Pavlova, O.V., Efimov, D.A., Vlasov, T.D.: Searching for prognostic criteria of students' academic success. *Univ. Manag.: Pract. Anal.* **21** **2**(108), 163–175 (2017)
4. Strenze, T.: Intelligence and socioeconomic success: a metaanalytic review of longitudinal research. *Intelligence* **35**(5), 401–426 (2007)
5. Zhu, D., Hodgkinson, I., Wang, Q.: Academic performance and financial forecasting performance: a survey study. *J. Behav. Exp. Fin.* **20** (2018)
6. Krushel, E.G., Stepanchenko, I.V., Panfilov, A.E., Kharitonov, I.M., Berisheva, E.D.: Forecasting model of small city depopulation processes and possibilities of their prevention. In: Kravets, A., Shcherbakov, M., Kultsova, M., Iijima, T. (eds.) *Knowledge-Based Software Engineering. JCKBSE 2014. Communications in Computer and Information Science*, vol. 466. Springer, Cham (2014)

7. Kharitonov, I.M., Krushel, E.G., Panfilov, A.E., Stepanchenko, I.V.: Trend forecasting model of quality of university graduates training on the example of Kamyshin technological institute (branch) of Volgograd state technical university. *J. Adv. Res. Dyn. Control Syst.* **10** 7 (Special issue), 1846–1852 (2018)
8. Oladokun, V.O., Adebajo, A.T., Charles-Owaba, O.E.: Predicting students' academic performance using artificial neural network: a case study of an engineering course. *Pacific J. Sci. Technol.* **9**(1), 72–79 (2008)
9. Zamkov, O., Peresetsky, A.: Russian Unified National Exams (UNE) and Academic Performance of ICEF HSE students, vol. 30 (2), pp. 93–114. Sinergia Press (2013)
10. Lialikova, V.I., Khatskevich, G.A.: Forecasting of students' learning success at the university based on data from entrance exams. *Vesnik of Yanka Kupala state university of Grodno. Series 2. Mathematics. Physics. Inform. Comput. Technol. Control* **2**(177), 70–73 (2014)
11. Poldin, O.V.: Predicting success in college on the basis of the results of unified national exam. *Appl. Econ.* **1**(21), 56–69 (2011)
12. Breiter, A., Stauke, E.: Assessment information systems for decision support in schools a case study from Hungary. *Knowl. Manage. Educ. Innov.* **230**, 9–17 (2006)
13. Bogomolov, A.I., Derkachenko, V.N., Aryutkina, T.A.: Forecasting of students' performance in special disciplines based on regression equations. *University proceedings. Volga region. Soc. Sci.* **1**(9), 124–132 (2009)
14. Grankov, M.V., Al-Gabri, W.M.: Regression model of the performance of student's groups in higher education institution. *Eng. J. Don* **1** (2017)
15. Erguven, M.: Comparison of the efficiency of principal component analysis and multiple linear regression to determine students' academic achievement. In: *Application of Information and Communication Technologies. 6th International Conference*, pp. 1–5 (2012)
16. Kharitonov, I.M.: Modeling process of building curriculum based on formal presentation of academic discipline. *Open Educ.* **2–1**, 21–32 (2011)
17. Draper, N.R., Smith, H.: *Applied Regression Analysis*, 3rd ed, 736 p. Wiley (1998)
18. Burnham, K.P., Anderson, D.R.: *Model Selection and Multimodel Inference: A Practical Information-Theoretic Approach*, 496 p. Springer, New York (2002)
19. Orlova, I.V., Turundaevsky, V.B.: *Multivariate Statistical Analysis in the Economic Processes Study (Monograph. ed)*, 190 p. MESI, Moscow (2014)
20. Alexopoulos, E.: Introduction to multivariate regression analysis. *Hippokratia* **14**, 8–23 (2010)
21. Tyurin, A.G., Zuyev, I.O.: Cluster analysis, methods and algorithms of the clustering. *Herald of MSTU MIREA* **2**(3), 86–97 (2014)
22. Brijesh, K., Saurabh, P.: Mining educational data to analyze students' performance. *Int. J. Adv. Comp. Sci. Appl.* **2**(6), 63–69 (2011)
23. Lubna, M.: Prediction of student's performance by modelling small dataset size. *Int. J. Educ. Technol. Higher Educ.* **16**, 27 (2019)
24. Anh, D.N., Van Quang, N., Thuy, L.X.: Academic performance forecast for student success. In: *XIX National Conference: Some Selected Issues of Information Technology and Communication. Hanoi, Oct 1–2/2016*, pp. 31–36

Increasing Student Motivation by Using Dynamic Rating: Approach and Implementation as Part of the LMS Based on Open-Source Software



Mikhail Ivanov  and Victor Radygin 

Abstract The issue of choosing a modern learning management system for working with part-time students has been investigated in detail. The possibilities of integrating the most popular modern learning management systems with the digital environment of the university are disclosed. The disadvantages of using ready-made solutions are shown. The influence of the choice of a student performance monitoring system and its integration into the modern learning management system on the motivation of a virtual group of students is studied. The disadvantages of the credit rating system are shown. An approach based on a dynamic rating is proposed. The methodology and calculation formulas for calculating the student rank are given. The modern technologies of building web services and mobile applications are investigated. The choice of technological tools for building a modern learning management system at NRNU “MEPhI” is justified. The idea of a three-level modern learning management system is revealed. Examples of ready-made system elements and a description of e-architecture are given.

Keywords Modern electronic education · LMS · m-learning · Student motivation · Competitive approach · Ruby on rails · Dynamic rating

1 Introduction

Competition in the international market of higher education is growing every year. More and more countries are investing a lot of money in the fight for high places of their universities in the world arena. For example, the national educational development program «Excellence Initiative» started in Germany in 2007, national projects 211 and 985 started in China in 1992 [1]. Similar program 5–100 in Russia have

M. Ivanov (✉)

Financial University Under the Government of the Russian Federation, 49 Leningradsky Prospekt, 125993 Moscow, Russia
e-mail: MNIVanov@fa.ru

V. Radygin

National Research Nuclear University MEPhI, 31, Kashirskoe hwy, 115409 Moscow, Russia
e-mail: VYRadygin@mephi.ru

started by presidential decree in 2012. Such government actions of different countries are due to the fact that today it is extremely difficult for universities to win a competition for applicants, and sometimes even for their students [2]. An important factor in such conditions is the quality and methods of presenting materials to both students directly in the university educational process and remote potential consumers for advertising purposes.

On the other hand, mentality and new knowledge perception way of current generation requires new approaches in teaching. Primarily, today students have access to petabytes of ready-made information on the Internet. As a result, they are not ready to spend a long time studying lectures, no matter how interesting and in any electronic form they are presented. Their involvement in the educational process requires an interactive approach that uses dynamically changing learning, which constantly varies between studying new knowledge, solving practical problems, and computer games. The second need for modern youth is social communication in electronic form by social network format. Moreover, according to WeAreSocial.com 52% of global Internet traffic came from mobile devices in January 2018. 41% of Internet users belonging to the age group of 16–29 today do not use stationary devices in principle [3]. In such a situation, “classical” non-mobile LMSs are not able to fully respond to the challenges of society.

A special specific problem for many higher education institutions is the high inertia of new digital education technologies introduction, due to the inability of age-old faculty to fully respond to new challenges in the field of pedagogy. Today, for most Russian universities situation when the vast majority of teachers belong to age groups older than 60 years or younger than 40 years is characteristic. For example, according to results of monitoring the higher education effectiveness in the Russian University of Transport share of faculty members over 65 years old is more than 32%, at the National Research Nuclear University “MEPhI”—over 34% [4]. This fact dictates additional requirements for LMS, forcing to combine software of different input difficulty levels: from the minimum presentation of discipline in static page form and files set to the symbiosis of training simulators and courses in MOOC format. Ready-made LMSs or MOOC-systems do not provide such versatile functionality.

2 Literature Review

The problem of integrating LMS with university corporate networks and training simulators is very important.

The most popular proprietary LMSs among world-leading universities are Blackboard Learn from Blackboard company, Canvas (the system code is free, but usually universities use a paid support from Instructure company), Brightspace from D2L company. According to the site, edutechnica.com [5] share of American universities using these systems amounted to 72.6% of the total number of higher education institutions in the United States in the spring of 2019. Using the experience of such

systems in the USA university environment is shown in work [6]. Unfortunately, For Russian universities and many Universities from Asia and countries of post-Soviet space, limited in budget and choice of its spending items, the main problem of using these systems is their price and its completion cost for integration into the university corporate environment. Many authors point to this problem in their papers. For example, Alja-warneh, S. in his work [7], shows some reasons for the transition from the proprietary Blackboard Learn system to the free Moodle system at Isra University (Jordan). One of the product choice determinants is the financial component of license software in this paper. The inaccessibility of proprietary LMSs for most post-Soviet and Asian (except big-gest and world-famous) universities is also indicated by V. G. Gerasimova and others in their work [8] on the Russian Market of LMS. Decisions about the choice of free software are also shown in work [9] and many other authors.

For European and American universities, one of the disadvantages of proprietary systems is caused by their lagging behind the needs of modern students. One of the indirect evidence of this fact is the rapid disappearance of some LMSs from the US market in the past four years. A vivid example is the ANGEL system, which occupied 4.6% of the market in 2015 and was completely excluded in spring, 2019. A large number of works are devoted to comparing leading products in markets of proprietary and free learning management software. Statistical research among students of Tokyo University [10] showed advantages of the fast-paced system Moodle more in 2008.

It is worth noting that the Russian legislation in the field of personal data imposes severe restrictions on information that is allowed to be placed in a cloud format. Because of it, many cloud solutions are not usable for universities. However, many authors emphasize the need to use modern technologies of social networks in training. For example, De-Marcos, L., and others in their work [11] show the importance of teacher's work in social networks, even in the presence of existing LMS.

Thus, modern LMS, on the one hand, should be integrated with such means as Facebook, Twitter, VKontakte, etc. But on the other hand, it should offer its closed ana-logs of social networks' elements and be integrated into university social network. Citation of e-materials, links to specific lessons or their elements, collective discussions, "likes" and "dislikes" is extremely important for attracting and involving students, applicants, and even students' parents. It is important to understand that, although modern LMSs often include a number of pointed elements, their remoteness from the usual sphere of students' communication often leads to the fact that point-ed tools are ignored by both students and teachers. This aspect further increases the complexity and cost of full integration of "package" LMS in the university educational process. Unfortunately, none of the proprietary and free LMSs has such a contradictory set of capabilities, which creates a need for their own refinement of such systems after their deployment. Lack of internal communication tools of learning management basic platforms reveal in the authors of their works from many countries. For example, A. Juma and others in their work [12] suggest combining LMS-systems and social networks.

The most popular open-source LMSs among the world's leading universities are Moodle and Sakai. According to edutechnica.com [5], the share of American universities using these systems is 20.1% of the total number of US higher education institutions in the spring of 2019. The use of free software largely solves a question of the introduction cost of LMS. Nevertheless, the question of the need to make an additional refinement system remains relevant and to free software. But, on the other hand, the lack of modern means of supporting mobile data technologies in these systems is shown in the works of many Russian and foreign authors. For example, Hasan [13] point out the shortcomings of Moodle in their works.

It should be noted that all considered systems, both proprietary and free, offer to the user (course author) a single-level complexity model. In fact, all authors, regardless of their preparation, work with the same interface. The complexity of course preparation varies only due to content variety offered by the teacher. Unfortunately, as shown above, this approach is not acceptable for many Russian universities. The problem of involving inexperienced age users in the atmosphere of online learning requires the availability of simple means of making electronic courses. On the other hand, for professionals creating exclusive courses that are the face of the university, powerful and sophisticated tools are needed. For teachers, leading the same general subjects once to dozens of groups, easily scalable technology is required.

An alternative to dividing the LMS system into different levels of complexity is to create a powerful support service that provides faculty with necessary technical advice and assistance. The need for a powerful teacher support service for e-learning was proposed in the papers [14, 15]. The disadvantage of this approach is its high cost and teacher's binding to the workplace in process of course's creating (due to need of interacting with support service). This solution is particularly difficult for geographically distributed universities. For example, MEPhI has a big network of 17 subsidiaries and the Moscow area. Creating 18 electronic education support services re-quires tremendous financial costs. The introduction of multi-level in entering complexity LMS will significantly reduce these costs. Considering the lack of this variability in finished systems, it is relevant to create a university own LMS or to refine one of the free products.

It is also worth noting that today's work of the modern university is provided by dozens of information systems integrated into a single ERP system [16]. They solve a variety of questions from planning class schedules, to social work and direct interpersonal interaction in the style of social networks. LMS should be naturally embedded as a separate component of this uniform information space. A simple example is a need for data exchange between such ERP components the curriculum development module, schedule development module, student's accounting module, faculty staffing module, and LMS. Based on the curriculum, timetable, and teaching staff, many electronic courses are formed. Feedback is similar. LMS should not only offer students problems to solve, but also provide their assessment and uploading performance to appropriate modules for monitoring students contingent. Unfortunately, despite the presence of some standards in ready-made LMSs, for example, SCORM standard [17], modern requirements of the educational process in Russian universities make this integration difficult.

Summarizing this section, there are four requirements that determine the impossibility of using a ready-made LMS. The first reason is a requirement for full integration with the university corporate system, both in terms of transferring basic data of the educational process and in terms of integration with the corporate social network. The second problem is a requirement for integration with the most famous social networks while maintaining the possibility of creating a non-public course. The third aspect is a requirement for a different level of tools to create e-courses. And the last reason is a requirement for effective integration tools with educational software developed by the university.

3 Competition as a Way to Increase Student Motivation in Learning Management Systems

The difficult economic situation in most countries of the world dictates the need to consider various business models of educational activities even to leading universities. Some universities, such as the Massachusetts Institute of Technology, due to their reputation to limit students' admission only by a virtual group. Other universities, such as Arizona State University, are forced to work in a large-set business model, with following the separation of virtual and diversification of education into various groups according to the complexity of material presented. Moreover, today this model is most common for the majority of Russian universities. It requires effective ways to differentiate students for the purpose of following selection the best. At the same time, motivating support among the virtual group should be provided in the context of general education in junior courses with weaker primary level students.

One way to increase motivation can be competition. An important component of its provision is an effective assessment system integrated into LMS. Unfortunately, existing LMSs consider the task of maintaining student performance as secondary. Most of them provide the possibility of taking into account students' grades through elements of linear credit rating (point-rating) system, which is most often used in classical universities.

Modern universities are increasingly giving priority to the credit rating system. Papers of many authors, for example, [18, 19] reveal its advantages. Briefly, the advantages of this approach can be formulated as follows: the credit rating system encourages students to work continuously throughout the semester. Thus, students' habit "learn only in session" is eliminated. Moreover, this system can be used both in the case of the semester examination model and in the case of the model based on the student's choice of courses and their duration recommended by the Bologna process.

The accumulated experience of using this model in Russian universities allows concluding that this approach is most effective only when working with students of approximately the same level of training and motivation. The research held by authors at some universities showed that under conditions of strong differentiation

of students' motivation and basic training, the linear credit rating system becomes not only ineffective but, on contrary, reduces the motivation of students by end of the course.

Performance of first-year students studying from 2009 to 2014 in specialty "Computer Science and Computer engineering" at Moscow State Industrial University was considered as research's object. The linear credit rating system was used to train these students in a specified period. The training was carried out full-time using LMS. Students of only one specialty are considered in this analysis in order to reduce the factor of differences in approaches to training in different specialties. Introductory points normalized by relative maximum points and scatter of values in a given year were used to analyze the initial level of students' training.

The research results (Fig. 1) have two trends at the end of the semester. First, the main purpose of the linear credit rating system worked. Students for whom load intensity and course complexity were too big were successfully eliminated (significant increase in the left column of the histogram). The second trend is brightly negative. Considering students with academic performance above 20% of minimum, distribution of their numbers relative to average total points has become much more concentrated in 40% quantile. A decrease in the number of students as they move away from the average level to extreme values is very sharply. The number of students with above-average results has fallen to less than 20% in one semester. A similar situation is characteristic not only for this university and this specialty. Studies held in other universities and other specialties confirm this trend in most cases. The exception is universities with very high entrance points or small groups within the same specialty.

This example demonstrates the disadvantages of the linear credit rating system in which students gain points by sequential summation of successfully passed control

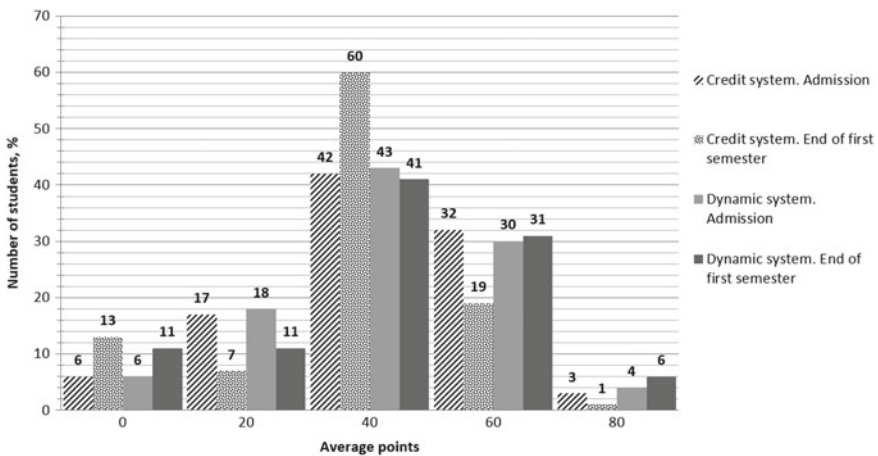


Fig. 1 Comparison of students' average point distributions at admission and the end of the first semester

measures. Thus, to increase students' motivation, it is necessary to develop a methodology for rating students and introduce approaches that increase their motivation. As a result, it is necessary to expand the capabilities of LMS associated with this aspect of the educational process.

4 The Dynamic Credit Rating System

The authors of this article with the assistance of Roganov [20] developed the dynamic credit rating system to eliminate disadvantages of the credit rating system for assessing students; dependence of assessment on time is its main operating mechanism. The system is based on five principles.

First of all, failure to do compulsory homework (which is not difficult) immediately leads to a noticeable decrease in rating. Their subsequent execution restores rating (fully or partially, depending on the delay).

The second base principle says that appraisals are carried out every two weeks (or several weeks), they have different weights and are accompanied by an assessment of students' current successes on the ten-point scale. Later appraisals are most significant.

The third principle is that all material of the semester is divided into 2–3 topics, each of them must be passed. Unfulfilled topic greatly reduces rating and amount of penalty increases with time. The subsequent performance of topics restores rating (depending on delay). The well-delivered topic brings a certain (non-decreasing over time) “bonus”.

The fourth principle is formulated as follows: attendance can be taken into account in ranking directly in the form of certain constant normalized value or influence only indirectly, due to a decrease in estimates of missing components.

The last principle is that the final academic performance at the end of the semester is taken into account due to the normalization of rating within the five-point segment.

Thus, a dynamic credit rating system includes four components. The first component is the current appraisal held every two or several weeks. Rating on a scale from 0 to 99 is set based on results of independent work, tests, work in the classroom and other parameters, excluding only assessment of homework. The most important second component is an obligatory simple individual homework (result is evaluated every two or several weeks). The third component is 2–3 obligatory activities per semester (depending on a number of modules), corresponding to large topics of course (held in form of writing control papers or passing colloquiums; if necessary, re-writing or re-taking are organized). The last component is intermediate appraisal (credit, graded credit, or exam), which is the final big topic of the semester (may not be passed by the student).

Contribution of appraisals to the rating is not equivalent: if more time current moment separates from grades moment, then it has less weight. This encourages students to pursue regular classes, as “old achievements are quickly forgotten,” and local success leads to an immediately visible increase in rating. If an appraisal event

is missed for a serious reason or other reasons for lack of ratings, the special rating calculation scheme is used to mitigate the effect of omission on the final result.

Obligatory homework must be completed on time. Contribution to the rating of tasks handed over on time is zero. Unfulfilled homework generates a penalty, the value of which increases with increasing time. Doing tasks within a reasonable time eliminates a penalty. If homework is done with a “long delay” in absence of serious reason explaining this, then a small but irremovable penalty is added to the rating.

The described scheme is aimed at developing students’ habits of completing homework. Experience using this approach shows that this happens quite quickly. It is important to note that homework should not be too large in volume, relatively simple, and different for different students. This can only be achieved by using specialized software tools that are part of LMS, and a reasonable amount and level of complexity should be done in accordance with the real possibilities of students.

Contribution to the rating of results of large topics doing is calculated according to the scheme very similar to taking into the account results of homework. The main difference is much more the importance of topics. In fact, their doing is the “repetition” examination session. Unfulfilled topic generates very noticeable penalty, which values in-creases with time. More time is given for re-submitting unfulfilled topic on time. Per-forming tasks eliminate penalties. With a very large “delay” without serious reason, a noticeable irremovable penalty is added to the rating.

Need to submit large topics is aimed at preparing students for a session, and eliminating its shock effect, allowing to gradually adapt to learning style at university.

The dynamic credit-rating system has been successfully used for 2 years (from 2014 to 2015) at the Faculty of Applied Mathematics and Theoretical Physics of Moscow State Industrial University to educate students of IT specialties in junior courses. To date, this approach is successfully applied in experimental mode for teaching students in the magistracy of the Institute of Nuclear Physics and Technology, NRNU “MEPhI”.

Effective factors of application dynamic rating and scheme for its calculation were identified during system using. In particular, a student’s first grading mark in the semester is determined after the first class of discipline, where students write “zero” independent work—so-called entrance control. Subsequent marks are set strictly systematically, at the end of every second week.

The grading mark is either a number from 0 to 99 or a sign of uncertainty, indicating an inability to classify the success of a particular student. The algorithm for determining the contribution of grading mark sequence to the rating is reduced to transforming the original sequence and finding the weighted average of marks of converted sequence. First of all, values of all numerical grading marks are reduced by 30, and the whole sequence of grading marks is divided into groups consisting of adjacent signs of uncertainty surrounded by some digital marks to left and right.

If the student does not have any grading marks at all, except for signs of uncertainty, then the first sign is evaluated as zero, two signs—minus 10, three signs—minus 20, more than three—minus 30 points. If the student has marks before missing obligatory activities and does not have one, then his marks are extrapolated: less than three signs of uncertainty continue with an arithmetic average of the last two marks (or one if it is

only one). Third and subsequent signs of uncertainty are replaced by zero if for first two signs of uncertainty replacement turned out to be non-negative, and minus 30 otherwise. If the student receives marks after missing one obligatory activity, a sign of uncertainty is replaced with an arithmetic average of three potential grades: last before omission and first two after omission. Each of two or more signs of uncertainty is replaced with an arithmetic average of the first three subsequent marks.

Following sequence of weights is used to calculate weighted sum:

1.0; 0.7; 0.4; 0.1; 0.05; 0.02; 0.01; 0.01; 0.01;...

The final formula for contribution to the rating of grading marks sequence can be determined as follows:

$$R_a = \frac{\sum_{i=1}^N w_{N-i+1} a_i}{\sum_{i=1}^N w_i}, \tag{1}$$

where N —number of obligatory activities;

a_i —marks converted according to the above rules;

w_i —weights.

Compulsory homework can be given every week or every two weeks, but the rating for their implementation is set only every two weeks. Homework is either fulfilled (set off) or unfulfilled, and thus mark for its implementation is binary (teacher can, for example, put plus sign in some electronic sheet at the time of assignment). In addition, it should be possible to indicate that failure to complete homework on time was due to serious reasons (seriously is determined by teacher).

Completed homework gives zero contribution to rating, if homework is delivered on time or delay does not exceed two weeks $t \geq 14$. The contribution to the rating is zero if it is indicated that failure to complete homework on time was due to serious reasons.

If homework is not completed, then its contribution is negative and is determined by piecewise linear function R_h , depending on a number of “delay” days:

$$R_h = \begin{cases} -0.2t & \text{if } t \leq 14, \\ -2.8 - 0.05(t - 14) & \text{if } 14 < t \leq 28, \\ -3.5 - 0.5(t - 28) & \text{if } 28 < t \leq 42, \\ -10.5 - 2(t - 42) & \text{if } t > 42, \end{cases} \tag{2}$$

where t —number of homework “delay” days.

A delay of more than 14 days is punishable by adding an unchangeable penalty equal to the minimum of 0.5 and the ratio of two to the number of homework is added to the rating.

Contribution to the rating of results of large topics submitting is similar to contribution of homework results and for each of them it is calculated using piecewise linear function R_h , depending on a number of “delay” days:

$$R_h = \begin{cases} -0.5t & \text{if } t \leq 21, \\ -10.5 - (t - 21) & \text{if } t > 21. \end{cases} \quad (3)$$

The excellent submitted topic gives further unchanged positive contributions to the rating of 20 points. Submitted (not excellent) topic gives zero contribution to rating. A topic that has not passed more than 30 days adds a penalty of -15 to the rating.

This technique works effectively only with special software that facilitates the calculation of ratings, provides graphical visualization and is understandable for students. Maximum achievable points according to semester results and predicted rating while maintaining the current level of performance must be shown to each student. Testing of the technique was carried out at Moscow State Industrial University.

Two cohorts of students were selected for testing: first-year students, who have not previously studied under the credit rating scheme, and second-year students who previously studied under the credit-rating scheme in the first year. The total number of students involved in the experiment was 96 in the second year and 108 in the first year.

The student survey conducted at the end of the semester showed that more than half of students positively evaluated the impact of the rating system on their involvement in the learning process. Analysis of first-year students' performance (Fig. 1) revealed a significant decrease in the tendency to "level out" all students, which may indicate the positive effect of the approach used.

5 Creating an Effective Learning Management System

The question of creating an effective LMS was considered by the authors on the example of one of Moscow's leading universities—NRNU MEPhI. Despite the fact that several effective LMSs based on the Moodle platform have existed in NRNU MEPhI for many years, for more effective promotion of this university in the international arena, a significant increase in the number and quality of electronic courses is required, especially in the most popular specialties. This requirement, together with identified shortcomings of Moodle LMS, determines the need to develop fundamentally new software.

Experience of leading Russian universities in the sphere of LMSs, such as the Higher School of Economics or the National University of Science and Technology MISIS has shown a high cost of integrating such systems into the university environment. At the same time, it is extremely difficult to achieve a number of identified requirements, for example, different complexity interfaces for creating courses. For these reasons, it was decided to consider an approach based on the development of its own software product.

One of the difficulties in integrating LMSs with ERP systems, social networks, and many virtual university simulators is a potential difference in development tools. For

scientific software that virtual simulators usually are, the most natural programming languages today are C++ and Python. For ERP class systems and social networks, web tools are used based on technologies such as PHP, Ruby on Rails, Django, etc. Today free solutions are most popular in universities of the Russian Federation.

Analysis of the most popular web frameworks allowed to determine the most suitable tool for NRNU MEPhI—Ruby on Rails framework [21, 22]. According to statistics from Australian independent agency Built With [23], the Ruby on Rails framework, to one degree or another, is the foundation of more than 1.5 million websites.

The effectiveness of using such technologies for university informatization is shown in the work [24]. It is worth noting that the choice of this system is also due to the three additional reasons. First of all, most of NRNU MEPhI internal network services are based on the Ruby on Rails framework. The second reason is that NRNU MEPhI has a large number of highly qualified Ruby on Rails programmers and experience in their training. The last but not the least reason is that the speed of development and modification of Ruby on Rails applications is higher than that of analogs on other popular frameworks.

Ajax—jQuery bundle was chosen to solve the problem of interactive user interaction. In addition, Websocket mechanisms were used to effectively implement feedback from client browser in web application [25].

The new LMS architecture also includes a mobile application based on Ruby language and Ruboto technology. Unity of programming language of web application and mobile application can significantly reduce the cost of maintaining the programmer's team.

The conceptual scheme of the created application includes three main aspects. The first aspect is the presence of three levels of interface complexity for creating and managing an electronic course and three performance accounting schemes and abilities to connect own algorithms in Ruby module form. The second aspect is the ability to connect training elements in form of IFrame, Ruby module, C-module integrated into Ruby, web module. The last aspect is supporting full integration through JSON-API with NRNU MEPhI systems for contingent accounting, scheduling, curriculum preparation, performance monitoring.

Three work options are offered to the teacher are creating a “community of discipline” according to the given template within an internal social network, creating a “community of discipline” with its own architecture within an internal social network, and creating an electronic course in LMS. Thus, the teacher gets the opportunity to quickly stratum in e-learning, gradually moving from a simpler level of presentation of materials to a more complex.

6 Conclusion

Thus, we can safely talk about the effectiveness of using free solutions in the field of electronic education for Russian universities. At the same time, to ensure the

university's high competitive ability in the international market, it is necessary to go beyond the framework of basic tools such as Moodle and Sakai and carry out our own development, often completely redesigning LMSs from scratch. When developing your own LMS, special attention should be paid to differences in the preparation of faculty and to ensure the possibility of trouble-free work even for employees who are poorly qualified in the IT field. Over time, this approach should provide enhancements to the overall digital culture of the staff and allow the transition to the construction of more complex and high-quality courses, both at the design and the substantive level.

The use of various technologies for assessing students' knowledge in the LMS allows them to flexibly respond to changes in the socio-cultural characteristics of students, ensuring high interest, regardless of their initial training.

References

1. Huang, F.: Building the world-class research universities: a case study of China. *High. Educ.* **70**(2), 203–215 (2015)
2. Agasisti, T., Shibanova, E., Platonova, D., Lisyutkin, M.: The Russian excellence initiative for higher education: a nonparametric evaluation of short-term results. *Int. Trans. Oper. Res.* **27**(4), 1911–1929 (2020)
3. Kemp, S.: Digital in 2018: World's internet users pass the 4 billion mark. Global Digital Report. Retrieved from <https://wearesocial.com/blog/2018/01/global-digital-report-2018> (2018)
4. Pugach, V.F.: Age of teachers in Russian universities: what is a problem? *High. Educ. Russia* **208**(1), 47–55 (2018)
5. Edutechnica. LMS Data—Spring 2019 Updates. Retrieved from <https://edutechnica.com/> (2019)
6. Machajewski, S., Steffen, A., Romero Fuerte, E., Rivera E.: Patterns in Faculty Learning Management System Use. *TechTrends* 1–7 (2018). <https://doi.org/10.1007/s11528-018-0327-0>
7. Aljawarneh, S.: Reviewing and exploring innovative ubiquitous learning tools in higher education. *J. Comput. High. Educ.* **32**(1), 57–73 (2020)
8. Gerasimova, V.G., Romanova, Y.D., Zhenova, N.A.: Russian market of LMS for higher education. *Astra Salvensis* **6**, 755–767 (2018)
9. Stankova, E.N., Barmasov, A.V., Dyachenko, N.V., Bukina, M.N., Barmasova, A.M., Yakovleva, T.Yu.: The use of computer technology as a way to increase efficiency of teaching physics and other natural sciences. In: *Lecture Notes in Computer Science (including subseries Lecture Notes in Artificial Intelligence and Lecture Notes in Bioinformatics)* 9789, pp. 581–594 (2016)
10. Miyazoe, T.: LMS-based EFL blended learning: Blackboard vs. Moodle. In: *JALT2007 Conference Proceedings*. Tokyo, Japan: JALT (2008)
11. De-Marcos, L., Domínguez, A., Saenz-De-Navarrete, J., Pagés, C.: An empirical study comparing gamification and social networking on e-learning. *Comput. Educ.* **75**, 82–91 (2014)
12. Juma, A., Rodríguez, J., Caraguay, J., Quiña-Mera, A., García-Santillán, I.: Integration and evaluation of social networks in virtual learning environments: A case study. *Commun. Comput. Inform. Sci.* **895**, 245–258 (2019)
13. Hasan, L.: Usability problems on desktop and mobile interfaces of the Moodle learning management system (LMS). In: *Proceedings of 2018 International Conference on E-Business and Applications, ICEBA 2018*, pp. 69–73 (2018)

14. Vershitskaya, E.R., Mikhaylova, A.V., Gilmanshina, S.I., Dorozhkin, E.M., Epaneshnikov, V.V.: Present-day management of universities in Russia: Prospects and challenges of e-learning. *Educ. Inform. Technol.* **25**(1), 611–621 (2020)
15. Mkrttchian, V., Kharicheva, D., Aleshina, E., Panasenko, S., Vertakova, Y., Gamidullaeva, L., Ivanov, M., Chernyshenko, V.: Avatar-based learning and teaching as a concept of new perspectives in online education in Post Soviet Union countries: theory, environment, approaches, tools. *Int. J. Virtual Personal Learn. Environ. (IJVPLE)* **10**(2), Article 5 (2020) (IGI Global, Hershey, PA, USA, 66–82)
16. Radygin, V.Y., Lukyanova, N.V., Kupriyanov, D.Yu.: LMS in university for in-class education: Synergy of free software, competitive approach and social networks technology. In: *Proceedings of the International Scientific-Practical Conference Information Technologies in Education of the XXI Century, (ITE-XXI)*, p. 020015. AIP Publishing, Melville, NY (2017)
17. Almurzayeva, B., Shunkeeva, O., Zhaltapova, A.: Contemporary forms of education assessment in organizations of Kazakhstan. *Przegląd Wschodnioeuropejski* **8**(2), 193–205 (2017)
18. Orekhov, E.F., Kostyuchenko, V.F.: Modernization of education—Hopes and realities. *Teoriya i Praktika Fizicheskoy Kultury* 2015-January(8), 3–5 (2015)
19. Alexandrov, A.I., Lukyanova, N.V., Radygin, V.Yu., Roganov, E.A.: Using dynamic rating system to improve the quality of teaching students in technical areas. *Young Scientist* **3**(83), 717–722 (2015)
20. Viswanathan, V.: Rapid web application development: a ruby on rails tutorial. *IEEE Softw.* **25**(6), 98–106 (2008)
21. McKenzie, P.: Weapons of Mass Assignment: a Ruby on Rails app highlights some serious, yet easily avoided, security vulnerabilities. *Queue* **9**(3), 40–48 (2011)
22. Built With. Framework Usage Distribution on the Entire. <https://trends.builtwith.com/framework/traffic/Entire-Internet> (2019)
23. Chunling, C.: Construction of the individualized college english learning management system using Ruby on Rails. In: *Proceedings of International Conference on Service Science, ICSS 2016-February (7400790)*, pp. 160–163 (2016)
24. Pimentel, V., Nickerson, B.G.: Communicating and displaying real-time data with WebSocket. *IEEE Internet Comput.* **16**(4), 45–53 (2012)
25. Bakhouyi, A., Dehbi, R., Banane, M., Talea, M.: A semantic web solution for enhancing the interoperability of E-learning systems by using next generation of SCORM specifications. *Int. J. Emerg. Technol. Learn.* **14**(11), 174–185 (2019)

Student Activity Cognitive Preference Registration in Dynamic Computer Testing Simulators



I. V. Shadrin 

Abstract The concept of organization of dynamic testing allowing a student to materialize their search activity when solving intellectual problems in the form of activities to transform objects in the virtual environment is proposed. Methods of registration of significant quantitative parameters allowing to identify priority ways of carrying out learning activities using the dynamic computer testing simulators are considered. Scenarios used in dynamic computer testing simulators actualizing different types of human intellectual activity are described.

Keywords Dynamic assessment · Education · Cognitive strategies

1 Introduction

At present, dynamic assessment of educational activity is of growing interest for practicing psychologists as well as for teachers of all levels of education. Various approaches to the organization of the dynamic assessment and methods of its practical application are described in literary sources [1–10]. However, the proposed concepts suggest that it is performed by a specialist (a psychologist or a competent teacher) who can direct student’s activities not by direct instructions but with the help of the leading questions and additional information from the subject area of the problem that is to be solved. Such people, controlling students’ activities for problem solution and dosing intervention in this activity depending on their success, are called mediators.

In the process of educational problem solution in which the use of the dynamic assessment has involved the registration of student’s activity is carried out in direct contact and required special training thus making it possible to notice particular features in behavior, speech, and knowledge of the subject area of the problem that is to be solved. This direct communication allows mediators to develop certain control actions, such as asking questions, giving indications, or providing additional information. These features make for the difficulties in mediator training. This makes

I. V. Shadrin (✉)

Krasnoyarsk State Pedagogical University named after V.P. Astafiev, 89 Ady Lebedevoy,
Krasnoyarsk 660049, Russia
e-mail: igor.v.shadrin@mail.ru

their mass character impossible and does not allow meeting the needs of educational institutions.

One of the observations, which are of interest for pedagogical practice, made by psychologists using methods of dynamic assessment, is the diagnosis of the students' cognitive activity manifesting itself in the way they react to control actions. The structure of such an interactive educational activity reflects the structure of student's mental processes, allows them to determine their priority methods of obtaining information from the surrounding world (cognitive strategies), their ability to identify, generalize, classify as well as use their search activity to form new mental functions, bring them to the next level of development and to explore the learning potential [4, 6, 8–13].

Thus, we can talk about a high social demand for training people of various age groups—from young children, continuing with school and university education, ending with advanced training and retraining of specialists. However, it would not be possible to meet the broader need of the educational system and supply it with the qualified personnel able to apply dynamic assessment in the practical pedagogical activity. It is essential to search for the means that could allow an ordinary teacher to use the dynamic assessment technologies in their daily activity, to supply them with a simple and affordable tool for individualized education based on the objectively recorded quantitative characteristics of the process of carrying out educational activity determined by the characteristics of the student's cognitive activity. Finding a solution to this problem is the center of attention of the scientists developing the direction of dynamic computer testing, creating dynamic computer testing simulators (DCTSs) [14–16]. We shall review what the DCTS is at the present stage of their development, review the range of their thematic application, the possibility to register learning activity indicators, and quantitative analysis used for the identification of cognitive preferences in students' educational activity.

2 The Methodology of Dynamic Computer Testing

DCTSs are computer programs that contain the following mandatory visual components:

- *The work area* is a part of the program interface available to the students for interactive engagement. In the process of educational problem solving, the student changes the condition of the work area and manipulates virtual objects. Depending on the type of the DCTS such objects may include graphs of functions [17], parts of images or musical compositions [18–20], words and phrases, or pointers to objects that are to be identified [21, 22]. The solution to the problem is a predetermined relative position of these objects, or, in the case of graphs of functions, the correspondence of the obtained function coefficients to the values requisite in the problem.

- *The task definition area* is a panel displaying the task (a problem) that is to be solved. In some DCTS the definition is textual (for instance, “complete the picture”) occupying a small area and not changing from task to task. In other types of DCTS, whose tasks require the user to identify elements, task definition can occupy a significant part of the program window and change with each attempt to solve it.
- *The control panel* is an area containing interface elements allowing you to change the condition of the work area. Such elements include buttons for controlling the equation coefficients for the graph plotted in the work area, buttons for selecting a fragment, a word, or a pointer, drop-down lists making the aforementioned process convenient, buttons for moving (setting) the selected element to the work area and for canceling the previously installed element. Depending on the type of DCTS tasks, the set of controls may vary.
- *The dashboard* is a panel containing interface elements allowing students to be fully aware of the current situation, come to the solution to the problem, and receive information on how their activity is assessed. An indicator showing the level achieved by a student is an obligatory dashboard element for all types of the DCTS and will be described below.
- In addition to the visual components, the DCTSs contain certain software blocks constituting student’s educational activity management system using evaluative feedback based on dynamic evaluation:
- *Task generator* is a block forming tasks of the same type differing in initial data and the initial situation in the work area. For tasks of the “Complete the picture” and “Set the sequence” types, the initial fragment sequence in the viewport is randomly set (using a random number generator), as well as the equation coefficients for the graph of the function. For the tasks of the “Establish the correspondence” kind, the pointer numbers in the task definition area, as well as the order of the corresponding work field elements, are randomized.
- *The dynamic assessment module* assesses a student’s action on a “correct—incorrect” scale each time an action is performed. On such a scale the ranking is based on the sign of approaching the goal of solving the problem. At each moment in time, the distance to the goal is known: the minimum number of actions required to achieve the condition of the work field corresponding to the solution of the problem. In case a student’s action has reduced the distance to the goal, the action is marked as “correct”, if the distance has been increased, it is marked as “incorrect”. Actions associated with viewing (scrolling through) the control panel elements are recorded by the system but are not evaluated since they do not bring the user closer to the solution of the problem or further away from it.
- *The feedback module* is a block responsible for the formation and implementation of control actions in the program interface. In the DCTS developed, the educational activity management system consists of two loops, for each of which certain program interface reactions are provided.
- The external control loop is used to assess the quality (independence) of the student’s activity in the process of solving the problem. It is a scale of discrete levels (from 1 to 10) which shows the grade for each task once it has been

completed. This assessment is directly related to the proportion of the student's correct actions. The bigger this proportion, the higher the level will be determined: 0–10% is the first level, 10–20% is the second level, etc. The achieved level is displayed on the dashboard and determines the operating mode of the internal control loop used to perform a dynamic assessment of the student's activity.

- Once the correctness of the action performed has been defined, depending on the type of the DCTS the following environmental reactions realizing evaluative feedback can be formed on the internal loop of educational activity management. The activation of these reactions (active/inactive) is determined by a random number generator. The higher the achieved level, the smaller the likelihood of the implementation of the corresponding environmental reaction. At the first level, the environment will react to every action performed while at the tenth level evaluative feedback is not available to the student. The operating mode is determined separately for each type of reaction.
- *The module used for logging student's activity and environmental reactions.* During the implementation of student's educational activity, the DCTS performs secret logging of the events. The electronic protocol (a relational database) records information about the content of student's actions, the time spent on its completion (decision making time), correctness, and generated environmental reactions.

Further, we shall review in more detail the environmental reactions that implement evaluative feedback based on the dynamic assessment of student's activity.

Changes in readings of the goal distance indicator. The current distance to the goal is shown on the dashboard. The student can check their correctness of what they do, based on the changes in the indicator readings and cancel the incorrect actions. This helps to come to a solution to the problem without having any idea of the problem domain. Next to the indicator often there is a fairy-tale character displaying joyful or sad emotions depending on the correctness of the student's actions.

“Actiogram” updates. An “actiogram” is an extended representation of the goal distance indicator. However, unlike it, displaying only the last change, the actiogram shows the history of changes in distance to the goal in the form of a step graph, unfolded to the scale of the actions taken.

Error eliminator. With this mode on, the educational activity management system cancels all changes made in the work area that do not correspond to the solution of the problem: it cancels the installation of incorrect correspondences, fragments of pictures, or musical works to be completed that are in the wrong place.

Dynamic highlighting of elements in the work area. Dynamic highlighting of elements in the work area highlights the correctly installed elements with green and the incorrectly installed elements with red. This allows the student to correct their mistakes.

The management system does not restrict the student in the choice of action allowing them to carry out the activity by the method of trial and error or use selective search, view fragments in the viewport or lay them all out on the work area. The system generates tasks of the same type, differing in initial data, allowing the student to improve their skills and achieve an error-free sequence of actions by encouraging

the student’s search activity in the context of the problematic environment uncertainty self-regulation. We shall note that to complete training in the DCTS, the student has to complete the task at the tenth level which means that they have to find a solution to the problem without making any erroneous actions in the absence of the environmental assessment of their actions.

Before we switch to the discussion of the possibilities of cognitive preference registration for the activity of those training with the DCTSs, we shall consider some scenarios implemented in it that actualize different types of human intellectual activity.

Identification of the complex system elements. This scenario is applied in the widest range of subject areas. The study of an object structure is implied in the most diverse areas of human activity: whether it is the study of the parts of a lathe, a musical instrument, or a window block. In the tasks of this type (Fig. 1), pointer numbers are randomly assigned in the task definition area while the set of names to be identified is formed in the work area. The student has to establish the correspondence between the pointers and the names by placing numbers in the work area. This scenario is suitable for studying (or testing the knowledge of) the object nomenclature and, for instance, for studying the table of derivatives (Figs. 2 and 3).

Figure 4 shows an example of the DCTS’ “Identification” task which is slightly different from those mentioned before. The student is asked to choose the index number as well as the name of the corresponding element. In this case, the student makes the choice of how the message is presented each time they do something: the name can be either heard or read by pressing the corresponding button of the program

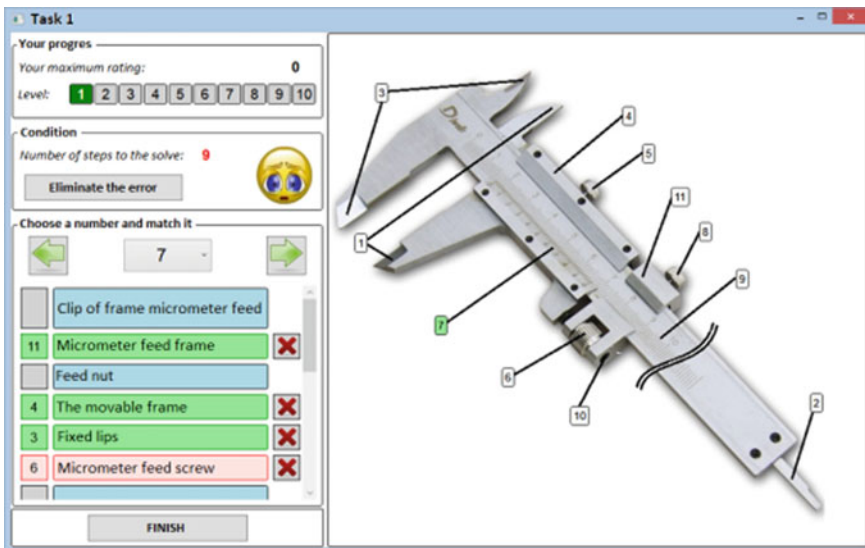


Fig. 1 DCTS: “Identification: Calipers”

Task 1

Your progress
Your maximum rating: 0
Level: 1 2 3 4 5 6 7 8 9 10

Condition
Number of steps to the solve: 47
Eliminate the error

Choose a number and match it
42

- Bushing, 1/2-module
- 25 Bevel gear, 12-tooth
- 11 Double connector connector peg, 3x3-module
- Gear, 16-tooth
- 41 Gear, 40-tooth

FINISH

Fig. 2 DCTS: "Identification: LEGO parts"

Task 1

SELECT THE DERIVATIVE NUMBERS CORRESPONDING TO THE FUNCTIONS

Level: 1 2 3 4 5 6 7 8 9 10

Condition

Select the number: 3

$f'(x) = \frac{1}{\sqrt{1-x^2}}$
 3 $f'(x) = -\sin x$
 8 $f'(x) = \frac{1}{\cos^2 x}$
 $f'(x) = \alpha^x \ln \alpha$
 4 $f'(x) = \frac{1}{x}$

Show errors FINISH

6	$f(x) = x^n$	1	$f(x) = \log_a x$
10	$f(x) = a^x$	4	$f(x) = \ln x$
8	$f(x) = \sin x$	5	$f(x) = \arcsin x$
3	$f(x) = \cos x$	9	$f(x) = \arccos x$
12	$f(x) = \operatorname{tg} x$	2	$f(x) = \operatorname{arctg} x$
7	$f(x) = \operatorname{ctg} x$	11	$f(x) = \operatorname{arctg} x$

Fig. 3 DCTS: "Identification: Table of derivatives"

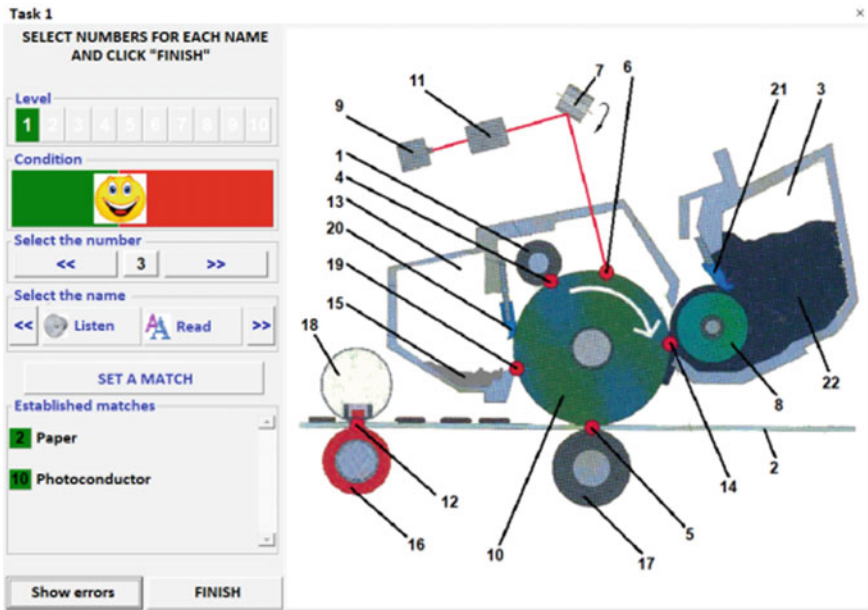


Fig. 4 DCTS: “Identification: Laser printer” with the option to select the method of name presenting

interface. A set of names appears in the work area only once the correspondence between the index number and the name selected has been established.

Sequence construction. This type of scenario is also used in the widest range of subject areas. Figure 5 pictures the task to construct a sequence of events forming a path of spaghetti to our table: from field plowing and wheat seed planting through ripening, harvesting, milling, and other procedures to table setting. It is possible to make such tasks in verbal form (Fig. 6) without using visual images for training high school students—it will significantly simplify the process of didactic material preparation and will make it accessible for the subject teacher.

Figure 7 shows a sequence of mathematical transformations used to find the value of a definite integral. The illustration above contains a blue “actiogram” showing a sequence of correct (upward graph, towards the Solution line) and incorrect (downward graph, towards the Initial condition line and below) student actions, as well as the red “statusogram” (a special representation of the level achieved, expanded to the scale of the tasks completed).

We shall note that a rather strict structure of sentences in some foreign languages (for example, English) makes it possible to use the described DCTS scenario for studying (or testing the knowledge of) the sentence structure by establishing the correct sequence of words. An example of such an environment designed for these purposes is shown in Fig. 8.

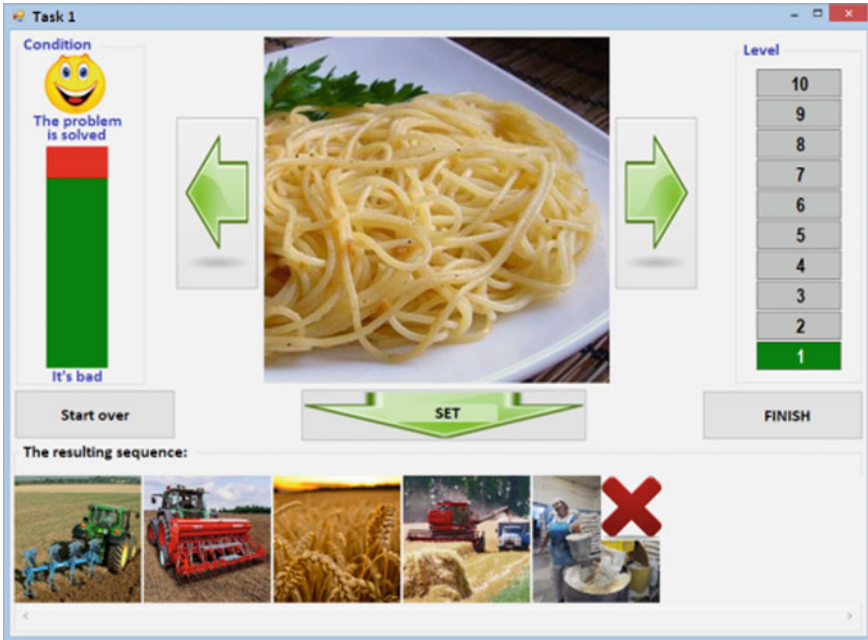


Fig. 5 DCTS: “Sequences: Spaghetti—from the field to the plate”

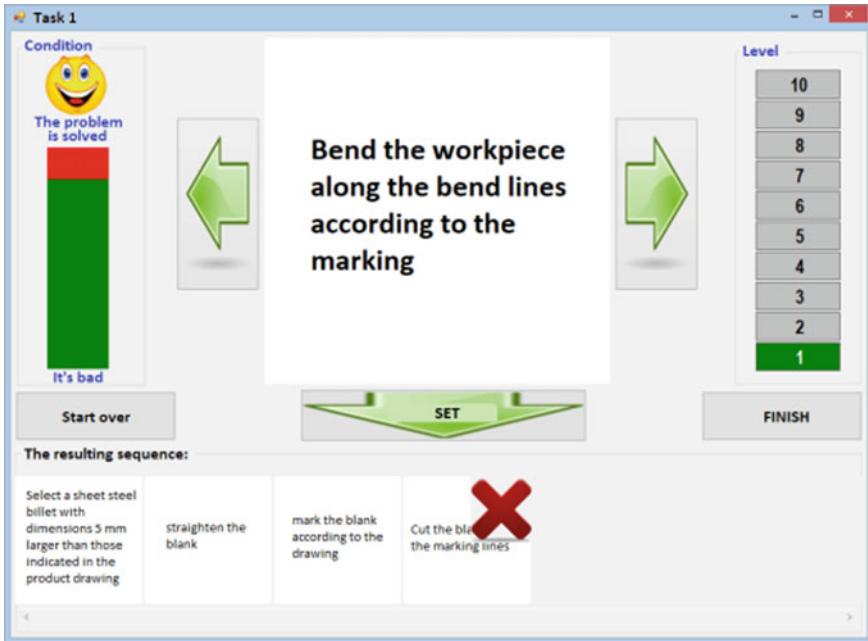


Fig. 6 DCTS: “Sequences: Making of a metal box”

Task 1

Fragment

$$= \frac{x^{\pi}}{2} + \frac{\sin(2x)}{4} \Big|_0^{\pi} = \frac{\pi}{2}$$

Statusgram

10
5
1

Actiongram

Solve

Beginning

It's bad

FINISH

$\int_0^{\pi} (x^3 + \sin(2x)) dx =$	$= \frac{x^4}{4} + \frac{1}{2} \int_0^{\pi} \sin(2x) d(2x)$	$= \left(\frac{x^4}{4} - \frac{1}{2} \cos(2x) \right) \Big _0^{\pi}$?
$\int_0^{\pi} \sin^2(x) dx =$	$= \int_0^{\pi} \frac{1 - \cos(2x)}{2} dx = \frac{1}{2} \int_0^{\pi} dx - \frac{1}{4} \int_0^{\pi} \cos(2x) d(2x)$	$= \frac{x}{2} \Big _0^{\pi} - \frac{\sin(2x)}{4} \Big _0^{\pi} = \frac{\pi}{2}$	
$\int_0^{\pi} \cos^2(x) dx =$	$= \int_0^{\pi} \frac{1 + \cos(2x)}{2} dx = \frac{1}{2} \int_0^{\pi} dx + \frac{1}{4} \int_0^{\pi} \cos(2x) d(2x)$?
$\int_0^{\pi} (x^3 + \sin(3x)) dx =$	$= \frac{x^4}{4} + \frac{1}{3} \int_0^{\pi} \sin(3x) d(3x)$	$= \frac{x^4}{4} - \frac{\cos(3x)}{3} \Big _0^{\pi} = \frac{\pi^4}{4} + \frac{2}{3}$	

Fig. 7 DCTS: “Sequence: Find the integral” (with “actiogram” displayed)

Puzzles. This scenario uses image construction from fragments. Images can be selected from some culturally independent areas (Fig. 9) or contain certain educational tasks. For instance, the task may be “Complete the technological chart for making a cutting board” (Fig. 10).

Having reviewed the DCTS scenarios, we would like to draw your attention to the fact that the process of finding a solution to the problem is, generally, the same for all of them. Regardless of the connected feedback modules, which, among other things, can actively intervene in the problem–solution process by canceling erroneous actions, the student can perform the following basic actions:

1. *Select elements in the viewport.* Using the “Left” and “Right” buttons, the students can select a fragment or a pointer number, sequentially going through them in the viewport. If a drop-list is available, one can access (open the viewport for) the certain required element without scrolling. For further discussion, we shall define these actions as “View previous”, “View next” and “Select view” respectively.
2. *Install elements within the work area.* Depending on the DCTS type, the installation of an element within the work area is performed either using a special button (the fragment selected is installed at the end of the constructed sequence) or by clicking the mouse button in the area that the element is supposed to be placed. We shall call this action the “Installation”.

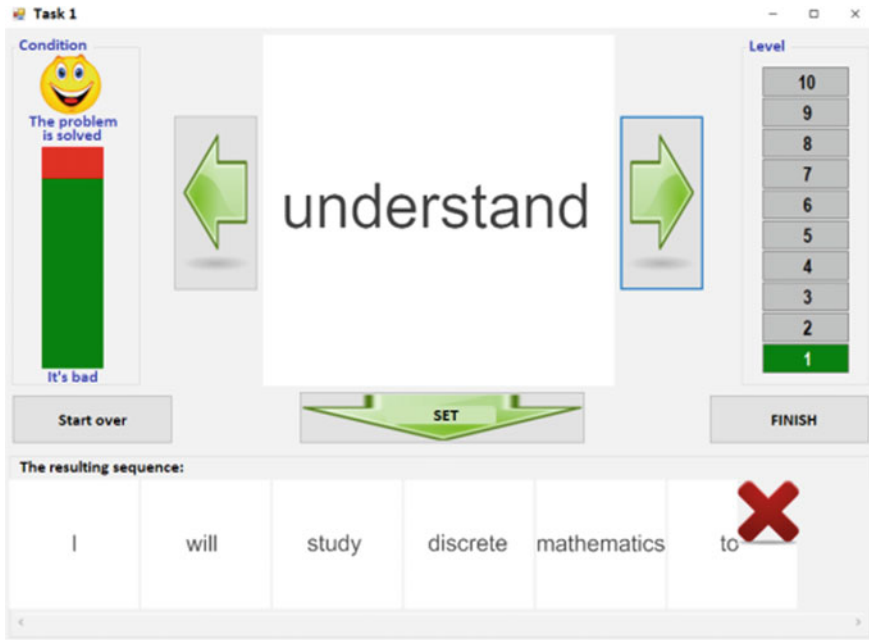


Fig. 8 DCTS: “Sequence: Make a sentence”

3. *Remove a previously installed fragment from the work area.* The student, focusing on the evaluative feedback indicators, realizing the dynamic assessment of their activity, can remove the previously installed fragments from the work area by placing them in the viewport to undo the previously made action. We shall call this action “Cancel”. Once canceled, the fragment can be installed in a different place in the work area or the student can select a different fragment.
4. *Press the “Finish” button.* When the student solves the problem, they inform the educational activity management system about it by pressing the “Finish” button. If the problem is really solved, the system determines a new level and generates the next task or makes a decision about training (testing) completion and reports it. If the problem is not solved (not all fragments required are installed or their position does not correspond to the solution), the management system reports this and requests that the student continue solving the problem. We shall call this action “Finish” and consider it correct in case the problem was solved, and incorrect if was not.

These actions are forming the system of student’s actions in the DCTS and are registered in the electronic protocol. The number of certain actions performed by the student while solving the problem as well as the frequency of transitions from one type of action to another (for instance, from viewing to installing or from installing to canceling) determines the structure of the student’s action system. This structure changes with the iterative solution of the same-type problems and is of particular

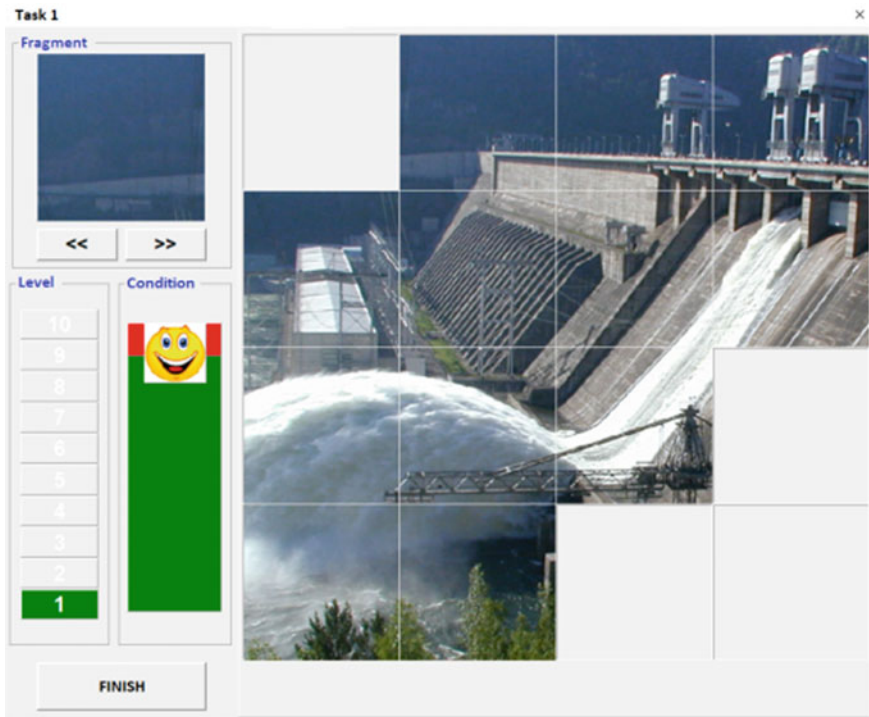


Fig. 9 DCTS: “Puzzle: Krasnoyarsk Dam”

interest in the framework of this study. We shall return to its consideration further when discussing the possibilities of students’ cognitive preference registration.

In addition to the student actions listed above, conducting this research on the use of the DCTS for diagnosing the educational activity, particular management elements were included in the interface. For instance, to determine the priority method for obtaining verbal information, the student was asked to choose between reading the message and listening to it, and for these actions the corresponding buttons were available. To diagnose a student’s self-esteem, we have added a tool that allows a student to independently assess the level of their performance. In some versions of the DCTSs, it is possible to review mistakes and cancel all erroneous fragments by clicking the corresponding button. However, all these functions only supplement the capabilities of the system and shall not be considered as major.

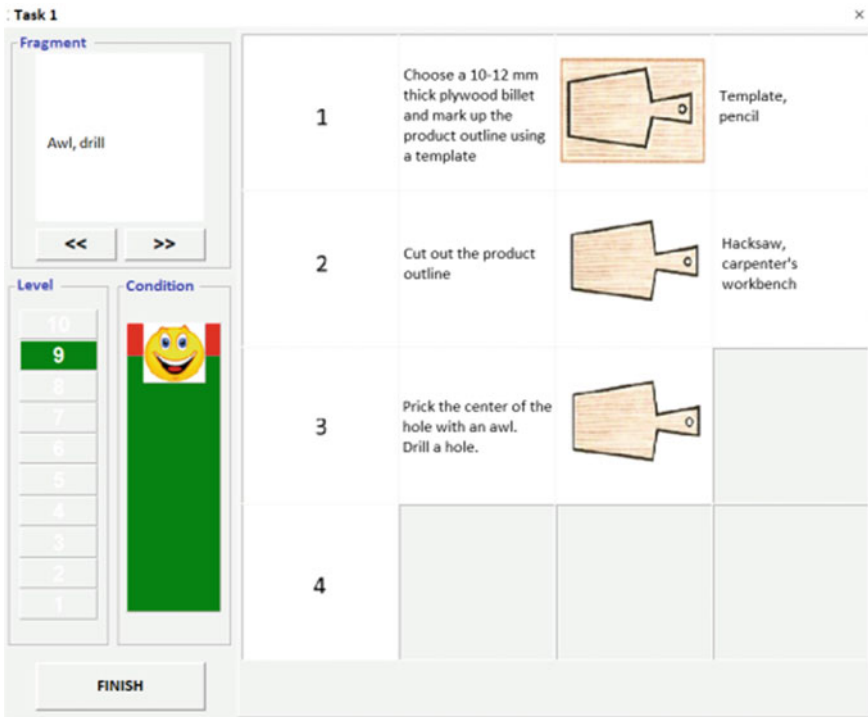


Fig. 10 DCTS: “Puzzle: process chart”

3 Results and Discussion

We shall review the possibilities of student’s cognitive preference registration in the process of analyzing their activity protocols in the DCTS. To obtain such an opportunity, a computer program was designed that extracts data from the protocols thus allowing them to be reviewed in various degrees of detail or generalization and to be presented in a visual form of charts, graphs, or diagrams. We shall generalize the results obtained during the experimental use of the DCTS and indicate the characteristic features of the educational activity implementation which, as a rule, is determined by the cognitive characteristics of the students involved.

Action system structure.

Figures 11 and 12 show oriented weighted graphs reflecting the structure of the students’ action system (we shall call them “Student 1” for Fig. 11 and “Student 2” for Fig. 12) during the completion of the first task in the DCTS. The vertices of the graph indicate the states of the student’s activity, the actions they perform: S_1 is for the installation of the fragment; S_2 is for cancellation; actions for scrolling through fragments to the left or the right are combined into the S_3 ; completion of the task is an absorbing state denoted by S_4 . The oriented edges of the graph describe the

Fig. 11 The action system structure of Student 1 when completing the first task

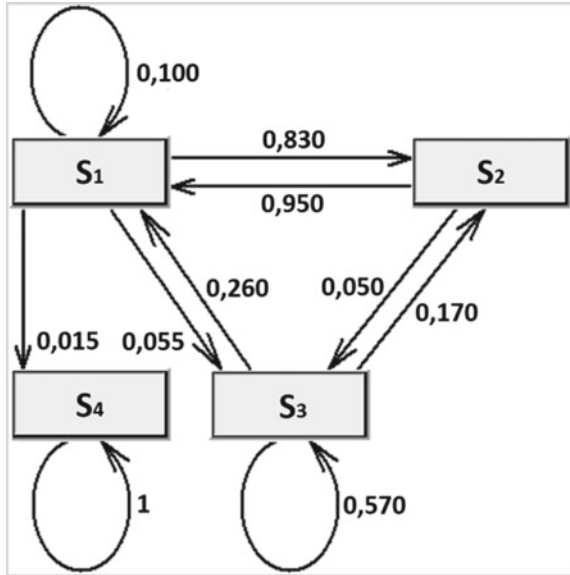
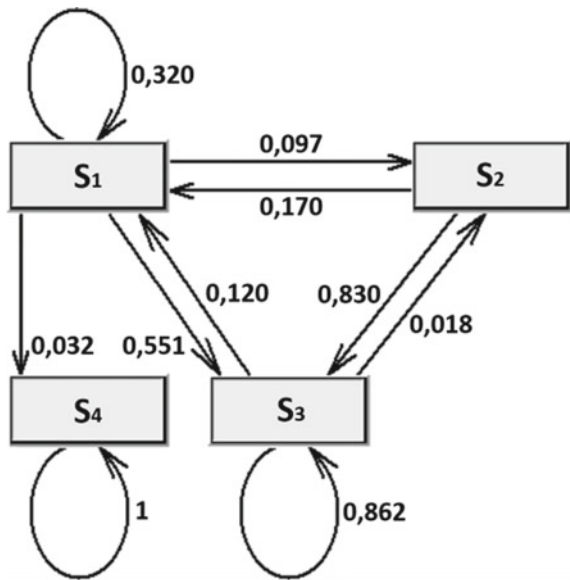


Fig. 12 The action system structure of Student 2 when completing the first task



transition between the states, and the weight of each of them is determined by the frequency of the corresponding transitions in the structure of the student’s action system.

We shall talk about the cognitive strategies or preferences of these students, which can be seen in the given figures. Based on the comparative analysis of these graphs, we

shall note that a characteristic feature of the activity of Student 1 is a high frequency of transitions from setting fragments to canceling and back (from S1 to S2 and back from S2 to S1). They tried to set fragments in different places of the work area and would cancel the installation immediately, focusing on the goal distance indicator.

Having canceled the installation of a fragment, Student 2, unlike Student 1, would rarely try to place it in a different position in the work area. More often than not, they would move on to find another fragment, the location of which they could guess. This can also be seen from the loop at the top of S3. Student 2 would look through the fragments a lot, trying to construct an image in their head, in their imagination, and thereby avoid erroneous actions in the work area.

Student 1 would also try to switch to this strategy to solve the problem. This can be seen in Fig. 13 which depicts the scale of time a student spent completing their actions. The values 1, 2, and 4 on the ordinate correspond to the states (the vertices of the previously described graph) S₁, S₂, and S₄. The S₃ state is divided into two values: 3.1 for scrolling to the previous fragment and 3.2 for scrolling to the next fragment.

With the overwhelming majority of transitions between the values 1 and 2, in the intervals between 150 and 250 s and between 480 and 630 s, attempts to view the proposed fragments and mentally form a complete picture occurred. However, the individual cognitive characteristics of Student 1 do not allow them to act in this mode.

The case of Student 2 is completely the opposite. One can see in Fig. 14 that on the basis of Student 2's activity lay the views (scrolling through fragments) to the left and the right. It means that this student analyzes the fragments presented, compares them, tries to determine the position of each in the constructed image. Only after that, they try to place the fragments in the work area.

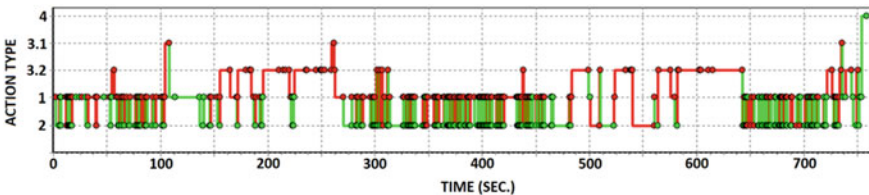


Fig. 13 Actions of Student 1 when completing the first task

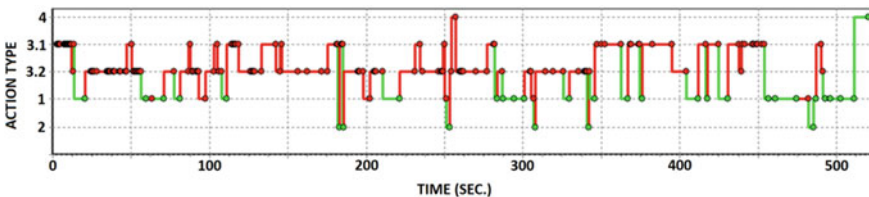
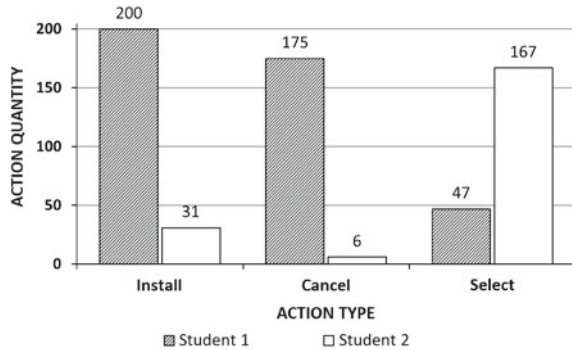


Fig. 14 Actions of Student 2 when completing the first task

Fig. 15 Quantitative parameters of Student 1 and Student 2 activity



Student 1 and Student 2 are the most representative ones, demonstrating two diametrically opposite ways of obtaining information from the environment. One tries to comprehend the environment through trial and error, searches for a solution to the problem directly, preferring the actual situation to a mental image, meanwhile the other tries to solve the problem by building a mental model and testing it in practice.

Having compared the quantitative characteristics of both students (Fig. 15), we shall note that 175 cancellations for Student 1 and 167 views for Student 2 vividly illustrate their strategies of choice. Thus, we can say that the analysis of the DCTS activity protocols allow students’ cognitive preference registration since such preferences are manifested in priority ways of search activity implementation in the process of intellectual problem solution.

The nature and dynamics of changes in the action system structure.

The students’ action system structure considered above describes the ways to achieve the local goal which is to solve the task with the assistance of the internal loop of the educational activity management system. The purpose of the external loop is to form such a structure of the student’s action system in which erroneous actions requiring the cancellation of the fragments installed will be excluded, and the S_2 vertex will be absent in the graph, or the weight of transitions to this state will be negligible. This corresponds to the tenth level of the student’s activity, at which they have to solve the problem in the absence of indicators of evaluative feedback.

Students of secondary school and universities took part in our experiments, and all of them have reached the tenth level. Each student acted in the mode most comfortable for them. Most of the participants would not change their strategies from task to task and thus achieved error-free performance in accordance with their cognitive preferences.

Students’ cognitive preferences defined the difference in the number of completed tasks and the time spent on training. For instance, Student 2 completed three tasks and spent twenty minutes to complete the training while Student 1 had to complete nineteen tasks and spend an hour. In Figs. 16 and 17 we can see a time sweep of these students’ actions made to complete the final task.

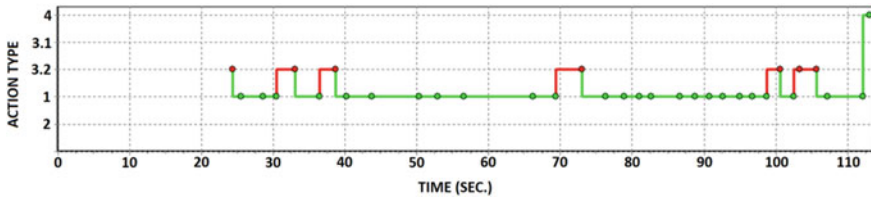


Fig. 16 Actions of Student 1 when completing the nineteenth task

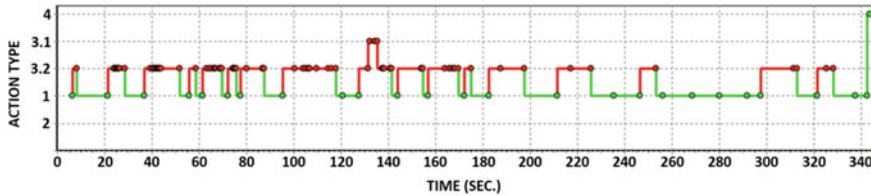


Fig. 17 Actions of Student 2 when completing the third task

We shall note that Student 1, having spent three times as much time on training, completed the task without any mistakes also three times faster than the other student. Unlike Student 2, they memorized the locations of almost every piece of the image that was to be constructed and acquired the skill of installing them. Student 1 identified the elements of the system starting with the fragments whose location was clear to them, as if these fragments were the crystallization centers, and then built the general picture around them.

Both students we studied are mentally and physically healthy people who have completed their university education. However, voluntary neuropsychological diagnostics of the development levels of their basic cognitive brain functions (BCBFs) conducted with the help of the method of the evoked potentials P300 has shown a reduced volume of operative memory and directed attention as well as impairment of recognition and differentiation processes in Student 2. Apparently, this very feature of their development determined the choice of the cognitive strategy used for finding solutions to the tasks assigned. There is no doubt that the implementation of manipulations with objects in the imagination allows for a more efficient problem-solving process and is a competitive advantage of an individual. However, people with deficiencies in the BCBFs development, if given the appropriate time and didactic resources, can achieve perfection in the problem-solving process for a certain subject area. This aspect of students' cognitive preference registration requires a separate study, model building for diagnostic automation, and will be useful for the vocational guidance of schoolchildren.

4 Conclusion

The results obtained illustrate the feasibility of the DCTSs for student's cognitive preference registration, and their massive application in the educational process will allow them to achieve learning goals in a mode comfortable for the student, as well as to individualize training in accordance with the objectively recorded cognitive activity features.

Acknowledgements The reported study was funded by RFBR, project number 20-07-00671.

References

1. Bosma, T., Hessels, M.G., Resing, W.C.: Teachers' preferences for educational planning: dynamic testing, teaching'experience and teachers' sense of efficacy. *Teach. Teacher Educ.* **28**(4), 560–567 (2012). <https://doi.org/10.1016/j.tate.2012.01.007>
2. Calero, M.D., Belen, G.M., Robles, M.A.: Learning potential in high IQ children: the contribution of dynamic assessment to the identification of gifted children. *Learn. Individual Differences* **21**(2), 176–181 (2011)
3. Feuerstein, R., Rand, Y., Hoffman, M.B.: Dynamic assessment of retarded performers: The Learning Potential Assessment Device, theory, instruments, and techniques. University Park Press, Baltimore, MD (1979)
4. Haywood, C.H., Lidz, C.S.: *Dynamic Assessment in Practice: Clinical and Educational Applications*. Cambridge University Press, New York (2007)
5. Lantolf, J.P., Poehner, M.E.: Dynamic assessment in the language classroom (CALPER Professional Development Document CPDD-0411). University Park: The Pennsylvania State University, Center for Advanced Language Proficiency Education and Research; 2004
6. Luria, A.R.: *The Working Brain*. Basic Books, New York (1973)
7. Resing, W.C.M.: Dynamic testing and individualized instruction: helpful in cognitive education? *J. Cogn. Educ. Psychol.* **12**(1), 81–95 (2013). <https://doi.org/10.1891/1945-8959.12.1.81>
8. Resing, W.C.M., Xenidou-Dervou, I., Steijn, W.M.P., Elliott, J.G.: A “picture” of children's potential for learning: Looking into strategy changes and working memory by dynamic testing. *Learn. Individual Differences* **22**(1), 144–150 (2012). <https://doi.org/10.1016/j.lindif.2011.11.002>
9. Resing, W.C.M., Elliott, J.G.: Dynamic testing with tangible electronics: Measuring children's change in strategy use with a series completion task. *Br. J. Educ. Psychol.* **81**(4), 579–605 (2011). <https://doi.org/10.1348/2044-8279.002006>
10. Sternberg, R.J., Grigorenko, E.L.: *Dynamic Testing: The Nature and Measurement of Learning Potential*. Cambridge University Press, New York (2002)
11. Hamers, J.H.M., Sijtsma, K., Ruijsenaars, A.J.J.M. (eds.): *Learning potential assessment: Theoretical, methodological, and practical issues*. Swets & Zeitlinger, Amsterdam (1993)
12. Resing, W.C.M.: Learning potential assessment: the alternative for measuring intelligence. *Educ. Child Psychol.* **14**, 68–82 (1997)
13. Vygotsky, L.S.: *Mind in Society: The Development of Higher Psychological Processes*. Harvard University Press, Cambridge, MA (1978)
14. Dyachuk, P.P., Brovka, N.V., Noskov, M.V., Peregudova, I.P.: Interactive self- regulation of educational activity in identification of complex objects. In the collection: Materials of the II International Scientific Conference. Siberian Federal University 2018. C, pp. 90–94

15. Bortnovsky, S.V., Dyachuk, P.P., Dyachuk, (Jr.) P.P.: Computer diagnostics of learning problem solving: effective and procedural aspects. *Open education* No. 3. S. pp. 8–14 (2011)
16. Dyachuk, P.P.: Dynamic computer testing. *Pedagogical Inform.* **3**, 3–8 (2005)
17. Dyachuk, P.P., Pustovalov, L.V., Surovtsev, V.M.: A control system for finding solutions to algorithmic problems. *Control Syst. Inform. Technol.* **3–2**(33), 258–263 (2008)
18. Bogomaz, I.V., Drozdova, L.N., Dyachuk, P.P., Shadrin, I.V.: Diagnostics of educational activities for the construction of spatial objects. *Bulletin of the Krasnoyarsk State Pedagogical University. V.P. Astafieva.* No. 2. S. pp. 33–38 (2011)
19. Drozdova, L.N., Dyachuk, I.P., Kudryavtsev, V.S.: Diagnostics of the dynamic parameters of educational activities in the design of sound objects. *Bulletin of the Krasnoyarsk State Pedagogical University. V.P. Astafieva.* No. 2. S. pp. 113–119 (2010)
20. Dyachuk, P.P., Kudryavtsev, V.S.: A synergistic approach to the management of puzzle music construction activities. *Bullet. Musical Sci.* **2**(4), S. 16–24 (2014)
21. Dyachuk, P., Dyachuk, P., Shadrin, I., Peregodova, I.: Dynamic adaptive testing and peculiarities of its use with medical students. *Electron. J. General Med.* T. 15. № 6. C. em84 (2018)
22. Dyachuk, P.P., Shadrin, I.V., Dyachuk, P.P., Peregodova, I.P.: Dynamic adaptive tests for identifying the structure of anatomical objects. *Comput. Sci. Educ.* **7**(296), 51–56 (2018)

Prospects of the Interdisciplinary Course “Computational Intelligence” in Engineering Education



Yuriy Skobtsov 

Abstract The experience of teaching lecture courses on genetic algorithms, evolutionary computing, and computational intelligence at a number of universities in Ukraine and St. Petersburg at the undergraduate and graduate levels is presented. The content of the new course “Computational Intelligence” (CI) is presented, which covers 5 main paradigms: artificial neural networks, evolutionary computing, fuzzy systems, swarm algorithms, and artificial immune systems. All 5 paradigms are successfully applied in solving many scientific and technical problems separately. However, modern trends require the development of hybrid systems where combinations of these paradigms are used. Hybrid systems are able to take advantage of the individual strengths of specific paradigms and compensate for the shortcomings of various CI paradigms. Various forms of hybridization of the components of computational intelligence are considered. On this basis, new powerful algorithms are developed to solve complex problems. The interdisciplinary character of CI is noted, which determines the prospects for its application in the development of cyber-physical systems using the processes of generalization, abstraction, and association inspired by nature. CI can be an important tool for multidisciplinary education and research.

Keywords Computational intelligence · Neural networks · Evolutionary computing · Swarm algorithms · Artificial immune systems · Hybrid systems · Interdisciplinary education · Cyber-physical systems

1 Introduction

In recent decades, a new direction in the theory and practice of artificial intelligence, evolutionary computing [1], has been rapidly developing. This term is usually used to generically describe search, optimization, or learning algorithms based on some formalized principles of natural evolutionary selection. On the other hand, the theory

Y. Skobtsov (✉)

Saint Petersburg State University of Aerospace Instrumentation, 67 Bol'shaya Morskaya Street, St. Petersburg, Russia

e-mail: ya_skobtsov@list.ru

of artificial neural networks and their many applications are developing even earlier and more rapidly [2]. The combining of these paradigms led to the formation of a new section “Computational Intelligence”. In this regard, the IEEE Neural Network Society changed its name in 2004 to the IEEE Computational Intelligence Society [3]. Computational intelligence (CI) [4] is currently one of the most actively developing areas in the field of computer science and technology and its methods are widely used in solving many scientific and technical problems.

2 Experience in Evolutionary Computation Teaching

The history of evolutionary computation (EC) began in the 60s of the XX century when various groups of scientists in the field of cybernetics independently studied the possibilities of applying the principles of biological systems evolution to solve various technical problems, usually requiring optimization problems. Thus, a new scientific direction was founded, which is now commonly called “evolutionary computation”. Genetic algorithms were originally developed for discreet optimization problems as a rather effective mechanism of combinatorial optimization. Unlike many other works, the goal of the author of GA—Holland [5] was not only the solution of specific problems but the study of the phenomenon of adaptation in biological systems and its application in computing systems. Moreover, a potential solution—an individual is presented by a chromosome that coded with binary code. A population contains a set of individuals. In the process of evolution, three main genetic operators are used: reproduction, crossover, and mutation.

Also in the 60s in Germany, Rechenberg [6] founded “evolutionary strategies” in solving the numerical optimization problem for the engineering of power lines. This scientific direction has developed independently for many years and important fundamental results were obtained here. In evolutionary strategies, a potential solution (an individual) is a vector of real numbers, a population consists of two individuals, and the main genetic operator is a mutation.

Fogel independently of other researchers founded evolutionary programming [7], where a potential solution is represented with the finite state machine. The main genetic operator here is also a mutation, which randomly changes the transition-output table of the state machine.

A little later, Koza at the Massachusetts Institute of Technology in the United States founded genetic programming [8]. Here, the LISP program, which has a tree structure, presents as an individual. On these structures, the genetic operators of crossover and mutations were developed.

Currently, these areas are combined into “evolutionary computation”, which are successfully used to solve many technical problems. At the same time, individual paradigms interact with each other by borrowing the best features from each other.

The first course “Genetic Algorithms” was developed by the author in the late 90s and tested at a number of universities in Ukraine as a course of choice. Further, this course was regularly taught to masters in the areas of Computer Science and

Computer Engineering. Further on this basis, the course “Evolutionary Computation” was created, which the author taught to masters of computer sciences at a number of universities in Ukraine. Initially, he included the following sections.

The first section outlines the basics of a simple genetic algorithm (GA), describes the genetic operators of reproduction, crossover, and mutation. The methods of potential solution representations for integers and real numbers are considered. The second section gives the mathematical foundations of GA: the theory of schemes, which shows the influence of genetic operators on the survival of individual groups of individuals that possess (or vice versa do not possess) certain properties.

The third section is devoted to combinatorial optimization problems. The traveling salesman problem is considered in detail as a basic problem for NP-complete problems. The main types of potential solution representations and problem-oriented genetic operators are described. The fourth section presents modern modifications and generalizations of GA. The various methods and strategies for implementing a simple GA are described. Various parent selection strategies, binary and arithmetic crossover operators and mutations, and methods for reducing the intermediate population are considered. Dynamical GAs with the changing number of individuals in the population are presented. Besides different methods for determining the life span are considered. Also, adaptive GAs, in which the probability of crossover and mutation is adjusted during evolution are presented.

In the fifth section, parallel genetic algorithms are described, the main types of parallelization and methods for their implementation are considered. The main types of parallel GAs are considered: global (“worker-master” model), distributed (“island model”), and cellular. The parallel global genetic algorithm based on the “work-master” model is described. A parallel genetic algorithm is presented, which is implemented according to the “island model” and its main parameters are presented. The sixth section is devoted to probabilistic and compact genetic algorithms, where the population is represented by a vector of gene probabilities.

The seventh section is devoted to genetic programming (GP). The foundations of the classical GP on tree structures are described, the operators of crossover and mutations in these structures are determined. A new direction of GP based on the linear graph model is presented, which allows one to efficiently solve many problems. Features of the implementation of the main stages of the GP are considered. Symbol regression is described in detail. The eighth section presents machine learning and classification systems based on EV, where products (or systems of rules) act as individuals. The Michigan and Pittsburgh approaches to solving this problem are described.

The ninth section outlines the basics of evolutionary strategies (ES), compares ES and GA. The tenth chapter discusses the basics of evolutionary programming based on the evolution of finite state machines. The eleventh section is devoted to the problems of the software implementation of evolutionary algorithms and contains a description of some software packages. In addition, issues of a hardware implementation of genetic algorithms are considered.

In this form, the course “Fundamentals of Evolutionary Computing” was taught for several years for masters at a number of Ukraine universities. It was published

in 2008 as a textbook with the stamp of the Ministry of Education and Science of Ukraine [9]. This publication summed up the first stage of the course.

Returning to the teaching experience, it should be said that at the second stage of the evolutionary computing course, the author tried to expand it to the computational intelligence course described above. An expanded and supplemented by swarm algorithms, the new course “Evolutionary Computing” was published at the INTUIT PH [10].

Since 2015 to date, the author taught similar courses at a number of universities in St. Petersburg: Peter the Great St. Petersburg Polytechnic University, St. Petersburg National Research University of Information Technologies, Mechanics and Optics, and St. Petersburg State University of Aerospace Instrumentation. As a result of the experience gained, the author came to the following 2-level teaching scheme: (1) In the framework of the bachelor’s program in the 4th year, the main EC paradigms and some CI sections are described; (2) In the master’s program in the 1st year, more “advanced” and complex CI sections are taught. So, the basic course in undergraduate studies contains the following sections:

1. The basics of GA.
2. Modifications and generalizations of GA.
3. An evolutionary approach to complexity evaluation for software projects.
4. Genetic programming.
5. Genetic algorithms for combinatorial optimization.
6. Evolutionary programming.
7. Evolutionary strategies.
8. Differential evolution.
9. The evolutionary method of software project planning.
10. Particle swarm optimization (PSO) algorithms.
11. Ant colony optimization (ACO) algorithms.
12. Artificial immune systems.

In addition to lectures, 7 laboratory works are proposed:

13. Simple GA.
14. GA search for extrema of functions with many variables.
15. Combinatorial optimization based on GA (the traveling salesman problem).
16. Symbolic regression.
17. Evolutionary strategy (extremum of the function with many variables).
18. Ant algorithm (traveling salesman problem).
19. PSO algorithm (extremum of the function with many variables).

In addition, a course project is carried out in the second semester. Themes of the course projects are mainly related to CI applications in software engineering. First of all, these are evolutionary methods for the complexity evaluation and of software project planning.

In the master’s program, the “advanced” course includes the following topics:

20. Multimodal evolutionary algorithms.

21. Multi-objective EA.
22. Constrained evolutionary optimization.
23. Parallel evolutionary algorithms.
24. Probabilistic GA first and higher orders.
25. Evolutionary methods of program testing.
26. Hardware implementation of EC.
27. Dynamic EC.
28. Hybridization of CI.
29. Advanced evolutionary combinatorial optimization (production schedules, SAT solvers).
30. CI for neural networks training.

The following laboratory works are foreseen:

31. Multimodal EA.
32. Multi-objective EA.
33. Constrained evolutionary optimization.
34. Parallel EA.

In general, the first 15 years of development turned out to be quite successful—the course was formed, 2 textbooks were published, more than 50 master’s works were completed using the mathematical apparatus of evolutionary calculations and computational intelligence in general. The course played a particularly significant role in postgraduate training—over 15 candidate dissertations and 1 doctoral thesis were prepared and defended using the mathematical apparatus of computational intelligence. The subjects of the dissertations were quite diverse: simulation and testing of digital circuits, processing, and recognition of medical images, guillotine cutting, medical expert systems, simulation of automated machine-building complexes, multi-objective optimization of production schedules, and others. Since CI has numerous applications in completely different areas, the CI apparatus significantly helped determine the choice of research topics. Next, we consider the prospects of the course “Computational Intelligence” in engineering education.

3 Computation Intelligence

Initially, CI is defined as a combination of fuzzy logic, neural networks, and genetic algorithms [4]. A broader definition of computational intelligence is the study of adaptive mechanisms that allow or facilitate intellectual behavior in complex, uncertain, and changing conditions. These adaptive mechanisms include artificial intelligence (AI) paradigms that demonstrate the ability to learn or adapt to new situations, generalize, discover, and associate [4]. CI paradigms use the natural phenomena models to solve complex problems and include neural networks, evolutionary computing, swarm intelligence, fuzzy systems, and artificial immune systems. These paradigms—components of CI are considered in more detail below.

Great attention is paid to the teaching of such courses in the USA and Europe, which is actively discussed in the press, for example [3]. Recently, leading universities in the world (especially the United States) have been paying increasing attention to interdisciplinary education and research. In particular, this concerns the well-known STEM program (science, technology, engineering, and mathematics), where an attempt was made to combine science, engineering, technology, and mathematics [3]. This is explained by the fact that, as a rule, computational intelligence courses are interdisciplinary in nature. Unfortunately, in Russia, this direction (and especially teaching) is not developing as fast as in other countries. Although recently, several good textbooks and monographs on CI have been published, for example [11, 12] and others. CI is the successor of artificial intelligence (AI) and determines the future computing nature. “Intelligence without computing is like birds without wings” [3]. CI, on the other hand, is different from AI. Some of the methods are common to CI and AI. CI can play a significant role in two main areas of interdisciplinary education and research in STEM, primarily, the extraction of knowledge from data and cyber-physical systems.

Currently, CI contains 5 main paradigms, namely: (1) artificial neural networks (ANN), (2) evolutionary computing (EV), (3) swarm intelligence (SI), (4) fuzzy systems (FS), and (5) artificial immune systems (AIS). All paradigms are developed on the basis of models of natural biological systems and processes, respectively: (1) the nervous system, (2) evolution, (3) swarm (flock) behavior, (4) human reasoning, (5) the mammalian immune system.

ANNs are developed in the form of parallel distributed network models based on a simulation of the learning process of the human brain [2]. Dozens of species of different ANNs have been proposed, among them the most popular are: a multilayer perceptron, networks with radial basis functions, and probabilistic neural networks [2]. Typically, ANNs consist of an input layer, an output layer, and one or more hidden layers. The number of hidden layers, the number of neurons in each layer, the neuron activation functions, and the learning algorithm are the main ones in the implementation of ANN to solve a specific problem.

EC is developed on the basis of a survival evolution model of the most adapted individuals [1]. The most popular here are genetic algorithms (GA) and genetic programming (GP). GA represents a class of stochastic search procedures based on the principles of natural genetics. Here, in the process of a solution search, an artificial evolution model is used, where each individual in the population represents a potential solution to the problem using a line known as a genome [1]. When using GA to solve a specific problem, it is necessary, first of all: to select (or develop) a representation of the genome—a potential solution, to determine a fitness function that allows evaluating the potential solution quality, to select (or develop) genetic selection, crossover operators and mutations. GP has much in common with GA but differs in the way it presents a potential solution. In the case of GA, the decision is often represented (encoded) by a string of numbers. On the other hand, a GP uses the representation of a computer program in the form of a tree structure that connects various inputs (leaves) through mathematical functions (nodes) at the output (root node) [1].

Swarm algorithms (SA) are also based on stochastic optimization, but they use models of the social behavior of a flock of birds, fish (insects swarm) [13–16]. The algorithm searches optimal value by sharing cognitive and social information among particles, each of which represents a potential solution. SA is used mainly in numerical optimization and has some advantages over evolutionary algorithms in terms of simpler implementation, faster convergence rate, and fewer parameters for tuning algorithms. For combinatorial optimization, and algorithms (ACO) are more often used, which also imitate social behavior and are based on stigmergy modeling (local environmental changing using pheromone) [16, 17].

FS models human reasoning and the formation of a concept in order to deal with inaccurate and uncertain information [18]. The combination of incomplete, inaccurate information and inaccurate nature in the decision-making process makes fuzzy logic very effective in complex engineering modeling, business, finance, and management systems that are otherwise difficult to model. The main problem in using FS is select the type of fuzzy membership functions, a rule base design that mimics the decision-making process, as well as the scaling factors used at the stages of fuzzification and defuzzification. These parameters and structures, in the general case, are based on trial and error and expert knowledge.

AIS is developed on the basis of the mechanical modeling of the natural immune system [19, 20]. All living organisms have the ability to resist and develop (partial or complete) immunity to pathogens or infections. These methods of CI have been developed based on the ideas and models of biological immune systems. AIS methods use various aspects of the immune system, such as pattern, matching, feature extraction, learning and memory, diversity, distributed processing, self-organization, and self-defense. The development of AIS consists of three main stages: the solution presentation, interaction evaluation, and the adaptation procedure. Various AIS algorithms were proposed based on models of natural immune systems, namely, the negative selection method, clonal selection, and models of continuous and discrete immune networks [15].

4 Hybridization of CI

The presented paradigms can be combined into hybrids, resulting in neuro-fuzzy systems, Neuro-Swarm systems, Fuzzy-PSO systems (particle swarm optimization), Fuzzy-GA systems, neuro-genetic systems, etc. Projects and developments using hybrid algorithms already exist in the literature [4]. Hybrid intelligent systems are developed by integrating two or more of these paradigms. Hybrid systems are able to take advantage of individual strengths and eliminate the shortcomings of various CI paradigms, thus offering powerful algorithms to solve complex problems. This is often used to solve complex real-world problems, where one method of CI is usually used to eliminate the shortcomings of another. For example, in adaptive neuro-fuzzy systems (ANFIS), the advantages of FS and ANS are manifested in combination for

setting membership functions, a rule base, and related parameters in accordance with the training data set.

Various forms of hybridization are used. The first consists of including components from one metaheuristic to another. The second form relates to systems that are sometimes referred to as a collaborative search. They consist of various information exchange algorithms. The third form is the integration of approximate and systematic (or complete) methods.

Exchange of components between metaheuristics. Hybridization is associated with the use of trajectory methods in population parameters. The most successful EC and ACO applications use local search procedures. The reason for this becomes apparent when analyzing the advantages of trajectory and population methods. The strength of population-based methods is, of course, based on the principles of recombination of solutions to obtain new ones. For example, in EC and Scatter Search algorithms [1], explicit recombination is performed by one or more re-combination operators. In ACO and EDA, the recombination is implicit, because new solutions are generated by distribution in the search space, which is a function of previous populations. This allows taking controlled steps in the search space, which, as a rule, are “larger” than the steps performed in the trajectory methods. As a rule, the decisions that result from recombination in population methods are usually more “different” from the parental individuals (than, say, using a move in a taboo search).

Cooperative search. The free form of hybridization is provided by a co-operative search [3, 4, 12], which consists of a search performed by various algorithms that exchange information about states, models, entire subtasks, solutions, or other characteristics of the search space. As a rule, joint search algorithms consist of parallel execution of search algorithms with different levels of communication. The algorithms may be different or instances of the same algorithm using different models or working with different parameter settings. The algorithms that make up the cooperative search engine can be all approximate, complete, or mixed.

5 Multidisciplinary Applications of CI

Applications of these hybrid methods of CI are contained in various fields of science and technology, for example, machine condition monitoring, fault detection and diagnosis [21]; intelligent production systems [21], biomedical applications in the healthcare system [22].

Note that there is a type of system that must act in advance taking into account the predicted state of the system in an unknown, uncertain, and changing environment. This is a guide to the development of intelligent autonomous systems. These systems form a wider class of newly created cyber-physical systems. In such systems, cyber resources representing computing, communication, and control are combined and matched to physical resources. To develop cyber-physical systems, often use the methods of CI, which have a unique ability to learn and adapt to new situations, using the processes of generalization, abstraction, and association peeped from nature.

Recently, the methods of CI are actively used in robotics, for example, a new direction “Evolutionary Robotics” has appeared. Moreover, CI methods are used both for solving problems of optimal path design, navigation, and training of individual robots and for collective behavior simulation and training of a robot group. For example, swarm and evolutionary algorithms are used to solve problems such as “box pushing”, where a group of robots must move a large object, which is significantly superior in weight and size to an individual robot. Swarm robotics studies how a large number of relatively simple physical agents (robots) can be organized in such a way that the desired collective behavior is achieved through local interactions between agents and agents with the environment. Swarm robotics deals with the problem of behavior design of individual robots and their interaction between themselves and the environment so that the desired collective behavior is achieved. Currently, there are no well-established approaches to the determination of group robot behavior at the lower level to achieve the desired collective behavior. Collective behavior is not just the sum of the behavior of individual agents of the collective, it is determined at the “social level”. This approach is also used to design robotic systems from various components. Note that all CI paradigms are actively used in robotics. This area is close to intelligent production systems, where the methods of CI are also widely used. In particular, such methods have been successfully applied to optimize production schedules [21, 23].

Currently, large volumes of data are collected in various forms in different areas, for example, related to business, science, technology, and biomedicine. An urgent problem is the processing of data of very large volumes to assess the current state of the system and identify early signs of any possible deterioration in the performance of systems. CI methods are ideal for applications such as tools for extracting knowledge from data for complex and often seemingly insoluble systems.

It should be noted the widespread use of CI methods, including hybrids, in computer-aided design (CAD) systems. For example, they are widely used in computer systems CAD [23], mainly at the stages of: (1) logical synthesis (design); (2) physical design (partitioning, placement, tracing); (3) testing. At the stage of synthesis of digital circuits, the methods of CI are applied at various levels: (1) transistor; (2) valve; (3) functional. In the synthesis of digital and analog circuits, CI algorithms are used to search for a circuit configuration in order to achieve its behavior in accordance with the specifications. Note that these methods allow problem-solving of not only para-metric but also structural synthesis, which was previously impossible. For the same reasons, CI methods have also been found to be effective in mechanical engineering CAD systems. CI methods, and especially hybrid systems, are effectively used in image processing and pattern recognition. In particular, they are used in segmentation and recognition of medical images [22, 24]. This determines their biomedical applications and their use in technical diagnostic systems, monitoring and predicting the behavior of complex production systems.

6 Conclusion

The growing interest in multidisciplinary education and research at universities using CI is obvious. There is also interest in the broad areas of cyberinfrastructure, cyber systems for understanding complex interdisciplinary systems and their development, as can be seen from various programs adopted at the federal level. There is a need to educate the next generation in such “cyber” areas and CI. CI can be an important tool for interdisciplinary education and research.

References

1. Simon D.: Evolutionary optimization algorithms: biologically-inspired and population-based approaches to computer intelligence, p. 742. Wiley (2013)
2. Haykin, S.: Neural Networks and Learning Machines, 3rd edn. Prentice Hall, New Jersey (2009)
3. Venayagamoorthy, G.K.: A Successful Interdisciplinary Course on Computational Intelligence, pp. 14–23. IEEE Computational Intelligence Magazine, Institute of Electrical and Electronics Engineers (IEEE) (2009)
4. Engelbrecht, A.P.: Computational Intelligence: Introduction, p. 597. Wiley (2007)
5. Holland, J.H.: Adaptation in Natural and Artificial Systems, p. 228. MIT Press, Cambridge, Michigan (1992)
6. Rechenberg, I.: Evolutionstrategie: Optimierung technischer Systeme nach Prinzipien der biologischen Evolution. Fromman-Holzboog, Stuttgart (1973)
7. Fogel, I.J., Owensm, A.J., Walsh, M.J.: Artificial Intelligence through Simulated Evolution. Wiley, New York (1966)
8. Koza, J.R.: Genetic Programming: On the Programming of Computers by means of Natural Selection. MIT, Cambridge (1992)
9. Skobtsov, Y.A.: Fundamentals of Evolutionary Computing, p. 326. DonNTU, Donetsk (2008)
10. Skobtsov, Y.A., Speransky, D.V.: Evolutionary Computation: Handbook, p. 331. The National Open University “INTUIT”, Moscow (2015) (in Russian)
11. Kureichik, V.V., Kureichik, V.M., Rodzin, S.I.: Theory of Evolutionary Computing, p. 260. Fizmatlit (2012) (in Russian)
12. Karpenko, A.P.: Modern search engine optimization algorithms. Nature-inspired Algorithms, p. 448. PH MSTU, Moscow (in Russian)
13. Eberhart, R., Shi, Y., Kennedy, J.: Swarm Intelligence, p. 512. Morgan Kaufmann (2010)
14. Bonabeau, E., Dorigo, M., Theraulaz, G.: Swarm intelligence: From Natural to Artificial Systems, p. 320. Oxford University Press, New York (1999)
15. Kandy, J., Eberhart, C.: Particle swarm intelligence. In: Proceedings of the IEEE International Conference on Neural Networks, pp. 1942–1948. (1995)
16. Dorigo, M.: Optimization, learning and natural algorithm. In: PhD Thesis. Politecnico di Milano (1992)
17. Dorigo, M., Bonabeau, E., Theraulaz, G.: Ant algorithms and stigmergy. Future Gener. Comput. Syst. **16**, 851–871 (2000)
18. Yen, J., Langari, R.: Fuzzy Logic: Intelligence, Control and Information. Prentice Hall, Upper Saddle River, NJ (2000)
19. Dasgupta, D.: Artificial Immune Systems and Their Applications, p. 344. Springer (1999)
20. Dasgupta, D., Luis, F.N.: Immunological Computation—Theory and Applications, p. 298. CRC, Boca Raton, FL (2009)

21. Skobtsov, Y., Chengar, O., Skobtsov, V., Pavlov, A.: Synthesis production schedules based on ant colony optimization method. In: Kacprzyk J., et al. (eds.) Proceedings of the 6th Computer Science Online Conference 2017 (CSOC2017), in Advances in Intelligent Systems and Computing, vol. 1 (573), pp. 456–465. Springer International Publishing Switzerland (2017)
22. El-Khatib, S., Skobtsov, Y., Rodzin, S.: Improved particle swarm medical image segmentation algorithm for decision making. In: Intelligent Distributed Computing XIII. IDC 2019. Studies in Computational Intelligence, vol. 868. Springer, Cham (2020)
23. Skobtsov, Y.A., Skobtsov, V.Y.: Evolutionary test generation methods for digital devices. In: Adamski M., et al. (eds.) Design of Digital Systems and Devices, p. 331–361. (Lecture Notes in Electrical Engineering, vol. 79). Springer-Verlag, Berlin (2011)
24. El-Khatib, S.A., Skobtsov, Y.A., Rodzin, S.I.: Theoretical and experimental evaluation of hybrid ACO-k-means image segmentation algorithm for MRI images using drift-analysis. *Procedia Comput. Sci.* **150**, 324 (2019)

Effective Tools and Technologies for Creating and Maintaining Web Resources Based on JavaScript Libraries



Ina Lukyanovich, Lidia Blinkova, and Uladzislau Sableuski

Abstract A set of structural elements is proposed that extends the functionality of the CMS visual editor, created on the basis of the ReactJS library. The tools and technologies used to create a learning system in English based on JavaScript libraries are described. The developed and applied tools significantly reduce the labor costs of developing web resources.

Keywords Web resources · JavaScript · ReactJS · Gutenberg API · CMS wordpress · DBMS MongoDB

1 Introduction

Creating and maintaining web resources still remains a laborious, costly task and requires, at the minimum, some web development skills. The development of tools and technologies for creating websites takes place in the following main areas: improving security (not considered in this article), reducing the degree of the creators' of the Internet content dependence on software developers, increasing the efficiency of programmers' work [1].

I. Lukyanovich (✉) · L. Blinkova · U. Sableuski
Belarusian State University, 4 Nezavisimosti Avenue, 220030 Minsk, Republic of Belarus
e-mail: lukianinna12345@gmail.com

L. Blinkova
e-mail: lidiablinkova@gmail.com

U. Sableuski
e-mail: vladsablevsky@gmail.com

2 Custom Library of Site Constructs Based on API CMS

The Website development based on the content management systems (CMS) greatly simplifies both the development and administration of resources for customer companies, thanks to a variety of plug-ins, templates, and other standard solutions. However, even to maintain a site created on the basis of CMS, you have to keep a specialist on your staff that has the necessary skills in web development or to contact the creators of the resource. In order to edit not only the content but also the page structure, in each developed CMS there are its own or integrated visual editors [2] and structural elements of web pages.

For CMS WordPress [3, 4] in particular, Gutenberg is such an editor [5], which allows one to create a page from the existing elements (Fig. 1) and develop custom blocks using the built-in Application Programming Interface (API). The term “block” is introduced to work in the Gutenberg content editor. A block is a functionally independent component of a page that can be used an unlimited number of times. Each paragraph, image, button, title, quote, video can be a separate block.

Besides buttons, the Gutenberg editor provides many other built-in block types such as columns, dividers, inline widgets, and other content types. There are also blocks available that allow you to embed services from third-party companies, including SoundCloud, Meetup.com, Reddit, TED, WordPress.tv, and many others. Currently, the built-in collection of Gutenberg has 66 blocks.

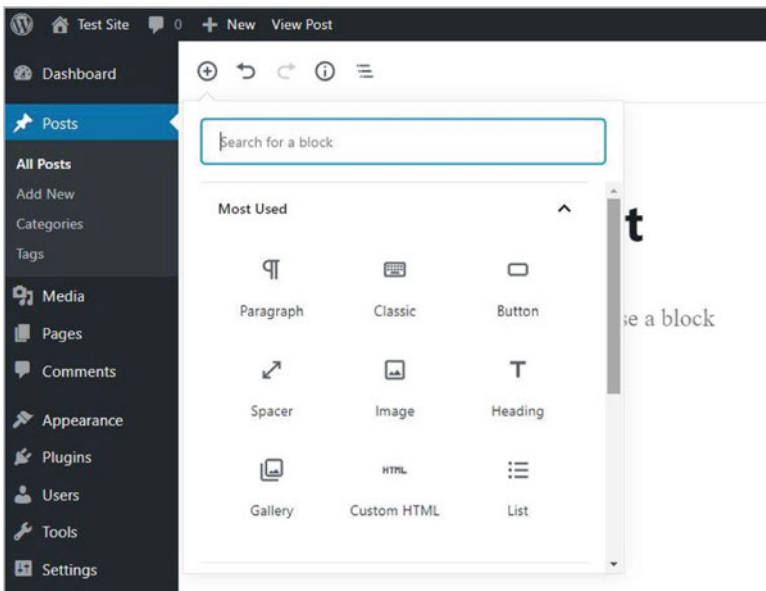


Fig. 1 Gutenberg visual content editor and its components: list, button, gallery, title, etc.

The advantage of the Gutenberg visual content editor is the clear and valid HTML of the inline blocks.

The weakness of almost all standard library blocks created by third-party developers is the fact that they are implemented without taking into account the integrability into the Document Object Model (DOM) [6] for sites of various types and purposes. Even with significant efforts of the creators of such libraries, they cannot fully meet the dynamically changing requirements of the subject area. The lack of flexibility—the degree of customization of properties—of system blocks makes editing ineffective (if any) and leads to the need to create new blocks.

However, we have to state that the system set of typical constructs of the Gutenberg editor does not allow one to obtain high-quality design solutions, either: its universal blocks are not suitable for the formation of the entire variety of web pages. Therefore, the development of sets of custom blocks is relevant.

The advantage of the Gutenberg visual content editor is a clean and valid HTML code of the built-in blocks. The development of their own structural elements is carried out using the ReactJS [7] JavaScript library, the peculiarities of working with the library are familiar to most Frontend developers. This library uses JSX [8], a JavaScript language extension that allows HTML-like code to coexist with JavaScript code.

When constructing blocks for pages and sites of various types [9], one should decompose page elements differently, determine their composition and nesting.

The Gutenberg open-source visual content editor API [5] is used to develop a library of reusable constructive elements of a single page website [9].

As a result of the decomposition of the elements of the site pages of this type, the following structural elements have been distinguished: design layout blocks, divided according to their purpose and technical characteristics; the main screen; the block of provided services or a unique trading offer; the recall block, etc.—the total of 26 blocks.

The elements of such a library should have the following abilities:

- to transform,
- to change their style,
- to edit the content of each block,
- to be adaptive,
- to appear in the editor block inside the admin toolbar.

The set of design elements is organized as a separate WordPress plugin so that it can be used on any websites running this CMS and CMS Drupal [10].

The library is a collection of JavaScript and Cascading Style Sheets (CSS) files. The only project PHP file describes the logic for connecting these files.

Let's consider the process of constructing a library element using the Progress-Section statistics block as an example, its design layout is shown in (Fig. 2).

Structurally, the block is made up of the background, (a color fill and an image with a transparent background), the left side of the block (title, subtitle, text block), and the right side of the block. The right side of the block (Fig. 3) contains a variable

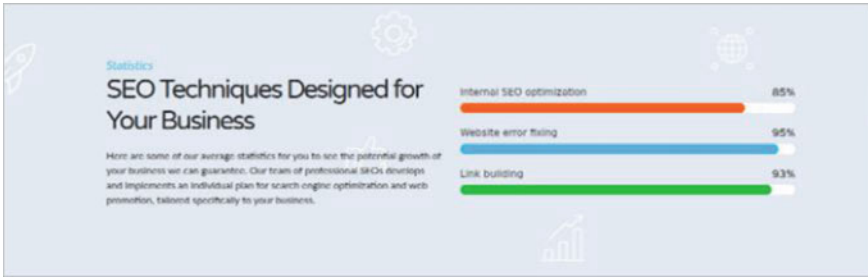


Fig. 2 Design layout of the ProgressSection statistics block

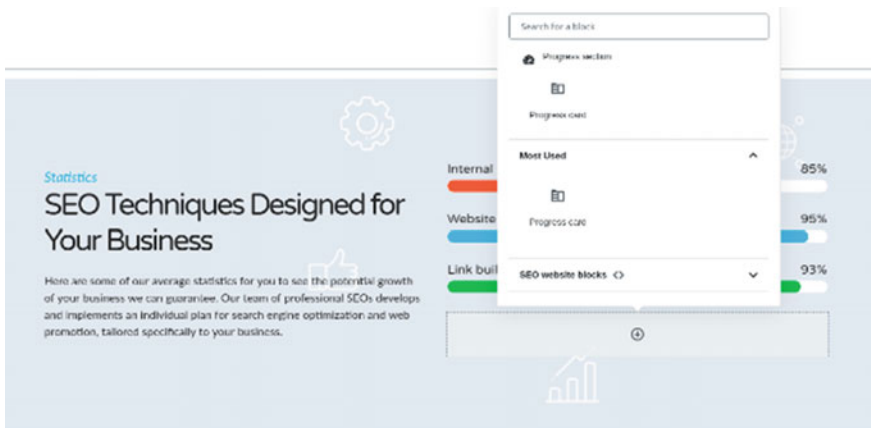
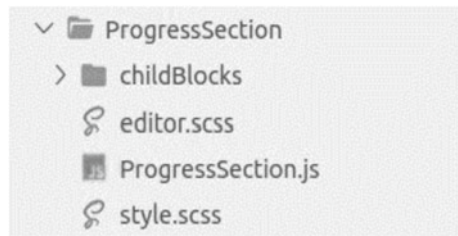


Fig. 3 The appearance of the ProgressSection block in the admin panel

number of child blocks—progress bars (color, text, completion percent). All of the listed structural elements of the block are editable.

The structure of the directory containing the statistics block is shown in Fig. 4. The parent block is described in the ProgressSection.js file. The child block code is located in the ProgressBar.js file, in the childBlocks folder.

Fig. 4 Directory structure of the statistics block



The appearance of the `ProgressSection` and `ProgressBar` blocks are defined in the SASS style files: `style.scss` and `editor.scss`.

The following attributes are set for the `ProgressSection` parent block:

- `id`—a unique identifier for the block that is generated by the default and can be used as a selector if it is necessary to change the DOM tree;
- `title`—the text title;
- `subTitle`—the text subtitle
- `info`—the text content of the block;
- `bgColor`—hexadecimal color code block fill;
- `bgImageURL`—link to the background image of the block.

The `ProgressSection` block consists of two React components [11]: the `View` component, which is responsible for the appearance of the block in the Gutenberg editor, and on the website page; the `Controls` component responsible for displaying the block settings in the parameter column in the Gutenberg editor.

Inside the `Controls` component, the logic for changing the background image and the fill color are described. To do this, special components that are part of the Gutenberg API editor are used in the controls component: the `MediaUpload` component, which is responsible for loading media files (in this case, images); a `ColorPicker` component that provides a choice of colors.

The appearance of the settings of the `ProgressSection` block is displayed in the editor, and this also requires writing an appropriate code.

About 200 lines of the code written to implement this element of a web page make it possible to manage all its parameters, to provide full controllability in the formation of various pages and sites.

An important property of the project is its integration with `webpack`, a static modular collector for JavaScript applications [12].

The builder is open-source and allows you to package, compile, and link all the resources required for a JavaScript project.

The collector has an entry point that it uses to build an internal dependency graph. After defining the entry point, the builder records which modules and libraries exist and how they are related. As a result, each dependency turns into files—packages. The output point indicates where the builder places the generated package files and how they name them. Loaders are special modules that allow you to handle various types of files. In this case, the project is divided into small modules [13].

The `webpack` builder configuration is described in the `webpack.config.js` file, which is located in the root directory of the project. `Webpack` is an open-source that allows you to solve many problems related to organizing the structure of the entire project.

The implementation of the website own structural elements greatly facilitates the administration of web resources, improves the quality, and reduces the development time by applying a set of pre-created components with their structure and logic, by changing some parameters and style.

3 MERN-Technology to Develop a Training System

Another important way to increase the efficiency of creating and maintaining sites and web applications written by using JavaScript libraries is the use of modular architecture and the development tools that allow one to implement such systems with minimal labor costs.

Let’s take a look at some of its key features using the English Learning System [14] web application. The teaching and testing web system for the English grammar is implemented on the basis of the methodology described in the book: “Collection of exercises for practical English grammar. A Practical English Grammar Programmed Workbook” R.W. Markley and E.W. Brockman with additional exercises by “L.A. Barmina and I.P. Verkhovskaya” [15].

The teaching system consists of several lessons. Each lesson contains questions that are divided into three types: text questions without an answer, questions that have one or more correct answers, and questions the answer to which must be entered from the keyboard (Fig. 5).

The creation of the second part of the English Language Learning System web application and the revision of its first part confirm the correct choice of MERN technology [16]. MERN technology, consisting of MongoDB, Express, React, Node.js, is one of the most popular tools for creating web applications. The technology reflects a modern approach to web development, in which at each level of the application, from client to server, the same language is used—JavaScript.

The MongoDB DBMS and the Postman application that fills it are of particular interest. MongoDB [17] is a document-oriented database management system (Fig. 7). The data in MongoDB are not written in tables and columns, as in a

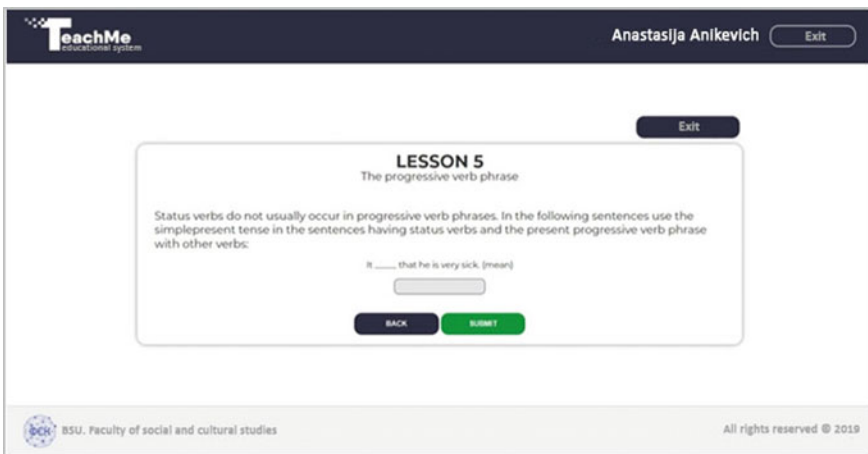


Fig. 5 The question the answer to which must be entered from the keyboard

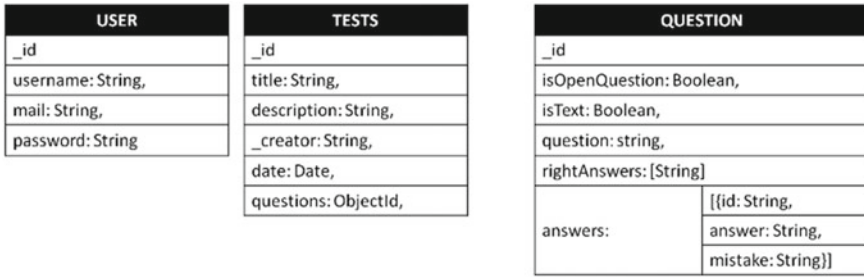


Fig. 6 Database scheme of the English language learning web application

relational database; instead, JSON-like documents with dynamic schemes are stored in MongoDB [18].

The MongoDB database may either not have any collections, or may contain a lot of collections. The collection is very similar to a traditional table and consists of zero or more documents. A document can be thought of as a string consisting of one or more fields that are similar to columns. The indexes in MongoDB are almost identical to those in relational databases. When any data are requested in MongoDB, the position of the record is returned, which can be counted, skipped a certain number of previous records without loading the data themselves [19].

The web application should store the information about the registered users, as well as about LESSONS added and QUESTIONS TO THEM.

Data storage is organized using the special Mongoose module, which provides a convenient interface for working with the MongoDB database.

The diagram (Fig. 6) shows the structure of the web application documents:

- The document storing the information about the user has the structure shown in the USER scheme. The document consists of the user’s name “username”, password “password”, email address—“email”. Almost all fields store a string type information, except for the `_id` field. The `_id` field is created automatically when an object is written to the database and is initialized with a unique value.
- The structure for web application lessons is presented in the TESTS scheme. The structure consists of the following fields: the title of the LESSON—“title”, a brief description of the lesson—“description”, the creator of the lesson—“creator”. The date field stores the date the lesson was created. The Questions field is initialized by the identifier of the required question.
- The document that stores questions of a web resource have the structure presented in the QUESTION scheme. The lesson has several types of questions, each of which has its own fields: for a text question—the field is Text, for an open question (the answer to which must be entered from the keyboard)—the field is Open Question. The Question field stores the wording of the question. The Right Answers field holds the correct answer. The Answers field stores an array of objects; `id` is a unique value by which the correct answer is determined. The Answer field

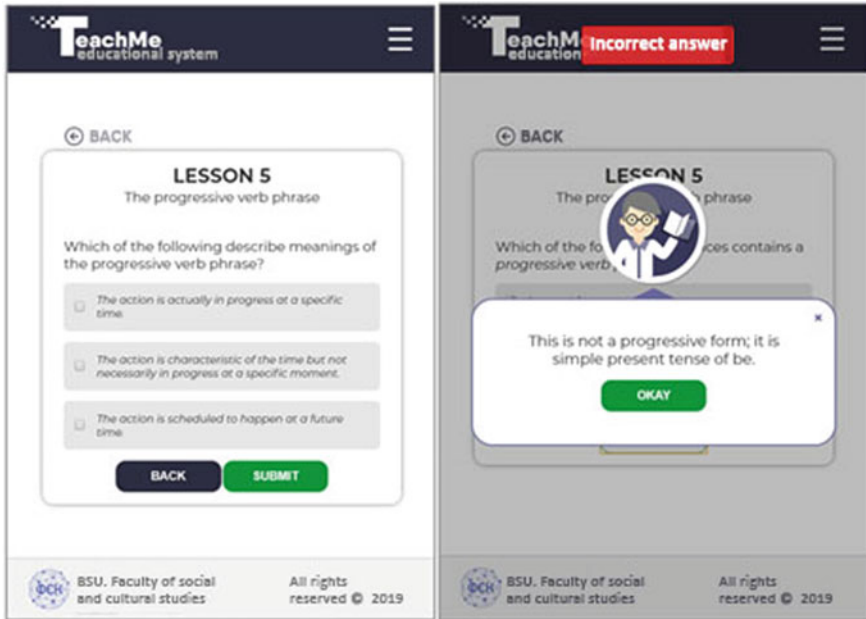


Fig. 7 A question and a hint to it on the iPad screen

contains the question, and in the Mistake field the text of the hint for this answer is stored.

When developing the application, a responsive layout was applied—a mobile version it is designed to be displayed both on the monitor screen and on the iPad and smartphone screens.

Responsive layout changes the design of the page depending on user behavior, platform, screen size, and device orientation and is an integral part of modern web development. It allows you to significantly save money and not to draw a new design for each resolution, but to change the size and location of individual elements.

To achieve responsiveness, grid layout, flexbox-technology, and media-queries were used.

Figure 7 presents a question and a hint to it on the iPad screen.

The Postman program [20] is used to add lessons and questions to the MongoDB database. The main purpose of this application is to create collections of POST requests to add a lesson to the application programming interface.

The database can be filled with third-party developers or subject specialists; the development of a special interface is not required to do this.

The developed web application is a universal module that can be used by students for self-study or distance learning [21].

4 Conclusion

Both the development of special APIs created to adapt the CMS to the current design tasks and the increased flexibility and availability of software products for front-end development contribute to reducing the dependence of the creators of the Internet content on software developers and to accelerating the implementation of web resources for various purposes.

The library of constructs for the formation of a one-page site presented in the work and “The Teaching System for English” created on the basis of MERN technology represent both of these trends. Custom libraries of site constructs, formed on the basis of the API, are applicable to many CMS, due to the generality of the toolkit—they can be used by site administrators to edit the content of an the Internet resource without involving a programmer. JavaScript libraries for front-end development, thanks to the improvement of visual tools for creating web resources, significantly reduce costs and speed up software implementation.

References

1. de Almeida Farzat, F., de Oliveira Barros, M., Horta Travassos, G.: Challenges on applying genetic improvement in JavaScript using a high-performance computer. *J. Softw. Eng. Res. Dev.* **6**, 12 (2018). <https://doi.org/10.1186/s40411-018-0056-2>
2. Elementor: #1 Free WordPress Page Builder. <https://elementor.com/>. Last accessed 28 Sept 2020
3. Heron, M., Hanson, V.L., Ricketts, I.: Open source and accessibility: advantages and limitations. *J. Interact. Sci.* **1**, 2 (2013). <https://doi.org/10.1186/2194-0827-1-2>
4. #1 WordPress Page Builder Plugin—WPBakery Page Builder. <https://wpbakery.com/>. Last accessed 28 Sept 2020
5. The new Gutenberg editing experience. <https://wordpress.org/gutenberg/>. Last accessed 28 Sept 2020
6. JavaScript and ECMA Specification. <https://www.w3resource.com/javascript/introduction/ECMA-and-javascript.php>. Last accessed 28 Sept 2020
7. Kulesza, R., de Sousa M.F., de Araújo, M.L.M., de Araújo, C.P., Filho, A.M.: Evolution of web systems architectures: a roadmap. In: Roesler V., Barrère E., Willrich R. (eds) *Special Topics in Multimedia, IoT and Web Technologies*. Springer, Cham (2020). https://doi.org/10.1007/978-3-030-35102-1_1
8. DOM Elements. <https://reactjs.org/docs/dom-elements.html>. Last accessed 28 Sept 2020
9. Tilda Publishen. <https://tilda.cc/ru/>. Last accessed 28 Sept 2020
10. Drupal for Developers. <https://www.drupal.org/developers>. Last accessed 28 Sept 2020
11. A declarative, efficient, and flexible JavaScript library for building user interfaces. <https://github.com/facebook/react>. Last accessed 28 Sept 2020
12. Concepts | webpack. <https://webpack.js.org/concepts/>. Last accessed 28 Sept 2020
13. Webpack—a bundler for javascript and friends. <https://github.com/webpack/webpack>. Last accessed 28 Sept 2020
14. Lukyanovich, I., Blinkova, L., Anikevich A.: Web application for independent work on English grammar with JavaScript libraries. In: Bolshakov A.A. (ed.) *Proceedings of the International Conference Mathematical Methods in Technique and Technologies—MMTT*, vol 12, pp.111–114. SPb Publishing house of Polytechnic University, (2019)

15. Marklee, R.W., et al.: Collection of exercises for practical English grammar. In: Bromine E.W. (ed.) *A Practical English Grammar Programmed Workbook*, p. 52. Collier Macmillan International, London (1977)
16. Bryce, C.: Security governance as a service on the cloud. *J. Cloud Comput.* **8**, 23 (2019). <https://doi.org/10.1186/s13677-019-0148-5>
17. Cornetta, G., Mateos, J., Touhafi, A., et al.: Design, simulation and testing of a cloud platform for sharing digital fabrication resources for education. *J. Cloud Comput.* **8**, 12 (2019). <https://doi.org/10.1186/s13677-019-0135-x>
18. Standard ECMA-404 The JSON Data Interchange Syntax 2nd edn. (December 2017). <https://www.ecma-international.org/publications/standards/Ecma-404.htm>. Last accessed 28 Sept 2020
19. Karl S. *The Little MongoDB Book*. Attribution-Noncommercial Unported license, p. 66. (2016)
20. The Collaboration Platform for API Development. <https://www.postman.com/>. Last accessed 28 Sept 2020
21. Onah, D.F.O., Pang, E.L.L., Sinclair, J.E.: Cognitive optimism of distinctive initiatives to foster self-directed and self-regulated learning skills: a comparative analysis of conventional and blended-learning in undergraduate studies. *Educ. Inf. Technol.* **25**, 4365–4380 (2020). <https://doi.org/10.1007/s10639-020-10172-w>